

Synthesis of Medium-Sized Oxygen and Nitrogen Heterocycles via Stevens
Rearrangement of Sulfonium Ylides and Formal Synthesis of (+)-Laurencin

by

Rongrong Lin

A thesis submitted in partial fulfillment of the requirements for the degree of

Doctor of Philosophy

Department of Chemistry
University of Alberta

© Rongrong Lin, 2017

Abstract

Medium-sized cyclic ether and amine motifs often constitute the framework of a variety of natural products with interesting biological activities. As a result, the construction of these heterocycles is an important subject in organic synthesis, which has triggered the development of many strategies. The Stevens [1,2]-shift of sulfonium ylides is a versatile way to form new C–C bonds, which could be applied in the synthesis of medium-sized heterocycles.

Chapter 1 is a review of recent developments on the generation of sulfonium ylides from metallocarbenes and sulfur nucleophiles and their subsequent transformations, including [2,3]-sigmatropic rearrangement, Stevens [1,2]-shift and S-H insertion. Background information on the metallocarbene generation *via* decomposition of α -diazocarbonyl compound is also discussed. However, synthetic applications using the Stevens [1,2]-shift of sulfonium ylides were under explored, which intrigued our investigation in this area.

A novel approach to medium-sized cyclic ethers was previously developed by the West group using a Stevens [1,2]-shift of a sulfonium ylide derived from a readily accessible six membered monothioacetal precursor. Chapter 2 provides a detailed discussion on an application of this methodology as the key step in an enantioselective formal synthesis of (+)-laurencin. The concise and efficient transformation offers a surprising degree of chirality transfer with observed retention of stereochemical configuration on the migrating carbon. The resulting sulfur bridge could be efficiently removed by reductive desulfurization.

An extension to this strategy to access medium-sized cyclic amines is described in Chapter 3. The substituted thiazolidine ring with a diazoketoester tether was prepared from readily available starting materials. Although the resulting diastereomeric products could not be separated, when they were subjected to the Stevens rearrangement conditions, the desired sulfur-bridged azepine was obtained in quantitative yield. This promising result proved the feasibility of the methodology. Additional investigation is currently in progress to study the stereoselectivity of this transformation. In the future, this methodology could be applied as the key step to synthesize *Stemona* alkaloids, such as stemoamide.

Preface

Review on the recent development of sulfonium ylide transformations in Chapter 1 will be published as Lin, R.; Atienza, B. J.; West, F. G., “Carbon-Carbon Bond Formation via Reactive Intermediates Generated from Trapping of Metallocarbenes with Nitrogen- and Sulfur-Based Nucleophiles,” *Manuscript in preparation* (invited short review for *Synthesis*). I was responsible for gathering literature reports and preparing the manuscript for the sulfur-based nucleophiles. Dr. Bren Jordan Atienza was responsible for the portion corresponding to the nitrogen-based nucleophiles (i.e., equal authorship). F. G. West was the supervisory author and was involved with concept formation and manuscript composition.

A significant portion of Chapter 2 was published in *Organic Letters* as Lin, R.; Cao, L.; F. G. West. *Org. Lett.*, **2017**, *19*, 552-555. Dr. Liya Cao was responsible for the methodology development and the initial route design for the formal synthesis. I was responsible for most work on the formal synthesis, preparation and characterization of compounds and preparing the manuscript. F. G. West was the supervisory author and was involved with concept formation and manuscript composition. A portion of Chapter 2 will be published in a full article as Cao, L.; Lin, R.; West, F. G. “Formation of Seven- and Eight-Membered Cyclic Ethers via Sulfonium Ylide Rearrangement and Application in the Formal Synthesis of (+)-Laurencin,” *Manuscript in preparation*. Dr. Liya Cao was responsible for the full-detailed development of methodology. I was responsible for the formal synthesis part including preparation and characterization of

compounds and the preparation of manuscript. Dr. F. G. West was the supervisory author and was involved with concept formation and manuscript composition.

Chapter 3 will be published as Lin, R.; Weilbeer, C.; Dorian, A.; West, F. G. "Formation of Medium-Sized Azacycles via the Stevens [1,2]-Shift of Sulfonium Ylides," *in preparation*. I was responsible for the synthetic design to access the required substrates, preparation and characterization of compounds, obtaining important preliminary results and preparing the manuscript. Dr. Claudia Weilbeer was responsible for further development of the methodology and synthetic design to access additional substrates, which was not included in this thesis. Andreas Dorian was responsible for the initial preparation of substrates as part of the undergraduate research project. Dr. F. G. West was the supervisory author and was involved with concept formation and manuscript composition.

Table of Contents

1 Chapter 1 Rearrangement of Sulfonium Ylides Derived from Diazocarbonyl Compounds.....	1
1.1 Introduction.....	1
1.2 Preparation of α -diazocarbonyl compounds.....	2
1.3 Reactivities of α -diazocarbonyl compounds	5
1.4 Structure and classification of metal carbenoids	7
1.5 Transition metal catalysis for decomposition of diazo compounds.....	11
1.5.1 Copper catalysis.....	11
1.5.2 Rhodium catalysis.....	15
1.6 Generation of sulfonium ylides.....	19
1.6.1 Deprotonation of sulfonium salts.....	19
1.6.2 Fluoride-induced desilylation of α -silylsulfonium salts.....	22
1.6.3 From carbenes generated thermally or photochemically	23
1.6.4 From metal carbenoids.....	24
1.7 An introduction on the Stevens rearrangement.....	24
1.7.1 Discovery	24
1.7.2 Mechanistic investigations on the Stevens rearrangement	25
1.8 Metallocarbene transformations with sulfur nucleophiles and synthetic applications	31
1.8.1 Reactivities of metallocarbenes with sulfur nucleophiles, an overview .	31
1.8.2 [2,3]-Sigmatropic rearrangement.....	32
1.8.3 The Stevens [1,2]-shift.....	43
1.8.4 S–H Insertions.....	55
1.8.5 Synthetic applications on the Stevens [1,2]-shift of sulfonium ylide	61
1.9 Conclusion	64
1.10 References.....	66

2	Chapter 2 Medium-Sized Cyclic Ethers via Stevens [1,2]-Shift of Mixed Monothioacetal Derived Sulfonium Ylides: Application to Formal Synthesis of (+)-Laurencin	73
2.1	Introduction.....	73
2.2	Previous total syntheses	75
2.2.1	Masamune's racemic total synthesis of (\pm)-laurencin	75
2.2.2	Murai's racemic total synthesis of (+)-laurencin	77
2.2.3	Overman's total synthesis of (+)-laurencin	80
2.2.4	Holmes' total synthesis of (+)-laurencin	82
2.2.5	Crimmins' total synthesis of (+)-laurencin.....	85
2.2.6	Kim's total synthesis of (+)-laurencin	87
2.2.7	Fujiwara's total synthesis of (+)-laurencin	88
2.3	Previous formal syntheses.....	90
2.3.1	Palenzuela's formal synthesis on Overman's intermediate	90
2.3.2	Pansare's formal synthesis of Palenzuela's intermediate	92
2.3.3	Martín's formal synthesis on Overman's intermediate.....	94
2.3.4	Hoffmann's formal synthesis of Holmes' intermediate.....	95
2.3.5	Crimmins' formal synthesis of Holmes' intermediate.....	97
2.3.6	Widenhoefer and Hong's formal synthesis of Kim's intermediate	98
2.4	Summary of the total and formal syntheses of (+)-laurencin	100
2.5	Results and discussion (a sulfonium ylide approach to the oxocene core).....	101
2.5.1	Preliminary consideration	101
2.5.2	Retrosynthetic analysis	103
2.5.3	Synthesis of the diazoketoester precursor (147) for the Stevens rearrangement	105
2.5.3.1	Preparation of acrylate ester 151, determination of enantiomeric ratio and absolute stereochemical configuration.....	105
2.5.3.2	Ring closing metathesis (RCM) and Michael addition.....	109
2.5.3.3	Formation of γ -lactone and reaction optimization	114

2.5.3.4	Synthesis of the substituted bicyclic 1,3-oxathiane	119
2.5.3.5	Retrosynthetic strategies to install the diazoketoester side chain .	123
2.5.3.6	Synthesis of the tethered diazoketoester moiety: strategy one	124
2.5.3.7	Synthesis of the tethered diazoketoester moiety: strategy two	126
2.5.4	Investigation of the Stevens [1,2]-shift.....	130
2.5.4.1	Preliminary results	130
2.5.4.2	Model study	133
2.5.4.3	Investigation on the key step.....	135
2.5.5	Synthesis of the Holmes intermediate 59.....	137
2.5.5.1	Reductive desulfurization	137
2.5.5.2	Olefin formation.....	140
2.5.5.3	Completion of the formal synthesis of (+)-laurencin.....	142
2.6	Conclusion and future directions	143
2.7	Experimental.....	149
2.7.1	General Information.....	149
2.8	References.....	193
3	Chapter 3 Medium-Sized Cyclic Amines via Stevens [1,2]-Shift of Sulfonium Ylides derived from Cyclic <i>N,S</i>-Acetals	201
3.1	Introduction.....	201
3.2	Applied strategies on azepine formation in the synthesis of stemoamide	202
3.2.1	Azepine formation by intramolecular cyclization of acyclic precursor	202
3.2.2	Azepine formation by [4+2] cycloaddition.....	205
3.2.3	Azepine formation by ring closing metathesis (RCM).....	206
3.3	Results and discussion	208
3.3.1	The proposal.....	208
3.3.2	Retrosynthetic strategy.....	210
3.3.3	Preparation of diazoketoester-thiazolidine substrate	211
3.4	Conclusion and future work.....	216

3.5	Experimental	221
3.5.1	General Information.....	221
3.6	References.....	231
Bibliography		235
Appendix I: Selected NMR Spectra (Chapter 2)		253
Appendix II: Selected NMR Spectra (Chapter 3).....		341

List of Schemes

Scheme 1.1 Wolff Rearrangement.....	1
Scheme 1.2 Regitz diazotransfer reaction.....	3
Scheme 1.3 One-pot preparation of diazoketoesters.....	4
Scheme 1.4 Catalytic inhibition by Lewis base	9
Scheme 1.5 Cyclopropanation reactions catalyzed by Cu(OTf) ₂	13
Scheme 1.6 Reduction of copper(II) to copper(I) by diazo compounds.....	13
Scheme 1.7 Synthesis of copper(I) α -carbonyl carbene complex	13
Scheme 1.8 Rh ₂ (OAc) ₄ catalyzed diazo decomposition and O–H insertion	15
Scheme 1.9 Base-induced generation of sulfonium ylide.....	20
Scheme 1.10 Formation of sulfur ylides and subsequent epoxidation reaction.....	21
Scheme 1.11 Base-induced sulfonium ylide formation and rearrangement	21
Scheme 1.12 Sulfonium ylide formation <i>via</i> fluoride-induced desilylation.....	22
Scheme 1.13 Sulfonium ylides derived from carbenes generated by photolysis.....	23
Scheme 1.14 The Stevens rearrangement of ammonium and sulfonium ylides.....	25
Scheme 1.15 Retention of configuration for the Stevens rearrangement.....	26
Scheme 1.16 Stevens rearrangement of chiral ammonium salt	27
Scheme 1.17 Radical pair pathways for the Stevens rearrangement	28
Scheme 1.18 Formation of homodimeric products during oxonium ylide rearrangement	29
Scheme 1.19 Copper-assisted mechanism for the Stevens rearrangement.....	30
Scheme 1.20 Reactions with propargyl sulfides.....	34
Scheme 1.21 Doyle-Kirmse reaction in water	35
Scheme 1.22 Hemin catalyzed Doyle-Kirmse reaction	36
Scheme 1.23 Doyle–Kirmse reaction catalyzed by electron-rich ferrate complex.....	38
Scheme 1.24 Cascade reaction initiated from sulfonium ylide.....	39
Scheme 1.25 Rhodium(II) catalyzed generation of sulfonium ylide and subsequent Sommelet–Hauser rearrangement.....	40

Scheme 1.26 Result of competing reaction pathways	41
Scheme 1.27 Oxindole synthesis via thia–Sommelet–Hauser rearrangement.....	42
Scheme 1.28 [2,3]-rearrangement of sulfonium ylide via in situ generated iodonium ylide	43
Scheme 1.29 The Stevens [1,2]-shift of sulfonium ylides derived from mixed cyclic thioacetals	44
Scheme 1.30 Early application of the Stevens [1,2]-shift of sulfonium ylides.....	44
Scheme 1.31 Synthesis of 1,4-oxathianes from 1,3-oxathiolanes	45
Scheme 1.32 Dirhodium tetraacetate catalyzed reaction of 1,4-oxathianes	46
Scheme 1.33 1,3-Dithiolane and 1,3-oxathiolane as starting materials.....	47
Scheme 1.34 Asymmetric Stevens [1,2]-shift of sulfonium ylide	48
Scheme 1.35 The competing pathway involving sulfonium ylide rearrangement.....	49
Scheme 1.36 Synthesis of tagetitoxin skeleton <i>via</i> photo-Stevens rearrangement.....	50
Scheme 1.37 Macrocyclic ring expansion <i>via</i> double Stevens rearrangement.....	51
Scheme 1.38 Intermolecular sulfonium ylide formation using spiro-thioketal	52
Scheme 1.39 Stevens rearrangement of intramolecularly generated sulfonium ylides	53
Scheme 1.40 Rearrangement of intramolecularly generated macrocyclic sulfonium ylides.....	54
Scheme 1.41 Sulfonium ylide rearrangement from disubstituted thietane	55
Scheme 1.42 Asymmetric S–H insertion generated from copper carbenoid	56
Scheme 1.43 Asymmetric S–H insertion reaction catalyzed by rhodium(II) complex and chiral spiro phosphoric acid.....	58
Scheme 1.44 S–H insertion reaction with trifluorodiazalkanes.....	59
Scheme 1.45 Copper catalyzed S–H insertion reaction with α -diazooesters	60
Scheme 1.46 Iron-based catalysis for S–H insertion reactions.....	61
Scheme 1.47 Synthetic applications of the Stevens [1,2]-shift of sulfonium ylides...	62
Scheme 1.48 Stevens [1,2]-shift of sulfonium ylide derived from <i>N,S</i> -acetal.....	62
Scheme 1.49 Asymmetric total syntheses of pyrrolizidine alkaloids	63

Scheme 1.50 Application of the Stevens [1,2]-shift in a formal synthesis of (+)- showdomycin	64
Scheme 2.1 Masamune's synthesis of oxocene 13, part one	76
Scheme 2.2 Masamune's total synthesis of (\pm)-laurencin, part two	77
Scheme 2.3 Murai's synthesis of intermediate 29	78
Scheme 2.4 Murai's synthesis of (+)-laurencin	79
Scheme 2.5 Overman's total synthesis of (+)-laurencin	81
Scheme 2.6 Yamaguchi lactonization and synthesis of the oxocene core	83
Scheme 2.7 Holmes' synthesis of (+)-laurencin	84
Scheme 2.8 Crimmins' asymmetric alkylation–ring closing metathesis approach	86
Scheme 2.9 Kim's total synthesis of (+)-laurencin	88
Scheme 2.10 . Fujiwara's total synthesis of (+)-laurencin	90
Scheme 2.11 Palenzuela's formal synthesis of Overman intermediate 43	92
Scheme 2.12 Pansare's formal synthesis on Palenzuela's intermediate	93
Scheme 2.13 Martín's formal synthesis of Overman's intermediate 43	95
Scheme 2.14 Hoffmann's approach to Holmes' intermediate 57	96
Scheme 2.15 Crimmin's formal synthesis of (+)-laurencin	98
Scheme 2.16 Widenhoefer and Hong's formal synthesis	99
Scheme 2.17 Previous work on the Stevens [1,2]-shift of ylide derived from acetal	101
Scheme 2.18 Stevens [1,2]-shift of ylide derived from mixed monothioacetal	102
Scheme 2.19 Preliminary results on formal synthesis of (+)-laurencin	103
Scheme 2.20 Retrosynthetic approach for the formal synthesis of (+)-laurencin	104
Scheme 2.21 Synthesis of acrylate ester 151	106
Scheme 2.22 Determination of enantiomeric ratio <i>via</i> Mosher ester derivatives	108
Scheme 2.23 Facially selective Michael addition	114
Scheme 2.24 Initial attempt at the formation of 1,3-oxathiane 149	115
Scheme 2.25 Synthesis of 150 from 170 and 167	118
Scheme 2.26 Step-wise synthesis of mercaptoalcohol 150	119
Scheme 2.27 Retrosynthetic analysis to approach 148	120

Scheme 2.28 Preparation of aldehyde 168 and dimethylacetal 174	120
Scheme 2.29 Epimerization of 178 to 148.....	123
Scheme 2.30 Retrosynthetic strategies to access diazoketoester 147	124
Scheme 2.31 Synthesis of ketoester 180.....	125
Scheme 2.32 Preparation of Weinreb amide 187.....	127
Scheme 2.33 Attempted protection of the axial hydroxyl group as PMB ether	128
Scheme 2.34 Acetate protection of the axial hydroxyl group.....	129
Scheme 2.35 Synthesis of diazoketoester 194	130
Scheme 2.36 Proposed mechanistic pathways.....	133
Scheme 2.37 Preparation of model compound 206	134
Scheme 2.38 The key step under optimized reaction conditions.....	136
Scheme 2.39 Elimination of the reaction pathway from 195 to 196	137
Scheme 2.40 Additional investigations into the reductive desulfurization.....	139
Scheme 2.41 Preparation of alcohols 213.....	141
Scheme 2.42 Olefination by the Chugaev elimination	142
Scheme 2.43 Completion of the formal synthesis	143
Scheme 2.44 Synthesis of ketone 58.....	143
Scheme 2.45 Potential transformation of the sulfur bridged cyclic ether.....	145
Scheme 2.46 Proposal for the use of radical clock to probe the mechanism for the Stevens rearrangement.....	146
Scheme 2.47 Proposal for the use of (<i>trans-trans</i>)-2-methoxy-3-phenylcyclopropyl substituent to differentiate reaction pathways	147
Scheme 2.48 Future applications of the Stevens rearrangement chemistry.....	148
Scheme 3.1 William's strategy for the synthesis of perhydroazaazulene core.....	202
Scheme 3.2 Sato and Chita's approach on the perhydroazaazulene core	203
Scheme 3.3 Intramolecular propargylic Barbier reaction	204
Scheme 3.4 Formation of azepine via cationic cyclization.....	204
Scheme 3.5 SmI ₂ promoted intramolecular cyclization.....	205
Scheme 3.6 . Formation of azepine <i>via</i> [4+2] cycloaddition	206

Scheme 3.7 Formation of azepine <i>via</i> ring closing metathesis	207
Scheme 3.8 Generation of medium-sized cyclic amines <i>via</i> Stevens [1,2]-shift of <i>N,S</i> -acetal derived sulfonium ylide	209
Scheme 3.9 Retrosynthetic plan for the formation of azepine.....	210
Scheme 3.10 Preparation of 4-amino-3-mercaptoputyric acid 54	211
Scheme 3.11 Preparation of pyrrolidone 61	212
Scheme 3.12 Synthesis of the diazoketoester side chain	213
Scheme 3.13 Stevens [1,2]-shift of sulfonium ylide derived from thiazolidine	214
Scheme 3.14 Preparation of dimethyl-substituted thiazolidine 68	215
Scheme 3.15 Stevens [1,2]-shift of sulfonium ylide derived from dimethyl substituted thiazolidine.....	216
Scheme 3.16 Future plan for the synthesis of azepines and azocanes using Stevens [1,2]-shift of sulfonium ylides	218
Scheme 3.17 Retrosynthetic analysis for the preparation of substrates 47.....	219
Scheme 3.18 Future application towards stemoamide.....	219
Scheme 3.19 Retrosynthesis for bicyclic thiazolidine 82	220

List of Figures

Figure 1.1 Classic routes to α -diazocarbonyl compounds.....	3
Figure 1.2 Reactivities of α -diazocarbonyl compounds.....	6
Figure 1.3 Singlet and triplet carbenes (methylene).....	7
Figure 1.4 Fischer carbene vs. Schrock carbene.....	8
Figure 1.5 Catalytic cycle for the generation of sulfonium ylides with metallocarbenes derived from α -diazocarbonyl precursors	9
Figure 1.6 Classification of metal carbenoids.....	10
Figure 1.7 Stability and reactivity of diazocarbonyl compounds	11
Figure 1.8 Copper(II) acetylacetonate complexes and fluorinated analogues.....	14
Figure 1.9 Structure of $\text{Rh}_2(\text{OAc})_4$	16
Figure 1.10 Ligand effect on rhodium(II) complexes (only one ligand was shown for clarity)	17
Figure 1.11 Structures of dirhodium(II) carbenes.....	18
Figure 1.12 Examples of onium ylides	19
Figure 1.13 Sulfonium ylides generated from metallocarbenes	32
Figure 2.1 Representative examples of marine natural products containing medium- sized ether core.....	74
Figure 2.2 Examples of eight-membered C15 acetogenins	75
Figure 2.3 Summary of the key disconnections to construct the oxocene core.....	100
Figure 3.1 Natural products containing a medium-sized cyclic amine.....	201

List of Tables

Table 1.1 Catalyst effect for the [2,3]-rearrangement of diazoketone 23	15
Table 1.2 Ligand effect on diazo transformations	17
Table 1.3 Highly enantioselective [2,3]-rearrangement of sulfonium ylides	34
Table 2.1 Determination of the absolute configurations.....	109
Table 2.2 Reaction optimization for the ring closing metathesis reaction.....	113
Table 2.3 Investigation into the one-pot synthesis of mercaptoalcohol 150.....	117
Table 2.4 Stereoselective formation of 1,3-oxathiane	122
Table 2.5 Structural assignment for 184 in comparison with 148 and 178	126
Table 2.6 Preliminary result on the Stevens rearrangement of sulfonium ylide.....	132
Table 2.7 Screening of reaction conditions using model substrate 206.....	135
Table 2.8 Reaction optimization for the reductive desulfurization: part one	138
Table 2.9 Reaction optimization for the reductive desulfurization: part two	140
Table 2.10 Comparison of ^1H NMR data of 59 with literature data	189
Table 2.11 Comparison of ^{13}C NMR data of 59 with literature data.....	190
Table 2.12 Comparison of ^1H NMR data of 58 with literature data.....	191
Table 2.13 Comparison of ^{13}C NMR data of 58 with literature data.....	192

List of Symbols and Abbreviations

$[\alpha]_D^{20}$	specific rotation at 20 °C and wavelength of sodium D line
δ	chemical shift
Å	angstrom
Ac	acetyl
Ac ₂ O	acetic anhydride
acac	acetylacetonate
acam	acetamidate
app	apparent (spectral)
aq	aqueous solution
Ar	aryl
Ar _F	3,5-bis(trifluoromethyl)phenyl
B:	unspecified base
9-BBN	9-borabicyclo(3.3.1)nonane
Bn	benzyl
BOM	benzyloxymethyl
br	broad (spectral)
Bu	butyl
Bz	benzoate
°C	degrees celsius
¹³ C	carbon-13
calcd	calculated
CAN	cerium ammonium nitrate
cap	caprolactamate
cat	indicates that the reagent was used in a catalytic amount
CDI	1,1-carbonyliimidazole
CIDNP	chemically induced dynamic nuclear polarization
cm ⁻¹	wave numbers

conc.	concentrated
Cp	cyclopentadienyl
CSA	camphorsulfonic acid
Cy	cyclohexyl
d	day(s); doublet (spectral)
DBU	1,8-diazabicyclo[5.4.0]undec-7-ene
DCC	1,3-dicyclohexylcarbodiimide
DCE	1,2-dichloroethane
dd	doublet of doublets (spectral)
ddd	doublet of doublet of doublets (spectral)
dddd	doublet of doublet of doublet of doublets (spectral)
dq	doublet of quartets (spectral)
DDQ	2,3-dichloro-5,6-dicyano-1,4-benzoquinone
DEB	diethylbenzene
DIBAL-H	diisobutylaluminum hydride
DMA	dimethylacetamide
DMAP	4-dimethylaminopyridine
DMF	<i>N,N</i> -dimethylformamide
DMP	Dess-Martin periodinane
DMSO	dimethylsulfoxide
<i>dr</i>	diastereomeric ratio
DVS	1,3-divinyl-1,1,3,3-tetramethyldisiloxane
EDG	electron-donating group
<i>ee</i>	enantiomeric excess
EI	electron impact (mass spectrometry)
ent	enantiomer
eq	equation
equiv.	equivalent (s)
<i>er</i>	enantiomeric ratio

ESI	electrospray ionization (mass spectrometry)
Et	ethyl
EtOAc	ethyl acetate
EtOH	ethanol
EWG	electron-withdrawing group
g	gram(s)
h	hour(s)
^1H	proton
hfacac	hexafluoroacetylacetonate
HMBC	heteronuclear multiple bond coherence (spectral)
HMPA	hexamethylphosphoramide
HRMS	high resolution mass spectrometry
h ν	light
Hz	hertz
IBX	<i>o</i> -iodoxybenzoic acid
Ipc	diisopinocampheyl
Ipr	1,3-bis(diisopropylphenyl)imidazol-2-ylidene
IR	infrared
<i>J</i>	coupling constant
KHMDS	potassium bis(trimethylsilyl)amide
L	litre(s); unspecified ligand
LA	Lewis acid
LiHMDS	lithium bis(trimethylsilyl)amide
M	molar
m	multiplet (spectral)
m/z	mass to charge ratio
M^+	molecular ion
<i>m</i> -CPBA	<i>meta</i> -chloroperbenzoic acid
Me	methyl

Mes	mesityl
mg	milligrams(s)
MHz	metahertz
min	minute(s)
μL	microlitre(s)
mL	millilitre (s)
ML _n	unspecified metal-ligand pair
mmol	millimole(s)
mol	mole(s)
MOM	methoxymethyl
mp	melting point
MS	molecular sieves
Ms	methanesulfonyl
μW	microwave(s)
NHC	<i>N</i> -heterocyclic carbene
nm	nanometer
NMO	<i>N</i> -methylmorpholine <i>N</i> -oxide
NMR	nuclear magnetic resonance
Nu	unspecified nucleophile
OAc	acetate
Oct ₃ P	trioctylphosphine
OMe	methoxy
OMOM	methoxymethyl ether
Ooct	octanoate
OTf	triflate
<i>i</i> -Pr	isopropyl
<i>p</i> -TsOH	<i>para</i> -toluenesulfonic acid
pfb	perfluorobutyrate
PG	protecting group

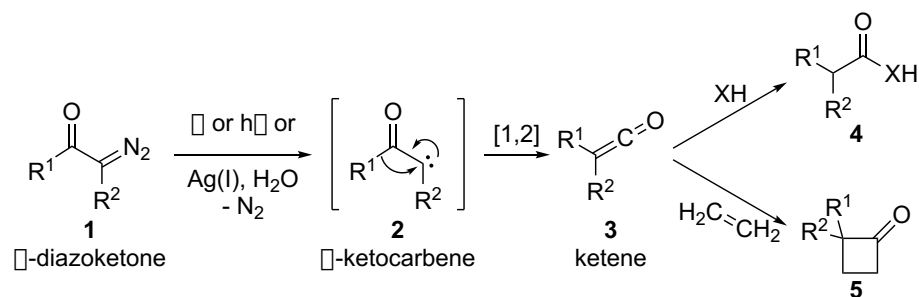
Ph	phenyl
Piv	pivaloyl
PMB	<i>para</i> -methoxybenzyl
PMP	<i>para</i> -methoxy phenyl
PNB	<i>para</i> -nitrobenzyl
ppm	parts per million
PPTS	pyridinium <i>p</i> -toluenesulfonate
PTSA	<i>p</i> -toluenesulfonic acid
Py	pyridine
q	quartet (spectral)
R	generalized alkyl group of substituent
Ra/Ni	Raney nickel
rac	racemic
R _f	retention factor (in chromatography)
rt	room temperature
s	singlet (spectral)
SEM	2-(trimethylsilyl)ethoxymethyl
t	triplet (spectral)
<i>T</i>	temperature
TBAF	tetrabutylammonium fluoride
TBAI	tetrabutylammonium iodide
TBDPS	<i>tert</i> -butyldiphenylsilyl
TBS	<i>tert</i> -butyldimethylsilyl
<i>t</i> Bu	<i>tert</i> -butyl
TES	triethylsilyl
Tf	trifluoromethanesulfonyl
TFA	trifluoroacetic acid
tfacac	trifluoroacetylacetonate
THF	tetrahydrofuran

THP	tetrahydropyran
TIPS	triisopropylsilyl
TLC	thin layer chromatography
TMS	trimethylsilyl
Tol	tolyl
TPA	triphenylacetate
TPAP	tetrapropylammonium perruthenate
TROESY	transverse rotating-frame overhauser enhancement spectroscopy
Ts	<i>para</i> -toluenesulfonyl
θ	dihedral angle (degree)

1 Chapter 1 Rearrangement of Sulfonium Ylides Derived from Diazocarbonyl Compounds

1.1 Introduction

α -Diazocarbonyl compounds are among the most versatile building blocks in organic synthesis with a broad spectrum of applications in natural product synthesis.¹ The first recorded α -diazocarbonyl compound was ethyldiazoacetate, which was synthesized by Curtius² in 1883 *via* diazotization of glycine ethyl ester. In 1902, Wolff^{3a} demonstrated the first example of an α -diazocarbonyl rearrangement by forming phenyl acetic acid from diazoacetophenone in the presence of silver(I) oxide and water. The process was believed to involve the generation of a carbene (**2**) followed by a [1,2]-shift to produce a reactive ketene intermediate (**3**), which was captured by various nucleophiles to form carboxylic acid derivatives (**4**) or reacted with olefins to yield cyclobutanones (**5**). Later, this process became known as the Wolff rearrangement.^{3b-c} Besides the use of silver salts, the Wolff rearrangement can also be promoted by thermolysis, photolysis and transition metal catalysis.



Scheme 1.1 Wolff Rearrangement

In late 1920s, Arndt and Eistert⁴ discovered a method of making α -diazocarbonyl compounds *via* acylation of diazomethane with acyl chlorides. Since then, various methodologies for the preparation of α -diazocarbonyl compounds have been reported. The decomposition of α -diazocarbonyl compounds generates high-energy species that

can be further reacted to form diverse products. Generation of carbenes from α -diazocarbonyl compounds with transition metal catalysts (Rh or Cu) is the most commonly employed method. The transient metalcarbene intermediates can undergo a broad range of transformations, such as Wolff rearrangements, C-H insertions, X-H insertions (X = O, N, S), cyclopropanation of olefins and ylide formation (Section 1.2.2.).¹ These transformations have been shown to be very useful tools in the synthesis of natural products. In this chapter, the main focus will be on the formation of sulfonium ylides from reactive metalcarbenes generated from α -diazocarbonyl compounds and their applications in accessing complex molecular structures.

1.2 Preparation of α -diazocarbonyl compounds

α -Diazocarbonyl compounds can be prepared using a variety of methods starting from various organic functionalities.^{1,5} The classic routes that lead to the formation of α -diazocarbonyl compounds are schematically presented in Figure 1.1. In the well-known Arndt-Eistert⁴ homologation reaction, an acyl chloride is generated from the corresponding carboxylic acid and then reacts with diazomethane to form an α -diazoketone (path A). This type of acylation reaction allows quick access to α -diazocarbonyl compounds from carboxylic acid precursors, but appropriate safety precautions must be taken due to the toxic and explosive nature of diazomethane. α -Amino compounds such as amino acids can undergo direct diazotization reactions with *in situ* generated nitrous acid to yield the desired α -diazocarbonyl compounds (path B). Ethyl diazoacetate is typically produced using this method from the ethyl ester of glycine.⁶ Dehydrogenation of hydrazones with oxidizing reagents (heavy-metal-based oxidants^{7a} or metal free variants^{7b}) can also be used (path C).

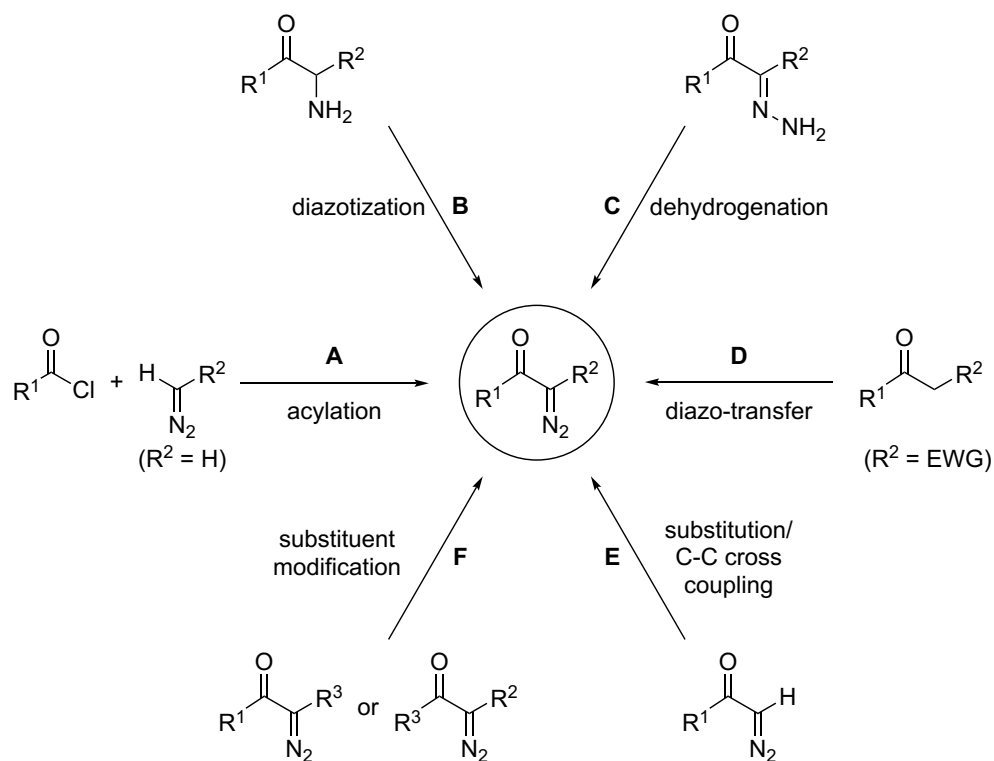
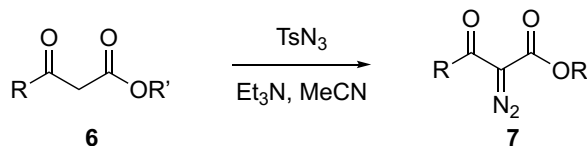


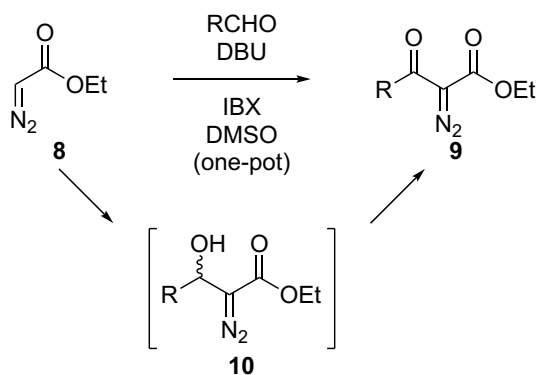
Figure 1.1 Classic routes to α -diazocarbonyl compounds

Diazotransfer of tosyl azide to the activated α -methylene position, typically known as the Regitz diazotransfer,⁸ is another commonly employed method (path D, Figure 1.1). The α -methylene position is typically activated by two flanking carbonyl functionalities or one carbonyl and one other electron withdrawing group. As depicted in Scheme 1.2, α -diazo- β -ketoester (**7**) is generated from β -ketoester (**6**) in the presence of tosyl azide under basic conditions. The Regitz diazotransfer has been applied to the synthesis of substrates in Chapter 3.



Scheme 1.2 Regitz diazotransfer reaction

Electrophilic substitution and transition metal catalyzed C–C cross coupling at the diazo carbon atom of α -diazocarbonyl compounds (path E, Figure 1.1) is an alternative strategy for further functionalization. A variety of methodologies were developed under this category. A typical example is the aldol-type C–C coupling of an α -diazocarbonyl precursor with various electrophiles, such as aldehydes and imines. For example, Steel and Erhunmwunse⁹ reported an efficient one-pot synthesis of α -diazo- β -dicarbonyl compound (**9**), which involved aldol-type addition of ethyl diazoacetate (**8**) to an aldehyde in the presence of DBU and subsequent *in situ* oxidation of **10** by IBX (Scheme 1.3). The one-pot two-step sequence demonstrated effective conversion of aldehydes to the corresponding α -diazo- β -dicarbonyl products. It can also serve as an alternative route to the traditional diazo transfer reaction. This method has been applied to give access to precursors used in the key step of a formal synthesis, and will be discussed in Chapter 2. In addition, under neutral or mildly basic conditions, direct substituent modification at either side of the diazocarbonyl group is also another strategy to access functionalized α -diazocarbonyl compounds (path F, Figure 1.1).



Scheme 1.3 One-pot preparation of diazoketoesters

1.3 Reactivities of α -diazocarbonyl compounds

It has been over 100 years since the discovery of the first α -diazocarbonyl compound – ethyl diazoacetate. As shown in Section 1.3, many methods are available to access this class of compounds. The reactivities of α -diazocarbonyl compounds and their synthetic applications have also been investigated extensively. Decomposition of α -diazocarbonyl compounds can provide reactive carbene intermediates with the loss of nitrogen. In early examples, free carbenes were often generated under thermal or photochemical conditions with diazo compounds and displayed unselective reactivity profiles due to their highly reactive nature.¹⁰ After the advent of copper catalysts¹¹ and dirhodium(II) complexes¹² for generating metal-stabilized carbenes, also known as metallocarbenes or metal carbenoids, α -diazocarbonyl compounds have emerged as versatile building blocks in organic synthesis.

Metallocarbenes derived from α -diazocarbonyl precursors are Fischer-type carbenes, and exhibit highly electrophilic characteristics at the carbon center.^{13,15} Thus, such metallocarbenes can participate in a variety of reactions with nucleophiles. The reactivity of α -diazocarbonyl compounds is summarized in Figure 1.2. The metallocarbene generated from α -diazocarbonyl compounds can react with diazocarbonyl substrate to result in dimerization (path A, Figure 1.2). In many cases, the diazo compounds are slowly added to the reaction mixtures to prevent the undesired dimerization pathway. Dilution of the reaction mixture is also another way to prevent dimerization.

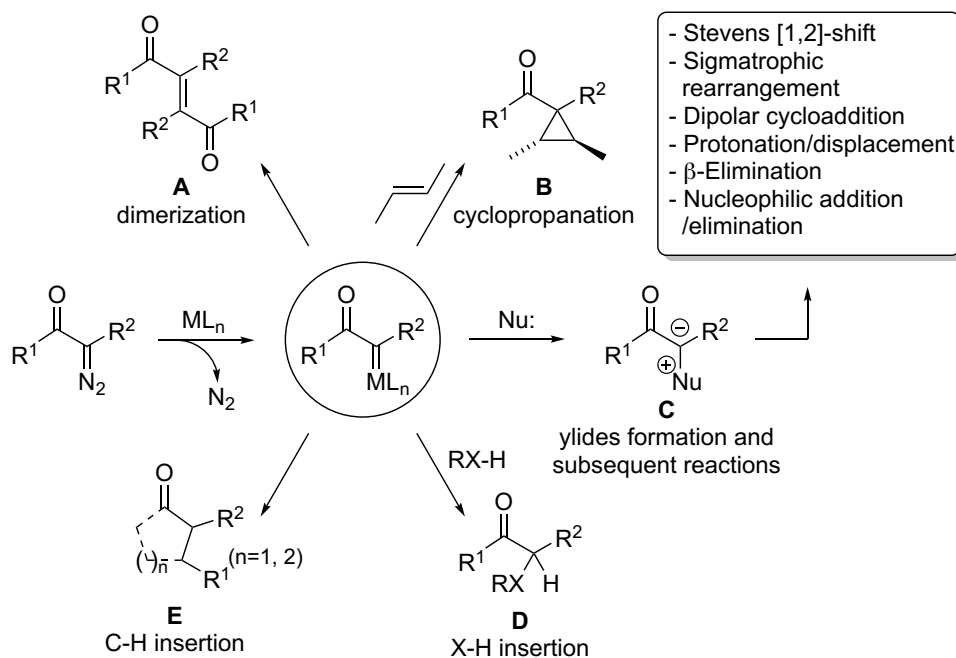


Figure 1.2 Reactivities of α -diazocarbonyl compounds

Inter- or intramolecular reactions of metallocarbenes with olefins yield cyclopropanes (path B, Figure 1.2).^{1,5} Intramolecular insertion of carbenes into unactivated C–H bonds (path E with an extended carbon chain on R¹) has often been used as a C–C bond forming strategy to form five-membered rings (four-membered and six-membered rings are also possible).^{1,5c} On the other hand, insertion of carbenes into X–H bonds (X = O, N, S, Se, P or Hal) can provide X–C bonds (path D).^{1,5a,5c} When the metallocarbene is generated in the presence of a Lewis basic heteroatom (N, O or S), the corresponding onium ylide is readily formed (path C). Common examples of such Lewis bases are ethers, carbonyls, amines, imines and sulfides. Depending on the type of ylide and the nature of the substituent, a variety of subsequent reactions can occur, such as a Stevens [1,2]-shift, sigmatropic rearrangement, dipolar cycloaddition, etc. Ylide transformations generated from α -diazocarbonyl compounds have thus become a vibrant and exciting field of research. Given the central role played by sulfonium ylides in the research described in this thesis, their generation and subsequent transformations will be the primary focus of this chapter.

1.4 Structure and classification of metal carbenoids

Carbenes^{14a} are charge neutral species bearing one divalent carbon atom with two nonbonding valence electrons. They can be classified as singlet or triplet carbenes, depending on the electronic configuration of the two nonbonding electrons. Reactions of free carbenes can have rather limited synthetic value owing to their high reactivity and consequent low selectivity. The most elementary example is the extremely reactive methylene (:CH₂), which can be generated by direct photolytic decomposition of diazomethane and has been described as “the most indiscriminate reagent known in organic chemistry” (Figure 1.3).^{14b} It was not until the introduction of the transition metal carbene complex by Fischer in 1964¹⁵ that this class of reactive species emerged as valuable intermediates in synthetic organic chemistry.

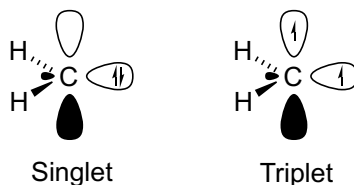


Figure 1.3 Singlet and triplet carbenes (methylene)

Carbenes can be stabilized *via* a formal metal-carbon double bond (Figure 1.4).¹⁶ The carbene unit donates the nonbonding electrons to an empty metal orbital to form the metal-carbon σ -bond, and back donation of the d-electrons from the metal to the electron-deficient carbene carbon atom forms a π -bond. When the back bonding is moderate, with low-valent late transition metals, the carbenoid is electrophilic at the carbon atom and it is referred to as a Fischer carbene. On the other hand, when the back bonding is strong, with high-valent early transition metals, the carbenoid is nucleophilic at the carbon atom and it is referred to as a Schrock carbene.

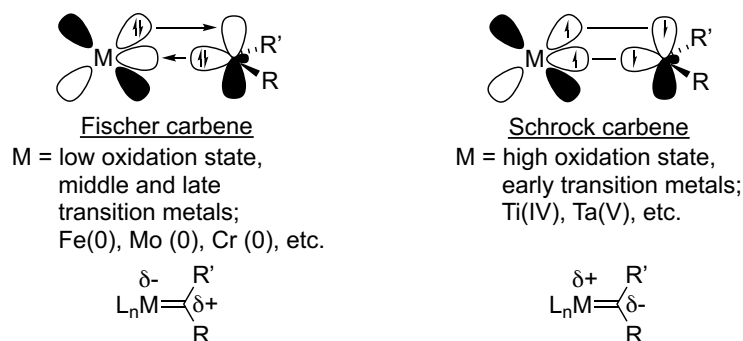


Figure 1.4 Fischer carbene vs. Schrock carbene

The mechanism for decomposition of diazo compounds by copper bronze was first suggested in 1952 by Yates.¹⁷ As shown in Figure 1.5, coordinative unsaturation of Lewis acidic transition metal salts, such as a $Rh_2(OAc)_4$ and Cu(I) complex, to α -diazocarbonyl precursor **11** leads to intermediate **12**. Extrusion of nitrogen then affords the metal-stabilized carbene **13**, which is electrophilic at the carbon center. Attack of a sulfur nucleophile on the electrophilic metallocarbene provides the metal-associated sulfonium ylide **14**,^{1,5,18} which then undergoes dissociation of the metal to generate a free sulfonium ylide **15** and the catalytically active ML_n . The free ylide then undergoes further transformations and ML_n reacts with another molecule of **11**. Alternatively, the metal catalyst may remain associated with the ylide during the subsequent transformations, which could lead to asymmetric induction when chiral ligands are used.^{19a}

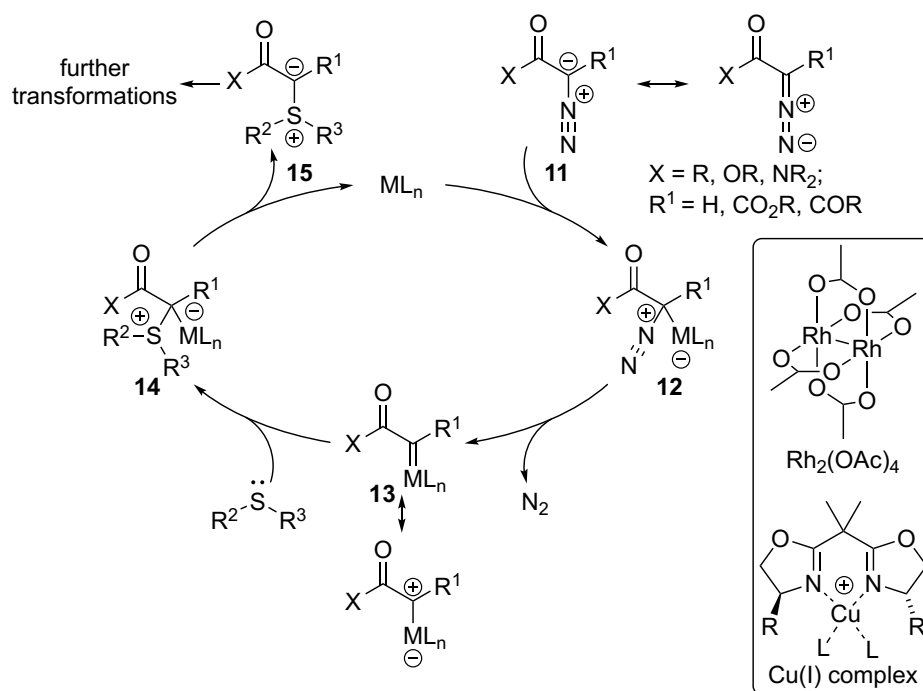
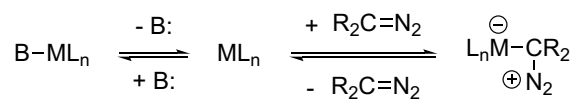


Figure 1.5 Catalytic cycle for the generation of sulfonium ylides with metallocarbenes derived from α -diazocarbonyl precursors

Oxygen and nitrogen nucleophiles have also been demonstrated to react with metallocarbenes to give oxonium and ammonium ylides, respectively. It is also noteworthy that due to the coordinative unsaturation of the metal catalyst, Lewis basic moieties (B:) can associate with the metal catalyst and inhibit diazo decomposition, as shown in Scheme 1.4.¹ Sulfides, amines and nitriles are examples of inhibitors. However, it is the stability of B-ML_n complex that determines the degree of inhibition for diazo compound association.¹ Dichloromethane and 1,2-dichloroethane are often used as solvents for metallocarbene generation because of their limited capacity to coordinate to the metal complexes.



Scheme 1.4 Catalytic inhibition by Lewis base

In addition, the reactivity of transition metal-stabilized carbenes is greatly influenced by the substituents on the α -diazocarbonyl compounds. Hence, the metal carbenoid intermediates have been classified into three major groups: acceptor/acceptor-, acceptor- and acceptor/donor-carbenoids (Figure 1.6).^{19b} The terms acceptor and donor refer, respectively, to the electron withdrawing and donating capability of the substituents at the metal center by resonance. Electron deficient carbene centers are destabilized by acceptor groups and thus the acceptor/acceptor- and acceptor-carbenoids are highly reactive towards nucleophiles. However, a donor group stabilizes the electron deficient metal carbene, and attenuates the reactivity of the acceptor/donor carbene, making it more selective.²⁰

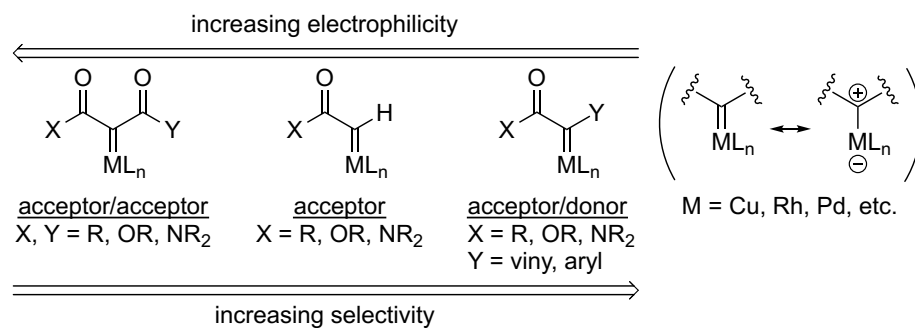


Figure 1.6 Classification of metal carbenoids

The reactivity of the transition metal catalysts is dependent on the Lewis acidity of the catalysts and the nucleophilicity of the diazo compounds (Figure 1.7).^{1,19b,21} The formal negative charge on the diazo carbon can be delocalized and stabilized by electron withdrawing carbonyl groups. However, the diazo compounds with two flanking carbonyl groups on the diazo carbon atom are more stable towards transition metal catalyzed decomposition than those with one carbonyl group.¹⁸ Less reactive acceptor/acceptor or acceptor type diazo compounds generally demand higher temperatures to undergo reactions with transition metal catalysts. Solvents such as 1,2-dichloroethane, benzene, and toluene are often employed to achieve higher

temperatures for the decomposition of diazomalonates and diazoacetoacetates; otherwise, dichloromethane is used.²²

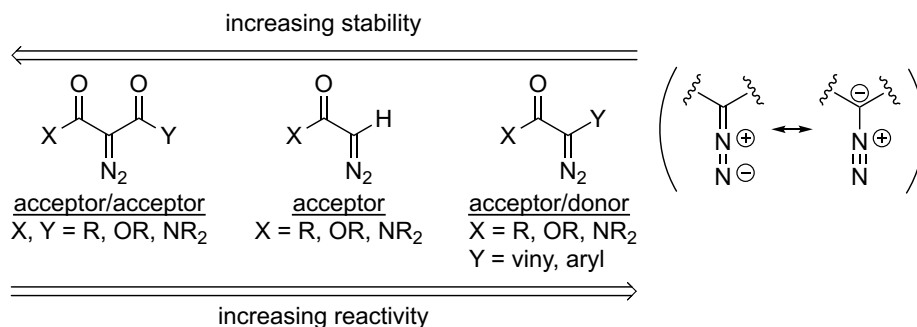


Figure 1.7 Stability and reactivity of diazocarbonyl compounds

1.5 Transition metal catalysis for decomposition of diazo compounds

The first recorded example of a transition metal mediated reaction of a diazo compound was accomplished by Silberrad and Roy²³ in 1906, in which copper dust was used to accelerate the decomposition of ethyl diazoacetate. Since then, a variety of late transition metal complexes (Cu, Rh, Pd, Co, Ru, etc.) have been developed. Among various metallocarbenes, those formed with copper and rhodium complexes are exceptionally prominent and attracted the most attention in the synthetic community due to their effectiveness and versatility. This section provides a basic background of the commonly used transition metal catalysis (Rh, Cu, etc.) in metal carbenoid transformations.

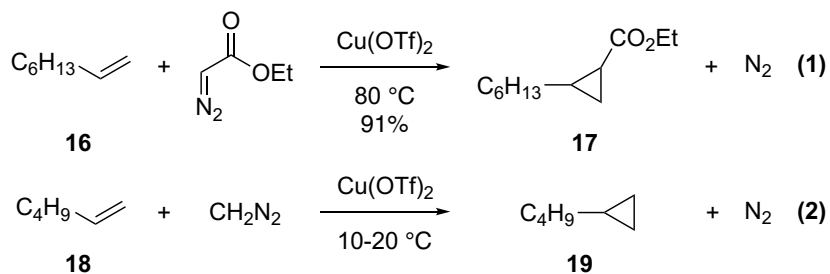
1.5.1 Copper catalysis

Copper catalyzed diazo decomposition, discovered over a century ago,²³ continues to be frequently applied in organic synthesis. Copper bronze and copper(II) sulfate were the earliest copper catalysts employed for diazo decomposition.^{1,10b} However,

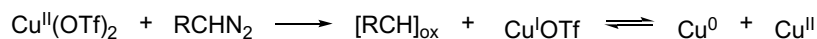
insolubility of these catalysts in the reaction medium limited their usage in diazo decomposition. Copper(II) acetylacetonate $[\text{Cu}(\text{acac})_2]$ ²⁴ and phosphite complexes of copper(I) chloride²⁵ were later developed as soluble alternatives to copper bronze and copper(II) sulfate. Synthesis of copper(II) complexes with chiral salicylaldimine ligands by Nozaki and coworkers²⁶ was the beginning of a modern era of asymmetric metallocarbene transformations.²⁷ Since then, the number of reports on various copper catalysts has shown exponential growth. However, the actual oxidation state of the active copper catalyst employed in the metallocarbene generation remained controversial for some time and both copper(I) and copper(II) were originally believed to be catalytically active.²⁸

In 1973, Kochi and coworkers^{29a} introduced homogeneous copper(I) trifluoromethanesulfonate (CuOTf) as a highly efficient catalyst for the decomposition of diazo compounds, and consequently influenced the basic understanding of copper catalysis for diazo decomposition, as well as metallocarbene mediated cyclopropanation reactions.²⁹ The authors established that copper(I) rather than copper(II) is catalytically competent. The nominally employed copper(II) complexes were reduced to copper(I) derivatives by a sacrificial amount of the diazo compound, which was supported by some important experimental observations as discussed below.

When $\text{Cu}(\text{OTf})_2$ was used as a heterogeneous catalyst for the cyclopropanation of 1-octene (**16**) and 1-hexene (**18**) with diazo compounds, the desired cyclopropane products **17** and **19**, respectively, were formed in good yields (Scheme 1.5). Diazomethane reacts at lower temperature, whereas ethyl diazoacetate requires elevated reaction temperature. However, the reaction mixture was darkened to completely black at the end. Furthermore, addition of excess $\text{Cu}(\text{OTf})_2$ afforded a clear pale blue solution, from which CuOTf was isolated as crystalline complex with 1,5-cyclooctadiene. Based on the two observations, it was concluded that $\text{Cu}(\text{OTf})_2$ was first reduced by the diazo compound to generate CuOTf *in situ* (Scheme 1.6), which was believed to catalyze the metal carbenoid formation. The dark coloration was due to the presence of colloidal copper(0) *via* disproportionation.

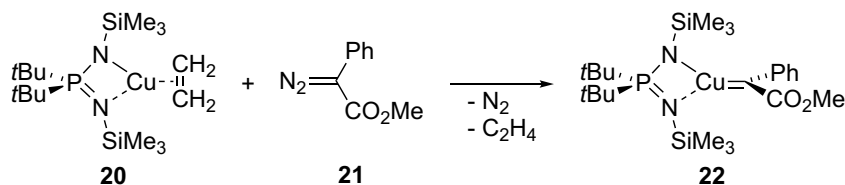


Scheme 1.5 Cyclopropanation reactions catalyzed by Cu(OTf)₂



Scheme 1.6 Reduction of copper(II) to copper(I) by diazo compounds

Therefore, a sacrificial quantity of the diazo compound is consumed to reduce Cu(II) to Cu(I), and consequently the overall yield is diminished. In some cases, Cu(II) was reduced to Cu(I) by phenylhydrazine³⁰ or diisobutylaluminum hydride³¹ *in situ* before adding the diazo substrates. However, the structure for the copper(I) carbenoid generated *via* decomposition of diazocarbonyl compounds was unknown until 2001. Straub and Hofmann³² characterized a copper(I) α -carbonyl carbene complex (Scheme 1.7) with a highly basic, sterically demanding, iminophosphanamide ligand. The reaction of the copper-ethylene complex (**20**) with 2-phenyl-2-diazoacetate (**21**) generated a copper carbenoid (**22**), which was unambiguously assigned and characterized spectroscopically.



Scheme 1.7 Synthesis of copper(I) α -carbonyl carbene complex

Although Cu(I) is accepted to be the active catalyst, Cu(II) complexes are generally employed due to their stability and ease of handling.³³ The electronic effects of the ligand associated with Cu(II) center can be altered, which had led to the development of various copper complexes. Copper(II) acetylacetonate complexes [e.g., Cu(acac)₂]²⁴ are often employed as catalysts for diazo decomposition due to their unique characteristics and their capability to be altered electronically without affecting the overall geometry of the copper complex.^{34a} The fluorinated analogues, such as Cu(tfacac)₂ and Cu(hfacac)₂ (Figure 1.8), are also commonly employed catalysts for diazo decomposition. They exhibit greater reactivity at significantly lower reaction temperatures. Only one of the two bidentate acetylacetonate ligands is presumed to remain associated to the metal center upon reductive activation from Cu(II) to Cu(I).¹

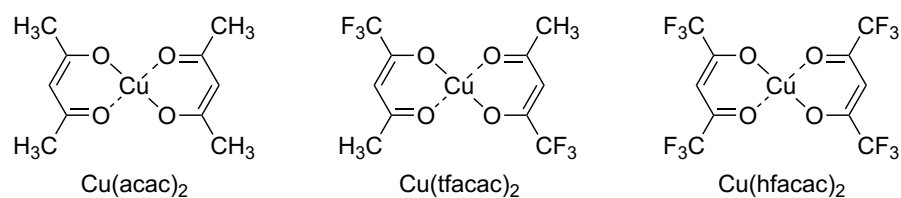
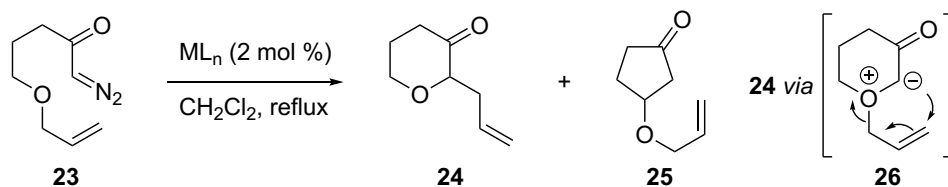


Figure 1.8 Copper(II) acetylacetonate complexes and fluorinated analogues

Clark and Krowiak³⁵ demonstrated the relationship between the electron demands of the ligand and the reactivity of copper carbenoid derived from diazoketone **23** (Table 1.1). Compound **24** was generated *via* oxonium ylide **26** formation followed by a [2,3]-sigmatropic rearrangement, whereas compound **25** was formed *via* the competing C–H insertion reaction. Cu(acac)₂ and its fluorinated analogues, Cu(tfacac)₂ and Cu(hfacac)₂, were shown to be more effective than Rh₂(OAc)₄ for ylide formation and rearrangement, suggesting the copper carbenoids are more electrophilic in nature. Incorporation of more fluorine atoms in the acetylacetonate ligand generally increases the electrophilicity and reactivity of the transient copper carbenoid, and therefore promotes the oxonium ylide formation rather than the competing C–H insertion.

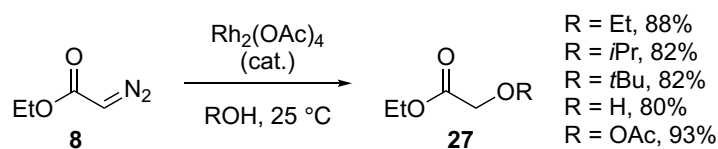


Entry	Catalyst	%Yield of 24	%Yield of 25
1	$Rh_2(OAc)_4$	41	18
2	$Cu(acac)_2$	61	12
3	$Cu(tfacac)_2$	78	0
4	$Cu(hfacac)_2$	83	0

Table 1.1 Catalyst effect for the [2,3]-rearrangement of diazoketone **23**

1.5.2 Rhodium catalysis

In 1973, the same year when Kochi and coworkers^{29a} established the catalytically active copper species, rhodium(II) acetate was first introduced by Teyssié³⁶ as another effective catalyst for diazo decomposition. The rhodium carbenoid generated from ethyl diazoacetate (**8**) readily underwent O–H insertion with alcohols, water or acetic acid to form **27** (Scheme 1.8). Since then, there has been a great surge of interest in exploiting the reactivity of rhodium carbenoids. The air stable rhodium(II) complexes later emerged as highly effective catalysts for a broad spectrum of α -diazocarbonyl decomposition and subsequent metalcarbene transformations.^{1,5,21,27b,37a}



Scheme 1.8 $Rh_2(OAc)_4$ catalyzed diazo decomposition and O–H insertion

The prototypical structure of rhodium(II) carboxylate³⁸ resembles the shape of a “paddle wheel” with a Rh–Rh single bond in the center and four bridging carboxylate ligands around the circumference (Figure 1.9). As a result, only one vacant axial coordination site per rhodium atom is available for ligand coordination to form a complex with octahedral geometry. From the side view on the right, the paddle wheel has electron rich circumference and electron deficient center. However, only one binding site at a time is catalytically active and Lewis basic inhibitors may impede reactivity by coordinating to the second binding site.^{39b}

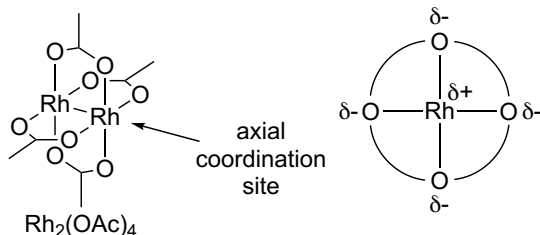


Figure 1.9 Structure of $\text{Rh}_2(\text{OAc})_4$

$\text{Rh}_2(\text{OAc})_4$ serves as the parent compound to access a variety of dirhodium(II) complexes through ligand exchange with substituted acetates or substituted acetamides (chiral or achiral).³⁴ Varying the electronic properties of the bridging ligand may be used to manipulate the reactivity of rhodium carbenes and the general trend is depicted in Figure 1.10.^{27b} Fluorine substitution in $\text{Rh}_2(\text{pfb})_4$ increases the electrophilicity of the catalyst, which leads to high reactivity in diazo decomposition, but poor stereo- and regiocontrol. On the other hand, $\text{Rh}_2(\text{acam})_4$ and $\text{Rh}_2(\text{cap})_4$ typically exhibit higher selectivities.^{27b}

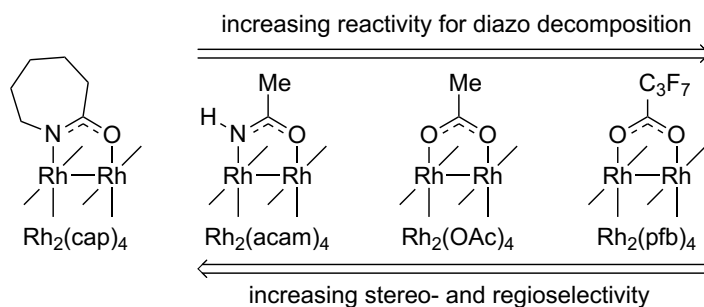
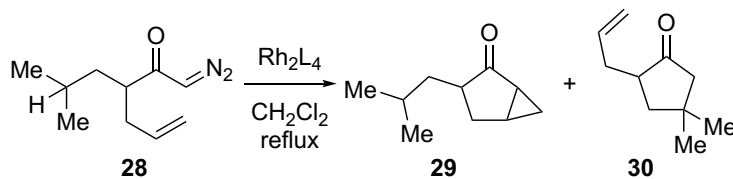


Figure 1.10 Ligand effect on rhodium(II) complexes (only one ligand was shown for clarity)

Padwa and Doyle³⁹ further demonstrated the electronic effects of ligands on the reactivity of the catalysts. Competition between C–H insertion on the tertiary carbon and cyclopropanation was investigated using diazoketone **28** in the presence of different rhodium(II) complexes (Table 1.2). Cyclopropanation product **29** and C–H insertion product **30** were both produced with $\text{Rh}_2(\text{OAc})_4$, demonstrating low chemoselectivity (entry 2). Interestingly, exclusive formation of either **29** or **30** was observed using $\text{Rh}_2(\text{cap})_4$ and $\text{Rh}_2(\text{pfb})_4$, respectively.



Entry	Catalyst	Yield %	29	30
1	$\text{Rh}_2(\text{OAc})_4$	97	44	56
2	$\text{Rh}_2(\text{pfb})_4$	56	0	100
3	$\text{Rh}_2(\text{cap})_4$	76	100	0

Table 1.2 Ligand effect on diazo transformations

Rhodium(II) complexes have wide range of synthetic applications, but the transient highly reactive rhodium(II) carbene intermediates have long defied characterization, and their structural information was initially based on various computational and kinetic studies.⁴⁰ A stable rhodium(II) carbene complex with an *N*-heterocyclic carbene (NHC) ligand (**31**, Figure 1.11) was isolated and characterized by X-ray crystallography in 2001,⁴¹ but it lacked the prototypical reactivity of an electrophilic rhodium carbene. In 2013, Davies and Berry⁴² generated a metastable rhodium(II) carbenoid intermediate with donor/acceptor substituent (**32**), which was stable for about 20 h in chloroform at 0 °C. The donor/acceptor carbenoids, with more attenuated reactivities than the acceptor-only carbenoids, were characterized by nuclear magnetic resonance spectroscopy (NMR) and optical spectroscopy. Very recently, the first X-ray crystal structure of reactive dirhodium donor/donor carbene complex (**33**) was obtained by Fürstner,^{43a} which was an important milestone for understanding rhodium-catalyzed diazo transformations. The carbene moiety was shown to occupy an axial coordination site on the dirhodium core in a staggered conformation with respect to O–Rh–O unit. The Rh–Rh–C axis is almost linear (176.9°). This investigation was further extended to the development of X-ray structures of various reactive donor/donor (**34**) and donor/acceptor (**35**) rhodium carbenes^{43b}

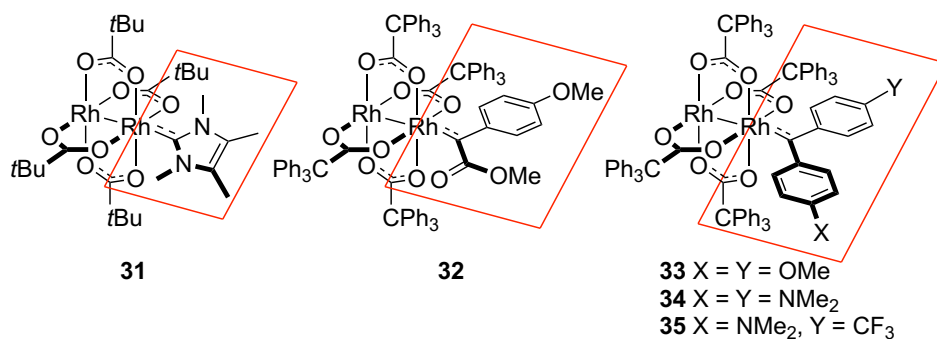


Figure 1.11 Structures of dirhodium(II) carbenes

1.6 Generation of sulfonium ylides

Ylides are neutral dipolar compounds in which a positively charged heteroatom is directly attached to a negatively charged carbon atom (Figure 1.12). One very well-known example is the phosphonium ylide (**36**), which is often used as a reagent in Wittig reactions. In the past few decades, the diverse transformations of oxonium (**37**), ammonium (**38**) and sulfonium (**39**) ylides have attracted considerable attention because of the parallel discoveries of efficient methods to generate them.¹⁸ Sulfonium ylides are often easier to prepare than the corresponding oxonium or ammonium ylides due to the enhanced stabilization by the vacant d-orbitals of the sulfur atoms.⁴⁴ Some sulfonium ylides are even stable enough for isolation and characterization, but consequently require elevated temperature to undergo further rearrangements. A general overview of the sulfonium ylide generation will be covered in this section.

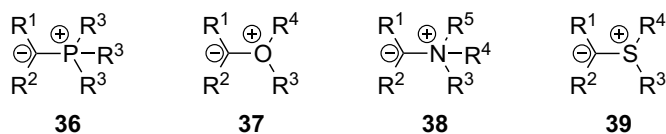
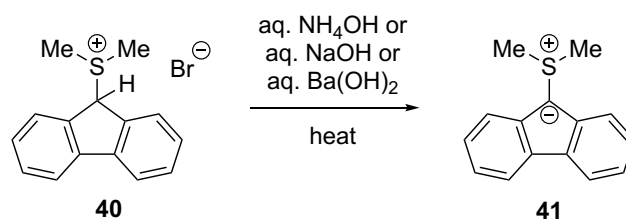


Figure 1.12 Examples of onium ylides

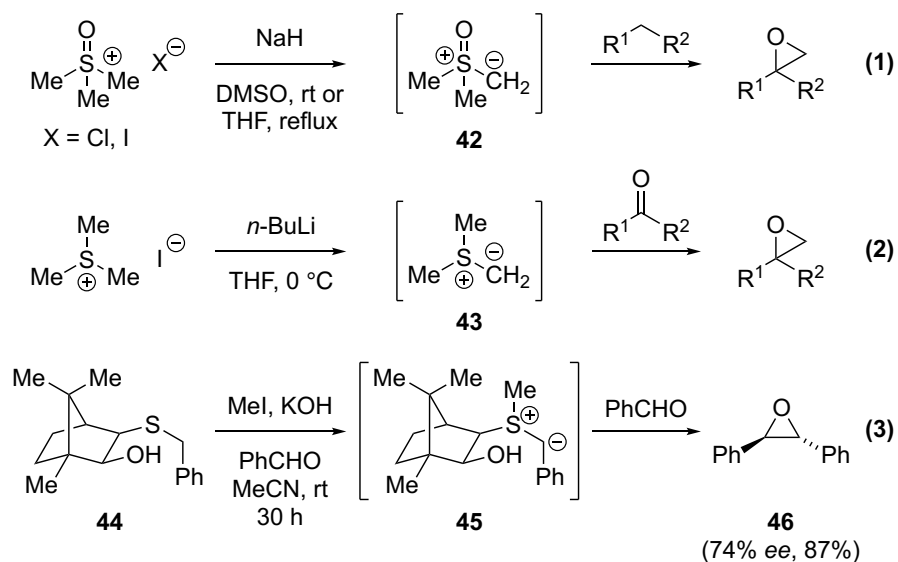
1.6.1 Deprotonation of sulfonium salts

The ylides are traditionally generated by deprotonating the α -proton of the corresponding sulfonium salts with strong bases.⁴⁵ The carbon atom next to the sulfonium salt often requires an electron withdrawing group to facilitate the deprotonation and stabilize the resulting sulfonium ylide. One of the earliest examples of base-induced sulfonium ylide generation was reported by Ingold and Jessop (Scheme 1.9),⁴⁶ by treating colorless sulfonium salt **40** with aqueous bases. Sulfonium ylide **41** was obtained as a yellow crystalline solid, and was sufficiently stable for isolation.



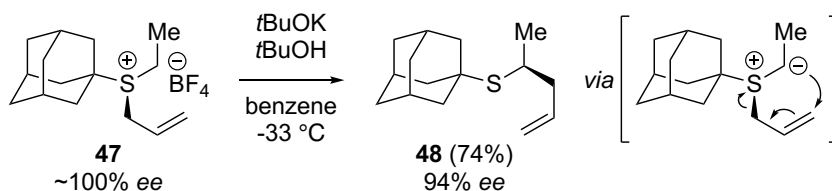
Scheme 1.9 Base-induced generation of sulfonium ylide

In 1962, Corey and Chaykovsky^{47a} reported a method to generate dimethylsulfoxonium methyllide (**42**) and dimethylsulfonium methyllide (**43**) *via* deprotonation of the corresponding halide salts. Both sulfur ylides (**42** and **43**) can react with aldehydes and ketones to form epoxides (eq 1 and 2, Scheme 1.10)^{47b} and this process is referred to as the Corey–Chaykovsky epoxidation. This reaction is widely used in organic synthesis to generate epoxides. Upon attaching a chiral group to the sulfur atom of the sulfonium ylide, it undergoes asymmetric epoxidation or aziridination.⁴⁸ For example, Hugang and coworkers⁴⁹ reported an easy one-pot procedure to generate enantioenriched epoxides (eq 3, Scheme 1.10) by tethering a camphor-derived moiety to sulfonium ylide **45**. Ylide **45** was generated *in situ via* methylation of **44** followed by deprotonation in the presence of potassium hydroxide. Subsequent reaction of **45** with benzaldehyde accounts for a stoichiometric enantioselective epoxidation to afford epoxide **46** with good enantiomeric excess (*ee*).



Scheme 1.10 Formation of sulfur ylides and subsequent epoxidation reaction

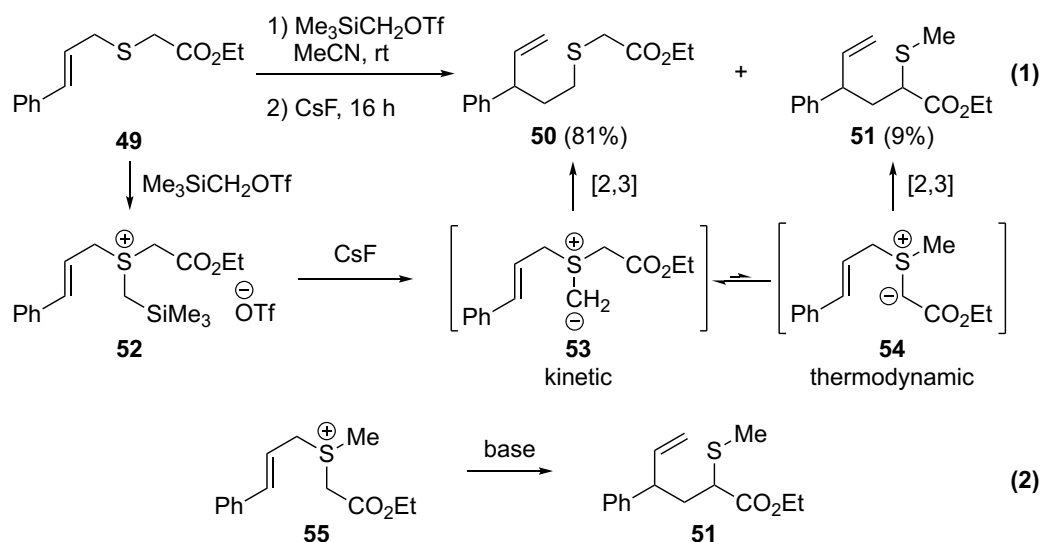
Another extensively explored area of sulfonium ylide chemistry is the [2,3]-rearrangement of allyl sulfonium ylide. Trost⁵⁰ studied the base-induced allyl sulfonium ylide generation and its [2,3]-rearrangement starting from enantiomerically pure sulfonium salt **47** (Scheme 1.11). Good chirality transfer from sulfur to carbon was observed in this rearrangement process and provided product **48** in 74% yield with 94% *ee*.



Scheme 1.11 Base-induced sulfonium ylide formation and rearrangement

1.6.2 Fluoride-induced desilylation of α -silylsulfonium salts

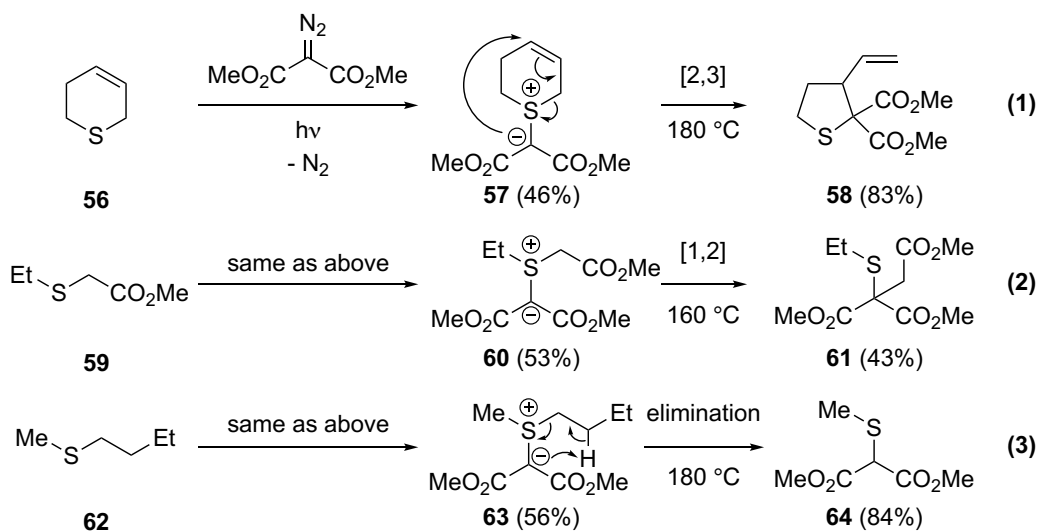
The above-mentioned base-induced deprotonation method can only be efficiently applied to the sulfonium salts that have one set of α -protons available for deprotonation. However, regioselectivity problems occur when more than one α -proton is available for base deprotonation. Fluoride-induced desilylation of α -silylsulfonium salts was developed⁵¹ as an alternative strategy, which can generate sulfonium ylides regioselectively under non-basic conditions (eq 1, Scheme 1.12).^{51b} Allylic α -silyl sulfonium salt **52** was formed *in situ* from sulfide **49**. Cesium fluoride assisted desilylation followed by a [2,3]-rearrangement produced **50** in 81% yield *via* **53**. Equilibration of ylide **53** to thermodynamically stable ylide **54** afforded 9% of **51** after a [2,3]-rearrangement. In this case, only a minor extent of ylide equilibration occurred based on the observed product ratio, illustrating the advantage of regioselective ylide formation provided by the desilylation method. In contrast, a base-assisted deprotonation strategy using non-silylated sulfonium salt **55** will produce **51** as the major product (eq 2, Scheme 1.12).



Scheme 1.12 Sulfonium ylide formation *via* fluoride-induced desilylation

1.6.3 From carbenes generated thermally or photochemically

Although the reactions of ylides derived from free carbenes often result in the formation of multiple products with low yields, successful sulfonium ylide generation and rearrangement with reasonable yields was observed in some cases. Ando and coworkers extensively investigated such reactions (Scheme 1.13).⁵² Bis(methoxycarbonyl)carbene is generated from direct pyrolysis of dimethyl diazomalonate, and it reacts with allyl sulfide **56**, benzyl sulfide **59** or alkyl sulfide **62** to generate the corresponding sulfonium ylides **57**, **60**, and **63**, respectively in moderate yields. Sulfonium ylides that are substituted with two flanking dicarbonyl groups at the ylide carbon are usually stable enough to be isolated and characterized. However, upon heating to elevated temperatures, interesting reactivities of sulfonium ylides were observed. A [2,3]-sigmatropic rearrangement of cyclic allylic sulfonium ylide **57** provided ring contraction product **58** (eq 1, Scheme 1.13).^{52a} Ylide **60** underwent a Stevens [1,2]-shift (eq 2, Scheme 1.13) to give rearranged product **61**. (The Stevens rearrangement is discussed in detail in Section 1.7). In the presence of a β -hydrogen, α,β -elimination (eq 3) can take place to give **64** in high yield.^{52b}



Scheme 1.13 Sulfonium ylides derived from carbenes generated by photolysis

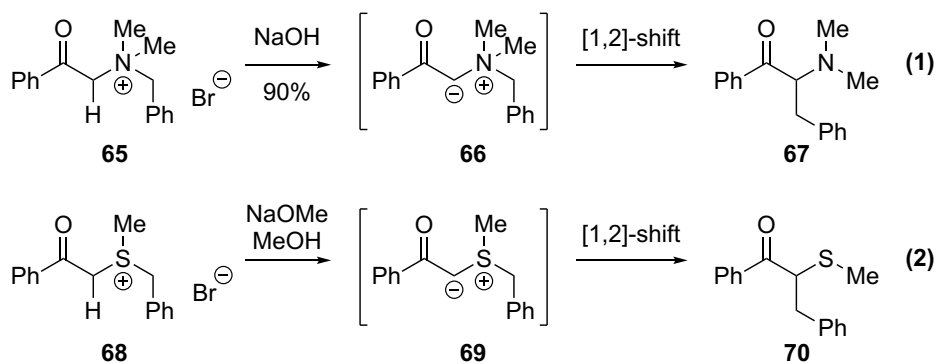
1.6.4 From metal carbenoids

By far the most preferred method for the generation of sulfur ylides is to react metallocarbenes with sulfur nucleophiles.^{1,5a,5d,18} This reaction proceeds under neutral reaction conditions and tolerates a wide range of functional groups, whereas the base-induced generation from sulfonium salts is intolerable for base-sensitive groups. Additionally, the use of metallocarbenes could assure the location of the ylide carbon, whereas the deprotonation can be unselective. As a result, the generation of sulfonium ylides from metallocarbenes derived from α -diazocarbonyl compounds has received great attention, and has been extensively investigated.^{1,18} To demonstrate the versatility of this method, representative examples have been highlighted in the remainder of Chapter 1. Furthermore, priority has been given to the developments in the past decade (Section 1.8). It is also noteworthy to introduce the Stevens rearrangement or Stevens [1,2]-shift, as it is one of the most important classes of transformations by sulfonium ylides.

1.7 An introduction on the Stevens rearrangement

1.7.1 Discovery

The [1,2]-shift of an ammonium ylide was first observed by Stevens and Thomson in 1928.^{53a} Deprotonation of ammonium salt **65** under basic conditions afforded product **67** via a [1,2]-shift of an ammonium ylide intermediate **66** (eq 1, Scheme 1.14). Similar reaction conditions were later applied to sulfonium salt **68**, which reacted in an analogous fashion to give product **70** (eq 2, Scheme 1.14).^{53b} The migrating group for both cases was the benzyl group.

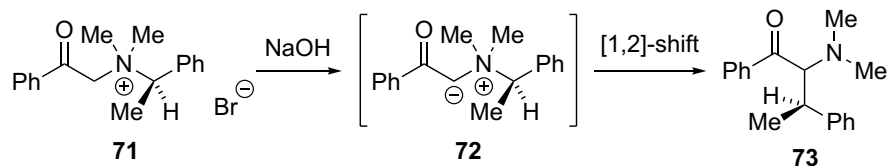


Scheme 1.14 The Stevens rearrangement of ammonium and sulfonium ylides

1.7.2 Mechanistic investigations on the Stevens rearrangement

The mechanism of the Stevens rearrangement has been a topic of investigation and debate since its discovery.⁵⁴ It remained controversial for many years and triggered many mechanistic studies. In general, three mechanistic pathways can be envisaged for the Stevens rearrangement: (a) a concerted [1,2]-sigmatropic rearrangement, (b) homolytic bond cleavage to give a radical pair followed by rapid recombination of the radical pair or (c) heterolytic bond cleavage to give a zwitterion pair followed by rapid recombination of the ion pair.

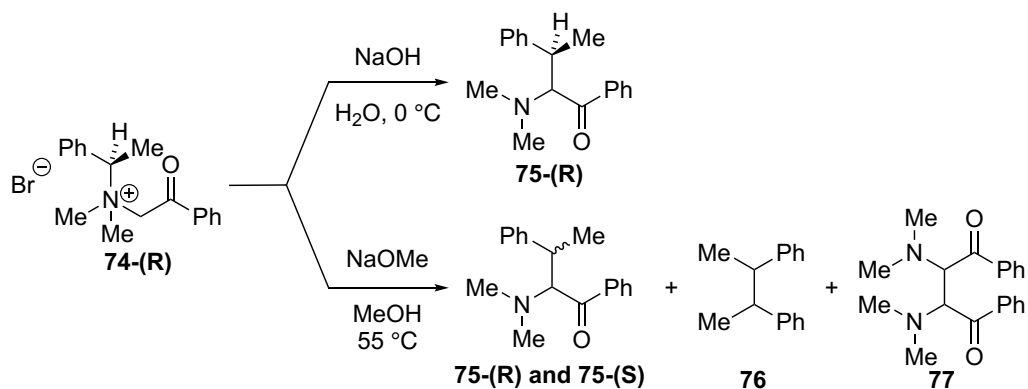
Treatment of a mixture of ammonium salts with base did not provide any cross-over products, indicating that the benzyl migration is an intramolecular process.⁵⁵ In 1947, Kenyon reported the first stereoselective example of the Stevens rearrangement using optically active ammonium salt **71** (Scheme 1.15).⁵⁶ Under basic conditions, an optically active product (**73**) was isolated, which was formed via the Stevens [1,2]-shift of the chiral center in **72** with a net retention of configuration at the migrating benzylic carbon atom.



Scheme 1.15 Retention of configuration for the Stevens rearrangement

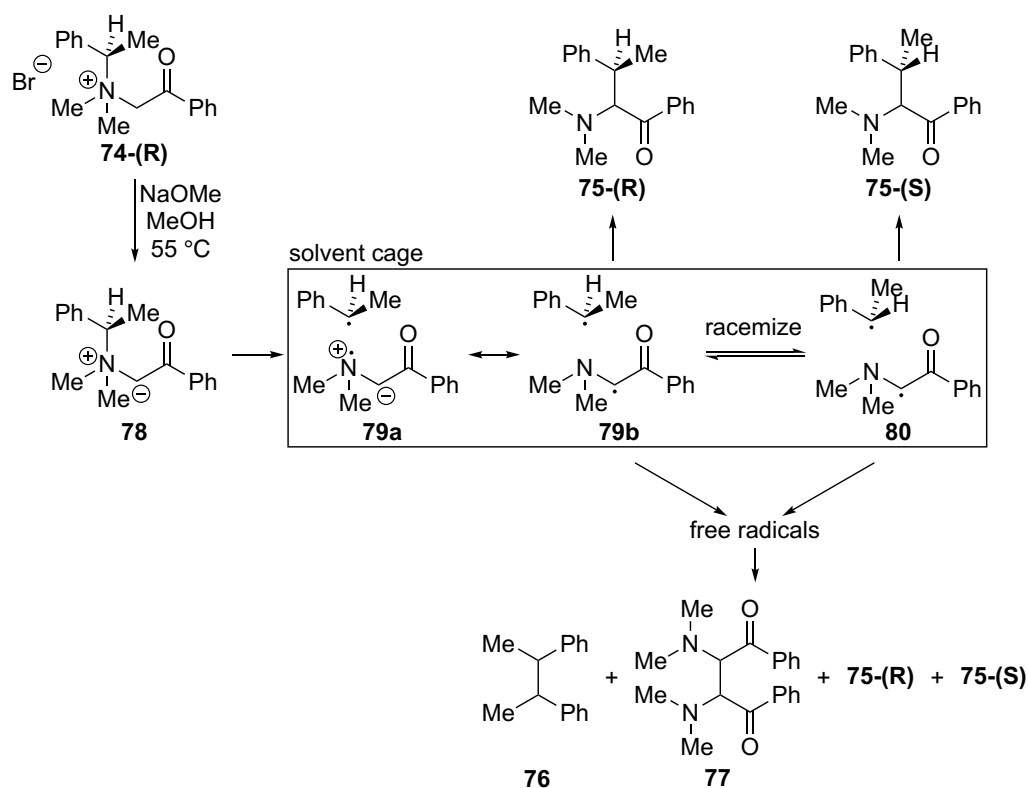
In the case of ylide rearrangements involving a total of four electrons, a concerted suprafacial [1,2]-shift with net retention of configuration of the migrating group is an orbital symmetry forbidden process that violates the Woodward–Hoffmann rules.⁵⁷ Thus, the Stevens rearrangement is suggested to undergo a step-wise mechanism.

In 1975, Ollis and coworkers^{58c} performed mechanistic investigations on the Stevens rearrangement process. After a series of elegant experiments, it was proposed that the Stevens rearrangement proceeds *via* a radical pair mechanism.⁵⁸ A chiral ammonium salt **74-(R)** underwent a Stevens rearrangement in the presence of aqueous sodium hydroxide at 0 °C to give **75-(R)** with 99% net retention of configuration (Scheme 1.15). However, treating the same starting material with sodium methoxide in methanol at 55 °C resulted in 56% net retention of configuration. In addition, small quantities of diastereomeric mixtures of dimer **76** and **77** were also isolated, supporting the proposal that the reaction involves radical pair intermediates. CIDNP (Chemically Induced Dynamic Nuclear Polarization) effects also suggest the formation of radical pair intermediates,^{58b} consistent with the findings by other research groups.^{52b,59}



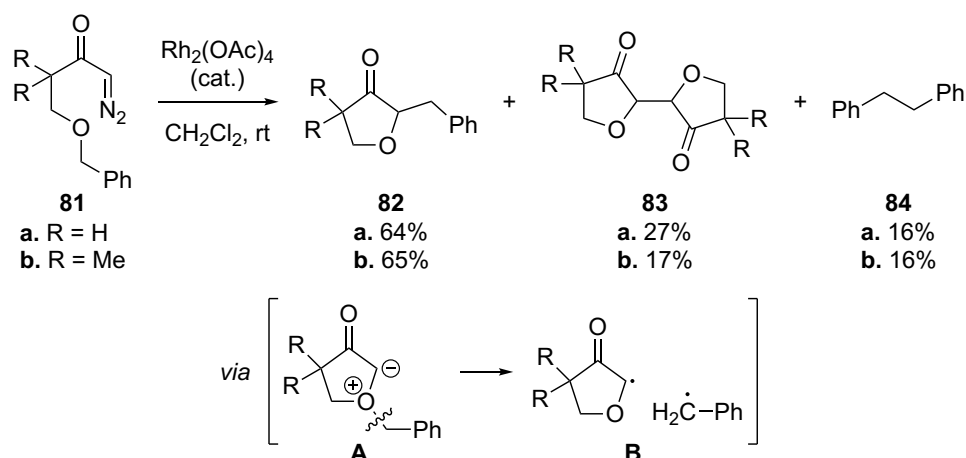
Scheme 1.16 Stevens rearrangement of chiral ammonium salt

By compiling all the experimental evidence, the mechanism of the Stevens rearrangement was reported as depicted in Scheme 1.17. *In situ* generated ammonium ylide **78** underwent bond homolysis to form radical pair **79a**, which can also be depicted as radical pair **79b** lacking charge separation and with the unpaired electron on carbon. At this point, radical pair **80** can undergo fast recombination to deliver **75-(R)** or racemize to radical pair **81** and then recombine to give a 1:1 mixture of **75-(S)** and **75-(R)**. Elevated temperature and low solvent viscosity would facilitate the diffusion of the radicals out of the solvent cage, which would also be consistent the formation of homodimeric product **76** and **77**. In contrast, the reaction is highly stereoselective when carried out at low temperature in viscous solvents.



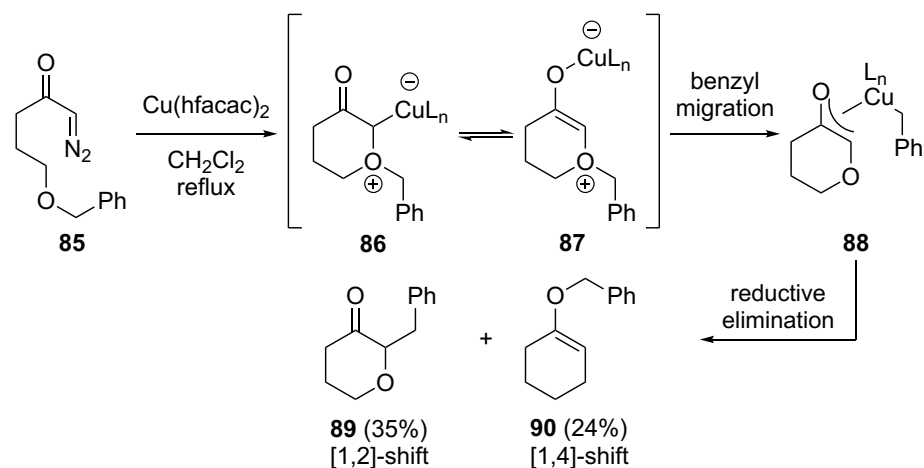
Scheme 1.17 Radical pair pathways for the Stevens rearrangement

Evidence for the radical pair mechanism was also provided by West and coworkers^{59a} during their study of oxonium ylide rearrangements (Scheme 1.18). Rhodium catalyzed Stevens rearrangements of diazoketones **81** went smoothly to provide the desired [1,2]-shift products **82** as the major products. However, isolation of significant quantities of homodimers **83** and **84** indicated formation of radical pair **B** through C–O bond homolysis of oxonium ylide **A**. Low viscosity solvents such as dichloromethane facilitate the escape of radical pair **B** from the solvent cage, which led to the dimeric products (**83** and **84**). Furthermore, the Stevens rearrangement of analogous ammonium ylides was also investigated, and formation of similar homodimers such as **84** was observed.^{59b}



Scheme 1.18 Formation of homodimeric products during oxonium ylide rearrangement

Interestingly, West and coworkers^{59c} demonstrated that the reactivity of ω -alkoxy diazo ketone substrates, such as **85**, is highly sensitive to the catalyst used. The observation of no homodimer formation using a copper catalyst instead of Rh₂(OAc)₄ led to the proposal of an alternative metal-assisted mechanism for the Stevens rearrangement process (Scheme 1.19). Copper catalyzed decomposition of diazoketone **85** provided the copper-associated intermediates **86** and **87**, which could give rise to oxa- π -allyl complex **88** after benzyl migration. Finally, the reductive elimination step furnished [1,2]- and [1,4]-shift products **89** and **90**, respectively.



Scheme 1.19 Copper-assisted mechanism for the Stevens rearrangement

Although the mechanism for the Stevens rearrangement still remains controversial, a few important conclusions can be drawn from previous observations. Variation of solvent, temperature, catalyst, migrating group and substrate substantially influence the Stevens rearrangement process. In many cases, a radical pair mechanism was proposed due to observed dimerized products. However, the absence of such a homodimer does not rule-out the radical pair mechanism. The observed high degree of chirality transfer can be attributed to the fast recombination of the radical pair in the solvent cage relative to bond rotation or diffusion from the cage. The metal catalyst could also be involved in the mechanistic pathway. Despite the uncertainties of the actual mechanism, the Stevens rearrangement of sulfonium ylides has been extensively studied for its synthetic applications.

1.8 Metallocarbene transformations with sulfur nucleophiles and synthetic applications

1.8.1 Reactivities of metallocarbenes with sulfur nucleophiles, an overview

Metallocarbenes can react readily with an available sulfur nucleophile to effect sulfur ylide formation.^{4,18} Examples of such sulfur nucleophiles include sulfides or thiols, sulfoxides and thiocarbonyls, which form sulfonium, sulfoxonium and thiocarbonyl ylides, respectively. However, the rearrangement of sulfoxonium and thiocarbonyl ylides has been underexplored in comparison with that of sulfonium ylides. Recent developments of transformations involving sulfonium ylides generated by metal catalyzed decomposition of α -diazocarbonyl compounds is discussed in the following sections.

Different substituents on the sulfur atom can affect the outcome of subsequent transformations. For example, when an allylsulfide is used as a nucleophile, the resulting sulfonium ylide (**91**) is prone to [2,3]-rearrangement to afford **A**, while the sulfonium ylide derived from thiol (**92**) is prone to proton-transfer to afford apparent S-H insertion products **B** (Figure 1.13). Ylide **93** can undergo a Stevens [1,2]-shift or an α' , β -elimination depending on the nature of the R^3 and R^4 groups on the sulfur atom. In contrast, if the carbenoid is substituted with two electron-withdrawing groups (i.e., $R^2 = \text{EWG}$), the resulting sulfonium ylide is isolable and will rearrange only under forcing conditions. All of these transformations can occur inter- and intramolecularly to build molecular complexity.

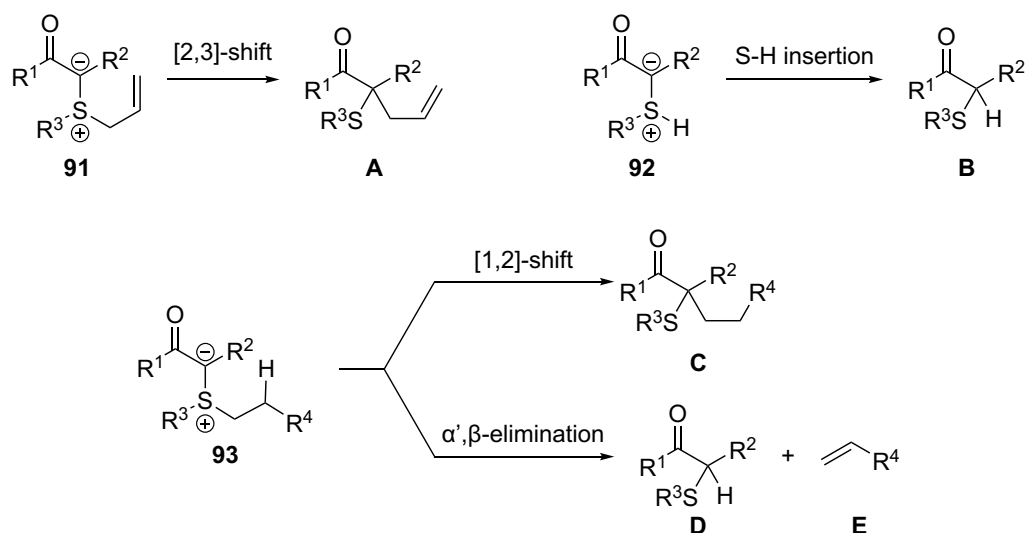


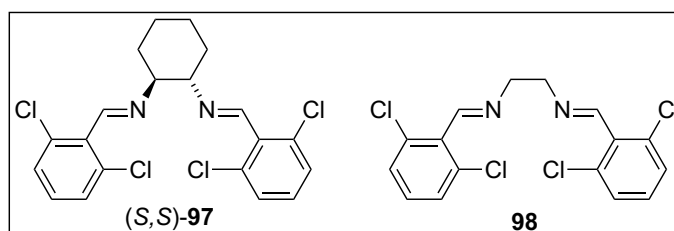
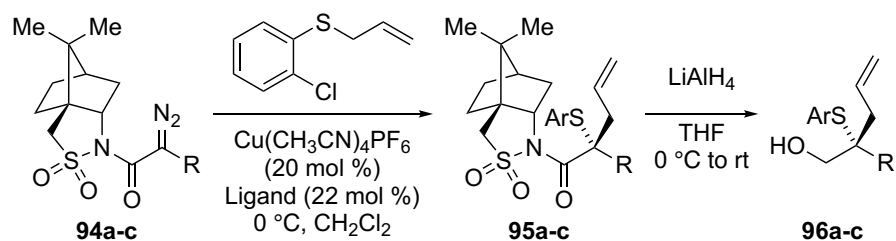
Figure 1.13 Sulfonium ylides generated from metallocarbenes

Although rhodium and copper catalysts are used to effect diazo decomposition and ylide formation in most cases, other transition metal catalysts such as iridium and iron have also been employed periodically.³⁷ Asymmetric induction was accomplished through substrate control and/or by using chiral ligands on the metal catalyst.^{27,34}

1.8.2 [2,3]-Sigmatropic rearrangement

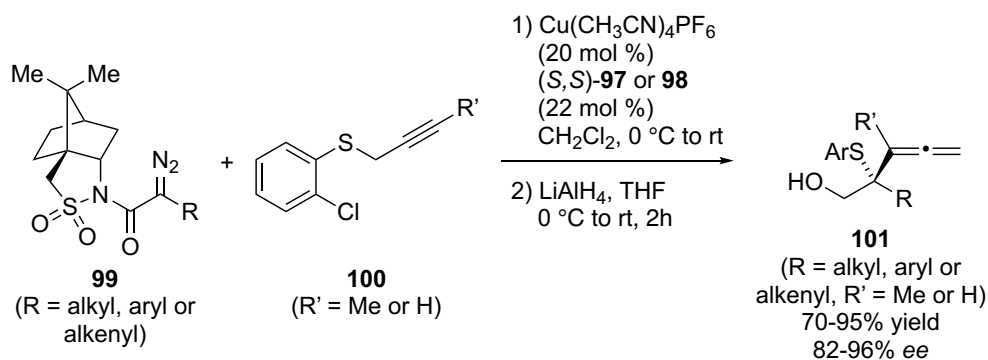
[2,3]-Sigmatropic rearrangements of allyl sulfonium ylides is a powerful and versatile bond reorganization process, which has attracted the attention of the synthetic community.^{1,5a,18,60} [2,3]-shifts of allyl sulfonium ylides that are formed *via* metal catalysis are referred to as the Doyle–Kirmse reaction.⁶¹ When an aromatic unsaturated double bond is involved in the [2,3]-rearrangement, the reaction is known as the Sommelet–Hauser rearrangement.⁶² Although the formation of allyl sulfonium ylide can occur inter- or intramolecularly, most of the developments in the past decade were on the intermolecular processes, in which the diazo group and the sulfur nucleophile were on different molecules.

In 2005, Wang and coworkers⁶³ reported a highly stereoselective [2,3]-sigmatropic rearrangement of sulfonium ylides (Doyle–Kirmse reaction), whereas previous literature precedent⁶⁴ on relevant asymmetric catalysis only showed moderate enantioselectivity. A double asymmetric induction approach was examined using a diazo substrate containing Oppolzer's camphor sultam in combination with a chiral copper(I) complex. The optimal enantioselectivity was obtained using *o*-chlorophenylallyl sulfide with chiral Schiff base ligand (*S,S*)-**97** (entry 1, Table 1.3) and the chiral auxiliary was subsequently removed from rearranged products **95** by LiAlH₄ reduction to give alcohols **96** as final isolated products. Interestingly, both (*S,S*)-**97** and (*R,R*)-**97** afforded alcohol **96a** with the same absolute configuration for the major enantiomer (entry 2, Table 1.3) and the usage of achiral ligand **98** improved the enantioselectivity (entry 3, Table 1.3), suggesting that the asymmetric induction in this process is dictated by the chiral auxiliary instead of the chiral ligand for the copper(I) complex. Diazo compounds with α -aryl, alkyl and alkenyl substituents can also afford the corresponding alcohols in high yields and high *ee*. The absolute configuration was confirmed by X-ray crystallography. The scope of the sulfide in this process was also extended to propargyl sulfides (**99**), which yielded the corresponding allenyl alcohols **101** in good yields and high enantioselectivity (Scheme 1.20).



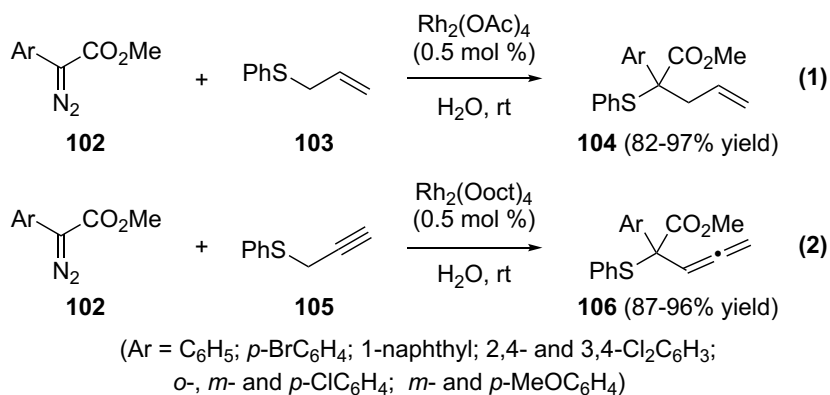
Entry	Ligand	R	Yield (%)	ee (%)
1	(S,S)-97	Ph (a)	70	90
2	(R,R)-97	Ph (a)	70	80
3	98	Ph (a)	72	92
4	(S,S)-97	Me (b)	81	86
5	98	Me (b)	67	82
6	(S,S)-97	CH=CHPh (c)	82	95
7	98	CH=CHPh (c)	78	85

Table 1.3 Highly enantioselective [2,3]-rearrangement of sulfonium ylides



Scheme 1.20 Reactions with propargyl sulfides

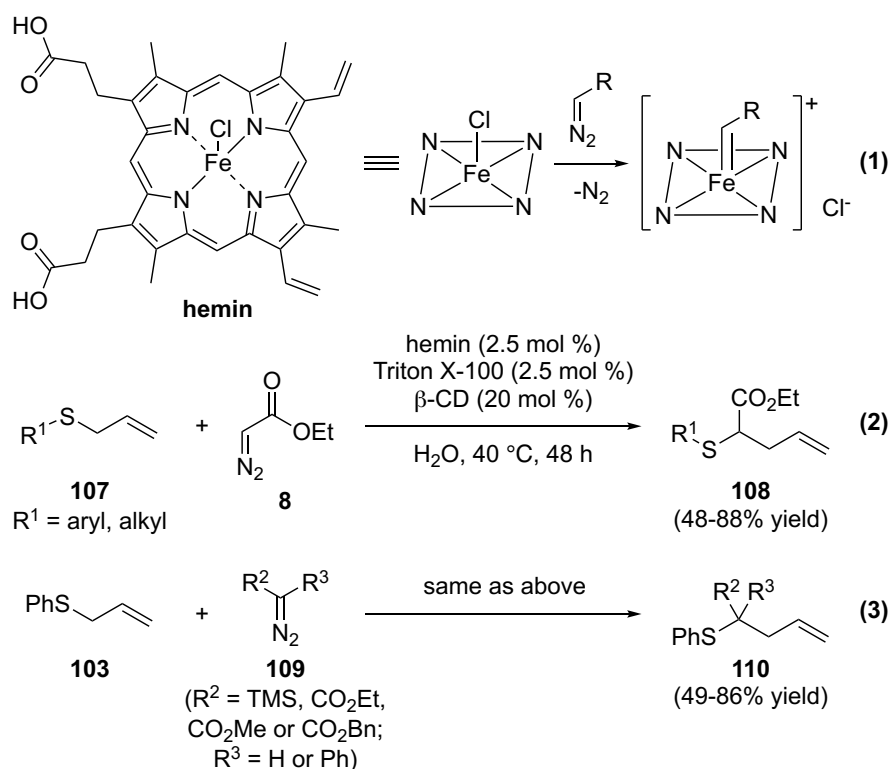
The Doyle–Kirmse reaction is usually conducted in anhydrous organic solvent under inert atmosphere due to the high reactivity of metal carbenoid intermediate. However, Wang and coworkers⁶⁵ demonstrated that the reaction works efficiently in water using rhodium(II) catalyst. Rhodium(II) catalyzed decomposition of various aryldiazoacetates (**102**) in the presence of allyl phenyl sulfide (**103**) or phenyl propargyl sulfide (**105**) using tap water as a solvent provided the corresponding [2,3]-rearranged products **104** and **106** in excellent yields (eq 1 and 2, Scheme 1.21). In cases when the reagents were insoluble, small amounts of toluene or dichloromethane were used to dissolve the reagents before subjecting them to the reaction conditions. The water soluble dirhodium(II) tetraacetate [Rh₂(OAc)₄] was observed to be an effective catalyst for the allyl phenyl sulfide case (eq 1), whereas hydrophobic dirhodium(II) tetraoctanoate [Rh₂(Ooct)₄] reduced the reaction time with phenyl propargyl sulfide (eq 2). Unfortunately, employment of chiral rhodium(II) catalyst in water resulted in only moderate enantioselectivity.



Scheme 1.21 Doyle-Kirmse reaction in water

The successful application of water as the solvent for rhodium catalyzed sulfonium ylide generation led to the exploration of other suitable transition metal catalysts that are capable of catalyzing reactions in water. Recently, Pan and coworkers⁶⁶ reported the use of aqueous hemin (eq 1, Scheme 1.22), a type of iron porphyrin, as a catalyst for the Doyle–Kirmse reaction. Cyclodextrin (β-CD) additive and non-ionic surfactant

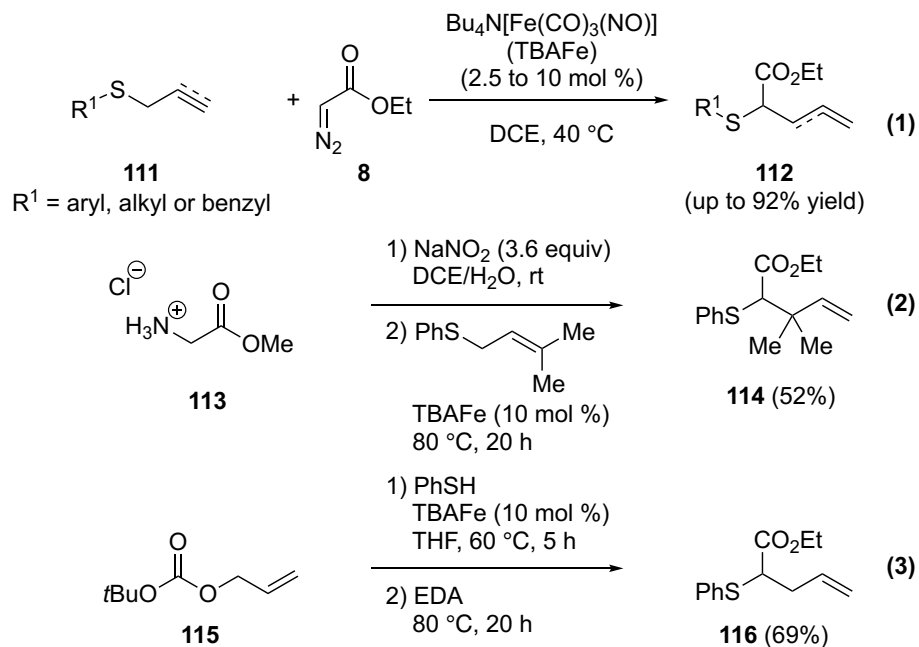
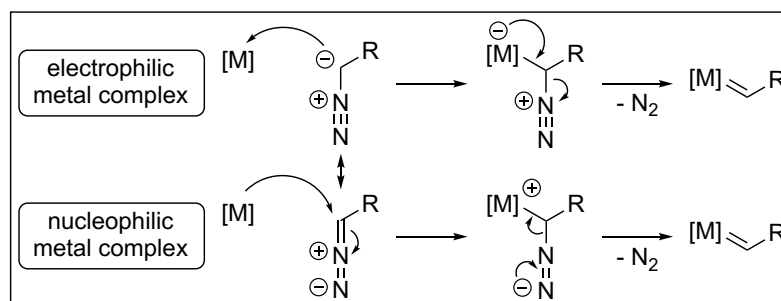
Triton X-100 were necessary for the formation of the desired iron carbenoid and the subsequent rearrangement of the sulfonium ylide (Scheme 1.22). The iron carbenoid was initially formed from ethyl diazoacetate (**8**) in the presence of various aryl and alkyl substituted allyl sulfides (**107**) to provide the rearranged products **108** in good yields (eq 2). Different types of diazo compounds, especially acceptor/donor and acceptor type diazo compounds, were compatible with the reaction conditions (eq 3). However, higher reaction temperatures (80 °C) and longer reaction times (20 h) are needed to transform the acceptor/donor carbenoid.



Scheme 1.22 Hemin catalyzed Doyle-Kirmse reaction

Iron-porphyrin-bound carbenoids can also be formed using a myoglobin-based biocatalyst in potassium phosphate buffer (pH 8), which was also shown to have high catalyst efficiency for the Doyle-Kirmse reaction with various allylic and propargylic sulfides and α -diazoesters.^{67a} The iron catalysts used for diazo decomposition often

belong to the class of oxidized metal catalysts with Lewis acidic metal centers. In 2012, Plietker and coworkers^{67b} demonstrated the first example of using electron-rich ferrate complexes for carbene transfer reactions (Scheme 1.23). Diazo decomposition in the presence of these nucleophilic metal complexes is believed to proceed initially *via* addition to the C=N bond followed by metallocarbene formation and extrusion of nitrogen gas, in contrast to the mechanism using electrophilic metal complexes. Nevertheless, the catalytic systems were robust enough to tolerate a broad range of functional groups (eg. alcohols, amines, and olefins). Good to excellent yields of products **112** were obtained with aryl, alkyl and benzyl substituted allylic sulfides and propargyl sulfides (**111**, eq 1). Trimethylsilyl diazomethane and dimethyl diazomalonate can also be used instead of ethyl diazoacetate (**8**). Most importantly, the authors demonstrated two one-pot procedures to expand the potential synthetic utilities of the catalytic system. The first one consisted of the *in situ* formation of ethyl diazoacetate from the reaction of glycine methyl ester hydrochloride **113** with sodium nitrite and a subsequent Doyle–Kirmse reaction to give product **114** (eq 2). This reaction was conducted with a bi-phasic mixture of dichloroethane and water, demonstrating great stability of the catalyst. The second one-pot procedure is a sequential sulfenylation/Doyle–Kirmse reaction (eq 3), featuring the *in situ* formation of an allylic sulfide intermediate from allylic carbonate **115**, followed by the reaction with ethyl diazoacetate to furnish the phenyl allyl sulfide **116**.

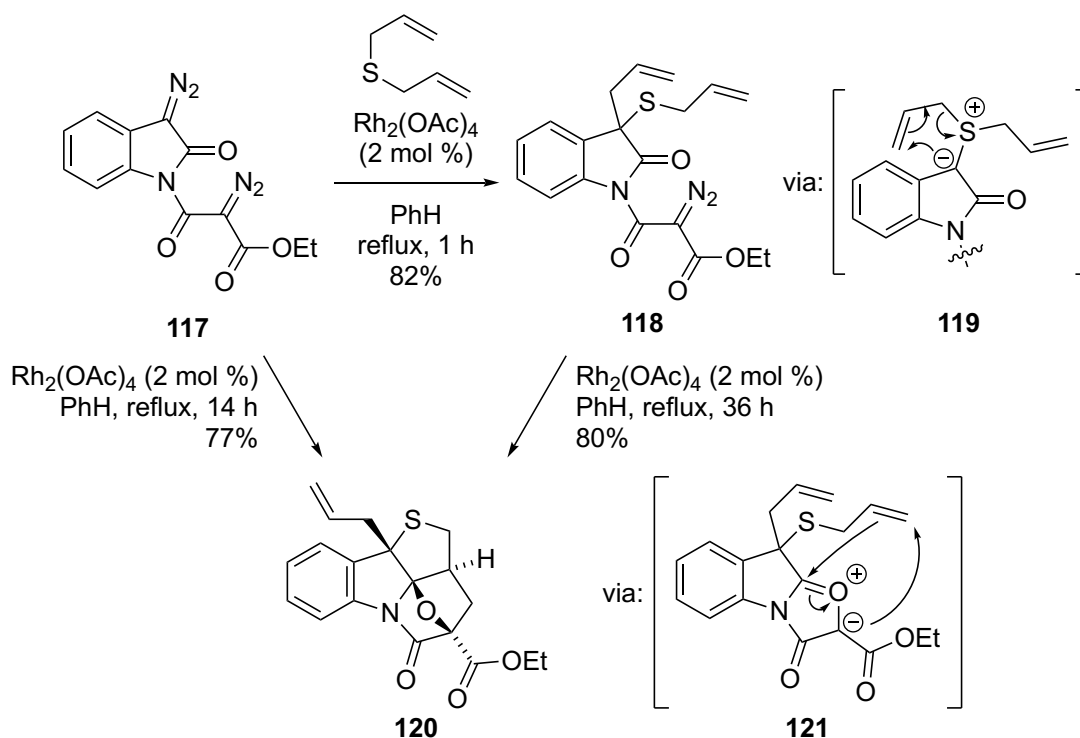


Scheme 1.23 Doyle–Kirmse reaction catalyzed by electron-rich ferrate complex

In addition, the first example of a silver-catalyzed Doyle-Kirmse reaction was reported by Davies and coworkers in 2009.⁶⁸ Silver triflate (AgOTf) was reported to be an efficient catalyst for carbenoid generation, and lead to the formation various allyl- or propargyl sulfonium ylides that could subsequently undergo [2,3]-rearrangements.

Very recently, Padwa and Bonderoff⁶⁹ reported a rhodium-catalyzed cascade reaction involving a sulfonium ylide to illustrate its capability to build up molecular complexity using metallocarbenes. The desired cascade sequence was initiated from bis-diazolactam **117**, bearing acceptor/acceptor and donor/acceptor diazo moieties on the same molecule (Scheme 1.24). Upon heating the reaction mixture in toluene for one

hour in the presence of dirhodium tetraacetate catalyst, **118** was formed *via* a [2,3]-rearrangement of allyl sulfonium ylide **119** derived from the donor/acceptor rhodium carbenoid. When **118** was subjected to the same reaction conditions, product **120** was generated *via* an intramolecular carbonyl ylide formation/cycloaddition cascade (**121**). However, prolonged heating (36 hours versus 1 hour) was required for the formation of **120**. In addition, **117** can be converted to **120** directly in a one-pot procedure without isolating **118**. This was achieved by employing identical reaction conditions for the formation of **118**, and increasing the reaction time to 14 hours. A 77% yield was obtained for the one-pot procedure, whereas the two-step protocol afforded **120** in an overall yield of only 65%.

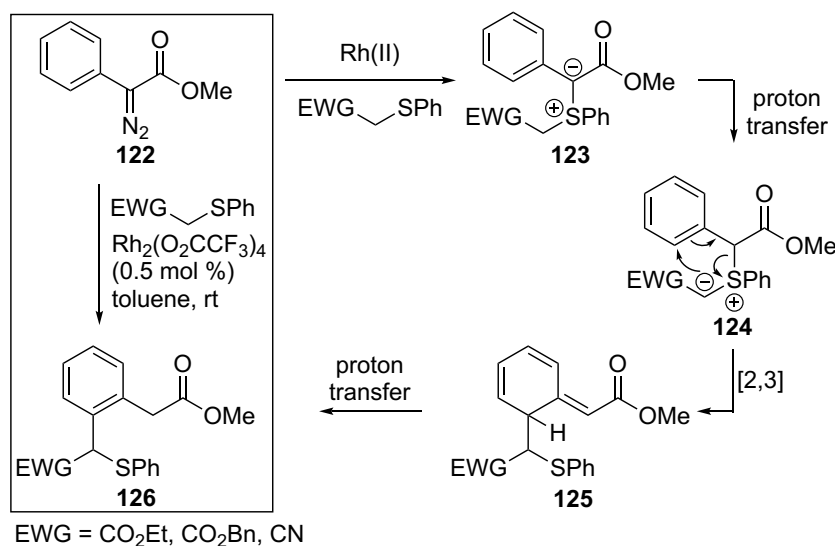


Scheme 1.24 Cascade reaction initiated from sulfonium ylide

In addition to the Doyle-Kirmse reaction highlighted in the many examples described above, the Sommelet-Hauser rearrangement of sulfonium ylides is another

attractive reaction, in which an aromatic π -bond is involved. This reaction is a unique approach to introduce ortho-substituents on arylacetates. The required sulfonium ylide is typically generated *via* deprotonation of the corresponding sulfonium salt with strong base or desilylation of α -silylsulfonium salts (Section 1.6.1 and 1.6.2). Recent studies have demonstrated that the Sommelet–Hauser rearrangement can also proceed under transition metal catalyzed conditions.

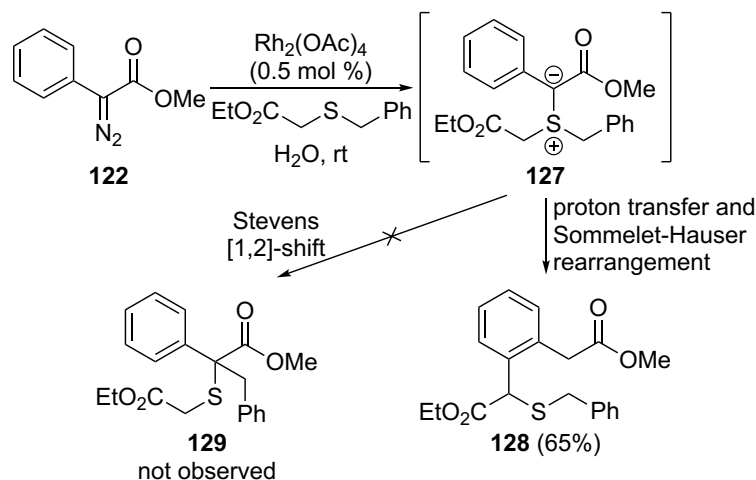
The first example of a rhodium (II) catalyzed Sommelet–Hauser rearrangement of sulfonium ylide was reported by Wang and coworkers (Scheme 1.25).^{70a} Formation of the donor/acceptor rhodium carbenoid in the presence of a thioether provided sulfonium ylide **123**. Proton transfer would then give rise to ylide **124**, which underwent consecutive [2,3]-sigmatropic dearomatization and rearomatization to form ortho-substituted product **126** in good yield.



Scheme 1.25 Rhodium(II) catalyzed generation of sulfonium ylide and subsequent Sommelet–Hauser rearrangement

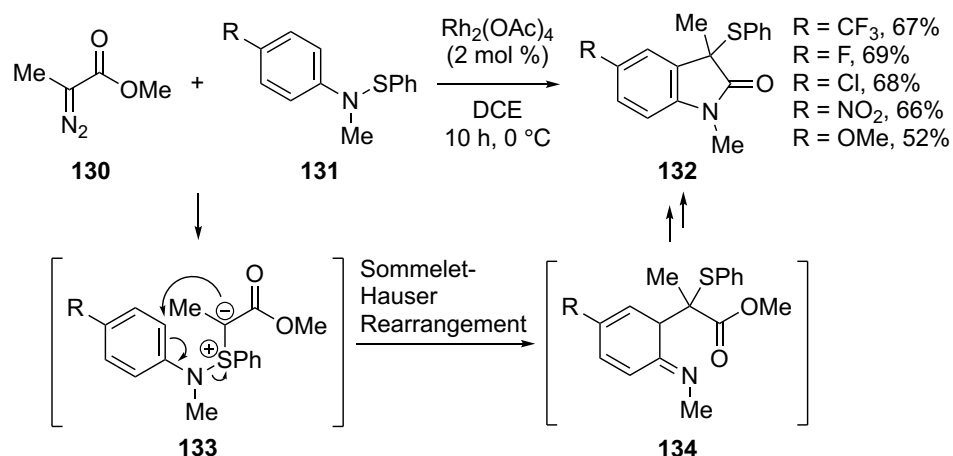
When ethyl benzylthioacetate is used (Scheme 1.26), the sulfonium ylide **127** can potentially undergo two pathways. However, the reaction only afforded **128** in 65% yield. Product **129** from the Stevens [1,2]-shift of the benzyl group was not observed,

indicating that the Sommelet–Hauser rearrangement process is more facile than the competing Stevens [1,2]-shift.



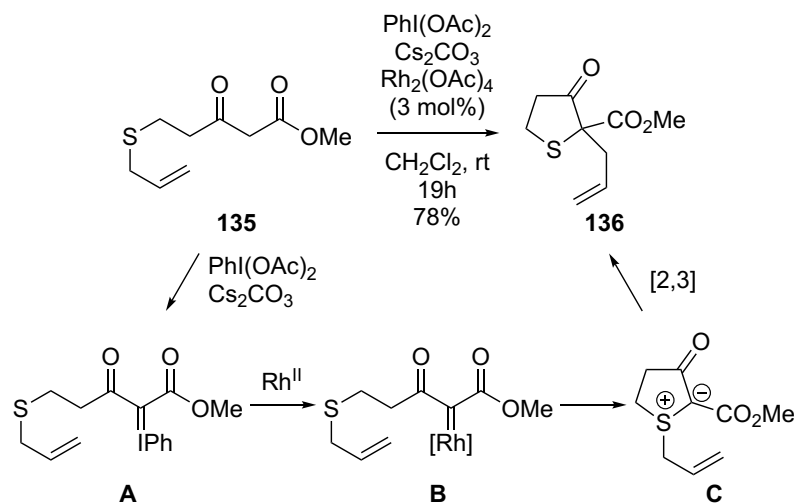
Scheme 1.26 Result of competing reaction pathways

Later, Wang and coworkers extended this methodology to prepare a series of (3-methylthio)oxindoles from α -diazocarbonyl compound **130** and sulfenamides **131** (Scheme 1.27).^{70b} It is notable that sulfonium ylide **133** is an intermediate in the Gassman oxindole synthesis,⁷¹ but was generated under rhodium catalyzed conditions in this specific example. Furthermore, the Sommelet–Hauser rearrangement of **133** provided imine intermediate **134**, which underwent rearomatization/cyclization to provide substituted oxindoles **132** as racemic mixture. Attempts to develop an enantioselective variant of this reaction with chiral dirhodium catalysts were unsuccessful.



Scheme 1.27 Oxindole synthesis via thia-Sommelet-Hauser rearrangement

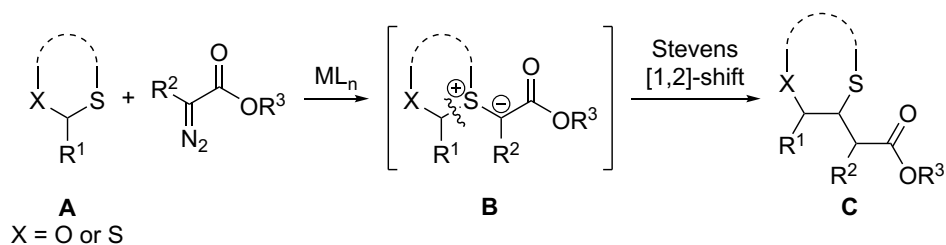
All examples described so far required the prior formation of diazocarbonyl substrates, which was then treated with a metal catalyst to effect sulfonium ylide formation and subsequent rearrangement. Interestingly, West and Murphy^{72a} demonstrated the first example of using iodonium ylides^{72b} as surrogates for diazoketoesters (Scheme 1.28). In this one-pot process, diazoketoester **135** was treated with iodobenzene diacetate [PhI(OAc)₂] and cesium carbonate at room temperature to generate phenyliodonium ylide **A**. Rhodium carbene **B** was subsequently formed in the presence of Rh₂(OAc)₄ in the reaction mixture, followed by intramolecular formation of sulfonium ylide **C** and [2,3]-sigmatropic rearrangement to provide product **136** in 78% yield. Overall, this methodology allows for the direct conversion of β-ketoester substrate to sulfonium ylide *via in situ* generation of iodonium ylide and metalcarbene intermediate. The [2,3]-rearrangement product is efficiently generated from the sulfonium ylide intermediate.



Scheme 1.28 [2,3]-rearrangement of sulfonium ylide via in situ generated iodonium ylide

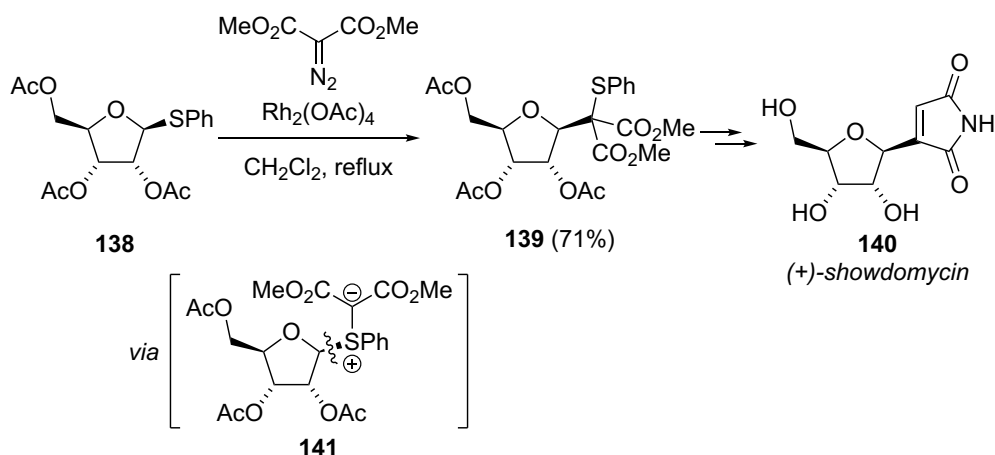
1.8.3 The Stevens [1,2]-shift

The discovery and mechanism of the Stevens [1,2]-shift has already been covered in Section 1.7. The Stevens [1,2]-shift of sulfonium ylides, generated by the reaction of metallocarbenes and sulfur nucleophiles, is a versatile C–C bond forming strategy and has received considerable attention in recent literature.^{6a,4,18} In particular, the transformation of sulfonium ylide **B** derived from *O,S*- and *S,S*-acetals (**A**) has been investigated extensively in the past decade (Scheme 1.29). When the cyclic mixed thioacetal is used, the Stevens [1,2]-shift of the anomeric carbon can result in a one-carbon ring expansion product (**C**) with the formation of a new C–C bond. An intramolecular variant on the ylide formation is also possible when the diazo moiety is tethered in proximity with the sulfur atom on the same molecule. In this section, recent developments in this area are discussed.



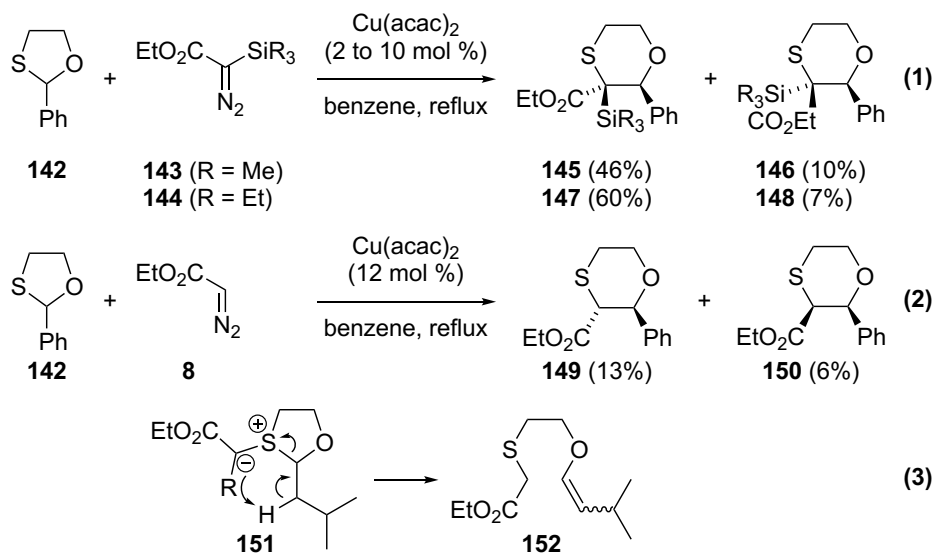
Scheme 1.29 The Stevens [1,2]-shift of sulfonium ylides derived from mixed cyclic thioacetals

An early benchmark example of the Stevens [1,2]-shift of sulfonium ylides derived from monothioacetals was reported by Kametani and coworkers (Scheme 1.30).⁷³ Rhodium catalyzed decomposition of dimethyl diazomalonate in the presence of monothioacetal **138** provided sulfonium ylide **141** that underwent a subsequent Stevens [1,2]-shift to furnish product **139**. This stereoselective C-glycosylation reaction has served as the key transformation in the total synthesis of (+)-showdomycin (**140**). Retention of the stereochemical configuration at the anomeric center was observed in this process. Since then, extensive investigations in this area have led to the development of many useful methodologies that are potentially applicable to the synthesis of complex molecular architectures.



Scheme 1.30 Early application of the Stevens [1,2]-shift of sulfonium ylides

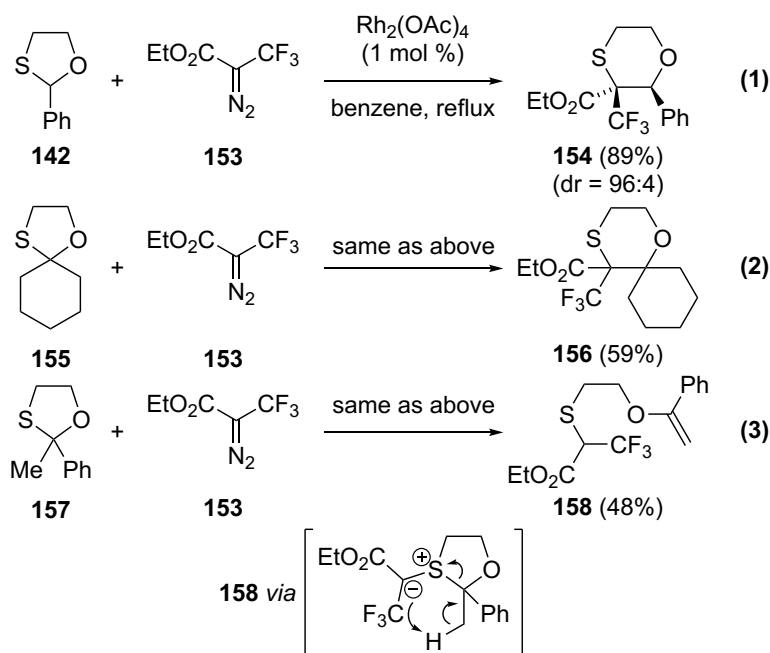
In 2005, Porter and coworkers⁷⁴ reported the conversion of 1,3-oxathiolanes to 1,4-oxathianes *via* a Stevens [1,2]-shift (Scheme 1.31). When diazo(trimethylsilyl)acetate ethyl ester (**143**) or diazo(triethylsilyl) acetate ethyl ester (**144**) was used, the desired ring expansion products were formed in good yields favoring the *cis*-isomer (**145** and **147**, eq 1). However, these products were prone to varying degrees of desilylation, and the more robust triethylsilyl group is preferred. On the other hand, when ethyl diazoacetate (**8**) was used, significant reductions in yields were observed (eq 2). Side reactions with the copper carbenoid and the sulfur atom in products **149** and **150** occurred when excess amounts of ethyl diazoacetate (**8**) were used due to a lack of discrimination between the sulfur atoms in the starting material and product. They thus concluded that the silyl groups play important roles to attenuate those side reactions by making the sulfur atom in the 1,4-oxathiane product more sterically hindered. In cases where the anomeric carbon was substituted with an alkyl group, a low yield of elimination product (**152**) was formed instead of the ring expansion product.



Scheme 1.31 Synthesis of 1,4-oxathianes from 1,3-oxathiolanes

Later, Zhu and coworkers⁷⁵ reported a variant to Porter's methodology. They found dirhodium tetraacetate to be a superior catalyst to copper(II) acetylacetonate. Ethyl

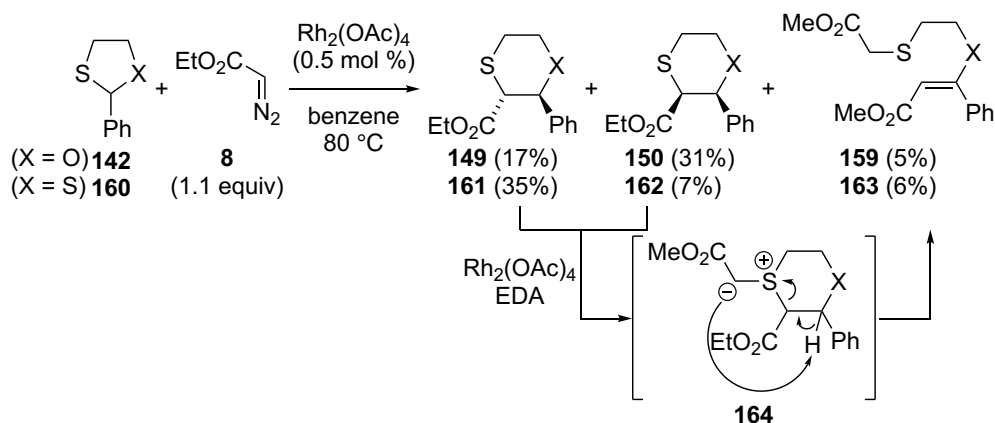
3,3,3-trifluoromethyl-2-diazopropionate (**153**) was used instead of diazo(triethylsilyl) acetate (**144**, Scheme 1.31) to give the corresponding 1,4-oxathiane **154** in high yields and excellent diastereoselectivity with the relative stereochemistry confirmed by X-ray crystallography (eq 1, Scheme 1.32). This reaction is also feasible for 1,3-oxathiolanes with various aryl groups on the anomeric center. Interestingly, when spiro 1,3-oxathiolane **155** was used, the desired [1,2]-shift product (**156**) was formed in only 59% yield due to a competing eliminative pathway of the product with an available β -hydrogen atom (eq 2). However, 1,3-oxathiolane **157** provided exclusively the elimination product (**158**) under the same reaction conditions, possibly due to the favorable five-membered transition state (eq 3). Overall, this methodology provided access to various trifluoromethyl containing 1,4-oxathiolanes.



Scheme 1.32 Dirhodium tetraacetate catalyzed reaction of 1,4-oxathianes

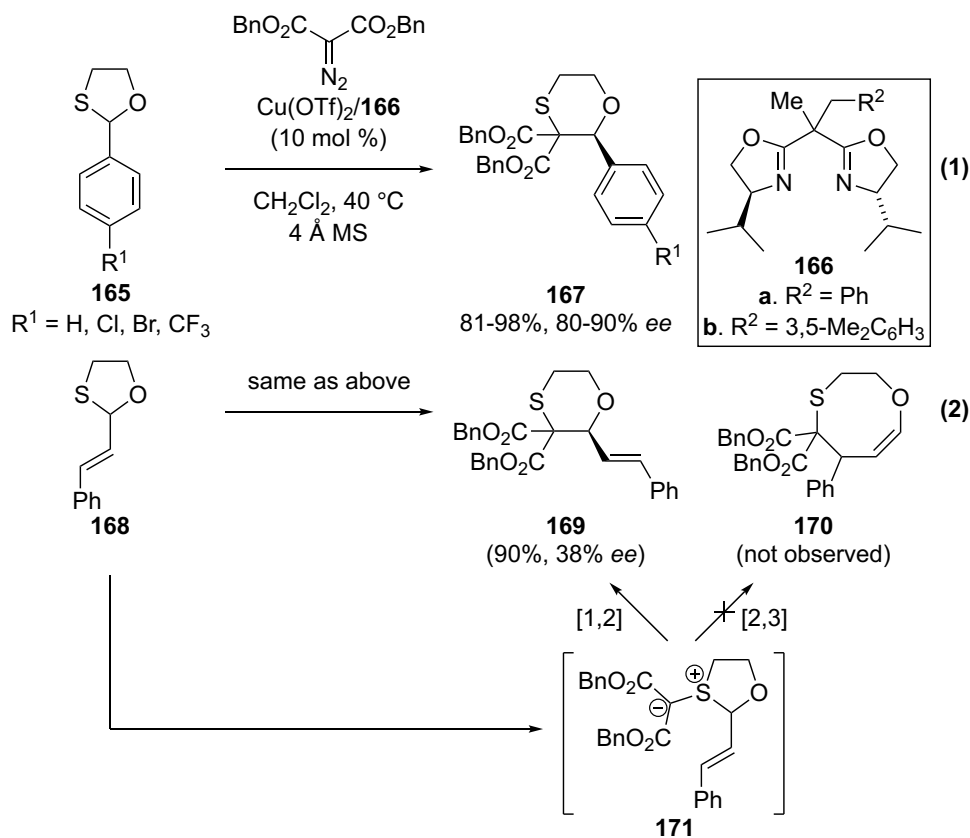
Kostikov and coworkers⁷⁶ have shown that 1,3-oxathiolane **142** and 1,3-dithiolane **160** were both suitable substrates to form ring expansion products **149/150** and **161/162** respectively *via* a Stevens [1,2]-shift (Scheme 1.33). Notably, improved yields of **149**

and **150** were obtained using dirhodium tetraacetate as the catalyst, whereas the use of copper(II) acetylacetonate as the catalyst resulted in poor yields in Porter's work (eq 2, Scheme 1.31).⁷⁴ The sulfur atom in the product was shown to undergo further reactions with the rhodium carbene to effect sulfonium ylide (**164**) formation, and a subsequent elimination reaction would generate enol ether **159** and vinyl sulfide **163**.



Scheme 1.33 1,3-Dithiolane and 1,3-oxathiolane as starting materials

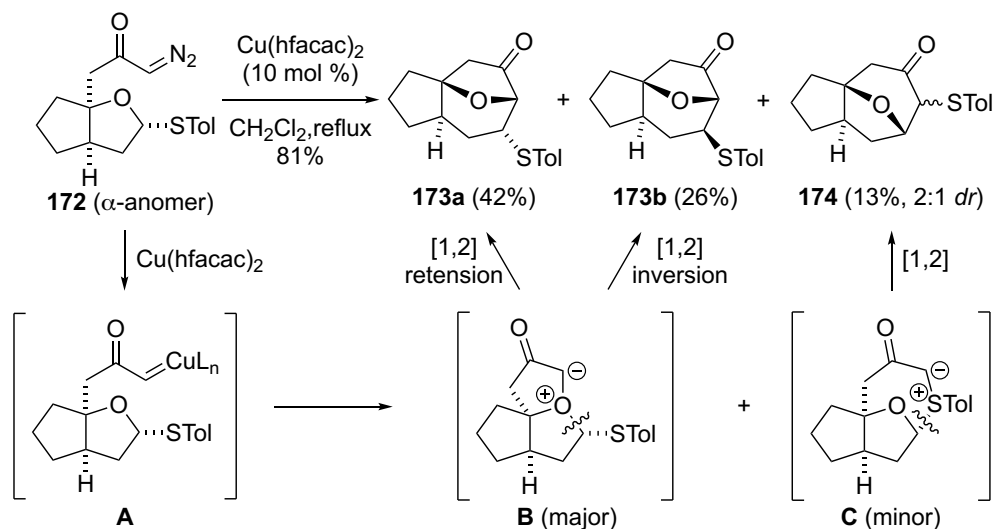
In 2009, Tang and coworkers^{77a} reported the first examples of catalytic asymmetric Stevens [1,2]-shifts of sulfonium ylides derived from 1,3-oxathiolanes (**165**) using copper (II) triflate with a chiral side-armed bisoxazoline^{77b} ligand **166** (eq 1, Scheme 1.34). In this work, enantioenriched 1,4-oxathianes (**167**) were synthesized in excellent yields and high enantioselectivity up to 90% *ee*, and the products were unambiguously assigned by X-ray crystallography. Optimal results were obtained using copper complexes with side-armed bisoxazoline ligands **166a/166b**, dibenzyl diazomalonates, and benzene rings substituted with electron-withdrawing groups (Cl, Br, CF_3). It was proposed that the chiral Cu(I) complex remains associated with the malonate group of the sulfonium ylide intermediate to induce enantioselectivity.⁷⁷ Interestingly, substrate **168** underwent a Stevens [1,2]-shift cleanly under these reaction conditions to give 1,4-oxathiane **169** in 90% yield, whereas the product resulting from the competing [2,3]-rearrangement process (**170**) was not observed (eq 2).



Scheme 1.34 Asymmetric Stevens [1,2]-shift of sulfonium ylide

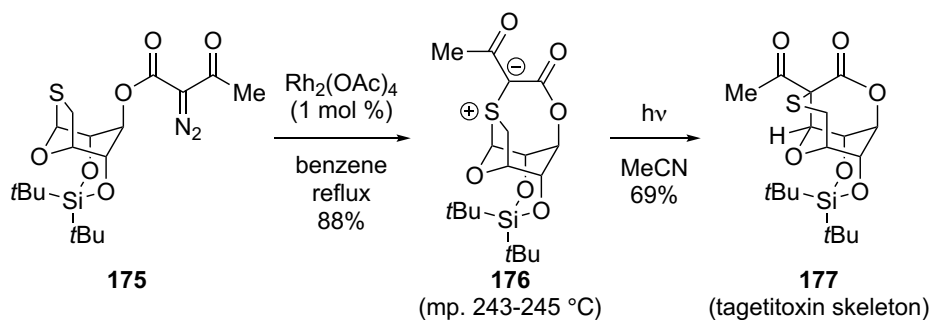
Examples described so far involved the Stevens [1,2]-shift of intermolecularly generated sulfonium ylides. However, intramolecular variants using cyclic mixed thioacetals with pendant diazocarbonyl side chains have also been reported, and have shown great versatility towards the synthesis of complex scaffolds. While trying to synthesize ether-bridged cycloheptane ring systems, West and coworkers⁷⁸ observed a competing pathway involving a rearrangement of the sulfonium ylide (Scheme 1.35). A bicyclic monothioacetal (**172**, α -anomer) with a pendent diazocarbonyl side chain was synthesized and isolated from the corresponding β -anomer. Upon treatment of **172** with $\text{Cu}(\text{hfacac})_2$, five-membered oxonium ylide intermediate **B** was formed from copper carbenoid **A**, followed by a Stevens [1,2]-shift of the ylide to provide desired products **173a** and **173b** in 68% yield. However, an interesting minor side product **174**

was also observed, presumably formed *via* the Stevens [1,2]-shift of sulfonium ylide **C**. The preference for oxonium ylide formation over sulfonium ylide formation can be attributed to the ring sizes. Nonetheless, [1,2]-shifts of ylides **B** and **C** have produced epimeric mixtures of products with erosion of stereochemical configuration at the migrating anomeric center, strongly suggesting a stepwise mechanism involving either radicals or ion pairs.



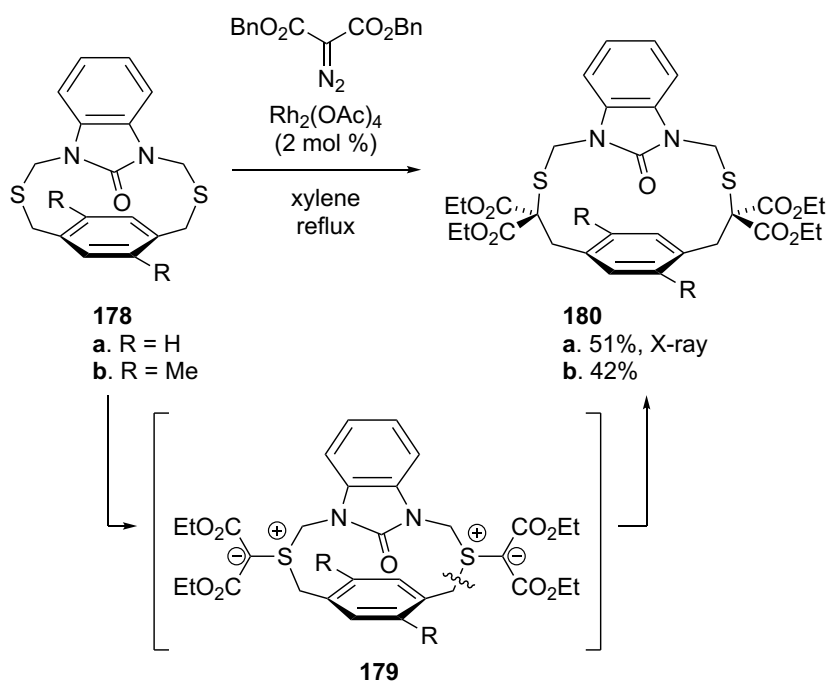
Scheme 1.35 The competing pathway involving sulfonium ylide rearrangement

Intramolecular Stevens rearrangements of sulfonium ylides derived from monothioacetals was recently applied in the synthesis of the core structure of RNA polymerase inhibitor tagetitoxin by Porter and coworkers (Scheme 1.36).⁷⁹ Catalytic decomposition of bicyclic 1,3-oxathiolane **175** furnished remarkably stable and isolable sulfonium ylide **176**. However, attempts to induce a Stevens rearrangement of **176** under thermal conditions in various solvents led to recovery of starting materials. Decomposition of **176** was observed with prolonged heating times. Interestingly, the less commonly employed photo-Stevens rearrangement effectively completed the desired conversion to tetracycle **177**, providing the core structure of tagetitoxin.



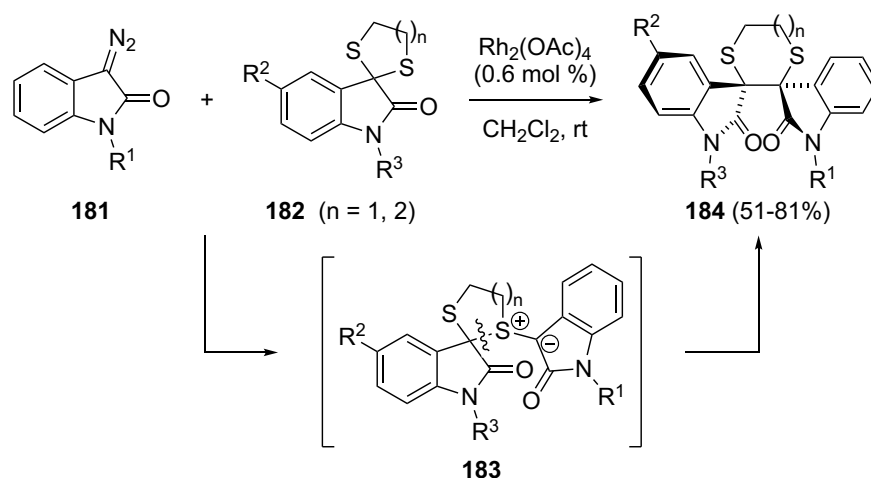
Scheme 1.36 Synthesis of tagetitoxin skeleton *via* photo-Stevens rearrangement

Macrocyclic ring expansion *via* Stevens rearrangement of sulfonium ylides is also an area of active investigation with a few recently reported examples. In 2006, Diver and coworkers⁸⁰ synthesized benzimidazolidinone cyclophanes through an intermolecular rhodium (II) catalyzed double Stevens rearrangement (Scheme 1.37). In this process, starting thiacyclophanes **178** were converted to the ring expansion products **180** in the presence of dirhodium tetraacetate and diethyl diazomalonate in refluxing xylene. Diazo decomposition was believed to occur at lower temperatures than the Stevens [1,2]-shift. Indeed, bis(sulfur ylide) intermediate **179** was isolated as a white precipitate when the reaction was carried out in lower temperatures (refluxing 1,2-dichloroethane and benzene). Subsequent heating of **179** in xylene afforded **180**, which was unambiguously assigned by X-ray crystallography. It is worth noting that bond cleavage of the sulfur-benzylic carbon bond was favored over the sulfur-acetal carbon bond to provide the observed regioselectivity.



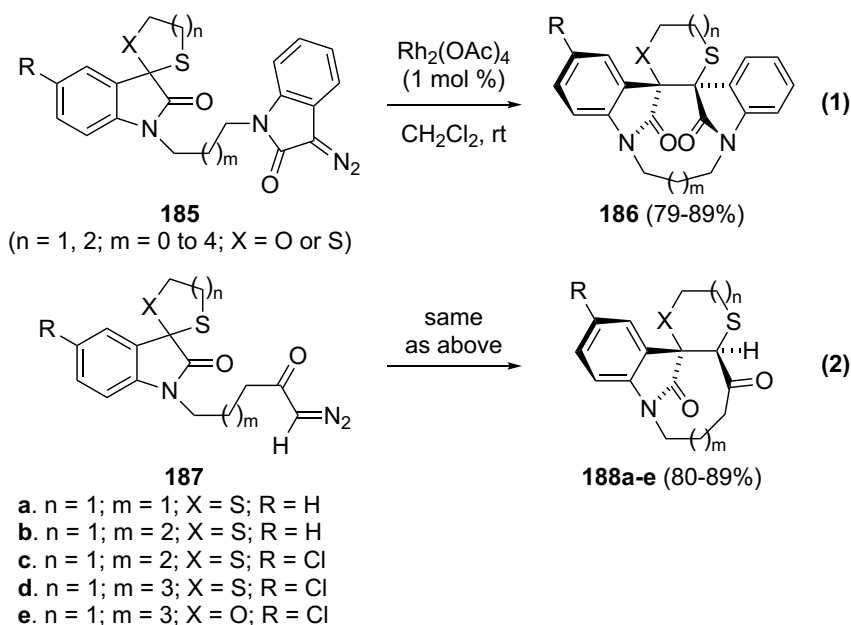
Scheme 1.37 Macrocyclic ring expansion *via* double Stevens rearrangement

Recently, Muthusamy and coworkers^{81a} demonstrated the first example of a Stevens rearrangement using spirocyclic thioketals (Scheme 1.38). Rhodium(II) catalyzed decomposition of diazoamides **181** in the presence of spiro-1,3-dithiolaneoxindole (**182**, n = 1) or spiro-1,3-dithianeoxindole (**182**, n = 2) was initially investigated. Intermolecular formation of sulfonium ylide **183** followed by a Stevens rearrangement afforded the desired dispiro oxindoles (**184**) in high yields as single diastereomers with the two oxindole rings in the *anti*-orientation.



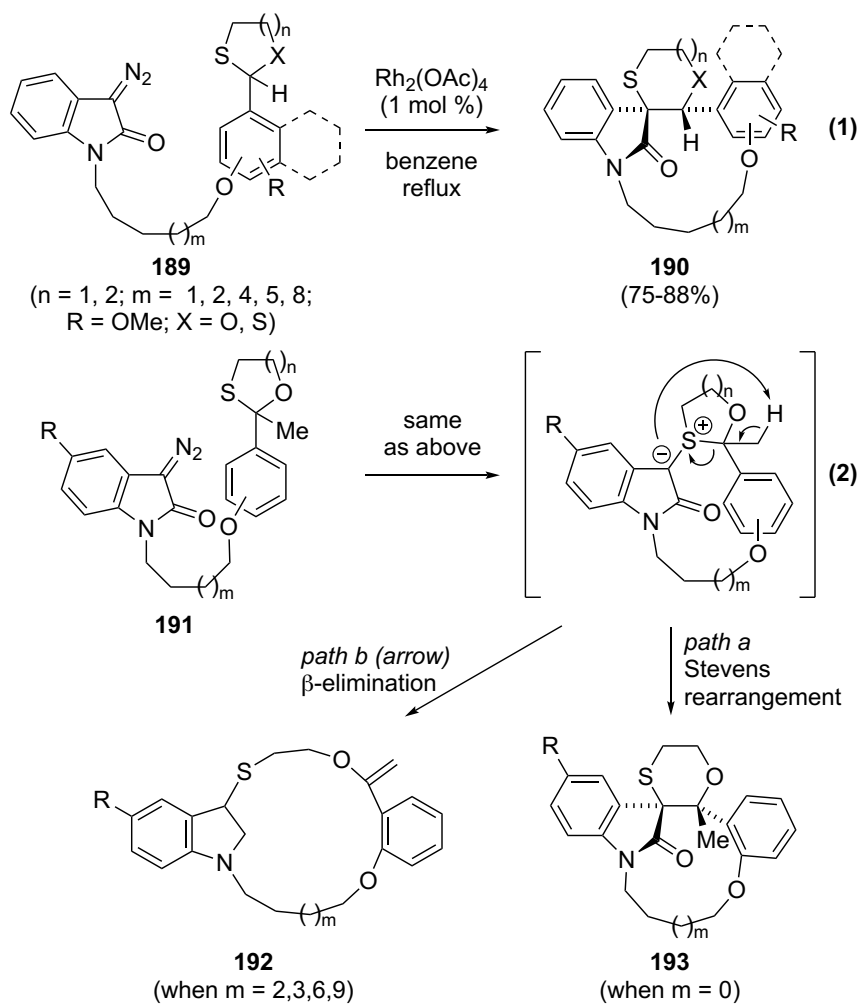
Scheme 1.38 Intermolecular sulfonium ylide formation using spiro-thioketal

Three years later, Muthusamy and coworkers^{81b} further extended the applicability of this methodology, and reported an intramolecular variant to access macrocyclic sipro- and dispiro-oxindoles through ring expansion reactions of 9- to 13-membered sulfonium ylides. In this case, the diazoamide and spiro-ketal moieties were tethered on the same molecule (**185**), and the desired rearrangement occurred to provide macrocyclic dispiro-1,4-dithianeoxindole and dispiro-1,4-oxathianeoxindoles (**186**) as single diastereomers in high yields (eq 1, Scheme 1.39). When the spiro-thioketals bearing pendant α -diazoketones (**187a-e**) were used as starting materials, spiro-1,4-dithianeoxindoles **188a-e** were also formed efficiently as single diastereomers (eq 2). However, lower diastereoselectivities were observed in other cases.



Scheme 1.39 Stevens rearrangement of intramolecularly generated sulfonium ylides

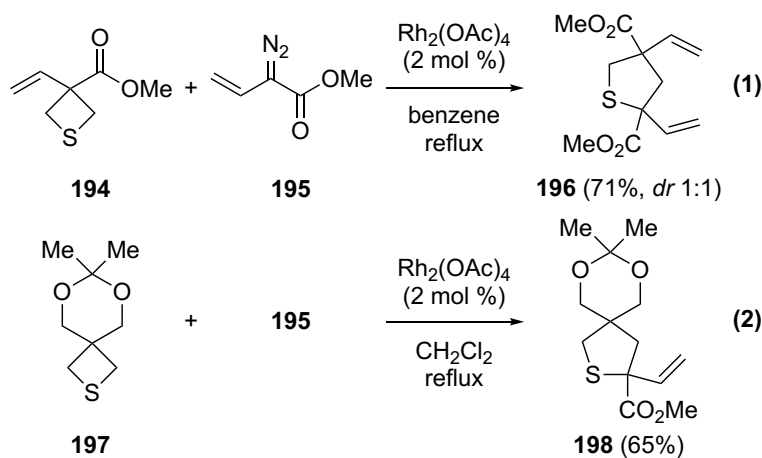
In 2017, the investigation on the Stevens rearrangement of intramolecularly generated sulfonium ylides from spiro-thioacetals was further extended to include 11- to 21-membered macrocyclic sulfonium ylide intermediates.^{81c} Various cyclic *S,S*- and *O,S*-acetals with pendant diazoamides were prepared with different chain lengths. Under the optimized conditions, the starting *S,S*- and *O,S*-acetals (**189**) provided the desired macrocycles **190** in high yields as single diastereomers (eq 1, Scheme 1.40). When 1,3-oxathiolane derived from acetophenone with a long chain length (**191**) was used, the product from the Stevens rearrangement was not observed. Instead, an interesting tetracyclic macrocycle **192** was formed in high yield (eq 2). As such, two reaction pathways were considered for the observed product formation with tetra-substituted anomeric centers. When the chain length is small ($m = 0$), a Stevens rearrangement of the transient sulfonium ylide intermediate occurred to provide macrocycle **193** (path a), whereas a longer chain length ($m = 2,3,6,9$) resulted in β -elimination (path b) to form macrocycle **192** with an exocyclic olefin.



Scheme 1.40 Rearrangement of intramolecularly generated macrocyclic sulfonium ylides

Lastly, an application of the Stevens rearrangement was reported by Zakarian and coworkers⁸² towards the synthesis of sesquiterpene *Nuphar* thioalkaloids with a 2,2,4,4-tetrasubstituted thiolane core. Although the target was to develop a general strategy to access all four stereoisomers of the 2,2,4,4-tetrasubstituted thiolane subunit, only the strategic ring expansion *via* the Stevens rearrangement is discussed here. The anticipated Stevens rearrangement of intermolecularly generated sulfonium ylide derived from disubstituted thietane **194** and diazoester **195** successfully provided the desired ring-expansion product **196**, but no diastereoselectivity was observed (eq 1,

Scheme 1.41). Spiro-bicyclic thietane **197** can also react in a similar fashion to give product **198** *via* a Stevens rearrangement (eq 2). Products **196** and **198** were both important intermediates toward the synthesis of thioalkaloids.

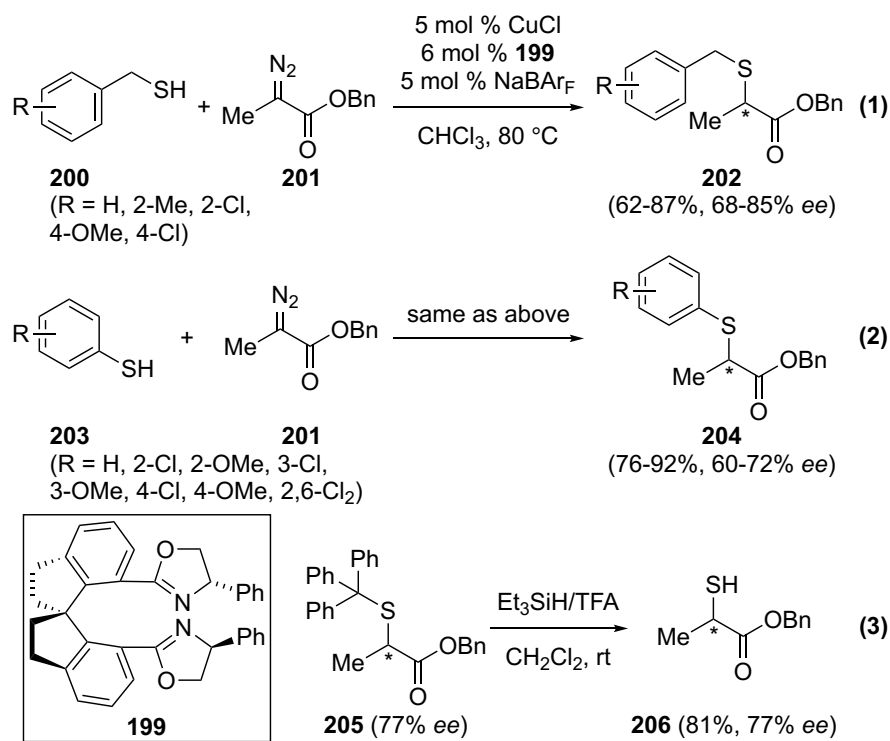


Scheme 1.41 Sulfonium ylide rearrangement from disubstituted thietane

1.8.4 S–H Insertions

Catalytic S–H insertion of α -diazocarbonyl compounds with thiols represents a useful way to introduce sulfur-containing substituents to the α -position of carbonyl compounds through C–S bond formation.^{37a} Recent development in this area has been focused on the catalytic enantioselective S–H insertion reactions between α -diazoesters and thiols using transition metal catalysts. As noted in previous literature precedents, the observed low asymmetric induction in catalytic S–H insertion reactions is mainly attributed to the high stability of the transient sulfonium ylide. It may allow the degeneration of the metal-complexed ylide to the free ylide and thus result in reduced enantioselectivity. In 2009, Zhou and coworkers⁸³ achieved the first example of this asymmetric variant to access chiral α -sulfenylated carbonyl compounds with high enantioselectivity (Scheme 1.42). The copper complex with chiral spiro bisoxazoline ligand (**199**) was found to be the most effective catalyst in providing the highest

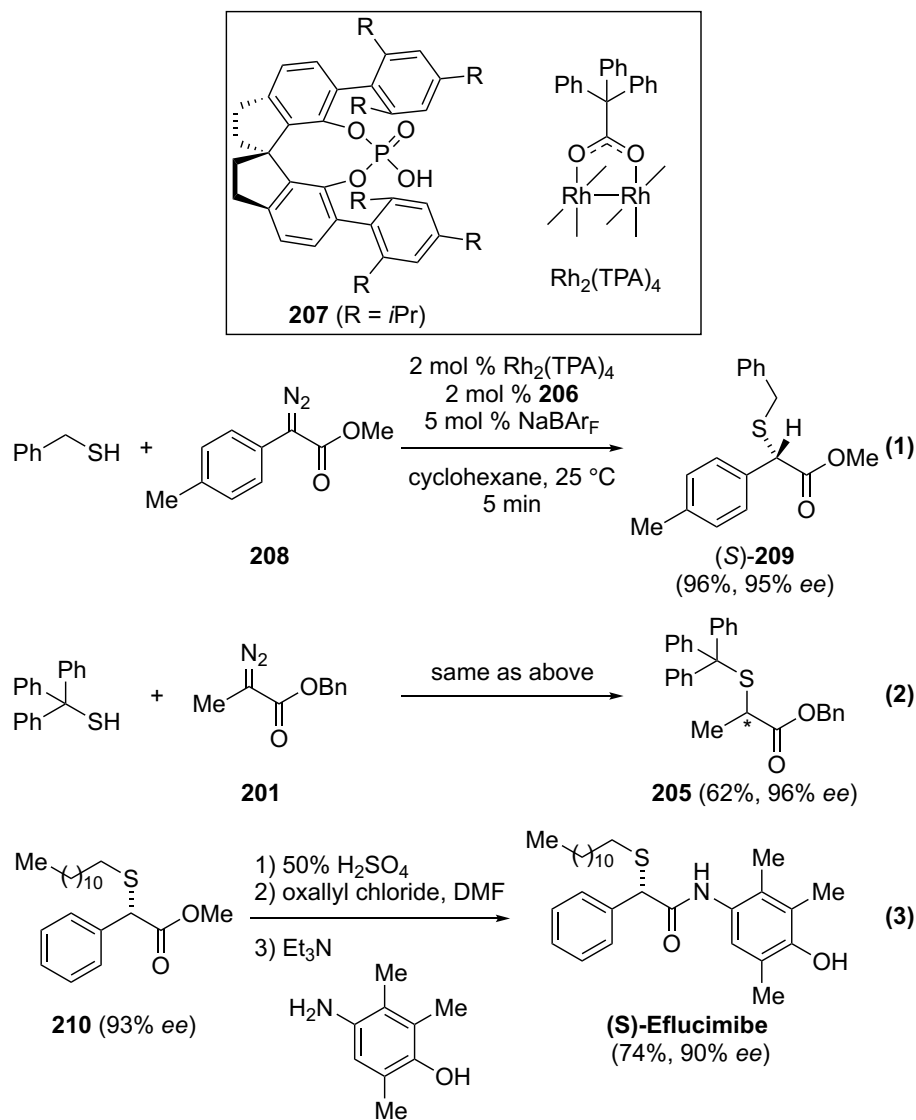
reactivity and enantioselectivity. Catalytic decomposition of benzyl 2-diazopropanoate (**201**) in the presence of various benzyl mercaptans (**200**) and phenyl mercaptans (**203**) was investigated, and was shown to afford corresponding α -sulfenylated carbonyl products **202** and **204** with high *ee* (eq 1 and eq 2). The methodology was applied to synthesize a trityl analog (**205**) with 77% *ee*. Deprotection of the trityl group under acidic conditions afforded α -mercaptoester **206** without diminishing the enantiopurity (eq 3), demonstrating the potential utility of this methodology.



Scheme 1.42 Asymmetric S–H insertion generated from copper carbenoid

Recently, Zhou and coworkers⁸⁴ performed further investigations and reported a highly enantioselective S–H insertion reaction *via* cooperative catalysis of achiral dirhodium complexes and chiral spiro phosphoric acids (Scheme 1.43). The best yield and enantioselectivity were observed when a combination of rhodium(II) triphenylacetate dimer [Rh₂(TPA)₄] and spiro phosphoric acid (**207**) was used. Various

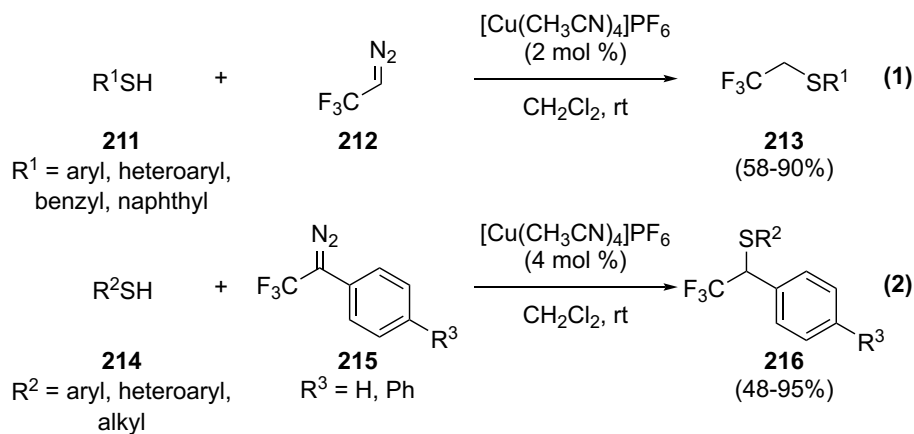
methyl phenyldiazoacetate complexes with different substitutions on the phenyl group were shown to react efficiently with benzyl mercaptan under optimized reaction conditions. For example, the reaction of diazoacetate **208** with benzyl mercaptan afforded chiral α -sulfenylated carbonyl product **209** in excellent yield and enantioselectivity (eq 1, Scheme 1.43). It is worth noting that the trityl protected product **205**, generated with 77% *ee* in the previous copper catalyzed conditions (eq 3, Scheme 1.42), was formed with 96% *ee* in this case (eq 2, Scheme 1.43), demonstrating the superior enantioselectivity offered by the catalytic system. To further probe the synthetic utility, a short three-step synthesis on (*S*)-eflucimbe was accomplished from the S–H insertion product **210** (eq 3, Scheme 1.42) through hydrolysis and amidation steps.



Scheme 1.43 Asymmetric S–H insertion reaction catalyzed by rhodium(II) complex and chiral spiro phosphoric acid

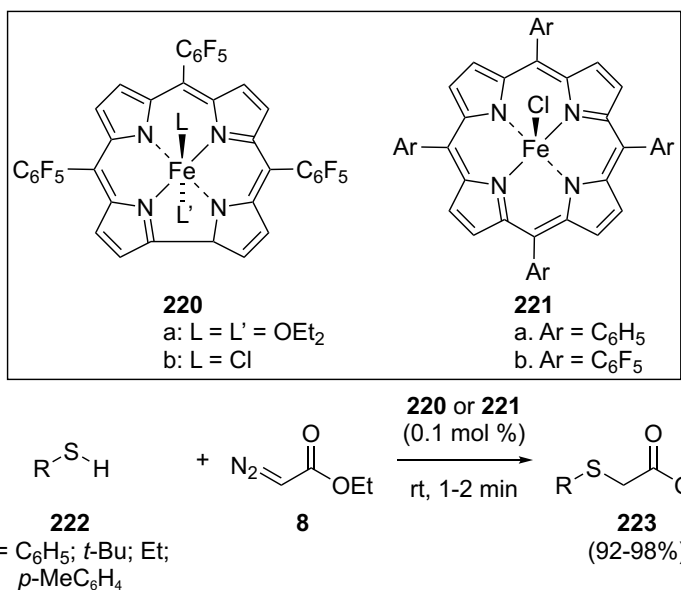
The achievement of asymmetric S–H insertion into metallocarbenes was definitely a remarkable milestone. In addition, several other recent examples on the development of catalytic S–H insertion reactions have also broadened the synthetic utility of this process. Recently, Gouverneur and coworkers⁸⁵ have reported a copper-catalyzed S–H insertion reaction with trifluorodiazalkanes to access various trifluoromethyl-containing sulfides (Scheme 1.44). [Cu(CH₃CN)₄]PF₆ was found to be the most

effective catalyst during reaction optimization. 2,2,2-Trifluoro-1-diazoethane (**212**) was initially examined under the optimized reaction conditions, and provided the desired S-H insertion products **213** using various thiols (**211**) in high yields (eq 1). The process was then applied to generate branched trifluoroalkyl products (eq 2) using 1-aryl-2,2,2-trifluoro-1-diazoethane (**215**). Various aryl, heteroaryl, and alkyl groups on the sulfur atom afforded **216** in good yields, except 4-methoxy or 4-nitro substituted benzyl mercaptan. On the other hand, when a nitro group was installed at R³, the reaction did not provide the desired product.



Scheme 1.44 S–H insertion reaction with trifluorodiazoalkanes

[Cu(CH₃CN)₄]PF₆ was then proven to be an effective catalyst for the S–H insertion reactions with α-diazoesters by Ollevier and coworkers (Scheme 1.45).⁸⁶ Benzyl mercaptan and various substituted thiophenols (**217**) were investigated in the reaction with different α-diazoketoester (**218**) under the optimal reaction conditions using 5 mol% of [Cu(CH₃CN)₄]PF₆ in dichloromethane at room temperature. Desired S–H insertion products **219** were formed in high yields.

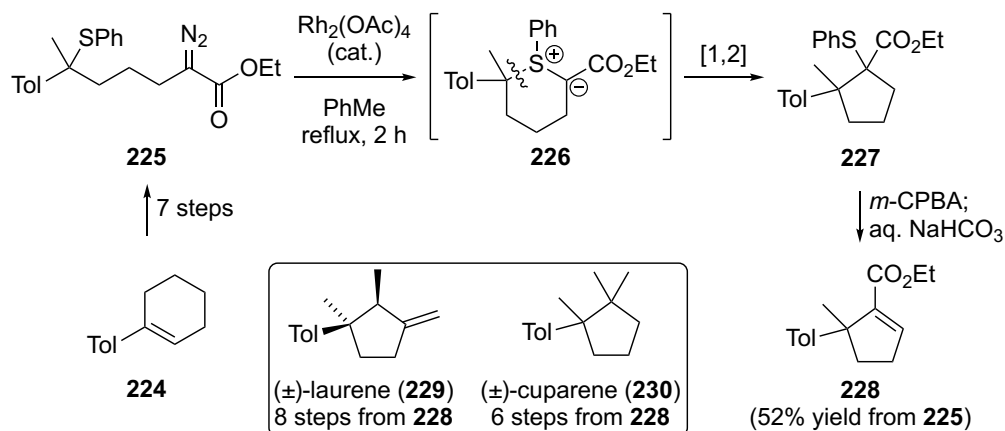


Scheme 1.46 Iron-based catalysis for S–H insertion reactions

1.8.5 Synthetic applications on the Stevens [1,2]-shift of sulfonium ylide

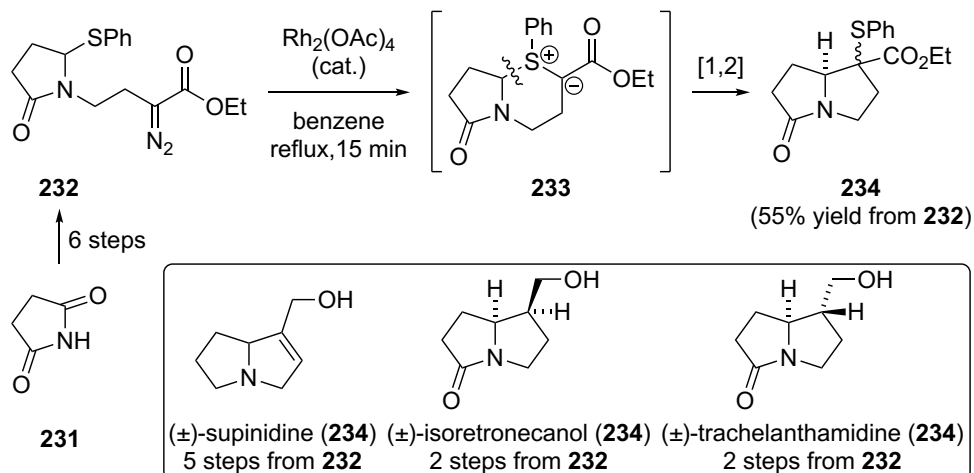
To the best of our knowledge, there were only limited literature precedent on the total synthesis of natural products employing the Stevens [1,2]-shift of sulfonium ylide generated from metallocarbene and sulfide. In 1980s, Kametani's group contributed a series of important reports in this area,^{73,89,90,91} which they referred to as the intramolecular carbenoid displacement reaction (ICD).

In 1985, Kametani and coworkers^{89a} reported the synthesis of (±)-cuparene (**230**) using Stevens [1,2]-shift of an intramolecularly generated sulfonium ylide as the key step. The starting sulfide with a pendant diazoketoester (**225**) was prepared from cyclohexene derivative **224**. Upon treatment with Rh₂(OAc)₄ in refluxing benzene, diazoketoester **225** was converted to the desired [1,2]-shift product **227** *via* sulfonium ylide intermediate **226**, followed by oxidative elimination to afford substituted cyclopentene **228** in 52% overall yield. Intermediate **228** could be converted to (±)-cuparene (**230**). Later, the same group reported the synthesis of (±)-laurene (**230**) from intermediate **228**.^{89b}



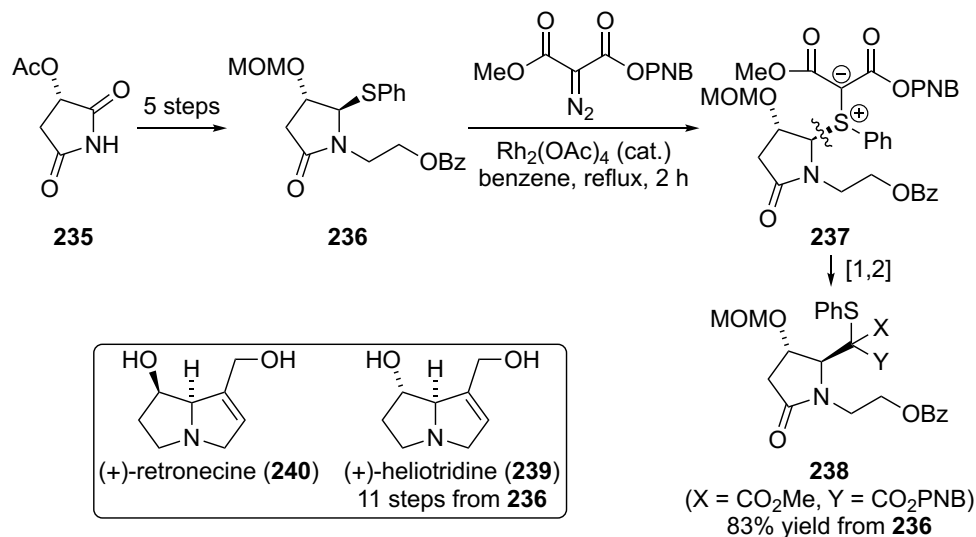
Scheme 1.47 Synthetic applications of the Stevens [1,2]-shift of sulfonium ylides

In 1985, the same authors extended the methodology to the synthesis of pyrrolizidine alkaloids⁹⁰ (Scheme 1.48). In this case, the sulfur nucleophile was part of an *N,S*-acetal (**232**) which led to the formation of a bicyclic sulfonium ylide intermediate (**233**). The desired [1,2]-shift product was formed in 55% yield as a mixture of inseparable diastereomers (**234**), which was converted into three pyrrolizidine alkaloids (**234**, **235** and **236**).



Scheme 1.48 Stevens [1,2]-shift of sulfonium ylide derived from *N,S*-acetal

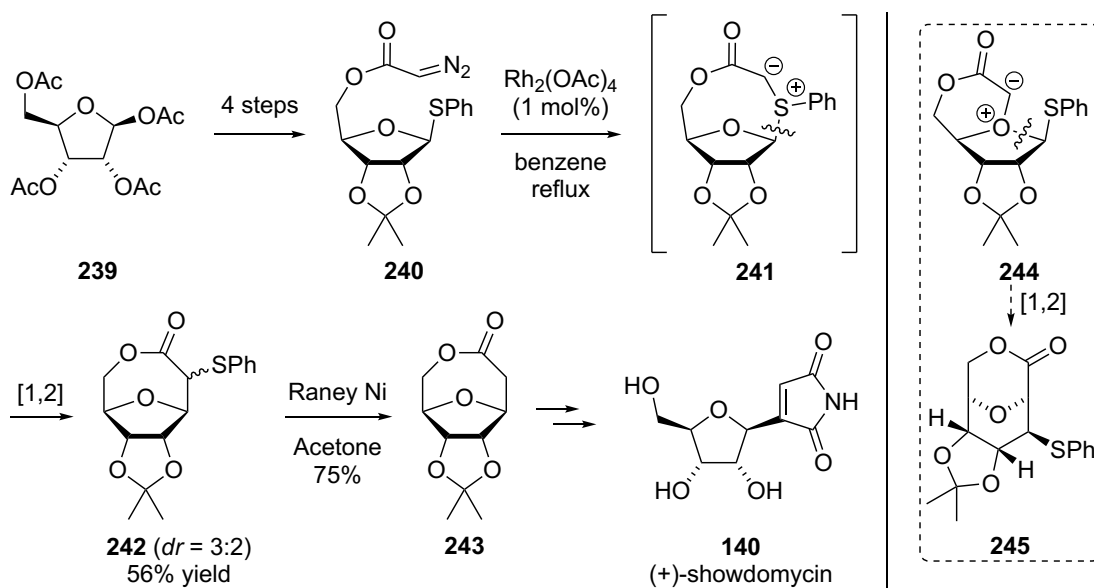
Later, this strategy was applied to the asymmetric total synthesis of (+)-heliotridine (**239**) and (+)-retronecin (**240**)⁹¹ (Scheme 1.49). The required *trans*-substituted pyrrolidone (**236**) was prepared from optically active succinimide **235** derived from (*S*)-malic acid. Rh₂(OAc)₄ catalyzed decomposition of methyl *p*-nitrobenzyl α-diazomalonate in the presence of sulfide **236** led to the intermolecular formation of sulfonium ylide **237**, which underwent an efficient [1,2]-shift to afford product **238** in 83% yield. Although the stereochemical configuration of product **238** was not determined, subsequent derivatization of **238** led to natural products **239** and **240** with known stereochemistry. As such, the Stevens [1,2]-shift occurred with retention of stereochemical configuration. Later, a variant of this methodology using monothioacetal substrate was applied to the synthesis of (+)-showdomycin⁷³ (Section 1.8.3, Scheme 1.30) by the same group.



Scheme 1.49 Asymmetric total syntheses of pyrrolizidine alkaloids

In 1993, Kim and coworkers⁹² published a formal synthesis of (+)-showdomycin using the Stevens [1,2]-shift of an intramolecularly generated sulfonium ylide derived from monothioacetal (Scheme 1.50). Diazoester **240** was prepared from a known ribofuranose derivative (**239**). When diazoester **240** was treated with Rh₂(OAc)₄ in

refluxing benzene, product **242** was isolated as a 3:2 mixture of inseparable diastereomers in 56% yield. In this process, product **242** was resulted from an eight-membered sulfonium ylide (**241**). Interestingly, the plausible competing pathway involving the formation of six-membered oxonium ylide **244** (see Section 1.8.3, Scheme 1.35 for a similar example) and the corresponding [1,2]-shift product (**245**) was not observed. Lactone **242** was then treated with Raney nickel to afford desulfurized product **243**, which is an advanced intermediate⁹³ towards (+)-showdomycin **140**.



Scheme 1.50 Application of the Stevens [1,2]-shift in a formal synthesis of (+)-showdomycin

1.9 Conclusion

Sulfonium ylides are reactive intermediates that could undergo various transformations depending on the substitution patterns. The catalytic generation of sulfonium ylides from α -diazocarbonyl compounds and sulfur nucleophiles using a transition metal catalyst is a mild and efficient method to generate these reactive

intermediates. This chapter has highlighted recent developments on the formation of sulfonium ylides from metallocarbenes and sulfur nucleophiles and their subsequent transformations, including [2,3]-rearrangements, Stevens [1,2]-shifts and S-H insertions. Among these transformations, the Stevens rearrangement is a versatile C-C bond forming strategy that has attracted considerable attention. Many of the recent developments on the Stevens rearrangement of sulfonium ylides were derived from cyclic *O,S*-, *S,S*-acetals, which could afford heterocyclic products *via* ring expansion or ring contraction. However, synthetic application employing the Stevens rearrangement of sulfonium ylides as the key step was underexplored with only a limited number of reports. As a result, we decided to investigate the Stevens [1,2]-shift of sulfonium ylides derived from cyclic *O,S*- and *N,S*-acetals as an ring expansion strategy to access eight-membered heterocycles and apply the methodology in natural product synthesis. In Chapter 2, our efforts toward a formal synthesis of (+)-laurencin employing this strategy will be discussed. The successful completion of this asymmetric formal synthesis will add a valuable example to enrich the field of sulfur ylide Stevens rearrangement chemistry. In Chapter 3, a novel methodology involving the Stevens [1,2]-shift of sulfonium ylides derived from a cyclic *N,S*-acetals to generate medium-sized azacycles will be discussed. This methodology could be potentially employed as the key step in the synthesis of *Stemona* alkaloids.

1.10 References

1. a) Curtius, T. *Ber.* **1883**, *16*, 2230–2231. b) Curtius, T. *J. Prakt. Chem.* **1888**, *38*, 396–440.
2. a) Wolff, L. *Justus Liebigs Ann. Chem.* **1902**, *325*, 129–195. For selected reviews, see: b) Kirmse, W. *Eur. J. Org. Chem.* **2002**, *2002*, 2193–2256. c) Candeias, N. R.; Trindade, A. F.; Gois, P. M. P.; Afonso, C. A. M. *The Wolff Rearrangement*; 2014; Vol. 3.
3. a) Arndt, F.; Eistert, B.; Amede, J. *Ber.* **1928**, *61B*, 1949–1953. b) Arndt, F.; Amende, J. *Ber.* **1928**, *61B*, 1122–1124. c) Arndt, F.; Eistert, B.; Partale, W. *Ber.* **1927**, *60B*, 1364–1370.
4. Doyle, M. P.; McKervey, M. A.; Ye, T. *Modern Catalytic Methods for Organic Synthesis with Diazo Compounds*; Wiley-Interscience: New York, 1998.
5. a) Ford, A.; Miel, H.; Ring, A.; Slattery, C. N.; Maguire, A. R.; McKervey, M. A. *Chem. Rev.* **2015**, *115*, 9981–10080. b) Maas, G. *Angew. Chem. Int. Ed.* **2009**, *48*, 8186–8195. c) Ye, T.; Mckervey, M. A. *Chem. Rev.* **1994**, *94*, 1091–1160; d) Zhang, Z.; Wang, J. *Tetrahedron* **2008**, *64*, 6577–6605.
6. a) Womack, E. B.; Nelson, A. B. *Org. Synth.* **1963**, *4*, 424–426. b) Womack, E. B.; Nelson, A. B. *Org. Synth.* **1955**, *3*, 392–393.
7. a) Holton, T. L.; Shechter, H. *J. Org. Chem.* **1995**, *60*, 4725–4729. b) Javed, M. I.; Brewer, M. *Org. Lett.* **2007**, *9*, 1789–1792.
8. a) Regitz, M. *Angew. Chem. Int. Ed. Engl.* **1967**, *6*, 733–749. b) Regitz, M. *Synthesis*, **1972**, *7*, 351–373.
9. Erhunmwunse, M. O.; Steel, P. G. *J. Org. Chem.* **2008**, *73*, 8675–8677.
10. a) Marchand, A. P.; Brockway, N. M. *Chem. Rev.* **1974**, *74*, 431–469. b) Dave, V.; Varnhoff, E. W. *Org. React. (N. Y.)* **1970**, *18*, 217–401.
11. a) Andrews, G.; Evans, D. A. *Tetrahedron Lett.* **1972**, *13*, 5121–5124. b) Ando, W.; Yagihara, T.; Kondo, S.; Nakayama, K.; Yamato, H.; Nakaido, S.; Migita, T. *J. Org. Chem.* **1971**, *36*, 1732–1736 and references cited therein.

12. a) Pirrung, M. C.; Liu, H.; Morehead, A. T., Jr. *J. Am. Chem. Soc.* **2002**, *124*, 1014–1023. b) Doyle, M. P.; Tamblyn, W. H.; Bagheri, V. *J. Org. Chem.* **1981**, *46*, 5094–5102 and references cited therein.
13. a) Dötz, K. H.; Stendel, J., Jr. *Chem. Rev.* **2009**, *109*, 3227–3274. b) Zhao, Y.; Wang, J. *Synlett* **2005**, No. 19, 2886–2892.
14. a) von E. Doering, W.; Hoffmann, A. K. *J. Am. Chem. Soc.* **1954**, *76*, 6162–6165. b) von E. Doering, W.; Buttery, R. G.; Laughlin, R. G.; Chaudhuri, N. *J. Am. Chem. Soc.* **1956**, *78*, 3224–3224.
15. Fischer, E. O.; Maasböl, A. *Angew. Chem. Int. Ed. Engl.* **1964**, *3*, 580–581.
16. Schubert, U. *Coord. Chem. Rev.* **1984**, *55*, 261–286.
17. Yates, P. *J. Am. Chem. Soc.* **1952**, *74*, 5376–5381.
18. *Nitrogen, Oxygen and Sulfur Ylide Chemistry*; Clark, J. S., Ed.; Oxford University Press: Oxford, 2002.
19. a) Hodgson, D. M.; Pierard, F. Y. T. M.; Stuppel, P. A. *Chem. Soc. Rev.* **2001**, *30*, 50–61. b) Davies, H. M. L.; Beckwith, R. E. J. *Chem. Rev.* **2003**, *103*, 2861–2903.
20. Davies, H. M. L.; Morton, D. *Chem. Soc. Rev.* **2011**, *40*, 1857–1869.
21. Doyle, M. P. *Chem. Rev.* **1986**, *86*, 919–939.
22. Doyle, M. P., In *Comprehensive Organometallic Chemistry II*; Hegedus, L. S., Ed.; Pergamon Press, New York, 1995; Vol. 12, pp 421–468.
23. Silberrad, O.; Roy, C. S. *J. Chem. Soc. Trans.* **1906**, *89*, 179–182.
24. Nozaki, H.; Moriuti, S.; Yamabe, M.; Noyori, R. *Tetrahedron Lett.* **1966**, *7*, 59–63.
25. Moser, W. R. *J. Am. Chem. Soc.* **1969**, *1171*, 1135–1140.
26. Nozaki, H.; Moriuti, S.; Takaya, H.; Noyori, R. *Tetrahedron Lett.* **1966**, *7*, 5239–5244.
27. For some selected review on asymmetric catalysis with metallocarbenes, see: a) ref 17b. b) Doyle, M. P.; Forbes, D. C. *Chem. Rev.* **1998**, *16*, 911–935. c) Doyle, M. P. *Chem. Rev.* **1986**, *86*, 919–939.

28. For a review, see: Wulfman, D. S.; Linstrumelle, G.; Cooper, C. F., In *The Chemistry of Diazonium and Diazo Groups, Part 2*; Patai, S., Ed.; Wiley, New York, 1978; Chapter 18.
29. a) Salomon, R. G.; Kochi, J. K. *J. Am. Chem. Soc.* **1973**, *95*, 3300–3310. b) Solomon, R. G.; Kochi, J. K. *J. Chem. Soc., Chem. Commun.* **1972**, 559–560.
30. a) Fritschi, H.; Leutenegger, U.; Pfaltz, A. *Helv. Chim. Acta* **1988**, *71*, 1553–1565. b) Lowenthal, R. E.; Abiko, A.; Masamune, S. *Tetrahedron Lett.* **1990**, *31*, 6005–6008.
31. Dauben, W. G.; Hendricks, R. T.; Luzzio, M. J.; Ng, H. P. *Tetrahedron Lett.* **1990**, *31*, 6969–6972.
32. Straub, B. F.; Hofmann, P. *Angew. Chem. Int. Ed.* **2001**, *40*, 1288–1290.
33. Salomon, R. G.; Kochi, J. K. *J. Am. Chem. Soc.* **1973**, *95*, 1889–1897.
34. a) Padwa, A.; Austin, D. J. *Angew. Chem. Int. Ed. Engl.* **1994**, *33*, 1797–1815. b) Doyle, M. P. *J. Org. Chem.* **2006**, *71*, 9253–9260.
35. Clark, J. S.; Krowiak, S. A. *Tetrahedron Lett.* **1993**, *34*, 4385–4388.
36. Paulissen, R.; Reimlinger, H.; Hayez, E.; Hubert, A. J.; Teyssié, P. *Tetrahedron Lett.* **1973**, *14*, 2233–2236.
37. Gillingham, D.; Fei, N. *Chem. Soc. Rev.* **2013**, *42*, 4918–4931.
38. For reviews on rhodium(II) carboxylates, see: a) Adly, F. G.; Ghanem, A. *Chirality* **2014**, *26*, 692–711. b) Merlic, C. A.; Zechman, A. L. *Synthesis* **2003**, *34*, 1137–1156; c) Boyar, E. B.; Robinson, S. D. *Coord. Chem. Rev.* **1983**, *50*, 109–208.
39. Padwa, A.; Austin, D. J.; Price, A. T.; Semones, M. A.; Doyle, M. P.; Protopopova, M. N.; Winchester, W. R.; Tran, A. *J. Am. Chem. Soc.* **1993**, *115*, 8669–8680.
40. For selected examples, see: a) Nakamura, E.; Yoshikai, N.; Yamanaka, M. *J. Am. Chem. Soc.* **2002**, *124*, 7181–7192. b) Pirrung, M. C.; Liu, H.; Morehead, A. T. *J. Am. Chem. Soc.* **2002**, *124*, 1014–1023. c) Pirrung, M. C.; Morehead, A. T. *J. Am. Chem. Soc.* **1996**, *118*, 8162–8163.

41. Snyder, J. P.; Padwa, A.; Stengel, T.; Arduengo, A. J.; Jockisch, A.; Kim, H.-J. *J. Am. Chem. Soc.* **2001**, *123*, 11318–11319 and references cited therein.
42. Kornecki, K. P.; Briones, J. F.; Boyarskikh, V.; Fullilove, F.; Autschbach, J.; Schrote, K. E.; Lancaster, K. M.; Davies, H. M. L.; Berry, J. F. *Science* **2013**, *342*, 351–354.
43. a) Werlé, C.; Goddard, R.; Philipps, P.; Farès, C.; Fürstner, A. *J. Am. Chem. Soc.* **2016**, *138*, 3797–3805. b) Werlé, C.; Goddard, R.; Fürstner, A. *Angew. Chem. Int. Ed.* **2015**, *54*, 15452–15456.
44. *Ylide Chemistry*; Johnson, A. W., Ed.; Academic Press: New York, 1966; pp 306–366.
45. *Sulfur Ylides: Emerging Synthetic Intermediates*; Trost, B. M.; Melvin, L. S., Eds.; Academic Press: New York, 1975; pp 13–36.
46. Jessop, J. A.; Ingold, C. K. *J. Chem. Soc.* **1930**, 713–718.
47. a) Corey, E. J.; Chaykovsky, M. *J. Am. Chem. Soc.* **1965**, *87*, 1353–1364. b) Corey, E. J.; Chaykovsky, M. *J. Am. Chem. Soc.* **1962**, *84*, 867–868.
48. a) Aggarwal, V. K.; Winn, C. L. *Acc. Chem. Res.* **2004**, *37*, 611–620. b) Gololobov, Y. G.; Nesmeyanov, A. N.; Lysenko, V. P.; Boldeskul, I. E. *Tetrahedron* **1987**, *43*, 2609–2651.
49. Li, A.-H.; Dai, L.-X.; Hou, X.-L.; Huang, Y.-Z.; Li, F.-W. *J. Org. Chem.* **1996**, *61*, 489–493.
50. Trost, B. M.; Hammen, R. M. *J. Am. Chem. Soc.* **1973**, *95*, 962–964.
51. a) Vedejs, E.; West, F. G. *Chem. Rev.* **1986**, *86*, 941–955. b) Vedejs, E.; Martinez, G. R. *J. Am. Chem. Soc.* **1979**, *101*, 6452–6454.
52. a) Ando, W.; Kondo, S.; Nakayama, K.; Ichibori, K.; Kohoda, H.; Yamato, H.; Imai, I.; Nakaido, S.; Migita, T. *J. Am. Chem. Soc.* **1972**, *94*, 3870–3876. b) Ando, W.; Yagihara, T.; Tozune, S.; Imai, I.; Suzuki, J.; Toyama, T.; Nakaido, S.; Migita, T. *J. Org. Chem.* **1972**, *37*, 1721–1727. For a review, see: c) Ando, W. *Acc. Chem. Res.* **1977**, *10*, 179–185.

53. a) Stevens, T. S.; Creighton, E. M.; Gordon, A. B.; MacNicol, M. *J. Chem. Soc.* **1928**, 3193–3197. b) Thomson, T.; Stevens, T. S. *J. Chem. Soc.* **1932**, 69–73.
54. Pine, S. H. *J. Chem. Educ.* **1971**, 99–102.
55. Thomas, B.; Stevens, S. *J. Chem. Soc.* **1930**, 2107–2119.
56. Campbell, B. A.; Houston, A. H.; Kenyon, J. *J. Chem. Soc.* **1947**, 93–95.
57. Woodward, R. B.; Hoffmann, R. *Angew. Chem. Int. Ed. Engl.* **1969**, *8*, 781–853.
58. a) Chantrapromma, K.; Ollis, W. D.; Sutherland, I. O. *J. Chem. Soc. Perkin Trans. I* **1983**, 1049–1061. b) Ollis, W. D.; Rey, M.; Sutherland, I. O. *J. Chem. Soc. Perkin Trans. I* **1983**, 1009–1027. c) Ollis, W. D.; Rey, M.; Sutherland, I. O. *J. Chem. Soc. Chem. Commun.* **1975**, 543–545.
59. a) Eberlein, T. H.; West, F. G.; Tester, R. W. *J. Org. Chem.* **1992**, *57*, 3479–3482. b) West, F. G.; Naidu, B. N. *J. Am. Chem. Soc.* **1993**, *115*, 1177–1178. c) West, F. G.; Naidu, B. N.; Tester, R. W. *J. Org. Chem.* **1994**, *59*, 6892–6894.
60. For selected reviews, see: a) Zhang, Y.; Wang, J. *Coord. Chem. Rev.* **2010**, *254*, 941–953. b) Li, A.-H.; Dai, L.-X.; Aggarwal, V. K. *Chem. Rev.* **1997**, *97*, 2341–2372. c) Vedejs, E. *Acc. Chem. Res.* **1984**, *17*, 358–364.
61. a) Kirmse, W.; Kapps, M. *Chem. Ber.* **1968**, *101*, 994–1003. b) Doyle, M. P.; Griffin, J. H.; Chinn, M. S.; van Leusen, D. *J. Org. Chem.* **1984**, *49*, 1917–1925. c) Doyle, M. P.; Tamblyn, W. H.; Bagheri, V. *J. Org. Chem.* **1981**, *46*, 5094–5102.
62. a) Sommelet, M. *Compt. Rend.* **1937**, *205*, 56–58. b) Kantor, S. W.; Hauser, C. R. *J. Am. Chem. Soc.* **1951**, *73*, 4122–4131. c) Hauser, C. R.; Kantor, S. W.; Brasen, W. R. *J. Am. Chem. Soc.* **1953**, *75*, 2660–2663.
63. Ma, M.; Peng, L.; Li, C.; Zhang, X.; Wang, J. *J. Am. Chem. Soc.* **2005**, *127*, 15016–15017.
64. For selected examples, see: a) Nishibayashi, Y.; Ohe, K.; Uemura, S. *J. Chem. Soc., Chem. Commun.* **1995**, 1245–1246. b) Zhang, X.; Qu, Z.; Ma, Z.; Shi, W.;

- Jin, X.; Wang, J. *J. Org. Chem.* **2002**, *67*, 5621–5625. c) McMillen, D. W.; Varga, N.; Reed, B. A.; King, C. *J. Org. Chem.* **2000**, *65*, 2532–2536.
65. Liao, M.; Wang, J. *Green Chem.* **2007**, *9*, 184–188.
66. Xu, X.; Li, C.; Tao, Z.; Pan, Y. *Green Chem.* **2017**, *19*, 1245–1249.
67. a) Tyagi, V.; Sreenilayam, G.; Bajaj, P.; Tinoco, A.; Fasan, R. *Angew. Chem. Int. Ed.* **2016**, *55*, 13562–13566. b) Holzwarth, M. S.; Alt, I.; Plietker, B. *Angew. Chem. Int. Ed.* **2012**, *51*, 5351–5354.
68. Davies, P. W.; Albrecht, S. J. C.; Assanelli, G. *Org. Biomol. Chem.* **2009**, *7*, 1276–1279.
69. Bonderoff, S. A.; Padwa, A. *J. Org. Chem.* **2017**, *82*, 642–651.
70. a) Liao, M.; Peng, L.; Wang, J. *Org. Lett.* **2008**, *10*, 693–696. b) Li, Y.; Shi, Y.; Huang, Z.; Wu, X.; Xu, P.; Wang, J.; Zhang, Y. *Org. Lett.* **2011**, *13*, 1210–1213.
71. Gassman, P. G.; van Bergen, T. J. *J. Am. Chem. Soc.* **1974**, *96*, 5508–5512.
72. a) Murphy, G. K.; West, F. G. *Org. Lett.* **2006**, *8*, 4359–4361. b) Müller, P. *Acc. Chem. Res.* **2004**, *37*, 243–251.
73. Kametani, T.; Kawamura, K.; Honda, T. *J. Am. Chem. Soc.* **1987**, *109*, 3010–3017.
74. Ioannou, M.; Porter, M. J.; Saez, F. *Tetrahedron* **2005**, *61*, 43–50.
75. Zhu, S.; Xing, C.; Zhu, S. *Tetrahedron* **2006**, *62*, 829–832.
76. Stepanov, A. V.; Molchanov, A. P.; Magull, J.; Vidović, D.; Starova, G. L.; Kopf, J.; Kostikov, R. R. *Tetrahedron* **2006**, *62*, 3610–3618.
77. a) Qu, J.-P.; Xu, Z.-H.; Zhou, J.; Cao, C.-L.; Sun, X.-L.; Dai, L.-X.; Tang, Y. *Adv. Synth. Catal.* **2009**, *351*, 308–312. b) Liao, S.; Sun, X. L.; Tang, Y. *Acc. Chem. Res.* **2014**, *47*, 2260–2272.
78. a) Murphy, G. K.; West, F. G. *Org. Lett.* **2005**, *7*, 1801–1804. b) Murphy, G. K.; Marmsäter, F. P.; West, F. G. *Can. J. Chem.* **2006**, *84*, 1470–1486.
79. a) Mortimer, A. J. P.; Aliev, A. E.; Tocher, D. A.; Porter, M. J. *Org. Lett.* **2008**, *10*, 5477–5480. b) Mortimer, A. J. P.; Plet, J. R. H.; Obasanjo, O. A.; Kaltsoyannis, N.; Porter, M. J. *Org. Biomol. Chem.* **2012**, *10*, 8616–8627.

80. Ellis-Holder, K. K.; Peppers, B. P.; Kovalevsky, A. Y.; Diver, S. T. *Org. Lett.* **2006**, *8*, 2511–2514.
81. a) Muthusamy, S.; Selvaraj, K. *Tetrahedron Lett.* **2013**, *54*, 6886–6888. b) Muthusamy, S.; Selvaraj, K.; Suresh, E. *Asian J. Org. Chem.* **2016**, *5*, 162–172. c) Muthusamy, S.; Selvaraj, K.; Suresh, E. *Eur. J. Org. Chem.* **2016**, *2016*, 1849–1859.
82. Lu, P.; Herrmann, A. T.; Zakarian, A. *J. Org. Chem.* **2015**, *80*, 7581–7589.
83. Zhang, Y.-Z.; Zhu, S.-F.; Cai, Y.; Mao, H.-X.; Zhou, Q.-L. *Chem. Commun.* **2009**, 5362–5364.
84. Xu, B.; Zhu, S.-F.; Zhang, Z.-C.; Yu, Z.-X.; Ma, Y.; Zhou, Q.-L. *Chem. Sci.* **2014**, *5*, 1442–1448.
85. Hyde, S.; Veliks, J.; Liégault, B.; Grassi, D.; Taillefer, M.; Gouverneur, V. *Angew. Chem. Int. Ed.* **2016**, *55*, 3785–3789.
86. Keipour, H.; Jalba, A.; Delage-Laurin, L.; Ollevier, T. *J. Org. Chem.* **2017**, *82*, 3000–3010.
87. Aviv, I.; Gross, Z. *Chem. Eur. J.* **2008**, *14*, 3995–4005.
88. Tyagi, V.; Bonn, R. B.; Fasan, R. *Chem. Sci.* **2015**, *6*, 2488–2494.
89. a) Kametani, T.; Kawamura, K.; Tsubuki, M.; Honda, T. *J. Chem. Soc. Chem. Commun.* **1985**, 1324–1325. b) Kametani, T.; Kawamura, K.; Tsubuki, M.; Honda, T. *J. Chem. Soc. Perkin Trans. I* **1988**, 193–199.
90. a) Kametani, T.; Yukawa, H.; Honda, T. *J. Chem. Soc. Chem. Commun.* **1986**, 651–652. b) Kametani, T.; Yukawa, H.; Honda, T. *J. Chem. Soc. Perkin Trans. I* **1988**, 833–837.
91. a) Kametani, T.; Yukawa, H.; Honda, T. *J. Chem. Soc. Chem. Commun.* **1988**, 685–687. b) Kametani, T.; Yukawa, H.; Honda, T. *J. Chem. Soc. Perkin Trans. I* **1990**, 571–577.
92. Kim, G.; Kang, S.; Kim, S. N. *Tetrahedron Lett.* **1993**, *34*, 7627–7628.
93. Sato, T.; Hayakawa, Y.; Noyori, R. *Bull. Chem. Soc. Jpn.* **1984**, *57*, 2515–2525.

2 Chapter 2 Medium-Sized Cyclic Ethers via Stevens [1,2]-Shift of Mixed Monothioacetal Derived Sulfonium Ylides: Application to Formal Synthesis of (+)-Laurencin

2.1 Introduction

Medium-sized cyclic ether moieties occur frequently in marine natural products.^{1,2} Examples include seven- to nine-membered cyclic ethers (**1–3**) and ladder-frame polyethers such as brevetoxin A (**4**), as illustrated in Figure 2.1, some of which exhibit important biological activities.² Unlike five- or six-membered rings, medium-sized cyclic ethers are generally difficult to construct by standard cyclization methods.^{3a,b} The synthetic challenge is attributed to the inherent difficulties of the formation of medium-sized rings from acyclic precursors due to enthalpic and entropic factors, with the eight-membered rings at the nadir on the plot of reaction rate versus ring size in the example of lactone formation.^{3a,c} Because of the inherent challenges, tremendous synthetic efforts have been devoted to the development of new methodologies where examples of these elegant approaches can be summarized into three categories: C–C bond formation, C–O bond formation, and rearrangement of an existing cyclic precursor.⁴

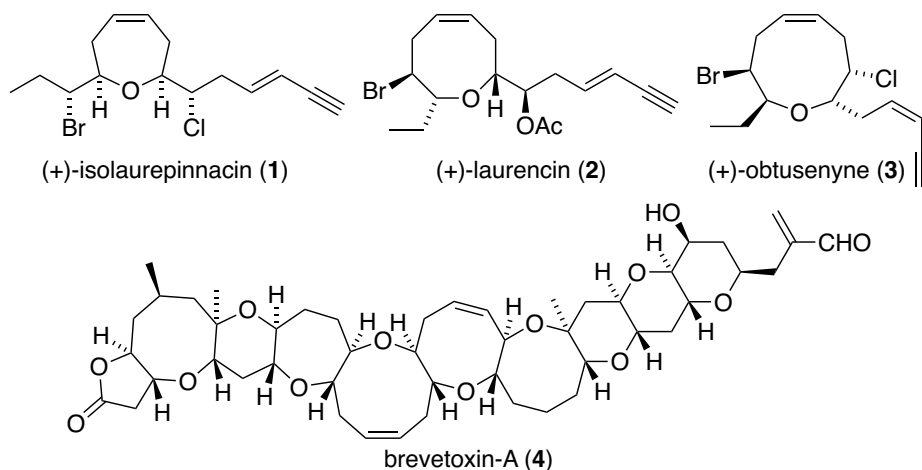


Figure 2.1 Representative examples of marine natural products containing medium-sized ether core

Red algae of the genus *Laurencia* produce medium-sized cyclic ethers as secondary metabolites, which typically possess a C_{15} skeleton (also known as C_{15} acetogenins or C_{15} nonterpenoids) with one or more halogen atoms and a terminal conjugated enyne moiety.^{1,2} Among all of the C_{15} acetogenins isolated from the *Laurencia* genus, the group containing eight-membered cyclic ethers is by far the largest, comprising of over ninety derivatives.^{1,2} The first medium-sized ring ether isolated from *Laurencia* is (+)-laurencin, which was isolated by Irie and coworkers^{5a} from *Laurencia glandulifera* in 1965, but its isolation and structural elucidation were not reported in detail until 1968.^{5b} The stereochemical configuration was later confirmed by X-ray crystallography.⁶ Since then, numerous C_{15} acetogenins have been isolated and characterized, some examples being shown in Figure 2.2.^{1,2} In 1967, biological investigations showed that (+)-laurencin (2) prolonged the sleep-time in pentobarbitone-anaesthetized mice by inhibiting the metabolism of pentobarbitone.⁷ Similar halogenated derivatives, such as 7, exhibited significant antistaphylococcal activity.^{2a}

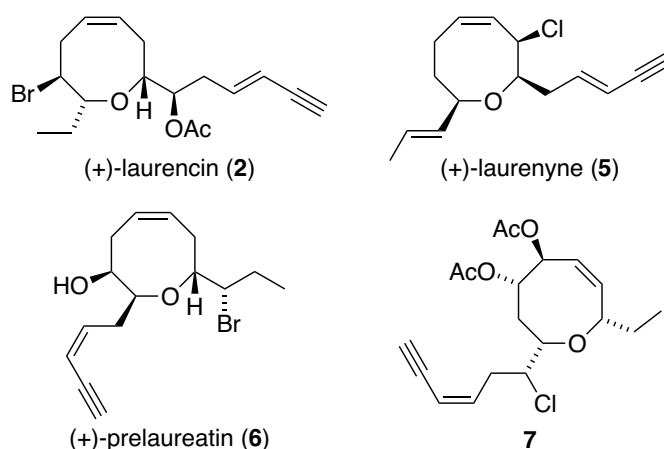


Figure 2.2 Examples of eight-membered C15 acetogenins

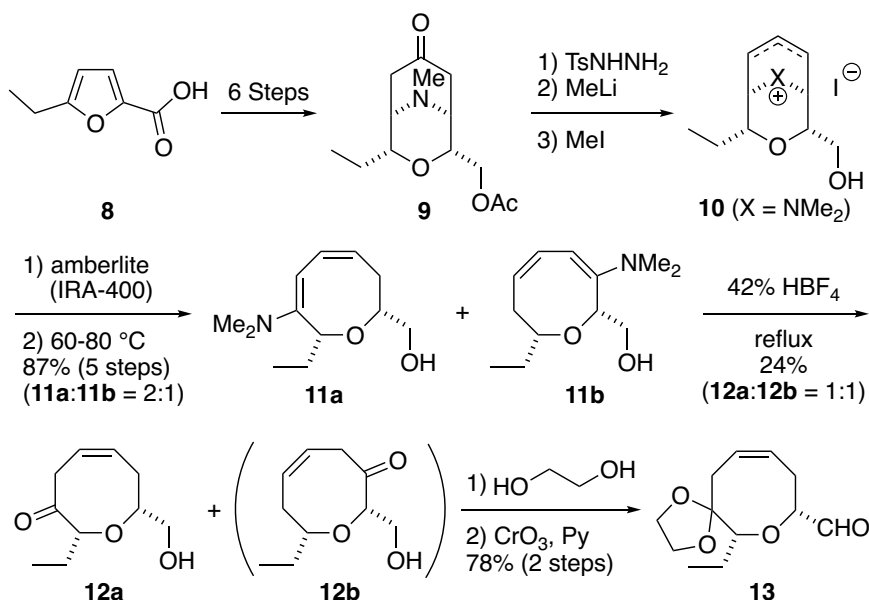
(+)-Laurencin (**2**) has attracted considerable attention in the synthetic community since its isolation in 1965. This molecule contains an oxocene core with a remote double bond, four stereogenic centers and an enyne subunit. Construction of the oxocene core in a stereoselective fashion is one of main formidable challenges that attracted the attention of the synthetic community. Laurencin has thus served as a testing ground for various methodologies towards the synthesis of medium-sized cyclic ethers. To date, 7 total syntheses and 6 formal syntheses of this molecule have been reported, using various strategic approaches.^{9,13,19,24-26,33,35,36,40,45,46,52} These syntheses are reviewed in this chapter with emphasis on the key transformations to construct the eight-membered cyclic ethers. We have also achieved a formal synthesis of (+)-laurencin via Stevens [1,2]-shift of mixed monothioacetal derived sulfonium ylides and the investigational details are also described later in this chapter.

2.2 Previous total syntheses

2.2.1 Masamune's racemic total synthesis of (\pm)-laurencin

The first total synthesis of (\pm)-laurencin (Scheme 2.1 and 2.2) was accomplished by the Masamune group in 1977,^{9a} and the experimental details were published in

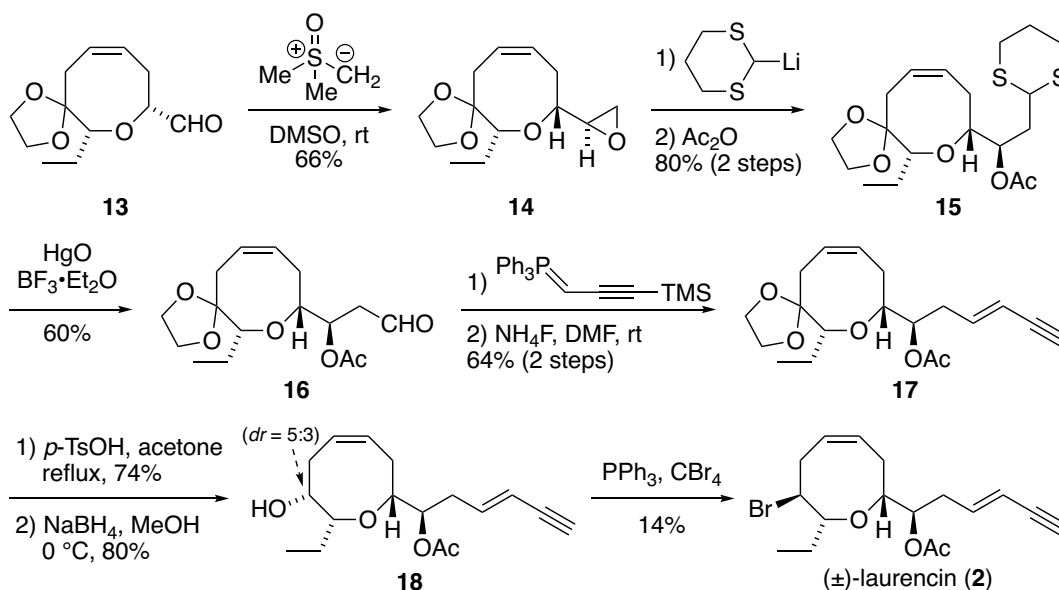
subsequent reports.^{9c,9d} Synthesis of intermediate **13** was described in an early report in 1975.^{9b} Bicyclic ketone **9** was derived from 5-ethyl-2-furoic acid **8** in 6 steps. **9** was converted to an isomeric mixture of olefins **10** by a Shapiro reaction¹⁰ followed by methylation with methyl iodide. Hofmann elimination of **10** followed by a facile [1,5]-hydride shift under the action of heat afforded a mixture of dienamines **11a** and **11b**.¹¹ Hydrolysis of **11a** and **11b** in refluxing 42% fluoroboric acid solution in water yielded a separable mixture of cyclic unconjugated enones **12a** and **12b**. Enone **12a** was converted to aldehyde **13** *via* acetalization of the ketone and oxidation of the primary alcohol.



Scheme 2.1 Masamune's synthesis of oxocene **13**, part one

In 1977, the Masamune group completed the total synthesis of (\pm)-laurencin from intermediate **13**.^{9a} Intermediate **13** first converted to epoxide **14** by a Corey-Chaykovsky¹² epoxidation reaction. Regioselective epoxide-opening with lithiated dithiane followed by acetylation of the resulting alcohol yielded oxocene **15**. Removal of the dithiane group by mercury oxide (HgO) in the presence of boron trifluoride diethyl etherate (BF₃·Et₂O) afforded aldehyde **16**, which was subjected to Wittig

olefination and desilylation to give selectively the *E*-olefin (**17**). Deprotection of the acetal under acidic conditions and reduction of the resulting ketone with sodium borohydride (NaBH₄) provided a 5:3 mixture of epimeric alcohols with the desired alcohol **18** as the major epimer. Finally, bromination of alcohol **18** in the presence of triphenylphosphine (PPh₃) and carbon tetrabromide (CBr₄) furnished (±)-laurencin in 14% yield.



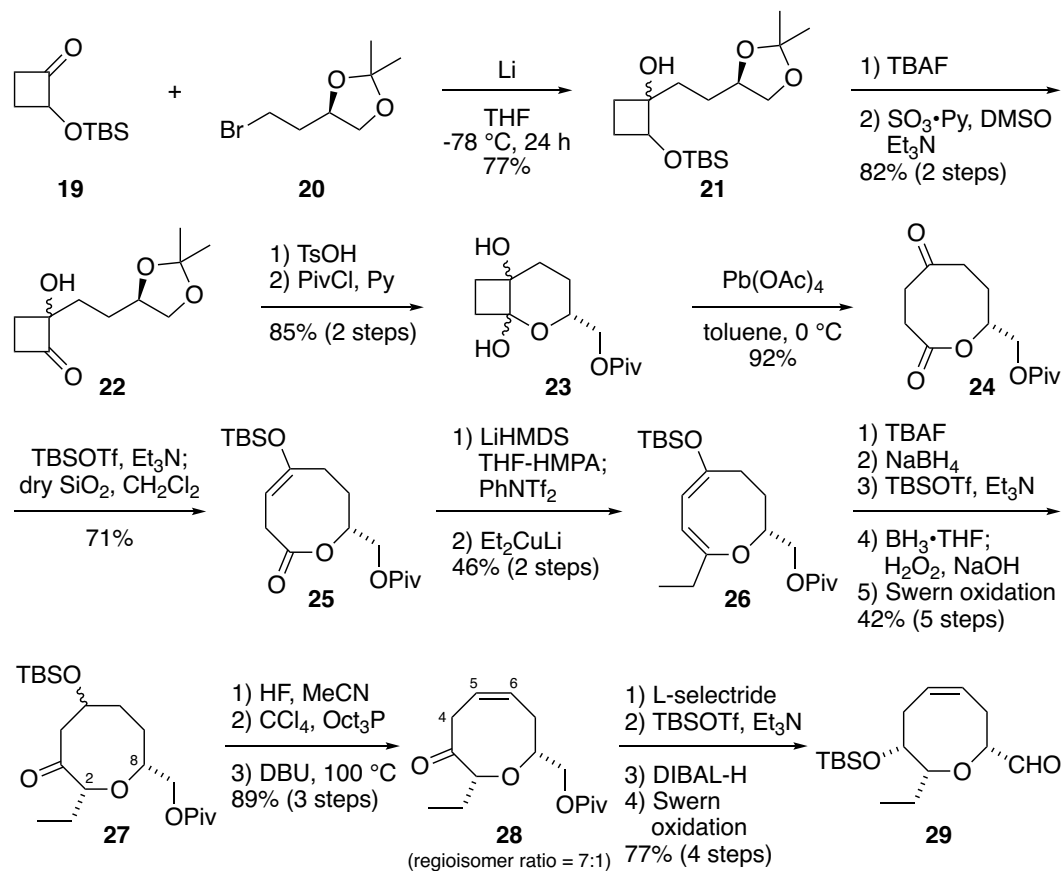
Scheme 2.2 Masamune's total synthesis of (±)-laurencin, part two

2.2.2 Murai's racemic total synthesis of (+)-laurencin

In 1992, fifteen years after Masamune's racemic total synthesis of laurencin, the Murai group accomplished the first asymmetric total synthesis of (+)-laurencin.¹³ The authors utilized a novel ring expansion reaction to access an eight-membered lactone, that was transformed into the desired oxocane ring *via* cyclic enol triflate formation followed by alkylation with an organocuprate reagent¹⁴ as shown below.

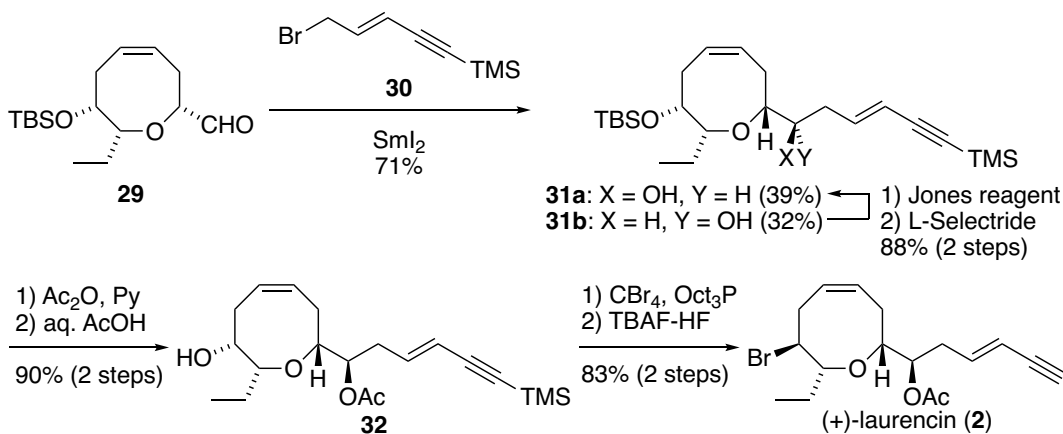
Construction of the oxocane core commenced with the reaction of chiral alkyl bromide **20**¹⁵ and silyloxycyclobutanone **19**¹⁶ in the presence of lithium (Scheme 2.3). The resulting diastereomeric mixture of alcohols (**21**) was treated with tetrabutyl

ammonium fluoride (TBAF) followed by oxidation to give cyclobutanone **22**. Deprotection of the acetal group under acidic conditions yielded a bicyclic triol, of which the primary alcohol was selectively protected as the pivalate ester to furnish bicyclic diol **23** in 85% yield. Upon treatment with lead tetraacetate [Pb(OAc)₄], oxidation of diol **23** provided ring expansion product **24**. The ketone group was then converted to silyl enol ether **25**. Deprotonation at the lactone α -position of **25** with lithium bis(trimethylsilyl)amide (LiHMDS) followed by a reaction with *N*-phenyl-bis(trifluoromethanesulfonylimide) (PhNTf₂) afforded the corresponding enol triflate, which was alkylated by lithium diethylcuprate (Et₂CuLi) to provide dienol ether **26**.



Scheme 2.3 Murai's synthesis of intermediate **29**

The silyl enol ether was converted to β -silyloxy ketone **27** via a five-step sequence involving desilylation with TBAF, NaBH₄ reduction, *tert*-butyldimethylsilyl (TBS) protection, hydroboration/oxidation and Swern oxidation.¹⁷ During the last Swern oxidation step, the treatment of triethylamine resulted in the epimerization at the α -position of the ketone and provided **27** exclusively in the 2,8-*cis*-configuration. The remote double bond for the oxocene was then installed via a three-step sequence, with the last step involving a base-mediated elimination that provided a mixture of the desired C5-C6 olefin **28** and the C4-C5 regioisomer in a ratio of 7:1. It is interesting to note that in the elimination step, the conjugated enone product (C4-C5 olefin) was formed only as a minor product, which could be isomerized to unconjugated enone **28** with DBU at high temperatures. The C4-C5 olefin can be isolated and isomerized to **28** upon treatment with 1,8-diazabicyclo(5.4.0)undec-7-ene (DBU). Ketone **28** was then converted to aldehyde **29** in four-steps and set the stage for the installation of the enyne side chain.



Scheme 2.4 Murai's synthesis of (+)-laurencin

The enyne side chain was installed via a SmI₂-mediated coupling reaction¹⁸ with **30** to provide a mixture of epimeric alcohols **31a** and **31b** (Scheme 2.4). Alcohol **31b**, with the undesired stereochemistry, was oxidized followed by reduction with L-Selectride to afford exclusively the desired stereochemical configuration (**31a**). Acetylation and

deprotection of the TBS group provided alcohol **32**. The final conversion in the synthesis of (+)-laurencin was achieved through bromination with $\text{CBr}_4/\text{Oct}_3\text{P}$ and desilylation with TBAF.

2.2.3 Overman's total synthesis of (+)-laurencin

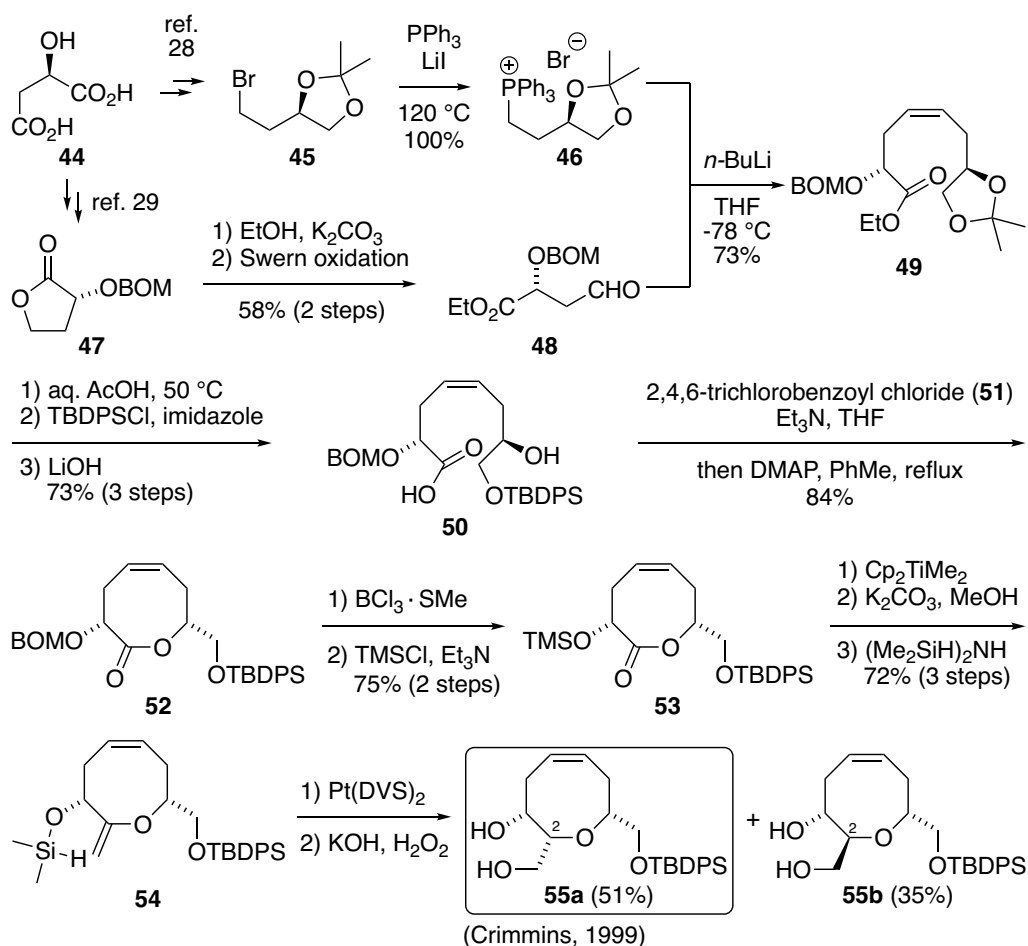
Shortly after the synthesis reported by Murai, Overman published another asymmetric total synthesis of (+)-laurencin in 1995.¹⁹ The commonly employed strategy to construct eight-membered cyclic ethers was through ring expansion reactions, which have been used in the previous two syntheses. However, the focus of Overman's synthesis was on the challenging direct construction of the oxocene core from an acyclic precursor *via* a Prins-type acetal-vinylsulfide cyclization pathway (Scheme 2.5).²⁰

The enantioenriched precursor (**39**) necessary for the key acetal-vinylsulfide cyclization step was synthesized from SEM protected allyl ether **33**. The first step involved an asymmetric allylation reaction using a modified version of Brown's method,²¹ in which the sequential reaction of allyl ether **33** with *sec*-BuLi, (-)-*B*-methoxydiisopinocampheylborane (**34**), and propionaldehyde generated a homoallylic alcohol in 95% *ee*, which was subsequently protected as *tert*-butyldimethylsilyl (TBDMS) ether (**35**). Hydroboration of **35** with 9-borabicyclo(3.3.1)nonane (9-BBN) followed by Suzuki coupling²² with 1-bromo-1-(phenylthio)ethene (**36**) afforded the desired adduct, which was then desilylated with tetra-butylammonium fluoride (TBAF) to yield alcohol **37**. Acetalization of **37** with α -bromo ether **38** and a subsequent change of protecting group from SEM to acetyl afforded the desired precursor (**39**) for the key step.

The Prins-cyclization of acetate **39** in the presence of three equivalents of boron trifluoride diethyl etherate ($\text{BF}_3 \cdot \text{Et}_2\text{O}$) at low temperatures effectively furnished oxocene **41** with the desired 2,8-*cis* configuration. This cyclization is believed to occur *via* oxocarbenium intermediate **40**. Raney-nickel desulfurization followed by replacement of protecting groups from acetyl to TBDMS and deprotection of the

2.2.4 Holmes' total synthesis of (+)-laurencin

In 1997, Holmes and coworkers published a seminal report on the total synthesis of (+)-laurencin.²⁶ The authors utilized a Yamaguchi lactonization²⁷ as the key step to construct the oxocane core. The remote double bond in the *cis*-configuration was constructed through Wittig olefination of the phosphonium ylide derived from phosphonium salt **46**, with aldehyde **48**, both of which could be synthesized from (*R*)-malic acid **44** (Scheme 2.6).^{28,29} The resulting *Z*-olefin **49** was subjected to a three-step protecting group manipulation, involving deprotection of the acetonide, selective protection of the primary alcohol as the TBDPS ether and hydrolysis of the ethyl ester to provide the required precursor for lactonization (**50**). The desired eight-membered lactone **52** was prepared in high yield under Yamaguchi lactonization conditions.²⁷ However, the minor nine-membered lactone product (10:1 ratio) was also formed *via* migration of the silyl group from the primary to the secondary hydroxyl group followed by lactonization. Replacement of the benzyloxymethyl acetal (BOM) group with a trimethyl silyl (TMS) group then permitted the separation of the eight- and nine-membered lactones.

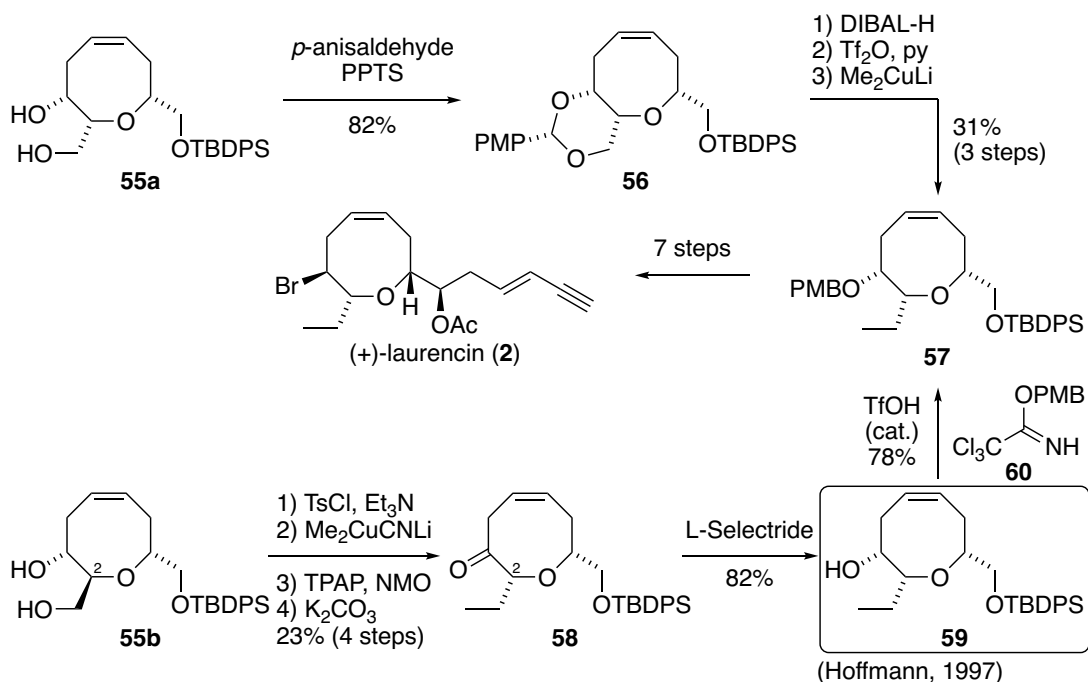


Scheme 2.6 Yamaguchi lactonization and synthesis of the oxocene core

The third stereogenic center was installed on **53** by a pathway involving lactone methylenation and intramolecular hydrosilation. Methylenation with the Petasis reagent³⁰ afforded an enol ether that was subsequently converted to silane **54**.³¹ The key intramolecular hydrosilation reaction³² of **54** was achieved using catalyst bis(1,3-divinyl-1,1,3,3-tetramethyldisiloxane)platinum (0) [Pt(DVS)₂] and the product was then oxidized with basic hydrogen peroxide to provide diols **55a** and **55b** in 51% and 35% yield respectively. **55a** was also synthesized later in a formal synthesis of (+)-laurancin by Crimmins and coworkers (Section 2.3.3).³³

Although diol **55a** was the desired intermediate containing the correct configuration at C2, both **55a** and **55b** were used to complete the total synthesis of (+)-laurancin

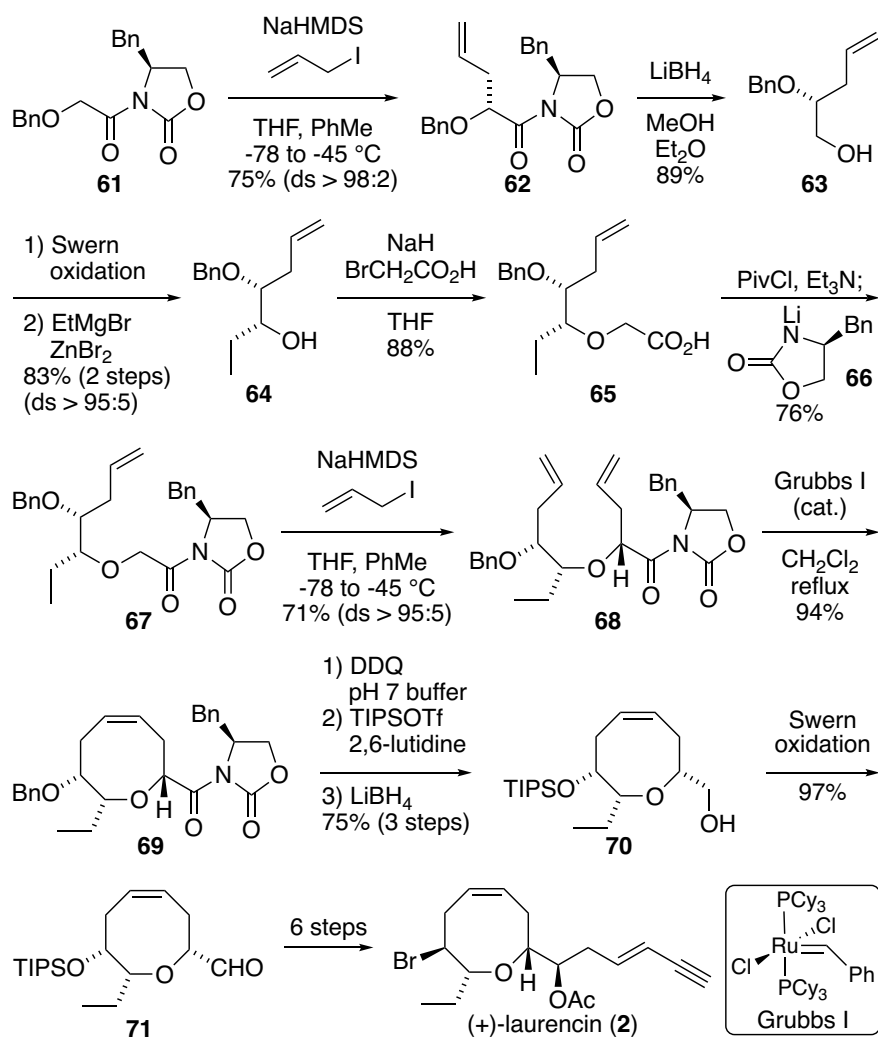
through oxocene **57** (Scheme 2.7). Diol **55a** was converted to *p*-methoxybenzylidene acetal **56**. Subsequent DIBAL-H reduction afforded a primary alcohol that was tosylated and methylated with Me₂CuLi to generate oxocene **57**. On the other hand, the configuration at C2 in **55b** could be epimerized to the correct configuration in four steps. Selective tosylation of the primary hydroxyl group followed by methylation furnished the ethyl substituent. The secondary hydroxyl group was then oxidized with tetrapropylammonium perruthenate (TPAP) and *N*-methylmorpholine *N*-oxide (NMO),³⁴ and the resulting ketone was epimerized at the α -position under basic conditions to provide ketone **58** with the correct configuration at C2. Ketone **58** was reduced with L-Selectride to give alcohol **59**, was then protected as a *p*-methoxybenzyl ether (**57**), identical to the one synthesized from **55a**. The synthesis of alcohol **59** was later accomplished by Hoffmann and coworkers using a different approach (Section 2.3.2).³⁵ The advanced intermediate oxocene **57** was converted to (+)-laurencin in seven steps.



Scheme 2.7 Holmes' synthesis of (+)-laurencin

2.2.5 Crimmins' total synthesis of (+)-laurencin

In 1999, Crimmins and Emmitte³⁶ reported an asymmetric total synthesis of (+)-laurencin, utilizing an asymmetric aldol reaction and ring closing metathesis^{33,37} as the key transformations to strategically access the oxocene ring. The synthesis began with alkylation of the sodium enolate of oxazolidinone **61** with allyl iodide to provide acyl oxazolidinone **62** (Scheme 2.8). The chiral auxiliary was then removed with lithium borohydride (LiBH₄) to yield alcohol **63**. Swern oxidation¹⁷ followed by chelation-controlled addition of ethylmagnesium bromide³⁸ afforded alcohol **64**. Two critical stereocenters that will eventually occupy adjacent positions on the oxocene ring are set at this point. The sodium alkoxide of **64** was alkylated with bromoacetic acid to yield acid **65**. Treatment of **65** with pivaloyl chloride allowed *in situ* generation of the mixed pivalic anhydride, which was then reacted with lithiated oxazolidinone **66** to provide acyl oxazolidinone **67**. Treatment of the sodium enolate of **67** with allyl iodide furnished the necessary diene (**68**) for oxocene formation *via* ring-closing metathesis.



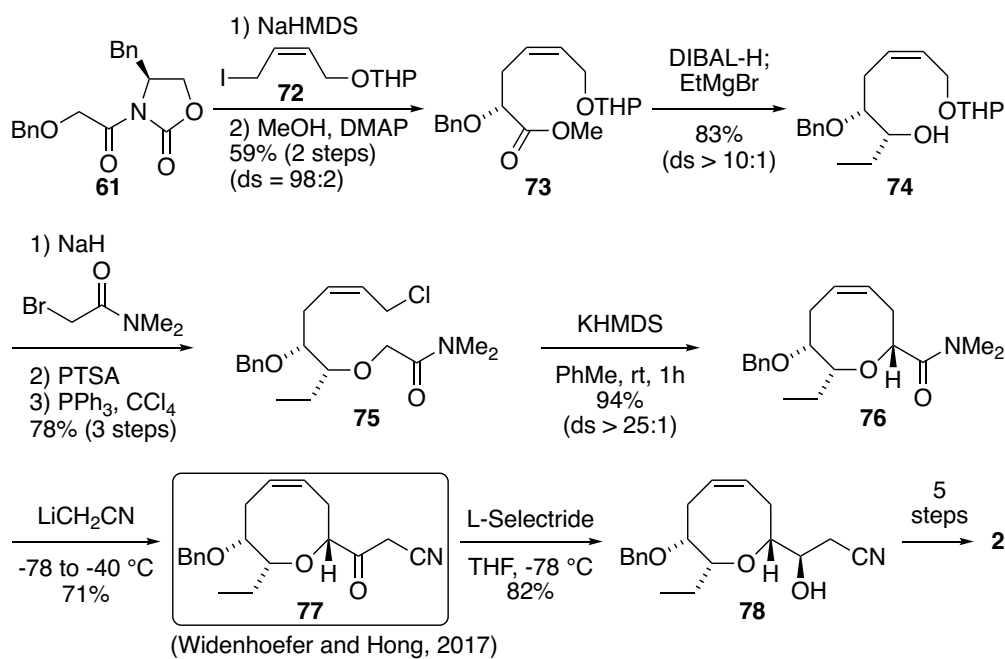
Scheme 2.8 Crimmins' asymmetric alkylation–ring closing metathesis approach

Upon exposure of diene **68** to ring closing metathesis conditions with Grubbs first generation precatalyst,³⁹ the desired oxocene **69** was formed in high yield. Although it is general difficult to form medium-sized rings from acyclic precursors as discussed at the beginning of this chapter, the construction of the oxocene *via* ring-closing metathesis is efficient. Subsequent replacement of the benzyl group (Bn) with a triisopropylsilyl (TIPS) group was necessary to avoid the partial isomerization of the *trans* olefin when the benzyl ether was removed after the incorporation of the enyne side chain. Reductive removal of the chiral auxiliary with lithium borohydride (LiBH₄)

afforded alcohol **70**, that was further oxidized under Swern oxidation conditions¹⁷ to furnish aldehyde **71**, which was then converted to (+)-laurencin in six steps.

2.2.6 Kim's total synthesis of (+)-laurencin

In 2005, Kim's group⁴⁰ achieved a total synthesis of (+)-laurencin utilizing an olefin symmetry-dependent internal alkylation reaction⁴¹ to construct the oxocene ring. The first stereocenter was installed in a similar way to the protocol reported by Crimmins' team,^{33,36} starting with the same oxazolidinone **61** (Scheme 2.9). The sodium enolate of **61** was alkylated with known allylic iodide **72**⁴² to yield the corresponding allylation product. The chiral auxiliary was subsequently removed by methanolysis in the presence of 4-dimethylaminopyridine (DMAP).⁴³ The resulting α -alkoxy methyl ester **73** was subjected to a one-pot diisobutylaluminum hydride (DIBAL-H) reduction and chelation-controlled nucleophilic addition⁴⁴ of ethylmagnesium chloride to generate *syn*-diol **74**. The key precursor (**75**) for the internal alkylation reaction was then synthesized in a three-step sequence: *O*-alkylation with *N,N*-dimethyl bromoacetamide, removal of tetrahydropyran (THP) ether under acidic conditions, and chlorination in the presence of triphenyl phosphine (PPh₃) and carbon tetrachloride (CCl₄).



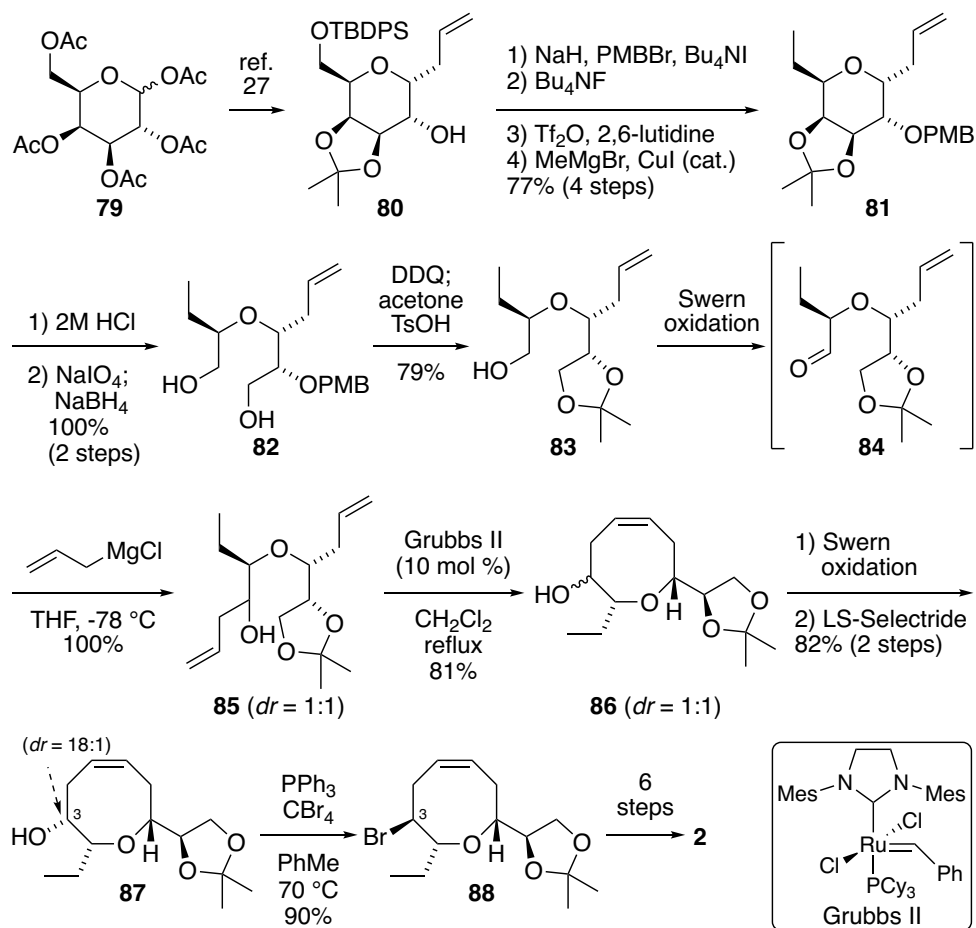
Scheme 2.9 Kim's total synthesis of (+)-laurencin

Upon treatment of **75** with potassium bis(trimethylsilyl)amide (KHMDS) at room temperature, the desired intramolecular alkylation reaction afforded oxocene **76** with excellent diastereoselectivity, furnishing the third stereocenter. Subsequent addition of the lithium anion of acetonitrile to α -alkoxy amide **76** afforded ketone **77**, which was subjected to stereo- and chemoselective reduction with L-Selectride to furnish alcohol **78**, completing the installation of the fourth stereocenter. The formation of ketone **77** *via* addition of the acetonitrile anion to the α -alkoxy amide was an unprecedented pathway. The total synthesis was then completed in five additional steps from alcohol **78**. On the other hand, ketone **77** has been recently synthesized by Widenhoefer and Hong⁴⁵ in a formal synthesis of (+)-laurencin (Section 2.3.6).

2.2.7 Fujiwara's total synthesis of (+)-laurencin

Fujiwara and coworkers accomplished the total synthesis of (+)-laurencin from a sugar derivative in 2005.⁴⁶ The key strategy to form the eight-membered cyclic ether

was by a *C*-glycoside ring-cleavage/ring-closing olefin metathesis process. First, β -D-galactose pentaacetate (**79**) was converted to **80** following the known procedure published from the same group.⁴⁷ Protection of the alcohol as the *p*-methoxybenzyl (PMB) ether and removal of the *tert*-butyldiphenylsilyl (TBDPS) ether afforded a primary alcohol, which was then triflated and methylated⁴⁸ to furnish the ethyl side-chain (**81**). After hydrolysis of the acetonide under acidic conditions, the resulting diol was subjected to oxidative cleavage with sodium periodate (NaIO₄), followed by a one-pot reduction with NaBH₄ to provide diol **82**. Subsequent deprotection of the PMB group with DDQ followed by acetonide formation afforded primary alcohol **83**. Swern oxidation¹⁷ and a one-pot allylation of the resulting aldehyde **84** with allyl magnesium chloride generated a 1:1 diastereomeric mixture of alcohols **85**. Surprisingly, the addition of a Grignard reagent to an α -alkoxy aldehyde in this case is completely unselective with no chelation control. Ring closing metathesis of **85** with Grubbs second generation precatalyst⁴⁹ effectively generated the desired oxocenes **86** as a 1:1 mixture of diastereomers. Sequential Swern oxidation¹⁷ and lithium trisiamylborohydride (LS-Selectride) reduction afforded **87** as the predominant diastereomer (*dr* = 18:1) with the correct configuration at C3. After bromination with PPh₃/CBr₄, stereochemical inversion at C4 afforded bromide **88**, which was then transformed to (+)-laurencin (**2**) in 6 steps.



Scheme 2.10 . Fujiwara's total synthesis of (+)-laurencin

2.3 Previous formal syntheses

To date, six formal syntheses of (+)-laurencin have been achieved by interception of various advanced intermediates from the reported total syntheses (Section 2.2), highlighting the different methodologies for the stereoselective construction of eight-membered cyclic ethers. These approaches are reviewed in this section.

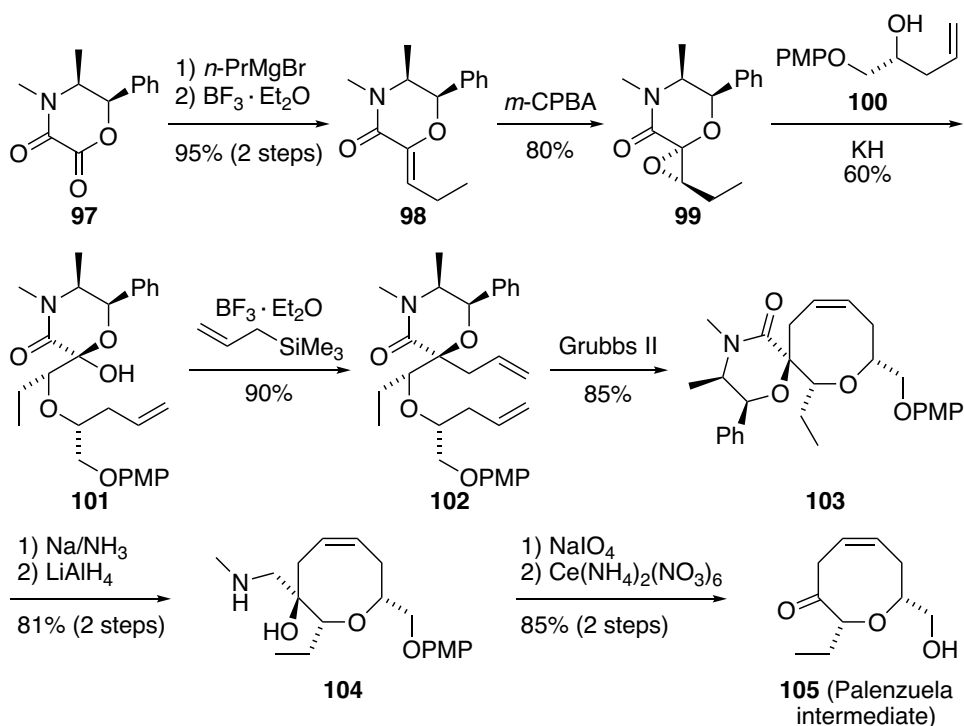
2.3.1 Palenzuela's formal synthesis on Overman's intermediate

In 1996, Palenzuela and coworkers²⁴ accomplished the first asymmetric formal synthesis of (+)-laurencin by intercepting intermediate **43** from the Overman synthesis

(Scheme 2.11).¹⁹ The stereochemistry of the carbon atom adjacent to the ether oxygen atom was controlled by means of a hetero Diels–Alder reaction. The oxocane core was formed *via* epoxide opening by a sulfone anion as shown below.

The key hetero Diels–Alder reaction between monoactivated diene **89** and aldehyde **90**⁵⁰ occurred efficiently in the presence of $\text{BF}_3 \cdot \text{Et}_2\text{O}$ and afforded product **91** with good diastereoselectivity.⁵¹ The desired α, α' -*cis* adduct was generated as the major diastereomer. Due to the liability of the silyl enol ether moiety, the mixture of diastereomers (**91**) was directly subjected to ozonolysis, reduction and esterification conditions, and was then separated by high-performance liquid chromatography (HPLC) to give **92**. Protection of the hydroxyl group and reduction of the ester yielded a primary alcohol, which was then tosylated and treated with lithium aluminum hydride (LiAlH_4) to afford intermediate **93**. The acetonide moiety in **93** was then converted to an epoxide (**94**) in three steps. In the presence of lithium diisopropyl amine (LDA), an intramolecular epoxide opening of **94** with the *in situ* generated sulfone anion afforded oxocane **95** in 60% yield. Swern oxidation,¹⁷ followed by elimination with DBU under heating conditions furnished oxocene **58** as the only product. The conjugated enone was presumed to form initially, but was isomerized to unconjugated enone **58** in the presence of DBU at elevated temperatures. Similar result was also obtained previously in Murai's synthesis.¹³ The corresponding side chain of **96** was installed *via* sequential desilylation, Swern oxidation and Horner–Wadsworth–Emmons olefination. Stereoselective reduction with L-Selectride followed by protection and DIBAL reduction afforded Overman's intermediate **43** (Section 2.2.3).¹⁹

which was subsequently opened by the potassium salt of chiral alcohol **100**,⁵⁴ furnishing highly-substituted hemiacetal **101**. A Lewis acid promoted allylation reaction occurred with complete stereocontrol, in which the allyl group was delivered from the less hindered face of the oxocarbenium intermediate and yielded diene **102**. Ring closing metathesis using Grubbs second generation precatalyst⁴⁹ generated the desired oxocene **103**. The ephedrine portion in morpholinone was readily removed with dissolving metal reduction (Na/NH_3),^{53a,b} and the resulting amide was reduced with lithium aluminum hydride (LiAlH_4) to afford amino alcohol **104**. Palenzuela's intermediate **105** (Section 2.3.1)²⁶ was then achieved by treatment with sodium periodate (NaIO_4) followed by removal of the *p*-methoxyphenyl (PMP) group.

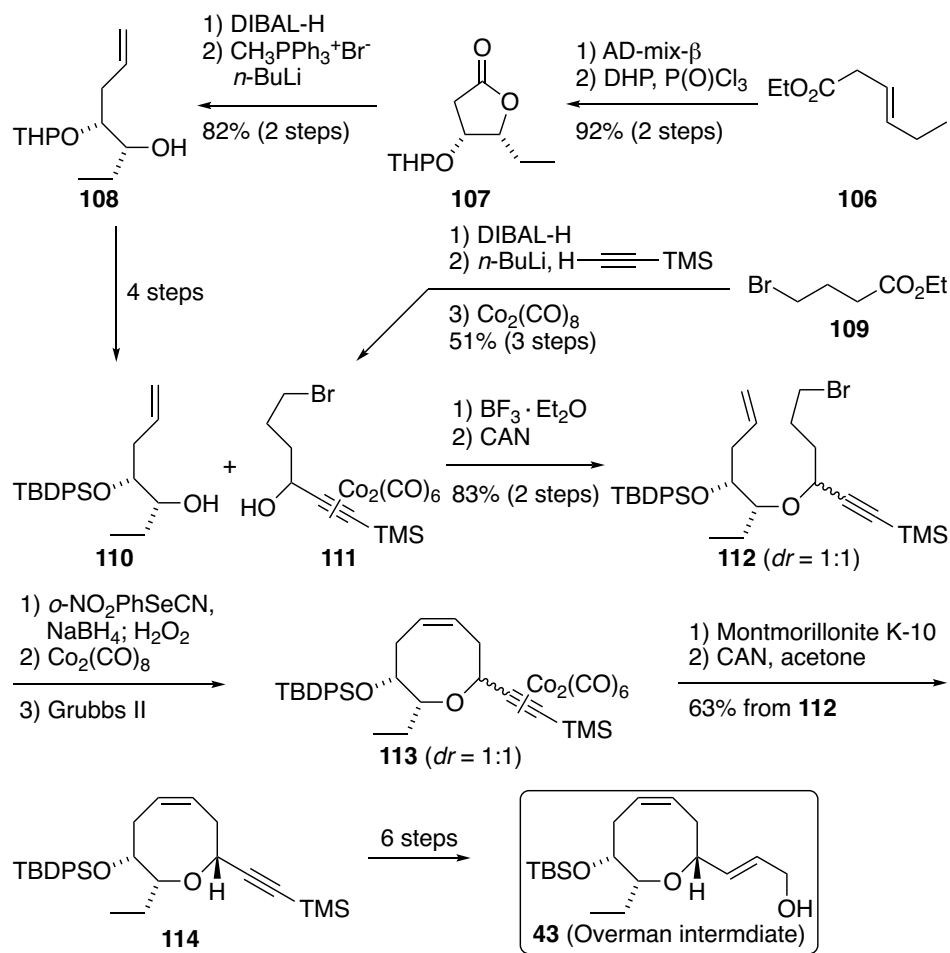


Scheme 2.12 Pansare's formal synthesis on Palenzuela's intermediate

2.3.3 Martín's formal synthesis on Overman's intermediate

The second synthesis of Overman's intermediate **43** (Section 2.2.3)¹⁹ was achieved by Martín and coworkers in 2008,²⁵ using an intermolecular Nicholas reaction⁵⁵ to access an unsaturated linear ether that was converted to the oxocene by ring closing metathesis (Scheme 2.13).⁵⁶ The enantioenriched alcohol **110** was synthesized from ethyl (*E*)-3-hexenoate (**106**). Sharpless asymmetric dihydroxylation⁵⁷ of **106** with spontaneous formation of the butyrolactone followed by tetrahydropyran (THP) protection afforded lactone **107**. Reduction of **107** with DIBAL-H yielded a lactol that was directly submitted to Wittig olefination conditions to provide **108**. A subsequent change of protecting groups furnished **100** in four steps. The Co₂(CO)₆-complexed propargylic alcohol **111** was made from ethyl 4-bromobutyrate (**109**) in three standard transformations.

When **110** and **111** were treated with boron trifluoride diethyl etherate (BF₃·Et₂O), the desired Nicholas reaction afforded a 1:1 mixture of diastereomeric ethers **112** after cleavage of the cobalt complex with ceric ammonium nitrate (CAN). The alkyl bromide moiety was then converted to a terminal olefin by a variant of the Grieco elimination reaction.⁵⁸ In this step, treatment of the *o*-nitrophenylselenocyanate with NaBH₄ generated a selenide anion, which reacted with the alkyl bromide to provide the corresponding selenide. Subsequent oxidation of the selenide to selenoxide with hydrogen peroxide (H₂O₂) followed by facile elimination afforded the terminal olefin. The diene was subjected to ring closing metathesis with Grubbs second generation precatalyst⁴⁹ to furnish the oxocene (**113**). The mixture of diastereomers were treated with montmorillonite K-10, followed by removal of the cobalt complex to provide the *cis* isomer **114** in quantitative yield, and thus completed the installation of the third stereogenic center. Intermediate **114** was then transformed into Overman's intermediate **43**¹⁹ in six steps.



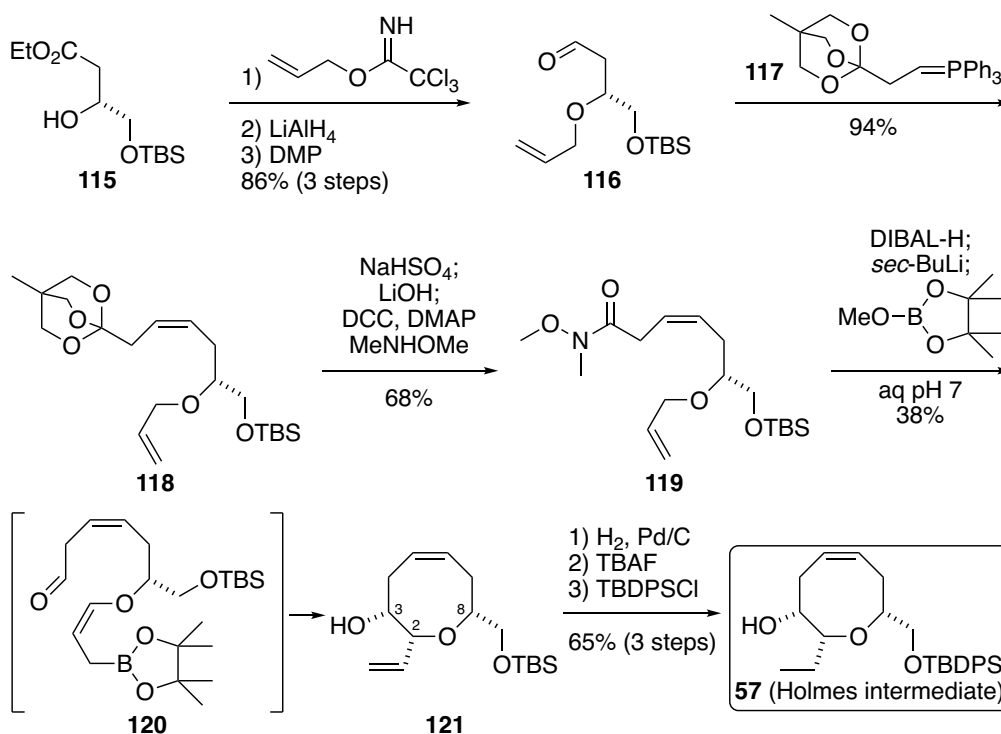
Scheme 2.13 Martín's formal synthesis of Overman's intermediate **43**

2.3.4 Hoffmann's formal synthesis of Holmes' intermediate

In 1997, after Holmes' total synthesis of (+)-laurencin,²⁶ Hoffmann and Krüger³⁵ published a formal synthesis of (+)-laurencin by intercepting Holmes' intermediate **59**. An intramolecular allylboration of an aldehyde⁵⁹ was employed as the key step for the construction of the oxocene ring (Scheme 2.14).

The synthesis began with enantioenriched alcohol **115**,⁶⁰ which was protected as the allyl ether, followed by reduction with lithium aluminum hydride (LiAlH_4) and oxidation with Dess-Martin periodinane (DMP)⁶¹ to provide aldehyde **116**. Subsequent Wittig olefination of **116** with reagent **117**⁶² afforded the desired olefin **118** with a *Z/E*

ratio of 96:4.⁶³ The bicyclic orthoester moiety was transformed into Weinreb amide **119** in a one-pot process, involving sequential deprotection of the orthoester, base hydrolysis, and coupling with *N,O*-dimethylhydroxylamine (MeNHOMe). Weinreb amide **119** was then subjected to sequential DIBAL-H reduction, *sec*-BuLi transmetalation, borylation with a pinacol borate ester, and liberation of the aldehyde and allylboronate with pH 7 buffer solution. In this process, the *in situ* generated intermediate **120** readily underwent intramolecular cyclization to form the desired oxocene ring **121** as a single diastereomer with the 2,3,8-*cis* configuration in moderate yield. Selective hydrogenation of the terminal olefin and replacement of protecting groups furnished Holmes' intermediate **57** (Section 2.2.4).²⁶

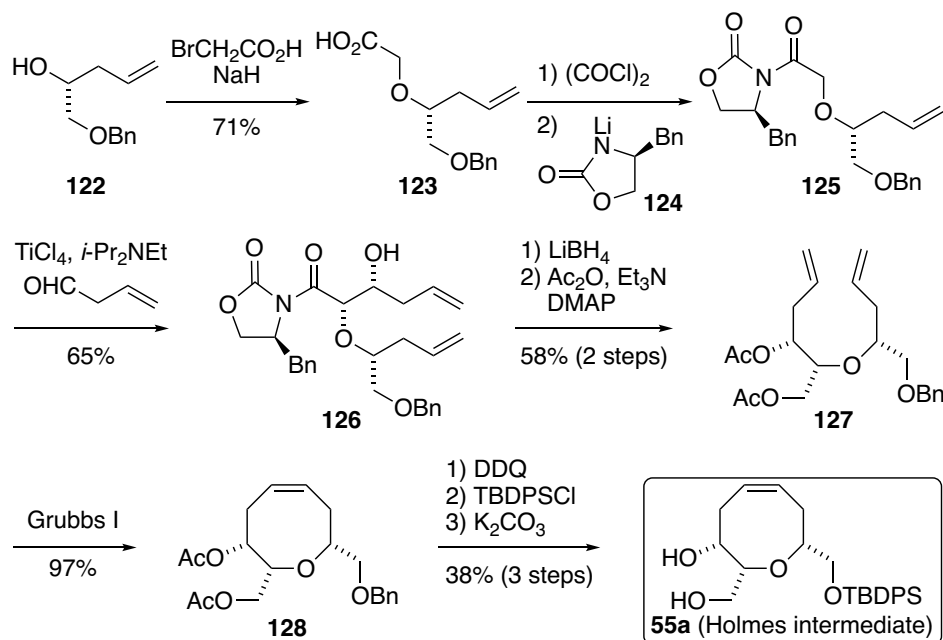


Scheme 2.14 Hoffmann's approach to Holmes' intermediate 57

2.3.5 Crimmins' formal synthesis of Holmes' intermediate

In 1999, the Crimmins group³³ reported another formal synthesis of (+)-laurencin *via* the interception of Holmes' intermediate **55a** (Section 2.2.4).²⁶ An asymmetric aldol addition and a ring closing metathesis reaction were employed for the construction of the oxocene core. This strategy was later applied in the total synthesis of (+)-laurencin reported by the same group (Section 2.2.5).³⁶

Alkoxyacetic acid **123** was prepared by reacting chiral alcohol **122** with bromoacetic acid in the presence of sodium hydride (Scheme 2.15). Acid **123** was then treated with oxalyl chloride, and the resulting acid chloride was reacted with lithiated chiral oxazolidinone **124** to form acyl oxazolidinone **125**. Subsequently, titanium tetrachloride (TiCl₄) mediated enolization with Hunig's base⁶⁴ followed by an aldol reaction with 3-butenal provided diene **126**. Removal of the chiral auxiliary with lithium borohydride (LiBH₄), followed by acetylation of the resulting diol provided diene **127**. Ring closing metathesis using Grubbs first generation precatalyst³⁹ afforded the desired oxocene **128**. After replacement of protecting groups and removal of the acetate in three steps, Holmes intermediate **55a**²⁶ was synthesized, thereby completing the formal synthesis of (+)-laurencin.



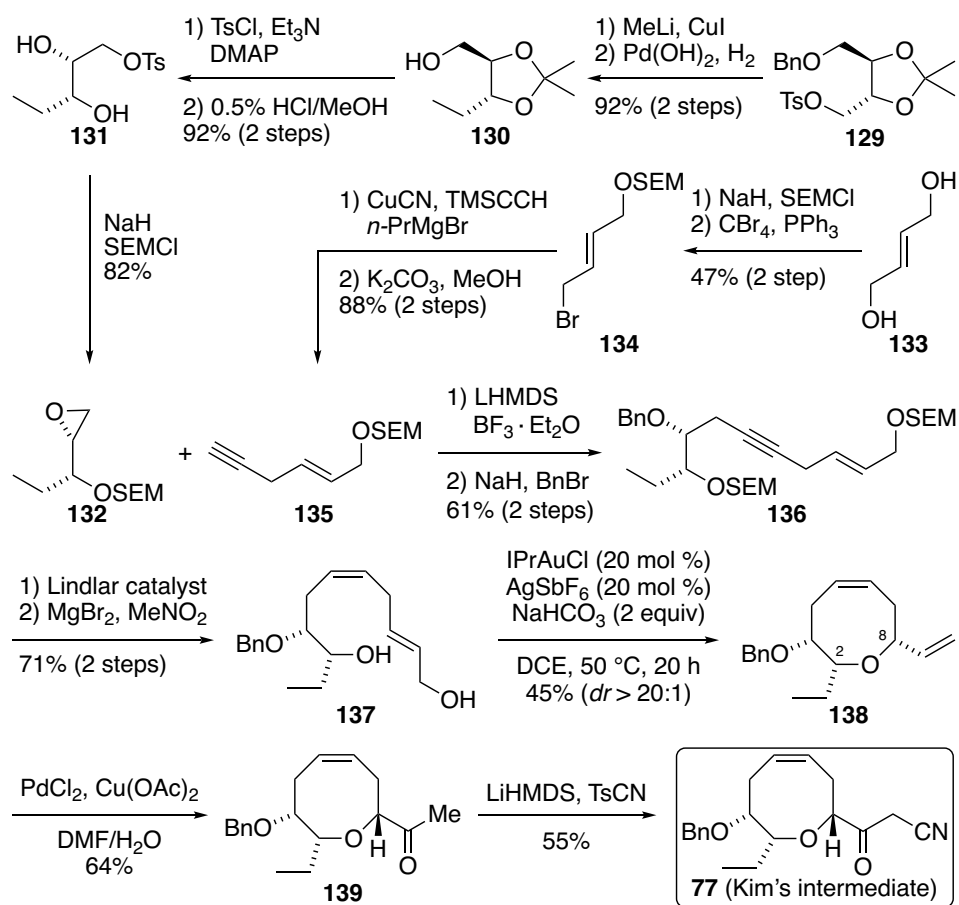
Scheme 2.15 Crimmin's formal synthesis of (+)-laurencin

2.3.6 Widenhoefer and Hong's formal synthesis of Kim's intermediate

The latest literature precedent on the formal synthesis of (+)-laurencin was reported by Widenhoefer and Hong.⁴⁵ The authors employed a gold(I) catalyzed intramolecular dehydrative alkoxylation reaction⁶⁵ as the key step to access an advanced intermediate from Kim's total synthesis (Section 2.2.7).⁴⁰ The synthesis commenced with the preparation of epoxide **132** and alkyne **135** (Scheme 2.16). Epoxide **132** was prepared from the D-threitol derived acetonide **129**.⁶⁶ Methylation of **129** followed by debenzoylation provided alcohol **130**. Conversion of alcohol **130** to the corresponding tosylate followed by acetonide deprotection under acidic conditions afforded diol **131**. Treatment of **131** with excess sodium hydride and 2-(trimethylsilyl)ethoxymethyl chloride (SEMCl) yielded epoxide **132** in one step.

The terminal alkyne **135** was synthesized from (*E*)-2-butene-1,4-diol **133**. Mono-SEM protection of **133** followed by bromination afforded bromide **134**, which was then coupled with ethynyltrimethylsilane (TMSCCH) and desilylated under basic conditions to provide terminal alkyne **135**.

Alkynylation of epoxide **132** was achieved by lithiation of **135** followed by transmetalation with boron trifluoride diethyl etherate and a reaction with **132**.⁶⁷ The resulting homopropargylic alcohol was benzylated to afford enyne **136**. Hydrogenation of the alkyne with Lindlars catalyst followed by SEM deprotection with magnesium bromide afforded ω -hydroxy allylic alcohol **137**. Under the optimized reaction conditions, the gold(I) catalyzed dehydrative alkoxylation reaction provided the desired 2,8-*cis*-oxocene **138** with high diastereoselectivity. Wacker oxidation of the terminal olefin in **138** provided methylketone **139**, which then underwent α -cyanation to form α -cyano ketone **77** with all spectral data in good agreement with those reported by Kim.⁴⁰



Scheme 2.16 Widenhofer and Hong's formal synthesis

2.4 Summary of the total and formal syntheses of (+)-laurencin

The six total syntheses and seven formal syntheses of (+)-laurencin have been summarized in Section 2.2 and Section 2.3, respectively. Stereocontrolled construction of the oxocene core was a challenging task, but a number of approaches were successfully employed. Among all of the syntheses, only the first two total syntheses by Masamune^{9a} and Murai¹³ employed ring expansion reactions of bicyclic precursors to furnish the oxocene core, whereas all other syntheses utilized acyclic precursors through various retrosynthetic bond disconnections (Scheme. 2.17). Among them, the total synthesis by Holmes and co-workers²⁶ stands as a seminal example, and two formal syntheses have been achieved^{33,35} *via* interception of advanced intermediates described by the Holmes team. Although a handful of methodologies were available to construct eight-membered cyclic ethers, there was still room to develop alternative complementary methods.

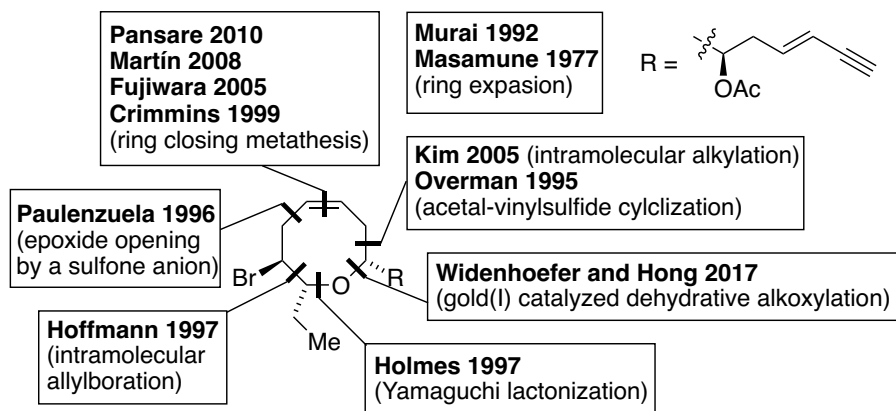
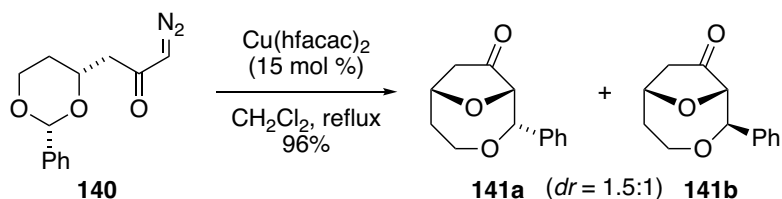


Figure 2.3 Summary of the key disconnections to construct the oxocene core

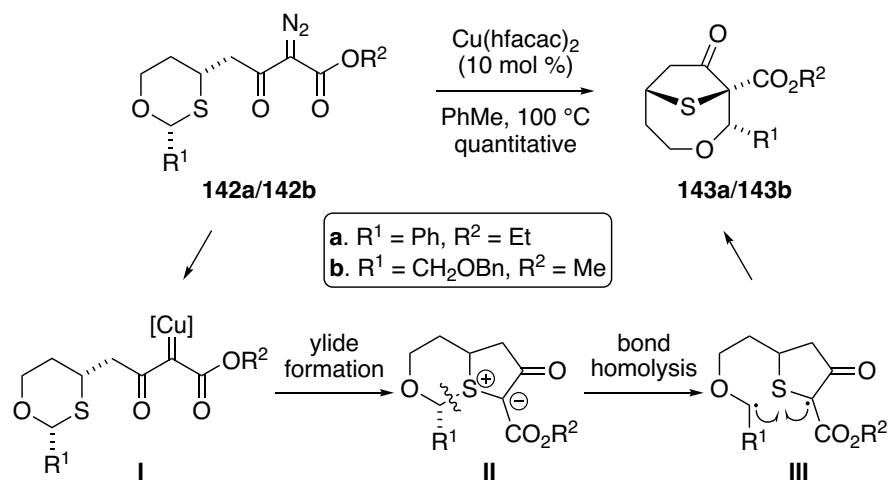
2.5 Results and discussion (a sulfonium ylide approach to the oxocene core)

2.5.1 Preliminary consideration



Scheme 2.17 Previous work on the Stevens [1,2]-shift of ylide derived from acetal

The West group has previously reported that ylides derived from the readily accessible acetal **140** with pendent diazoketone moieties (Scheme 2.17) underwent an efficient Stevens [1,2]-shift to furnish the oxygen bridged cyclic ethers **141a** and **141b** in the presence of $\text{Cu}(\text{hfacac})_2$,⁶⁸ but further elaboration to monocyclic medium-ring ethers was impeded by the difficulty in removing the bridging ether moiety. However, if an analogous transformation could be carried out *via* a sulfonium ylide derived from a six-membered mixed monothioacetal (1,3-oxathiane),⁶⁹ the resulting sulfur bridged oxacycle would be amenable to reductive desulfurization to leave a functionalized oxocane. In previous work by Dr. Liya Cao,⁷⁰ 1,3-oxathianes **142a/142b** were prepared as model substrates to evaluate this approach. When subjected to catalytic $\text{Cu}(\text{hfacac})_2$ in toluene at 100 °C, the corresponding sulfur bridged cyclic ethers **143a/143b** were obtained in quantitative yields (Scheme 2.18). In notable contrast to the earlier acetal case, rearrangement products **143** were isolated as single diastereomers. While the doubly stabilized diazoketoesters **142a/142b** underwent clean conversion to the desired sulfur-bridged oxacycles, the corresponding monostabilized diazoketones either failed to furnish the products or did so with low stereoselectivity.⁷⁰



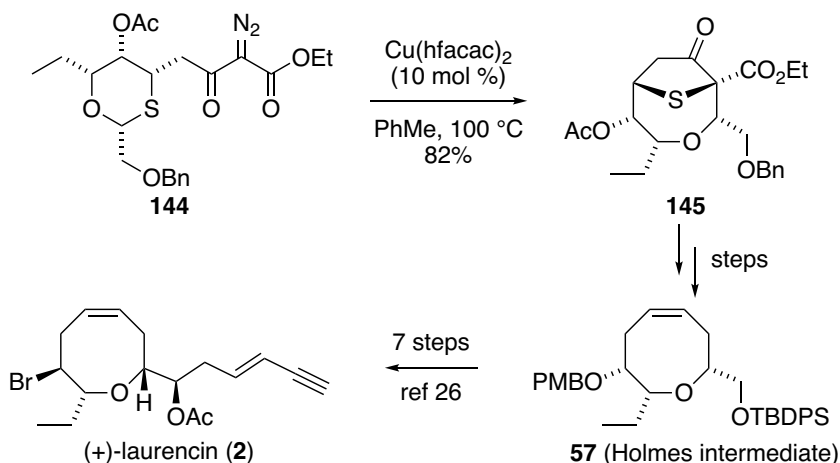
Scheme 2.18 Stevens [1,2]-shift of ylide derived from mixed monothioacetal

Prior work suggests that the major pathway in [1,2]-shifts should occur with stereochemical retention (i.e., to give **143a/143b** rather than the epimeric products).^{68c,71} However, these products cannot be obtained as crystalline solids, preventing unambiguous structural assignment by X-ray diffraction analysis, and TROESY experiments provided inconsistent correlations. Nonetheless, these products were tentatively assigned as shown, in analogy to the more substituted example (**145**, Scheme 2.19) as well as the product from the key step of the formal synthesis (**195**, Scheme 2.38)

The sequence is presumed to occur *via* formation of metalcarbene intermediate **I** followed by ring closure *via* attack of the nucleophilic sulfur atom on the electrophilic carbenoid center to afford sulfonium ylide **II** (Scheme 2.18). The Stevens [1,2]-shift is believed to be a stepwise process,⁷² and a homolytic mechanism proceeding through biradical intermediates such as **III** has been implicated in [1,2]-shifts involving ammonium^{73a} and oxonium^{73b} ylides. However, rearrangement *via* heterolysis cannot be ruled out in the case of acetal-derived ylides and has been invoked in some previous examples.^{69a,d,f} Regardless of mechanism, the high degree of chirality transfer during migration of the anomeric carbon with either a strongly stabilizing phenyl substituent (**142a**) or a weakly stabilizing benzyloxymethyl substituent (**142b**) inspired confidence

that this strategy could be adapted to the synthesis of more complex targets such as laurencin. Furthermore, such an application would permit correlation of advanced intermediates with known compounds and thus provide definitive information regarding the stereochemical outcome of the [1,2]-shift.

It was shown in preliminary studies⁷⁰ that a highly substituted 1,3-oxathiane tethered with a diazoketoester moiety (**144**) underwent the Stevens [1,2]-shift to provide sulfur-bridged oxacycle **145** in 82% yield as a single diastereomer (Scheme 2.19). Encouraged by this result, we carried out further investigations into the convenient and stereoselective route to medium-sized cyclic ethers *via* the Stevens [1,2]-shift of simple monothioacetal precursors, and successfully applied this methodology in a formal synthesis of (+)-laurencin by intercepting Holmes' intermediate **57**²⁶ (Scheme 2.18). Detailed studies are described in the subsequent sections.

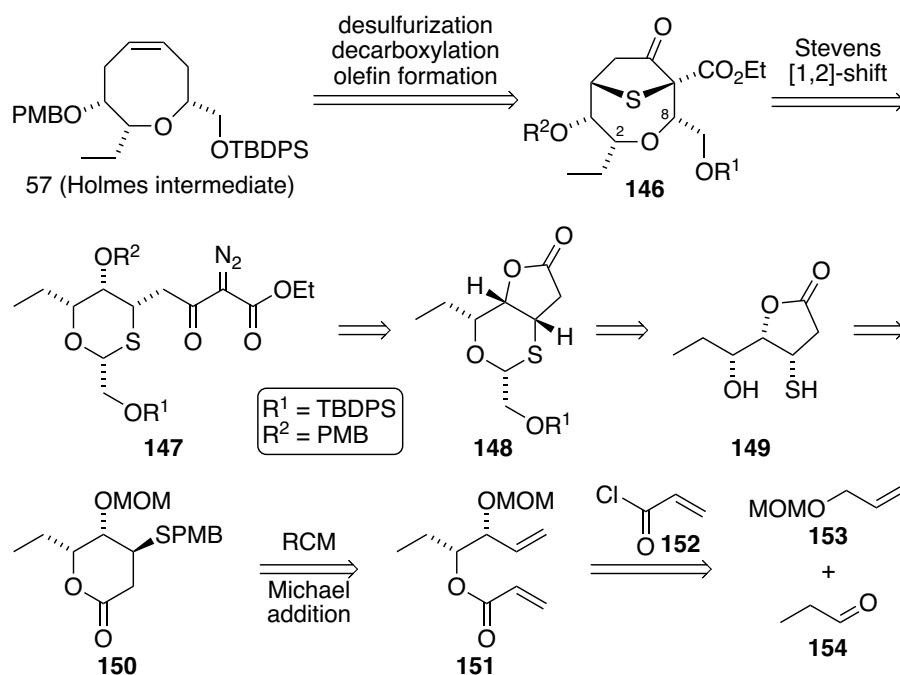


Scheme 2.19 Preliminary results on formal synthesis of (+)-laurencin

2.5.2 Retrosynthetic analysis

We envisioned that the sulfur bridged eight-membered cyclic ether **146** could be converted to the Holmes' intermediate **57**²⁶ *via* sequential reductive desulfurization of the sulfur bridge, decarboxylation and olefin formation reactions (Scheme 2.20). Compound **146** is the expected product from diazoketoester **147** *via* the stereoselective

Stevens [1,2]-shift of an intramolecularly generated sulfonium ylide. The highly functionalized 1,3-oxathiane substrate (**147**) required for the key [1,2]-shift step required a multistep synthetic route to install the necessary substituents and stereocenters. The diazoketoester moiety in **147** can be prepared from the corresponding bicyclic 1,3-oxathiane **148**. Intermediate **148** can be obtained from a stereoselective Lewis acid mediated 1,3-oxathiane formation from mercaptoalcohol **149**, which is the product of the deprotection and isomerization of δ -lactone **150**. Compound **150** was envisioned to come from acrylate ester **151** *via* ring-closing metathesis (RCM) and stereoselective Michael addition. The starting acrylate ester **151**, containing two stereocenters, could be prepared *via* asymmetric allylboration/oxidation of **153** with aldehyde **154**, followed by coupling of the resulting homoallylic alcohol with acryloyl chloride **152**.



Scheme 2.20 Retrosynthetic approach for the formal synthesis of (+)-laurencin

In the proposed approach, the absolute stereochemistry is set in the asymmetric allylboration/oxidation process and the facially selective Michael addition to the rigid

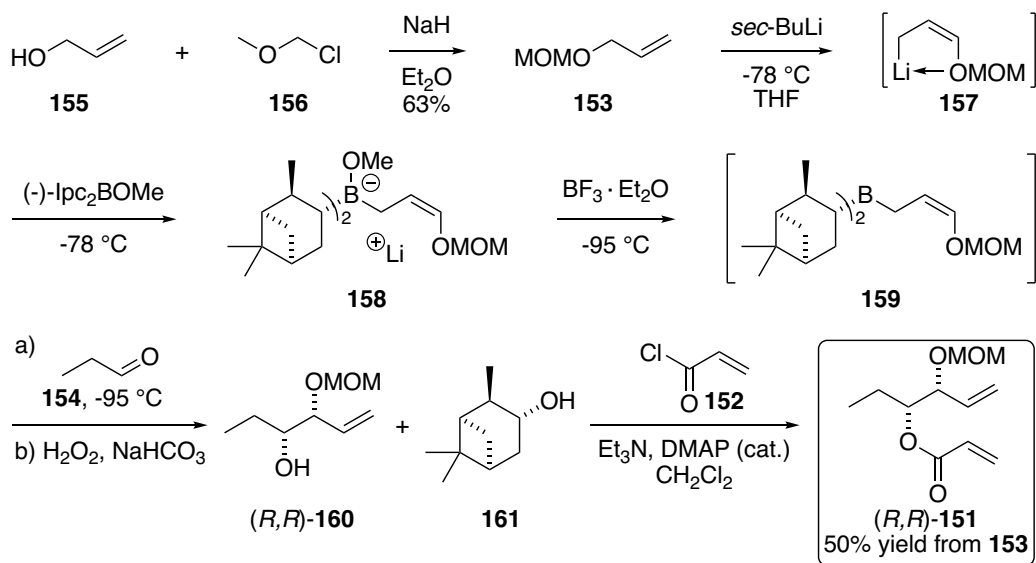
dihydropyran ring (product from RCM of **151**). The final stereocenter would then be installed by the stereoselective formation of monothioacetal **148**, with the silyloxy methyl substituent (CH_2OR^1 , $\text{R}^1 = \text{TBDPS}$) occupying the equatorial position of the anomeric carbon. We hypothesized that the Stevens [1,2]-shift of the highly substituted 1,3-oxathiane **147** could occur with stereochemical retention to form the expected 2,8-*cis*-oxocane **146**. In addition, as noted in Holmes' intermediate **57**, the primary and secondary hydroxyl groups are protected with, respectively, *p*-methoxybenzyl (PMB) and *t*-butyldiphenylsilyl (TBDPS) groups. Therefore, it is necessary to install these protecting groups during the synthesis (i.e., $\text{R}^1 = \text{TBDPS}$ and $\text{R}^2 = \text{PMB}$). However, we had to take into account the possibility that the bulky silyl group could affect the Stevens [1,2]-shift due to its proximity to the migrating anomeric carbon atom. On the other hand, while the stereocenters are not highly prone to stereochemical erosion with the designed route, we need to pay attention to the stereochemical configurations of each intermediate as the reactions proceed forward.

2.5.3 Synthesis of the diazoketoester precursor (**147**) for the Stevens rearrangement

2.5.3.1 Preparation of acrylate ester **151**, determination of enantiomeric ratio and absolute stereochemical configuration

As depicted in Scheme 2.21, the starting acrylate ester **151** was prepared from allyl alcohol **155**, which was first converted to 1-(methoxymethoxy)-2-propene (**153**) following the procedure described by Yamamoto and coworkers.⁷⁴ Compound **153** was then subjected to Brown's asymmetric allylboration and oxidation conditions²¹ with a slight modification. In this process, **153** was treated with *sec*-butyllithium at $-78\text{ }^\circ\text{C}$ to form the organolithium intermediate **157**. After addition of (-)-*B*-methoxydiisopinocampheylborane [(-)-Ipc₂BOMe], borate **158** was formed *in situ*. The reaction mixture was further cooled to $-95\text{ }^\circ\text{C}$ and followed by addition of boron trifluoride diethyl etherate, which is known to react with borates⁷⁵ to generate the

corresponding trialkylborane (**159**) which was immediately treated with propanal **154**. After oxidation with hydrogen peroxide, the enantioenriched homoallylic alcohol (*R,R*)-**160** was generated along with isopinocampheol **161**. However, (*R,R*)-**160** is slightly volatile⁷⁴ and has a similar R_f value to **161** by thin layer chromatography (TLC), making it difficult to achieve complete separation by column chromatography. Attempted isolation at this stage only resulted in diminished overall yield. As a result, the final organic layer containing the mixture of (*R,R*)-**160** and **161** was directly treated with triethylamine (Et_3N), 4-dimethylaminopyridine (DMAP) and acryloyl chloride **152** to afford the corresponding acrylate esters, which were subsequently separated by column chromatography to afford the desired acrylate ester (*R,R*)-**151** in 50% overall yield.

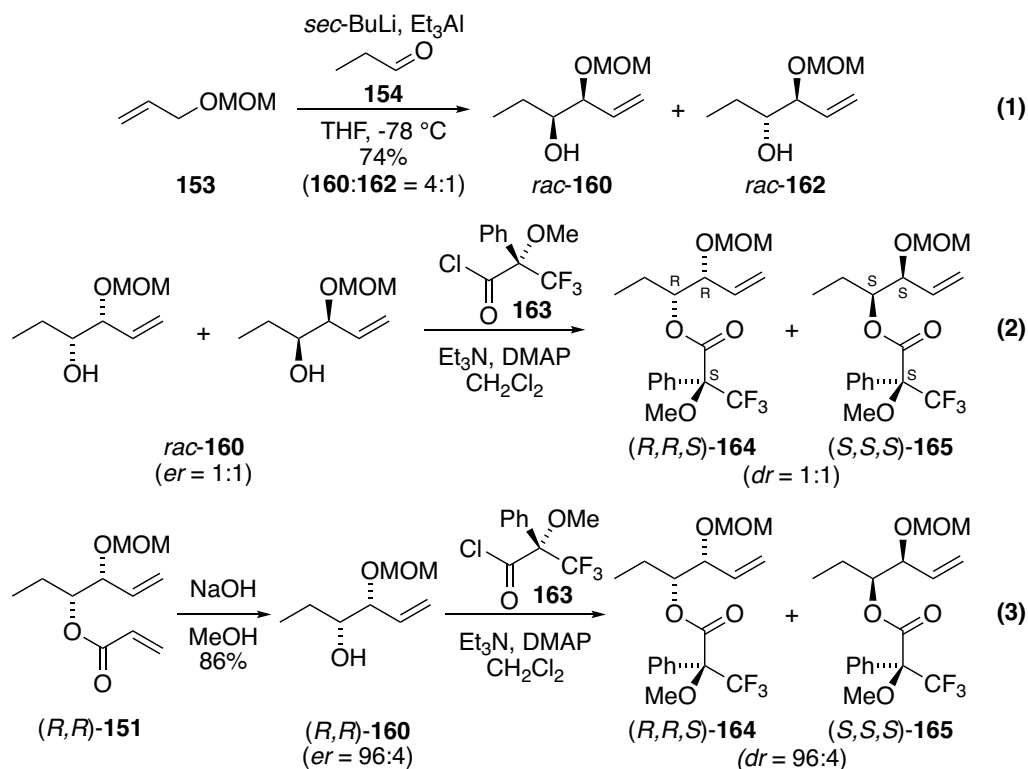


Scheme 2.21 Synthesis of acrylate ester **151**

Although (*R,R*)-**160** was synthesized following the well-established asymmetric allylboration and oxidation protocol,²¹ optimization of the reaction condition was necessary because the procedure required one-pot addition of many reagents. For the optimal reaction outcome, the *sec*-butyllithium solution was titrated in the first step of the synthesis of each batch of materials. Boron trifluoride diethyl etherate ($\text{BF}_3 \cdot \text{Et}_2\text{O}$)

and propionaldehyde (EtCHO) were purified by distillation prior to use. (-)-*B*-Methoxydiisopinocampheylborane was purchased from Sigma-Aldrich as five gram bottles. Due to the hygroscopic nature of this reagent, all of the contents from one bottle were consumed for the generation of each batch of (*R,R*)-**151**. In general, the optimized reaction (as described in the experimental section) was carried out five times to generate enough material to complete the formal synthesis.

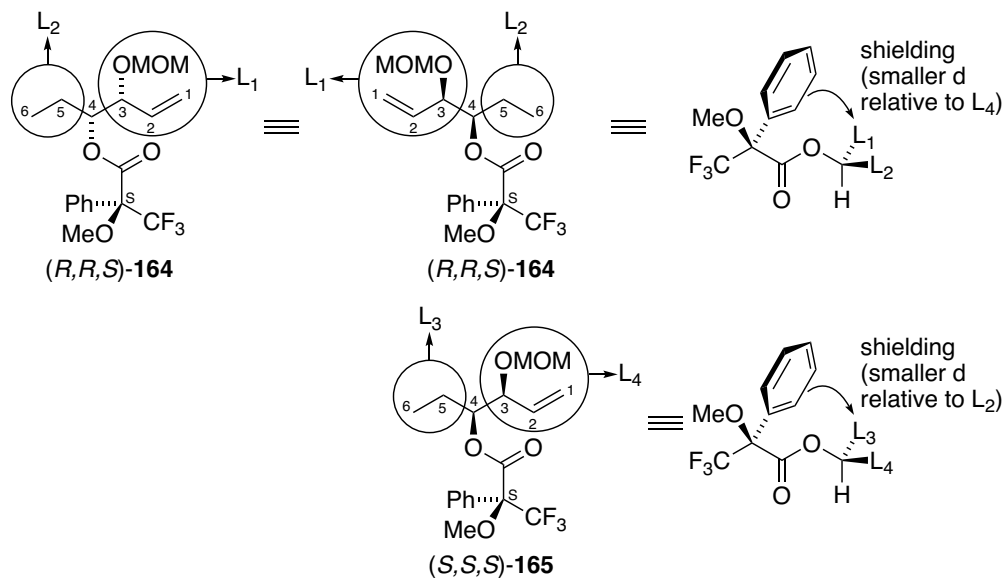
With acrylate ester (*R,R*)-**151** in hand, the next task was to determine the enantiomeric ratio (Scheme 2.22). (*R,R*)-**151** was hydrolyzed to homoallylic alcohol (*R,R*)-**160** under basic conditions (eq 3). The racemic homoallylic alcohol *rac*-**160** was also synthesized from **153** as described by Yamamoto and coworkers⁷⁴ (eq 1). Both *rac*-**160** and (*R,R*)-**160** were converted to the corresponding Mosher esters⁷⁶ using the commercially available acid chloride **163** from Sigma-Aldrich (eq 2 and eq 3). This reaction resulted in the formation of two diastereomeric Mosher esters (*R,R,S*)-**164** and (*S,S,S*)-**165** in each case (eq 2 and eq 3). Since diastereomers have different physical and spectroscopic properties, (*R,R,S*)-**164** and (*S,S,S*)-**165** displayed distinctive chemical shifts in terms of their ¹H and ¹⁹F NMR spectra (refer to the attached spectra in the appendix). The diastereomeric ratios obtained from the integration of clearly resolved resonances could therefore be used to measure enantiomeric ratios of the starting alcohols *rac*-**160** and (*R,R*)-**160**. In the event, the enantiomeric ratio of (*R,R*)-**160** was determined to be 96:4.



Scheme 2.22 Determination of enantiomeric ratio *via* Mosher ester derivatives

In addition, the Mosher ester analysis⁷⁶ also permitted the determination of the absolute configuration. By analyzing the upfield or downfield shift for a number of analogous pairs of protons in the diastereomeric esters, the absolute configuration of the original secondary alcohol could be reliably deduced.^{76b,c} In particular, (*R,R,S*)-**164** and (*S,S,S*)-**165** were represented in the same conformations as described by Mosher^{76b} in Table 2.1, in which the trifluoromethyl (CF₃) group and C-H bond of the secondary alcohol were coplanar with the carbonyl group. If the configuration at C4 is correctly assigned in the major diastereomer (*R,R,S*)-**164**, the phenyl group would be in close proximity to the L₁ side chain, which would impose an anisotropic shielding effect on the protons within the L₁ substructure. Analogously, L₃ in the minor diastereomer (*S,S,S*)-**165** would be shielded in the same way. As shown in the observed chemical shifts in Table 2.1, L₁ protons in (*R,R,S*)-**164** had lower chemical shifts than the same set of protons in (*S,S,S*)-**165**, whereas the chemical shifts for the terminal methyl

protons (H-6) in (*S,S,S*)-**165** were shifted upfield relative to the methyl protons in (*R,R,S*)-**164**. Since these observations were consistent with the initially assigned structures, the absolute configuration at C4 was determined to be *R*. As the *syn*-diol derivative was produced in the allylboration step, the absolute configurations of the two stereocenters in the homoallylic alcohol (*R,R*)-**160** were determined to be *R* and *R*.



δ in ppm (^1H NMR, CDCl_3)

compound	H-2	H-1(A)	H-1(B)	acetal (A)	acetal (B)	H-3	H-6
(<i>R,R,S</i>)- 164	5.57	5.27-5.24	5.22	4.55	4.43	4.14-4.10	0.96
(<i>S,S,S</i>)- 165	5.68	5.37-5.35	5.35-5.33	4.68	4.55	4.20-4.16	0.84
				L_1/L_4			L_2/L_3

Table 2.1 Determination of the absolute configurations

2.5.3.2 Ring closing metathesis (RCM) and Michael addition

With acrylate ester (*R,R*)-**151** in hand, the next task was to investigate the ring closing metathesis reaction to form dihydropyranone **166**. However, ring-closing metathesis using ester-linked dienes can potentially be inefficient due to catalyst deactivation *via* formation of the undesired complex between the ester carbonyl oxygen

and the metal center.⁷⁷ Fürstner and Langemann^{77a} reported the use of titanium(IV) isopropoxide [Ti(*i*OPr)₄] as a Lewis acid additive to coordinate to the ester group, and disrupt the coordination to the metal center.

Grubbs 2nd generation precatalyst (**A**)⁴⁹ was initially employed, producing the desired product **166** in 76% isolated yield after heating in toluene at 80 °C (entry 1, Table 2.2). We envisioned that the yield of ring closing metathesis (RCM) to make six-membered ring could be improved. However, while the introduction of Ti(O*i*Pr)₄^{77a} lowered the reaction temperature, there was no improvement in the yield (entry 2).

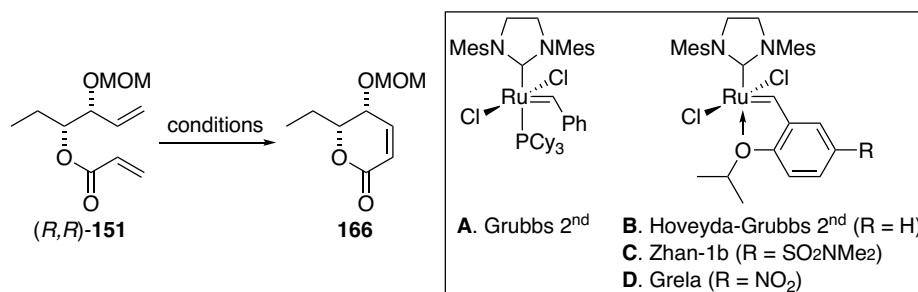
We then shifted our attention to using an alternative catalyst for the RCM of the acrylate ester. The moisture and air stable Hoveyda-Grubbs second generation precatalyst (**B**)⁷⁸ was investigated on a small-scale reaction. A higher temperature was necessary for the reaction to occur within a reasonable time frame, as indicated by the detection of only trace amounts of product by thin layer chromatography (TLC) after refluxing in dichloromethane for 16 hours (entry 3). Another reaction was then conducted directly in toluene at 80 °C (entry 4) with portion-wise addition of the precatalyst into the reaction mixture, and afforded **166** in 92% yield as a transparent dark oil. The attempt to reduce the precatalyst loading resulted in prolonged heating time to achieve full conversion, which also lead to diminished product yield, possibly due to product decomposition or side reactions (entry 5). The reaction was then scaled-up progressively to generate materials for the investigation of the frontline reactions (entries 6-9). In general, the reaction was monitored by thin layer chromatography (TLC), and the precatalyst was added in small portions to the reaction mixture as solutions in toluene. As the scale became larger, a longer reaction time of about four days was necessary to achieve full conversion (entries 7 and 8), and higher precatalyst loading resulted in a better isolated yield (entry 7 vs. entry 8).

Both Grubbs second generation precatalyst (**A**)⁴⁹ and Hoveyda-Grubbs second generation precatalyst (**B**)⁷⁸ were commercially available from Sigma-Aldrich in similar price ranges. For economic considerations, it would be beneficial to find more active metathesis precatalyst that could provide good product yields in relatively short

reaction times and low catalyst loadings. The nitro-substituted Hoveyda-Grubbs second generation precatalyst, also known as the Grela's catalyst (**D**),⁷⁹ was shown to be more reactive than both **A** and **B**. The introduction of an electron-withdrawing group on the aromatic ring *para* to the of the isopropoxy group is believed to reduce its chelating ability to the ruthenium center and facilitate initiation of the catalytic cycle.^{79a} Unfortunately, catalyst **D** was not commercially available during this time and the attempted synthesis following literature procedure afforded catalyst **D** with low purity. At the same time, we were pleased to find a less expensive alternative, the Zhan-1b (**C**) catalyst,⁸⁰ with an electron-withdrawing dimethylsulfonamide group *para* to the isopropoxy group.

Catalyst **C** was directly tested on a large scale reaction (entry 9) and afforded the desired product in shorter reaction times in comparison to the reaction in entry 10. However, the active pre-catalyst and the product (**166**) had displayed very similar R_f values in a range of solvent mixtures, making them difficult to separate by flash column chromatography when the catalyst was not totally consumed. The slight greenish appearance of the final product was also an indication that traces of the pre-catalyst were present, which might contribute to the high yield of 92%. We subsequently tried to reduce the catalyst loading while frequently monitoring the reaction progress by TLC (thin layer chromatography). For each reaction, the reaction mixture was added with about 1–2 mol% precatalyst everytime and stirred for a certain period of time before the addition of more precatalyst until the starting martial was totally consumed. The total precatalyst loading was reduced to 8.8 mol% and provided **166** in 85% yield in 29 hours. Additional optimization was also performed as shown (entry 11 to entry 14). Increasing the reaction temperature to 100 °C was shown to reduce the reaction time (entry 12). However, the starting material is not strongly UV-active and might overlap with side products, making TLC (thin layer chromatography) an unreliable method for reaction monitoring. We then shifted to GC (gas chromatography) for reaction monitoring, which could potentially provide more accurate information on the relative percentages of starting material and product in the reaction mixture. Eventually, the

catalyst loading could be reduced to 2.1 mol% to afford dihydropyranone **166** in good yield over relatively short reaction times (19 hours) in comparison to other condition (entry 14).

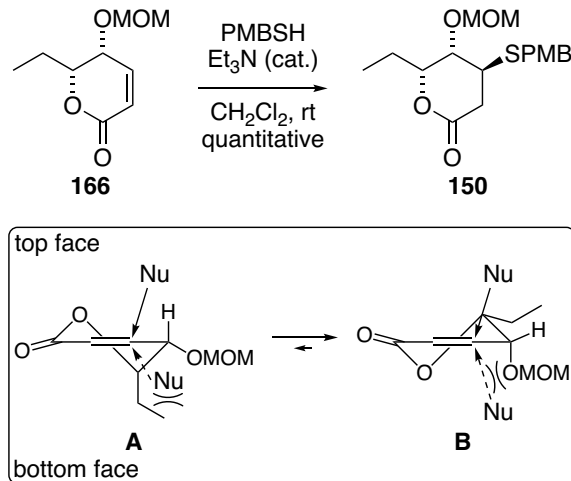


entry	catalyst (mol%) ^a	scale	solvent ^b	T (°C)	time	yield (%) ^c
1	A (5.0 mol%)	100 mg (0.47 mmol)	PhMe	80	38 h	76
2 ^{77a}	A (10.0 mol%) Ti(OiPr)₄ (30.0 mol%)	100 mg (0.47 mmol)	CH ₂ Cl ₂	reflux	39 h	76
3	B (3.7 mol%)	50 mg (0.22 mmol)	CH ₂ Cl ₂ / PhMe ^d	reflux	32 h	31 ^e
4	B (5.4 mol%)	100 mg (0.47 mmol)	PhMe	80	32 h	92 ^f
5	B (3.7 mol%)	100 mg (0.47 mmol)	PhMe	80	112 h	59
6	B (6.3 mol%)	212 mg (0.99 mmol)	PhMe	80	42 h	80
7	B (9.0 mol%)	550 mg (2.57 mmol)	PhMe	80	90 h	82
8	B (5.0 mol%)	632 mg (2.95 mmol)	PhMe	80	94 h	76
9	C (11.0 mol%)	725 mg (3.38 mmol)	PhMe	80	69 h	92 ^{f,g}
10	C (8.8 mol%)	1.00 g (5.00 mmol)	PhMe	80	29 h	85 ^g
11	C (5.4 mol%)	380 mg (1.77 mmol)	PhMe	80	96 h	82 ^g
12	C (2.7 mol%)	300 mg (1.40 mmol)	PhMe	100	21 h	79
13	C (2.2 mol%)	300 mg (1.40 mmol)	PhMe	100	30 h	80 ^h
14	C (2.1 mol%)	265 mg (1.24 mmol)	PhMe	100	19 h	82 ^h

^a The catalyst was added in 1 to 2 mol% portions as a solution in the same reaction solvent and the reaction progress was monitored by TLC. ^b [] = 0.02 M. ^c Isolated yield. ^d Only a trace amount of product was observed by TLC using 1 mol% of catalyst in CH₂Cl₂ at reflux overnight. PhMe and more catalyst was added to the dried-out residue and heated at refluxed for additional 16 hours. ^e The rest of the mass balance consisted of a mixture of products. ^f Decomposed catalyst residue might be presented in the final product as it was a transparent dark oil. ^g The final product had a slightly greenish color, possibly due to the presence of traces of catalyst. ^h Reaction was monitored by GC instead of TLC.

Table 2.2 Reaction optimization for the ring closing metathesis reaction

When the α,β -unsaturated lactone **166** was treated with 4-methoxybenzyl mercaptan (PMBSH), the desired Michael addition went cleanly to afford **150** in quantitative yield as a single diastereomer (Scheme 2.23). Although TROESY experiments did not provide direct evidence for the relative stereochemistry of the SPMB group, the assigned configuration of **150** could be explained by the conformational analysis of starting lactone **166**. In both half-chair conformations **A** and **B**, the top face offers a less hindered trajectory for the incoming sulfur nucleophile in comparison to the bottom face, making the attack from top face more favorable. In addition, this reaction also worked efficiently on various scales including gram-scale.



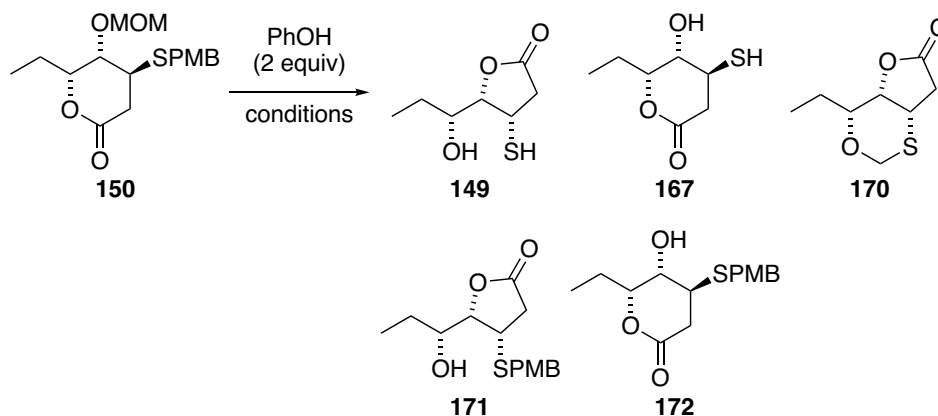
Scheme 2.23 Facially selective Michael addition

2.5.3.3 Formation of γ -lactone and reaction optimization

It was anticipated that both methoxy methyl ether (MOM) and *p*-methoxybenzyl (PMB) groups could be cleaved in a single reaction as both of them are labile under acidic conditions. Treatment of lactone **150** in refluxing trifluoroacetic acid (TFA) in the presence of phenol as the scavenger afforded a mixture of products. After a quick chromatographic purification, ^1H and ^{13}C NMR of the major fraction indicated both **149** and **167** (also determined by HRMS analysis) along with intractable mixture of products. The inseparable mixture of lactones (**149** and **167**) was directly treated with

2.24 was repeated first (entry 1). After careful separation, three products were isolated, γ -lactone **149**, δ -lactone **167** and 1,3-oxathiane **170**. Compound **170** was possibly formed *via* the sequence of MOM transfer to the sulfur atom, removal of the PMB group, formation of the γ -lactone and formation of monothioacetal. The generation of about a 1:1 ratio of **149** to **167** could explain the low yield that was obtained in the initial investigation (Scheme 2.24) as **167** was the unproductive side product for the subsequent 1,3-oxathiane formation. Increasing the heating time was shown to increase the relative ratio of δ -lactone **167** over γ -lactone **149** (entry 2 and 3). A similar result was observed when anisole was used as the scavenger instead of phenol (entry 4). Other solvent systems were also investigated. For example, when a 1:1 mixture of tetrahydrofuran and TFA was used, 93% of **172** was formed after heating at 60 °C overnight (entry 5). Treatment of **150** with 10 equivalents of TFA in refluxing toluene formed a mixture of **171**, **172** and **170** (entry 6).

Although it was difficult to generalize a definitive explanation for the product distribution, some important conclusions can be drawn from the observations. Firstly, the PMB group could be removed only under forcing conditions (heating in neat TFA). Secondly, prolonged heating favors the formation of the 6-membered lactone over the 5-membered lactone (i.e., yields of **167/149** in entries 1-4 versus yields of **172/171** in entries 5 and 6).



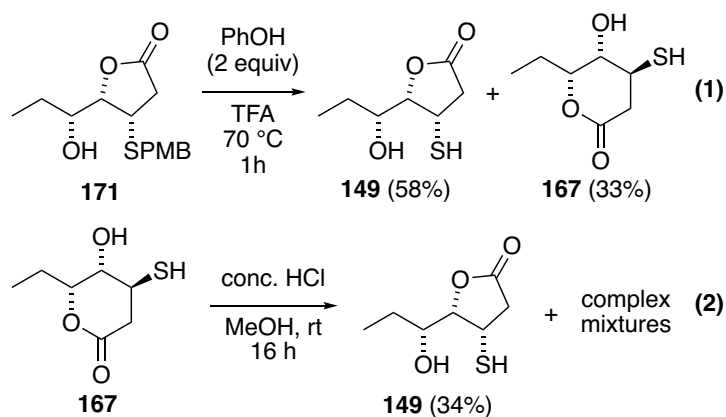
entry	solvent	<i>T</i> (°C)	time	yield (%) ^a				
				149	167	171	172	170
1	TFA	70	1 h	38	42	-	-	10
2	TFA	70	2 h	26	58	-	-	~10 ^b
3	TFA	70	2.5 h	10	81	-	-	-
4	TFA, anisole (3 equiv) ^c	70	3 h	16	73	-	-	3
5	TFA/THF (1:1)	60	16 h	-	-	-	93	-
6	PhMe, TFA (10 equiv)	reflux	1 h	-	-	50	35	11

^a Isolated yield. ^b Product **169** contained some impurities. ^c Anisole was used instead of phenol.

Table 2.3 Investigation into the one-pot synthesis of mercaptoalcohol **150**

In addition, two more experiments were performed as shown in Scheme 2.25. Re-subjecting γ -lactone **171** to the initially investigated reaction conditions resulted in the formation of both **149** and **167** (eq 1), indicating that heating contributed to the formation of the undesired δ -lactone **167**. During column chromatography, two important observations were made. Immediately after the column chromatography, the ¹H NMR spectrum of **167** often contained a small amount of γ -lactone **149**. When **167** was stored in open flasks at room temperature, periodic NMR analysis showed that the relative ratio of γ -lactone **149** in ¹H NMR increased over time. These findings indicated that **167** might be converted to **149** under weakly acidic conditions. We envisioned the translactonization to be an acid-assisted process, which might go to completion under

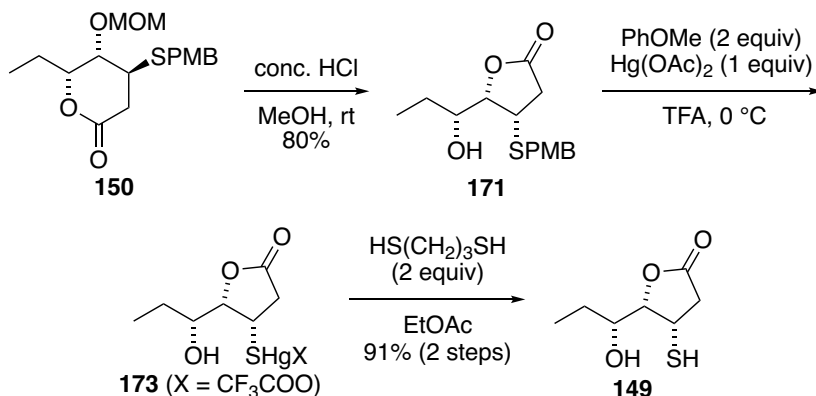
strongly acidic conditions. However, when **167** was treated with HCl, a disappointing 34% yield of **149** was formed along with a complex mixture of products (eq 2).



Scheme 2.25 Synthesis of 150 from 170 and 167

As the removal of both MOM and PMB groups in one step was inefficient, we explored an alternative route to access mercaptoalcohol **149** (Scheme 2.26). By subjecting **150** to acidic conditions at room temperature, the MOM ether was selectively hydrolyzed, then underwent isomerization to generate γ -lactone **171**. In order to avoid further isomerization to the undesired δ -lactone, the PMB group needed to be removed at lower temperatures. After surveying the literature, we found an efficient method for S-PMB group removal by mercury salt,^{81a} a process which has been applied to the selective cleavage of the PMB group from a protected-cysteine residue in complex peptide synthesis.⁸¹ In the reported protocol,⁸¹ Hg(TFA)₂ was generated *in situ* from a solution of Hg(OAc)₂ in TFA, which could cleave PMB thioether effectively, due to the high affinity of sulfur atom to mercury salt. However, the use of Hg(OAc)₂ in AcOH led to diminished yield. To our delight, this method worked well for the synthesis of **149** as shown below. Compound **171** was dissolved in cold trifluoroacetic acid in the presence anisole as the scavenger. Upon addition of an equimolar amount of mercury acetate, mercaptide **173** was formed immediately while the spot for **171** on the TLC plate was completely replaced by a baseline spot. Without

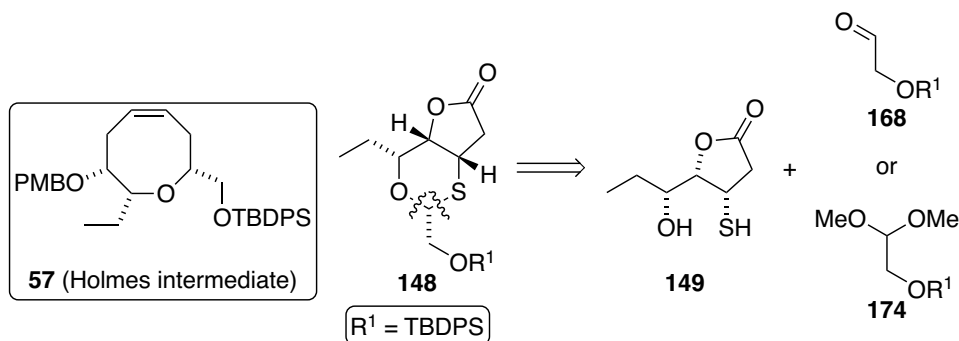
isolation, the mercuric ion **173** was precipitated with 1,3-propanedithiol as a white-gray solid and subsequently generated mercaptoalcohol **149**. The three-step sequence to remove MOM and PMB worked efficiently, even for the gram-scale reaction, to deliver mercaptoalcohol **149** in good yields without forming any of the undesired 6-membered lactone isomers.



Scheme 2.26 Step-wise synthesis of mercaptoalcohol **150**

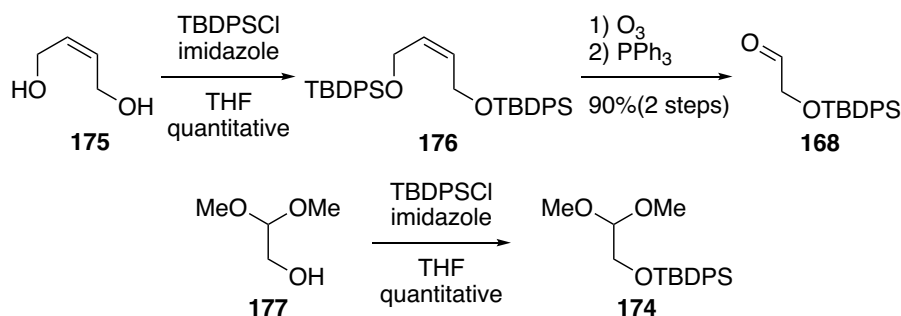
2.5.3.4 Synthesis of the substituted bicyclic 1,3-oxathiane

With mercaptoalcohol **149** in hand, the conversion to bicyclic 1,3-oxathiane **148** was investigated next. Recall that the primary hydroxyl group is protected as *t*-butyldiphenylsilyl (TBDPS) ether in the target Holmes intermediate **57**²⁶ (Scheme 2.27). Hence, the important fragment for the generation of 1,3-oxathiane **148** would come from either aldehyde **168** or dimethylacetal **174** with a TBDPS group at R¹.



Scheme 2.27 Retrosynthetic analysis to approach 148

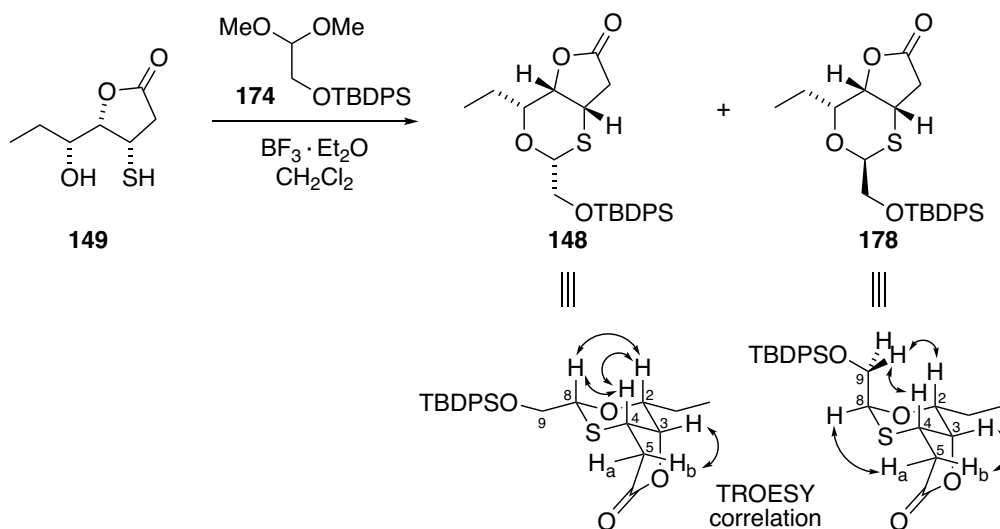
The initial investigation into the 1,3-oxathiane formation was conducted using aldehyde **168** (Scheme 2.24), which was prepared from *cis*-2-butene-1,4-diol (**175**) via TBDPS protection and ozonolysis (Scheme 2.28). After achieving the finalized synthetic route for γ -lactone **149**, dimethylacetal **174** was employed instead of **168**. Compound **174** was synthesized by protecting 2,2-dimethoxyethanol (**177**) as the TBDPS ether.



Scheme 2.28 Preparation of aldehyde **168** and dimethylacetal **174**

Treatment of mercaptoalcohol **149** with dimethyl acetal **174** yielded an epimeric mixture of separable 1,3-oxathianes **148** and **179** (Table 2.4). The stereochemistry of the anomeric center was assigned based on the observed TROESY correlation as depicted in Table 2.4. The TROESY spectra of the major diastereomer showed obvious correlations of H₈–H₂ and H₄–H₂, which is consistent with the all-*cis* configuration (**148**) in the presumed chair conformation of the six-membered ring. On the other hand, the observed correlations of H₂–H₉, H₄–H₉ and H₈–H_{5a} on the TROESY spectra of the minor diastereomer indicated the C₈-*trans* relative configuration (**178**) with respect to the configurations at C₂ and C₄. The process of 1,3-oxathiane formation was thus favoring the equatorial disposition of the substituent at the anomeric carbon in the presumed chair confirmation.

The reaction was performed multiple times with the goal of achieving optimal yield and diastereoselectivity. Some examples are shown in Table 2.4. When the reaction was conducted at -10 °C, 50% of **148** and 20% **178** were obtained (entry 1). After increasing the equivalents of reagents and reducing the reaction temperature to -78 °C, the overall yield and diastereoselectivity were also improved (entry 3). The diastereoselectivity was further improved when the reaction mixture was left in the -78 °C cooling bath longer (entry 4). The optimal reaction condition was achieved on a relatively large scale reaction (entry 5) in which the reaction mixture was stirred at -78 °C for three hours and gradually warmed to 5 °C over 3.5 hours to achieve 90% yield of **148**.



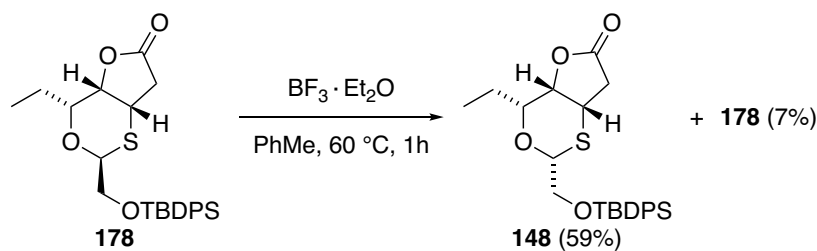
entry	$\text{BF}_3 \cdot \text{Et}_2\text{O}$	174	T (°C)	time ^b	yield (%) ^a	
					148	178
1	1.2 equiv	1.2 equiv	-10	1 h	50	20
2	1.2 equiv	1.6 equiv	-78	0.5 h	51 ^c	24 ^c
3	2.4 equiv	2.0 equiv	-78	1 h	73	13
4	2.2 equiv	2.0 equiv	-78	2.5 h	75	11
5 ^d	2.1 equiv	2.0 equiv	-78	3 h ^e	90	6

^a Isolated yield. ^b Cooling bath was removed and reaction mixture was allowed to warm up to room temperature before work-up. ^c Yield was corrected based on recovered starting material. ^d 570 mg (3.23 mmol) scale reaction. ^e Additional 1.0 equiv of $\text{BF}_3 \cdot \text{Et}_2\text{O}$ and 0.5 equiv of **174** was added and reaction mixture was gradually warmed up to 5 °C in 3.5 h.

Table 2.4 Stereoselective formation of 1,3-oxathiane

We envisioned that the undesired diastereomer **178**, generated during the optimization process, could be epimerized to 1,3-oxathiane **148**. Initially, no conversion of **178** to **148** was observed when it was submitted to the same reaction conditions as for its formation ($\text{BF}_3 \cdot \text{Et}_2\text{O}$ and **174** at -78 °C in dichloromethane). However, after heating the reaction mixture at reflux for 2 hours, the formation of a small amount of **148** was detected by TLC, indicating the desired epimerization occurs at elevated temperatures. After a few more attempts, the optimal result was obtained

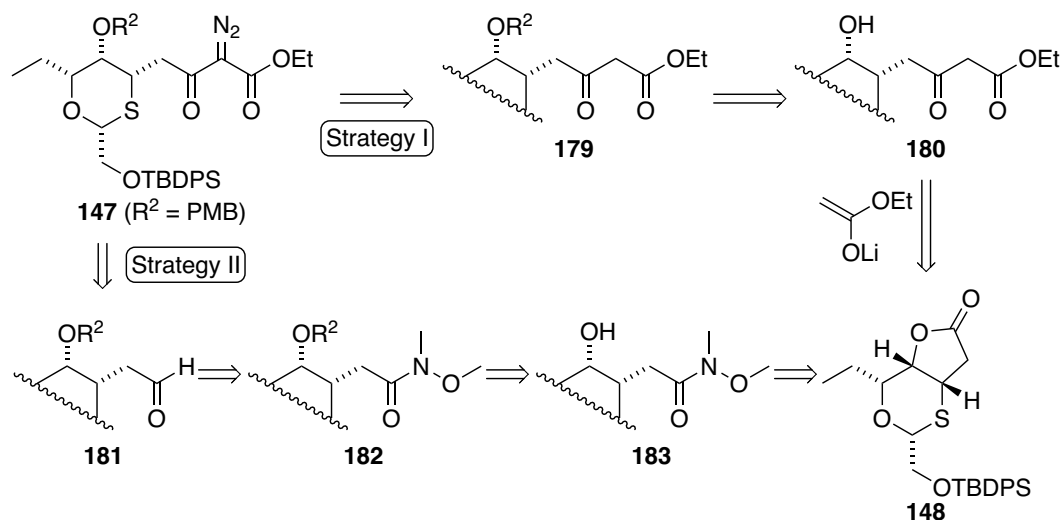
when **178** was heated at 60 °C in toluene for 1 hour in the presence of 1 equivalent of $\text{BF}_3 \cdot \text{Et}_2\text{O}$ (Scheme 2.29), and 59% yield of **148** was obtained along with recovered **178** in 7% yield. This allowed us to recycle and epimerize all of the 1,3-oxathiane **178** that was previously generated during the reaction optimization to the desired anomer **148**.



Scheme 2.29 Epimerization of 178 to 148

2.5.3.5 Retrosynthetic strategies to install the diazoketoester side chain

With the desired 1,3-oxathiane ring (**148**) in hand, the next step was to install the diazoketoester side chain (**147**). There are a variety of methods to generate α -diazocarbonyl compounds, as previously mentioned in Chapter 1. We envisioned two strategic routes to generate **147** from **148** (Scheme 2.30). In the first strategy, the diazoketone is generated *via* a Regitz diazotransfer reaction on β -ketoester **179**, which could be formed by protecting the secondary hydroxyl group in **180**. The β -ketoester functionality in **180** could be generated by Claisen condensation of **148** with lithium enolate. For the second strategy, we were inspired by the efficient one-pot synthesis of an α -diazo- β -dicarbonyl compound from an aldehyde substrate, as reported by Steel and Erhunmwunse.⁸² Aldehyde **181** is thus an important intermediate, which could be generated from Weinreb amide **183** after hydroxyl protection and amide (**182**) reduction. The lactone function in **148** could be converted into amide **182** by treatment with the *N,O*-dimethylhydroxylamine anion. Although the route for the first strategy is ultimately one-step shorter in comparison to the second strategy, both routes were explored, and details are shown in the subsequent sections.

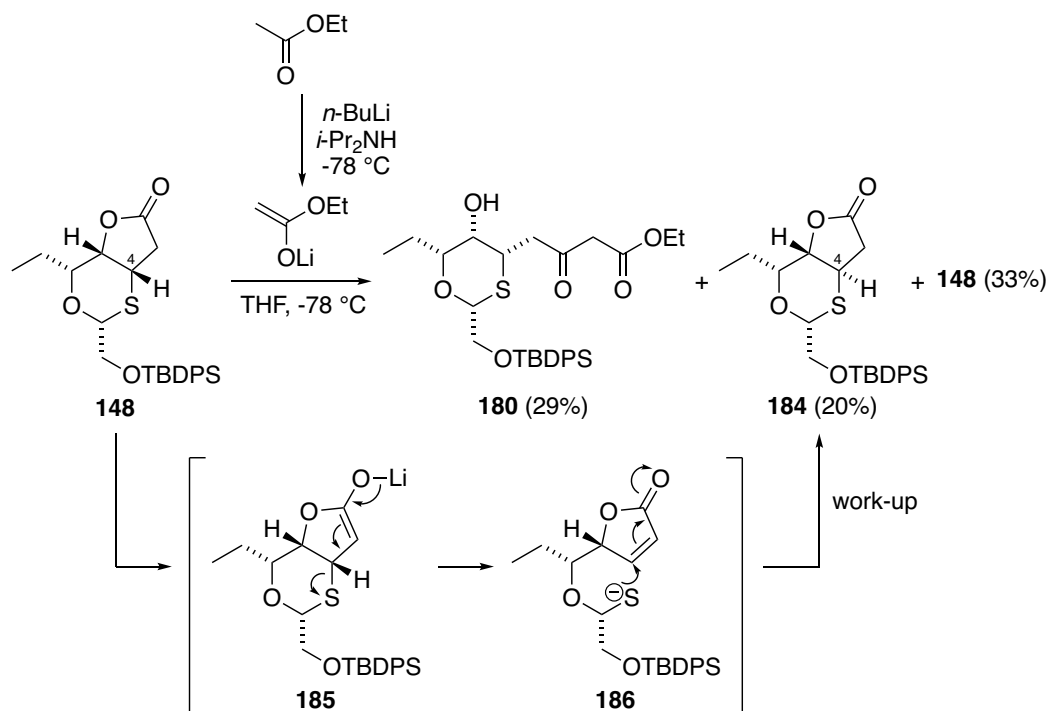


Scheme 2.30 Retrosynthetic strategies to access diazoketoester 147

2.5.3.6 Synthesis of the tethered diazoketoester moiety: strategy one

The shorter route to access the targeted diazoketoester intermediate was investigated first. The first step of this route involves the synthesis of β -ketoester **180** *via* a Claisen condensation of a lithium enolate with lactone **148** (Scheme 2.31). The lithium enolate was generated by deprotonation of ethyl acetate with lithium diisopropylamide (LDA). Lactone **148** was then added to the reaction mixture containing the lithium enolate. After work-up, two products were isolated, along with 33% recovered starting material. The first product was the desired β -ketoester **180**, which was obtained in 29% yield. Isolation of a significant amount of a second product intrigued us. This compound did not have the signals that correspond to an ethyl ester side chain in its ^1H NMR spectrum, but possessed a molecular weight identical to the starting lactone **148** by high resolution mass spectroscopy (HRMS). Its ^1H and ^{13}C NMR spectra were similar in comparison to those of lactone **148**, but all the signals were slightly shifted, strongly suggesting the second product to be an isomer of lactone **148**. We envisioned that the only possible site to participate in the reaction pathway was the α -position of the lactone ring in **148**. Deprotonation of the α -proton under strongly basic conditions would generate enolate **185**, which has a suitable leaving group at the β -position. Subsequent C-S bond

cleavage followed by re-closure of the ring *via* Michael addition (**186**) would yield *trans*-fused bicyclic compound **184**, which is a C4 epimer of the starting lactone **148**.



Scheme 2.31 Synthesis of ketoester **180**

More evidence was gathered to support the stereochemical assignment for lactone **184**. The observed TROSEY correlation between H2 and H8 indicated a 2,8-*cis*-configuration (Table 2.5). Although the presumed twisted chair conformation for the six-membered ring does not have an additional unique pair of spatially adjacent protons to support the proposed structure by TROESY, some useful information could be drawn from the ¹H NMR coupling constants. The approximate dihedral angles between the vicinal protons could be determined using the corresponding vicinal coupling constants on the Karplus curve.⁸³ In particular, the observed vicinal coupling constant for H3-H2 was 9.2 Hz, indicating a dihedral angle of around 20°, whereas the coupling constant of 6.5 Hz for H3-H4 indicated a dihedral angle of around 130°. These values were consistent with the 2,3-*cis*- and 3,4-*trans*-configuration as illustrated in the twisted

chair conformation in Table 2.5. The coupling constant versus dihedral angle information for 1,3-oxathianes **148** and **178** are also listed for comparison.

148		178		184	
J ($^1\text{H NMR}$)	θ	J ($^1\text{H NMR}$)	θ	J ($^1\text{H NMR}$)	θ
$J_{\text{H3,H2}} = 1.8 \text{ Hz}$	$\sim 60^\circ$	$J_{\text{H3,H2}} = 2.1 \text{ Hz}$	$\sim 60^\circ$	$J_{\text{H3,H2}} = 9.2 \text{ Hz}$	$\sim 20^\circ$
$J_{\text{H3,H4}} = 4.0 \text{ Hz}$	$\sim 60^\circ$	$J_{\text{H3,H4}} = 7.8 \text{ Hz}$	$\sim 40^\circ$	$J_{\text{H3,H4}} = 6.6 \text{ Hz}$	$\sim 130^\circ$

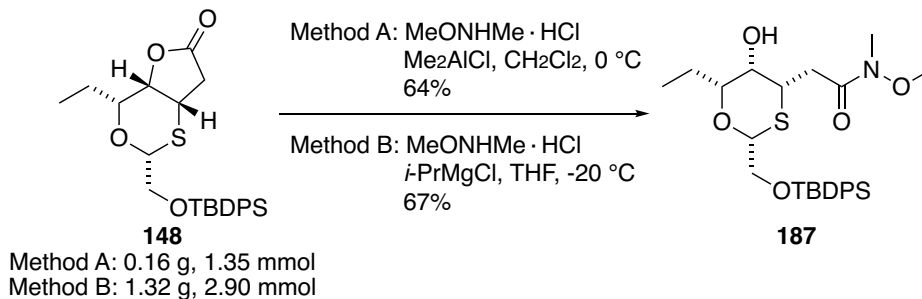
Table 2.5 Structural assignment for 184 in comparison with 148 and 178

In light of these results, the first approach with its Claisen condensation step was deemed unsuitable for the overall synthesis, as stereochemical erosion occurred under strongly basic conditions. Therefore, no further investigation into strategy one was performed, and we shifted our attention to the alternative second strategy.

2.5.3.7 Synthesis of the tethered diazoketoester moiety: strategy two

Although the second strategy required an extra step to convert the lactone ring to the diazoketoester (Scheme 2.30), this route led to the generation of the diazoketoester without any erosion of stereochemistry, and investigational details are discussed in this section.

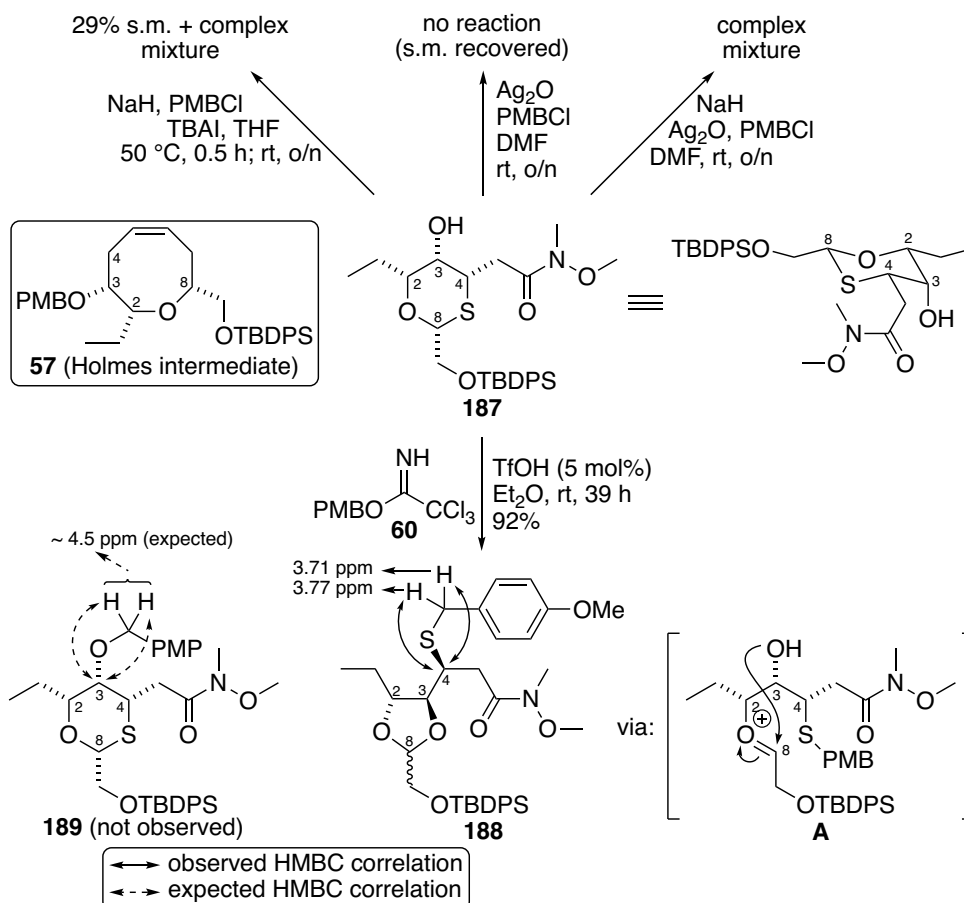
The lactone ring in **148** can be opened with *N,O*-dimethylhydroxylamine to afford the corresponding Weinreb amide.⁸⁴ Dimethylaluminum chloride⁸⁵ and *N,O*-dimethylhydroxylamine were initially employed for a small-scale reaction and afforded γ -hydroxy Weinreb amide **187** in 64% yield (method A, Scheme 2.32). However, formation of an emulsion during the work-up step could be problematic for reactions performed at larger scales. We then examined the use of isopropyl magnesium chloride with *N,O*-dimethylhydroxylamine, and the reaction worked smoothly to provide Weinreb amide **187** in 67% yield for a gram-scale reaction under the optimized conditions (method B).



Scheme 2.32 Preparation of Weinreb amide 187

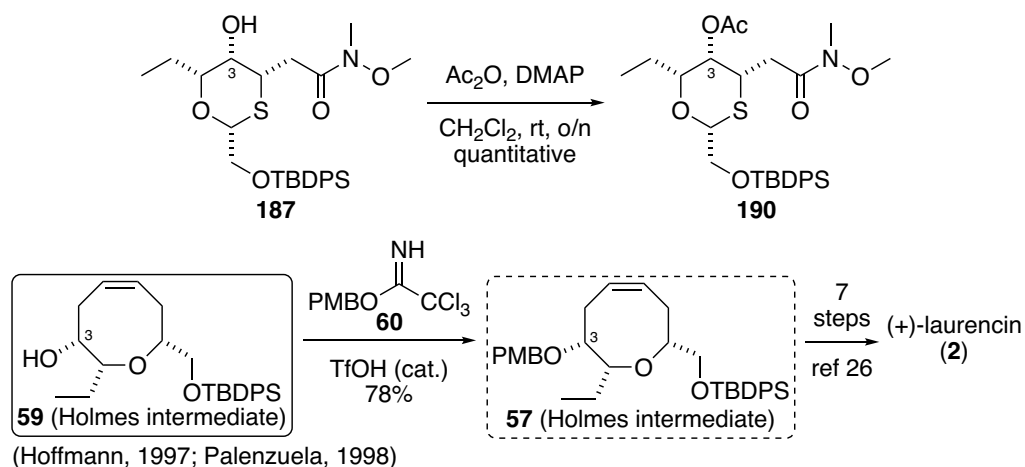
A secondary hydroxyl group was also formed during the Weinreb amide synthesis. This hydroxyl group at C3 is in the axial position of the presumed chair conformation of the six-membered 1,3-oxathiane ring (Scheme 2.33). As the C3-hydroxyl group in the final Holmes intermediate (**57**)²⁶ was protected as a PMB ether, we envisaged the direct installation of PMB group on alcohol **180**. However, when *p*-methoxybenzyl chloride (PMBCl) was used as the electrophile, no reaction occurred under neutral conditions while a complex mixture of products was obtained under basic conditions. We also tested the method of using 4-methoxybenzyl-2,2,2-trichloroacetimidate (**60**) under mildly acidic conditions. This reaction afforded a single product in high yield, which we initially believed to be **189**. The expected chemical shift for the benzylic protons next to the oxygen atom in **189** should be around 4.5 ppm on the ¹H NMR

spectrum, and the benzylic protons would also show an HMBC correlation to the C3 carbon atom. However, the observed chemical shift for the benzylic protons were 3.71 and 3.77 ppm, and they showed an HMBC correlation with the C4 carbon atom. The benzylic carbon atom was evidently not attached to the oxygen atom. The observed data was consistent with the five-membered acetal **188**, which was formed in three sequential transformations. Under mildly acidic condition, the PMB group was installed on the more accessible sulfur atom to afford a sulfonium ion, that subsequently opened-up to give oxocarbenium ion **A**. The former axial hydroxyl group could then react intramolecularly with the oxocarbenium ion to generate acetal **188**, a five membered *O,O*-acetal.



Scheme 2.33 Attempted protection of the axial hydroxyl group as PMB ether

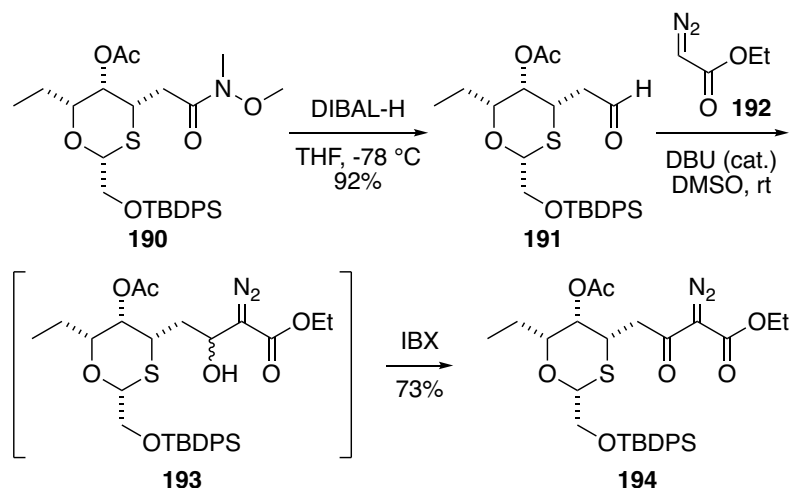
The difficulties encountered while trying to introduce the PMB group might be attributed to steric hindrance around the axial hydroxyl group. We thus imagined that a smaller group might be more easily accommodated. Treatment of **187** with acetic anhydride (Ac_2O) in the presence of DMAP afforded acetate **190** in quantitative yield (Scheme 2.34). If acetate **190** was used as an intermediate to synthesize target compound **57**, two additional late-stage steps had to be introduced to exchange the protecting group. After re-examining Holmes' total synthesis,²⁶ alcohol **59** was found to be another fully characterized intermediate that was converted to **57** by PMB protection, then converted to (+)-laurencin (**2**) in seven steps. We could thus introduce one extra step of C3-acetate removal at the end of the synthesis to access alcohol **59**. On the other hand, **59** has also been synthesized previously by Hoffmann³⁵ and Palenzuela²⁴ *via* different approaches (Section 2.3.4 and Section 2.3.1), which provided us additional literature data for comparison. To this end, the target of the formal synthesis was changed to alcohol **59**.



Scheme 2.34 Acetate protection of the axial hydroxyl group

Reduction of Weinreb amide **190** with DIBAL-H afforded the corresponding aldehyde **191** in 92% yield (Scheme 2.35). While all steps prior to the formation of **191**

could be carried out on gram scale or higher, DIBAL-H reduction of **190** was restricted to scales of 0.5 g or less to avoid potential competing reductive removal of the acetate group. Aldehyde **191** was subjected to ethyl diazoacetate (EDA, **192**) in the presence of 1,8-diazabicyclo[5.4.0]undec-7-ene (DBU) and 2-iodoxybenzoic acid (IBX) to furnish the key diazoketoester substrate **194**.⁸² This one-pot procedure involved the addition of EDA to aldehyde **191** to generate the transient diazoester intermediate **193**, which was rapidly oxidized upon addition of IBX to furnish the diazoketoester side chain.



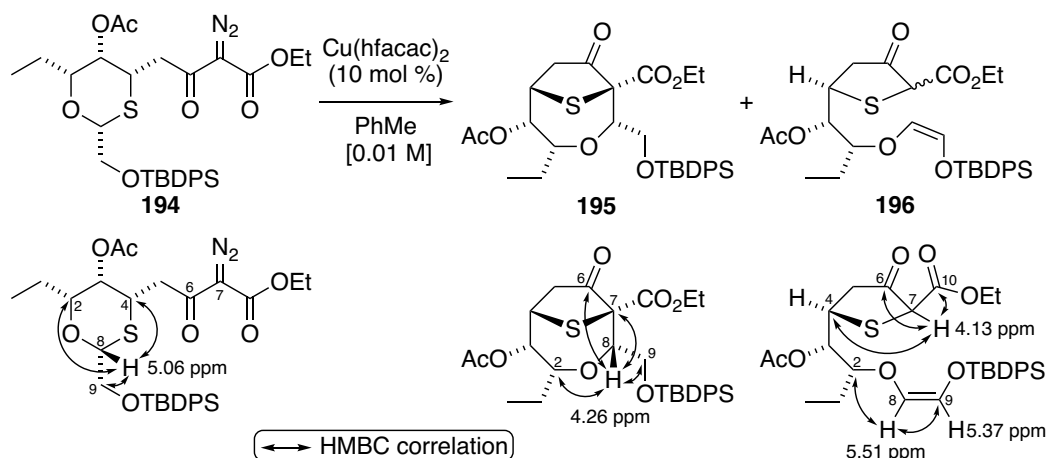
Scheme 2.35 Synthesis of diazoketoester **194**

2.5.4 Investigation of the Stevens [1,2]-shift

2.5.4.1 Preliminary results

The key sulfonium ylide rearrangement was examined next, under the standard conditions employed with **142a**, **142b** and **144** (Scheme 2.18 and 2.19). Upon heating in toluene at 100 °C in the presence of Cu(hfacac)₂, **194** provided a mixture of two products, one of which being the desired bicyclic oxocane **195** (entry 1, Table 2.6). The ¹H NMR spectrum for the mixture contained many overlapping signals, but the second

product had a pair of vicinal protons that appeared as distinctive doublets at 5.51 and 5.37 ppm. Additionally, the second product also had the same molecular weight as oxocane **195** by HRMS analysis. Nonetheless, the reaction outcome in this case was drastically different to the reaction of **144** under the same reaction conditions. In order to characterize the second product and confirm the result obtained in entry one, the first reaction was repeated on a larger-scale (entry 2 and entry 3). After careful chromatographic purification, the desired oxocane **195** was obtained as a single diastereomer in only minor amounts (16%), and the predominant second product (43%) was isolated as a 2:1 mixture of epimers at C7 (entry 3). The structure was determined to be monocyclic olefins **196** using a combination of 1D and 2D NMR experiments. For example, the previously mentioned vicinal protons were H8 and H9, and H8 showed correlation with C9 and C2 by HMBC. The small coupling constant for H8 and H9 was indicative of a *cis*-olefin. A singlet at 4.13 ppm in the ¹H NMR spectrum was assigned to H7, which also correlated with C4, C6 and C10 by HMBC. On the other hand, the structural assignment of **195** was further supported by the spectroscopic data of H8. In the starting diazoketoester **194**, H8 had chemical shift of 5.06 ppm in the ¹H NMR and showed correlations to C2 and C4, whereas in product **195**, the signal for H8 was at 4.26 ppm in the ¹H NMR and H8 showed correlation with C6, C7, C9 and C2. In addition, isolation of **196** as a pure product was complicated by its instability when subjected to silica gel chromatography, and this undoubtedly contributed to the diminished material balance.



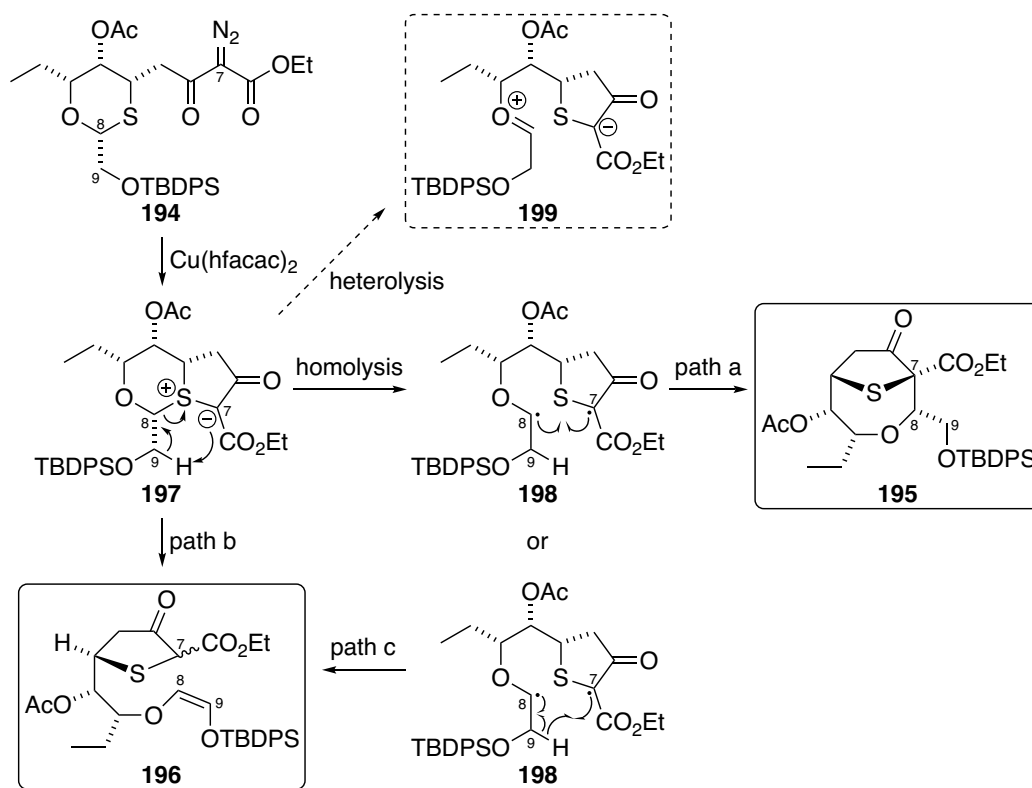
entry	scale	T (°C)	time (h)	yield (%) ^a	
				195	196^b
1	17.6 mg (0.029 mmol)	100	0.5	25	14
2	59.8 mg (0.098 mmol)	100	0.5	15	41
3	63.0 mg (0.103 mmol)	100	1	16	48 (<i>dr</i> = 2:1)
4	30.0 mg (0.049 mmol)	80	0.5	18	11 ^d

^a Isolated yield. ^b **196** was not very stable for column chromatography. ^c A mixture of **195** and **196** was obtained after column purification and the yield was determined by ¹H NMR. ^d Two chromatographic separations were performed.

Table 2.6 Preliminary result on the Stevens rearrangement of sulfonium ylide

For mechanistic considerations, a few pathways were proposed to rationalize the observed product formation. Upon the formation of sulfonium ylide **197** from diazoketoester **194** via a transient metalcarbene, the desired Stevens [1,2]-shift could occur through a homolytic mechanism proceeding through biradical intermediate **198** to generate **195** (path a, Scheme 2.36). Product **196** was presumed to form via α',β -elimination of intermediate sulfonium ylide **197** (path b). The α',β -elimination process has been noted in previous examples.⁸⁶ However, the elimination could also occur after bond homolysis via intramolecular abstraction of the hydrogen radical (path c). Nonetheless, in the case of the TBDPS-substituted substrate (**194**), α',β -elimination was the favorable pathway over the Stevens [1,2]-shift under the same reaction

conditions employed with benzyl-substituted substrate **144** (Scheme 2.19). The bulky silyl group might orient the β -proton in a favorable geometry for the elimination to take place.

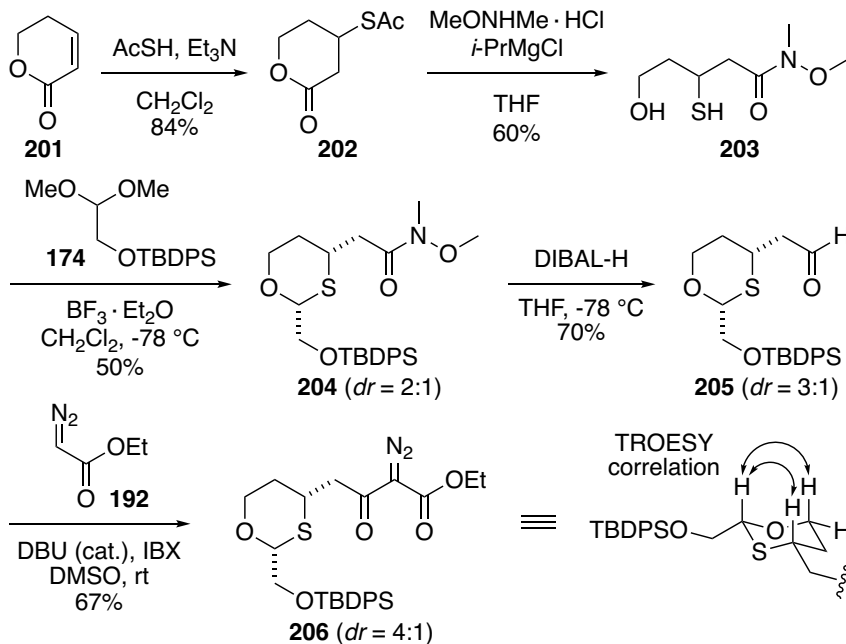


Scheme 2.36 Proposed mechanistic pathways

2.5.4.2 Model study

In an effort to find conditions that favored formation of **195**, we surveyed alternative conditions using the simplified model compound **206**, which was prepared from 5,6-dihydropyran-2-one **201** (Scheme 2.37). Michael addition with thioacetic acid afforded lactone **202**, and subsequent lactone ring opening with *N,O*-dimethylhydroxylamine in the presence of isopropylmagnesium chloride yielded mercaptoalcohol **203**. Sequential 1,3-oxathiane formation, DIBAL-H reduction and a one-pot coupling reaction with ethyl diazoacetate **192** furnished the desired model compound **206** as a 4:1 mixture of

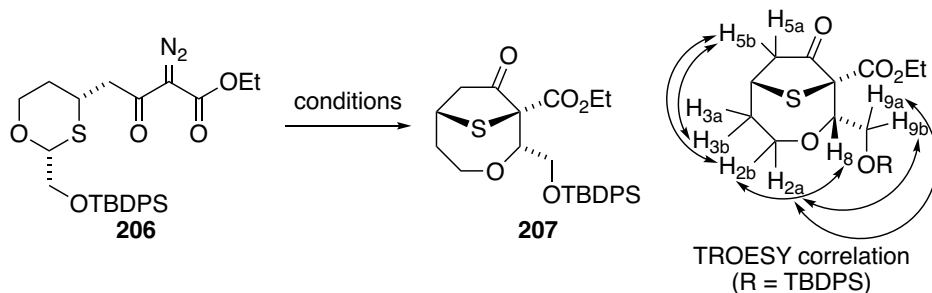
inseparable diastereomers. The major diastereomer had the *cis*-configuration for the two substituents on the six-membered ring, which was supported by the observed TROESY correlation.



Scheme 2.37 Preparation of model compound **206**

The model compound **206** was then used as the substrate to screen the reaction conditions (Table 2.7). The original reaction conditions only afforded the desired product **207** in 23% yield (entry 1). A complex mixture of products was obtained when dirhodium tetraacetate [$\text{Rh}_2(\text{OAc})_4$] was used as the catalyst (entry 2). As discussed in Chapter 1, Cu(I) is the active catalyst for diazo decomposition (Section 1.5.1). By stirring a mixture of 10 mol% $\text{Cu}(\text{OTf})_2$ and 10 mol% indole at room temperature for one hour, Cu(I) could be generated *in situ* (entry 3).⁸⁷ After addition of the diazoketoester **206**, the reaction mixture was stirred for 16 hours at room temperature and 16 hours at reflux. However, this method generated **207** in only 11% yield. In the end, we found that the formation of the desired [1,2]-shift product **207** could be achieved at relatively low temperatures (CH_2Cl_2 at reflux), albeit at the cost of longer

reaction times (entry 4). Product **207** was isolated as a single diastereomer in 84% yield, but it was difficult to determine the relative stereochemistry with the observed TROESY correlations.



entry	catalyst	solvent	T ($^{\circ}\text{C}$)	time	yield (%) ^a
					207
1	Cu(hfacac) ₂ (10 mol%)	PhMe	100	0.5 h	23
2	Rh ₂ (OAc) ₂ (5 mol%)	CH ₂ Cl ₂	reflux	16 h	- ^b
3	Cu(OTf) ₂ (10 mol%)	CH ₂ Cl ₂	rt	16 h	11
	indole (10 mol%)		reflux	16 h	
4	Cu(hfacac) ₂ (10 mol%)	CH ₂ Cl ₂	reflux	16 h	84

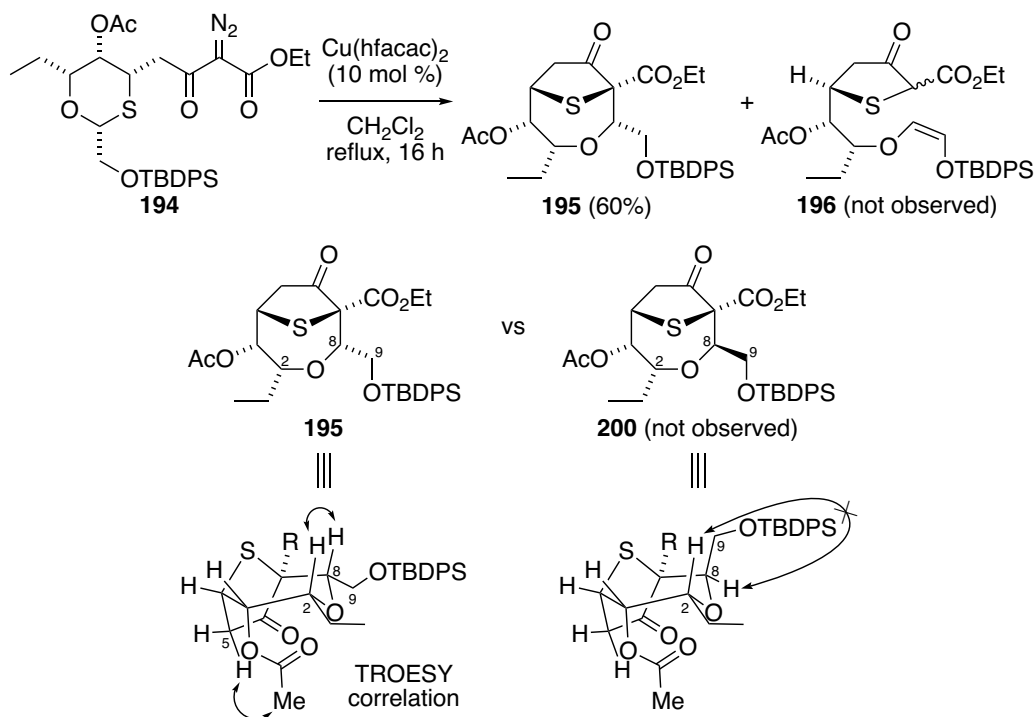
^a Isolated yield. ^b The rest of the mass balance was complex mixture. ^c Complex mixture was obtained.

Table 2.7 Screening of reaction conditions using model substrate 206

2.5.4.3 Investigation on the key step

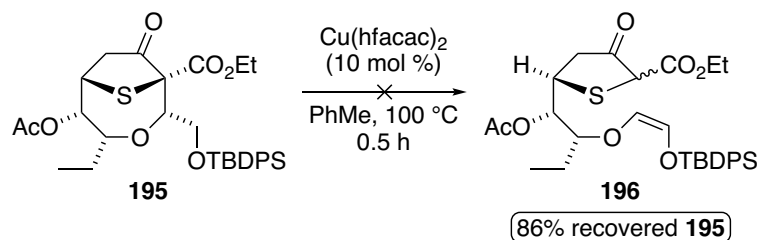
When **194** was subjected to the optimized conditions (entry 4, Table 2.7), the desired oxocane **195** was obtained in an acceptable yield (60%), uncontaminated with side-product **196** (Scheme 2.38). Most importantly, as in the model series, **196** was isolated as a single diastereomer. However, in this case, TROESY analysis provided unambiguous evidence for migration of the anomeric center with retention, an assignment that was confirmed through later correlation to the Holmes intermediates **58** and **59**. This result strongly suggests that the stereoselective rearrangement of model substrates **142a/142b** (Scheme 2.18) and **206** (Table 2.7) also occurred with retention,

as there is no plausible reason why the presence of fewer substituents on the oxathiane ring would result in a complete stereochemical reversal to migration with inversion.



Scheme 2.38 The key step under optimized reaction conditions

In addition, no conversion of **195** to **196** was observed when it was resubmitted to the original reaction conditions [$\text{Cu}(\text{hfacac})_2$ in toluene at 100 °C], as shown in Scheme 2.39. Only unreacted **195** was recovered in 86% yield, indicating that **195** resulted from a competing reactivity pathway of the sulfonium ylide intermediate rather than from a secondary reaction of the initially formed [1,2]-shift product.

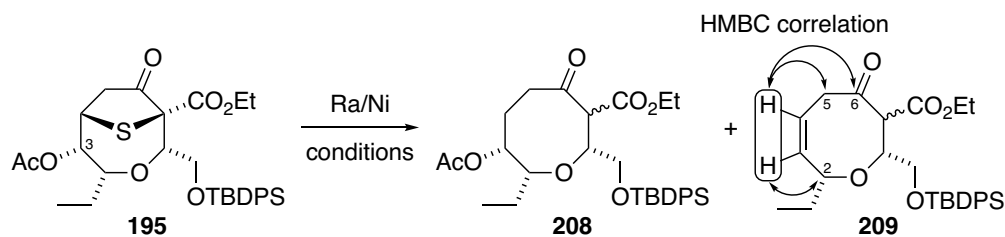


Scheme 2.39 Elimination of the reaction pathway from **195** to **196**

2.5.5 Synthesis of the Holmes intermediate **59**

2.5.5.1 Reductive desulfurization

Having successfully formed the sulfur-bridged oxocane **195**, it was now necessary to carry out the remaining transformations: reductive desulfurization, decarboxylation and olefin formation. The reductive desulfurization to remove the sulfur bridge was investigated first. When **195** was treated with Raney nickel 2800 in acetone, only 15% of the desired oxocane **209** was obtained, along with an unknown side product (entry 1, Table 2.8). The use of deactivated Raney nickel (pretreated by refluxing for two hours in acetone prior to the addition of **195**) did not improve the yield. When **195** was stirred with Raney nickel in EtOH at 0 °C, the yield of the desired product **209** was increased to 31% along with the same side product (entry 2). In this case, the side product was isolated in high purity and was determined to be oxocene **209**; formed *via* undesired elimination of the C3 acetate group. After a few more trials, improved yield of **208** was obtained when THF was used as the solvent (entry 5). However, the undesired elimination product **209** was also generated in 33%.



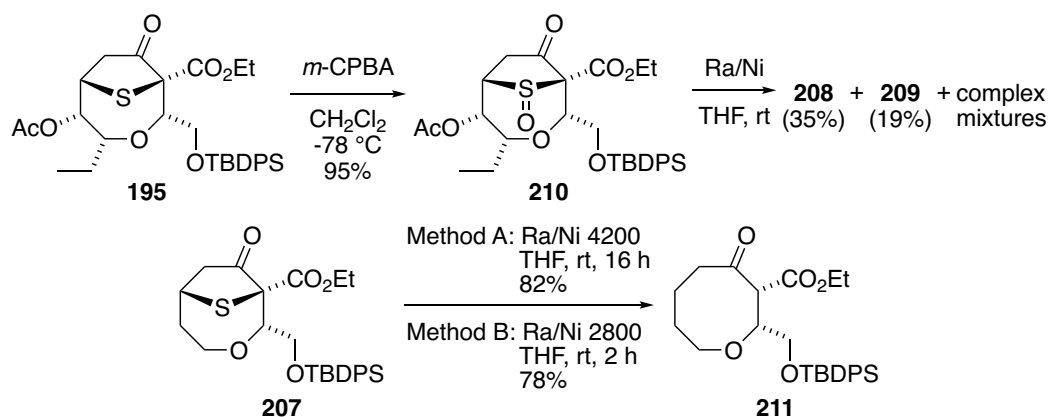
entry	Ra/Ni ^a	solvent	T (°C)	time	Yield (%) ^b	
					208	209
1	2800	acetone	rt	1 h	17	15
2	2800	EtOH	0	0.5 h	31	22
3	4200	EtOH	-20	15 min	10	5
4	2800	acetone	-20 to 0	1 h	11	6
5	2800	THF	rt	2 h	49	33

^a Raney nickel 2800 and 4200 were commercially available by Sigma Aldrich. The amount of Raney nickel used for each entry was around 30 to 40 times by weight based on the weight of starting material. ^b Isolated yield.

Table 2.8 Reaction optimization for the reductive desulfurization: part one

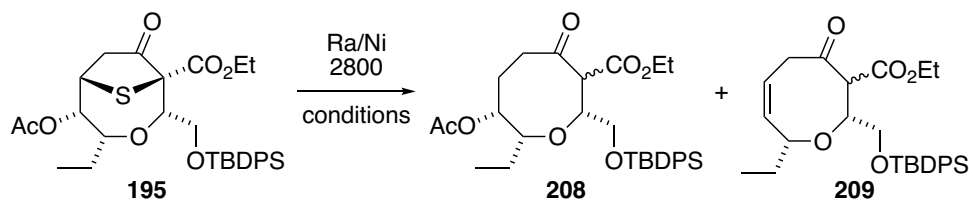
Formation of a significant amount of elimination product is undesired. In order to improve the overall productivity of the desulfurization step, we explored an alternative pathway. The sulfoxide group was also known to be readily cleaved in the presence of Raney nickel.⁸⁸ To test this strategy, the sulfide in **195** was converted to the corresponding sulfoxide (**210**) in the presence of *m*-chloroperoxybenzoic acid (*m*-CPBA) (Scheme 2.40). However, when the same reaction conditions (entry 5, Table 2.8) were applied using **210** as the starting material, the desired product **208** was obtained in only 35% yield. The undesired side product **209** was still formed in 19% yield, suggesting this alternative pathway to be ineffective. Additional reactions were carried out on the model sulfur-bridged oxacycle **207**, obtained from the model study of the key step, to test the two grades of Raney nickel reagent (4200 and 2800) that were purchased from Sigma-Aldrich. Oxocane **211** could be obtained in good yields using both Raney nickel reagents, but longer reaction times were needed when using

Raney nickel 4200, demonstrating the superior reactivity of Raney nickel 2800 for the entitled transformation. Formation of oxocane **211** in high yields further demonstrated the potential applicability of this methodology as an effective route for the synthesis of medium-sized cyclic ethers.



Scheme 2.40 Additional investigations into the reductive desulfurization

We envisioned that the residual basic content in Raney nickel might also lead to the elimination of the C3-acetate group. The reaction was further optimized as shown in Table 2.9. When a mixture of buffer (pH 5.0) and EtOH was used as solvent (entry 1, Table 2.9), similar yield to the reaction using THF as solvent (entry 5, Table 2.8) was obtained. The yield of **208** could be further improved by using 1.0 M AcOH and EtOH as solvent (entry 2, Table 2.9). Finally, we found that by using a 1:2 mixture of acetate buffer (pH = 4.6) and EtOH as solvent, Raney nickel desulfurization afforded the desired product **208** in 71% yield along with only 10% yield of elimination product **209** (entry 4).



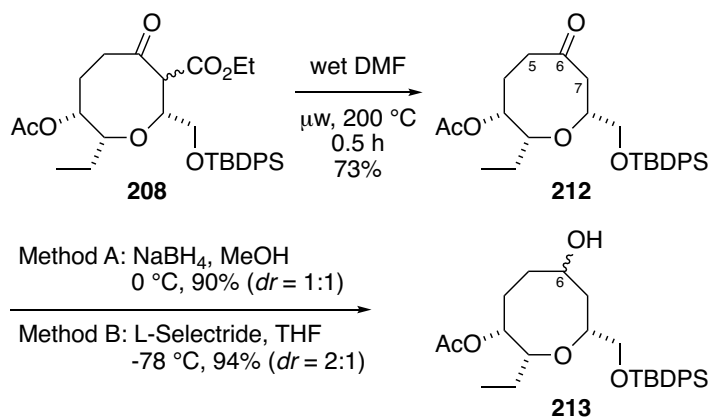
entry	solvent ^a	<i>T</i> (°C)	time	Yield (%) ^b	
				208	209
1	buffer (pH 5.0) ^c /EtOH (1:2)	rt	0.5 h	50	24
2	1.0 M AcOH/EtOH (1:2)	rt	0.5 h	67	trace ^d
3	buffer (pH 4.6) ^e /EtOH (1:2)	rt	1 h	70	trace ^d
4	buffer (pH 4.6) ^e /EtOH (1:2)	rt	0.5 h	71	10

^a Solvent ratios were by volume. ^b Isolated yield. ^c Potassium biphthalate sodium hydroxide buffer solution in pH 5.0. ^d **209** was isolated along with unidentified mixture of products. ^e Acetate buffer solution in pH 4.6.

Table 2.9 Reaction optimization for the reductive desulfurization: part two

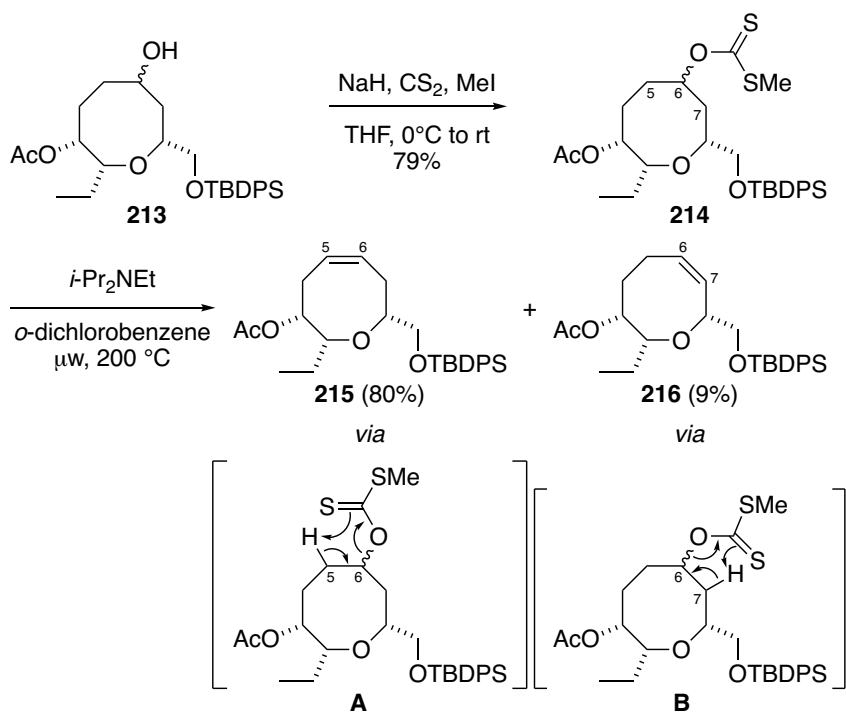
2.5.5.2 Olefin formation

The next task was to convert oxocane **208** to the desired oxocene by introducing the C5–C6 double bond. Oxocane **208** was first subjected to decarboxylation *via* microwave heating in aqueous DMF to afford ketone **212** in 73% yield (Scheme 2.41).⁸⁹ At this point, the ketone group could be converted to the corresponding endocyclic alkene using many different methods. However, regioselectivity could be a potential concern, as both the C5–C6 and C6–C7 double bonds could be formed. With that in mind, we started investigating olefination using Chugaev elimination.⁹⁰ Ketone **212** was first reduced with L-Selectride to form a 2:1 epimeric mixture of inseparable alcohols **213** (Method B). Sodium borohydride could also be used in the reduction step (Method A), but the diastereoselectivity was lower than with L-Selectride.



Scheme 2.41 Preparation of alcohols 213

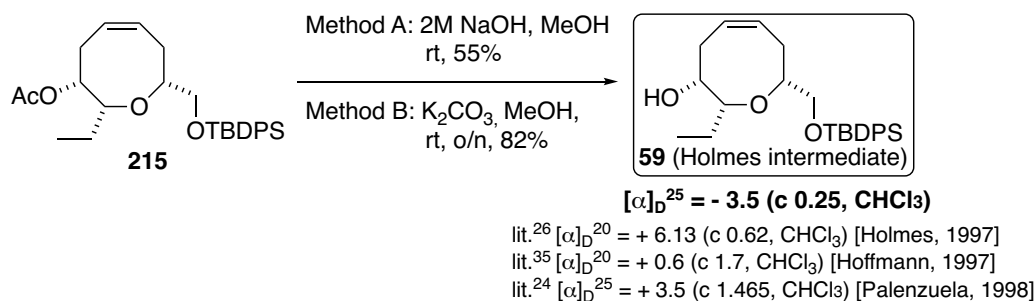
The epimeric mixture of alcohols **213** was converted into the xanthate esters **214** by sequential addition of sodium hydride (NaH), carbon disulfide (CS_2) and methyl iodide (MeI) (Scheme 2.43). Conversion to xanthate **214** set the stage for Chugaev elimination,⁹⁰ which was carried out by microwave heating ($200\text{ } ^\circ\text{C}$) in *o*-dichlorobenzene, furnishing two elimination products as a 9:1 mixture of the desired C5–C6 olefin **215** and the C6–C7 regioisomer **216**, which were readily separable by chromatography.



Scheme 2.42 Olefination by the Chugaev elimination

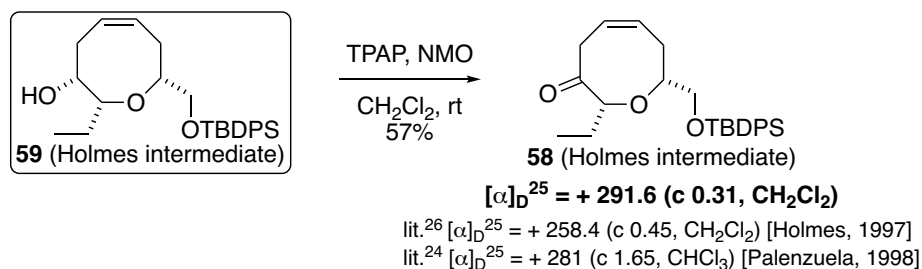
2.5.5.3 Completion of the formal synthesis of (+)-laurencin

To complete the formal synthesis of laurencin, **215** was subjected to acetate cleavage to provide **59**, which was previously reported by Holmes and coworkers.²⁶ While spectral data were in complete agreement (see comparison tables provided at the end of Section 2.7, Table 2.10 and Table 2.11), the specific rotation had the opposite sign as that reported in the original work and in the work by Hoffmann³⁵ and Palenzuela.²⁴ In all cases the absolute value of the rotation was small, allowing for significant error.



Scheme 2.43 Completion of the formal synthesis

Notably, another fully characterized advanced intermediate of laurencin, ketone **58**²⁶ had a much larger specific rotation. Alcohol **59** could be oxidized to **58** using tetrapropylammonium perruthenate (TPAP) and *N*-methylmorpholine *N*-oxide (NMO), and the spectral data were once again in full agreement (see comparison tables provided at the end of Section 2.7, Table 2.12 and Table 2.13). Moreover, the specific rotation was also in good agreement with the published values.^{26,24}



Scheme 2.44 Synthesis of ketone 58

2.6 Conclusion and future directions

We have described a novel, stereoselective route to functionalized medium-sized cyclic ethers *via* Stevens [1,2]-shift of sulfonium ylides derived from mixed monothioacetals (1,3-oxathianes). The substituted 1,3-oxathianes can be prepared *via* a short sequence. The relative and absolute stereochemical configurations were established by an asymmetric allylboration/oxidation (Section 2.5.3.1), a facially

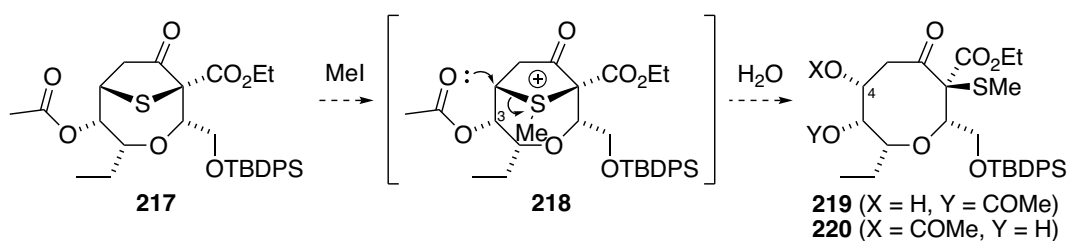
selective Michael addition (Section 2.5.3.2) and a stereoselective acetal formation (Section 2.5.3.4). In order to synthesize the requisite diazoketoester functionality from a γ -lactone ring, the Claisen condensation pathway (Section 2.5.3.6) and the Weinreb amide pathway (Section 2.5.3.7) were investigated. The former pathway was abandoned due to the formation of a product with erosion of stereochemistry. In the Weinreb amide approach, the desired diazoketoester side chain was readily synthesized. However, problems were encountered while trying to protect the axial hydroxyl group, which could not be converted to the desired PMB ether in compliance with the target Holmes intermediate. Alternatively, we protected the axial hydroxyl group as an acetate, which required an added hydrolysis at the end to synthesize another Holmes intermediate.

Interesting results were obtained during the investigation of the key step (Section 2.5.4). It was found that at elevated reaction temperatures, the major product was formed *via* α' , β -elimination of the sulfonium ylide, in competition with the desired Stevens [1,2]-shift. After surveying the reaction conditions using a model compound, the optimized reaction conditions were found to be in refluxing dichloromethane. Very importantly, the stereochemical information at the anomeric center is retained during migration. Subsequently, the sulfur-bridge could be efficiently removed with Raney nickel in a buffered solution to afford the oxocane ring. After the decarboxylation, the desired olefin was formed using the Chugaev elimination. In the event, an epimeric mixture of xanthate esters were subjected to microwave heating to provide a 9:1 mixture of olefin regioisomers with the desired isomer formed as the major isomer. At the end, two advanced intermediates from the Holmes' total synthesis of (+)-laurencin were achieved, adding another successful example to enrich the field of sulfur ylide Stevens rearrangement chemistry.

In conclusion, we utilized a highly stereoselective Stevens rearrangement as the key transformation to form the oxocane core of (+)-laurencin, which is a unique approach in comparison to the earlier synthesis discussed in Sections 2.2 and 2.3 (Figure 2.3). In some of previous syntheses that utilized the C–C bond formation as the key

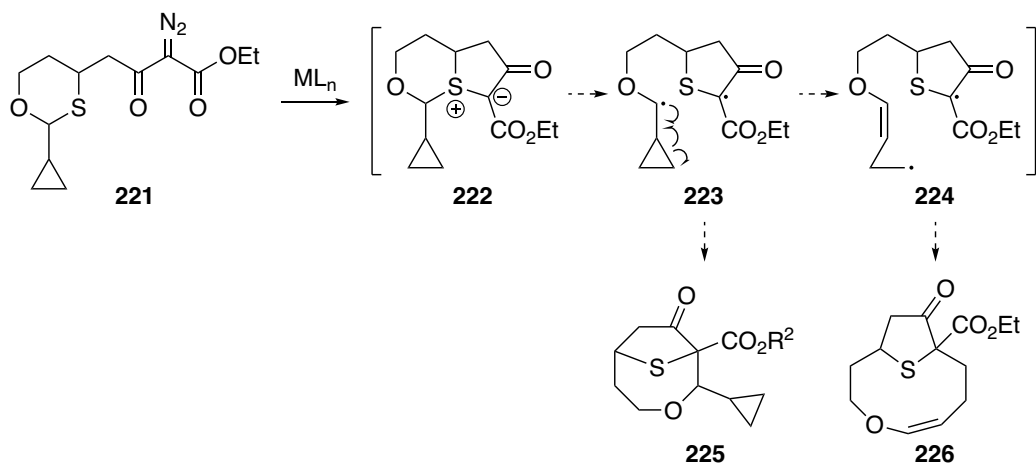
transformation to the eight-membered cyclic ethers, the formation of C–C bond were not stereoselective because the resulting C–C bond did not contain any stereocenters. Examples in this category including the ring closing metathesis approach used by Pansare, Martin, Fujiwara and Crimmins, and the sulfone anion epoxide opening approach by Paulenzuela. On the other hand, in the syntheses devised by Kim and Overman, the intramolecular alkylation and acetal-vinylsulfide cyclization reactions, respectively, allowed the stereoselective formation of C–C bond with one stereocenter. The intramolecular allylboration approach by Hoffmann led to the stereoselective formation of two stereocenters. In our Stevens rearrangement approach, the six-membered monothioacetal was efficiently transformed into an eight-membered cyclic ether with the formation of a new C–C bond and the stereochemical configuration of the migrating anomeric carbon is retained. The strategy worked efficiently on the simple model substrates and the highly substituted complex monothioacetal substrates, demonstrating the overall feasibility of this approach as a general and robust way to form eight-membered cyclic ethers.

In our approach to form eight membered cyclic ether, the product for the Stevens arrangement was a sulfur-bridged eight-membered cyclic ether and the sulfur bridge was subsequently removed. However, the sulfur bridge could potentially offer other possible interesting transformations. For example, if sulfide **217** was methylated, the resulting sulfonium intermediate (**218**) could undergo ring opening with the adjacent acetate group at C3. After aqueous work-up, a mixture of secondary alcohols **219** and **220** could be formed along with the generation of a new stereocenter at C4, which could be further transformed to build molecular complexity.



Scheme 2.45 Potential transformation of the sulfur bridged cyclic ether

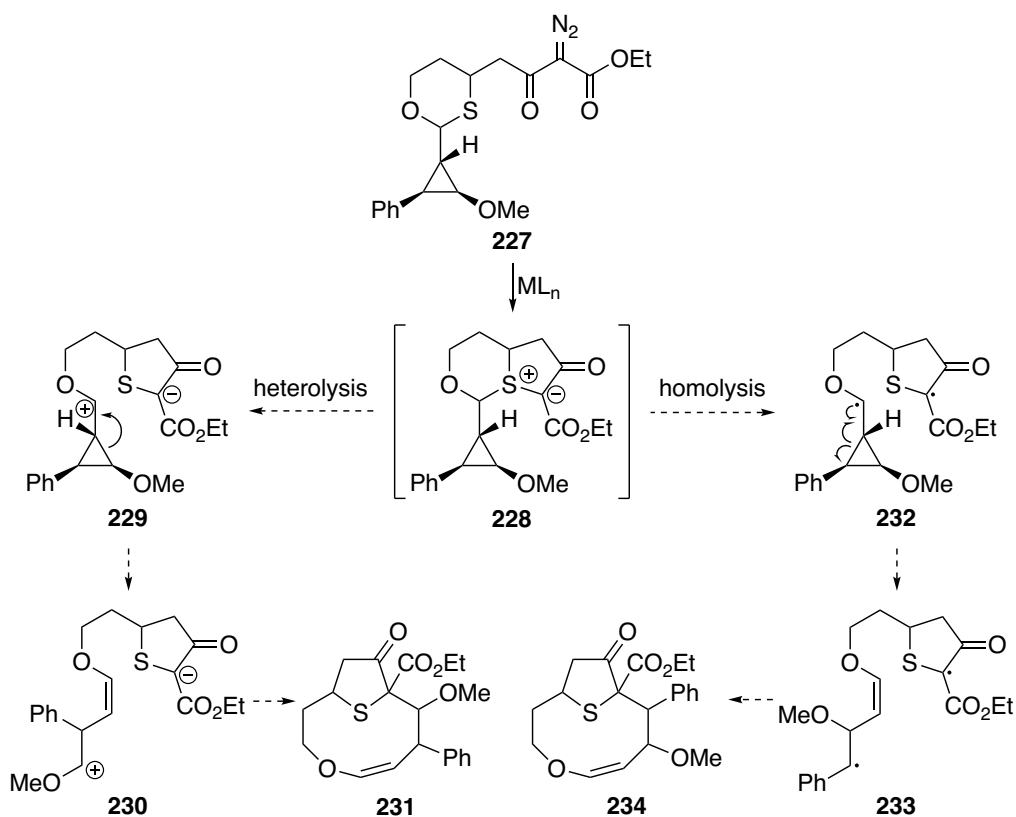
Future investigations could also be dedicated to resolve the actual mechanism involved in the Stevens rearrangement involving monothiacetal substrates, as this stepwise process could undergo both homolytic and heterolytic pathways involving biradical and zwitterionic intermediates, respectively. One possibility is to install a cyclopropane ring next to the migrating anomeric center, in which the cyclopropylcarbinyl moiety which could serve as a radical probe⁹¹ (Scheme 2.45). If the [1,2]-shift involves biradical intermediate **223**, the cyclopropane ring might be opened to afford biradical **224** and subsequently generate product **226**. However, it is also possible that the recombination of biradical **223** is faster than the cyclopropane ring opening to generate [1,2]-shift product **225**. Nevertheless, the result from this approach could provide valuable mechanistic insights.



Scheme 2.46 Proposal for the use of radical clock to probe the mechanism for the Stevens rearrangement

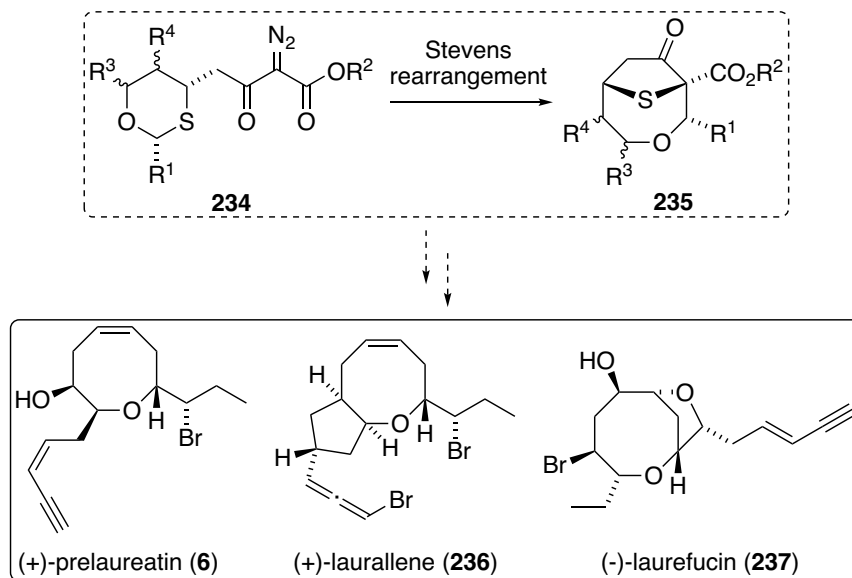
Alternatively, (*trans-trans*)-2-methoxy-3-phenylcyclopropyl group could be installed at the anomeric position (**227**) to distinguish between radical and carbocation intermediates (Scheme 2.46).⁹² In this design, the phenyl group could stabilize a radical more efficiently than the methoxy group, while carbocations are more stabilized by the methoxy group. Therefore, the cyclopropane ring opening occurs with high

regioselectivity under distinctive reaction pathways involving radical and carbocation intermediates, which will furnish different products reflecting the nature of the active intermediates in the reaction mechanism. In particular, if sulfonium ylide **228** undergoes heterolytic cleavage of the C-S bond, cyclopropylcarbinyl cation **229** would undergo ring opening towards the methoxy group to generate zwitterionic intermediate **230** and provide product **231**. On the other hand, if homolytic cleavage is involved, the cyclopropylcarbinyl radical would undergo ring opening towards the phenyl group to form biradical **233**, which recombines to furnish product **234**. This investigation could provide important mechanistic evidence to differentiate homolytic and heterolytic pathways.



Scheme 2.47 Proposal for the use of (*trans-trans*)-2-methoxy-3-phenylcyclopropyl substituent to differentiate reaction pathways

Despite the actual mechanism, the Stevens rearrangement worked efficiently with both simple and highly functionalized 1,3-oxathiane substrates having a pendant diazoketoester group. We believe this methodology could be amenable towards the synthesis of other interesting natural products containing medium-sized cyclic ether framework, including prelaurenatin (**6**),⁹³ laurallene (**236**),⁹³ and laurefucin (**237**).⁹⁴



Scheme 2.48 Future applications of the Stevens rearrangement chemistry

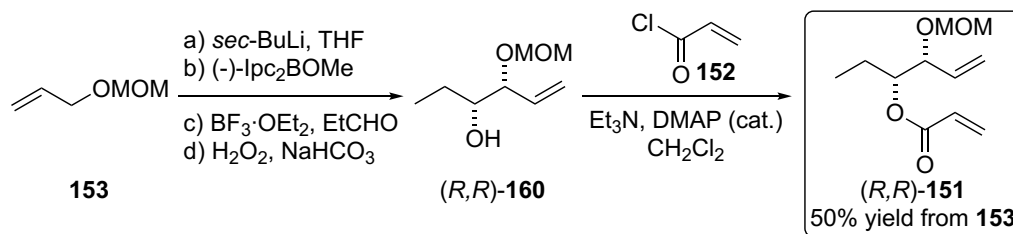
Having successfully synthesized functionalized oxocanes, we envisioned a similar methodology to access medium-sized azacycles, which is another important structural motif occurred in natural products. Efforts towards the synthesis of medium-sized azacycles *via* Stevens [1,2]-shifts will be described in Chapter 3.

2.7 Experimental

2.7.1 General Information

Reactions were conducted in oven-dried (120 °C) or flame-dried glassware under a positive argon or nitrogen atmosphere unless otherwise stated. Transfer of anhydrous solvents or mixtures was accomplished with oven-dried syringes or via cannulae. Solvents were distilled before use: methylene chloride (CH₂Cl₂) from calcium hydride; tetrahydrofuran (THF), diethylether (Et₂O) from sodium/benzophenone ketyl; toluene (PhMe) from sodium metal; dimethylsulfoxide (DMSO) from calcium hydride. BF₃·Et₂O was distilled before use. Propionaldehyde was dried over 4Å molecular sieves overnight and distilled before use. All other solvents and commercially available reagents were either purified by standard procedures or used without further purification. Thin layer chromatography (TLC) was performed on glass plates precoated with 0.25 mm Kiesegel 60 F₂₅₄ (Merck); the stains for TLC analysis were conducted with 2.5% *p*-anisaldehyde in AcOH-H₂SO₄-EtOH (1:3:90) and further heating until development of color. Flash chromatography columns were packed with 230-240 mesh silica gel and performed with the indicated eluents. Microwave heating was carried out in a Biotage Initiator microwave reactor using 0.5-2 mL microwave vials. Reaction temperature was determined through measurement of the vial surface temperature using an infrared sensor, then correction of internal temperature by the unit's processor using a proprietary algorithm. Proton Nuclear magnetic resonance (¹H NMR) spectra were recorded at 500 MHz or 700 MHz in indicated deuterated solvents and coupling constants (*J*) were reported in Hertz (Hz). Splitting patterns were designated as s, singlet; d, doublet; t, triplet; q, quartet; m, multiplet; br, broad; dd, doublet of doublets, etc. The chemical shifts were reported on the δ scale (ppm) and the spectra were referenced to residual solvent peaks: CDCl₃ (7.26 ppm for ¹H NMR; 77.16 ppm for ¹³C NMR). Carbon nuclear magnetic resonance spectra (¹³C NMR) were recorded at 125 MHz and the chemical shifts were reported to the nearest 0.1 ppm to reflect the digital resolution of the data. In some cases, two nearly overlapping resonances were reported to the nearest 0.01 ppm to distinguish them from each other.

Infrared (IR) spectra were recorded neat and reported in cm^{-1} . Mass spectra were recorded by using ESI or EI as specified in each case. Values for specific rotation ($[\alpha]_{\text{D}}^{25}$) were reported in units of $\text{deg cm}^2 \text{g}^{-1}$.

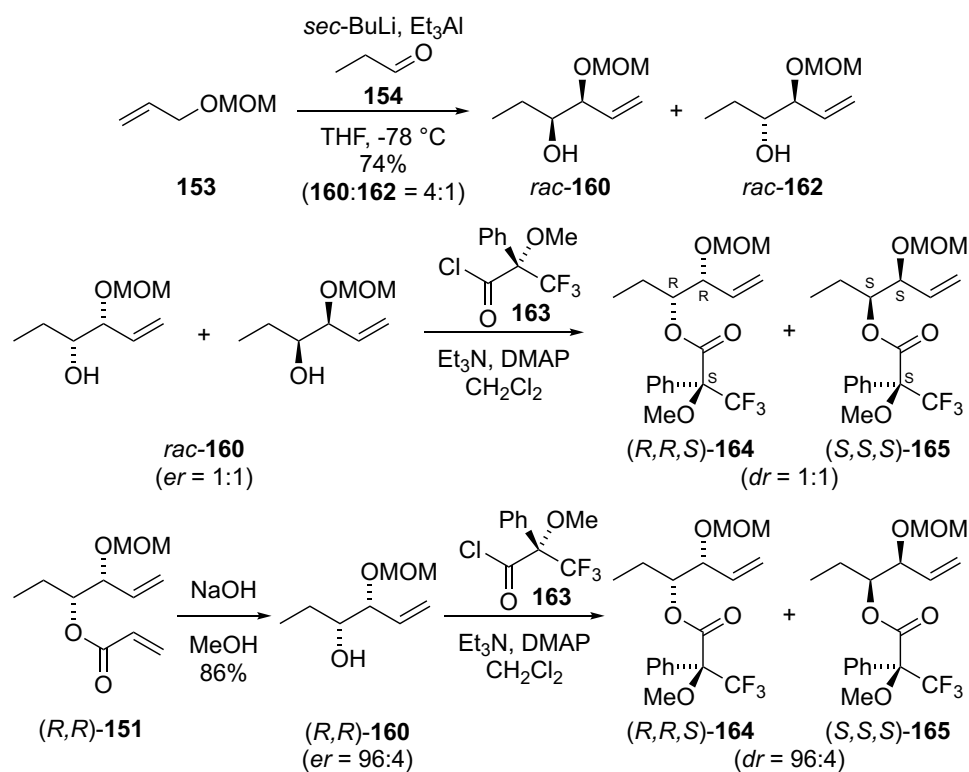


1-(Methoxymethoxy)-2-propene **153** was prepared following procedure described by Yamamoto and coworkers.⁷⁴ Homoallylic alcohol (*R,R*)-**160** was prepared by the procedure described by Brown and co-workers²¹ with modifications as described below.

Acrylate ester (*R,R*)-151. To a solution of **153** (1.85 g, 18.1 mmol) in THF (40 mL) at -78 °C was added *sec*-BuLi (1.35 M in cyclohexane, 12.3 mL, 16.5 mmol) dropwise over 30 minutes. After stirring at -78 °C for additional 30 minutes, a solution of (-)-*B*-methoxydiisopinocampheylborane (Aldrich, 5.24 g, 16.6 mmol) in THF (17 mL) was added dropwise over 30 minutes and the mixture was stirred for 1 h before cooling to about -95 °C in MeOH/liquid nitrogen bath. BF₃·Et₂O (3.00 mL, 23.7 mmol) was then added dropwise followed by a solution of propionaldehyde (1.17 mL, 15.8 mmol) in THF (10 mL). The mixture was stirred at -95 °C for 3 h and then allowed to warm up gradually overnight in the cooling bath to a final temperature of about 5 °C. The solvent was removed under vacuum and the residue was dissolved in CH₂Cl₂ (100 mL). The solution was cooled to 0 °C and added 30% H₂O₂ solution (30 mL) and saturated NaHCO₃ solution (60 mL). The mixture was stirred for 6 h at room temperature. The aqueous layer was extracted with CH₂Cl₂ (2×40 mL). The combined organic layers were washed with brine (100 mL), dried with anhydrous MgSO₄ and filtered to provide

a solution of crude product ((*R,R*)-**160** and its erythro diastereomer) and isopinocampyl alcohol in CH₂Cl₂. To this solution was added trimethylamine (13.6 mL, 97.7 mmol) and 4-dimethylmethylaminopyridine (0.60 g, 4.9 mmol) at 0 °C, followed by dropwise addition of acryloyl chloride **152** (7.00 mL, 86.4 mmol). The mixture was stirred for an additional 30 minutes at room temperature and poured into water (150 mL). The aqueous layer was extracted with CH₂Cl₂ (2×20 mL). The combined organic layers were washed with saturated NH₄Cl solution (2×100 mL), brine (100 mL), dried over anhydrous MgSO₄, filtered and concentrated. Careful column chromatography (silica gel, 5% EtOAc/hexanes) provided (*R,R*)-**151** (1.69 g, 50% for 2 steps) as a colorless oil: R_f 0.32 (10% EtOAc/hexanes); [α]_D²⁵ = - 55.3 (c 1.96, CHCl₃); IR (cast film) 3081, 2972, 2940, 2887, 1725, 1638, 1620, 1406, 1296, 1270, 1196, 1149, 1095, 1038 cm⁻¹; ¹H NMR (500 MHz, CDCl₃) δ 6.43 (dd, *J* = 17.2, 1.5 Hz, 1H), 6.17 (dd, *J* = 17.3, 10.4 Hz, 1H), 5.83 (dd, *J* = 10.4, 1.5 Hz, 1H), 5.69 (ddd, *J* = 17.2, 10.4, 7.5 Hz, 1H), 5.34-5.30 (m, 1H), 5.30-5.28 (m, 1H), 5.02 (ddd, *J* = 8.6, 5.7, 4.4 Hz, 1H), 4.68 (d, *J* = 6.8 Hz, 1H), 4.51 (d, *J* = 6.8 Hz, 1H), 4.16-4.21 (m, 1H), 3.35 (s, 3H), 1.79-1.70 (m, 1H), 1.67-1.57 (m, 1H), 0.92 (t, *J* = 7.5 Hz, 3H); ¹³C NMR (125 MHz, CDCl₃) δ 166.1, 134.2, 131.0, 128.7, 119.8, 94.0, 77.6, 76.4, 55.7, 23.6, 9.7; HRMS (ESI, [M+Na]⁺) calcd for C₁₁H₁₈O₄Na 237.1097, found: *m/z* 237.1095.

Note: Due to the hygroscopic nature of (-)-*B*-methoxydiisopinocampheylborane, the reagent bottle was sealed with septum immediately after the first opening and was purged with argon. THF was then added to the bottle to dissolve the whole content and the solution was transferred to a syringe. The reagent bottle was weighed before and after to obtain the actual weight of reagent used in the reaction. Complete separation of the major threo diastereomer (*R,R*)-**151** with the minor erythro diastereomer was achieved by column chromatography. Determination of the enantiomeric ratio for (*R,R*)-**151** and the absolute configuration is described below.



Racemic alcohol *rac*-160. A modified procedure⁷⁴ was applied. To a solution of **153** (1.00 g, 9.79 mmol) in THF (50.0 mL) at -78 °C was added *sec*-BuLi (1.1M in cyclohexane, 9.5 mL, 10.5 mmol) dropwise by syringe. After stirring at -78 °C for 30 minutes, Et₃Al (1.0M in hexanes, 10.5 mL, 10.5 mmol) was added followed by addition of propionaldehyde (0.70 mL, 9.8 mmol). The mixture was warmed up to 0 °C and quenched by slow addition of saturated NH₄Cl solution (30 mL). The resulting mixture was filtered through a celite pad and rinsed with Et₂O (20 mL). The aqueous layer was extracted with Et₂O (2×20 mL). The combined organic layers were washed with brine (50 mL), dried with anhydrous MgSO₄, filtered and concentrated to give an inseparable mixture of threo and erythro 1,2-diol derivatives (1.69 g, 74%, *dr* = 4:1 by ¹H NMR). The alcohols were converted to the corresponding acrylate esters (racemic mixture of **151** and their erythro diastereomers) to allow separation by column chromatography as described above to provide a racemic mixture of **151** as a colorless oil (0.93 g, 44% for 2 steps). The racemic mixture of **151** was then hydrolyzed with NaOH as described below to provide *rac*-**160** as a yellow oil.

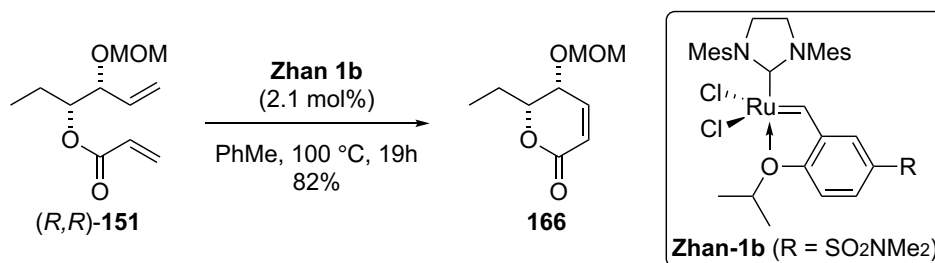
Alcohol (*R,R*)-160. To a solution of (*R,R*)-**151** (from the asymmetric allylboration step, 50 mg, 0.23 mmol) in methanol (2.0 mL) was added 3M NaOH solution (0.54 mL, 1.6 mmol) and the mixture was stirred at room temperature for 2 h before adding into a mixture of Et₂O (10 mL) and saturated NH₄Cl solution (10 mL). The aqueous layer was extracted with Et₂O (2×10 mL). The combined organic layers were washed with brine (15 mL), dried over anhydrous MgSO₄, filtered and concentrated to provide (*R,R*)-**160** (32 mg, 86%) as a yellow oil: *R_f* 0.28 (20% EtOAc/hexanes); IR (cast film) 3464, 3079, 2962, 2936, 2887, 1642, 1153, 1137, 1041, 970, 922 cm⁻¹; ¹H NMR (500 MHz, CDCl₃) δ 5.74-5.65 (m, 1H), 5.34-5.32 (m, 1H), 5.30 (ddd, *J* = 6.5, 1.7, 0.7 Hz, 1H), 4.74 (d, *J* = 6.7 Hz, 1H), 4.58 (d, *J* = 6.7 Hz, 1H), 3.87 (dd, *J* = 7.3, 7.3 Hz, 1H), 3.47 (dddd, *J* = 8.4, 6.7, 3.7, 3.7 Hz, 1H), 3.40 (s, 3H), 2.51 (d, *J* = 3.7 Hz, 1H), 1.64-1.55 (m, 1H), 1.48-1.38 (m, 1H), 1.00 (t, *J* = 7.5 Hz, 3H); ¹³C NMR (125 MHz, CDCl₃) δ 135.1, 120.0, 94.1, 81.2, 74.8, 55.9, 25.7, 10.0; HRMS (ESI, [M+Na]⁺) calcd for C₈H₁₆O₃Na 183.0992, found: *m/z* 183.0995.

Mosher esters⁷⁶ (*R,R,S*)-164 and (*S,S,S*)-165. General Procedure. To a solution of the alcohol (*R,R*)-**160** or *rac*-**160** (9 mg, 0.06 mmol) in CH₂Cl₂ (1.0 mL) at room temperature was added triethylamine (16 μL, 0.11 mmol) and 4-dimethylaminopyridine (one small crystal). (*R*)-(-)-MPTA-Cl (Aldrich, 22 mg, 0.087 mmol) was added and the mixture was stirred at room temperature for 4 h. The solvent was then removed under vacuum. Et₂O (2 mL) was added to the residue to precipitate out trimethylamine HCl salt, which was then filtered out and rinsed forward with excess Et₂O. The filtrate was concentrated and quick column chromatography by a short plug (silica gel, 10% EtOAc/hexanes) provided a mixture of (*R,R,S*)-**164** and (*S,S,S*)-**165**. The diastereomeric ratios of (*R,R,S*)-**164** and (*S,S,S*)-**165** obtained from ¹H NMR and ¹⁹F NMR spectra would dictate the enantiomeric ratios of the starting alcohols ((*R,R*)-**160** or *rac*-**160**). (Note: column chromatography was performed quickly on a short plug to avoid potential separation of (*R,R,S*)-**164** and (*S,S,S*)-**165**. As a result, the ¹H NMR spectra may contain peaks from impurities or reagents.) The absolute configurations of

the two stereogenic centers for (*R,R*)-**160** were also determined to be *R* and *R*, using method described by Mosher and co-workers.^{76b}

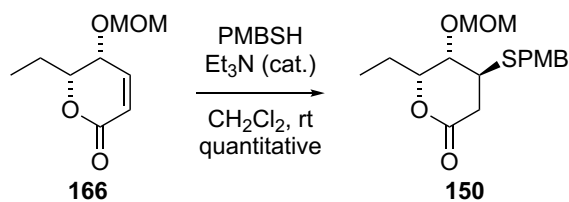
(*R,R,S*)-**164**: R_f 0.55 (20% EtOAc/hexanes); ^1H NMR (500 MHz, CDCl_3) δ 7.60-7.57 (m, 2H), 7.42-7.39 (m, 3H), 5.57 (ddd, $J = 17.0, 10.7, 7.6$ Hz, 1H), 5.27-5.24 (m, 1H), 5.22 (ddd, $J = 9.7, 1.5, 0.9$ Hz, 1H), 5.11 (ddd, $J = 8.0, 6.1, 4.3$ Hz, 1H), 4.55 (d, $J = 7.0$ Hz, 1H), 4.43 (d, $J = 7.0$ Hz, 1H), 4.14-4.10 (m, 1H), 3.21 (s, 3H), 1.88-1.76 (m, 1H), 1.72-1.56 (m, 1H), 0.96 (t, $J = 7.5$ Hz, 3H); ^{19}F NMR (469 MHz, CDCl_3) δ 71.42.

(*S,S,S*)-**165**: R_f 0.55 (20% EtOAc/hexanes); ^1H NMR (500 MHz, CDCl_3) δ 7.60-7.57 (m, 2H), 7.42-7.39 (m, 3H), 5.68 (ddd, $J = 17.6, 10.0, 7.8$ Hz, 1H), 5.37-5.35 (m, 1H), 5.35-5.33 (m, 1H), 5.13 (ddd, $J = 8.0, 6.6, 4.0$ Hz, 1H), 4.68 (d, $J = 6.7$ Hz, 1H), 4.55 (d, $J = 6.7$ Hz, 1H), 4.20-4.16 (m, 1H), 3.30 (s, 3H), 1.88-1.76 (m, 1H), 1.72-1.56 (m, 1H), 0.84 (t, $J = 7.5$ Hz, 3H); ^{19}F NMR (469 MHz, CDCl_3) δ 71.30.

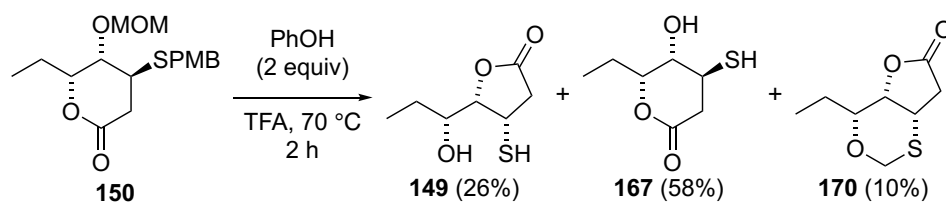


Dihydropyranone 166 (entry 3). Degassed toluene (60 mL) was added to (*R,R*)-**151** (0.265 g, 1.24 mmol) in the reaction flask. The mixture was heated to reflux and further degassed by bubbling with nitrogen using a long needle for 1 h. The mixture was then cooled to 100 °C and a solution of Zhan-1b (8.6 mg, 0.012 mmol) in toluene (10 mL) was added by cannula. After stirring at 100 °C for 4 h, a solution of Zhan-1B (11 mg, 0.014 mmol) in toluene (10.0 mL) was added by cannula. The mixture was stirred at 100 °C for 15 h and then cooled to room temperature. The solvent was removed under vacuum. Column chromatography (silica gel, 20%, 30%, 35% EtOAc/hexanes) provided **166** (0.190 g, 82%) as a slightly tanned oil: R_f 0.19 (40% EtOAc/hexanes);

$[\alpha]_D^{25} = -228.0$ (c 1.64, CHCl_3); IR (cast film) 3066, 2972, 2940, 2888, 1721, 1631, 1465, 1381, 1253, 1150, 1113, 1092, 1025, 919, 826 cm^{-1} ; ^1H NMR (500 MHz, CDCl_3) δ 7.02 (dd, $J = 9.7, 5.5$ Hz, 1H), 6.14 (d, $J = 9.7$ Hz, 1H), 4.73 (d, $J_{AB} = 7.0$ Hz, 1H), 4.67 (d, $J_{AB} = 7.0$ Hz, 1H), 4.28 (ddd, $J = 8.2, 6.0, 2.8$ Hz, 1H), 4.01 (dd, $J = 5.5, 2.8$ Hz, 1H), 3.36 (s, 3H), 2.02-1.92 (m, 1H), 1.86-1.77 (m, 1H), 1.06 (t, $J = 7.5$ Hz, 3H); ^{13}C NMR (125 MHz, CDCl_3) δ 163.6, 143.7, 123.6, 96.4, 81.8, 66.9, 56.0, 23.4, 9.8; HRMS (ESI, $[\text{M}+\text{Na}]^+$) calcd for $\text{C}_9\text{H}_{14}\text{O}_4\text{Na}$ 209.0784, found: m/z 209.0782.



δ -Lactone 150. To a solution of **166** (0.756 g, 4.06 mmol) in CH_2Cl_2 (40 mL) at room temperature was added triethylamine (0.11 mL, 0.81 mmol) and *p*-methoxybenzothiol (0.90 mL, 6.5 mmol). After stirring at room temperature overnight, the solvent was removed under vacuum. Column chromatography (silica gel, 25%, 30%, 35% EtOAc/hexanes) provided **150** (1.35 g, quantitative yield) as a colorless oil: R_f 0.33 (40% EtOAc/hexanes); $[\alpha]_D^{25} = -3.5$ (c 1.78, CHCl_3); IR (cast film) 2968, 2937, 2837, 1736, 1610, 1512, 1249, 1150, 1024 cm^{-1} ; ^1H NMR (500 MHz, CDCl_3) δ 7.26-7.23 (m, 2H), 6.88-6.84 (m, 2H), 4.61 (d, $J_{AB} = 7.1$ Hz, 1H), 4.54 (d, $J_{AB} = 7.1$ Hz, 1H), 4.52 (ddd, $J = 8.0, 5.9, 1.8$ Hz, 1H), 3.80 (s, 3H), 3.78 (d, $J_{AB} = 13.8$ Hz, 1H), 3.73 (d, $J_{AB} = 13.8$ Hz, 1H), 3.70 (d, $J = 3.0, 1.8$ Hz, 1H), 3.35 (s, 3H), 3.16 (ddd, $J = 7.2, 4.0, 3.1$ Hz, 1H), 2.99 (dd, $J = 17.7, 7.2$ Hz, 1H), 2.46 (dd, $J = 17.7, 4.0$ Hz, 1H), 1.92-1.82 (m, 1H), 1.71-1.61 (m, 1H), 1.00 (t, $J = 7.5$ Hz, 3H); ^{13}C NMR (125 MHz, CDCl_3) δ 169.4, 159.2, 130.1, 129.2, 114.3, 95.8, 79.9, 73.1, 56.3, 55.5, 39.1, 35.6, 33.0, 24.3, 9.8; HRMS (EI, M^+) calcd for $\text{C}_{17}\text{H}_{24}\text{O}_5\text{S}$ 340.1345, found: m/z 340.1343.



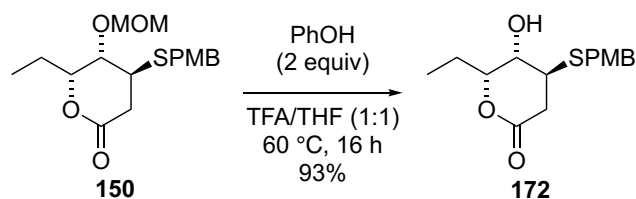
δ -lactone 167. To a solution of **150** (206 mg, 0.605 mmol) in trifluoroacetic acid (3 mL) at room temperature was added phenol (115 mg, 1.22 mmol). After stirring at 70 °C for 2 h, the reaction mixture was cooled to room temperature. The solvent was removed under vacuum and the residue was diluted with CH₂Cl₂ (30 mL). Saturated NaHCO₃ solution (20 mL) was added and the aqueous layer was extracted with CH₂Cl₂ (2×20 mL). The combined organic layers were washed with brine (30 mL), dried over anhydrous MgSO₄, filtered and concentrated. Column chromatography (silica gel, 10%, 20%, 25% EtOAc/CH₂Cl₂) provided **149** (28 mg, 26%) as a clear and colorless oil. The rest of fractions were combined and the second column chromatography was performed to provide **167** (62 mg, 58% yield) as a slightly yellow oil and **170** (11 mg, 10% yield) as a yellow oil.

149: characterization data was provided at the end of the reaction for PMB deprotection of **171**.

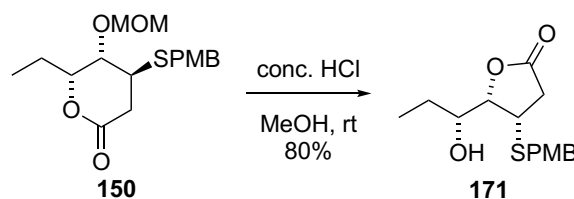
167: *R_f* 0.27 (20% EtOAc/ CH₂Cl₂); IR (cast film) 3403 (br), 2978, 2943, 1787, 1168 cm⁻¹; ¹H NMR (500 MHz, CDCl₃) δ 5.44 (ddd, *J* = 7.5, 5.9, 4.6 Hz, 1H), 4.64 (dd, *J* = 6.8, 4.6 Hz, 1H), 3.89-3.80 (m, 1H), 2.98 (dd, *J* = 17.7, 8.5 Hz, 1H), 2.61 (dd, *J* = 17.7, 7.6 Hz, 1H), 1.97-1.88 (m, 1H), 1.88-1.78 (m, 1H), 1.81 (d, *J* = 8.1 Hz, 1H), 1.02 (t, *J* = 7.5 Hz, 3H); ¹³C NMR (125 MHz, CDCl₃) δ 173.1, 80.9, 78.9, 38.8, 35.1, 23.2, 9.3; HRMS (ESI, [M+Na]⁺) calcd for C₇H₁₂O₃SNa 199.0399, found: *m/z* 199.0400.

170: *R_f* 0.60 (20% EtOAc/ CH₂Cl₂); IR (cast film) 2975, 2938, 1787, 1179, 1076 cm⁻¹; ¹H NMR (500 MHz, CDCl₃) δ 4.82 (d, *J_{AB}* = 11.0 Hz, 1H), 4.80 (d, *J_{AB}* = 11.0 Hz, 1H), 4.20 (dd, *J* = 3.6, 1.8 Hz, 1H), 3.93 (d, *J* = 6.1, 3.6 Hz, 1H), 3.44 (ddd, *J* = 8.2, 5.7, 1.8 Hz, 1H), 2.94 (d, *J* = 17.3, 6.1 Hz, 1H), 2.43 (d, *J* = 17.3 HZ, 1H), 1.94-1.83 (m, 1H), 1.77-1.66, (m, 1H), 1.02 (t, *J* = 7.5 Hz, 3H); ¹³C NMR (125 MHz, CDCl₃) δ 174.4,

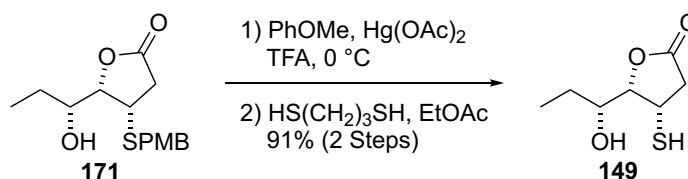
79.1, 73.6, 69.2, 38.5, 37.6, 25.6, 10.0; HRMS (EI, M^+) calcd for $C_8H_{12}O_3S$ 188.0507, found: m/z 188.0508.



δ -lactone 172. To a solution of **150** (55 mg, 0.16 mmol) in trifluoroacetic acid (1 mL) and THF (4 mL) at room temperature was added phenol (33 mg, 0.35 mmol). After stirring at 60 °C for 1 h, no conversion was observed by TLC. More trifluoroacetic acid (3 mL) was added to the reaction mixture. After stirring at 60 °C for 16 h, the reaction mixture was cooled to room temperature. The mixture was diluted with Et_2O (10 mL). The organic layer was washed with saturated $NaHCO_3$ solution (3 \times 15 mL) and the aqueous layer was extracted with Et_2O (2 \times 10 mL). The combined organic layers were washed with brine (20 mL), dried over anhydrous $MgSO_4$, filtered and concentrated. Column chromatography (silica gel, 20% $EtOAc$ /hexanes) provided **172** (45 mg, 93%) as a clear and colorless oil: R_f 0.44 (40% $EtOAc$ / hexanes); IR (cast film) 3410 (br), 2975, 2943, 2840, 1788, 1610, 1513, 1465, 1223, 1168 cm^{-1} ; 1H NMR (500 MHz, $CDCl_3$) δ 7.24-7.20 (m, 2H), 6.91-6.87 (m, 2H), 4.98 (ddd, $J = 7.2, 7.2, 2.3$ Hz, 1H), 4.30 (dd, $J = 8.0, 2.3$ Hz, 1H), 3.81 (s, 3H), 3.75 (d, $J_{AB} = 14.0$ Hz, 1H), 3.70 (d, $J_{AB} = 14.0$ Hz, 1H), 3.58 (ddd, $J = 11.2, 9.2, 8.0$ Hz, 1H), 2.68 (dd, $J = 17.7, 9.2$ Hz, 1H), 2.47 (dd, $J = 17.7, 11.2$ Hz, 1H), 1.77-1.64 (m, 2H), 0.80 (t, $J = 7.5$ Hz, 3H); ^{13}C NMR (125 MHz, $CDCl_3$) δ 173.7, 159.5, 130.0, 129.7, 114.6, 80.0, 79.1, 55.5, 40.8, 37.0, 35.0, 23.4, 9.3; HRMS (ESI, $[M+Na]^+$) calcd for $C_{15}H_{20}O_4SNa$ 319.0975, found: m/z 319.0972.



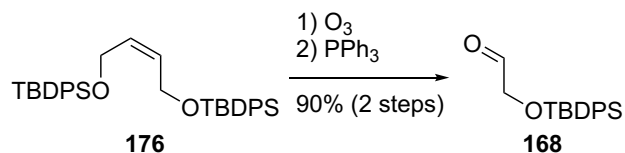
δ -Lactone 171. To a solution of **150** (1.57g, 4.79 mmol) in MeOH (35 mL) at 10 °C was added conc. HCl (8.0 mL, 48 mmol) and the mixture was stirred at room temperature for 20 h. The solvent was removed under vacuum and the residue was diluted with EtOAc (20 mL). Saturated NaHCO₃ solution (20 mL) was added and the aqueous layer was extracted with EtOAc (2×20 mL). The combined organic layers were washed with brine (30 mL), dried over anhydrous MgSO₄, filtered and concentrated. Column chromatography (silica gel, 3%, 5% EtOAc/CH₂Cl₂) provided **171** (1.14 g, 80%) as a clear and colorless oil. (Note: the crude concentrated can be carried forward directly to the subsequent reaction without purification by column chromatography.) R_f 0.44 (20% EtOAc/CH₂Cl₂); $[\alpha]_D^{25} = +36.4$ (c 2.28, CHCl₃); IR (cast film) 3467 (br), 2964, 2937, 1779, 1610, 1512, 1249, 1176, 1032; ¹H NMR (500 MHz, CDCl₃) δ 7.24-7.20 (m, 2H), 6.88-6.85 (m, 2H), 4.23 (dd, $J = 7.6, 2.4$ Hz, 1H), 3.84-3.79 (m, 1H), 3.81 (s, 3H), 3.77 (d, $J_{AB} = 13.9$ Hz, 1H), 3.72 (d, $J_{AB} = 13.9$ Hz, 1H), 3.50 (ddd, $J = 9.5, 9.5, 7.6$ Hz, 1H), 2.68 (dd, $J = 17.4, 10.0$ Hz, 1H), 2.62 (dd, $J = 17.4, 9.1$ Hz, 1H), 1.73 (d, $J = 5.4$ Hz, 1H), 1.62-1.44 (m, 2H), 0.92 (t, $J = 7.4$ Hz, 3H); ¹³C NMR (125 MHz, CDCl₃) δ 175.2, 159.3, 130.0, 129.5, 114.4, 83.1, 72.8, 55.5, 41.3, 36.6, 36.4, 26.2, 10.2; HRMS (ESI, $[M+Na]^+$) calcd for C₁₅H₂₀O₄SNa 319.0975, found: m/z 319.0968.



Mercaptoalcohol 149. To a solution of **171** (1.63 g, 4.50 mmol) in trifluoroacetic acid (25 mL) was added anisole (1.0 mL, 9.0 mmol) and the mixture was cooled to 0 °C in

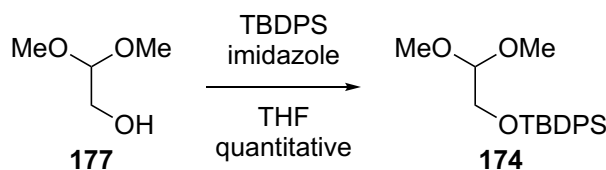
an ice water bath. Mercury acetate (1.51 g, 4.72 mmol) was added in one portion as a solid to give a clear yellow solution. Reaction completed after stirring at 0 °C for 5 minutes and solvent was removed under vacuum. The resulting residue was diluted with EtOAc (30 mL) followed by the addition of 1,3-propanedithiol (0.68 mL, 6.8 mmol). A grey-white solid started to precipitate out of the solution slowly and the slurry was stirred at room temperature overnight. The solid was filtered off and the filtrate was added to saturated NaHCO₃ solution (25 mL). The aqueous layer was extracted with EtOAc (2×25 mL). The combined organic layers were washed with brine (30 mL), dried over anhydrous MgSO₄, filtered and concentrated. Column Chromatography (silica gel, 20%, 30%, 40%, 45% EtOAc/hexanes) provided **149** (0.72 g, 91%) as a slightly yellow oil: *R_f* 0.28 (40% EtOAc/hexanes); [α]_D²⁵ = - 42.5 (*c* 2.37, CHCl₃); IR (cast film) 3446 (br), 2966, 2937, 1774, 1182 cm⁻¹; ¹H NMR (500 MHz, CDCl₃) δ 4.43, (dd, *J* = 7.3, 3.0 Hz, 1H), 4.10 (dddd, *J* = 8.0, 5.1, 5.1, 3.0 Hz, 1H), 3.71 (dddd, *J* = 9.2, 9.2, 9.2, 7.3 Hz, 1H), 2.93 (dd, *J* = 17.4, 8.7 Hz, 1H), 2.73 (dd, *J* = 17.4, 9.1 Hz, 1H), 2.00 (d, *J* = 9.8 Hz, 1H), 1.74 (d, *J* = 5.1 Hz, 1H), 1.73-1.59 (m, 2H), 1.03 (t, *J* = 7.4 Hz, 3H); ¹³C NMR (125 MHz, CDCl₃) δ 174.9, 83.7, 72.9, 39.7, 35.9, 26.3, 10.1; HRMS (ESI, [M+Na]⁺) calcd for C₇H₁₂O₃SNa 199.0399, found: *m/z* 199.0397.

(Note: the filter cake contains mercury salt and was discarded in designated mercury waste container for later disposal.)

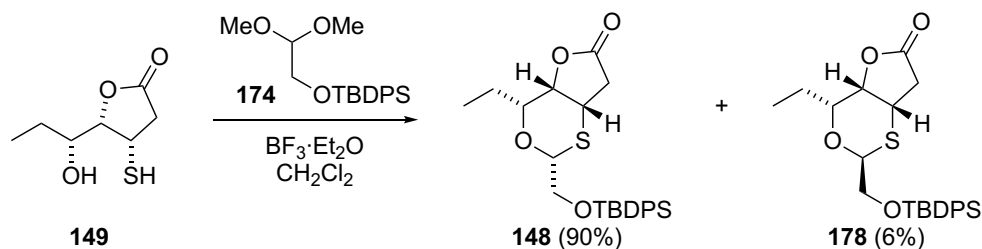


Aldehyde 168. To a solution of **176** (4.68 g, 8.29 mmol) in CH₂Cl₂ (120 mL) at -78 °C was bubbled a mixture of ozone/O₂ until the solution turned light blue. Nitrogen was then bubbled through the solution until the reaction mixture turned colorless. Triphenylphosphine (2.01g, 7.66 mmol) was then added to the cold solution and the mixture was gradually warmed to room temperature. The solvent was removed under

vacuum. Column chromatography (silica gel, 5%, 8% EtOAc/hexanes) provided **168** (4.45g, 90% yield) as a thick colorless oil: R_f 0.37 (10% EtOAc/hexanes); IR (cast film) 3072, 3050, 2957, 2932, 2890, 2858, 2710, 1738, 1428, 1112 cm^{-1} ; ^1H NMR (400 MHz, CDCl_3) δ 9.73 (t, $J = 0.9$ Hz, 1H), 7.68-7.63 (m, 4H), 7.48-7.37 (m, 6H), 4.21 (d, $J = 0.9$ Hz, 2H), 1.10 (s, 9H); ^{13}C NMR (125 MHz, CDCl_3) δ 201.8, 135.7, 132.7, 130.2, 128.1, 70.2, 26.9, 19.4; HRMS (ESI, $[\text{M}+\text{Na}]^+$) calcd for $\text{C}_{18}\text{H}_{22}\text{O}_2\text{SiNa}$ 321.1281, found: m/z 321.1277.



Dimethylacetal 174. To a solution of 2,2-dimethoxyethanol **177** (Alfa Aesar, 2.54 g, 24.0 mmol) and imidazole (2.12 g, 31.5 mmol) in THF (50 mL) at 0 °C was added *tert*-butyldiphenylchlorosilane (8.1 mL, 32 mmol) dropwise and the mixture was warmed up to room temperature. After stirring at room temperature for 4 h, the mixture was added to saturated NH_4Cl solution (50 mL) and extracted with Et_2O (3×40 mL). The combined organic layer was washed with brine (80 mL), dried with anhydrous MgSO_4 , filtered and concentrated. Column chromatography (silica gel, 2%, 4% EtOAc/hexanes) provided **174** (8.23 g, quantitative yield) as a thick colorless oil: R_f 0.52 (10% EtOAc/hexanes); IR (cast film) 3072, 3050, 2932, 2894, 2858, 1590, 1473, 1428, 1113, 1063, 824 cm^{-1} ; ^1H NMR (400 MHz, CDCl_3) δ 7.71-7.66 (m, 4H), 7.45-7.35 (m, 6H), 4.42 (t, $J = 5.3$ Hz, 1H), 3.67 (d, $J = 5.3$ Hz, 1H), 3.36 (s, 6H), 1.07 (s, 9H); ^{13}C NMR (125 MHz, CDCl_3) δ 135.8, 133.6, 130.0, 127.8, 104.7, 64.3, 54.4, 27.0, 19.4; HRMS (ESI, $[\text{M}+\text{Na}]^+$) calcd for $\text{C}_{20}\text{H}_{28}\text{O}_3\text{SiNa}$ 367.1700, found: m/z 367.1698.



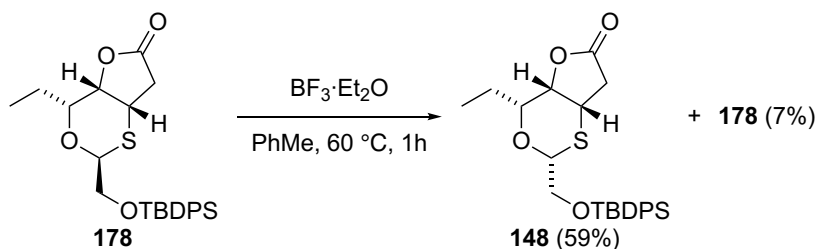
1,3-Oxathiane 148. To a solution of **149** (0.570 g, 3.23 mmol) in CH_2Cl_2 (32.0 mL) at -78°C was added acetal **174** (2.23 g, 6.47 mmol) via syringe and rinsed forward with CH_2Cl_2 (2.0 mL). $\text{BF}_3 \cdot \text{Et}_2\text{O}$ (0.86 mL, 6.79 mmol) was added dropwise via syringe in 30 minutes to result in a clear light yellow solution. The reaction was stirred at -78°C for 4 hours and then allowed to warm up gradually in the dry ice/acetone bath. Reaction completed after 3 hours while bath temperature reached around 5°C . Saturated NaHCO_3 solution (70 mL) was added at low temperature and the mixture was warmed up to room temperature. The aqueous layer was extracted with CH_2Cl_2 (2×50 mL). The combined organic layers were washed with brine (70 mL), dried over anhydrous MgSO_4 , filtered and concentrated. Column chromatography (silica gel, 20%, 30%, 35%, 40% EtOAc/hexanes) provided **148** (1.33g, 90%) and **178** (90.0 mg, 6%) as slightly yellow oils.

148: R_f 0.43 (40% EtOAc/hexanes); $[\alpha]_D^{25} = -73.8$ (c 2.09, CHCl_3); IR (cast film) 3071, 3050, 2962, 2932, 2858, 1793, 1776, 1428, 1173, 1152, 1114 cm^{-1} ; ^1H NMR (500 MHz, CDCl_3) δ 7.70-7.65 (m, 4H), 7.46-7.41 (m, 2H), 7.41-7.36 (m, 4H), 4.93 (dd, $J = 6.0, 5.3$ Hz, 1H), 4.18 (dd, $J = 4.0, 1.8$ Hz, 1H), 3.97-3.93 (m, 1H), 3.94 (dd, $J = 10.9, 6.0$ Hz, 1H), 3.74 (dd, $J = 10.9, 5.3$ Hz, 1H), 3.47 (ddd, $J = 8.2, 5.7, 1.8$ Hz, 1H), 2.94 (dd, $J = 17.3, 6.4$ Hz, 1H), 2.43 (dd, $J = 17.3, 0.8$ Hz, 1H), 1.90-1.80 (m, 1H), 1.75-1.66 (m, 1H), 1.06 (s, 9H), 1.01, (t, $J = 7.5$ Hz, 3H); ^{13}C NMR (125 MHz, CDCl_3) δ 174.5, 135.7(5), 135.7(2), 133.2(5), 133.1(6), 129.9(5), 129.9(2), 127.8(7), 127.8(5), 82.6, 79.6, 73.3, 66.0, 38.7, 38.1, 26.9, 25.4, 19.4, 10.1; HRMS (ESI, $[\text{M}+\text{Na}]^+$) calcd for $\text{C}_{25}\text{H}_{32}\text{O}_4\text{SSiNa}$ 479.1683, found: m/z 479.1676.

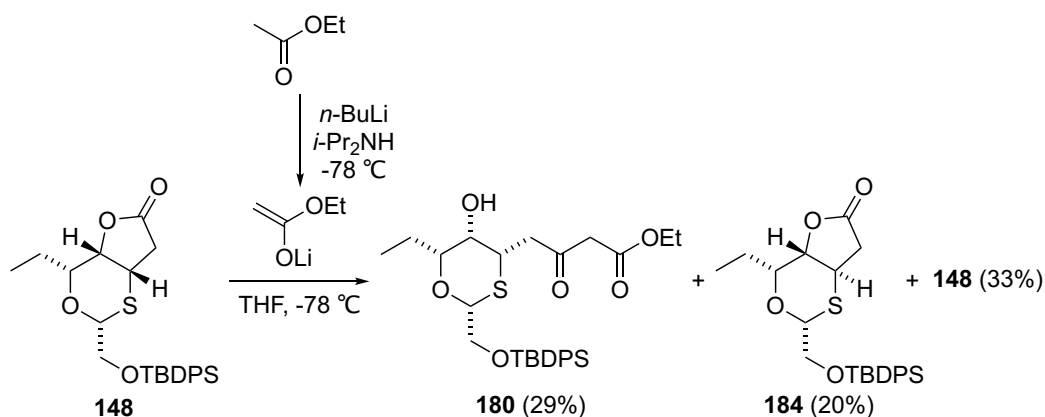
(Note: TROESY experiment was conducted using acetone-d₆ as solvent to resolve some of the overlapped signals.) ¹H NMR (500 MHz, acetone-d₆) δ 7.76-7.72 (m, 4H), 7.49-7.41 (m, 6H), 5.12 (dd, *J* = 6.0, 4.8 Hz, 1H), 4.41 (dd, *J* = 3.6, 1.7 Hz, 1H), 4.18 (d, *J* = 6.0, 3.6 Hz, 1H), 3.93 (dd, *J* = 10.9, 6.0 Hz, 1H), 3.75 (dd, *J* = 10.9, 4.8 Hz, 1H), 3.70 (ddd, *J* = 8.3, 5.5, 1.7 Hz, 1H), 3.15 (dd, *J* = 17.2, 6.0 Hz, 1H), 2.26 (d, *J* = 17.2 Hz, 1H), 1.08-1.63 (m, 2H), 1.06 (s, 9H), 1.00 (t, *J* = 7.4 Hz, 3H)

178: *R_f* 0.59 (40% EtOAc/hexanes); IR (cast film) 3071, 3049, 2961, 2932, 2858, 1786, 1156, 1114, 1088, 823, 702 cm⁻¹; ¹H NMR (500 MHz, CDCl₃) δ 7.70-7.65 (m, 4H), 7.48-7.43 (m, 2H), 7.43-7.38 (m, 4H), 5.21 (dd, *J* = 5.8, 5.8 Hz, 1H), 4.49 (dd, *J* = 7.8, 2.1 Hz, 1H), 4.04 (ddd, *J* = 8.0, 5.9, 2.0 Hz, 1H), 3.95 (dd, *J* = 11.1, 6.3 Hz, 1H), 3.81 (ddd, *J* = 9.0, 7.8, 6.7 Hz, 1H), 3.79 (dd, *J* = 11.1, 5.3 Hz, 1H), 2.91 (dd, *J* = 18.0, 9.0 Hz, 1H), 2.74 (dd, *J* = 18.0, 6.6 Hz, 1H), 1.74-1.57 (m, 2H), 1.07 (s, 9H), 0.96 (t, *J* = 7.4 Hz, 3H); ¹³C NMR (125 MHz, CDCl₃) δ 174.8, 135.7(6), 135.7(3), 133.0, 130.0(9), 130.0(8), 128.0, 77.4, 76.8, 72.5, 65.0, 35.9, 35.2, 26.9, 24.2, 19.4, 10.0; HRMS (ESI, [M+Na]⁺) calcd for C₂₅H₃₂O₄SSiNa 478.1683, found: *m/z* 479.1677.

(Note: TROESY experiments were conducted using acetone-d₆ and C₆D₆ as solvents to resolve some of the overlapped signals.) ¹H NMR (500 MHz, acetone-d₆) δ 7.76-7.72 (m, 4H), 7.51-7.42 (m, 6H), 5.21 (dd, *J* = 7.3, 5.2 Hz, 1H), 4.57 (dd, *J* = 6.4, 1.9 Hz, 1H), 4.18 (dd, *J* = 11.2, 7.3 Hz, 1H), 4.11-4.05 (m, 2H), 3.84 (dd, *J* = 11.2, 5.2 Hz, 1H), 3.03 (dd, *J* = 17.7, 8.1 Hz, 1H), 2.51 (dd, *J* = 17.7, 4.2 Hz, 1H), 1.70-1.56 (m, 2H), 1.07 (s, 9H), 0.98 (t, *J* = 7.5 Hz, 3H); ¹H NMR (500 MHz, C₆D₆) δ 7.77-7.71 (m, 4H), 7.21-7.19 (m, 6H), 5.00 (dd, *J* = 6.3, 5.3 Hz, 1H), 3.81 (dd, *J* = 11.0, 6.3 Hz, 1H), 3.70 (dd, *J* = 11.0, 5.3 Hz, 1H), 3.62-3.58 (m, 2H), 2.79 (ddd, *J* = 8.9, 7.4, 6.2 Hz, 1H), 2.30 (dd, *J* = 17.9, 6.0 Hz, 1H), 2.16 (dd, *J* = 17.9, 9.0 Hz, 1H), 1.72-1.61 (m, 1H), 1.46-1.35 (m, 1H), 1.15 (s, 9H), 0.79 (t, *J* = 7.5 Hz, 3H).



Epimerization of 148. To a solution of **148** (0.103 g, 0.226 mmol) in toluene (2.3 mL) was added $\text{BF}_3 \cdot \text{Et}_2\text{O}$ (30 μL , 0.24 mmol) and the mixture was stirred at 60 $^\circ\text{C}$ for 30 minutes. The reaction mixture was cooled to room temperature and added to a mixture of saturated NaHCO_3 (5 mL) and CH_2Cl_2 (5 mL). The aqueous layer was extracted with CH_2Cl_2 (2 \times 5 mL). The combined organic layers were washed with brine (10 mL), dried over anhydrous MgSO_4 , filtered and concentrated. Column chromatography (silica gel, 20%, 30%, 35%, 40% EtOAc/hexanes) provided **148** (60.5 mg, 59%) and recovered **178** (7.6 mg, 7%) as clear and slightly yellow oils. Spectral data for **148** and **178** were shown above.

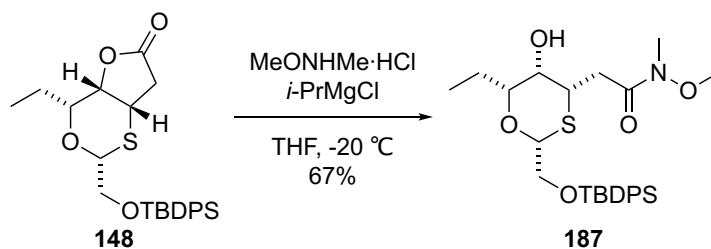


Ketoester 180 and 1,3-oxathiane 184. To a solution of diisopropylamine (22 μL , 0.16 mmol) in THF (0.5 mL) at -78 $^\circ\text{C}$ was added $n\text{-BuLi}$ (2.5 M solution in THF, 60 μL , 0.15 mmol). After stirring at -78 $^\circ\text{C}$ for 10 minutes, EtOAc (13 mL, 0.13 mmol) was added and the mixture was stirred at -78 $^\circ\text{C}$ for 10 minutes. A solution of **148** (58 mg, 0.13 mmol) in THF (1.0 mL) was then added. After stirring for 0.5 h, the mixture was

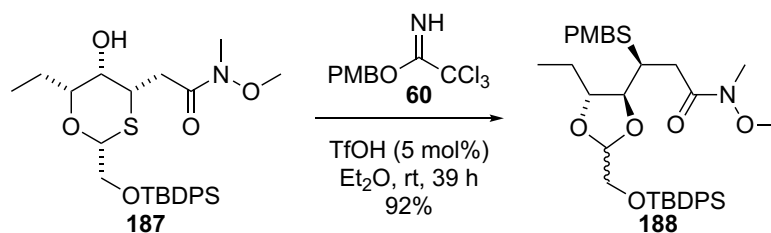
warmed up to 0 °C and added with saturated NH₄Cl solution (10 mL). The layers were separated and the aqueous layer was extracted with Et₂O (2×10 mL). The combined organic layers were washed with brine (15 mL), dried over anhydrous MgSO₄, filtered and concentrated. Column chromatography (silica gel, 10%, 15%, 20%, 30%, 40% EtOAc/hexanes) provided **184** (12 mg, 20%), **180** (20 mg, 29%) as colorless oil. Unreacted **180** (19 mg, 33%) was also recovered.

184: R_f 0.72 (40% EtOAc/hexanes); IR (cast film) 3071, 3050, 2961, 2931, 2858, 1786, 1428, 1148, 1114 cm⁻¹; ¹H NMR (500 MHz, CDCl₃) δ 7.71-7.66 (m, 4H), 7.47-7.42 (m, 2H), 7.42-7.37 (m, 4H), 4.95 (dd, *J* = 5.9, 4.8 Hz, 1H), 4.27 (dd, *J* = 9.2, 6.6 Hz, 1H), 3.93 (dd, *J* = 11.0, 5.9 Hz, 1H), 3.77 (ddd, *J* = 8.4, 8.4, 6.6 Hz, 1H), 3.76 (dd, *J* = 11.0, 4.8 Hz, 1H), 3.35 (ddd, *J* = 8.9, 8.9, 3.3 Hz, 1H), 2.86 (dd, *J* = 17.8, 8.4 Hz, 1H), 2.65 (dd, *J* = 17.8, 8.9 Hz, 1H), 1.88-1.79 (m, 1H), 1.62-1.51 (m, 1H), 1.06 (s, 9H), 1.01 (t, *J* = 7.5 Hz, 3H); ¹³C NMR (125 MHz, CDCl₃) δ 174.5, 135.8(0), 135.7(9), 133.3, 133.2, 130.0(1), 129.9(9), 127.9(0), 127.8(8), 80.2, 79.1, 76.8, 66.4, 36.0, 33.8, 26.9, 26.3, 19.4, 9.6; HRMS (ESI, [M+Na]⁺) calcd for C₂₅H₃₂O₄SSiNa 479.1683, found: m/z 479.1676.

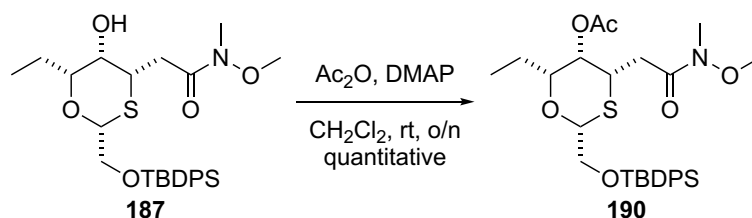
180: R_f 0.59 (40% EtOAc/hexanes); IR (cast film) 3526 (br), 3071, 3049, 2962, 2931, 2858, 1742, 1719, 1428, 1113 cm⁻¹; ¹H NMR (500 MHz, CDCl₃) δ 7.71-7.66 (m, 4H), 7.46-7.35 (m, 6H), 4.96 (dd, *J* = 5.7, 4.8 Hz, 1H), 4.20 (q, *J* = 7.1 Hz, 2H), 3.88 (dd, *J* = 10.9, 5.7 Hz, 1H), 3.74 (dd, *J* = 10.9, 4.8 Hz, 1H), 3.78-3.69 (m, 1H), 3.46 (d, *J*_{AB} = 15.5 Hz, 1H), 3.44 (d, *J*_{AB} = 15.5 Hz, 1H), 3.43-3.39 (m, 1H), 3.29 (dd, *J* = 8.1, 5.6 Hz, 1H), 3.07 (dd, *J* = 18.3, 8.7 Hz, 1H), 2.60 (dd, *J* = 18.3, 4.8 Hz, 1H), 2.41 (d, *J* = 12.5 Hz, 1H), 1.74-1.61 (m, 1H), 1.61-1.49 (m, 1H), 1.28 (t, *J* = 7.1 Hz, 3H), 1.06 (s, 9H), 0.93 (t, *J* = 7.5 Hz, 3H); ¹³C NMR (125 MHz, CDCl₃) δ 200.3, 166.9, 135.8(4), 135.7(7), 133.3(5), 133.3(3), 129.9(2), 129.8(9), 127.8(5), 127.8(4), 127.8(0), 127.7(9), 84.7, 84.0, 65.9, 64.5, 61.7, 49.8, 44.8, 43.0, 26.9, 25.3, 19.4, 14.2, 9.8; HRMS (ESI, [M+Na]⁺) calcd for C₂₉H₄₀O₆SSiNa 567.2207, found: m/z 567.2199.



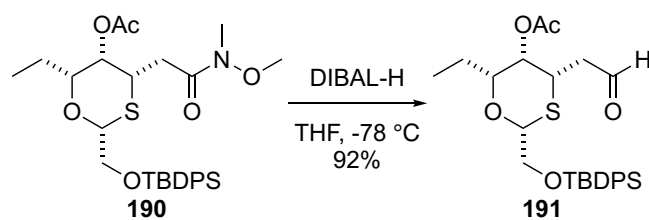
Alcohol 187. To a solution of **148** (1.33 g, 2.90 mmol) in THF (30 mL) at room temperature was added *N,O*-dimethylhydroxylamine (0.71 g, 7.3 mmol) in one portion. The mixture was cooled in a bath of about $-20\text{ }^\circ\text{C}$ (dry ice/acetone). *i*-PrMgCl (2.0 M in THF, 7.3 mL, 15 mmol) was added to the reaction mixture dropwise by syringe in 30 minutes while maintaining the bath temperature at around $-20\text{ }^\circ\text{C}$. After stirring for 15 minutes, the mixture was added to saturated NH_4Cl solution (60 mL) and the precipitate was dissolved with additional water (18 mL). The layers were separated and the aqueous layer was extracted with EtOAc ($2\times 60\text{ mL}$). The combined organic layers were washed with brine (80 mL), dried over anhydrous MgSO_4 , filtered and concentrated. Column chromatography (silica gel, 20%, 30%, 40%, 45% EtOAc/hexanes) provided **187** (1.011 g, 65%) as a colorless oil: R_f 0.27 (40% EtOAc/hexanes); $[\alpha]_D^{25} = +19.6$ (c 2.54, CHCl_3); IR (cast film) 3529 (br), 3072, 3050, 2962, 2933, 2858, 1664, 1428, 1389, 1114 cm^{-1} ; $^1\text{H NMR}$ (500 MHz, CDCl_3) δ 7.71-7.68 (m, 4H), 7.45-7.41 (m, 2H), 7.40-7.36 (m, 4H), 4.97 (dd, $J = 5.9, 4.6\text{ Hz}$, 1H), 3.89 (dd, $J = 11.0, 5.9\text{ Hz}$, 1H), 3.75 (dd, $J = 11.0, 4.6\text{ Hz}$, 1H), 3.76-3.73 (m, 1H), 3.70 (s, 3H), 3.49 (br d, $J = 12.5\text{ Hz}$, 1H), 3.31 (dd, $J = 8.2, 5.5\text{ Hz}$, 1H), 3.19 (s, 3H), 2.93 (dd, $J = 16.8, 9.1\text{ Hz}$, 1H), 2.49 (dd, $J = 16.8, 4.6\text{ Hz}$, 1H), 2.45 (d, $J = 12.5\text{ Hz}$, 1H), 1.74-1.64 (m, 1H), 1.60-1.51 (m, 1H), 1.06 (s, 9H), 0.94 (t, $J = 7.5\text{ Hz}$, 3H); $^{13}\text{C NMR}$ (125 MHz, CDCl_3) δ 171.4, 135.7(7), 135.7(5), 133.4, 129.9, 129.8, 127.8(0), 127.7(9), 84.6, 84.1, 66.0, 64.8, 61.5, 44.3, 34.0, 32.2, 26.8, 25.3, 19.4, 9.9; HRMS (ESI, $[\text{M}+\text{Na}]^+$) calcd for $\text{C}_{27}\text{H}_{39}\text{NO}_5\text{SSiNa}$ 540.2210, found: m/z 540.2210.



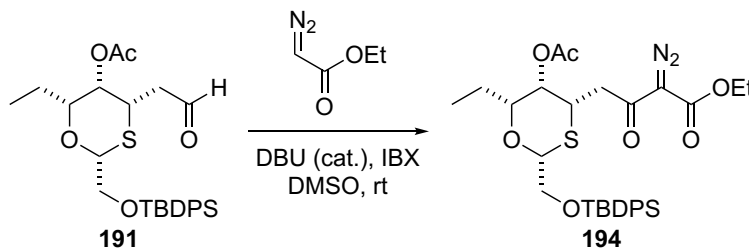
Acetal 188. To a solution of **187** (136 mg, 0.263 mmol) in Et₂O (3.0 mL) at room temperature was added 4-methoxybenzyl-2,2,2-trichloroacetimidate (0.16 mL, 0.79 mmol) and trifluoromethanesulfonic acid (1.0 μL, 0.013 mmol). Reaction did not complete after stirring at room temperature for 23 h. More 4-methoxybenzyl-2,2,2-trichloroacetimidate (0.16 mL, 0.79 mmol) was added. After stirring at room temperature for 16 h, saturated NaHCO₃ solution (10 mL) was added to the reaction flask. The aqueous layer was extracted with Et₂O (3×10 mL). The combined organic layers were washed with brine (20 mL), dried over anhydrous MgSO₄, filtered and concentrated. Column chromatography (silica gel, 1%, 3%, 5% 10% EtOAc/CH₂Cl₂) provided **188** (155 mg, 92% yield) as a slightly yellow oil: R_f 0.49 (40% EtOAc/hexanes); IR (cast film) 3072, 3050, 2961, 2933, 2858, 1665, 1512, 1441, 1114 cm⁻¹; ¹H NMR (500 MHz, CDCl₃) δ 7.71-7.67 (m, 4H), 7.42-7.33 (m, 6H), 7.29-7.26 (m, 2H), 6.87-6.82 (m, 2H), 5.21 (app t, *J* = 3.6 Hz, 1H), 3.79 (s, 3H), 3.77 (d, *J*_{AB} = 13.3 Hz, 1H), 3.71 (d, *J*_{AB} = 13.3 Hz, 1H), 3.77-3.72 (m, 1H), 3.69 (s, 3H), 3.65-3.62 (m, 3H), 3.21 (s, 3H), 3.16 (ddd, *J* = 9.8, 6.6, 2.0 Hz, 1H), 3.08-3.98 (m, 1H), 2.91-2.83 (m, 1H), 1.44-1.33 (m, 1H), 1.33-1.21 (m, 1H), 1.03 (s, 9H), 0.82 (t, *J* = 7.4 Hz, 3H); ¹³C NMR (125 MHz, CDCl₃) δ 172.3, 158.9, 135.8, 133.6(5), 133.6(3), 130.9, 130.4, 129.7(1), 129.7(2), 114.1, 104.4, 83.2, 81.0, 65.7, 61.5, 55.4, 42.5, 37.6, 36.2, 32.4, 26.9, 25.6, 19.4, 10.3; HRMS (ESI, [M+Na]⁺) calcd for C₃₅H₄₇NO₆SSiNa 660.2786, found: *m/z* 660.2772.



Weinreb amide 190. To a solution of **187** (1.011 g, 1.95 mmol) in CH₂Cl₂ (40 mL) at room temperature was added 4-dimethylaminopyridine (0.48 g, 3.9 mmol) and acetic anhydride (0.55 mL, 5.9 mmol). After stirring at room temperature for 20 h, the mixture was added to saturated NaHCO₃ solution (100 mL). the aqueous layer was extracted with CH₂Cl₂ (2×100 mL). The combined organic layers were washed with brine (100 mL), dried over anhydrous MgSO₄, filtered and concentrated. Column chromatography (silica gel, 30%, 40%, 45%, 50% EtOAc/hexanes) provided **14** (1.057 g, quantitative yield) as a colorless oil: *R_f* 0.34 (40% EtOAc/hexanes); [α]_D²⁵ = - 11.7 (*c* 1.37, CHCl₃); IR (cast film) 3071, 3049, 2962, 2933, 2858, 1739, 1665, 1428, 1235, 1114 cm⁻¹; ¹H NMR (500 MHz, CDCl₃) δ 7.72-7.66 (m, 4H), 7.45-7.40 (m, 2H), 7.40-7.35 (m, 4H), 5.09-5.05 (m, 2H), 3.98 (dd, *J* = 10.9, 6.3 Hz, 1H), 3.89 (ddd, *J* = 8.8, 5.6, 1.9 Hz, 1H), 3.78 (dd, *J* = 10.9, 4.8 Hz, 1H), 3.64 (s, 3H), 3.44 (ddd, *J* = 8.3, 4.9, 1.1 Hz, 1H), 3.18 (s, 3H), 2.68 (dd, *J* = 16.4, 8.8 Hz, 1H), 2.41 (dd, *J* = 16.4, 5.5 Hz, 1H), 2.15 (s, 3H), 1.59-1.49 (m, 1H), 1.46-1.36 (m, 1H), 1.06 (s, 9H), 0.95 (t, *J* = 7.5 Hz, 3H); ¹³C NMR (125 MHz, CDCl₃) δ 171.1, 170.8, 135.8(0), 135.7(7), 133.5(1), 133.4(6), 129.8(6), 129.8(1), 127.8(1), 127.7(9), 84.9, 82.6, 66.1(3), 66.1(1), 61.4, 41.3, 33.7, 32.4, 26.9, 25.3, 20.9, 19.4, 10.0; HRMS (ESI, [M+Na]⁺) calcd for C₂₉H₄₁NO₆SSiNa 582.2316, found: *m/z* 582.2316.

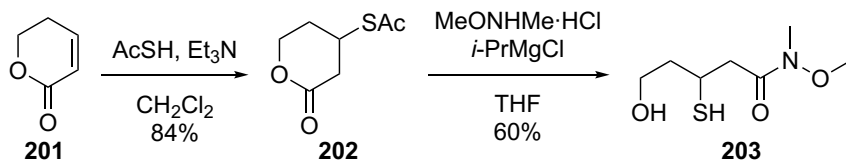


Aldehyde 191. To a solution of **190** (0.579 g, 1.03 mmol) in THF (10 mL) at -78 °C was added DIBAL-H solution (1.0 M in THF, 1.55 mL, 1.55 mmol) dropwise by syringe in 30 minutes. Reaction completed after stirring at -78 °C for 10 minutes and was quenched by addition of saturated Rochelle salt solution (25 mL) at low temperature. The mixture was then warmed up to room temperature gradually to give a cloudy mixture, which was filtered through a pad of celite and rinsed with Et₂O (25 mL). The aqueous layer was extracted with Et₂O (2×25 mL). The combined organic layers were washed with brine (35 mL), dried over anhydrous MgSO₄, filtered and concentrated. Column chromatography (silica gel, 20%, 25%, 30%, 35% EtOAc/hexanes) provided **191** (0.476 g, 92%) as a light yellow oil: *R_f* 0.30 (20% EtOAc/hexanes); [α]_D²⁵ = -9.3 (*c* 0.24, CHCl₃); IR (cast film) 3071, 3049, 2961, 2932, 2858, 2729, 1738, 1235, 1113, 1092 cm⁻¹; ¹H NMR (500 MHz, CDCl₃) δ 9.70 (br s, 1H), 7.71-7.66 (m, 4H), 7.45-7.41 (m, 2H), 7.40-7.36 (m, 4H), 5.07 (dd, *J* = 5.9, 5.3 Hz, 1H), 4.98 (br dd, *J* = 1.4, 1.4 Hz, 1H), 3.98 (dd, *J* = 10.8, 6.1 Hz, 1H), 3.86 (ddd, *J* = 7.7, 6.2, 1.9 Hz, 1H), 3.78 (dd, *J* = 10.9, 5.2 Hz, 1H), 3.43 (ddd, *J* = 8.3, 5.1, 0.9 Hz, 1H), 2.69 (dd, *J* = 18.1, 7.7 Hz, 1H), 2.45 (ddd, *J* = 18.1, 6.2, 1.0 Hz, 1H), 2.16 (s, 3H), 1.61-1.50 (m, 1H), 1.45-1.36 (m, 1H), 1.06 (s, 9H), 0.94 (t, *J* = 7.5 Hz, 3H); ¹³C NMR (125 MHz, CDCl₃) δ 198.3, 171.3, 135.8(1), 135.7(6), 133.4, 133.3, 129.9(1), 129.8(6), 127.8(4), 127.8(2), 85.0, 82.5, 66.0, 65.9, 45.6, 39.3, 26.9, 25.2, 20.9, 19.4, 9.9; HRMS (ESI, [M+Na]⁺) calcd for C₂₇H₃₆O₅SSiNa 523.1945, found: *m/z* 523.1943.



Diazoketoester 194. DMSO (2.0 mL) was added to **191** (0.200 g, 0.400 mmol) and the mixture was stirred at room temperature for about 20 minutes to achieve a

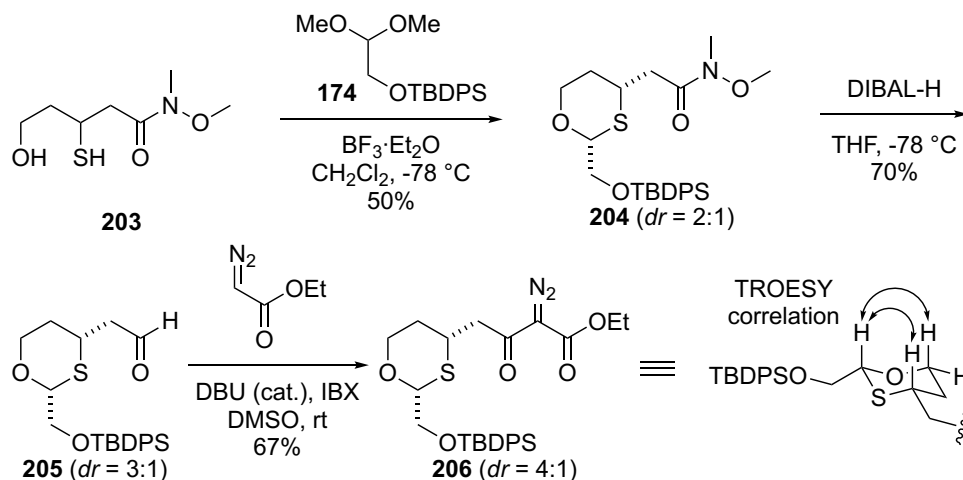
homogeneous solution. To a solution of ethyl diazoacetate (EDA, 51 μL , 0.48 mmol) in DMSO (5.0 mL) in another reaction flask was added DBU (6 μL , 0.04 mmol) and the mixture was cooled in an ice water bath. The solution of **15** in DMSO was then added to the reaction flask by syringe. The resulting reaction mixture was allowed to warm up to room temperature gradually and then stirred for 21 h. 45 wt% IBX (0.50 g, 0.80 mmol; Aldrich, contained benzoic acid and isophthalic acid as stabilizers in a total amount of 55 wt%) was added to reaction mixture in one portion as a solid and dissolution occurred in \sim 20 minutes to afford a light yellow solution. Reaction completed after stirring at room temperature for 6 h. Reaction mixture was added to saturated NaHCO_3 solution (20 mL) and extracted with CH_2Cl_2 (3×20 mL). The combined organic layers were washed with brine (30 mL), dried over anhydrous MgSO_4 , filtered and concentrated. Column chromatography (silica gel, 10%, 13% EtOAc/hexanes) provided **16** (0.179 g, 73%) as a light yellow oil: R_f 0.33 (20% EtOAc/hexanes); $[\alpha]_D^{25} = +4.2$ (c 1.12, CHCl_3); IR (cast film) 3071, 3049, 2962, 2933, 2858, 2137, 1738, 1717, 1654, 1428, 1235, 1115, 1026 cm^{-1} ; ^1H NMR (500 MHz, CDCl_3) δ 7.71-7.66 (m, 4H), 7.45-7.40 (m, 2H), 7.40-7.35 (m, 4H), 5.06 (dd, $J = 6.2, 5.0$ Hz, 1H), 5.00 (br dd, $J = 1.4, 1.4$ Hz, 1H), 4.27 (q, $J = 7.2$ Hz, 2H), 3.97 (dd, $J = 11.0, 6.2$ Hz, 1H), 3.95 (ddd, $J = 9.1, 5.2, 1.8$ Hz), 3.78 (dd, $J = 11.0, 4.9$ Hz, 1H), 3.43 (ddd, $J = 8.3, 5.0, 0.9$ Hz, 1H), 3.26 (dd, $J = 17.7, 9.1$ Hz, 1H), 2.71 (dd, $J = 17.7, 5.3$ Hz, 1H), 2.15 (s, 3H), 1.60-1.50 (m, 1H), 1.45-1.35 (m, 1H), 1.32 (t, $J = 7.2$ Hz, 3H), 1.06 (s, 9H), 0.94 (t, $J = 7.4$ Hz, 3H); ^{13}C NMR (125 MHz, CDCl_3) δ 189.3, 171.4, 161.2, 135.8(2), 135.7(8), 133.5, 133.4, 129.8(7), 129.8(2), 127.8(3), 127.8(0), 85.0, 82.5, 66.1, 65.8, 61.6, 41.2, 40.8, 26.9, 25.3, 20.9, 19.4, 14.5, 10.0 (diazo carbon not detected); HRMS (ESI, $[\text{M}+\text{Na}]^+$) calcd for $\text{C}_{31}\text{H}_{40}\text{N}_2\text{O}_7\text{SSiNa}$ 635.2218, found: m/z 635.2217.



Lactone 202. To a solution of **201** (Aldrich, 1.185 g, 12.08 mmol) in CH_2Cl_2 (15 mL) was added triethylamine (0.17 mL, 1.2 mmol) and thioacetic acid (1.28 mL, 18.2 mL) at room temperature. After stirring at room temperature for 16 h, the starting material was completely consumed. Saturated NaHCO_3 solution (30 mL) was then added to the reaction flask and the mixture was warmed up to room temperature. The aqueous layer was extracted with CH_2Cl_2 (2×30 mL). The combined organic layers were washed with brine (60 mL), dried over anhydrous MgSO_4 , filtered and concentrated. Column chromatography (silica gel, 30%, 35%, 40%, 45% EtOAc/hexanes) provided **204** (1.78 g, 84%) as a yellow oil: R_f 0.40 (33% EtOAc/hexanes); IR (cast film) 2972, 2915, 1741, 1691, 1476, 1401, 1354, 1255, 1218, 1119, 1070, 956 cm^{-1} ; ^1H NMR (500 MHz, CDCl_3) δ 4.46 (ddd, $J = 11.7, 5.4, 4.6$ Hz, 1H), 4.36 (ddd, $J = 11.7, 8.9, 3.9$ Hz, 1H), 3.91 (dddd, $J = 8.9, 8.9, 6.5, 4.9$ Hz, 1H), 3.00 (ddd, $J = 17.8, 6.5, 1.1$ Hz, 1H), 2.58 (dd, $J = 17.8, 8.9$ Hz, 1H), 2.35 (s, 3H), 2.29–2.21 (m, 1H), 1.93 (dddd, $J = 13.7, 8.9, 8.9, 4.6$ Hz, 1H); ^{13}C NMR (125 MHz, CDCl_3) δ 194.4, 168.7, 67.7, 36.3, 35.3, 30.8, 29.1; HRMS (ESI, $[\text{M}+\text{Na}]^+$) for $\text{C}_7\text{H}_{10}\text{O}_3\text{SNa}$ calcd 197.0243, found: m/z 197.0242.

Mercaptoalcohol 203. To a solution of **202** (1.77 g, 10.2 mmol) in THF (100 mL) at room temperature was added *N,O*-dimethylhydroxylamine (5.55 g, 56.9 mmol) in one portion. The mixture was cooled in a bath of about -20 °C (dry ice/acetone). *i*-PrMgCl (2.0 M in THF, 58.0 mL, 116 mmol) was added to the reaction mixture dropwise by syringe in 50 minutes while maintaining the bath temperature at around -20 °C. After stirring for 10 minutes, the mixture was added to saturated NH_4Cl solution (120 mL) and the precipitate was dissolved with additional water (10 mL). The mixture was neutralized with the addition of HCl solution. The layers were separated and the

aqueous layer was extracted with EtOAc (2×100 mL). The combined organic layers were washed with brine (150 mL), dried over anhydrous MgSO₄, filtered and concentrated. Column chromatography (silica gel, 60%, 70% EtOAc/CH₂Cl₂) provided **203** (1.18 g, 60%) as a colorless oil: R_f 0.25 (70% EtOAc/CH₂Cl₂); IR (cast film) 3419 (br), 2938, 2546, 1650, 1464, 1429, 1389, 1179, 1114, 1051, 996 cm⁻¹; ¹H NMR (500 MHz, CDCl₃) δ 3.83-3.77 (m, 2H), 3.71 (s, 3H), 3.53-3.49 (m, 1H), 3.20 (s, 3H), 2.83-2.78 (m, 2H), 1.97-1.92 (m, 1H), 1.89 (d, *J* = 7.3 Hz, 1H), 1.85-1.80 (m, 1H) (OH proton not detected); ¹³C NMR (125 MHz, CDCl₃) δ 172.3, 61.6, 60.6, 42.0, 41.2, 33.2, 32.4; HRMS (ESI, [M+Na]⁺) for C₇H₁₅NO₃Na calcd 216.0665, found: *m/z* 216.0665.



1,3-Oxathiane 204. To a solution of **203** (0.765 g, 3.96 mmol) in CH₂Cl₂ (40 mL) at -78 °C was added acetal **174** (3.41 g, 9.90 mmol) via syringe and rinsed forward with CH₂Cl₂ (2.0 mL). BF₃·Et₂O (1.50 mL, 11.9 mmol) was then added dropwise via syringe. The reaction was stirred at -78 °C for 15 minutes and warmed up gradually to 0 °C. Saturated NaHCO₃ solution (50 mL) was then added to the reaction flask and the mixture was warmed up to room temperature. The aqueous layer was extracted with CH₂Cl₂ (2×40 mL). The combined organic layers were washed with brine (60 mL), dried over anhydrous MgSO₄, filtered and concentrated. Column chromatography (silica gel, 40%, 45%, 50% EtOAc/hexanes) provided **204** (0.94 g, 50%) as an

inseparable mixture of *cis* **204** and *trans* **204** isomers as a colorless oil. (Diastereomeric ratio of 2:1 was determined by integration of the acetal protons in the ^1H NMR spectrum. Assignment of protons and carbons to the individual isomers was accomplished through analysis of a combination of COSY, HSQC, and HMBC spectra of the mixture.) R_f 0.33 (40% EtOAc/hexanes); IR (cast film) 3071, 3049, 2933, 2858, 1666, 1472, 1428, 1386, 1112, 999, 704 cm^{-1} ; HRMS (ESI, $[\text{M}+\text{Na}]^+$) for $\text{C}_{25}\text{H}_{35}\text{NO}_4\text{SSiNa}$ calcd 496.1948, found: m/z 496.1954.

cis **204** (major diastereomer): ^1H NMR (500 MHz, CDCl_3) δ 7.70-7.66 (m, 4H), 7.44-7.40 (m, 2H), 7.40-7.35 (m, 4H), 4.95 (dd, $J = 6.1, 4.7$ Hz, 1H), 4.18 (ddd, $J = 12.1, 4.1, 2.3$ Hz, 1H), 3.89 (ddd, $J = 11.0, 6.1$ Hz, 1H), 3.73 (dd, $J = 11.0, 4.7$ Hz, 1H), 3.68 (s, 3H), 3.58 (ddd, $J = 12.4, 12.4, 2.1$ Hz, 1H), 3.62-3.54 (m, 1H), 3.19 (s, 3H), 2.66-2.54 (m, 2H), 1.91 (dddd, $J = 13.7, 2.3, 2.3, 2.3$ Hz, 1H), 1.65-1.58 (m, 1H), 1.06 (s, 9H); ^{13}C NMR (125 MHz, CDCl_3) δ 171.4, 135.8, 133.5(2), 133.4(8), 129.8(2), 129.8(1), 127.8(1), 127.8(0), 84.5, 69.7, 66.6, 61.5, 38.2, 37.7, 30.2, 32.2, 26.9, 19.5.

Partial *trans* **204** (minor diastereomer): ^1H NMR (500 MHz, CDCl_3) δ 7.70-7.66 (m, 4H), 7.44-7.40 (m, 2H), 7.40-7.35 (m, 4H), 5.03 (dd, $J = 6.5, 4.9$ Hz, 1H), 3.96 (dd, $J = 11.0, 6.6$ Hz, 1H), 3.97-3.93 (m, 1H), 3.81-3.76 (m, 1H), 3.74-3.72 (m, 1H), 3.71 (s, 3H), 3.62-3.54 (m, 1H), 3.20 (s, 3H), 3.12-3.05 (m, 1H), 2.82 (dd, $J = 15.6, 7.8$ Hz, 1H), 2.20 (dddd, $J = 14.3, 11.0, 4.2, 4.2$ Hz, 1H), 1.65-1.58 (m, 1H), 1.06 (s, 9H); ^{13}C NMR (125 MHz, CDCl_3) δ 171.4, 135.7, 133.5, 129.8, 127.8, 79.2, 66.3, 64.2, 61.6, 36.4, 33.7, 32.5, 30.2, 26.9, 19.4.

Aldehyde 205. To a solution of **204** (0.406 g, 0.857 mmol, mixture of *cis* **204** and *trans* **204** isomers, 2:1) in THF (10 mL) at -78 $^\circ\text{C}$ was added DIBAL-H solution (1.0 M in THF, 1.20 mL, 1.20 mmol) dropwise by syringe. Reaction was completed after stirring at -78 $^\circ\text{C}$ for 10 minutes. The reaction was quenched by addition of saturated Rochelle salt solution (30 mL) at low temperature. The mixture was then warmed up to room temperature gradually to give a cloudy mixture, which was filtered through a short pad

of celite and rinsed with Et₂O (30 mL). The resulting aqueous layer was extracted with Et₂O (2×30 mL). The combined organic layers were washed with brine (40 mL), dried over anhydrous MgSO₄, filtered and concentrated. Column chromatography (silica gel, 10%, 15%, 20%, 30% EtOAc/hexanes) provided **205** (0.285 g, 80%) as an inseparable mixture of *cis* **205** and *trans* **205** isomers as a colorless oil. (Diastereomeric ratio of 3:1 was determined by integration of the acetal protons in the ¹H NMR spectrum. Assignment of protons and carbons to the individual isomers was accomplished through analysis of a combination of COSY, HSQC, and HMBC spectra of the mixture.) R_f 0.50 (30% EtOAc/hexanes); IR (cast film) 3071, 3049, 2932, 2858, 2724, 1725, 1472, 1428, 1390, 1112, 703 cm⁻¹; HRMS (ESI, [M+Na]⁺) for C₂₃H₃₀O₃SSiNa calcd 437.1577, found: m/z 437.1576.

cis **205** (major diastereomer): ¹H NMR (500 MHz, CDCl₃) δ 9.78 (t, *J* = 1.6 Hz, 1H), 7.70-7.65 (m, 4H), 7.45-7.35 (m, 6H), 4.95 (dd, *J* = 5.9, 5.2 Hz, 1H), 4.18 (ddd, *J* = 12.1, 4.1, 2.2 Hz, 1H), 3.90 (dd, *J* = 10.9, 5.9 Hz, 1H), 3.73 (dd, *J* = 10.9, 5.2 Hz, 1H), 3.58 (ddd, *J* = 12.2, 12.2, 2.1 Hz, 1H), 3.63-3.52 (m, 1H), 2.62 (ddd, *J* = 7.2, 4.4, 1.6 Hz, 1H), 1.83 (dddd, *J* = 13.6, 2.4, 2.4, 2.4 Hz, 1H), 1.70-1.60 (m, 1H), 1.06 (s, 9H); ¹³C NMR (125 MHz, CDCl₃) δ 199.5, 135.8, 133.4, 129.8(7), 129.8(6), 127.8(4), 127.8(2), 84.6, 69.6, 66.4, 49.8, 35.8, 32.9, 26.9, 19.4.

Partial *trans* **205** (minor diastereomer): ¹H NMR (500 MHz, CDCl₃) δ 9.77 (t, *J* = 1.5 Hz, 1H), 7.70-7.65 (m, 4H), 7.45-7.35 (m, 6H), 4.97 (dd, 6.4, 4.9 Hz, 1H), 3.98-3.92 (m, 1H), 3.76-3.70 (m, 1H), 3.63-3.52 (m, 1H), 3.03 (ddd, *J* = 17.4, 8.3, 1.9 Hz, 1H), 2.80 (ddd, *J* = 17.4, 6.7, 1.5 Hz, 1H), 2.20 (dddd, *J* = 14.2, 11.0, 4.3, 4.3 Hz, 1H), 1.60-1.52 (m, 1H), 1.06 (s, 9H); ¹³C NMR (125 MHz, CDCl₃) δ 200.0, 135.8, 133.5, 129.9, 127.9, 79.1, 66.3, 64.0, 47.6, 31.6, 30.1, 26.9, 19.4.

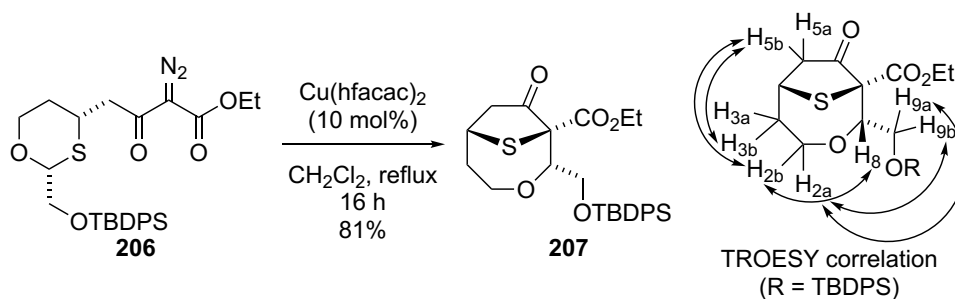
Diazoketoester 206. DMSO (3.3 mL) was added to **205** (0.273 g, 0.658 mmol, mixture of *cis* **205** and *trans* **205** isomers, 3:1) and the mixture was stirred at room temperature for about 20 minutes to achieve a homogeneous solution. To a solution of ethyl

diazoacetate (83 μ L, 0.79 mmol) in DMSO (3.3 mL) in another reaction flask was added DBU (10 μ L, 0.067 mmol) and the mixture was cooled in an ice water bath. The solution of **205** in DMSO was then added to the reaction flask by syringe. The resulting reaction mixture was allowed to warm up to room temperature gradually and then stirred for 21 h. 45 wt% IBX (0.660 g, 1.06 mmol; Aldrich, contained benzoic acid and isophthalic acid as stabilizers in a total amount of 55 wt%) was added to reaction mixture in one portion as a solid and dissolution occurred in \sim 20 minutes to afford a light yellow solution. Reaction completed after stirring at room temperature for additional 6 h. The reaction mixture was added to saturated NaHCO₃ solution (25 mL) and extracted with CH₂Cl₂ (3 \times 25 mL). The combined organic layers were washed with brine (40 mL), dried over anhydrous MgSO₄, filtered and concentrated. Column chromatography (silica gel, 10%, 15%, 20% EtOAc/hexanes) provided **5c** (0.232 g, 67%) as an inseparable mixture of *cis* **206** and *trans* **206** isomers as a colorless oil. (Diastereomeric ratio of 4:1 was determined by integration of the acetal protons in the ¹H NMR spectrum. Assignment of protons and carbons to the individual isomers was accomplished through analysis of a combination of COSY, HSQC, and HMBC spectra of the mixture.) R_f 0.38 (20% EtOAc/hexanes); IR (cast film) 3071, 3048, 2960, 2931, 2858, 2136, 1717, 1655, 1309, 1132, 1112 cm⁻¹; HRMS (ESI, [M+Na]⁺) for C₂₇H₃₄N₂O₅SSiNa calcd 549.1850, found: m/z 549.1845.

cis **206** (major diastereomer): ¹H NMR (500 MHz, CDCl₃) δ 7.69-7.66 (m, 4H), 7.44-7.35 (m, 6H), 4.94 (dd, *J* = 6.2, 4.6 Hz, 1H), 4.30 (q, *J* = 7.2 Hz, 2H), 4.17 (ddd, *J* = 12.1, 4.1, 2.3 Hz, 1H), 3.88 (dd, *J* = 11.0, 6.2 Hz, 1H), 3.72 (dd, *J* = 11.0, 4.6 Hz, 1H), 3.66-3.58 (m, 1H), 3.58 (ddd, *J* = 12.1, 12.1, 2.1 Hz, 1H), 3.06 (dd, *J*_{AM} = 16.7 Hz, *J*_{AX} = 7.4 Hz, 1H), 3.01 (dd, *J*_{MA} = 16.7 Hz, *J*_{MX} = 6.5 Hz, 1H), 1.88-1.81 (m, 1H), 1.70-1.60 (m, 1H), 1.33 (t, *J* = 7.2 Hz, 3H), 1.05 (s, 9H); ¹³C NMR (125 MHz, CDCl₃) δ 190.0, 161.3, 135.8, 133.5(2), 133.4(8), 129.8(1), 129.8(0), 127.8(1), 127.7(9), 84.6, 69.7, 66.6, 61.8, 46.0, 37.4, 33.1, 26.9, 19.5, 14.5 (diazo carbon not detected).

Partial *trans* **206** (minor diastereomer): ¹H NMR (500 MHz, CDCl₃) δ 7.69-7.66 (m, 4H), 7.44-7.35 (m, 6H), 5.11 (dd, *J* = 6.3, 4.6 Hz, 1H), 4.35-4.26 (m, 2H), 3.96 (ddd, *J*

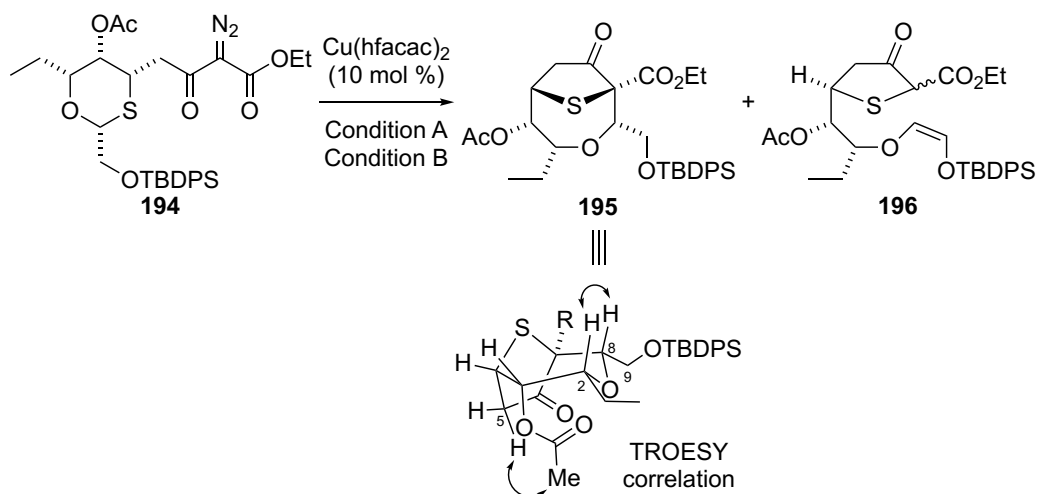
= 12.3, 4.0, 4.0 Hz, 1H), 3.90 (dd, $J = 10.9, 6.3$ Hz, 1H), 3.82 (ddd, $J = 11.9, 11.9, 2.3$ Hz, 1H), 3.73 (dd, $J = 16.0, 8.5$ Hz, 1H), 3.70 (dd, $J = 10.9, 4.6$ Hz, 1H), 3.66-3.58 (m, 1H), 3.16 (dd, $J = 16.0, 6.4$ Hz, 1H), 2.22 (dddd, $J = 14.4, 11.7, 4.3, 4.3$ Hz, 1H) 1.63-1.58 (m, 1H), 1.33 (t, $J = 7.1$ Hz, 3H), 1.05 (s, 9H); ^{13}C NMR (125 MHz, CDCl_3) δ 190.5, 161.4, 135.8, 133.5, 129.8, 127.8, 79.4, 66.5, 64.4, 61.7, 43.5, 33.6, 30.0, 26.9, 19.5, 14.3.



Sulfur-bridged oxacycle 207. To a solution of $\text{Cu}(\text{hfacac})_2$ (0.021 g, 0.044 mmol) in CH_2Cl_2 (44 mL) at reflux was added a solution of **206** (0.231 g, 0.439 mmol, mixture of *cis* **206** and *trans* **206** isomers, 4:1) in CH_2Cl_2 (11 mL) dropwise through the condenser via syringe over 30 minutes. After stirring at reflux for 16 h, the starting material was completely consumed. The reaction mixture was then cooled to room temperature and solvent was removed under vacuum. Column chromatography (silica gel, 10%, 15%, 20% EtOAc/hexanes) provided **207** (0.177 g, 81%) as a colorless oil: R_f 0.29 (20% EtOAc/hexanes); IR (cast film) 3071, 3049, 2932, 2890, 2857, 1750, 1728, 1428, 1233, 1112, 1035 cm^{-1} ; ^1H NMR (500 MHz, CDCl_3) δ 7.71-7.67 (m, 4H), 7.44-7.41 (m, 2H), 7.41-7.37 (m, 4H), 4.61 (dd, $J = 7.9, 3.6$ Hz, 1H), 4.20 (ddd, $J = 13.4, 8.6, 4.6$ Hz, 1H), 4.12 (dd, $J = 11.4, 7.9$ Hz, 1H), 4.08 (dq, $J_{AM} = 10.8$ Hz, $J_{AX} = 7.2$ Hz, 1H), 4.05 (dd, $J_{MA} = 10.8$ Hz, $J_{MX} = 7.2$ Hz, 1H), 3.79 (dd, $J = 11.4, 3.6$ Hz, 1H), 3.67 (ddd, $J = 8.0, 6.4, 1.5$ Hz, 1H), 3.55 (ddd, $J = 13.6, 4.9, 4.9$ Hz, 1H), 3.04 (dd, $J = 17.9, 8.3$ Hz, 1H), 2.60 (d, $J = 17.9$ Hz, 1H), 2.13-2.08 (m, 1H), 1.96 (dddd, $J = 14.5, 8.4, 4.6, 1.7$ Hz, 1H), 1.05 (s, 9H); ^{13}C NMR (125 MHz, CDCl_3) δ 208.9, 165.6, 135.7(9), 135.7(4), 133.6, 133.4, 129.8, 127.8(1), 127.8(0), 82.5, 70.2, 62.8, 62.6, 62.3,

48.3, 38.6, 37.2, 26.9, 19.4, 13.9; HRMS (ESI, $[M+Na]^+$) for $C_{27}H_{34}O_5SSiNa$ calcd 521.1788, found: m/z 521.1783.

Note: $Cu(hfacac)_2 \cdot xH_2O$ (green solid) was purchased from Aldrich. A portion of the catalyst was dried under high vacuum over drierite for 16 h to give anhydrous $Cu(hfacac)_2$ (grey purple solid), which was used for all the reactions employing this catalyst. The remaining anhydrous catalyst was kept in a vial, purged with nitrogen and stored in the desiccator.



Compound 195 and 196. Condition A. To a solution of **194** (63 mg, 0.10 mmol) in toluene (10 mL) at 100 °C was added $Cu(hfacac)_2$ (4.9 mg, 0.010 mmol) as solid in one portion. After stirring the reaction mixture at 100 °C for 1 h, the starting material was completely consumed. The reaction mixture was then cooled to room temperature and the solvent was removed under vacuum. The resulting crude was immediately subjected to column chromatography (silica gel, 10%, 15%, 20%, 25% EtOAc/hexanes) to achieve partial separation and afforded **196** (fraction A, 15.8 mg) and a mixture of **195** and **196** (fraction B, 19.7 mg) as colorless oils in a combined overall yield of 59%. Final yields of **195** and **196** were calculated based on the ratio obtained from 1H NMR of fraction B (25.9 mg **196**, 43%, 9.6 mg **195**, 16%). A second column chromatography was not performed due to instability of **196**. **196** (fraction A)

was isolated as a mixture of diastereomers ($dr = 2:1$) and was used for characterization. (Diastereomeric ratio of 2:1 was determined by integration of the olefin protons in the ^1H NMR spectrum. Assignment of protons and carbons to the individual isomers was accomplished through analysis of a combination of COSY, HSQC, and HMBC spectra of the mixture.) R_f 0.37 (20% EtOAc/hexanes); IR (cast film) 3071, 3049, 2932, 2890, 2857, 1750, 1728, 1428, 1234, 1112, 1035; HRMS (ESI, $[\text{M}+\text{Na}]^+$) calcd for $\text{C}_{31}\text{H}_{40}\text{O}_7\text{SSiNa}$ 607.2156, found: m/z 607.2157.

196a (major diastereomer): ^1H NMR (700 MHz, CDCl_3) δ 7.72-7.68 (m, 4H), 7.45-7.41 (m, 2H), 7.41-7.36 (m, 4H), 5.51 (d, $J = 3.3$ Hz, 1H), 5.37 (d, $J = 3.3$ Hz, 1H), 5.17 (dd, $J = 6.9, 4.9$ Hz, 1H), 4.24-4.19 (m, 2H), 4.13 (s, 1H), 3.99 (app q, $J = 7.0$ Hz, 1H), 3.78 (ddd, $J = 7.5, 5.0, 5.0$ Hz, 1H), 3.00 (dd, $J = 17.7, 7.6$ Hz, 1H), 2.63 (dd, $J = 17.7, 6.3$ Hz, 1H), 2.07 (s, 3H), 1.65-1.59 (m, 2H), 1.28 (t, $J = 7.2$ Hz, 3H), 1.09 (s, 9H), 1.02 (t, $J = 7.3$ Hz, 3H); ^{13}C NMR (125 MHz, CDCl_3) δ 205.3, 170.2, 168.4, 135.5(8), 135.5(7), 132.9(9), 132.9(2), 130.6, 130.0(6), 130.0(2), 127.9, 127.8, 123.9, 82.7, 75.8, 62.5, 52.7, 42.8, 41.4, 26.7, 23.6, 20.9, 19.4, 14.2, 9.9.

196b (minor diastereomer): ^1H NMR (700 MHz, CDCl_3) δ 7.72-7.68 (m, 4H), 7.45-7.41 (m, 2H), 7.41-7.36 (m, 4H), 5.54 (d, $J = 3.3$ Hz, 1H), 5.40 (d, $J = 3.3$ Hz, 1H), 5.22 (dd, $J = 8.9, 3.5$ Hz, 1H), 4.24-4.19 (m, 2H), 4.04 (s, 1H), 3.85 (ddd, $J = 8.9, 7.8, 6.8$ Hz, 1H), 3.67 (ddd, $J = 8.2, 5.1, 3.5$ Hz, 1H), 2.83 (dd, $J = 17.7, 6.8$ Hz, 1H), 2.79 (dd, $J = 17.7, 7.8$ Hz, 1H), 2.10 (s, 3H), 1.65-1.53 (m, 2H), 1.28 (t, $J = 7.2$ Hz, 3H), 1.09 (s, 9H), 1.00 (t, $J = 7.3$ Hz, 3H); ^{13}C NMR (125 MHz, CDCl_3) δ 204.4, 170.2, 168.4, 135.6, 133.0, 132.9, 130.7, 130.0(7), 130.0(3), 127.9, 124.0, 82.5, 76.0, 62.6, 52.4, 41.4, 40.3, 26.7, 23.8, 20.9, 19.4, 14.1, 10.2.

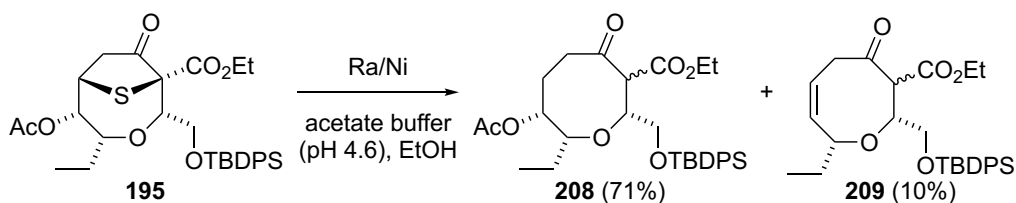
Spectral data for **195** was given at the end of **Condition B**.

Compound 195 and 196. Condition B. To a solution of $\text{Cu}(\text{hfacac})_2$ 6.7 mg, 0.014 mmol) in CH_2Cl_2 (14 mL) at reflux was added a solution of **194** (86 mg, 0.14 mmol) in CH_2Cl_2 (4 mL) dropwise through the condenser via syringe over 30 minutes. After stirring the reaction mixture at reflux for 16 h, the starting material was completely

consumed. The reaction mixture was then cooled to room temperature and the solvent was removed under vacuum. The resulting crude was purified by column chromatography (silica gel, 10%, 15%, 20%, 25% EtOAc/hexanes) to give **195** (49 mg, 60%) as a clear and colorless oil (**196** was not isolated in this case due to decomposition): R_f 0.29 (20% EtOAc/hexanes); $[\alpha]_D^{25} = +57.2$ (c 1.11, CHCl_3); IR (cast film) 3072, 3044, 2963, 2934, 2895, 1766, 1742, 1230, 1113, 1025, 705 cm^{-1} ; ^1H NMR (700 MHz, CDCl_3) δ 7.67-7.65 (m, 4H), 7.43-7.39 (m, 2H), 7.38-7.35 (m, 4H), 5.20 (dd, $J = 7.2, 3.4$ Hz, 1H), 4.60 (ddd, $J = 9.1, 3.8, 3.8$ Hz, 1H), 4.26 (dd, $J = 7.3, 3.1$ Hz, 1H), 4.09 (dq, $J = 10.8, 7.2$ Hz, 1H), 3.96 (dq, $J = 10.8, 7.2$ Hz, 1H), 3.87 (dd, $J = 8.7, 7.4$ Hz, 1H), 3.82 (dd, $J = 11.3, 3.2$ Hz, 1H), 3.76 (dd, $J = 11.3, 7.3$ Hz, 1H), 3.03 (d, $J = 18.9$ Hz, 1H), 2.66 (dd, $J = 18.8, 9.1$ Hz, 1H), 2.12 (s, 3H), 1.66-1.58 (m, 1H), 1.45-1.38 (m, 1H), 1.11 (t, $J = 7.2$ Hz, 3H), 1.04 (s, 9H), 1.01 (t, $J = 7.3$ Hz, 3H); ^{13}C NMR (125 MHz, CDCl_3) δ 206.3, 170.2, 165.6, 135.7(9), 135.7(5), 133.3(5), 133.3(4), 129.8(2), 129.7(7), 129.7(9), 127.7(7), 90.8, 84.8, 77.2, 64.6, 64.5, 62.2, 41.6, 38.8, 26.9, 25.2, 20.9, 19.3, 13.9, 10.7; HRMS (ESI, $[\text{M}+\text{Na}]^+$) calcd for $\text{C}_{31}\text{H}_{40}\text{O}_7\text{SSiNa}$ 607.2150, found: m/z 607.2156.

(Note: no conversion of **195** to **196** was observed when it was resubmitted to the original reaction conditions, as described below)

To a solution of **95** (7.2 mg, 0.012 mmol) in toluene (1.2 mL) at 100 °C was added $\text{Cu}(\text{hfacac})_2$ (0.6 mg, 0.01 mmol) as solid in one portion. After stirring the reaction mixture at 100 °C for 1 h, the reaction mixture was then cooled to room temperature and the solvent was removed under vacuum. Crude ^1H NMR did not show peaks corresponding to **196**. Column chromatography (silica gel, 10%, 15%, 20%, 25% EtOAc/hexanes) provided **195** (6.2 mg, 86%).

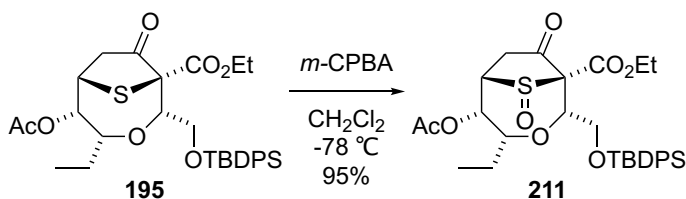


Oxocane 208. Raney nickel 2800 (Aldrich, ~300 mg suspended in water) was allowed to adhere to the tip of a stir bar and dipped quickly into acetate buffer (Aldrich, pH 4.6, 3×3 mL) and absolute EtOH (2×3 mL). The black solid was then rinsed off the stir bar into a clean vial with excess EtOH. (Note: caution must be taken during the washing process as Raney nickel is pyrophoric upon exposure to air.) Raney nickel was then allowed to settle at the bottom of the vial. To a solution of **195** (23 mg, 0.039 mmol) in reaction flask in EtOH and acetate buffer (pH 4.6) (3.8 mL, 2:1 EtOH/buffer, v/v) was added the pretreated Raney Nickel by pipette (add mainly the solid portion and avoid addition of too much EtOH). The mixture was stirred vigorously at room temperature for 30 minutes, filtered through a pad of Celite and rinsed with EtOAc (15 mL). The filter cake of Raney nickel residue was kept moist at all times and transferred immediately after the filtration into designated Raney nickel waste container (rinsed forward with water) for later disposal. The filtrate was washed with brine (20 mL) and the aqueous layer was extracted with EtOAc (2×15 mL). The combined organic layers were dried over anhydrous MgSO₄, filtered and concentrated. Column chromatography (silica gel, 5%, 10%, 15%, 20% EtOAc/hexanes) provided **208** (15 mg, 71%) as a colorless oil and **209** (2 mg, 10%) as a slightly yellow oil.

208: *R_f* 0.33 (20% EtOAc/hexanes); IR (CHCl₃) 3072, 3051, 2961, 2932, 2858, 1740, 1708, 1371, 1240, 1113, 1027 cm⁻¹; ¹H NMR (700 MHz, CDCl₃) δ 7.78-7.76 (m, 2H), 7.69-7.67 (m, 2H), 7.44-7.41 (m, 4H), 7.40-7.36 (m, 4H), 4.91 (ddd, *J* = 8.3, 4.0, 2.1 Hz, 1H), 4.35 (d, *J* = 9.7 Hz, 1H), 4.15 (q, *J* = 7.2 Hz, 2H), 4.10 (ddd, *J* = 9.7, 3.9, 2.9 Hz, 1H), 3.88 (d, *J* = 10.9, 4.0 Hz, 1H), 3.84 (dd, *J* = 10.9, 2.7 Hz, 1H), 3.22 (ddd, *J* = 8.4, 5.2, 2.2 Hz, 1H), 2.91 (ddd, *J* = 14.7, 8.9, 2.5 Hz, 1H), 2.48 (ddd, *J* = 14.7, 11.1, 2.5 Hz, 1H), 2.38 (dddd, *J* = 14.6, 10.9, 8.3, 2.5 Hz, 1H), 2.11 (s, 3H), 2.10-2.07 (m, 1H), 1.60-1.52 (m, 1H), 1.44-1.37 (m, 1H), 1.22 (t, *J* = 7.1 Hz, 3H), 1.06 (s, 9H), 0.82

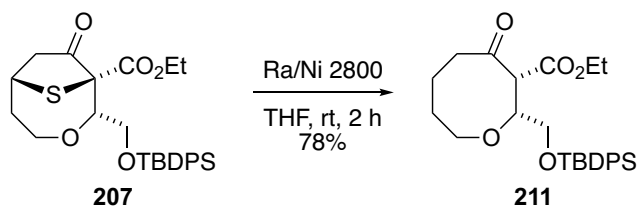
(t, $J = 7.5$ Hz, 3H); ^{13}C NMR (125 MHz, CDCl_3) δ 209.3, 168.0, 136.0, 135.7, 129.9, 129.8, 127.8, 127.7, 82.7, 81.8, 73.2, 66.5, 61.4, 59.4, 40.1, 27.2, 26.8, 25.6, 21.2, 19.5, 14.2, 10.4; HRMS (ESI, $[\text{M}+\text{Na}]^+$) calcd for $\text{C}_{31}\text{H}_{42}\text{O}_7\text{SiNa}$ 577.2592, found: m/z 577.2596.

209: R_f 0.50 (20% EtOAc/hexanes); IR (cast film) 3072, 3050, 2961, 2932, 2858, 1742, 1708, 1640, 1239, 1114 cm^{-1} ; ^1H NMR (500 MHz, CDCl_3) δ 7.73-7.66 (m, 4H), 7.45-7.34 (m, 6H), 5.59-5.56 (m, 2H), 4.24-4.28 (m, 1H), 4.18-4.09 (m, 3H), 3.95-3.89 (m, 1H), 3.75 (dd, $J = 10.6, 5.0$ Hz, 1H), 3.74 (d, $J = 6.3$ Hz, 1H), 3.65 (dd, $J = 10.6, 4.3$ Hz, 1H), 2.94-2.89 (m, 1H), 1.71-1.60 (m, 1H), 1.24 (t, $J = 7.1$ Hz, 3H), 1.04 (s, 9H), 0.96 (t, $J = 7.3$ Hz, 3H); ^{13}C NMR (125 MHz, CDCl_3) δ 203.6, 169.1, 135.8, 135.7, 135.2, 133.4, 133.3, 129.8(8), 129.8(4), 127.9, 127.8, 121.9, 83.0, 77.9, 66.2, 61.4, 60.4, 43.0, 28.7, 26.8, 19.4, 14.2, 10.0; HRMS (ESI, $[\text{M}+\text{Na}]^+$) calcd for $\text{C}_{29}\text{H}_{38}\text{O}_5\text{SiNa}$ 517.2381, found: m/z 517.2370.



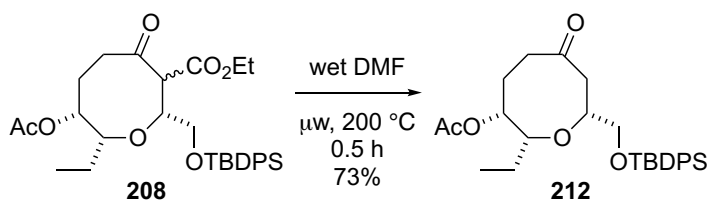
Sulfoxide 211. To a solution of **195** (16 mg, 0.028 mmol) in CH_2Cl_2 (1 mL) at $-78\text{ }^\circ\text{C}$ was added a solution of *m*-chloroperbenzoic acid (77 wt%, 10 mg, 0.046 mmol) in CH_2Cl_2 (1 mL). After stirring at $-78\text{ }^\circ\text{C}$ for 20 minutes, the starting material was completely consumed. Saturated NaHCO_3 solution (5 mL) was added to the reaction flask and the mixture was warmed up to room temperature. The aqueous layer was extracted with CH_2Cl_2 (2 \times 5 mL). The combined organic layers were washed with brine (10 mL), dried over anhydrous MgSO_4 , filtered and concentrated. Column chromatography (silica gel, 2%, 4%, 5% MeOH/ CH_2Cl_2) provided **211** (16 mg, 95%) as a colorless oil: R_f 0.29 (2% MeOH/ CH_2Cl_2); IR (cast film) 3072, 3049, 2963, 2933, 2858, 1770, 1747, 1429, 1226, 1114 cm^{-1} ; ^1H NMR (500 MHz, CDCl_3) δ 7.65-7.61 (m,

4H), 7.45-7.35 (m, 6H), 5.39 (dd, $J = 8.1, 2.8$ Hz, 1H), 4.35 (dd, $J = 7.2, 3.4$ Hz, 1H), 4.17 (dq, $J = 10.7, 7.2$ Hz, 1H), 4.11-4.06 (m, 1H), 4.06 (dq, $J = 10.7, 7.2$ Hz, 1H), 3.82 (dd, $J = 11.4, 7.2$ Hz, 1H), 3.72 (dd, $J = 11.4, 3.4$ Hz, 1H), 3.52 (ddd, $J = 8.8, 4.0, 2.8$ Hz, 1H), 3.20 (dd, $J = 19.2, 9.1$ Hz, 1H), 3.12 (dd, $J = 19.2, 1.8$ Hz, 1H), 2.15 (s, 3H), 1.71-1.59 (m, 1H), 1.48-1.39 (m, 1H), 1.16 (t, $J = 7.2$ Hz, 3H), 1.03 (s, 9H), 0.97 (t, $J = 7.5$ Hz, 3H); ^{13}C NMR (125 MHz, CDCl_3) δ 204.4, 169.9, 135.7(3), 135.6(9), 132.9(1), 132.8(8), 130.0(2), 129.9(5), 127.9(1), 127.8(7), 85.6, 85.5, 84.4, 68.8, 63.9, 63.1, 58.9, 37.2, 26.9, 25.1, 20.7, 19.2, 14.0, 10.3; HRMS (ESI, $[\text{M}+\text{Na}]^+$) calcd for $\text{C}_{31}\text{H}_{40}\text{O}_8\text{SSiNa}$ 623.2105, found: m/z 623.2110.



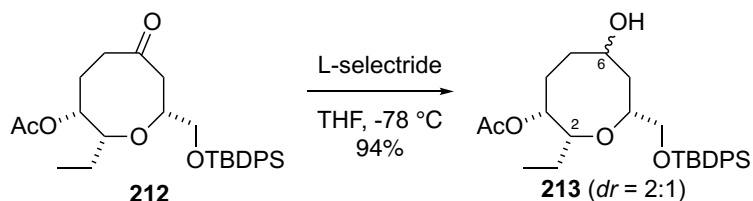
Oxocane 211. Raney nickel 2800 (Aldrich, ~300 mg suspended in water) was allowed to adhere to the tip of a stir bar and dipped quickly into saturated NH_4Cl solution (2 mL), water (2×2 mL) and THF (3×2 mL). The black solid was then rinsed off the stir bar into a clean vial with excess THF. Raney nickel was then allowed to settle at the bottom of the vial. To a solution of **207** (25 mg, 0.051 mmol) in THF (2 mL) was added the pretreated Raney nickel by pipette (add mainly the solid portion and avoid addition of too much THF). The mixture was stirred vigorously at room temperature for 2 h, filtered through a pad of Celite and rinsed with EtOAc (5 mL). The filtrate was washed with brine (20 mL) and the aqueous layer was extracted with EtOAc (2×5 mL). The combined organic layers were dried over anhydrous MgSO_4 , filtered and concentrated. Column chromatography (silica gel, 5%, 10%, 15%, 20%, 25% EtOAc/hexanes) provided **211** (19 mg, 78%) as a colorless oil: R_f 0.39 (20% EtOAc/hexanes); IR (cast film) 3072, 3049, 2931, 2858, 1742, 1712, 1428, 1113 cm^{-1} ; ^1H NMR (700 MHz, CDCl_3) δ 7.73-7.62 (m, 4H), 7.46-7.32 (m, 6H), 4.21 (ddd, $J = 10.3, 4.7, 4.0$ Hz, 1H),

4.14 (dq, $J = 10.8, 7.1$ Hz, 1H), 4.09 (dq, $J = 10.8, 7.1$ Hz, 1H), 3.87 (d, $J = 10.3$ Hz, 1H), 3.91-3.84 (m, 1H), 3.75-3.71 (m, 2H), 3.58 (ddd, $J = 12.2, 5.7, 3.7$ Hz, 1H), 2.75 (ddd $J = 12.6, 9.8, 3.0$ Hz, 1H), 2.53 (ddd, $J = 12.6, 8.5, 3.5$ Hz, 1H), 2.02-1.93 (m, 1H), 1.87-1.74 (m, 2H), 1.74-1.62 (m, 1H), 1.20 (t, $J = 7.1$ Hz, 3H), 1.06 (s, 9H); ^{13}C NMR (125 MHz, CDCl_3) δ 208.2, 168.1, 135.8, 135.7, 133.4(3), 133.3(8), 129.8 (4), 129.8(2), 127.8(2), 127.8 (0), 77.9, 70.5, 66.5, 62.1, 61.3, 41.7, 28.1, 26.9, 24.2, 19.4, 14.1; HRMS (ESI, $[\text{M}+\text{Na}]^+$) calcd for $\text{C}_{27}\text{H}_{36}\text{O}_5\text{SiNa}$ 491.2224, found: m/z 491.2220.



Ketone 212. To a solution of ketoester **208** (18 mg, 0.032 mmol) in DMF (0.6 mL) in a 2 mL Biotage microwave vial was added H_2O (15 μL , 0.80 mmol). The vial was sealed and subjected to microwave irradiation (200 $^\circ\text{C}$) in a Biotage Initiator microwave reactor for 30 min. (See the general information for description of temperature monitoring in microwave reactions.) The reaction mixture was cooled to room temperature and added to a mixture of CH_2Cl_2 (10 mL) and water (5 mL). The resulting organic layer was washed with water (3 \times 5 mL). The aqueous layer was combined, saturated with sodium chloride and extracted with CH_2Cl_2 (3 \times 10 mL). The combined organic layers were dried over anhydrous MgSO_4 , filtered and concentrated. Column chromatography (silica gel, 15%, 20%, 25%, 30% EtOAc/hexanes) provided **212** (11 mg, 73%) as a colorless oil: R_f 0.25 (20% EtOAc/hexanes); $[\alpha]_D^{25} = +32.9$ (c 0.8, CHCl_3); IR (cast film) 3072, 3049, 2962, 2932, 2858, 1736, 1701, 1428, 1242, 1113, 1081 cm^{-1} ; ^1H NMR (700 MHz, CDCl_3) δ 7.70-7.67 (m, 4H), 7.45-7.41 (m, 2H), 7.40-7.36 (m, 4H), 4.78 (ddd, $J = 10.3, 4.5, 2.3$ Hz, 1H), 3.81 (dd, $J = 10.5, 5.0$ Hz, 1H), 3.74-3.70 (m, 1H), 3.63 (dd, $J = 10.3, 6.4$ Hz, 1H), 3.03 (ddd, $J = 9.0, 4.2, 2.5$ Hz, 1H), 2.97 (dd, $J = 10.8, 10.8$ Hz, 1H), 2.58 (ddd, $J = 16.2, 6.9, 2.4$ Hz, 1H), 2.55

(dd, $J = 11.0, 2.0$ Hz, 1H), 2.50 (dddd, $J = 13.4, 13.4, 10.7, 2.7$ Hz, 1H), 2.40 (ddd, $J = 16.1, 13.4, 2.5$ Hz, 1H), 2.07 (s, 3H), 1.98 (dddd, $J = 13.9, 6.9, 4.5, 2.4$ Hz, 1H), 1.54-1.48 (m, 1H), 1.36-1.29 (m, 1H), 1.06 (s, 9H), 0.81 (t, $J = 7.4$ Hz, 3H); ^{13}C NMR (125 MHz, CDCl_3) δ 214.1, 170.6, 135.8(4), 135.7(7), 133.5, 133.4, 129.9, 127.8(5), 127.8(3), 82.7, 80.9, 74.8, 66.8, 45.7, 41.2, 27.0, 25.6(7), 25.6(5), 21.2, 19.4, 10.3; HRMS (ESI, $[\text{M}+\text{Na}]^+$) calcd for $\text{C}_{28}\text{H}_{38}\text{O}_5\text{SiNa}$ 505.2381, found: m/z 505.2388.



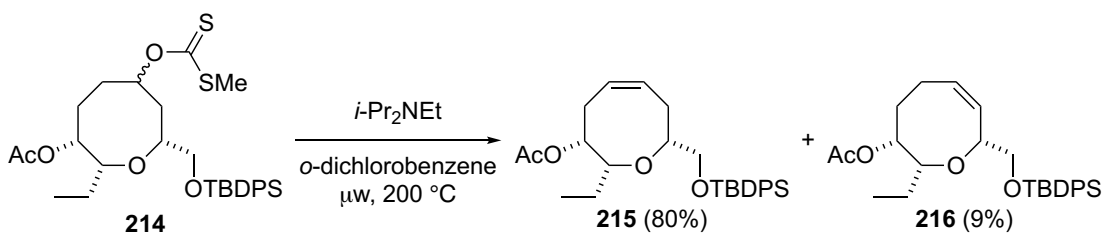
Alcohols 213. To a solution of **212** (14 mg, 0.029 mmol) in THF (1.0 mL) at $-78\text{ }^\circ\text{C}$ was added L-Selectride (0.06 mL, 0.06 mmol, 1.0 M in THF) dropwise and the mixture was stirred for 5 minutes at $-78\text{ }^\circ\text{C}$. After completion of reaction, saturated NH_4Cl solution (10 mL) and EtOAc (10 mL) was added. The aqueous layer was extracted with EtOAc (3×10 mL). The combined organic layers were washed with brine (15 mL), dried with anhydrous MgSO_4 , filtered and concentrate. Column chromatography (silica gel, 30%, 35%, 40%, 45% EtOAc/hexanes) provided **213** (13 mg, 94%) as a mixture of inseparable C6 epimers as a colorless oil. (Diastereomeric ratio of 2:1 was determined by integration of the C2 proton in the ^1H NMR spectrum. Assignment of protons and carbons to the individual isomers was accomplished through analysis of a combination of COSY, HSQC, and HMBC spectra of the mixture: R_f 0.34 (40% EtOAc/hexanes); IR (cast film) 3452 (br), 3072, 3051, 2961, 2931, 2858, 1736, 1259, 1243, 1113, 1025, 704 cm^{-1} ; HRMS (ESI, $[\text{M}+\text{Na}]^+$) calcd for $\text{C}_{28}\text{H}_{40}\text{O}_5\text{SiNa}$ 507.2537, found: m/z 507.2534.

213 (major diastereomer): ^1H NMR (700 MHz, CDCl_3) δ 7.71-7.67 (m, 4H), 7.45-7.40 (m, 2H), 7.40-7.35 (m, 4H), 4.96-4.89 (m, 1H), 4.09 (br s, 1H), 4.08-4.03 (m, 1H), 3.79-3.73 (m, 2), 3.57-3.50 (m, 1H), 3.38 (ddd, $J = 8.6, 5.1, 2.0$ Hz, 1H), 2.27-2.22 (m,

accomplished through analysis of a combination of COSY, HSQC, and HMBC spectra of the mixture.) R_f 0.65 (40% EtOAc/hexanes); IR (cast film) 3071, 3050, 2960, 2931, 2858, 1737, 1428, 1239, 1113, 1080, 1052 cm^{-1} ; HRMS (ESI, $[\text{M}+\text{Na}]^+$) calcd for $\text{C}_{30}\text{H}_{42}\text{O}_5\text{S}_2\text{SiNa}$ 597.2135, found: m/z 597.2144.

214 (major diastereomer): ^1H NMR (500 MHz, CDCl_3) δ 7.72-7.64 (m, 4H), 7.46-7.35 (m, 6H), 6.06-5.98 (m, 1H), 4.97-4.93 (m, 1H), 3.79-3.67 (m, 2H), 3.61-3.50 (m, 1H), 3.35 (ddd, $J = 8.5, 5.0, 1.9$ Hz, 1H), 2.56 (s, 3H), 2.40-2.18 (m, 2H), 2.08 (s, 3H), 2.06-1.83 (m, 4H), 1.61-1.47 (m, 1H), 1.45-1.34 (m, 1H), 1.05 (s, 9H), 0.83 (t, $J = 7.5$ Hz, 3H); ^{13}C NMR (125 MHz, CDCl_3) δ 214.8, 170.8, 135.8(5), 135.8(3), 133.6, 133.5, 129.8(5), 129.8(4), 127.8, 82.7, 81.0, 77.8, 72.8, 66.0, 33.1, 27.0, 25.7, 25.3, 24.5, 21.3, 19.3, 19.1, 10.6.

214 (minor diastereomer): ^1H NMR (500 MHz, CDCl_3) δ 7.72-7.64 (m, 4H), 7.46-7.35 (m, 6H), 5.73 (dddd, $J = 9.8, 9.8, 3.4, 3.4$ Hz, 1H), 4.93-4.90 (m, 1H), 3.79-3.67 (m, 1H), 3.61-3.50 (m, 2H), 3.24 (ddd, $J = 8.0, 5.3, 2.5$ Hz, 1H), 2.51 (s, 3H), 2.40-2.18 (m, 2H), 2.08 (s, 3H), 2.06-1.83 (m, 3H), 1.72-1.64 (m, 1H), 1.61-1.47 (m, 1H), 1.45-1.34 (m, 1H), 1.05 (s, 9H), 0.82 (t, $J = 7.3$ Hz, 3H); ^{13}C NMR (125 MHz, CDCl_3) δ 214.9, 170.7, 135.8(1), 135.7(9), 133.7, 133.5, 129.9, 127.9, 84.8, 84.3, 81.0, 72.8, 67.0, 36.1, 27.3, 27.0, 26.9, 25.5, 21.2, 19.3, 19.0, 10.6.

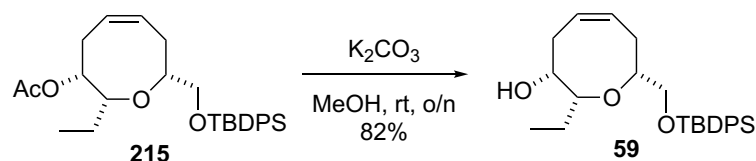


Oxocene 215. To a solution of xanthate ester **214** (10 mg, 0.017 mmol) in $o\text{-dichlorobenzene}$ (2.0 mL) in a 2 mL Biotage microwave vial was added $i\text{-Pr}_2\text{NEt}$ (3 μL , 0.02 mmol). The vial was purged with N_2 and sealed. The resulting mixture was subjected to microwave irradiation (200°C) in a Biotage Initiator microwave reactor

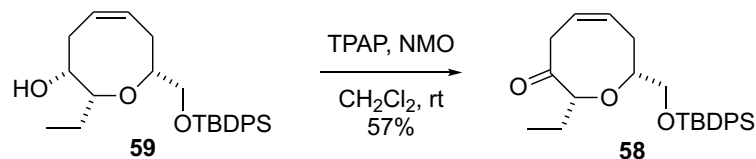
for 30 min. (See the general information for description of temperature monitoring in microwave reactions.) The reaction mixture was cooled to room temperature and directly subjected to column chromatography (silica gel, 2%, 4%, 6% EtOAc/hexanes) to give **215** (major, 6.5 mg) and **216** (minor, 0.7 mg) as colorless oils in a combined overall yield of 89%.

215: R_f 0.34 (20% EtOAc/hexanes); $[\alpha]_D^{25} = +11.3$ (c 0.26, CHCl_3); IR (cast film) 3071, 3048, 3022, 2960, 2931, 2859, 1736, 1428, 1240, 1113 cm^{-1} ; ^1H NMR (700 MHz, CDCl_3) δ 7.69-7.66 (m, 4H), 7.44-7.40 (m, 2H), 7.39-7.36 (m, 4H), 5.93-5.88 (m, 1H), 5.74 (dddd, $J = 10.3, 10.3, 6.7, 1.7$ Hz, 1H), 4.91 (ddd, $J = 11.2, 5.2, 2.6$ Hz, 1H), 3.81 (dd, $J = 10.1, 5.1$ Hz, 1H), 3.55 (dd, $J = 10.1, 7.6$ Hz, 1H), 3.55-3.52 (m, 1H), 3.39-3.34 (m, 1H), 2.70 (app q, $J = 11.1$ Hz, 1H), 2.43 (ddd, $J = 14.0, 8.5, 0.9$ Hz, 1H), 2.35-2.29 (m, 1H), 2.22-2.26 (m, 1H), 2.06 (s, 3H), 1.48-1.41 (m, 1H), 1.30-1.23 (m, 1H), 1.06 (s, 9H), 0.81 (t, $J = 7.4$ Hz, 3H); ^{13}C NMR (125 MHz, CDCl_3) δ 171.0, 135.8(0), 135.7(5), 133.8, 133.7, 131.0, 129.8(1), 129.7(9), 128.3, 127.8, 83.2, 82.0, 76.9, 67.0, 31.8, 29.5, 27.0, 25.5, 21.3, 19.4, 10.7; HRMS (ESI, $[\text{M}+\text{Na}]^+$) calcd for $\text{C}_{28}\text{H}_{38}\text{O}_4\text{SiNa}$ 489.2432, found: m/z 489.2426.

216: R_f 0.37 (20% EtOAc/hexanes); IR (CHCl_3) 3072, 3050, 3014, 2960, 2931, 2857, 1737, 1428, 1240, 1113 cm^{-1} ; ^1H NMR (700 MHz, CDCl_3) δ 7.76-7.74 (m, 2H), 7.72-7.69 (m, 2H), 7.43-7.40 (m, 2H), 7.39-7.36 (m, 4H), 5.76 (dddd, $J = 11.7, 8.3, 8.3, 1.3$ Hz, 1H), 5.43 (ddd, $J = 11.7, 3.2, 1.7$ Hz, 1H), 5.09 (ddd, $J = 6.0, 4.0, 2.0$ Hz, 1H), 4.23-4.19 (m, 1H), 3.74 (dd, $J = 10.5, 6.9$ Hz, 1H), 3.67 (dd, $J = 10.5, 4.7$ Hz, 1H), 3.52 (ddd, $J = 9.0, 4.6, 2.1$ Hz, 1H), 3.07-3.00 (m, 1H), 2.09 (s, 3H), 1.94 (dddd, $J = 14.6, 6.4, 6.4, 2.4$ Hz, 1H), 1.82 (dddd, $J = 13.3, 8.9, 6.7, 2.4$ Hz, 1H), 1.67-1.58 (m, 1H), 1.54-1.48 (m, 1H), 1.06 (s, 9H), 0.98 (t, $J = 7.5$ Hz, 3H); ^{13}C NMR (125 MHz, CDCl_3) δ 171.0, 136.0, 135.8, 134.0, 133.8, 130.9, 129.6(9), 129.6(6), 129.6(1), 127.7(4), 127.6(9), 81.7, 81.0, 71.9, 66.8, 30.7, 26.6, 25.5, 21.5, 21.4, 19.4, 10.8; HRMS (ESI, $[\text{M}+\text{Na}]^+$) calcd for $\text{C}_{28}\text{H}_{38}\text{O}_4\text{SiNa}$ 489.2432, found: m/z 489.2438.

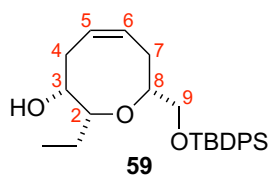


Alcohol 59. To a solution of **215** (4.3 mg, 9.2 μmol) in MeOH (1.0 mL) was added K_2CO_3 (5 mg, 0.04 mmol). After stirring at room temperature vigorously for 3 h, a clear solution was obtained. More K_2CO_3 (5 mg, 0.04 mmol) was added and the mixture was stirred at room temperature overnight (19 h). Solvent was then removed under vacuum and the residue was diluted with EtOAc (5 mL). Saturated NH_4Cl solution (5 mL) was added and the aqueous layer was extracted with EtOAc (3 \times 5 mL). The combined organic layers were washed with brine (15 mL), dried over anhydrous MgSO_4 , filtered and concentrated. Column chromatography (silica gel, 5%, 10%, 15% EtOAc/hexanes) provided **59** (3.2 mg, 82%) as a colorless oil: R_f 0.32 (20% EtOAc/hexanes); $[\alpha]_D^{25} = -3.5$ (c 0.25, CHCl_3); IR (cast film) 3451 (br), 3071, 3048, 3018, 2960, 2930, 2858, 1428, 1114, 1078, 825 cm^{-1} ; ^1H NMR (500 MHz, CDCl_3) δ 7.76-7.66 (m, 4H), 7.45-7.40 (m, 2H), 7.40-7.36 (m, 4H), 5.80-5.70 (m, 2H), 3.72 (dd, $J = 13.0, 8.3$ Hz, 1H), 3.69-3.61 (m, 1H), 3.56-3.50 (m, 2H), 3.40 (ddd, $J = 9.4, 4.4, 1.5$ Hz, 1H), 2.51 (ddd, $J = 12.8, 8.9, 8.9$ Hz, 1H), 2.38 (ddd, $J = 13.9, 8.2, 2.7$ Hz, 1H), 2.34-2.26 (m, 2H), 1.66-1.57 (m, 1H), 1.45-1.36 (m, 1H), 1.06 (s, 9H), 0.87 (t, $J = 7.4$ Hz, 3H); ^{13}C NMR (125 MHz, CDCl_3) 135.6, 133.6, 129.6(5), 129.6(3), 129.5, 129.1, 127.6(4), 127.6(2), 82.3, 81.1, 74.3, 66.4, 33.5, 30.4, 26.9, 25.9, 19.2, 10.5; HRMS (ESI, $[\text{M}+\text{Na}]^+$) calcd for $\text{C}_{26}\text{H}_{36}\text{O}_3\text{SiNa}$ 447.2326, found: m/z 447.2319.



Ketone 58. To a solution of **59** (5.5 mg, 0.013 mmol) in CH_2Cl_2 (1 mL) at room temperature was added activated powdered 4 \AA molecular sieves (20 mg) and *N*-

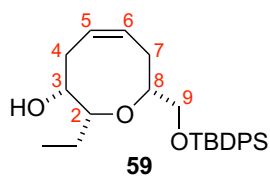
methylmorpholine *N*-oxide (4.6 mg, 0.039 mmol). After stirring at room temperature for 10 minutes, tetrapropylammonium perruthenate (0.6 mg, 1 μ mol) was added. The mixture was further stirred at room temperature and monitored by TLC until completion (1 h). The initial green reaction mixture darkened as the reaction proceeded. The mixture was then diluted with 1 mL EtOAc and filtered through a short plug of silica gel and rinsed with EtOAc (1.0 mL) three times. The filtrate was concentrated to give **58** (3 mg, 57%) as a clear and colorless oil: R_f 0.53 (20% EtOAc/hexanes); $[\alpha]_D^{25} = +291.6$ (*c* 0.31, CH₂Cl₂), IR (cast film) 3072, 3051, 3026, 2961, 2932, 2858, 1718, 1428, 1113, 824 cm⁻¹; ¹H NMR (700 MHz, CDCl₃) δ 7.69-7.66 (m, 4H), 7.45-7.42 (m, 2H), 7.40-7.37 (m, 4H), 5.79-5.75 (m, 1H), 5.63-5.58 (m, 1H), 3.86 (ddd, $J = 12.2, 7.4, 2.0$ Hz, 1H), 3.77 (dd, $J = 10.3, 5.7$ Hz, 1H), 3.71 (dd, $J = 8.7, 4.3$ Hz, 1H), 3.58 (dd, $J = 10.3, 6.7$ Hz, 1H), 3.50 (dddd, $J = 6.5, 6.5, 6.5, 2.2$ Hz, 1H), 2.76 (dd, $J = 12.2, 6.9$ Hz, 1H), 2.40 (ddd, $J = 14.8, 8.4, 2.3$ Hz, 1H), 2.33 (ddd, $J = 14.6, 7.2, 7.2$ Hz, 1H), 1.72-1.65 (m, 1H), 1.57-1.50 (m, 1H), 1.06 (s, 9H), 0.90 (t, $J = 7.4$ Hz, 3H); ¹³C NMR (125 MHz, CDCl₃) δ 214.0, 135.6(0), 135.5(8), 133.5, 133.4, 129.7(3), 129.7(1), 128.6, 127.6(9), 127.6(8), 125.8, 87.1, 84.1, 66.2, 41.0, 29.9, 26.8, 26.1, 19.2, 10.0; HRMS (ESI, [M+Na]⁺) calcd for C₂₆H₃₄O₃SiNa 445.2169, found: m/z 445.2163.



Entry	Signal Assignment ^a	Synthetic 59 (700 MHz, CDCl ₃)	Lit. ²⁶ (500 MHz, CDCl ₃)	Lit. ²⁴ (400 MHz, CDCl ₃)
1	Ar-H	7.76-7.66 (m, 4H)	7.69-7.67 (m, 4H)	7.68 (m, 4H)
2	Ar-H	7.45-7.40 (m, 2H) 7.40-7.36 (m, 4H)	7.43-7.36 (m, 6H)	7.45-7.36 (m, 6H)
3	5+6	5.80-5.70 (m, 2H)	5.80-5.70 (m, 2H)	5.81-5.70 (m, 2H)
4	9a	3.72 (dd, <i>J</i> = 13.0, 8.3 Hz, 1H)	3.72 (dd, <i>J</i> = 13.0, 8.3 Hz, 1H)	3.73 (dd, <i>J</i> = 12.8, 8.3 Hz, 1H)
5	3	3.69-3.61 (m, 1H)	3.67-3.63 (m, 1H)	3.65 (m, 1H)
6	8+9b	3.56-3.50 (m, 2H)	3.54-3.52 (m, 2H)	3.53 (m, 2H)
7	2	3.40 (ddd, <i>J</i> = 9.4, 4.4, 1.5 Hz, 1H)	3.40 (ddd, <i>J</i> = 9.2, 4.4, 1.6 Hz, 1H)	3.40 (dd, <i>J</i> = 9.2, 4.4 Hz, 1H)
8	4a	2.51 (ddd, <i>J</i> = 12.8, 8.9, 8.9 Hz, 1H)	2.51 (dt, <i>J</i> = 12.6, 9.0 Hz, 1H)	2.53 (m, 1H)
9	7a	2.38 (ddd, <i>J</i> = 13.9, 8.2, 2.7 Hz, 1H)	2.42-2.28 (m, 3H)	2.27-2.42 (m, 3H)
10	7b+4b	2.34-2.26 (m, 2H)		
11	OH	Not detected	1.65 (d, <i>J</i> = 10.3 Hz, 1H)	1.72 (br s, 1H)
12	CH ₂ CH ₃	1.66-1.57 (m, 1H) 1.45-1.36 (m, 1H)	1.65-1.59 (m, 1H) 1.43-1.38 (m, 1H)	1.68-1.60 (m, 1H) 1.45-1.37 (m, 1H)
13	C(CH ₃) ₃	1.06 (s, 9H)	1.06 (s, 9H)	1.07 (s, 9H)
14	CH ₂ CH ₃	0.87 (t, <i>J</i> = 7.4 Hz, 3H)	0.87 (t, <i>J</i> = 7.4 Hz, 3H)	0.87 (t, <i>J</i> = 7.4 Hz, 3H)

^a The assignment was based on synthetic **59**.

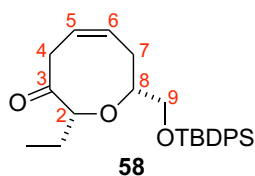
Table 2.10 Comparison of ¹H NMR data of **59 with literature data**



Entry	Signal Assignment ^a	Synthetic 59 ^b (126 MHz, CDCl ₃)	Lit. ²⁶ (50 MHz, CDCl ₃)	Lit. ²⁴ (100 MHz, CDCl ₃)
1	Ar-C	135.6	135.6	135.6
2	Ar-C (quartnary)	133.6	133.6	133.6
3	Ar-C	129.6(5) 129.6(3)	129.6	129.6
4	5	129.5	129.4	129.5
5	6	129.1	129.1	129.1
6	Ar-C	127.6(4) 127.6(2)	127.6	127.7 127.6
7	2	82.3	82.3	82.3
8	8	81.1	81.1	81.1
9	3	74.3	74.3	74.3
10	9	66.4	66.4	66.4
11	4	33.5	33.5	33.5
12	7	30.4	30.4	30.4
13	C(CH ₃) ₃	26.9	26.9	26.9
14	CH ₂ CH ₃	25.9	25.9	25.9
15	C(CH ₃) ₃	19.2	19.2	19.2
16	CH ₂ CH ₃	10.5	10.5	10.5

^a The assignment was based on synthetic **59**. ^b The spectra were referenced to residual solvent peaks of CDCl₃ to 77.06 ppm instead of 77.16 ppm for the purpose of comparison.

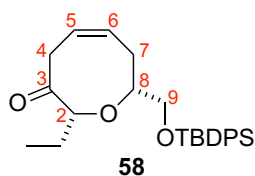
Table 2.11 Comparison of ¹³C NMR data of **59 with literature data**



Entry	Signal Assignment ^a	Synthetic 58 (700 MHz, CDCl ₃)	Lit. ²⁶ (250 MHz, CDCl ₃)	Lit. ²⁴ (400 MHz, CDCl ₃)
1	Ar-H	7.69-7.66 (m, 4H)	7.70-7.76 (m, 4H)	7.67 (d, <i>J</i> = 6.9 Hz, 4H)
2	Ar-H	7.45-7.42 (m, 2H) 7.40-7.37 (m, 4H)	7.44-7.34 (m, 6H)	7.37-7.45 (m, 6H)
3	6	5.79-5.75 (m, 1H)	5.83-5.73 (m, 1H)	5.77 (m, 1H)
4	5	5.63-5.58 (m, 1H)	5.66-5.56 (m, 1H)	5.61 (dt, <i>J</i> = 10.6, 7.2 Hz, 1H)
5	4a	3.86 (ddd, <i>J</i> = 12.2, 7.4, 2.0 Hz, 1H)	3.87 (ddd, <i>J</i> = 12.2, 7.4, 1.8 Hz, 1H)	3.87 (ddd, <i>J</i> = 12.2, 7.4 Hz, 1H)
6	9a	3.77 (dd, <i>J</i> = 10.3, 5.7 Hz, 1H)	3.78 (dd, <i>J</i> = 9.9, 5.8 Hz, 1H)	3.78 (dd, <i>J</i> = 10.1, 5.7 Hz, 1H)
7	2	3.71 (dd, <i>J</i> = 8.7, 4.3 Hz, 1H)	3.69 (dd, <i>J</i> = 8.5, 4.2 Hz, 1H)	3.71 (dd, <i>J</i> = 8.6, 4.3 Hz, 1H)
8	9b	3.58 (dd, <i>J</i> = 10.3, 6.7 Hz, 1H)	3.59 (dd, <i>J</i> = 9.9, 6.6 Hz, 1H)	3.58 (dd, <i>J</i> = 10.1, 6.8 Hz, 1H)
9	8	3.50 (dddd, <i>J</i> = 6.5, 6.5, 6.5, 2.2 Hz, 1H)	3.52-3.43 (m, 1H)	3.51 (m, 1H)
10	4b	2.76 (dd, <i>J</i> = 12.2, 6.9 Hz, 1H)	2.76 (dd, <i>J</i> = 12.2, 2.8 Hz, 1H) ^b	2.76 (dd, <i>J</i> = 12.2, 6.8 Hz, 1H)
11	7	2.40 (ddd, <i>J</i> = 14.8, 8.4, 2.3 Hz, 1H) 2.33 (ddd, <i>J</i> = 14.6, 7.2, 7.2 Hz, 1H)	2.45-2.56 (m, 2H)	2.36 (m, 2H)
12	CH ₂ CH ₃	1.72-1.65 (m, 1H) 1.57-1.50 (m, 1H)	1.75-1.54 (m, 2H)	1.69 (m, 1H) 1.54 (m, 1H)
13	C(CH ₃) ₃	1.06 (s, 9H)	1.06 (s, 9H)	1.07 (s, 9H)
14	CH ₂ CH ₃	0.90 (t, <i>J</i> = 7.4 Hz, 3H)	0.88 (t, <i>J</i> = 7.2 Hz, 3H)	0.90 (t, <i>J</i> = 7.4 Hz, 3H)

^a The assignment was based on synthetic **58**.

Table 2.12 Comparison of ¹H NMR data of **58 with literature data**



Entry	Signal Assignment ^a	Synthetic 58 ^b (126 MHz, CDCl ₃)	Lit. ²⁶ (50 MHz, CDCl ₃)	Lit. ²⁴ (100 MHz, CDCl ₃)
1	3	214.0	214.0	214.0
2	Ar-C	135.6(0) 135.5(8)	135.6 135.6	135.7 135.6
3	Ar-C (quaternary)	133.5 133.4	133.5 133.4	133.5 133.4
4	Ar-C	129.7(3) 129.7(1)	129.7	129.7
5	6	128.6	128.6 ^c	128.6
6	Ar-C	127.6(9) 127.6(8)	127.7 ^c	127.7
7	5	125.8	125.8 ^c	125.8
8	2	87.1	87.1	87.1
9	8	84.1	84.1	84.1
10	9	66.2	66.2	66.2
11	4	41.0	41.0	41.0
12	7	29.9	29.9	29.9
13	C(CH ₃) ₃	26.8	26.6	26.8
14	CH ₂ CH ₃	26.1	26.1	26.1
15	C(CH ₃) ₃	19.2	19.2	19.2
16	CH ₂ CH ₃	10.0	10.0	10.0

^a The assignment was based on synthetic **58**. ^b The spectra were referenced to residual solvent peaks of CDCl₃ to 77.06 ppm instead of 77.16 ppm for the purpose of comparison. ^c The reported assignment was 5-C. ^d The reported assignment was 6-C. ^e The reported assignment was Ar-C.

Table 2.13 Comparison of ¹³C NMR data of **58 with literature data**

2.8 References

1. Harizani, M.; Ioannou, E.; Roussis, V. In *Progress in the Chemistry of Organic Natural Products*; Kinghorn, A. D., Falk, H., Gibbons, S., Kobayashi, J., Eds.; Springer International Publishing: Switzerland, **2016**; Vol. 102, pp 91–252.
2. a) Zhou, Z. F.; Menna, M.; Cai, Y. S.; Guo, Y. W. *Chem. Rev.* **2015**, *115*, 1543–1596. b) Wanke, T.; Philippus, A. C.; Zatelli, G. A.; Vieira, L. F. O.; Lhullier, C.; Falkenberg, M. *Rev. Bras. Farmacogn.* **2015**, *25*, 569–587. c) Yasumoto, T.; Murata, M. *Chem. Rev.* **1993**, *93*, 1897–1909.
3. a) Galli, C.; Mandolini, L. *Eur. J. Org. Chem.* **2000**, 3117–3125. b) Illuminati, G.; Mandolini, L.; Masci, B. *J. Am. Chem. Soc.* **1975**, *97*, 4960–4966. c) Illuminati, G.; Mandolini, L. *Acc. Chem. Res.* **1981**, *14*, 95–102.
4. For selected reviews, see: a) Martín, T.; Padrón, J. I.; Martín, V. S. *Synlett* **2013**, *25*, 12–32. b) Kim, D. *Synlett* **2013**, *25*, 33–57. c) Kleinke, A. S.; Webb, D.; Jamison, T. F. *Tetrahedron* **2012**, *68*, 6999–7018. d) Rainier, J. D. In *Metathesis in Natural Product Synthesis: Strategies, Substrates and Catalysts*; Cossy, J., Arseniyadis, S., Meyer, C., Eds.; Wiley–VCH Verlag: Weinheim, 2010; pp 87–127. e) Tori, M.; Mizutani, R. *Molecules* **2010**, *15*, 4242–4260. f) Fujiwara, K. *Top. Heterocycl. Chem.* **2006**, *5*, 97–148. g) Snyder, N. L.; Haines, H. M.; Peczu, M. W. *Tetrahedron* **2006**, *62*, 9301–9320. h) Yet, L. *Chem. Rev.* **2000**, *100*, 2963–3007. i) Hoberg, J. O. *Tetrahedron* **1998**, *54*, 12631–12670. j) Murai, A. *Stud. Nat. Prod. Chem.* **1996**, *19*, 411–461. k) Elliott, M. C. *Contemp. Org. Synth.* **1994**, *1*, 457–474. (l) Roxburgh, C. J. *Tetrahedron* **1993**, *49*, 10749–10784.
5. a) Irie, T.; Suzuki, M.; Masamune, T. *Tetrahedron Lett.* **1965**, *6*, 1091–1099. b) Irie, T.; Suzuki, M.; Masamune, T. *Tetrahedron* **1968**, *24*, 4193–4205.
6. a) Cameron, A. F.; Cheung, K. K.; Ferguson, G.; Robertson, J. M. *Chem. Commun.* **1965**, *24*, 638. b) Cameron, A. F.; Cheung, K. K.; Ferguson, G.; Monteath Robertson, J. *J. Chem. Soc. B* **1969**, *12*, 559–564.

7. Kaul, P. N.; Kulkarni, S. K.; Kurosawa, E. *J. Pharm. Pharmacol.* **1978**, *30*, 589–590.
8. Kladi, M.; Vagias, C.; Stavri, M.; Rahman, M. M.; Gibbons, S.; Roussis, V. *Phytochem. Lett.* **2008**, *1*, 31–36.
9. a) Murai, A.; Murase, H.; Matsue, H.; Masamune, T. *Tetrahedron Lett.* **1977**, *18*, 2507–2510. b) Masamune, T.; Matsue, H. *Chem. Lett.* **1975**, 895–898. c) Masamune, T.; Matsue, H.; Murase, H. *Bull. Chem. Soc. Jpn.* **1979**, *52*, 127–134. d) Masamune, T.; Murase, H.; Matsue, H.; Murai, A. *Bull. Chem. Soc. Jpn.* **1979**, *52*, 135–141.
10. Shapiro, R. H.; Heath, M. J. *J. Am. Chem. Soc.* **1967**, *89*, 5734–5735.
11. Paquette, L. A.; Begland, R. W.; Storm, P. C. *J. Am. Chem. Soc.* **1968**, *90*, 6148–6153.
12. Corey, E. J.; Chaykovsky, M. *J. Am. Chem. Soc.* **1965**, *87*, 1353–1364.
13. Tsushima, K.; Murai, A. *Tetrahedron Lett.* **1992**, *33*, 4345–4348.
14. a) Tsushima, K.; Araki, K.; Murai, A. *Chem. Lett.* **1989**, 1313–1316. b) Tsushima, K.; Murai, A. *Chem. Lett.* **1990**, 761–764.
15. Mori, K.; Takigawa, T.; Matsuo, T. *Tetrahedron* **1979**, *35*, 933–940.
16. Murai, A.; Ono, M.; Masamune, T. *J. Chem. Soc. Chem. Commun.* **1977**, 573–574.
17. a) Mancuso, A. J.; Huang, S.-L.; Swern, D. *J. Org. Chem.* **1978**, *43*, 2480–2482. b) Mancuso, A. J.; Swern, D. *Synthesis* **1981**, 165–185.
18. Souppe, J.; Namy, J. L.; Kagan, H. B. *Tetrahedron Lett.* **1982**, *23*, 3497–3500.
19. Bratz, M.; Bullock, W. H.; Overman, L. E.; Takemoto, T. *J. Am. Chem. Soc.* **1995**, *117*, 5958–5966.
20. Blumenkopf, T. A.; Bratz, M.; Castañeda, A.; Look, G. C.; Overman, L. E.; Rodriguez, D.; Thompson, A. S. *J. Am. Chem. Soc.* **1990**, *112*, 4386–4399.
21. Brown, H. C.; Jadhav, P. K.; Bhat, K. S. *J. Am. Chem. Soc.* **1988**, *110*, 1535–1538.
22. Miyaura, N.; Suzuki, A. *Chem. Rev.* **1995**, *95*, 2457–2483.

23. Ito, Y.; Hirao, T.; Saegusa, T. *J. Org. Chem.* **1978**, *43*, 1011–1013.
24. a) Mujica, M. T.; Afonso, M. M.; Galindo, A.; Palenzuela, J. A. *Synlett* **1996**, 983–984. b) Mujica, M. T.; Afonso, M. M.; Galindo, A.; Palenzuela, J. A. *J. Org. Chem.* **1998**, *63*, 9728–9738.
25. Ortega, N.; Martín, V. S.; Martín, T. *J. Org. Chem.* **2010**, *75*, 6660–6672.
26. Burton, J. W.; Clark, J. S.; Derrer, S.; Stork, T. C.; Bendall, J. G.; Holmes, A. B. *J. Am. Chem. Soc.* **1997**, *119*, 7483–7498.
27. Inanaga, J.; Hirata, K.; Saeki, H.; Katsuki, T.; Yamaguchi, M. *Bull. Chem. Soc. of Jpn.* **1979**, *52*, 1989–1993.
28. a) Mori, K.; Watanabe, H. *Tetrahedron Lett.* **1984**, *52*, 6025–6026. b) Barth, M.; Bellamy, F. D.; Renaut, P.; Samreth, S.; Schuber, F. *Tetrahedron* **1990**, *46*, 6731–6740. c) Meyers, A. I.; Lawson, J. P.; Walker, D. G.; Linderman, R. J. *J. Org. Chem.* **1986**, *51*, 5111–5123.
29. Collum, D. B.; McDonald III, J. H.; Still, W. C. *J. Am. Chem. Soc.* **1980**, *102*, 2118–2120.
30. a) Petasis, N. A.; Bzowej, E. I. *J. Am. Chem. Soc.* **1990**, *112*, 6392–6394. b) Petasis, N. A.; Lu, S.-P.; Bzowej, E. I.; Fu, D.-K.; Staszewski, J. P.; Akritopoulou-Zanze, I.; Patane, M. A.; Hu, Y.-H. *Pure Appl. Chem.* **1996**, *68*, 667–670.
31. Taomao, K.; Nakagawa, Y.; Arai, H.; Higuchi, N.; Ito, Y. *J. Am. Chem. Soc.* **1988**, *110*, 3712–3714.
32. Tamao, K.; Nakagawa, Y.; Ito, Y. *Organometallics* **1993**, *12*, 2297–2308.
33. Crimmins, M. T.; Choy, A. L. *J. Am. Chem. Soc.* **1999**, *121*, 5653–5660.
34. a) Ley, S. V.; Norman, J.; Griffith, W. P.; Marsden, S. P. *Synthesis*. **1994**, 639–666. b) Griffith, W. P.; Ley, S. V.; Whitcombe, G. P.; White, A. D. *J. Chem. Soc. Chem. Commun.* **1987**, 1625–1627.
35. Krüger, J.; Hoffmann, R. W. *J. Am. Chem. Soc.* **1997**, *119*, 7499–7504.
36. Crimmins, M. T.; Emmitte, K. A. *Org. Lett.* **1999**, *1*, 2029–2032.
37. Crimmins, M. T.; Choy, A. L. *J. Org. Chem.* **1997**, *62*, 7548–7549.

38. Asami, M.; Kimura, R. *Chem. Lett.* **1985**, 1211–1222.
39. Schwab, P.; Grubbs, R. H.; Ziller, J. W. *J. Am. Chem. Soc.* **1996**, *118*, 100–110.
40. Baek, S.; Jo, H.; Kim, H.; Kim, H.; Kim, S.; Kim, D. *Org. Lett.* **2005**, *7*, 75–77.
41. Kim, H.; Choi, W. J.; Jung, J.; Kim, S.; Kim, D. *J. Am. Chem. Soc.* **2003**, *125*, 10238–10240.
42. Holton, R. A.; Zoeller, J. R. *J. Am. Chem. Soc.* **1985**, *107* 7, 2124–2131.
43. Su, D.-W.; Wang, Y.-C.; Yan, T.-H. *Tetrahedron Lett.* **1999**, *40*, 4197–4198.
44. Burke, S. D.; Deaton, D. N.; Olsen, R. J.; Armistead, D. M.; Blough, B. E. *Tetrahedron Lett.* **1987**, *28*, 3905–3906.
45. Lanier, M. L.; Park, H.; Mukherjee, P.; Timmerman, J. C.; Ribero, A. A.; Widenhoefer, R. A.; Hong, J. *Chem. Eur. J.* **2017**, *23*, 7180–7184.
46. Fujiwara, K.; Yoshimoto, S.; Takizawa, A.; Souma, S. I.; Mishima, H.; Murai, A.; Kawai, H.; Suzuki, T. *Tetrahedron Lett.* **2005**, *46*, 6819–6822.
47. Fujiwara, K.; Souma, S.; Mishima, H.; Murai, A. *Synlett* **2002**, 1493–1495.
48. Kotsuki, H.; Kadota, I.; Ochi, M. *Tetrahedron Lett.* **1989**, *30*, 1281–1284.
49. Scholl, M.; Ding, S.; Lee, C. W.; Grubbs, R. H. *Org. Lett.* **1999**, *1*, 953–956.
50. Hubschwerlen, C.; Specklin, J.-L.; Higelin, J. *Org. Synth.* **1995**, *72*, 1.
51. Stereoselectivity was dictated by an endo-Cram approach of the diene to the aldehyde, see: a) Danishefsky, S.; Kobayashi, S.; Kerwin Jr, J. F. *J. Org. Chem.* **1982**, *47*, 1981–1983. b) Danishefsky, S. J.; Pearson, W. H.; Harvey, D. F.; Maring, C. J.; Springer, J. P. *J. Am. Chem. Soc.* **1985**, *107*, 1256–1268.
52. Adsool, V. a; Pansare, S. V. *Org. Biomol. Chem.* **2008**, *6*, 2011–2015.
53. a) Pansare, S.; Adsool, V. A. *Org. Lett.* **2006**, *8*, 5897–5899. b) Pansare, S. V.; Ravi, R. G.; Jain, R. P. *J. Org. Chem.* **1998**, *63*, 4120–4124. c) Pansare, S. V.; Shinkre, B. A.; Bhattacharyya, A. *Tetrahedron* **2002**, *58*, 8985–8991.
54. Crimmins, M. T.; Tabet, E. A. *J. Am. Chem. Soc.* **2000**, *122*, 5473–5476.
55. Lockwood, R. F.; Nicholas, K. M. *Tetrahedron Lett.* **1977**, *18*, 4163–4166.
56. a) Ortega, N.; Martín, T.; Martín, V. S. *Eur. J. Org. Chem.* **2009**, 554–563. b) Ortega, N.; Martín, T.; Martín, V. S. *Org. Lett.* **2006**, *8*, 871–873.

57. a) Jacobsen, E. N.; Markó, I.; Mungall, W. S.; Schröder, G.; Sharpless, K. B. *J. Am. Chem. Soc.* **1988**, *110*, 1968–1970. b) Kolb, H. C.; VanNieuwenhze, M. S.; Sharpless, K. B. *Chem. Rev.* **1994**, *94*, 2483–2547.
58. a) Burke, S. D.; Voight, E. A. *Org. Lett.* **2001**, *3*, 237–240. b) Grieco, P. A.; Gilman, S.; Nishizawa, M. *J. Org. Chem.* **1976**, *41*, 1485–1486. c) Sharpless, K. B.; Young, M. W. *J. Org. Chem.* **1974**, *40*, 947–949.
59. a) Hoffmann, R. W.; Münster, I. *Tetrahedron Lett.* **1995**, *36*, 1431–1434. b) Hoffmann, R. W.; Münster, I. *Liebigs Ann. Chem.* **1997**, 1143–1150.
60. Saito, S.; Ishikawa, T.; Kuroda, A.; Koga, K.; Moriwake, T. *Tetrahedron* **1992**, *48*, 4067–4086.
61. Dess, D. B.; Martin, J. C. *J. Org. Chem.* **1983**, *48*, 4155–4156.
62. Corey, E. J.; Shimoji, K. *J. Am. Chem. Soc.* **1983**, *105*, 1662–1664.
63. Keinan, E.; Sinha, S. C.; Singh, S. P. *Tetrahedron* **1991**, *47*, 4631–4638.
64. Evans, D. A.; Rieger, D. L.; Bilodeau, M. T.; Urpi, F. *J. Am. Chem. Soc.* **1991**, *113*, 1047–1049.
65. Biannic, B.; Aponick, A. *Euro. J. Org. Chem.* **2011**, *2011*, 6605–6617.
66. Suzuki, T.; Matsumura, R.; Oku, K.-I.; Taguchi, K.; Hagiwara, H.; T., H.; Ando, M. *Tetrahedron Lett.* **2001**, *42*, 65–67.
67. Yamaguchi, M.; Hirao, I. *Tetrahedron Lett.* **1983**, *24*, 4, 391–394.
68. a) Tester, R. W.; West, F. G. *Tetrahedron Lett.* **1998**, *39*, 4631–4634. For additional examples on formation of oxygen bridged medium-sized rings from acetal precursors via Stevens [1,2]-shift, see: b) Stewart, C.; McDonald, R.; West, F. G. *Org. Lett.* **2011**, *13*, 720–723. c) Murphy, G. K.; Marmsäter, F. P.; West, F. G. *Can. J. Chem.* **2006**, *84*, 1470–1486.
69. For precedents on Stevens [1,2]-shift using five-membered mixed monothioacetal (1,3-oxathiolane) as precursors, see: a) Qu, J. P.; Xu, Z. H.; Zhou, J.; Cao, C. L.; Sun, X. L.; Dai, L. X.; Tang, Y. *Adv. Synth. Catal.* **2009**, *351*, 308–312. b) Stepakov, A. V.; Molchanov, A. P.; Magull, J.; Vidović, D.; Starova, G. L.; Kopf, J.; Kostikov, R. R. *Tetrahedron* **2006**, *62*, 3610–3618. c)

- Zhu, S.; Xing, C.; Zhu, S. *Tetrahedron* **2006**, *62*, 829–832. d) Ioannou, M.; Porter, M. J.; Saez, F. *Tetrahedron* **2005**, *61*, 43–50. e) Ioannou, M.; Porter, M. J.; Saez, F. *Chem. Commun.* **2002**, *18*, 346–347. An addition example on intramolecular sulfonium ylide rearrangement: f) Kim, G.; Kang, S.; Soon, N. K. *Tetrahedron Lett.* **1993**, *34*, 7627–7628.
70. Cao, L. *Seven- and Eight-Membered Ether Formation via Sulfonium Ylide Rearrangement Processes and Application in an Approach to (+)-Laurencin*. PhD Thesis, University of Alberta, Alberta, 2010.
71. a) For evidence on retention of configuration for Stevens [1,2]-shift of ammonium ylide, see: Ollis, W. D.; Rey, M.; Sutherland, I. O. *J. Chem. Soc., Perkin Trans. 1*, **1983**, 1009–1027. For evidence on retention of configuration for Stevens [1,2]-shift of oxonium ylide, see: (b) Marmsäter, F. P.; Murphy, G. K.; West, F. G. *J. Am. Chem. Soc.* **2003**, *125*, 14724–14725.
72. For review on Stevens [1,2]-shifts with mechanistic discussion, see: a) Vanecko, J. A.; Wan, H.; West, F. G. *Tetrahedron* **2006**, *62*, 1043–1062. b) Markó, I. E. In *Comprehensive Organic Synthesis*; Trost, B. M., Fleming, I., Eds.; Pergamon: Oxford, 1991; Vol. 3, pp 913–974.
73. a) For evidence on stepwise radical pathway for Stevens [1,2]-shift, see: 35a). b) Eberlein, T. H.; West, F. G.; Tester, R. W. *J. Org. Chem.* **1992**, *57*, 3479–3482.
74. Yamamoto, Y.; Yatagai, H.; Saito, Y.; Maruyama, K. *J. Org. Chem.* **1984**, *49*, 1096–1104.
75. Brown, H. C.; Sinclair, J. A. *J. Organomet. Chem.* **1977**, *131*, 163–169.
76. a) Dale, J. A.; Dull, D. L.; Mosher, H. S. *J. Org. Chem.* **1969**, *34*, 2543–2549. b) Dale, J. A.; Mosher, H. S. *J. Am. Chem. Soc.* **1973**, *95*, 512–519. c) Hoye, T. R.; Jeffrey, C. S.; Shao, F. *Nat. Protoc.* **2007**, *2*, 2451–2458.
77. a) Fürstner, A.; Langemann, K. *J. Am. Chem. Soc.* **1997**, *119*, 9130–9136. b) Ghosh, A. K.; Cappiello, J.; Shin, D. *Tetrahedron Lett.* **1998**, *39*, 4651–4654.

78. Kingsbury, J. S.; Harrity, J. P. A.; Bonitatebus, P. J.; Hoveyda, A. H. *J. Am. Chem. Soc.* **1999**, *121*, 791–799.
79. a) Michrowska, A.; Bujok, R.; Harutyunyan, S.; Grela, K. *J. Am. Chem. Soc.* **2004**, *126*, 9318–9325. b) Grela, K.; Harutyunyan, S.; Michrowska, A. *Angew. Chem. Int. Ed.* **2002**, *41*, 4038–4040.
80. Preparation and application of Zhan-1B catalyst: Zhan, Z.-Y. J. U.S. Patent, **2007**, 20070043180.
81. a) Nishimura, O.; Kitada, C.; Fujino, M. *Chem. Pharm. Bull.* **1978**, *26*, 1576–1585. For an example of application in the peptide synthesis, see: b) Macmillan, D.; Anderson, D. W. *Org. Lett.* **2004**, *6*, 4659–4662.
82. Erhunmwunse, M. O.; Steel, P. G. *J. Org. Chem.* **2008**, *73*, 8675–8677. Ch 1
83. Karplus, M. *J. Am. Chem. Soc.* **1963**, *85*, 2870–2871.
84. Nahm, S.; Weinreb, S. M. *Tetrahedron Lett.* **1981**, *22*, 3815–3818.
85. Shimizu, T.; Osako, K.; Nakata, T. *Tetrahedron Lett.* **1997**, *38*, 2685–2688.
86. The α' , β -elimination process has been noted in ref 33b–d. For a review with examples of α' , β -elimination on sulfonium ylide, see: Padwa, A.; Hornbuckle, S. F. *Chem. Rev.* **1991**, *91*, 263–309.
87. Phipps, R. J.; Grimster, N. P.; Gaunt, M. J. *J. Am. Chem. Soc.* **2008**, *130*, 8172–8174.
88. Arnone, A.; Bravo, P.; Panzeri, W.; Viani, F.; Zanda, M. *Eur. J. Org. Chem.* **1999**, 117–127.
89. Curran, D. P.; Zhang, Q. *Adv. Synth. Catal.* **2003**, *345*, 329–332.
90. a) Chugaev, L. *Ber. Dtsch. Chem. Ges.* **1899**, *32*, 3332–3335. For selected recent examples of xanthate formation/Chugaev elimination used in organic synthesis, see: b) Lee, K.; Boger, D. L. *J. Am. Chem. Soc.* **2014**, *136*, 3312–3317. c) Nicolaou, K. C.; Ortiz, A.; Zhang, H.; Guella, G. *J. Am. Chem. Soc.* **2010**, *132*, 7153–7176. d) Padwa, A.; Zhang, H. *J. Org. Chem.* **2007**, *72*, 2570–2582.
91. Nonhebel, D. C. *Chem. Soc. Rev.* **1993**, *22*, 347–359.

92. Newcomb, M.; Chestney, D. L. *J. Am. Chem. Soc.* **1994**, *116*, 9753.
93. Crimmins, M. T.; Tabet, E. A. *J. Am. Chem. Soc.* **2000**, *122*, 5473–5476.
94. Snyder, S. A.; Brucks, A. P.; Treitler, D. S.; Moga, I. *J. Am. Chem. Soc.* **2012**, *134*, 17714–17721.

3 Chapter 3 Medium-Sized Cyclic Amines via Stevens [1,2]-Shift of Sulfonium Ylides derived from Cyclic *N,S*-Acetals

3.1 Introduction

The construction of medium-sized cyclic amines is an important subject in organic synthesis as these structural motifs often constitute the framework of a variety of natural products with interesting biological activities. Examples of their occurrence in nature include cephalotaxine (**1**),¹ otonecine (**2**)² and lycoposerramine T (**3**)³ and many others (Figure 3.1). Stemoamide (**4**)^{4,6} and stemonine (**5**)^{5,6} are *Stemona* alkaloids are found in various plant species of the *Stemonaceae* family,⁶ which often possess a characteristic pyrrolo[1,2-*a*]-azepine (**6**) (also known as the perhydroazaazulene) core. This polycyclic architecture has led to the development of many synthetic strategies.⁶ In particular, numerous efforts have been devoted to the efficient construction of stemoamide (**4**), which is the simplest *Stemona* alkaloid. This review briefly examines several synthetic approaches towards stemoamide (**4**), in order to provide a general understanding on the synthesis on fused azepines.

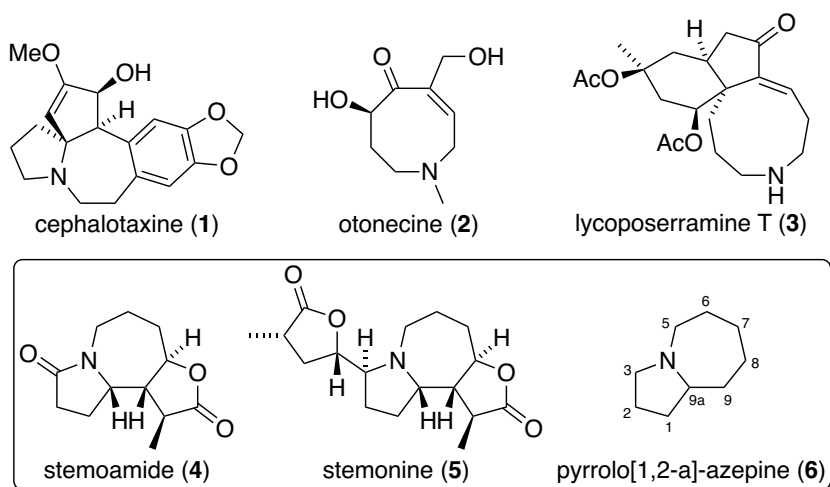
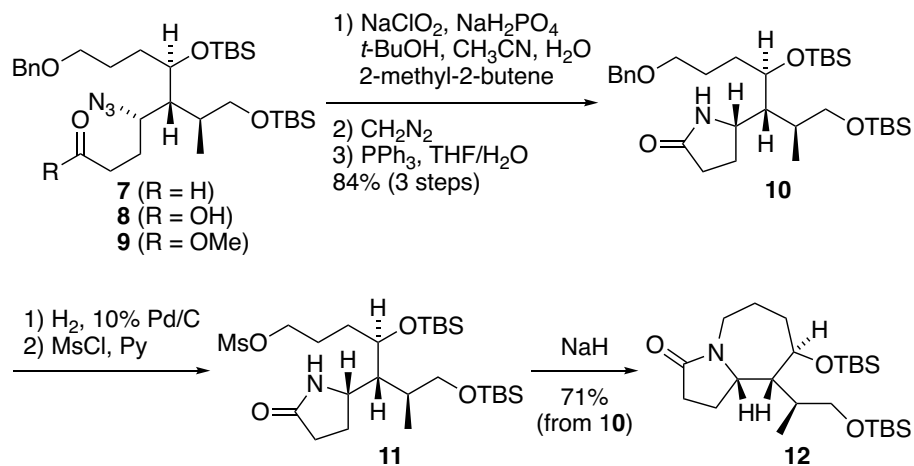


Figure 3.1 Natural products containing a medium-sized cyclic amine

3.2 Applied strategies on azepine formation in the synthesis of stemoamide

3.2.1 Azepine formation by intramolecular cyclization of acyclic precursor

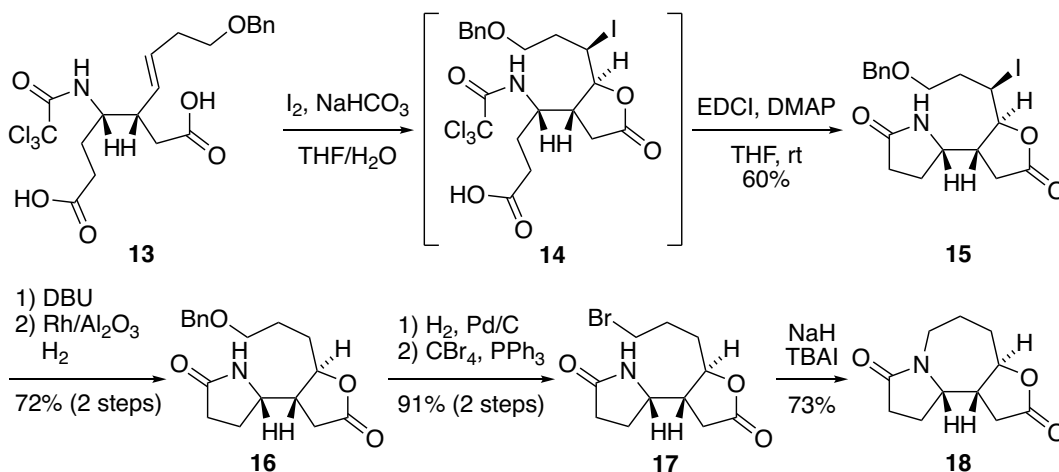
In 1994, Williams and coworkers published the first total synthesis of (-)-stemoamide.⁷ The pyrrolidone ring of the perhydroazaazulene system was formed by means of a Staudinger reaction,⁸ as depicted in Scheme 3.1. Sodium chlorite oxidation of aldehyde **7** followed by esterification of the resulting carboxylic acid **8** furnished methyl ester **9**. The Staudinger reaction between the azide and triphenylphosphine (PPh₃) afforded an iminophosphorane intermediate, which was then hydrolyzed to the amine followed by *in situ* cyclization with the ester moiety to provide lactam **10**. Removal of the benzyl group and treatment with methanesulfonyl chloride (MsCl) afforded mesylate **11**. The subsequent 7-*exo-tet* cyclization⁹ in the presence of sodium hydride (NaH) furnished azepine **12**. A similar transformation involving 7-*exo-tet* cyclization⁹ with pyrrolidone and mesylate to form the azepine ring has also been applied in three other syntheses.^{10,11,12}



Scheme 3.1 William's strategy for the synthesis of perhydroazaazulene core

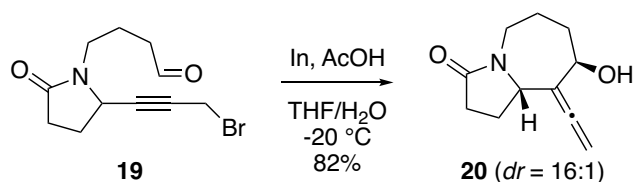
Another example of this approach was recently reported by Sato and Chida¹³ in their asymmetric total synthesis. Lactone **14** was formed *via* iodolactonation of bis(acid) **13**.

Without any isolation, lactone **14** was treated with 1-ethyl-3-(3-dimethylaminopropyl)-carbodiimide hydrochloride (EDCI·HCl) and 4-dimethylaminopyridine (DMAP) to afford pyrrolidone **15** followed by *in situ* cleavage of the trichloroacetyl group. Reduction of the alkyl iodide was achieved by elimination and hydrogenation to provide benzyl ether **16**, which was converted to bromide **17** in two steps. Upon treatment of **17** with sodium hydride (NaH) and tetrabutylammonium iodide (TBAI), 7-*exo-tet* cyclization⁹ furnished the desired azepine **18**.



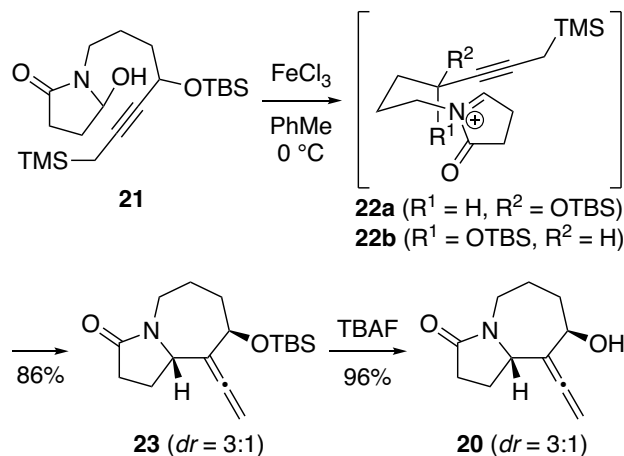
Scheme 3.2 Sato and Chita's approach on the perhydroazaazulene core

In 2009, Bates and Sridar¹⁴ reported a synthesis of (\pm)-stemoamide using an intramolecular Barbier reaction¹⁵ as the key step to form the azepine ring. The required aldehyde tethered with a propargylic bromide side chain (**19**) was derived from succinimide. After surveying different reagents and solvents, the optimized reaction conditions were found to be the use of indium in wet THF in the presence of acetic acid (Scheme 3.3). The desired allenic alcohol was generated in 82% yield with the relative stereochemistry determined by X-ray crystallography.



Scheme 3.3 Intramolecular propargylic Barbier reaction

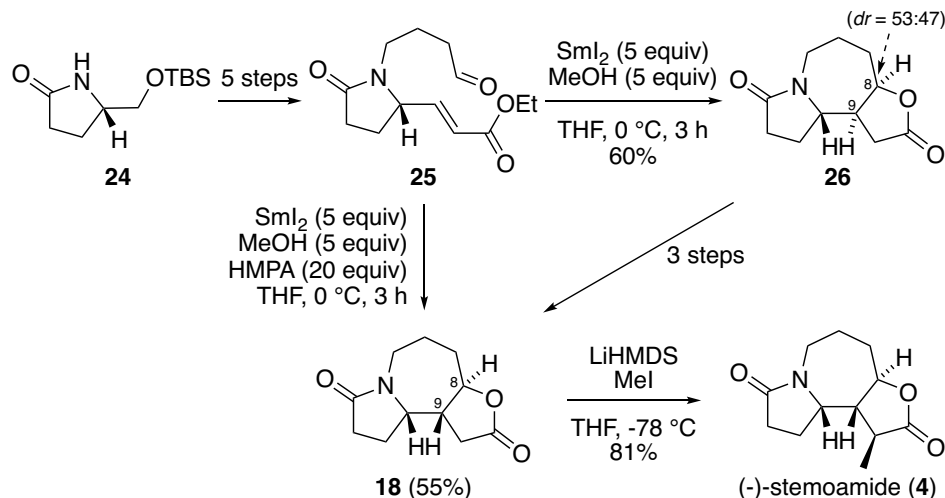
Later, the same racemic allenic alcohol (**20**) was synthesized by Hong and coworkers *via* an *N*-acyliminium cyclization pathway (Scheme 3.4).¹⁶ When the propargylsilane **21** was subjected to an FeCl₃-promoted cyclization, allenic product **23** was formed as a 3:1 mixture of diastereomers. The cyclization was presumed to proceed through the *in situ* generated iminium ion. After desilylation with tetrabutylammonium fluoride (TBAF), the diastereomeric mixture of allenic alcohols was separated by column chromatography to afford **20**. This process was subsequently applied to an asymmetric total synthesis of (-)-stemoamide by the same group.¹⁷



Scheme 3.4 Formation of azepine via cationic cyclization

In 2011, Honda and coworkers¹⁸ published an efficient synthesis of (-)-stemoamide (**4**) using an intramolecular samarium diiodide-promoted 7-*exo-trig* cyclization⁹ as the key step (Scheme 3.5). The required aldehyde **25** was synthesized from pyrrolidone **24** in 5 steps. Upon treatment with samarium diiodide (SmI₂), the *in situ* generated ketyl

radical underwent conjugate addition to the α,β -unsaturated ester followed by an intramolecular lactonization to afford tricyclic compound **26** as a mixture of inseparable epimers at C8. Although the desired configuration at C9 was not obtained in this case, partially separated **26** could be converted into (-)-stemoamide (**4**) in 4 steps. However, when the reaction was carried out in the presence of hexamethylphosphoramide (HMPA), the desired azepine **18** was isolated in 55% yield along with a trace amount of the C8 epimer. The synthesis was completed after the stereoselective methylation of **18** with methyl iodide (MeI) according to a literature procedure.²⁵

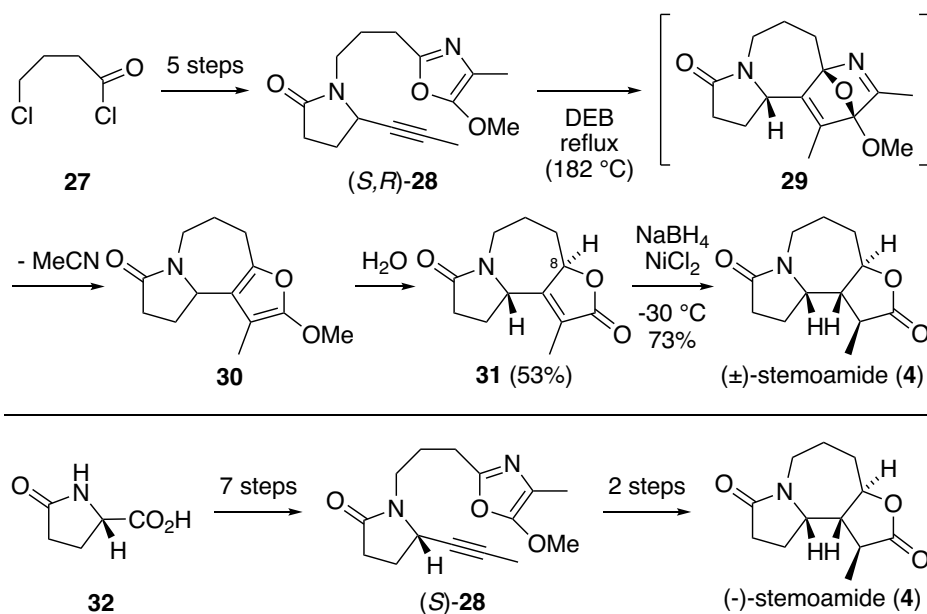


Scheme 3.5 SmI_2 promoted intramolecular cyclization

3.2.2 Azepine formation by [4+2] cycloaddition

An efficient strategy to synthesize stemoamide was developed by Jacobi's group (Scheme 3.6).²⁰ The authors published both racemic^{20a} and asymmetric^{20b} total syntheses of stemoamide, in which the key step involved an intramolecular Diels-Alder (IMDA)/retro-Diels-Alder process²¹ which allowed for the construction of the azepine-lactone unit in a single step. Acetylenic oxazole (*R,S*)-**28** was prepared from γ -chlorobutyryl chloride **27**.^{20a} When **28** was heated in diethylbenzene at reflux (185 °C),

the anticipated methoxyfuran **30** was generated along with the formation of acetonitrile. However, **30** was rapidly hydrolyzed to butenolide **31** upon isolation. The relative stereochemical configuration of butenolide **31** was confirmed by its subsequent conversion to (±)-stemoamide (**4**) with sodium borohydride (NaBH₄) and catalytic nickel(II) chloride (NiCl₂). Later, this strategy was applied in an asymmetric total synthesis using enantioenriched acetylenic oxazole (*S*)-**28**, which was derived from (*S*)-pyroglutamic acid **32** in 7 steps.^{20b}

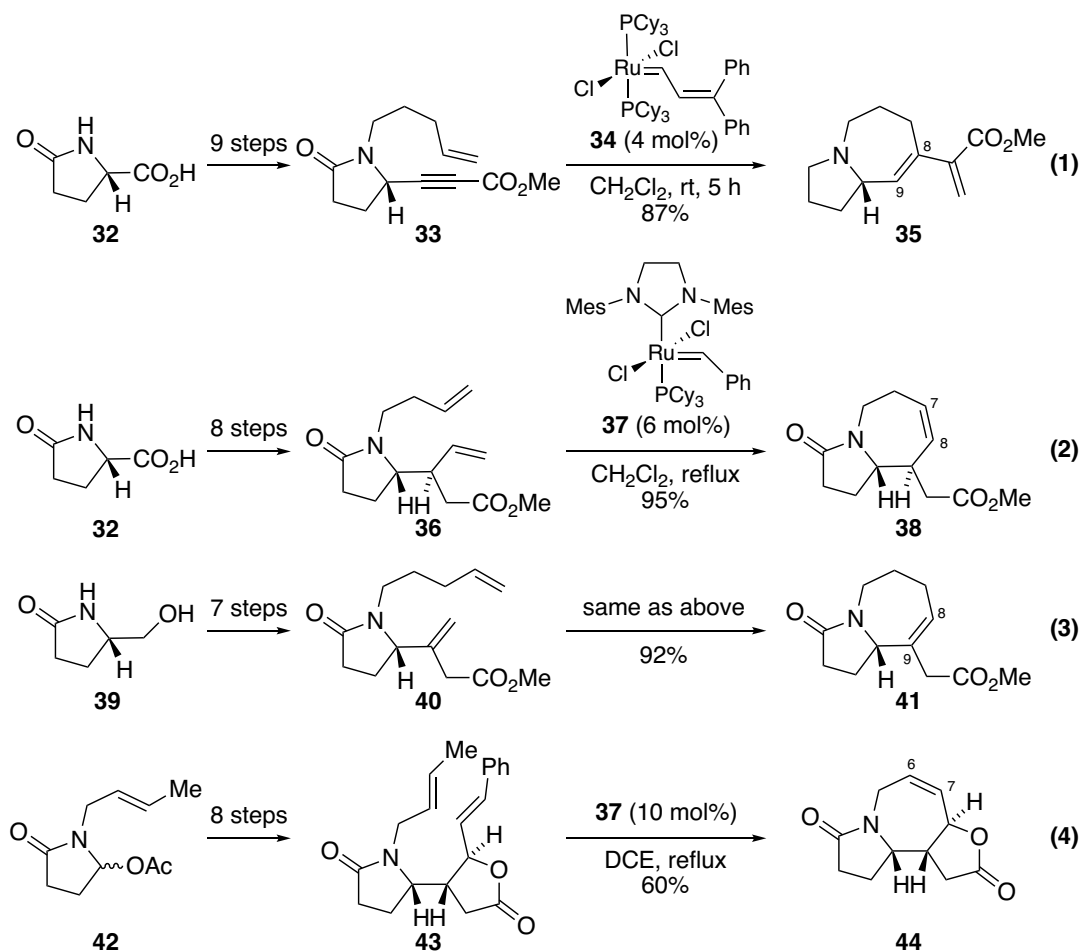


Scheme 3.6 . Formation of azepine *via* [4+2] cycloaddition

3.2.3 Azepine formation by ring closing metathesis (RCM)

Another frequently applied methodology to access the azepine ring of stemoamide is by ring closing metathesis (RCM). The pioneering work in this area was reported by Mori and Kinoshita (eq 1, Scheme 3.7).²² Enyne **33** was prepared from (*S*)-pyroglutamic acid **32** in 9 steps. When **33** was treated with a catalytic amount of **34**, the key intramolecular enyne metathesis²³ afforded diene **35** in 87% yield, furnishing the substituted azepine ring with a double bond at C8–C9. The resulting diene group was used for further transformations.

Later, Sibi and Subramanian²⁴ reported a total synthesis of (-)-stemoamide using ring closing metathesis as the key step to form the azepine ring with an olefin at C7–C8 (eq 2). The required diene **36** was also derived from (*S*)-pyroglutamic acid **32**. Similarly, in the total synthesis reported by Somfai and coworkers,²⁵ the key step involved ring closing metathesis of **40**, which was generated from pyrrolidone **39**. The desired azepine ring was constructed *via* formation of the C8–C9 double bond (eq 3).



In the three examples shown above (eq 1-3), the azepine ring was constructed from RCM of a diene precursor that contained a pyrrolidone ring, followed by the formation of the butyrolactone unit. However, in the asymmetric total synthesis reported by Olivo

and coworkers,²⁶ the azepine ring was formed after the construction of the butyrolactone unit (eq 4). In this synthesis, diene **43** was derived from pyrrolidone **42** and was converted to azepine **44** *via* the anticipated RCM reaction to complete the construction of the perhydroazaazulene-lactone unit.

There are several other methodologies for the construction of medium-sized cyclic amines²⁷ and ring closing metathesis is considered the most versatile and efficient method, which has been applied in many total syntheses.^{27c,28} However, the relative paucity of synthetic applications using the existing methodologies is notable. Many of the current synthetic methods remain very specific with less attention being paid to the aspect of stereocontrol.²⁸ As such, the development of a new strategy for the efficient synthesis of medium-sized cyclic amines is still in great demand. There are several unmet needs that new strategies might address. For example, it is important to have a wide substrate scope with functional groups that could be easily derivatized to other important building blocks. If such a process could offer stereoselectivity, then it could be applicable to the synthesis of natural products with stereocenters.

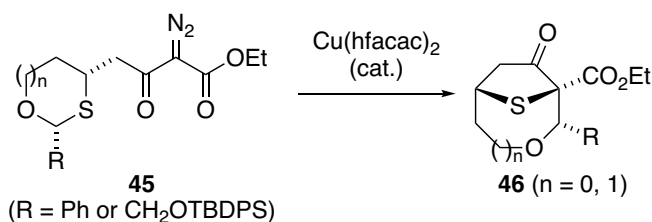
3.3 Results and discussion

3.3.1 The proposal

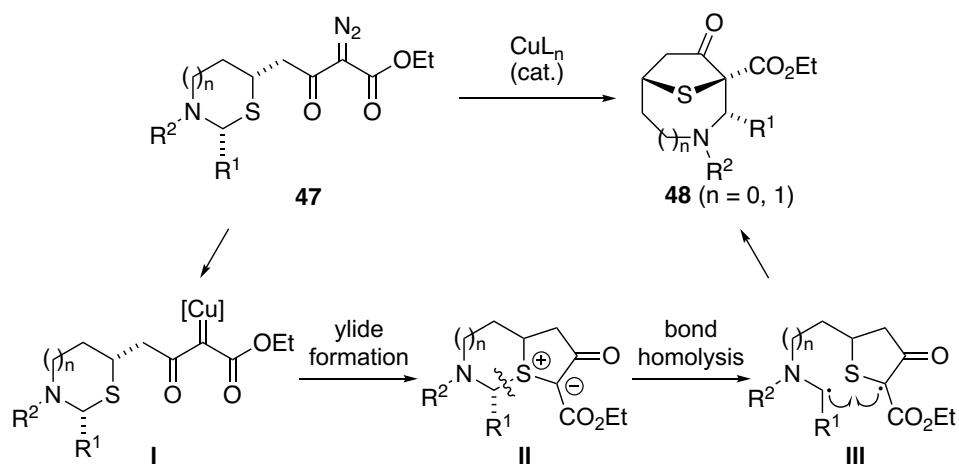
We have demonstrated that the Stevens [1,2]-shift of the sulfonium ylide derived from mixed monothioacetals (**45**) is an efficient method for the formation of eight-membered cyclic ethers (**46**) (Scheme 3.1).³⁰ The West group has previously demonstrated the efficient formation of seven-membered cyclic ethers using this methodology.²⁹ As an application, this methodology has been successfully employed in a formal synthesis of (+)-laurencin, as discussed in detail in Chapter 2.³⁰ As previously discussed in Chapter 1 (Section 1.9), Kametani and coworkers clearly demonstrated that the acetal carbon atom of an *N,S*-acetal derived sulfonium ylide could effectively undergo the Stevens [1,2]-shift.³¹ These results prompted us to investigate a similar pathway to access medium-sized cyclic amines (**48**) starting from

five- and six-membered *N,S*-acetals of type **47** (Scheme 3.8). In this way, treatment of **47** with a copper catalyst could form a fused bicyclic sulfonium ylide, which could hopefully undergo the Stevens [1,2]-shift to provide sulfur-bridged azacycle **48**. The [1,2]-shift is expected to be stereoselective, providing a product with stereochemical retention at the migrating anomeric carbon. The resulting sulfur bridge could then be cleaved by Raney nickel desulfurization to leave a functionalized azacycle.

Previous work



The proposal



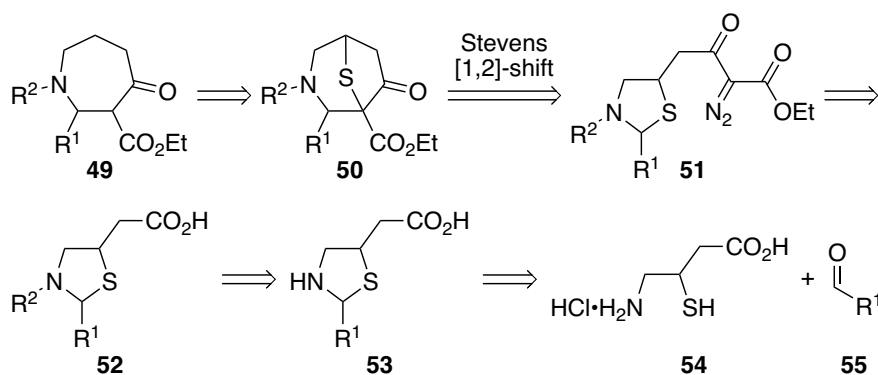
Scheme 3.8 Generation of medium-sized cyclic amines *via* Stevens [1,2]-shift of *N,S*-acetal derived sulfonium ylide

In the proposed pathway (Scheme 3.8), different substituents could be installed at R¹ and R² to access various functionalized seven- or eight-membered azacycles. In addition, the precursor also permits the ability to quickly probe substituent effects at the migrating carbon and at the nitrogen. However, a mixture of *cis* and *trans* thiazolidine products with respect to the carboxylic acid side chain might be obtained

at the end as the formation of five-membered *N,S*-acetal **56** could be unselective. The resulting mixture of anomers may not be separable by column chromatography. In spite of that, the investigation would provide an opportunity to validate the basic bond-formation strategy of our concept.

3.3.2 Retrosynthetic strategy

While the ultimate goal was utilize the Stevens [1,2]-shift as the key step in a natural product total synthesis, our first objective was to design an efficient synthetic route to access a variety of model diazoketoesters containing a thiazolidine ring (**51**). As shown in Scheme 3.10, azepine **49** could come from sulfur-bridged azacycle **50** via desulfurization. The key step to generate compound **50** could involve the Stevens [1,2]-shift of the sulfonium ylide derived from thiazolidine **51** with a tethered diazoketoester side chain. The diazoketoester group could come from the corresponding carboxylic acid (**52**) which, in turn, could be generated from thiazolidine **53**. Compound **53** could be generated from the reaction of aldehyde **55** and readily available 4-amino-3-mercaptobutyric acid **54**.



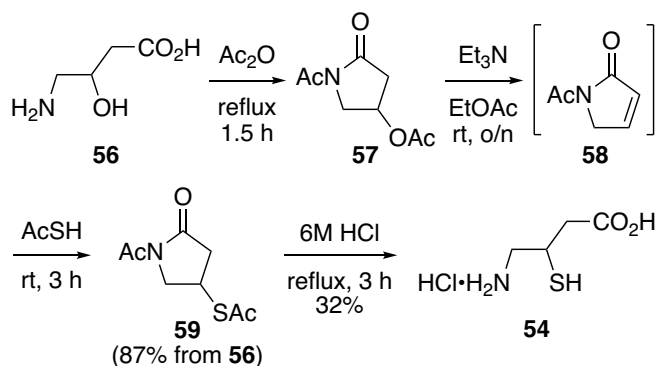
Scheme 3.9 Retrosynthetic plan for the formation of azepine

In the proposed approach, different substituents could be installed at R¹ and R² to generate a variety of interesting substituted diazoketoester-thiazolidine substrates. However, a mixture of *cis* and *trans* thiazolidine products with respect to the carboxylic

acid side chain might be obtained at the end as the formation of the five-membered *N,S*-acetal **56** could be unselective. In addition, the resulting mixture of anomers may not be separable by column chromatography. In spite of that, the investigation could provide some preliminary results to validate our concept and approach.

3.3.3 Preparation of diazoketoester-thiazolidine substrate

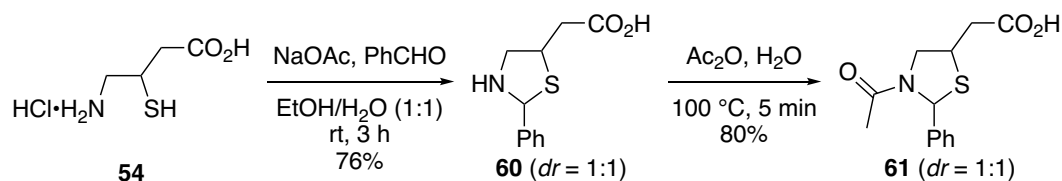
4-Amino-3-mercaptoprobutyric acid **54** was prepared from 4-amino-3-hydroxybutyric acid **55** following a known procedure (Scheme 3.10).³² In this process, compound **56** was converted to pyrrolidone **57** in refluxing acetic anhydride (Ac_2O). Treatment of compound **57** with triethylamine (Et_3N) afforded α,β -unsaturated γ -lactam **58** intermediate, which was directly treated with thioacetic acid (AcSH) to provide γ -lactam **59** in 87% overall yield. Compound **59** was then converted to 4-amino-3-mercaptoprobutyric acid **54** in a refluxing HCl solution.



Scheme 3.10 Preparation of 4-amino-3-mercaptoprobutyric acid **54**

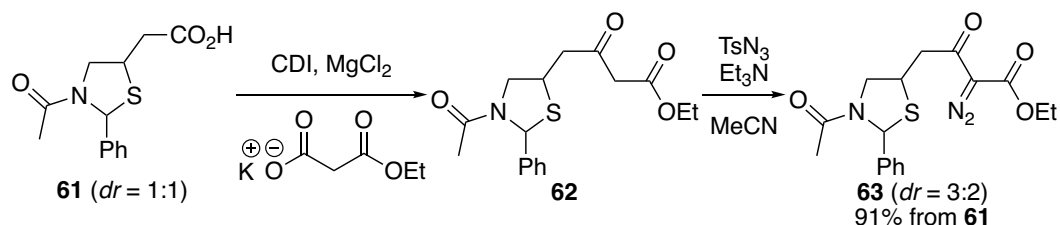
With 4-amino-3-mercaptoprobutyric acid **54** in hand, the next task was to form the thiazolidine ring with an aldehyde, so the resulting thiazolidine would contain a suitable substituent on the anomeric carbon for the Stevens rearrangement. We decided to use benzaldehyde for the initial investigation, because the strongly stabilizing phenyl substituent could lead to an effective [1,2]-shift of the acetal carbon, as previously shown in Sections 1.8.3 and 2.5.1. As such, compound **54** was treated with

benzaldehyde in the presence of sodium acetate (NaOAc) to afford thiazolidine **60** (Scheme 3.11). However, formation of the five membered *N,S*-acetal was not stereoselective and a 1:1 mixture of inseparable *cis*- and *trans*-isomers was obtained. We anticipated that these diastereomers could be separated by column chromatography at a later stage when the diazoketoester side chain was installed. In the presence of acetic anhydride (Ac₂O) and water at elevated temperatures, the acetyl group was installed on the secondary amine to provide a 1:1 mixture of thiazolidine **61**. An acetyl group was chosen because it is a commonly used amine protecting groups and could be installed easily; we could also see if the migration of the anomeric carbon next to an amide could occur efficiently once it was attached.



Scheme 3.11 Preparation of pyrrolidone 61

Upon obtaining the the substituted thiazolidine ring, the next task was to convert the carboxylic acid group into the corresponding diazoketoester, which was achieved in a two-step sequence (Scheme 3.12). In the first step, we utilized the homologation reaction reported by Masamune and coworkers³³ to synthesize β -ketoester **62** from carboxylic acid **61**. In this step, the carboxylic acid was converted into the corresponding imidazolide by 1,1'-carbonyldiimidazole (1,1'-CDI), which was treated with the magnesium ethyl malonate that was generated from magnesium chloride (MgCl₂) and potassium ethyl malonate. The resulting 1:1 mixture of diastereomeric β -ketoesters **62** was directly converted to diazoketoesters **63** using the Regitz diazotransfer reaction³⁴ in the presence of tosyl azide and triethylamine. Since we could not separate these diazoketoesters (**63**), the resultant 3:2 mixture of diastereomers was carried forward to the next step to see if the Stevens [1,2]-shift could occur.

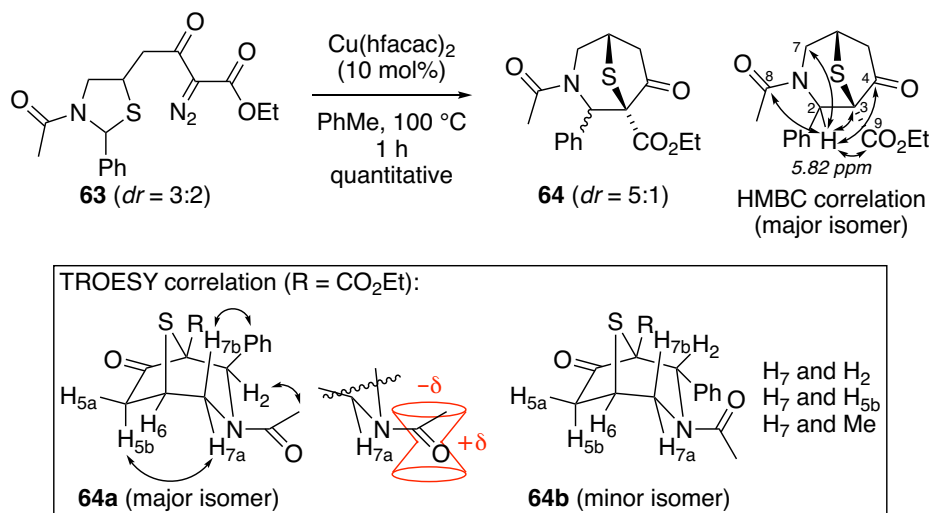


Scheme 3.12 Synthesis of the diazoketoester side chain

The Stevens [1,2]-shift was examined next (Scheme 3.13). Treatment of thiazolidines **63** with 10 mol% of $\text{Cu}(\text{hfacac})_2$ in toluene at 100 °C for 1 h afforded an inseparable mixture of two products, which showed the mass of the desired sulfur-bridged azepine (**64**) by HRMS analysis. These two products were diastereomers as the ^1H and ^{13}C NMR spectra displayed the same set of protons and carbons with slight differences in chemical shifts for the major and minor products. A combination of 1D and 2D NMR analyses were performed to assign these two diastereomers. For the major diastereomer, there was a distinctive singlet at 5.82 ppm in the ^1H NMR spectrum, which was assigned as H2. H2 showed correlations with C3, C4, C7, C8 and C9 by HMBC analysis, which further supported the structural assignment and inspired confidence that the desired Stevens [1,2]-shift did occur. For the minor diastereomer, the same HMBC correlations were observed for H2.

We also attempted to determine the relative configuration for both diastereomers based on the correlations displayed by TROESY analysis. For the major diastereomer, H5b was assigned to the proton at the endo position, because its vicinal coupling constant with H6 was ~ 0 Hz, indicating a dihedral angle of around 90° with H6. H5b also showed TROESY correlation with one of the geminal protons at C7. The other geminal proton at C7 had a zero vicinal coupling constant with H6 and was also correlated to the aromatic protons. A tentative structural assignment was made based on these observations, as shown in Scheme 3.14. In addition, H2 was also correlated to the acetyl protons. Interestingly, the ^1H NMR chemical shifts for H7a and H7b were at 4.79 ppm and 3.36 ppm, respectively (i.e., they were separated by 1.43 ppm). We

hypothesized that H7b may be deshielded by anisotropy, because it was in close proximity to the deshielding region of the amide carbonyl group, as shown below.



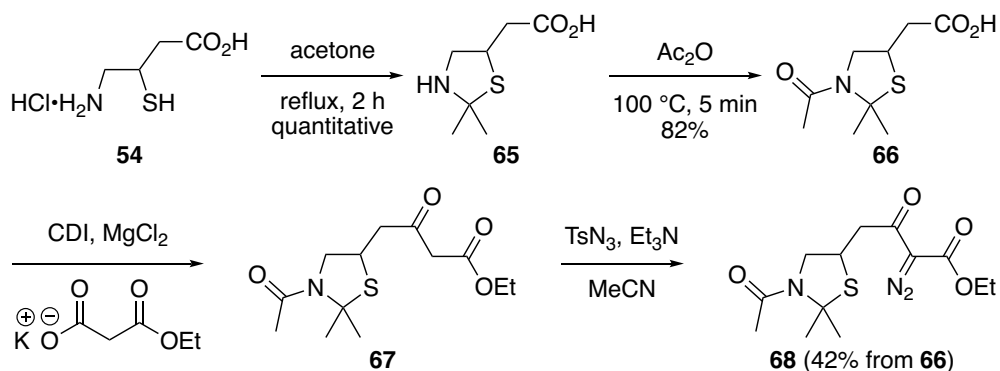
Scheme 3.13 Stevens [1,2]-shift of sulfonium ylide derived from thiazolidine

The minor diastereomer (**64b**) was presumed to be the C2 epimer of **64a**. However, it was difficult to gather enough evidence to support this assignment for two reasons. First of all, the diastereotopic protons H7a and H7b gave an overlapped multiplet on the ¹H NMR spectrum. As a result, the observed TROESY correlations for H7a and H7b to H2, H5b and Me could not be differentiated. Secondly, the ¹H NMR signals for the minor diastereomer (**64b**) was much weaker than that of the major diastereomer (**64a**). Therefore, increasing the intensity of TROESY spectra led to significant overlap of cross peaks. In general, it is difficult to perform TROESY analysis of a minor component in a mixture.

Although we have not obtained definitive assignments of the relative stereochemistry for the product, the quantitative yield of this process definitely proved the feasibility of the approach. In addition, the diastereomeric ratio of 5:1 indicated stereochemical inversion for one of the diastereomers in the Stevens [1,2]-shift, as the diastereomeric ratio for the starting material was 3:2. It would be ideal if the

diastereomeric pyrrolidones **63** could be separated and submitted to the reaction conditions separately to provide evidence for stereoselectivity of the anticipated rearrangement.

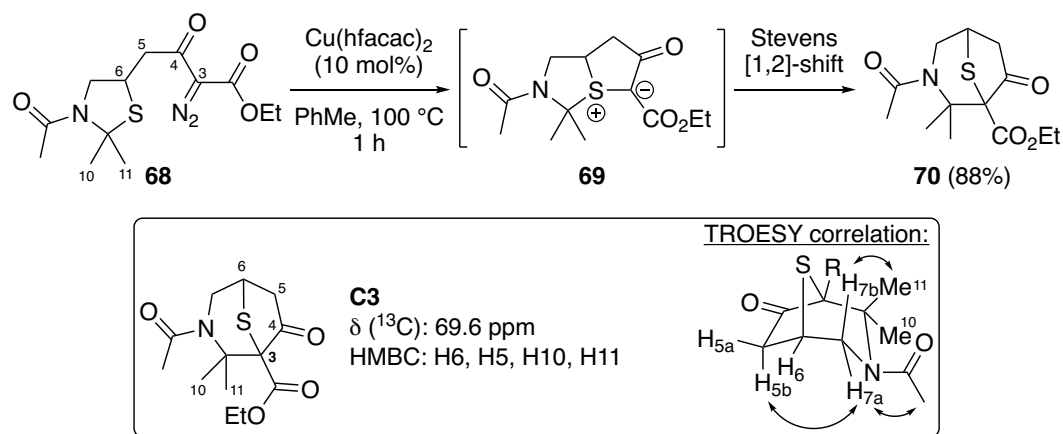
After the preliminary proof of concept, we shifted our attention to prepare the dimethyl-substituted thiazolidine (**68**), which could be prepared as a single product and provide cleaner NMR spectra without any complications from a mixture of diastereomers (Scheme 3.14). A similar route for the preparation of thiazolidine-diazoketoester **63** (Scheme 3.11 and 3.12) was employed here. The starting 4-amino-3-mercaptoputyric acid **54** was stirred in refluxing acetone to afford thiazolidine **65** in quantitative yield. The secondary amine in **65** was then protected as the acetamide in the presence of acetic anhydride and water to afford acid **66**. Compound **66** was subjected to the Masamune homologation³³ and provided β -ketoester **67**, which was subjected to the Regitz diazotransfer conditions in the presence of tosyl azide (TsN_3) and triethylamine (Et_3N) to afford diazoketoester-thiazolidine **68** in an overall yield of 42%. The low yield was mainly from the homologation step, which has not been optimized. We envision the yield could be improved after optimization of the reaction conditions.



Scheme 3.14 Preparation of dimethyl-substituted thiazolidine 68

The dimethyl-substituted thiazolidine was then subjected to the Stevens rearrangement conditions. To our delight, the anticipated [1,2]-shift of a sterically

congested dimethyl-substituted anomeric carbon occurred smoothly to afford the desired azepine product (**70**) in 88% yield, providing validation of the strategic concept and demonstrating its applicability to substrates lacking conjugative destabilization at the migrating center. In this case, the spectra were much easier to analyze in comparison to the first example, in which a mixture of diastereomeric product was isolated (Scheme 3.13). The structural assignment was also supported by the observed HMBC correlation of C3 with protons H6, H5, H10 and H11. TROESY experiment also provided additional data to support the assignment.



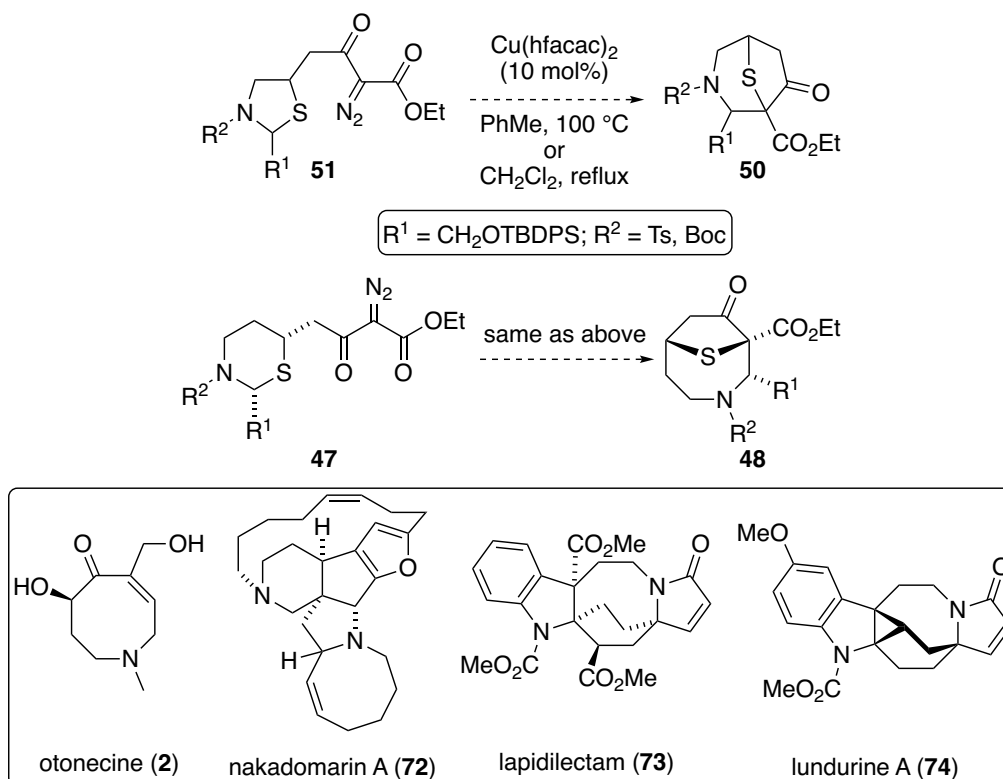
Scheme 3.15 Stevens [1,2]-shift of sulfonium ylide derived from dimethyl substituted thiazolidine

3.4 Conclusion and future work

In summary, we have described a novel method to generate functionalized medium-sized azacycles *via* Stevens [1,2]-shift of sulfonium ylides derived from thiazolidines. In the two examples previously described, the thiazolidine compound tethered to a diazoketoester side chain could be readily prepared, and thiazolidine underwent efficient conversion to the azepine product of Stevens [1,2]-shift. During our preliminary investigations, treatment of the thiazolidine-diazoketoester substrate in the presence of a catalytic amount of Cu(hfacac)_2 at elevated temperatures afforded products whose spectral data are fully consistent with the bridged bicyclic azepines

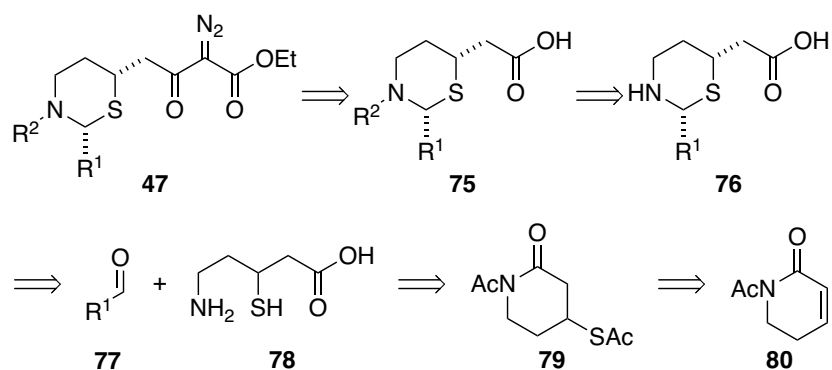
expected from the Stevens [1,2]-shift of sulfonium ylides. This result demonstrated the feasibility of the designed route towards medium-sized azacycles. We have obtained preliminary results on two successful examples using this approach. In these examples, migration of the anomeric carbon with either a strongly stabilizing phenyl substituent or a sterically congested dimethyl substituent inspired confidence that this strategy could be applied to the synthesis of other substituted azepines. Further studies on the substrate scope and additional applications of this method are currently under investigation in the West group. Some possible avenues of future work in this area are described below.

An important goal is to further expand the substrate scope by installing different functional substituents at R¹ and R² (Scheme 3.16) and extend the method to the synthesis of substituted eight-membered azacycles (azocanes). Some examples of natural products containing this framework are otonocine (**2**),² nakadomarine A (**72**),³⁵ lapidilectam (**73**)³⁶ and lundurine A (**74**).³⁷ An efficient route (see below) could be designed to access a variety of six-membered *N,S*-acetal substrates **47**, which could be subjected to the optimized reaction conditions for the Stevens rearrangement to see if the desired azocanes **48** could be generated. If the *cis*- and *trans*-isomers of **47** could be separated by column chromatography, they could be subjected to the optimized reaction conditions to generate azocane **48** to provide further information on the stereoselectivity of the process.



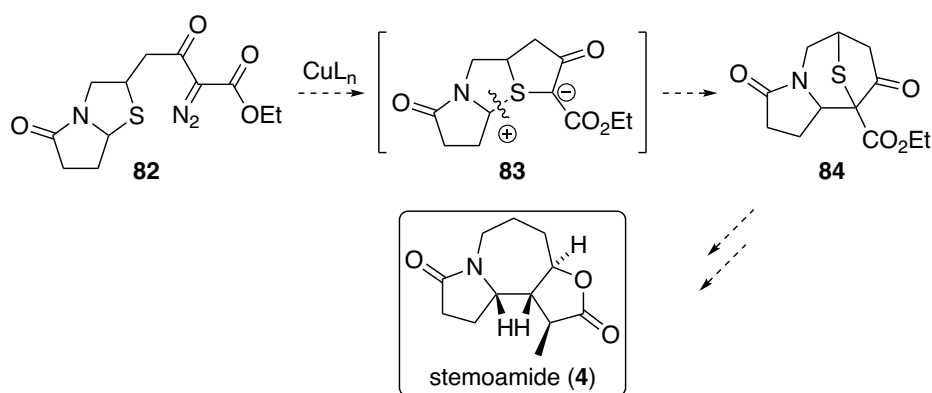
Scheme 3.16 Future plan for the synthesis of azepines and azocanes using Stevens [1,2]-shift of sulfonium ylides

We envisioned a route to synthesize the required diazo substrates (**47**) (Scheme 3.17). The strategy is similar in comparison to the synthesis of the five membered *N,S*-acetals. The diazoketoester group in **47** could be synthesized *via* the Masamune homologation³³ followed by Regitz diazotransfer,³⁴ starting from carboxylic acid **75**. Different protecting groups (R^2) could be installed on amine **76**, which could be readily synthesized by reaction of amino mercaptan **78** and aldehyde **77**. Compound **78** is an important precursor that could be synthesized from lactam **69** under acidic conditions, such as in refluxing HCl solution. Compound **79** could be generated by the Michael addition of thioacetic acid to α,β -unsaturated lactam **80**, which could be prepared by a known procedure.^{38a} Alternatively, compound **80** could be obtained by acetate protection of 5,6-dihydropyridin-2(1H)-one **81**.^{38b,c}



Scheme 3.17 Retrosynthetic analysis for the preparation of substrates **47**

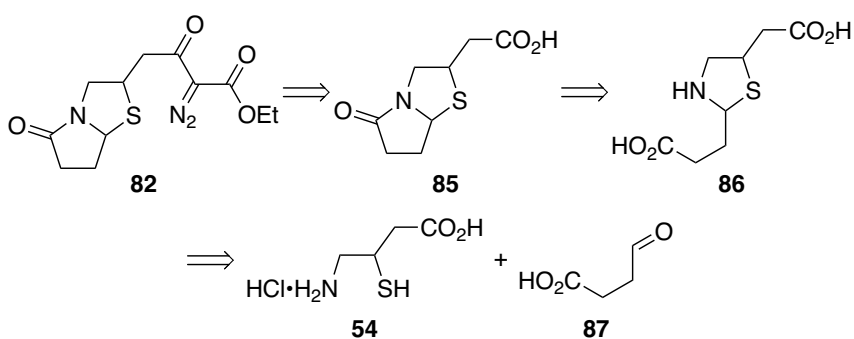
The chemistry described in this chapter could potentially be applied as the key step in the synthesis of the *Stemona* alkaloids possessing a perhydroazaazulene framework (Scheme 3.18). We envision that bicyclic model substrate **82** could be prepared (see below). Catalytic decomposition of the diazo compound would lead to tricyclic sulfonium ylide **83**, followed by Stevens [1,2]-shift to provide perhydroazaazulene **84**. If such a process could be developed and optimized, the resulting product **84** could be further converted to stemoamide **4**.



Scheme 3.18 Future application towards stemoamide

A retrosynthetic proposal for the synthesis of bicyclic thiazolidine-diazoketoester **82** is depicted in Scheme 3.19. Again, the Masamune homologation³³/Regitz

diazotransfer³⁴ sequence could be used to convert carboxylic acid **85** into diazoketoester **83**. The pyrrolidone ring could be generated from **86** via an intramolecular coupling reaction of the amine and carboxylic acid groups in the presence of a coupling reagent, such as DCC. Compound **86** could be prepared from 4-amino-3-mercaptopropanoic acid **54** and the known aldehyde **87**.³⁹ There are a few concerns in the proposed pathways. A mixture of *cis*- and *trans*-isomers would be formed in the acetal formation step and the separation by column would be difficult to achieve due to the presence of two carboxylic acid groups. In addition, the anticipated intramolecular coupling reaction of **86** to form a pyrrolidone ring might be problematic due to regiocontrol. However, the mixtures of isomers (**86**) could be subjected to intramolecular coupling reactions. We envision that the behavior of *cis*- and *trans*-isomer in the coupling reaction might be different, which could provide certain quantities of **85** to be converted to diazoketoester **82** and test the subsequent Stevens rearrangement. Moreover, the apparent stereoselectivity observed in the rearrangement of **63** (3:2 mixture to 5:1 mixture) leaves open the possibility that both isomers of **82** might converge upon the same diastereomeric major product. An additional advantage of examining bicyclic substrates such as this is that there should be a better chance of determining the relative stereochemical configurations of these rigid systems.



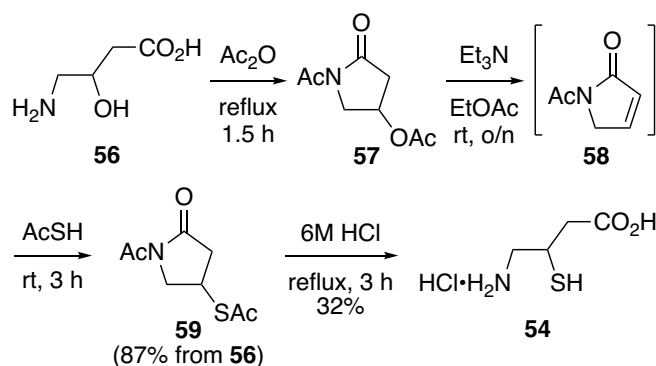
Scheme 3.19 Retrosynthesis for bicyclic thiazolidine 82

3.5 Experimental

3.5.1 General Information

Reactions were conducted in oven-dried (120 °C) or flame-dried glassware under a positive argon or nitrogen atmosphere unless otherwise stated. Transfer of anhydrous solvents or mixtures was accomplished with oven-dried syringes. Solvents were distilled before use: acetonitrile (MeCN) from calcium hydride; tetrahydrofuran (THF) from sodium/benzophenone ketyl; toluene (PhMe) from sodium metal. All other solvents and commercially available reagents were used without further purification. Thin layer chromatography (TLC) was performed on glass plates precoated with 0.25 mm Kiesegel 60 F₂₅₄ (Merck); the stains for TLC analysis were conducted with 2.5% *p*-anisaldehyde in AcOH-H₂SO₄-EtOH (1:3:90) and further heating until development of color. Flash chromatography columns were packed with 230-240 mesh silica gel and performed with the indicated eluents. Proton Nuclear magnetic resonance (¹H NMR) spectra were recorded at 500 MHz or 700 MHz in indicated deuterated solvents and coupling constants (*J*) were reported in Hertz (Hz). Splitting patterns were designated as s, singlet; d, doublet; t, triplet; q, quartet; m, multiplet; br, broad; dd, doublet of doublets, etc. The chemical shifts were reported on the δ scale (ppm) and the spectra were referenced to residual solvent peaks: CDCl₃ (7.26 ppm for ¹H NMR; 77.16 ppm for ¹³C NMR); CD₃OD (3.33 ppm for ¹H NMR; 77.16 ppm for ¹³C NMR); DMSO-d₆ (2.49 ppm for ¹H NMR; 39.5 ppm for ¹³C NMR); D₂O (4.80 ppm for ¹H NMR). Carbon nuclear magnetic resonance spectra (¹³C NMR) were recorded at 125 MHz and the chemical shifts were reported to the nearest 0.1 ppm to reflect the digital resolution of the data. In some cases, two nearly overlapping resonances were reported to the nearest 0.01 ppm to distinguish them from each other. Infrared (IR) spectra were recorded neat and reported in cm⁻¹. Mass spectra were recorded by using ESI.

(Note: The peak around 206 ppm in ¹³C NMR experiments using 700 MHz NMR spectrometer is an artifact of the spectrometer.)

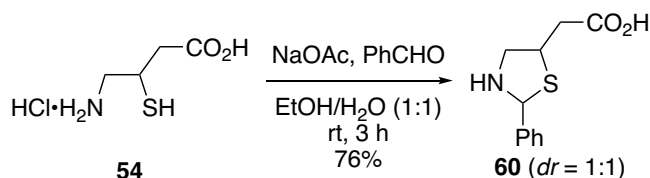


4-Amino-3-mercaptoputyric acid **54** was prepared from commercially available 4-amino-3-hydroxybutyric acid **55** (Sigma-Aldrich) following a known procedure³² with slight modifications.

Pyrrolidone 57. A solution of 4-amino-3-hydroxybutyric acid **54** (Sigma-Aldrich, 1.01g, 8.48 mmol) in acetic anhydride (4.00 mL, 42.0 mmol) was heated at refluxed for 1.5 h. The reaction mixture was then cooled to room temperature and concentrated under reduced pressure. The residue was subjected to azeotropic distillation with toluene (3×20 mL). EtOAc (3.5 mL) was added to the resulting oily residue followed by triethylamine (1.29 mL, 9.25 mmol). The reaction mixture was stirred at room temperature for 16 h to generate intermediate **58**. Thioacetic acid (0.66 mL, 1.09 mmol) was then added and the reaction was completed after stirring at room temperature for 3 h. Saturated NH_4Cl solution (20 mL) was added to the reaction flask and the aqueous layer was extracted with EtOAc (2×20 mL). The combined organic layers were washed with saturated NaHCO_3 solution (20 mL) and brine (30 mL), dried over anhydrous MgSO_4 , filtered and concentrated. Column chromatography (silica gel, 10%, 15%, 20% EtOAc/hexanes) provided **59** as a reddish brown oil (1.31 g, 78%): R_f 0.43 (40% EtOAc/hexane); IR (cast film) 3423 (br), 3000 (br), 1706, 1601, 1501, 1407 cm^{-1} ; ^1H NMR (500 Hz, CDCl_3) δ 4.21 (dd, $J = 12.4, 7.5$ Hz, 1H), 4.07 (dddd, $J = 8.5, 7.5, 6.1, 5.3$ Hz, 1H), 3.75 (dd, $J = 12.4, 5.3$ Hz, 1H), 3.09 (dd, $J = 18.0, 8.5$ Hz, 1H), 2.61 (dd, $J = 18.0, 6.1$ Hz, 1H), 2.51 (s, 3H), 2.36 (s, 3H); ^{13}C NMR (125 Hz, CDCl_3) δ 194.6,

172.6, 171.0, 51.1, 39.9, 33.5, 30.7, 25.0; HRMS (ESI, $[M+Na]^+$) calcd for $C_8H_{11}NO_3SNa$, 224.0352, found: m/z 224.0351.

4-Amino-3-mercaptopbutyric acid 54. To pyrrolidone **57** (6.97 g, 34.6 mmol) was added 6M HCl solution (4.4 mL) and a biphasic solution was formed at room temperature. Upon heating to reflux, a homogeneous solution was formed and was stirred for 3 h under reflux. After cooling to room temperature, EtOAc (20 mL) and water (20 mL) was added to the reaction mixture. The aqueous layer was concentrated under reduced pressure. The residue was subjected to azeotropic distillation with 2-propanol (2×20 mL) and toluene (2×20 mL). The product was recrystallized from 2-propanol (20 mL), filtered and dried under high vacuum to provide 4-amino-3-mercaptopbutyric acid **54** as a slightly pink solid, which contains one molecule of 2-propanol (2.54 g, 32%): IR (cast film) 2990, 2925, 1745, 1696, 1301 cm^{-1} ; 1H NMR (500 Hz, D_2O) δ 4.06 (septet, $J = 6.3$ Hz, 1H), 3.48-3.38 (m, 2H), 3.11 (dd, $J = 12.5$, 9.5 Hz, 1H), 2.91, (dd, 16.4, 5.5 Hz, 1H), 2.75 (dd, $J = 16.4$, 7.9 Hz, 1H), 1.21 (d, $J = 6.3$ Hz, 6H) (carboxylic acid proton was not observed due to exchange); ^{13}C NMR (125 Hz, D_2O) δ 176.0, 65.2, 46.2, 42.4, 34.9, 24.7; HRMS (ESI, $[M+H]^+$) calcd for $C_4H_{10}NO_2S$ 136.0428, found: m/z 136.0427.

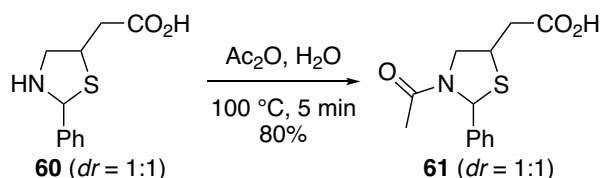


Thiazolidines 60. To a solution of **54** (674 mg, 2.91 mmol) in water (11 mL) was added sodium acetate (239 mg, 2.91 mmol), anhydrous ethanol (11 mL) and benzaldehyde (0.30 mL, 3.0 mmol). The reaction mixture was stirred at room temperature for 2 h and then cooled in an ice water bath. The precipitated crystals were collected by filtration. The solid was further dried under high vacuum to provide **60** as a white solid (491 mg, 76%). Product **60** was isolated as a mixture of *cis* **60** and *trans* **60** isomers. (Ratio of *cis* and *trans* **60** (1:1) was determined by integration of the acetal protons in the 1H

NMR spectrum. Assignment of protons and carbons to the individual isomers was accomplished through analysis of a combination of COSY, HSQC, and HMBC spectra of the mixture.) IR (cast film) 3500, 3031, 2800 (br), 1634, 1540, 1408 cm^{-1} ; HRMS (ESI, $[\text{M-H}]^-$) calcd for $\text{C}_{11}\text{H}_{12}\text{NO}_2\text{S}$ 222.0594, found: m/z 222.0595.

60 (diastereomer A): ^1H NMR (500 Hz, DMSO-d_6) δ 7.44-7.40 (m, 2H), 7.35-7.23 (m, 3H), 5.56 (s, 1H), 3.86-3.80 (m, 1H), 3.47 (dd, $J = 12.2, 6.0$ Hz, 1H), 2.68 (dd, $J = 16.6, 6.2$ Hz, 1H), 2.66 (dd, $J = 12.2, 6.6$ Hz, 1H), 2.52 (dd, $J = 16.6, 8.4$ Hz, 1H) (carboxylic acid proton was not observed due to exchange); ^{13}C NMR (125 Hz, DMSO-d_6) δ 173.0, 141.0, 128.2, 127.7, 127.3, 72.5, 57.6, 49.5, 40.2.

60 (diastereomer B): ^1H NMR (500 Hz, DMSO-d_6) δ 7.48-7.44 (m, 2H), 7.35-7.23 (m, 3H), 5.44 (s, 1H), 3.80-3.75 (m, 1H), 3.22 (dd, $J = 12.3, 2.0$ Hz, 1H), 3.00 (dd, $J = 12.3, 6.2$ Hz, 1H), 2.76 (dd, $J = 16.6, 6.9$ Hz, 1H), 2.54 (dd, $J = 16.6, 8.0$ Hz, 1H) (carboxylic acid proton was not observed due to exchange); ^{13}C NMR (125 Hz, DMSO-d_6) δ 172.9, 140.1, 128.1, 127.5, 127.0, 73.5, 57.2, 48.7, 41.5.

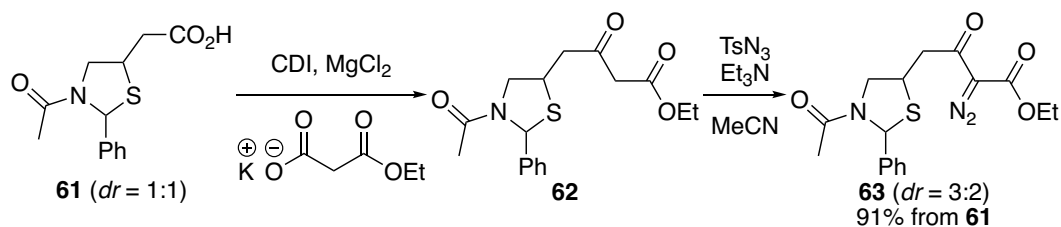


Thiazolidines 61. A solution of **60** (361 mg, 1.62 mmol) in acetic anhydride (0.76 mL, 8.1 mmol) and water (0.87 mL) was heated at 100 $^\circ\text{C}$ for 5 min and then cooled to room temperature. Solvent was removed under reduced pressure. The residue was subjected to azeotropic distillation with toluene (2×10 mL) and 2-propanol (10 mL). The crude solid was recrystallized from EtOH and water to provide **61** as a white solid (344 mg, 80%). Product **61** was isolated as a mixture of diastereomers. (Ratio of *cis* and *trans* **61** (1:1) was determined by integration of the acetal protons in the ^1H NMR spectrum. Assignment of protons and carbons to the individual isomers was accomplished through analysis of a combination of COSY, HSQC, and HMBC spectra of the

mixture.) IR (cast film) 3030, 3000 (br), 2934, 1725, 1653, 1608, 1415 cm^{-1} ; HRMS (ESI, $[\text{M-H}]^-$) calcd for $\text{C}_{13}\text{H}_{14}\text{NO}_3\text{S}$ 264.0700, found: m/z 264.0699.

60 (diastereomer A): ^1H NMR (500 Hz, CD_3OD) δ 7.41-7.19 (m, 5H), 6.42 (s, 1H), 4.19 (dd, $J = 12.3, 5.0$ Hz, 1H), 4.03 (dd, $J = 12.3, 5.8$ Hz, 1H), 3.97-3.91 (m, 1H), 2.82-2.58 (m, 2H), 2.19 (s, 3H) (carboxylic acid proton was not observed due to exchange); ^{13}C NMR (125 Hz, CD_3OD) δ 174.3, 171.4, 142.9, 130.0, 129.2, 127.0, 64.9, 56.8, 43.7, 39.5, 23.0.

60 (diastereomer B): ^1H NMR (500 Hz, CD_3OD) δ 7.41-7.19 (m, 5H), 6.29, (s, 1H), 4.16 (dd, $J = 11.0, 5.5$ Hz, 1H), 3.96 (dd, $J = 11.0, 5.0$ Hz, 1H), 3.91-3.83 (m, 1H), 2.82-2.58 (m, 2H), 1.93 (s, 3H) (carboxylic acid proton was not observed due to exchange); ^{13}C NMR (125 Hz, CD_3OD) δ 174.3, 172.1, 143.3, 129.4, 128.6, 126.6, 65.9, 56.1, 42.4, 39.5, 22.4.

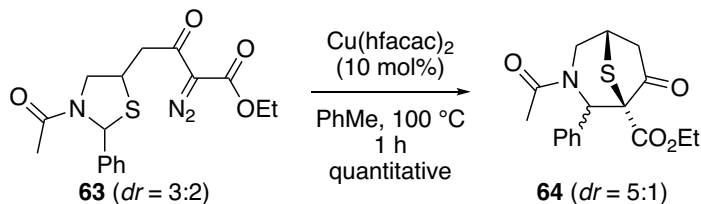


Diazoketoesters 63. To a solution of **61** (50 mg, 0.19 mmol) in THF (1.0 mL) at 0°C was added carbonyldiimidazole (37 mg, 0.23 mmol) in one portion. This reaction mixture (flask A) was stirred at room temperature for 2 h. In a separate flask (flask B), magnesium chloride (27 mg, 0.28 mmol) and potassium ethyl malonate (38 mg, 0.22 mmol) were stirred in THF (1.0 mL) at room temperature for 1.5 h. Flask B was cooled in an ice water bath and the content from flask A was added to flask B *via* syringe. The reaction mixture was stirred at room temperature for 16 h. EtOAc (10 mL) and 0.5 M HCl solution (10 mL) were then added to the reaction mixture. The aqueous layer was extracted with EtOAc (2×10 mL). The combined organic layer was washed with saturated NaHCO_3 solution (10 mL), brine (20 mL), dried with MgSO_4 , filtered and concentrated to provide crude **62**, which was directly carried forward to the next step.

To a solution of crude **62** in acetonitrile (1.8 mL) at room temperature was added triethylamine (25 μ L, 0.19 mmol) and *p*-toluenesulfonyl azide (27 μ L, 0.18 mmol). After stirring at room temperature for 16 h, the solvent was removed under reduced pressure. Column chromatography (silica gel, 50% EtOAc/hexanes) provided **63** as a yellow oil (61 mg, 91% from **62**). Product **63** was isolated as a mixture of diastereomers. (Ratio of *cis* and *trans* **63** (3:2) was determined by integration of the acetal protons in the ^1H NMR spectrum. Assignment of protons and carbons to the individual isomers was accomplished through analysis of a combination of COSY, HSQC, and HMBC spectra of the mixture.) R_f 0.18 (40% EtOAc/hexane); IR (cast film) 3050, 2982, 2931, 2138, 1715, 1656, 1399, 1313 cm^{-1} ; HRMS (ESI, $[\text{M}+\text{Na}]^+$) calcd for $\text{C}_{17}\text{H}_{19}\text{N}_3\text{O}_4\text{SNa}$ 384.0988, found: m/z 384.0988.

63 (major diastereomer): ^1H NMR (500 Hz, CDCl_3) δ 7.39-7.20 (m, 5H), 6.05 (s, 1H), 4.35-4.24 (m, 3H), 4.02-3.95 (m, 2H), 3.31-3.28 (m, 2H), 1.96 (s, 3H), 1.33 (t, $J = 7.1$ Hz, 3H); ^{13}C NMR (125 Hz, CDCl_3) δ 189.9, 168.6, 161.2, 141.7, 129.2, 128.3, 125.5, 65.0, 61.8, 54.8, 44.4, 41.1, 22.6, 14.5 (diazo carbon not detected).

63 (minor diastereomer): ^1H NMR (500 Hz, CDCl_3) δ 7.39-7.20 (m, 5H), 6.54 (s, 1H), 4.35-4.24 (m, 3H), 4.05 (dd, $J = 11.0, 5.8$ Hz, 1H), 3.80 (dd, $J = 11.0, 4.5$ Hz, 1H), 3.35 (dd, $J = 17.2, 6.1$ Hz, 1H), 3.12 (dd, $J = 17.2, 8.1$ Hz, 1H), 2.18 (s, 3H), 1.33 (t, $J = 7.1$ Hz, 3H); ^{13}C NMR (125 Hz, CDCl_3) δ 190.0, 169.7, 161.2, 141.3, 128.6, 127.9, 126.3, 63.5, 61.9, 55.2, 44.6, 42.1, 23.3, 14.5 (diazo carbon not detected).

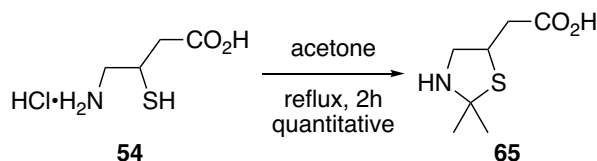


Azepine 64. To a solution of **63** (48 mg, 0.13 mmol) in toluene (7.0 mL) at 100 $^\circ\text{C}$ was added $\text{Cu}(\text{hfacac})_2$ (5.9 mg, 0.012 mmol) in one portion as a solid. After stirring at 100 $^\circ\text{C}$ for 1 h, the solvent was removed under reduced pressure. Column chromatography

(silica gel, 50%, 60%, 70% EtOAc/hexanes) provided **64** as a colorless oil (44.0 mg, quantitative yield). Product **64** was isolated as a mixture of diastereomers (5:1 ratio determined by ^1H NMR integration of benzylic methane proton): R_f 0.31 (70% EtOAc/hexane); IR (cast film) 3060, 2980, 2934, 1754, 1727, 1655, 1406, 1250 cm^{-1} ; HRMS (ESI, $[\text{M}+\text{Na}]^+$) calcd for $\text{C}_{17}\text{H}_{19}\text{NO}_4\text{SNa}$ 356.0927, found: m/z 356.0919.

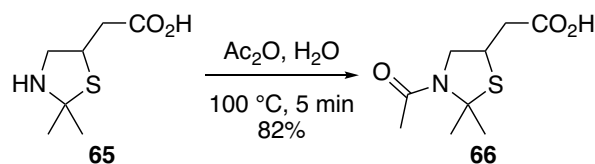
64a (major diastereomer): ^1H NMR (500 Hz, CDCl_3) δ 7.42-7.23 (m, 5H), 5.82 (s, 1H), 4.79 (dd, $J = 14.0, 3.7$ Hz, 1H), 4.28 (q, $J = 7.2$ Hz, 2H), 3.74-3.70 (m, 1H), 3.36 (d, $J = 14.0$ Hz, 1H), 2.98 (dd, $J = 17.7, 0.7$ Hz, 1H), 2.61 (d, $J = 17.7$ Hz, 1H), 2.13 (s, 3H), 1.27 (t, $J = 7.2$ Hz, 3H); ^{13}C NMR (125 Hz, CDCl_3) δ 203.8, 172.1, 166.0, 135.7, 128.8, 128.5, 128.1, 67.5, 63.2, 61.6, 44.3, 43.8, 21.8, 14.1.

64b (minor diastereomer): ^1H NMR (500 Hz, CDCl_3) δ 7.42-7.23 (m, 5H), 6.56 (s, 1H), 4.25-4.20 (m, 2H), 3.95-3.88 (m, 2H), 3.77-3.74 (m, 1H), 3.04 (dd, $J = 17.7, 6.1$ Hz, 1H), 2.56 (d, $J = 17.7$ Hz, 1H), 2.11 (s, 3H), 1.26 (t, $J = 7.2$ Hz, 3H); ^{13}C NMR (125 Hz, CDCl_3) δ 201.8, 170.5, 165.7, 136.4, 128.9, 128.3, 128.1, 68.1, 63.0, 55.8, 49.6, 43.3, 22.8, 14.1.

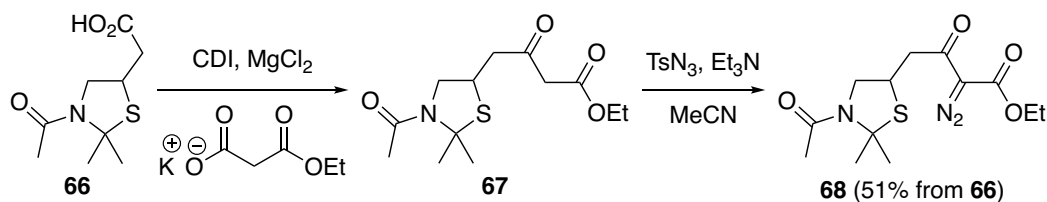


Thiazolidine 65. A solution of **54** (587 mg, 2.53 mmol) in acetone (45 mL) was heated to reflux and stirred for 2 h. The reaction mixture was concentrated to dryness. The crude solid was recrystallized from methanol and diethyl ether to provide **65** (523 mg, quantitative yield) as a fluffy white solid: mp 167-169 $^\circ\text{C}$; IR (cast film) 2929, 2900 (br), 2765, 1713, 1152 cm^{-1} ; ^1H NMR (500 Hz, CD_3OD) δ 4.22-4.14 (m, 1H), 3.96 (dd, $J = 12.4, 7.3$ Hz, 1H), 3.57 (dd, $J = 12.4, 7.2$ Hz, 1H), 2.91 (dd, $J = 17.3, 6.3$ Hz, 1H), 2.78 ($J = 17.3, 8.0$ Hz, 1H), 1.80 (s, 3H), 1.79 (s, 3H) (carboxylic acid proton was not observed due to exchange); ^{13}C NMR (125 Hz, CD_3OD) δ 174.0, 73.2, 52.1, 43.3, 40.2,

29.1, 28.9; HRMS (ESI, $[M+H]^+$) calcd for $C_7H_{14}NO_2S$ 176.0740, found: m/z 176.0738.

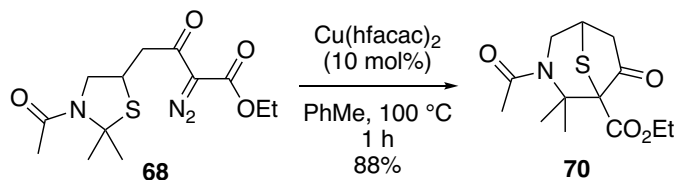


Thiazolidine 66. To acetic anhydride (0.92 mL, 9.7 mmol) was added **65** (103 mg, 0.486 mmol) as a solid in one portion. The resulting slurry was heated at 100 °C for 5 min to provide an orange solution. The reaction mixture was cooled to room temperature and water (0.18 mL, 9.7 mmol) was added to the reaction mixture. The resulting mixture was concentrated under reduced pressure. The residue was subjected to azeotropic distillation with toluene (3×1 mL). Column chromatography (silica gel, 2%, 3%, 4%, 5% MeOH/ CH_2Cl_2) provided **66** (86 mg, 82% yield) as a slightly yellow solid: mp 95-98 °C; R_f 0.25 (10% MeOH/ CH_2Cl_2); IR (cast film) 2977, 2932, 2850 (br), 1726, 1654, 1608, 1418, 1223 cm^{-1} ; 1H NMR (600 Hz, CD_3OD) δ 4.17 (dd, $J = 10.7, 5.6$ Hz, 1H), 2.79 (dddd, $J = 7.3, 7.3, 7.3, 5.6$ Hz, 1H), 3.65 (dd, $J = 10.7, 7.8$ Hz, 1H), 2.71 (dd, $J = 16.2, 7.3$ Hz, 1H), 2.59 (dd, $J = 16.2, 7.2$ Hz, 1H), 2.08 (s, 3H), 1.82 (s, 3H), 1.79 (s, 3H) (carboxylic acid proton was not observed due to exchange); ^{13}C NMR (125 Hz, CD_3OD) δ 174.4, 171.1, 73.6, 59.8, 30.3, 38.8, 30.0, 29.6, 25.3; HRMS (ESI, $[M-H]^-$) calcd for $C_9H_{14}NO_3S$ 216.070, found: m/z 216.0703.



Diazoketoester 68. To a solution of **66** (86 mg, 0.40 mmol) in THF (4.0 mL) at 0 °C was added carbonyldiimidazole (77 mg, 0.48 mmol) in one portion. This reaction mixture (flask A) was stirred at room temperature for 2 h. In a separate flask (flask B), magnesium chloride (56 mg, 0.59 mmol) and potassium ethyl malonate (80 mg, 0.47

mmol) were stirred in THF (4.0 mL) at room temperature for 1 h. Flask B was cooled in an ice water bath and the contents from flask A were added to flask B *via* syringe. After stirring at room temperature for 16 h, the solvent was removed under reduced pressure. Et₂O (200 mL) and 0.5 M HCl solution (6 mL) was then added to the residue. The aqueous layer was extracted with Et₂O (2×10 mL). The combined organic layers were washed with saturated NaHCO₃ solution (20 mL), brine (20 mL), dried with MgSO₄, filtered and concentrated. A quick chromatographic purification (5% MeOH/CH₂Cl₂) provided crude **67** as a yellow oil, which was directly carried forward to the next step. To a solution of crude **67** in acetonitrile (2.0 mL) at room temperature was added triethylamine (28 μL, 0.22 mmol) and *p*-toluenesulfonyl azide (34 μL, 0.22 mmol). After stirring at room temperature for 16 h, the solvent was removed under reduced pressure. Column chromatography (silica gel, 30%, 40%, 50% EtOAc/hexane) provided **68** as a clear colorless oil (52 mg, 42% yield): R_f 0.49 (5% MeOH/CH₂Cl₂); IR (cast film) 2980, 2932, 2140, 1716, 1649, 1163 cm⁻¹; ¹H NMR (500 Hz, CD₃OD) δ 4.31 (q, *J* = 7.2 Hz, 2H), 4.11 (dd, *J* = 10.2, 5.3 Hz, 1H), 3.87-3.81 (m, 1H), 3.56 (dd, *J* = 10.2, 8.0 Hz, 1H), 3.28 (dd, *J* = 17.5, 6.0 Hz, 1H), 3.19 (dd, *J* = 17.5, 7.9 Hz, 1H), 2.07 (s, 3H), 1.87 (s, 3H), 1.82 (s, 3H), 1.34 (t, *J* = 7.2 Hz); ¹³C NMR (125 Hz, CD₃OD) δ 190.0, 168.4, 161.2, 72.5, 61.9, 58.6, 43.6, 38.4, 30.0, 29.4, 25.8, 14.5 (diazo carbon not detected); HRMS (ESI, [M+Na]⁺) calcd for C₁₃H₁₉N₃O₄SNa 336.0988, found: *m/z* 336.0985.



Azepine 70. To a solution of **68** (17 mg, 0.056 mmol) in toluene (5.0 mL) at 100 °C was added Cu(hfacac)₂ (3 mg, 0.006 mmol) in one portion as a solid. After stirring at 100 °C for 1 h, the solvent was removed under reduced pressure. Column chromatography (silica gel, 40%, 50%, 60% EtOAc/hexanes) provided **70** as a

colorless oil (14 mg, 88% yield): R_f 0.32 (80% EtOAc/hexane); IR (cast film) 2983, 2963, 1763, 1741, 1668, 1256, 1132 cm^{-1} ; ^1H NMR (700 Hz, CDCl_3) δ 4.20 (q, $J = 7.2$ Hz, 2H), 3.89 (dd, $J = 12.9, 3.8$ Hz, 1H), 3.72 (dd, $J = 12.9, 1.5$ Hz, 1H), 3.55 (ddd, $J = 6.0, 3.8, 2.0$ Hz, 1H), 2.93 (dd, $J = 17.7, 6.2$ Hz, 1H), 2.57 (d, $J = 17.7$ Hz, 1H), 2.04 (s, 3H), 1.90 (s, 3H), 1.73 (s, 3H), 1.26 (t, $J = 7.2$ Hz, 3H); ^{13}C NMR (100 Hz, CDCl_3) δ 203.3, 173.8, 166.2, 69.6, 63.5, 62.3, 51.8, 43.7, 36.1, 26.3, 23.8, 19.0, 14.0; HRMS (ESI, $[\text{M}+\text{Na}]^+$) calcd for $\text{C}_{13}\text{H}_{19}\text{NO}_4\text{SNa}$ 308.0927, found: m/z 308.0927.

3.6 References

1. For a recent total synthesis on cephalotaxine, see: Ma, X. Y.; An, X. T.; Zhao, X. H.; Du, J. Y.; Deng, Y. H.; Zhang, X. Z.; Fan, C. A. *Org. Lett.* **2017**, *19*, 2965–2968 and references cited therein.
2. For total syntheses of otonecine, see: a) Vedejs, E.; Galante, R. J.; Goekjian, P. G. *J. Am. Chem. Soc.* **1998**, *120*, 3613–3622. b) Niwa, H.; Sakata, T.; Yamada, K. *Bull. Chem. Soc. Jpn.* **1994**, *67*, 2345–2347. c) Niwa, H.; Uosaki, Y.; Yamada, K. *Tetrahedron Lett.* **1983**, *24*, 5731–5732.
3. For a total synthesis on lycoposerramine T, see: Zaimoku, H.; Nishide, H.; Nishibata, A.; Goto, N.; Taniguchi, T.; Ishibashi, H. *Org. Lett.* **2013**, *15*, 2140–2143 and references cited therein.
4. Lin, W.-H.; Ye, Y.; Xu, R.-S. *J. Nat. Prod.* **1992**, *55*, 571–576.
5. For an example of total synthesis on stemonine, see: Williams, D. R.; Shamim, K.; Reddy, J. P.; Amato, G. S.; Shaw, S. M. *Org. Lett.* **2003**, *5*, 3361–3364 and references cited therein.
6. For selected reviews on *Stemona* alkaloids, see: a) Pilli, R. A.; Rosso, G. B.; de Oliveira, M. C. F. *Nat. Prod. Rep.* **2010**, *27*, 1908–1937. b) Pilli, R. A.; de Oliveira, M. C. F. *Nat. Prod. Rep.* **2000**, *17*, 117–127. c) Alibés, R.; Figueredo, M. *Eur. J. Org. Chem.* **2009**, 2421–2435. d) Greger, H. *Planta Med.* **2006**, *72*, 99–113.
7. Williams, D. R.; Reddy, J. P.; Amato, G. S. *Tetrahedron Lett.* **1994**, *35*, 6417–6420.
8. For a review, see: Gololobov, Y. G.; Kasukhin, L. F. *Tetrahedron* **1992**, *48*, 1353–1406.
9. a) Baldwin, J. E.; Thomas, R. C.; Kruse, L. I.; Silberman, L. *J. Org. Chem.* **1977**, *42*, 3846–3852. b) Baldwin, J. E. *J. Chem. Soc. Chem. Commun.* **1976**, 734–736.
10. Gao, P.; Tong, Z.; Hu, H.; Xu, P. F.; Liu, W.; Sun, C.; Zhai, H. *Synlett* **2009**, 2188–2190.
11. Bogliotti, N.; Dalko, P. I.; Cossy, J. *Synlett* **2006**, 2664–2666.
12. Kohno, Y.; Narasaka, K. *Bull. Chem. Soc. Jpn.* **1996**, *69*, 2063–2070.

13. Nakayama, Y.; Maeda, Y.; Hama, N.; Sato, T.; Chida, N. *Synthesis* **2016**, *48*, 1647–1654.
14. Bates, R. W.; Sridhar, S. *Synlett* **2009**, 1979–1981.
15. Bates, R. W.; Sridhar, S. *J. Org. Chem.* **2008**, *73*, 8104–8105 and references cited therein.
16. Wang, Y.; Zhu, L.; Zhang, Y.; Hong, R. *Angew. Chem. Int. Ed.* **2011**, *50*, 2787–2790.
17. Mi, X.; Wang, Y.; Zhu, L.; Wang, R.; Hong, R. *Synthesis* **2012**, *44*, 3432–3440.
18. Honda, T.; Matsukawa, T.; Takahashi, K. *Org. Biomol. Chem.* **2011**, *9*, 673–675.
19. a) Honda, T. *Chem. Pharm. Bull.* **2012**, *60*, 687–705. b) Szostak, M.; Fazakerley, N. J.; Parmar, D.; Procter, D. J. *Chem. Rev.* **2014**, *114*, 5959–6039. c) Nicolaou, K. C.; Ellery, S. P.; Chen, J. S. *Angew. Chem. Int. Ed.* **2009**, *48*, 7140–7165.
20. a) Jacobi, P. A.; Lee, K. *J. Am. Chem. Soc.* **1997**, *119*, 3409–3410. b) Jacobi, P. A.; Lee, K. *J. Am. Chem. Soc.* **2000**, *122*, 4295–4303.
21. For examples of previous development, see: a) Jacobi, P. A.; Blum, C. A.; DeSimone, R. W.; Udodong, U. E. S. *J. Am. Chem. Soc.* **1991**, *113*, 5384–5392. b) Jacobi, P. A.; Kacxmerek, C. S. R.; Udodong, U. E. *Tetrahedron* **1987**, *43*, 5475–5488 and references cited therein.
22. a) Kinoshita, A.; Mori, M. *Heterocycles* **1997**, *46*, 287–299. b) Kinoshita, A.; Mori, M. *J. Org. Chem.* **1996**, *61*, 8356–8357.
23. a) Mori, M. *Adv. Synth. Catal.* **2007**, *349*, 121–135. b) Mori, M. *Top. Organomet. Chem.* **1998**, *1*, 133–154.
24. Sibi, M. P.; Subramanian, T. *Synlett* **2004**, 1211–1214.
25. Torssell, S.; Wanngren, E.; Somfai, P. *J. Org. Chem.* **2007**, *72*, 4246–4249.
26. Olivo, H. F.; Tovar-Miranda, R.; Barragán, E. *J. Org. Chem.* **2006**, *71*, 3287–3290.
27. For selected review, see: a) Evans, P. A.; Holmes, A. B. *Tetrahedron* **1991**, *47*, 9131–9166. b) Yet, L. *Chem. Rev.* **2000**, *100*, 2963–3007. c) Nubbemeyer, U. *Top. Curr. Chem.* **2001**, *216*, 125–196. For selected recent examples, see: d) Baud, L. G.; Manning, M. A.; Arkless, H. L.; Stephens, T. C.; Unsworth, W. P. *Chem. Eur.*

- J.* **2017**, *23*, 2225–2230. e) Shaw, M. H.; Croft, R. A.; Whittingham, W. G.; Bower, J. F. *J. Am. Chem. Soc.* **2015**, *137*, 8054–8057. f) Nakamura, I.; Sato, Y.; Takeda, K.; Terada, M. *Chem. Eur. J.* **2014**, *20*, 10214–10219.
28. a) Deiters, A.; Martin, S. F. *Chem. Rev.* **2004**, *104*, 2199–2238. b) Sattely, E. S.; Cortex, G. A.; Moebius, D. C.; Schrock, R. R.; Hoveyda, A. H. *J. Am. Chem. Soc.* **2005**, *127*, 8526–8533.
29. Cao, L. *Seven- and Eight-Membered Ether Formation via Sulfonium Ylide Rearrangement Processes and Application in an Approach to (+)-Laurencin*. PhD Thesis, University of Alberta, Alberta, 2010.
30. Lin, R.; Cao, L.; West, F. G. *Org. Lett.* **2017**, *19*, 552–555.
31. a) Kametani, T.; Honda, T. *J. Chem. Soc. Chem. Commun.* **1986**, 651–652. b) Kametani, T.; Yukawa, H.; Honda, T. *J. Chem. Soc. Perkin Trans. I* **1988**, 833–837. c) Kametani, T.; Yukawa, H.; Honda, T. *J. Chem. Soc. Chem. Commun.* **1988**, 685–687. d) Kametani, T.; Yukawa, H.; Honda, T. *J. Chem. Soc. Perkin Trans. I* **1990**, 571–577.
32. Iwasaki, T.; Kondo, K.; Nakatani, T.; Yoshioka, R. US 5495012 A, February 27, 1996.
33. Brooks, D. W.; Lu, L. D.-L.; Masamune, S. *Angew. Chem. Int. Ed. Engl.* **1979**, *18*, 72–74.
34. a) Regitz, M. *Angew. Chem. Int. Ed. Engl.* **1967**, *6*, 733–749. b) Regitz, M. *Synthesis*, **1972**, *7*, 351–373.
35. For a recent total synthesis of nakadomarin A, see: Boeckman, R. K.; Wang, H.; Rugg, K. W.; Genung, N. E.; Chen, K.; Ryder, T. R. *Org. Lett.* **2016**, *18*, 6136–6139 and references cited therein.
36. Yap, W. S.; Gan, C. Y.; Low, Y. Y.; Choo, Y. M.; Etoh, T.; Hayashi, M.; Komiyama, K.; Kam, T. S. *J. Nat. Prod.* **2011**, *74*, 1309–1312.
37. Kirillova, M. S.; Muratore, M. E.; Dorel, R.; Echavarren, A. M. *J. Am. Chem. Soc.* **2016**, *138*, 3671–3674.

38. Compound **80** could be synthesized *via* a similar strategy: a) Fujii, T.; Yoshifuji, S.; Ikeda, K. *Chem. Pharm. Bull.* **1966**, *1427*, 2841–2845. For the preparation of compound **81**, see: b) Barcelos, R. C.; Pastre, J. C.; Vendramini-Costa, D. B.; Caixeta, V.; Longato, G. B.; Monteiro, P. A.; de Carvalho, J. E.; Pilli, R. A. *ChemMedChem* **2014**, *9*, 2725–2743. c) Zou, Y.; Yan, C.; Zhang, H.; Xu, J.; Zhang, D.; Huang, Z.; Zhang, Y. *Eur. J. Med. Chem.* **2017**, *138*, 313–319. C)
39. Lee, S.; Bae, M.; In, J.; Kim, J. H.; Kim, S. *Org. Lett.* **2017**, *19*, 254–257.
40. Jiang, Y.-Y.; Wang, Q.-Q.; Liang, S.; Hu, L.-M.; Little, R. D.; Zeng, C.-C. *J. Org. Chem.* **2016**, *81*, 4713–4719.

Bibliography

Chapter 1

1. a) Curtius, T. *Ber.* **1883**, *16*, 2230–2231. b) Curtius, T. *J. Prakt. Chem.* **1888**, *38*, 396–440.
2. a) Wolff, L. *Justus Liebigs Ann. Chem.* **1902**, *325*, 129–195. For selected reviews, see: b) Kirmse, W. *Eur. J. Org. Chem.* **2002**, *2002*, 2193–2256. c) Candeias, N. R.; Trindade, A. F.; Gois, P. M. P.; Afonso, C. A. M. *The Wolff Rearrangement*; 2014; Vol. 3.
3. a) Arndt, F.; Eistert, B.; Amede, J. *Ber.* **1928**, *61B*, 1949–1953. b) Arndt, F.; Amende, J. *Ber.* **1928**, *61B*, 1122–1124. c) Arndt, F.; Eistert, B.; Partale, W. *Ber.* **1927**, *60B*, 1364–1370.
4. Doyle, M. P.; McKervey, M. A.; Ye, T. *Modern Catalytic Methods for Organic Synthesis with Diazo Compounds*; Wiley-Interscience: New York, 1998.
5. a) Ford, A.; Miel, H.; Ring, A.; Slattery, C. N.; Maguire, A. R.; McKervey, M. A. *Chem. Rev.* **2015**, *115*, 9981–10080. b) Maas, G. *Angew. Chem. Int. Ed.* **2009**, *48*, 8186–8195. c) Ye, T.; Mckervey, M. A. *Chem. Rev.* **1994**, *94*, 1091–1160; d) Zhang, Z.; Wang, J. *Tetrahedron* **2008**, *64*, 6577–6605.
6. a) Womack, E. B.; Nelson, A. B. *Org. Synth.* **1963**, *4*, 424–426. b) Womack, E. B.; Nelson, A. B. *Org. Synth.* **1955**, *3*, 392–393.
7. a) Holton, T. L.; Shechter, H. *J. Org. Chem.* **1995**, *60*, 4725–4729. b) Javed, M. I.; Brewer, M. *Org. Lett.* **2007**, *9*, 1789–1792.
8. a) Regitz, M. *Angew. Chem. Int. Ed. Engl.* **1967**, *6*, 733–749. b) Regitz, M. *Synthesis*, **1972**, *7*, 351–373.
9. Erhunmwunse, M. O.; Steel, P. G. *J. Org. Chem.* **2008**, *73*, 8675–8677.
10. a) Marchand, A. P.; Brockway, N. M. *Chem. Rev.* **1974**, *74*, 431–469. b) Dave, V.; Varnhoff, E. W. *Org. React. (N. Y.)* **1970**, *18*, 217–401.

11. a) Andrews, G.; Evans, D. A. *Tetrahedron Lett.* **1972**, *13*, 5121–5124. b) Ando, W.; Yagihara, T.; Kondo, S.; Nakayama, K.; Yamato, H.; Nakaido, S.; Migita, T. *J. Org. Chem.* **1971**, *36*, 1732–1736 and references cited therein.
12. a) Pirrung, M. C.; Liu, H.; Morehead, A. T., Jr. *J. Am. Chem. Soc.* **2002**, *124*, 1014–1023. b) Doyle, M. P.; Tamblyn, W. H.; Bagheri, V. *J. Org. Chem.* **1981**, *46*, 5094–5102 and references cited therein.
13. a) Dötz, K. H.; Stendel, J., Jr. *Chem. Rev.* **2009**, *109*, 3227–3274. b) Zhao, Y.; Wang, J. *Synlett* **2005**, No. 19, 2886–2892.
14. a) von E. Doering, W.; Hoffmann, A. K. *J. Am. Chem. Soc.* **1954**, *76*, 6162–6165. b) von E. Doering, W.; Buttery, R. G.; Laughlin, R. G.; Chaudhuri, N. *J. Am. Chem. Soc.* **1956**, *78*, 3224–3224.
15. Fischer, E. O.; Maasböl, A. *Angew. Chem. Int. Ed. Engl.* **1964**, *3*, 580–581.
16. Schubert, U. *Coord. Chem. Rev.* **1984**, *55*, 261–286.
17. Yates, P. *J. Am. Chem. Soc.* **1952**, *74*, 5376–5381.
18. *Nitrogen, Oxygen and Sulfur Ylide Chemistry*; Clark, J. S., Ed.; Oxford University Press: Oxford, 2002.
19. a) Hodgson, D. M.; Pierard, F. Y. T. M.; Stupple, P. A. *Chem. Soc. Rev.* **2001**, *30*, 50–61. b) Davies, H. M. L.; Beckwith, R. E. J. *Chem. Rev.* **2003**, *103*, 2861–2903.
20. Davies, H. M. L.; Morton, D. *Chem. Soc. Rev.* **2011**, *40*, 1857–1869.
21. Doyle, M. P. *Chem. Rev.* **1986**, *86*, 919–939.
22. Doyle, M. P., In *Comprehensive Organometallic Chemistry II*; Hegedus, L. S., Ed.; Pergamon Press, New York, 1995; Vol. 12, pp 421–468.
23. Silberrad, O.; Roy, C. S. *J. Chem. Soc. Trans.* **1906**, *89*, 179–182.
24. Nozaki, H.; Moriuti, S.; Yamabe, M.; Noyori, R. *Tetrahedron Lett.* **1966**, *7*, 59–63.
25. Moser, W. R. *J. Am. Chem. Soc.* **1969**, *1171*, 1135–1140.
26. Nozaki, H.; Moriuti, S.; Takaya, H.; Noyori, R. *Tetrahedron Lett.* **1966**, *7*, 5239–5244.

27. For some selected review on asymmetric catalysis with metallocarbenes, see: a) ref 17b. b) Doyle, M. P.; Forbes, D. C. *Chem. Rev.* **1998**, *16*, 911–935. c) Doyle, M. P. *Chem. Rev.* **1986**, *86*, 919–939.
28. For a review, see: Wulfman, D. S.; Linstrumelle, G.; Cooper, C. F., In *The Chemistry of Diazonium and Diazo Groups, Part 2*; Patai, S., Ed.; Wiley, New York, 1978; Chapter 18.
29. a) Salomon, R. G.; Kochi, J. K. *J. Am. Chem. Soc.* **1973**, *95*, 3300–3310. b) Solomon, R. G.; Kochi, J. K. *J. Chem. Soc., Chem. Commun.* **1972**, 559–560.
30. a) Fritschi, H.; Leutenegger, U.; Pfaltz, A. *Helv. Chim. Acta* **1988**, *71*, 1553–1565. b) Lowenthal, R. E.; Abiko, A.; Masamune, S. *Tetrahedron Lett.* **1990**, *31*, 6005–6008.
31. Dauben, W. G.; Hendricks, R. T.; Luzzio, M. J.; Ng, H. P. *Tetrahedron Lett.* **1990**, *31*, 6969–6972.
32. Straub, B. F.; Hofmann, P. *Angew. Chem. Int. Ed.* **2001**, *40*, 1288–1290.
33. Salomon, R. G.; Kochi, J. K. *J. Am. Chem. Soc.* **1973**, *95*, 1889–1897.
34. a) Padwa, A.; Austin, D. J. *Angew. Chem. Int. Ed. Engl.* **1994**, *33*, 1797–1815. b) Doyle, M. P. *J. Org. Chem.* **2006**, *71*, 9253–9260.
35. Clark, J. S.; Krowiak, S. A. *Tetrahedron Lett.* 1993, *34*, 4385–4388.
36. Paulissen, R.; Reimlinger, H.; Hayez, E.; Hubert, A. J.; Teyssié, P. *Tetrahedron Lett.* **1973**, *14*, 2233–2236.
37. Gillingham, D.; Fei, N. *Chem. Soc. Rev.* **2013**, *42*, 4918–4931.
38. For reviews on rhodium(II) carboxylates, see: a) Adly, F. G.; Ghanem, A. *Chirality* **2014**, *26*, 692–711. b) Merlic, C. A.; Zechman, A. L. *Synthesis* **2003**, *34*, 1137–1156; c) Boyar, E. B.; Robinson, S. D. *Coord. Chem. Rev.* **1983**, *50*, 109–208.
39. Padwa, A.; Austin, D. J.; Price, A. T.; Semones, M. A.; Doyle, M. P.; Protopopova, M. N.; Winchester, W. R.; Tran, A. *J. Am. Chem. Soc.* **1993**, *115*, 8669–8680.

40. For selected examples, see: a) Nakamura, E.; Yoshikai, N.; Yamanaka, M. *J. Am. Chem. Soc.* **2002**, *124*, 7181–7192. b) Pirrung, M. C.; Liu, H.; Morehead, A. T. *J. Am. Chem. Soc.* **2002**, *124*, 1014–1023. c) Pirrung, M. C.; Morehead, A. T. *J. Am. Chem. Soc.* **1996**, *118*, 8162–8163.
41. Snyder, J. P.; Padwa, A.; Stengel, T.; Arduengo, A. J.; Jockisch, A.; Kim, H.-J. *J. Am. Chem. Soc.* **2001**, *123*, 11318–11319 and references cited therein.
42. Kornecki, K. P.; Briones, J. F.; Boyarskikh, V.; Fullilove, F.; Autschbach, J.; Schrote, K. E.; Lancaster, K. M.; Davies, H. M. L.; Berry, J. F. *Science* **2013**, *342*, 351–354.
43. a) Werlé, C.; Goddard, R.; Philipps, P.; Farès, C.; Fürstner, A. *J. Am. Chem. Soc.* **2016**, *138*, 3797–3805. b) Werlé, C.; Goddard, R.; Fürstner, A. *Angew. Chem. Int. Ed.* **2015**, *54*, 15452–15456.
44. *Ylide Chemistry*; Johnson, A. W., Ed.; Academic Press: New York, 1966; pp 306–366.
45. *Sulfur Ylides: Emerging Synthetic Intermediates*; Trost, B. M.; Melvin, L. S., Eds.; Academic Press: New York, 1975; pp 13–36.
46. Jessop, J. A.; Ingold, C. K. *J. Chem. Soc.* **1930**, 713–718.
47. a) Corey, E. J.; Chaykovsky, M. *J. Am. Chem. Soc.* **1965**, *87*, 1353–1364. b) Corey, E. J.; Chaykovsky, M. *J. Am. Chem. Soc.* **1962**, *84*, 867–868.
48. a) Aggarwal, V. K.; Winn, C. L. *Acc. Chem. Res.* **2004**, *37*, 611–620. b) Gololobov, Y. G.; Nesmeyanov, A. N.; Lysenko, V. P.; Boldeskul, I. E. *Tetrahedron* **1987**, *43*, 2609–2651.
49. Li, A.-H.; Dai, L.-X.; Hou, X.-L.; Huang, Y.-Z.; Li, F.-W. *J. Org. Chem.* **1996**, *61*, 489–493.
50. Trost, B. M.; Hammen, R. M. *J. Am. Chem. Soc.* **1973**, *95*, 962–964.
51. a) Vedejs, E.; West, F. G. *Chem. Rev.* **1986**, *86*, 941–955. b) Vedejs, E.; Martinez, G. R. *J. Am. Chem. Soc.* **1979**, *101*, 6452–6454.
52. a) Ando, W.; Kondo, S.; Nakayama, K.; Ichibori, K.; Kohoda, H.; Yamato, H.; Imai, I.; Nakaido, S.; Migita, T. *J. Am. Chem. Soc.* **1972**, *94*, 3870–3876. b)

- Ando, W.; Yagihara, T.; Tozune, S.; Imai, I.; Suzuki, J.; Toyama, T.; Nakaido, S.; Migita, T. *J. Org. Chem.* **1972**, *37*, 1721–1727. For a review, see: c) Ando, W. *Acc. Chem. Res.* **1977**, *10*, 179–185.
53. a) Stevens, T. S.; Creighton, E. M.; Gordon, A. B.; MacNicol, M. *J. Chem. Soc.* **1928**, 3193–3197. b) Thomson, T.; Stevens, T. S. *J. Chem. Soc.* **1932**, 69–73.
54. Pine, S. H. *J. Chem. Educ.* **1971**, 99–102.
55. Thomas, B.; Stevens, S. *J. Chem. Soc.* **1930**, 2107–2119.
56. Campbell, B. A.; Houston, A. H.; Kenyon, J. *J. Chem. Soc.* **1947**, 93–95.
57. Woodward, R. B.; Hoffmann, R. *Angew. Chem. Int. Ed. Engl.* **1969**, *8*, 781–853.
58. a) Chantrapromma, K.; Ollis, W. D.; Sutherland, I. O. *J. Chem. Soc. Perkin Trans. I* **1983**, 1049–1061. b) Ollis, W. D.; Rey, M.; Sutherland, I. O. *J. Chem. Soc. Perkin Trans. I* **1983**, 1009–1027. c) Ollis, W. D.; Rey, M.; Sutherland, I. O. *J. Chem. Soc. Chem. Commun.* **1975**, 543–545.
59. a) Eberlein, T. H.; West, F. G.; Tester, R. W. *J. Org. Chem.* **1992**, *57*, 3479–3482. b) West, F. G.; Naidu, B. N. *J. Am. Chem. Soc.* **1993**, *115*, 1177–1178. c) West, F. G.; Naidu, B. N.; Tester, R. W. *J. Org. Chem.* **1994**, *59*, 6892–6894.
60. For selected reviews, see: a) Zhang, Y.; Wang, J. *Coord. Chem. Rev.* **2010**, *254*, 941–953. b) Li, A.-H.; Dai, L.-X.; Aggarwal, V. K. *Chem. Rev.* **1997**, *97*, 2341–2372. c) Vedejs, E. *Acc. Chem. Res.* **1984**, *17*, 358–364.
61. a) Kirmse, W.; Kapps, M. *Chem. Ber.* **1968**, *101*, 994–1003. b) Doyle, M. P.; Griffin, J. H.; Chinn, M. S.; van Leusen, D. *J. Org. Chem.* **1984**, *49*, 1917–1925. c) Doyle, M. P.; Tamblyn, W. H.; Bagheri, V. *J. Org. Chem.* **1981**, *46*, 5094–5102.
62. a) Sommelet, M. *Compt. Rend.* **1937**, *205*, 56–58. b) Kantor, S. W.; Hauser, C. R. *J. Am. Chem. Soc.* **1951**, *73*, 4122–4131. c) Hauser, C. R.; Kantor, S. W.; Brasen, W. R. *J. Am. Chem. Soc.* **1953**, *75*, 2660–2663.
63. Ma, M.; Peng, L.; Li, C.; Zhang, X.; Wang, J. *J. Am. Chem. Soc.* **2005**, *127*, 15016–15017.

64. For selected examples, see: a) Nishibayashi, Y.; Ohe, K.; Uemura, S. *J. Chem. Soc., Chem. Commun.* **1995**, 1245–1246. b) Zhang, X.; Qu, Z.; Ma, Z.; Shi, W.; Jin, X.; Wang, J. *J. Org. Chem.* **2002**, *67*, 5621–5625. c) McMillen, D. W.; Varga, N.; Reed, B. A.; King, C. *J. Org. Chem.* **2000**, *65*, 2532–2536.
65. Liao, M.; Wang, J. *Green Chem.* **2007**, *9*, 184–188.
66. Xu, X.; Li, C.; Tao, Z.; Pan, Y. *Green Chem.* **2017**, *19*, 1245–1249.
67. a) Tyagi, V.; Sreenilayam, G.; Bajaj, P.; Tinoco, A.; Fasan, R. *Angew. Chem. Int. Ed.* **2016**, *55*, 13562–13566. b) Holzwarth, M. S.; Alt, I.; Plietker, B. *Angew. Chem. Int. Ed.* **2012**, *51*, 5351–5354.
68. Davies, P. W.; Albrecht, S. J. C.; Assanelli, G. *Org. Biomol. Chem.* **2009**, *7*, 1276–1279.
69. Bonderoff, S. A.; Padwa, A. *J. Org. Chem.* **2017**, *82*, 642–651.
70. a) Liao, M.; Peng, L.; Wang, J. *Org. Lett.* **2008**, *10*, 693–696. b) Li, Y.; Shi, Y.; Huang, Z.; Wu, X.; Xu, P.; Wang, J.; Zhang, Y. *Org. Lett.* **2011**, *13*, 1210–1213.
71. Gassman, P. G.; van Bergen, T. J. *J. Am. Chem. Soc.* **1974**, *96*, 5508–5512.
72. a) Murphy, G. K.; West, F. G. *Org. Lett.* **2006**, *8*, 4359–4361. b) Müller, P. *Acc. Chem. Res.* **2004**, *37*, 243–251.
73. Kametani, T.; Kawamura, K.; Honda, T. *J. Am. Chem. Soc.* **1987**, *109*, 3010–3017.
74. Ioannou, M.; Porter, M. J.; Saez, F. *Tetrahedron* **2005**, *61*, 43–50.
75. Zhu, S.; Xing, C.; Zhu, S. *Tetrahedron* **2006**, *62*, 829–832.
76. Stepakov, A. V.; Molchanov, A. P.; Magull, J.; Vidović, D.; Starova, G. L.; Kopf, J.; Kostikov, R. R. *Tetrahedron* **2006**, *62*, 3610–3618.
77. a) Qu, J.-P.; Xu, Z.-H.; Zhou, J.; Cao, C.-L.; Sun, X.-L.; Dai, L.-X.; Tang, Y. *Adv. Synth. Catal.* **2009**, *351*, 308–312. b) Liao, S.; Sun, X. L.; Tang, Y. *Acc. Chem. Res.* **2014**, *47*, 2260–2272.
78. a) Murphy, G. K.; West, F. G. *Org. Lett.* **2005**, *7*, 1801–1804. b) Murphy, G. K.; Marmsäter, F. P.; West, F. G. *Can. J. Chem.* **2006**, *84*, 1470–1486.

79. a) Mortimer, A. J. P.; Aliev, A. E.; Tocher, D. A.; Porter, M. J. *Org. Lett.* **2008**, *10*, 5477–5480. b) Mortimer, A. J. P.; Plet, J. R. H.; Obasanjo, O. A.; Kaltsoyannis, N.; Porter, M. J. *Org. Biomol. Chem.* **2012**, *10*, 8616–8627.
80. Ellis-Holder, K. K.; Peppers, B. P.; Kovalevsky, A. Y.; Diver, S. T. *Org. Lett.* **2006**, *8*, 2511–2514.
81. a) Muthusamy, S.; Selvaraj, K. *Tetrahedron Lett.* **2013**, *54*, 6886–6888. b) Muthusamy, S.; Selvaraj, K.; Suresh, E. *Asian J. Org. Chem.* **2016**, *5*, 162–172. c) Muthusamy, S.; Selvaraj, K.; Suresh, E. *Eur. J. Org. Chem.* **2016**, *2016*, 1849–1859.
82. Lu, P.; Herrmann, A. T.; Zakarian, A. *J. Org. Chem.* **2015**, *80*, 7581–7589.
83. Zhang, Y.-Z.; Zhu, S.-F.; Cai, Y.; Mao, H.-X.; Zhou, Q.-L. *Chem. Commun.* **2009**, 5362–5364.
84. Xu, B.; Zhu, S.-F.; Zhang, Z.-C.; Yu, Z.-X.; Ma, Y.; Zhou, Q.-L. *Chem. Sci.* **2014**, *5*, 1442–1448.
85. Hyde, S.; Veliks, J.; Liégault, B.; Grassi, D.; Taillefer, M.; Gouverneur, V. *Angew. Chem. Int. Ed.* **2016**, *55*, 3785–3789.
86. Keipour, H.; Jalba, A.; Delage-Laurin, L.; Ollevier, T. *J. Org. Chem.* **2017**, *82*, 3000–3010.
87. Aviv, I.; Gross, Z. *Chem. Eur. J.* **2008**, *14*, 3995–4005.
88. Tyagi, V.; Bonn, R. B.; Fasan, R. *Chem. Sci.* **2015**, *6*, 2488–2494.
89. a) Kametani, T.; Kawamura, K.; Tsubuki, M.; Honda, T. *J. Chem. Soc. Chem. Commun.* **1985**, 1324–1325. b) Kametani, T.; Kawamura, K.; Tsubuki, M.; Honda, T. *J. Chem. Soc. Perkin Trans. I* **1988**, 193–199.
90. a) Kametani, T.; Yukawa, H.; Honda, T. *J. Chem. Soc. Chem. Commun.* **1986**, 651–652. b) Kametani, T.; Yukawa, H.; Honda, T. *J. Chem. Soc. Perkin Trans. I* **1988**, 833–837.
91. a) Kametani, T.; Yukawa, H.; Honda, T. *J. Chem. Soc. Chem. Commun.* **1988**, 685–687. b) Kametani, T.; Yukawa, H.; Honda, T. *J. Chem. Soc. Perkin Trans. I* **1990**, 571–577.

92. Kim, G.; Kang, S.; Kim, S. N. *Tetrahedron Lett.* **1993**, *34*, 7627–7628.
93. Sato, T.; Hayakawa, Y.; Noyori, R. *Bull. Chem. Soc. Jpn.* **1984**, *57*, 2515–2525.

Chapter 2

1. Harizani, M.; Ioannou, E.; Roussis, V. In *Progress in the Chemistry of Organic Natural Products*; Kinghorn, A. D., Falk, H., Gibbons, S., Kobayashi, J., Eds.; Springer International Publishing: Switzerland, **2016**; Vol. *102*, pp 91–252.
2. a) Zhou, Z. F.; Menna, M.; Cai, Y. S.; Guo, Y. W. *Chem. Rev.* **2015**, *115*, 1543–1596. b) Wanke, T.; Philippus, A. C.; Zatelli, G. A.; Vieira, L. F. O.; Lhullier, C.; Falkenberg, M. *Rev. Bras. Farmacogn.* **2015**, *25*, 569–587. c) Yasumoto, T.; Murata, M. *Chem. Rev.* **1993**, *93*, 1897–1909.
3. a) Galli, C.; Mandolini, L. *Eur. J. Org. Chem.* **2000**, 3117–3125. b) Illuminati, G.; Mandolini, L.; Masci, B. *J. Am. Chem. Soc.* **1975**, *97*, 4960–4966. c) Illuminati, G.; Mandolini, L. *Acc. Chem. Res.* **1981**, *14*, 95–102.
4. For selected reviews, see: a) Martín, T.; Padrón, J. I.; Martín, V. S. *Synlett* **2013**, *25*, 12–32. b) Kim, D. *Synlett* **2013**, *25*, 33–57. c) Kleinke, A. S.; Webb, D.; Jamison, T. F. *Tetrahedron* **2012**, *68*, 6999–7018. d) Rainier, J. D. In *Metathesis in Natural Product Synthesis: Strategies, Substrates and Catalysts*; Cossy, J., Arseniyadis, S., Meyer, C., Eds.; Wiley–VCH Verlag: Weinheim, 2010; pp 87–127. e) Tori, M.; Mizutani, R. *Molecules* **2010**, *15*, 4242–4260. f) Fujiwara, K. *Top. Heterocycl. Chem.* **2006**, *5*, 97–148. g) Snyder, N. L.; Haines, H. M.; Peczu, M. W. *Tetrahedron* **2006**, *62*, 9301–9320. h) Yet, L. *Chem. Rev.* **2000**, *100*, 2963–3007. i) Hoberg, J. O. *Tetrahedron* **1998**, *54*, 12631–12670. j) Murai, A. *Stud. Nat. Prod. Chem.* **1996**, *19*, 411–461. k) Elliott, M. C. *Contemp. Org. Synth.* **1994**, *1*, 457–474. (l) Roxburgh, C. J. *Tetrahedron* **1993**, *49*, 10749–10784.
5. a) Irie, T.; Suzuki, M.; Masamune, T. *Tetrahedron Lett.* **1965**, *6*, 1091–1099. b) Irie, T.; Suzuki, M.; Masamune, T. *Tetrahedron* **1968**, *24*, 4193–4205.

6. a) Cameron, A. F.; Cheung, K. K.; Ferguson, G.; Robertson, J. M. *Chem. Commun.* **1965**, 24, 638. b) Cameron, A. F.; Cheung, K. K.; Ferguson, G.; Monteath Robertson, J. *J. Chem. Soc. B* **1969**, 12, 559–564.
7. Kaul, P. N.; Kulkarni, S. K.; Kurosawa, E. *J. Pharm. Pharmacol.* **1978**, 30, 589–590.
8. Kladi, M.; Vagias, C.; Stavri, M.; Rahman, M. M.; Gibbons, S.; Roussis, V. *Phytochem. Lett.* **2008**, 1, 31–36.
9. a) Murai, A.; Murase, H.; Matsue, H.; Masamune, T. *Tetrahedron Lett.* **1977**, 18, 2507–2510. b) Masamune, T.; Matsue, H. *Chem. Lett.* **1975**, 895–898. c) Masamune, T.; Matsue, H.; Murase, H. *Bull. Chem. Soc. Jpn.* **1979**, 52, 127–134. d) Masamune, T.; Murase, H.; Matsue, H.; Murai, A. *Bull. Chem. Soc. Jpn.* **1979**, 52, 135–141.
10. Shapiro, R. H.; Heath, M. J. *J. Am. Chem. Soc.* **1967**, 89, 5734–5735.
11. Paquette, L. A.; Begland, R. W.; Storm, P. C. *J. Am. Chem. Soc.* **1968**, 90, 6148–6153.
12. Corey, E. J.; Chaykovsky, M. *J. Am. Chem. Soc.* **1965**, 87, 1353–1364.
13. Tsushima, K.; Murai, A. *Tetrahedron Lett.* **1992**, 33, 4345–4348.
14. a) Tsushima, K.; Araki, K.; Murai, A. *Chem. Lett.* **1989**, 1313–1316. b) Tsushima, K.; Murai, A. *Chem. Lett.* **1990**, 761–764.
15. Mori, K.; Takigawa, T.; Matsuo, T. *Tetrahedron* **1979**, 35, 933–940.
16. Murai, A.; Ono, M.; Masamune, T. *J. Chem. Soc. Chem. Commun.* **1977**, 573–574.
17. a) Mancuso, A. J.; Huang, S.-L.; Swern, D. *J. Org. Chem.* **1978**, 43, 2480–2482. b) Mancuso, A. J.; Swern, D. *Synthesis* **1981**, 165–185.
18. Soupe, J.; Namy, J. L.; Kagan, H. B. *Tetrahedron Lett.* **1982**, 23, 3497–3500.
19. Bratz, M.; Bullock, W. H.; Overman, L. E.; Takemoto, T. *J. Am. Chem. Soc.* **1995**, 117, 5958–5966.
20. Blumenkopf, T. A.; Bratz, M.; Castañeda, A.; Look, G. C.; Overman, L. E.; Rodriguez, D.; Thompson, A. S. *J. Am. Chem. Soc.* **1990**, 112, 4386–4399.

21. Brown, H. C.; Jadhav, P. K.; Bhat, K. S. *J. Am. Chem. Soc.* **1988**, *110*, 1535–1538.
22. Miyaura, N.; Suzuki, A. *Chem. Rev.* **1995**, *95*, 2457–2483.
23. Ito, Y.; Hirao, T.; Saegusa, T. *J. Org. Chem.* **1978**, *43*, 1011–1013.
24. a) Mujica, M. T.; Afonso, M. M.; Galindo, A.; Palenzuela, J. A. *Synlett* **1996**, 983–984. b) Mujica, M. T.; Afonso, M. M.; Galindo, A.; Palenzuela, J. A. *J. Org. Chem.* **1998**, *63*, 9728–9738.
25. Ortega, N.; Martín, V. S.; Martín, T. *J. Org. Chem.* **2010**, *75*, 6660–6672.
26. Burton, J. W.; Clark, J. S.; Derrer, S.; Stork, T. C.; Bendall, J. G.; Holmes, A. *B. J. Am. Chem. Soc.* **1997**, *119*, 7483–7498.
27. Inanaga, J.; Hirata, K.; Saeki, H.; Katsuki, T.; Yamaguchi, M. *Bull. Chem. Soc. of Jpn.* **1979**, *52*, 1989–1993.
28. a) Mori, K.; Watanabe, H. *Tetrahedron Lett.* **1984**, *52*, 6025–6026. b) Barth, M.; Bellamy, F. D.; Renaut, P.; Samreth, S.; Schuber, F. *Tetrahedron* **1990**, *46*, 6731–6740. c) Meyers, A. I.; Lawson, J. P.; Walker, D. G.; Linderman, R. J. *J. Org. Chem.* **1986**, *51*, 5111–5123.
29. Collum, D. B.; McDonald III, J. H.; Still, W. C. *J. Am. Chem. Soc.* **1980**, *102*, 2118–2120.
30. a) Petasis, N. A.; Bzowej, E. I. *J. Am. Chem. Soc.* **1990**, *112*, 6392–6394. b) Petasis, N. A.; Lu, S.-P.; Bzowej, E. I.; Fu, D.-K.; Staszewski, J. P.; Akritopoulou-Zanze, I.; Patane, M. A.; Hu, Y.-H. *Pure Appl. Chem.* **1996**, *68*, 667–670.
31. Taomao, K.; Nakagawa, Y.; Arai, H.; Higuchi, N.; Ito, Y. *J. Am. Chem. Soc.* **1988**, *110*, 3712–3714.
32. Tamao, K.; Nakagawa, Y.; Ito, Y. *Organometallics* **1993**, *12*, 2297–2308.
33. Crimmins, M. T.; Choy, A. L. *J. Am. Chem. Soc.* **1999**, *121*, 5653–5660.
34. a) Ley, S. V.; Norman, J.; Griffith, W. P.; Marsden, S. P. *Synthesis*. **1994**, 639–666. b) Griffith, W. P.; Ley, S. V.; Whitcombe, G. P.; White, A. D. *J. Chem. Soc. Chem. Commun.* **1987**, 1625–1627.

35. Krüger, J.; Hoffmann, R. W. *J. Am. Chem. Soc.* **1997**, *119*, 7499–7504.
36. Crimmins, M. T.; Emmitte, K. A. *Org. Lett.* **1999**, *1*, 2029–2032.
37. Crimmins, M. T.; Choy, A. L. *J. Org. Chem.* **1997**, *62*, 7548–7549.
38. Asami, M.; Kimura, R. *Chem. Lett.* **1985**, 1211–1222.
39. Schwab, P.; Grubbs, R. H.; Ziller, J. W. *J. Am. Chem. Soc.* **1996**, *118*, 100–110.
40. Baek, S.; Jo, H.; Kim, H.; Kim, H.; Kim, S.; Kim, D. *Org. Lett.* **2005**, *7*, 75–77.
41. Kim, H.; Choi, W. J.; Jung, J.; Kim, S.; Kim, D. *J. Am. Chem. Soc.* **2003**, *125*, 10238–10240.
42. Holton, R. A.; Zoeller, J. R. *J. Am. Chem. Soc.* **1985**, *107* 7, 2124–2131.
43. Su, D.-W.; Wang, Y.-C.; Yan, T.-H. *Tetrahedron Lett.* **1999**, *40*, 4197–4198.
44. Burke, S. D.; Deaton, D. N.; Olsen, R. J.; Armistead, D. M.; Blough, B. E. *Tetrahedron Lett.* **1987**, *28*, 3905–3906.
45. Lanier, M. L.; Park, H.; Mukherjee, P.; Timmerman, J. C.; Ribero, A. A.; Widenhoefer, R. A.; Hong, J. *Chem. Eur. J.* **2017**, *23*, 7180–7184.
46. Fujiwara, K.; Yoshimoto, S.; Takizawa, A.; Souma, S. I.; Mishima, H.; Murai, A.; Kawai, H.; Suzuki, T. *Tetrahedron Lett.* **2005**, *46*, 6819–6822.
47. Fujiwara, K.; Souma, S.; Mishima, H.; Murai, A. *Synlett* **2002**, 1493–1495.
48. Kotsuki, H.; Kadota, I.; Ochi, M. *Tetrahedron Lett.* **1989**, *30*, 1281–1284.
49. Scholl, M.; Ding, S.; Lee, C. W.; Grubbs, R. H. *Org. Lett.* **1999**, *1*, 953–956.
50. Hubschwerlen, C.; Specklin, J.-L.; Higelin, J. *Org. Synth.* **1995**, *72*, 1.
51. Stereoselectivity was dictated by an endo-Cram approach of the diene to the aldehyde, see: a) Danishefsky, S.; Kobayashi, S.; Kerwin Jr, J. F. *J. Org. Chem.* **1982**, *47*, 1981–1983. b) Danishefsky, S. J.; Pearson, W. H.; Harvey, D. F.; Maring, C. J.; Springer, J. P. *J. Am. Chem. Soc.* **1985**, *107*, 1256–1268.
52. Adsool, V. a; Pansare, S. V. *Org. Biomol. Chem.* **2008**, *6*, 2011–2015.
53. a) Pansare, S.; Adsool, V. A. *Org. Lett.* **2006**, *8*, 5897–5899. b) Pansare, S. V.; Ravi, R. G.; Jain, R. P. *J. Org. Chem.* **1998**, *63*, 4120–4124. c) Pansare, S. V.; Shinkre, B. A.; Bhattacharyya, A. *Tetrahedron* **2002**, *58*, 8985–8991.
54. Crimmins, M. T.; Tabet, E. A. *J. Am. Chem. Soc.* **2000**, *122*, 5473–5476.

55. Lockwood, R. F.; Nicholas, K. M. *Tetrahedron Lett.* **1977**, *18*, 4163–4166.
56. a) Ortega, N.; Martín, T.; Martín, V. S. *Eur. J. Org. Chem.* **2009**, 554–563. b) Ortega, N.; Martín, T.; Martín, V. S. *Org. Lett.* **2006**, *8*, 871–873.
57. a) Jacobsen, E. N.; Markó, I.; Mungall, W. S.; Schröder, G.; Sharpless, K. B. *J. Am. Chem. Soc.* **1988**, *110*, 1968–1970. b) Kolb, H. C.; VanNieuwenhze, M. S.; Sharpless, K. B. *Chem. Rev.* **1994**, *94*, 2483–2547.
58. a) Burke, S. D.; Voight, E. A. *Org. Lett.* **2001**, *3*, 237–240. b) Grieco, P. A.; Gilman, S.; Nishizawa, M. *J. Org. Chem.* **1976**, *41*, 1485–1486. c) Sharpless, K. B.; Young, M. W. *J. Org. Chem.* **1974**, *40*, 947–949.
59. a) Hoffmann, R. W.; Münster, I. *Tetrahedron Lett.* **1995**, *36*, 1431–1434. b) Hoffmann, R. W.; Münster, I. *Liebigs Ann. Chem.* **1997**, 1143–1150.
60. Saito, S.; Ishikawa, T.; Kuroda, A.; Koga, K.; Moriwake, T. *Tetrahedron* **1992**, *48*, 4067–4086.
61. Dess, D. B.; Martin, J. C. *J. Org. Chem.* **1983**, *48*, 4155–4156.
62. Corey, E. J.; Shimoji, K. *J. Am. Chem. Soc.* **1983**, *105*, 1662–1664.
63. Keinan, E.; Sinha, S. C.; Singh, S. P. *Tetrahedron* **1991**, *47*, 4631–4638.
64. Evans, D. A.; Rieger, D. L.; Bilodeau, M. T.; Urpi, F. *J. Am. Chem. Soc.* **1991**, *113*, 1047–1049.
65. Biannic, B.; Aponick, A. *Euro. J. Org. Chem.* **2011**, *2011*, 6605–6617.
66. Suzuki, T.; Matsumura, R.; Oku, K.-I.; Taguchi, K.; Hagiwara, H.; T., H.; Ando, M. *Tetrahedron Lett.* **2001**, *42*, 65–67.
67. Yamaguchi, M.; Hirao, I. *Tetrahedron Lett.* **1983**, *24*, 4, 391–394.
68. a) Tester, R. W.; West, F. G. *Tetrahedron Lett.* **1998**, *39*, 4631–4634. For additional examples on formation of oxygen bridged medium-sized rings from acetal precursors via Stevens [1,2]-shift, see: b) Stewart, C.; McDonald, R.; West, F. G. *Org. Lett.* **2011**, *13*, 720–723. c) Murphy, G. K.; Marmsäter, F. P.; West, F. G. *Can. J. Chem.* **2006**, *84*, 1470–1486.
69. For precedents on Stevens [1,2]-shift using five-membered mixed monothioacetal (1,3-oxathiolane) as precursors, see: a) Qu, J. P.; Xu, Z. H.;

- Zhou, J.; Cao, C. L.; Sun, X. L.; Dai, L. X.; Tang, Y. *Adv. Synth. Catal.* **2009**, *351*, 308–312. b) Stepanov, A. V.; Molchanov, A. P.; Magull, J.; Vidović, D.; Starova, G. L.; Kopf, J.; Kostikov, R. R. *Tetrahedron* **2006**, *62*, 3610–3618. c) Zhu, S.; Xing, C.; Zhu, S. *Tetrahedron* **2006**, *62*, 829–832. d) Ioannou, M.; Porter, M. J.; Saez, F. *Tetrahedron* **2005**, *61*, 43–50. e) Ioannou, M.; Porter, M. J.; Saez, F. *Chem. Commun.* **2002**, *18*, 346–347. An addition example on intramolecular sulfonium ylide rearrangement: f) Kim, G.; Kang, S.; Soon, N. K. *Tetrahedron Lett.* **1993**, *34*, 7627–7628.
70. Cao, L. *Seven- and Eight-Membered Ether Formation via Sulfonium Ylide Rearrangement Processes and Application in an Approach to (+)-Laurencin*. PhD Thesis, University of Alberta, Alberta, 2010.
71. a) For evidence on retention of configuration for Stevens [1,2]-shift of ammonium ylide, see: Ollis, W. D.; Rey, M.; Sutherland, I. O. *J. Chem. Soc., Perkin Trans. 1*, **1983**, 1009–1027. For evidence on retention of configuration for Stevens [1,2]-shift of oxonium ylide, see: (b) Marmsäter, F. P.; Murphy, G. K.; West, F. G. *J. Am. Chem. Soc.* **2003**, *125*, 14724–14725.
72. For review on Stevens [1,2]-shifts with mechanistic discussion, see: a) Vanecko, J. A.; Wan, H.; West, F. G. *Tetrahedron* **2006**, *62*, 1043–1062. b) Markó, I. E. In *Comprehensive Organic Synthesis*; Trost, B. M., Fleming, I., Eds.; Pergamon: Oxford, 1991; Vol. 3, pp 913–974.
73. a) For evidence on stepwise radical pathway for Stevens [1,2]-shift, see: 35a). b) Eberlein, T. H.; West, F. G.; Tester, R. W. *J. Org. Chem.* **1992**, *57*, 3479–3482.
74. Yamamoto, Y.; Yatagai, H.; Saito, Y.; Maruyama, K. *J. Org. Chem.* **1984**, *49*, 1096–1104.
75. Brown, H. C.; Sinclair, J. A. *J. Organomet. Chem.* **1977**, *131*, 163–169.
76. a) Dale, J. A.; Dull, D. L.; Mosher, H. S. *J. Org. Chem.* **1969**, *34*, 2543–2549. b) Dale, J. A.; Mosher, H. S. *J. Am. Chem. Soc.* **1973**, *95*, 512–519. c) Hoye, T. R.; Jeffrey, C. S.; Shao, F. *Nat. Protoc.* **2007**, *2*, 2451–2458.

77. a) Fürstner, A.; Langemann, K. *J. Am. Chem. Soc.* **1997**, *119*, 9130–9136. b) Ghosh, A. K.; Cappiello, J.; Shin, D. *Tetrahedron Lett.* **1998**, *39*, 4651–4654.
78. Kingsbury, J. S.; Harrity, J. P. A.; Bonitatebus, P. J.; Hoveyda, A. H. *J. Am. Chem. Soc.* **1999**, *121*, 791–799.
79. a) Michrowska, A.; Bujok, R.; Harutyunyan, S.; Grela, K. *J. Am. Chem. Soc.* **2004**, *126*, 9318–9325. b) Grela, K.; Harutyunyan, S.; Michrowska, A. *Angew. Chem. Int. Ed.* **2002**, *41*, 4038–4040.
80. Preparation and application of Zhan-1B catalyst: Zhan, Z.-Y. J. U.S. Patent, **2007**, 20070043180.
81. a) Nishimura, O.; Kitada, C.; Fujino, M. *Chem. Pharm. Bull.* **1978**, *26*, 1576–1585. For an example of application in the peptide synthesis, see: b) Macmillan, D.; Anderson, D. W. *Org. Lett.* **2004**, *6*, 4659–4662.
82. Erhunmwunse, M. O.; Steel, P. G. *J. Org. Chem.* **2008**, *73*, 8675–8677. Ch 1
83. Karplus, M. *J. Am. Chem. Soc.* **1963**, *85*, 2870–2871.
84. Nahm, S.; Weinreb, S. M. *Tetrahedron Lett.* **1981**, *22*, 3815–3818.
85. Shimizu, T.; Osako, K.; Nakata, T. *Tetrahedron Lett.* **1997**, *38*, 2685–2688.
86. The α',β -elimination process has been noted in ref 33b–d. For a review with examples of α',β -elimination on sulfonium ylide, see: Padwa, A.; Hornbuckle, S. F. *Chem. Rev.* **1991**, *91*, 263–309.
87. Phipps, R. J.; Grimster, N. P.; Gaunt, M. J. *J. Am. Chem. Soc.* **2008**, *130*, 8172–8174.
88. Arnone, A.; Bravo, P.; Panzeri, W.; Viani, F.; Zanda, M. *Eur. J. Org. Chem.* **1999**, 117–127.
89. Curran, D. P.; Zhang, Q. *Adv. Synth. Catal.* **2003**, *345*, 329–332.
90. a) Chugaev, L. *Ber. Dtsch. Chem. Ges.* **1899**, *32*, 3332–3335. For selected recent examples of xanthate formation/Chugaev elimination used in organic synthesis, see: b) Lee, K.; Boger, D. L. *J. Am. Chem. Soc.* **2014**, *136*, 3312–3317. c) Nicolaou, K. C.; Ortiz, A.; Zhang, H.; Guella, G. *J. Am. Chem.*

- Soc.* **2010**, *132*, 7153–7176. d) Padwa, A.; Zhang, H. *J. Org. Chem.* **2007**, *72*, 2570–2582.
91. Nonhebel, D. C. *Chem. Soc. Rev.* **1993**, *22*, 347–359.
92. Newcomb, M.; Chestney, D. L. *J. Am. Chem. Soc.* **1994**, *116*, 9753.
93. Crimmins, M. T.; Tabet, E. A. *J. Am. Chem. Soc.* **2000**, *122*, 5473–5476.
94. Snyder, S. A.; Brucks, A. P.; Treitler, D. S.; Moga, I. *J. Am. Chem. Soc.* **2012**, *134*, 17714–17721.

Chapter 3

1. For a recent total synthesis on cephalotaxine, see: Ma, X. Y.; An, X. T.; Zhao, X. H.; Du, J. Y.; Deng, Y. H.; Zhang, X. Z.; Fan, C. A. *Org. Lett.* **2017**, *19*, 2965–2968 and references cited therein.
2. For total syntheses of otonecine, see: a) Vedejs, E.; Galante, R. J.; Goekjian, P. *J. Am. Chem. Soc.* **1998**, *120*, 3613–3622. b) Niwa, H.; Sakata, T.; Yamada, K. *Bull. Chem. Soc. Jpn.* **1994**, *67*, 2345–2347. c) Niwa, H.; Uosaki, Y.; Yamada, K. *Tetrahedron Lett.* **1983**, *24*, 5731–5732.
3. For a total synthesis on lycoposerramine T, see: Zaimoku, H.; Nishide, H.; Nishibata, A.; Goto, N.; Taniguchi, T.; Ishibashi, H. *Org. Lett.* **2013**, *15*, 2140–2143 and references cited therein.
4. Lin, W.-H.; Ye, Y.; Xu, R.-S. *J. Nat. Prod.* **1992**, *55*, 571–576.
5. For an example of total synthesis on stemonine, see: Williams, D. R.; Shamim, K.; Reddy, J. P.; Amato, G. S.; Shaw, S. M. *Org. Lett.* **2003**, *5*, 3361–3364 and references cited therein.
6. For selected reviews on *Stemona* alkaloids, see: a) Pilli, R. A.; Rosso, G. B.; de Oliveira, M. C. F. *Nat. Prod. Rep.* **2010**, *27*, 1908–1937. b) Pilli, R. A.; de Oliveira, M. C. F. *Nat. Prod. Rep.* **2000**, *17*, 117–127. c) Alibés, R.; Figueredo, M. *Eur. J. Org. Chem.* **2009**, 2421–2435. d) Greger, H. *Planta Med.* **2006**, *72*, 99–113.

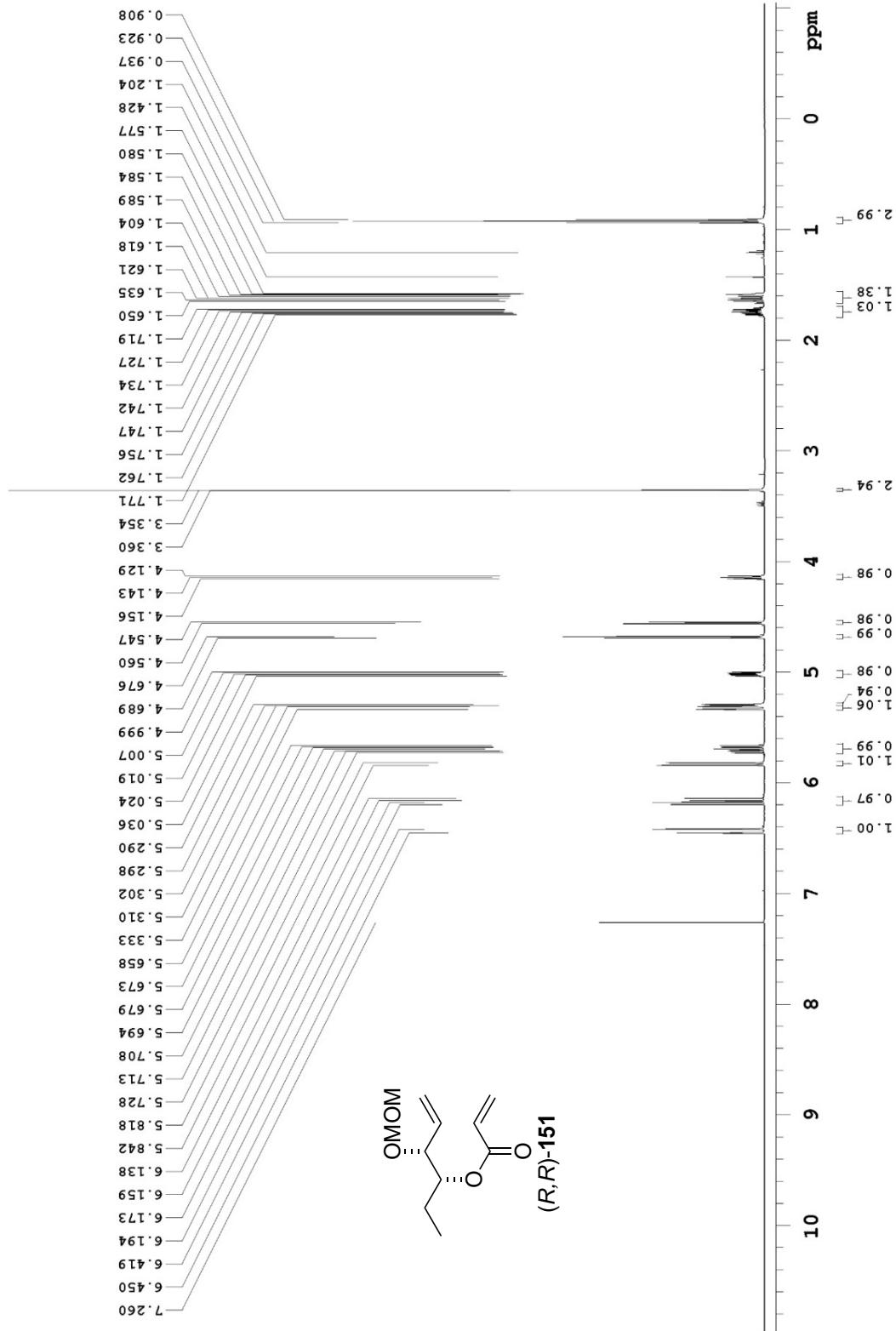
7. Williams, D. R.; Reddy, J. P.; Amato, G. S. *Tetrahedron Lett.* **1994**, *35*, 6417–6420.
8. For a review, see: Gololobov, Y. G.; Kasukhin, L. F. *Tetrahedron* **1992**, *48*, 1353–1406.
9. a) Baldwin, J. E.; Thomas, R. C.; Kruse, L. I.; Silberman, L. *J. Org. Chem.* **1977**, *42*, 3846–3852. b) Baldwin, J. E. *J. Chem. Soc. Chem. Commun.* **1976**, 734–736.
10. Gao, P.; Tong, Z.; Hu, H.; Xu, P. F.; Liu, W.; Sun, C.; Zhai, H. *Synlett* **2009**, 2188–2190.
11. Bogliotti, N.; Dalko, P. I.; Cossy, J. *Synlett* **2006**, 2664–2666.
12. Kohno, Y.; Narasaka, K. *Bull. Chem. Soc. Jpn.* **1996**, *69*, 2063–2070.
13. Nakayama, Y.; Maeda, Y.; Hama, N.; Sato, T.; Chida, N. *Synthesis* **2016**, *48*, 1647–1654.
14. Bates, R. W.; Sridhar, S. *Synlett* **2009**, 1979–1981.
15. Bates, R. W.; Sridhar, S. *J. Org. Chem.* **2008**, *73*, 8104–8105 and references cited therein.
16. Wang, Y.; Zhu, L.; Zhang, Y.; Hong, R. *Angew. Chem. Int. Ed.* **2011**, *50*, 2787–2790.
17. Mi, X.; Wang, Y.; Zhu, L.; Wang, R.; Hong, R. *Synthesis* **2012**, *44*, 3432–3440.
18. Honda, T.; Matsukawa, T.; Takahashi, K. *Org. Biomol. Chem.* **2011**, *9*, 673–675.
19. a) Honda, T. *Chem. Pharm. Bull.* **2012**, *60*, 687–705. b) Szostak, M.; Fazakerley, N. J.; Parmar, D.; Procter, D. J. *Chem. Rev.* **2014**, *114*, 5959–6039. c) Nicolaou, K. C.; Ellery, S. P.; Chen, J. S. *Angew. Chem. Int. Ed.* **2009**, *48*, 7140–7165.
20. a) Jacobi, P. A.; Lee, K. *J. Am. Chem. Soc.* **1997**, *119*, 3409–3410. b) Jacobi, P. A.; Lee, K. *J. Am. Chem. Soc.* **2000**, *122*, 4295–4303.
21. For examples of previous development, see: a) Jacobi, P. A.; Blum, C. A.; DeSimone, R. W.; Udodong, U. E. S. *J. Am. Chem. Soc.* **1991**, *113*, 5384–5392.

- b) Jacobi, P. A.; Kacxmerek, C. S. R.; Udodong, U. E. *Tetrahedron* **1987**, *43*, 5475–5488 and references cited therein.
22. a) Kinoshita, A.; Mori, M. *Heterocycles* **1997**, *46*, 287–299. b) Kinoshita, A.; Mori, M. *J. Org. Chem.* **1996**, *61*, 8356–8357.
23. a) Mori, M. *Adv. Synth. Catal.* **2007**, *349*, 121–135. b) Mori, M. *Top. Organomet. Chem.* **1998**, *1*, 133–154.
24. Sibi, M. P.; Subramanian, T. *Synlett* **2004**, 1211–1214.
25. Torssell, S.; Wanngren, E.; Somfai, P. *J. Org. Chem.* **2007**, *72*, 4246–4249.
26. Olivo, H. F.; Tovar-Miranda, R.; Barragán, E. *J. Org. Chem.* **2006**, *71*, 3287–3290.
27. For selected review, see: a) Evans, P. A.; Holmes, A. B. *Tetrahedron* **1991**, *47*, 9131–9166. b) Yet, L. *Chem. Rev.* **2000**, *100*, 2963–3007. c) Nubbemeyer, U. *Top. Curr. Chem.* **2001**, *216*, 125–196. For selected recent examples, see: d) Baud, L. G.; Manning, M. A.; Arkless, H. L.; Stephens, T. C.; Unsworth, W. P. *Chem. Eur. J.* **2017**, *23*, 2225–2230. e) Shaw, M. H.; Croft, R. A.; Whittingham, W. G.; Bower, J. F. *J. Am. Chem. Soc.* **2015**, *137*, 8054–8057. f) Nakamura, I.; Sato, Y.; Takeda, K.; Terada, M. *Chem. Eur. J.* **2014**, *20*, 10214–10219.
28. a) Deiters, A.; Martin, S. F. *Chem. Rev.* **2004**, *104*, 2199–2238. b) Sattely, E. S.; Cortex, G. A.; Moebius, D. C.; Schrock, R. R.; Hoveyda, A. H. *J. Am. Chem. Soc.* **2005**, *127*, 8526–8533.
29. Cao, L. *Seven- and Eight-Membered Ether Formation via Sulfonium Ylide Rearrangement Processes and Application in an Approach to (+)-Laurencin. PhD Thesis, University of Alberta, Alberta, 2010.*
30. Lin, R.; Cao, L.; West, F. G. *Org. Lett.* **2017**, *19*, 552–555.
31. a) Kametani, T.; Honda, T. *J. Chem. Soc. Chem. Commun.* **1986**, 651–652. b) Kametani, T.; Yukawa, H.; Honda, T. *J. Chem. Soc. Perkin Trans. I* **1988**, 833–837. c) Kametani, T.; Yukawa, H.; Honda, T. *J. Chem. Soc. Chem. Commun.* **1988**, 685–687. d) Kametani, T.; Yukawa, H.; Honda, T. *J. Chem. Soc. Perkin Trans. I* **1990**, 571–577.

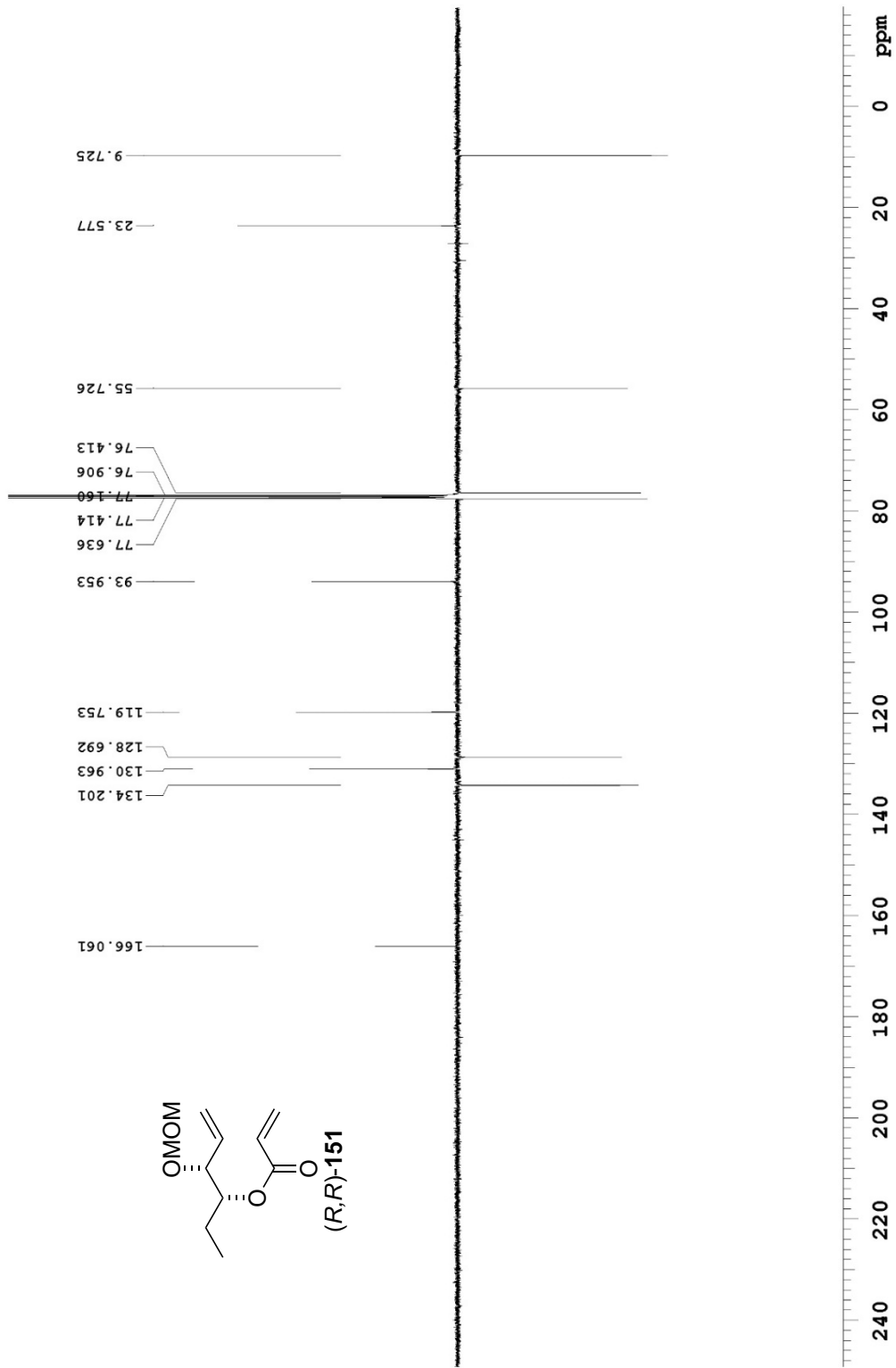
32. Iwasaki, T.; Kondo, K.; Nakatani, T.; Yoshioka, R. US 5495012 A, February 27, 1996.
33. Brooks, D. W.; Lu, L. D.-L.; Masamune, S. *Angew. Chem. Int. Ed. Engl.* **1979**, *18*, 72–74.
34. a) Regitz, M. *Angew. Chem. Int. Ed. Engl.* **1967**, *6*, 733–749. b) Regitz, M. *Synthesis*, **1972**, *7*, 351–373.
35. For a recent total synthesis of nakadomarin A, see: Boeckman, R. K.; Wang, H.; Rugg, K. W.; Genung, N. E.; Chen, K.; Ryder, T. R. *Org. Lett.* **2016**, *18*, 6136–6139 and references cited therein.
36. Yap, W. S.; Gan, C. Y.; Low, Y. Y.; Choo, Y. M.; Etoh, T.; Hayashi, M.; Komiyama, K.; Kam, T. S. *J. Nat. Prod.* **2011**, *74*, 1309–1312.
37. Kirillova, M. S.; Muratore, M. E.; Dorel, R.; Echavarren, A. M. *J. Am. Chem. Soc.* **2016**, *138*, 3671–3674.
38. Compound **80** could be synthesized *via* a similar strategy: a) Fujii, T.; Yoshifuji, S.; Ikeda, K. *Chem. Pharm. Bull.* **1966**, *1427*, 2841–2845. For the preparation of compound **81**, see: b) Barcelos, R. C.; Pastre, J. C.; Vendramini-Costa, D. B.; Caixeta, V.; Longato, G. B.; Monteiro, P. A.; de Carvalho, J. E.; Pilli, R. A. *ChemMedChem* **2014**, *9*, 2725–2743. c) Zou, Y.; Yan, C.; Zhang, H.; Xu, J.; Zhang, D.; Huang, Z.; Zhang, Y. *Eur. J. Med. Chem.* **2017**, *138*, 313–319. C)
39. Lee, S.; Bae, M.; In, J.; Kim, J. H.; Kim, S. *Org. Lett.* **2017**, *19*, 254–257.
40. Jiang, Y.-Y.; Wang, Q.-Q.; Liang, S.; Hu, L.-M.; Little, R. D.; Zeng, C.-C. *J. Org. Chem.* **2016**, *81*, 4713–4719.

Appendix I: Selected NMR Spectra (Chapter 2)

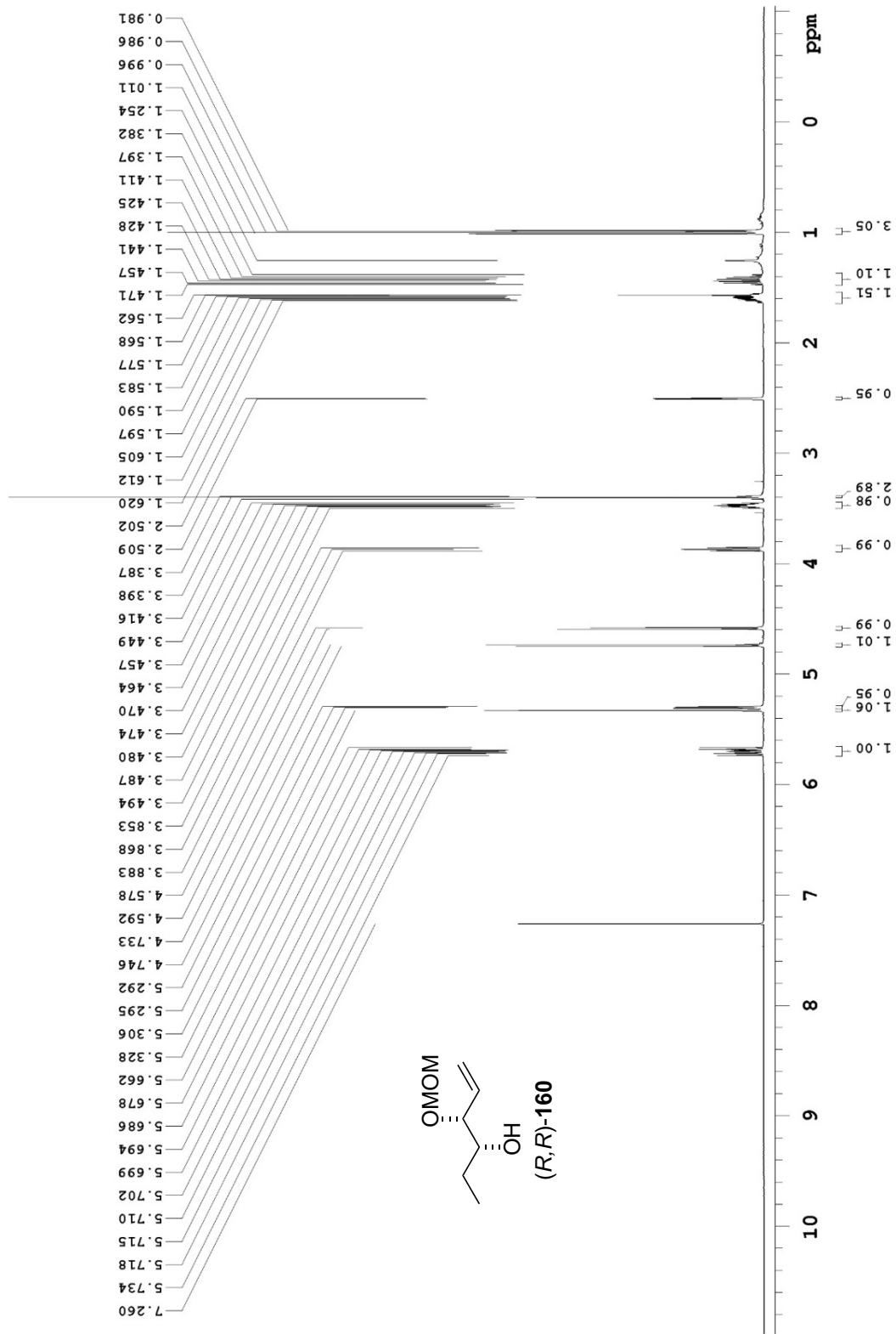
499.815 MHz H1 PRESAT in cdc13 (ref. to CDC13 @ 7.26 ppm), temp 27.7 C -> actual temp = 27.0 C, coldddual probe



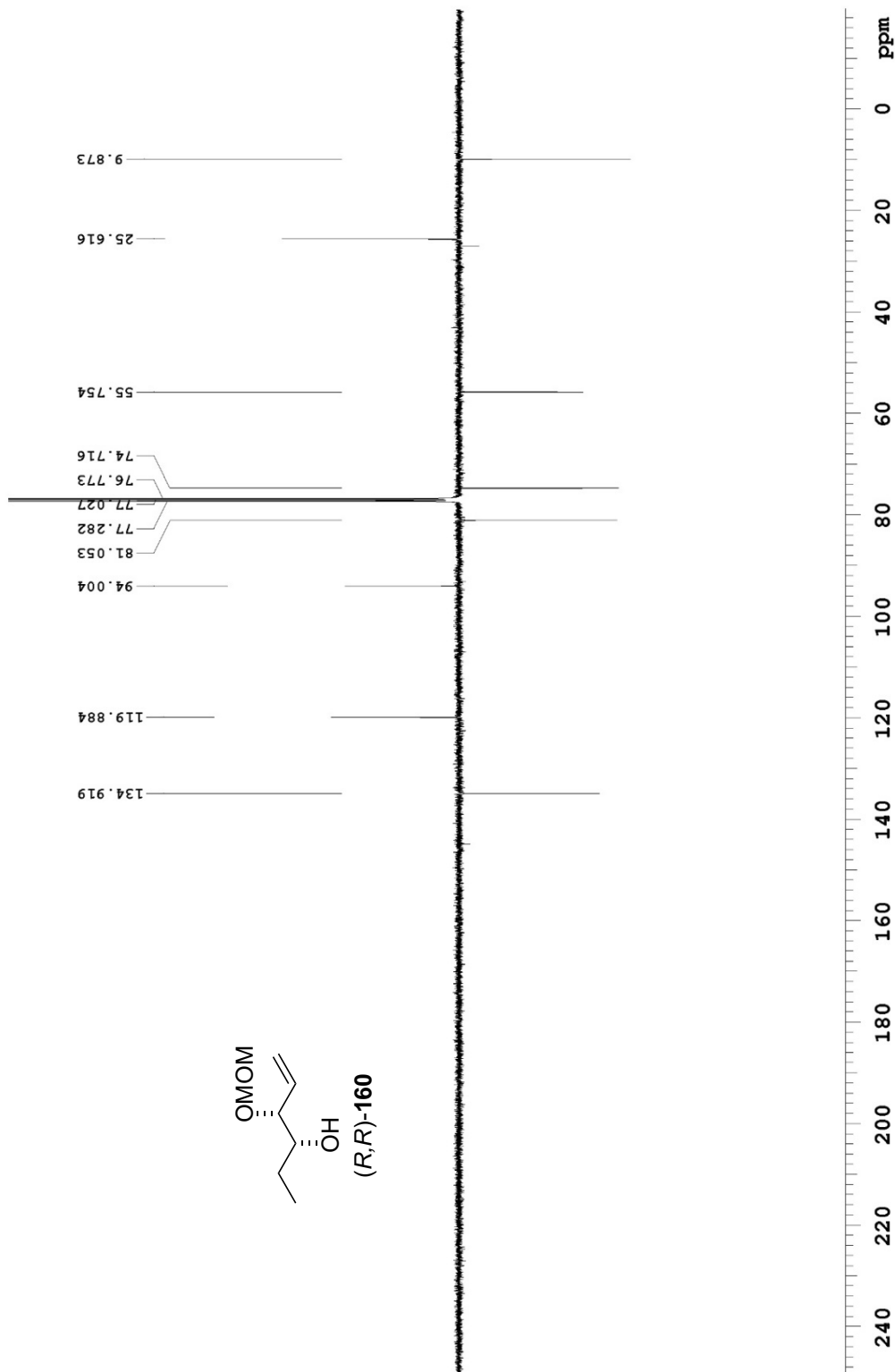
125.692 MHz C13[H1] APT_ad in cdcl3 (ref. to CDC13 @ 77.16 ppm), temp 27.7 C -> actual temp = 27.0 C, cold dual probe
 C & CH2 same, CH & CH3 opposite side of solvent signal



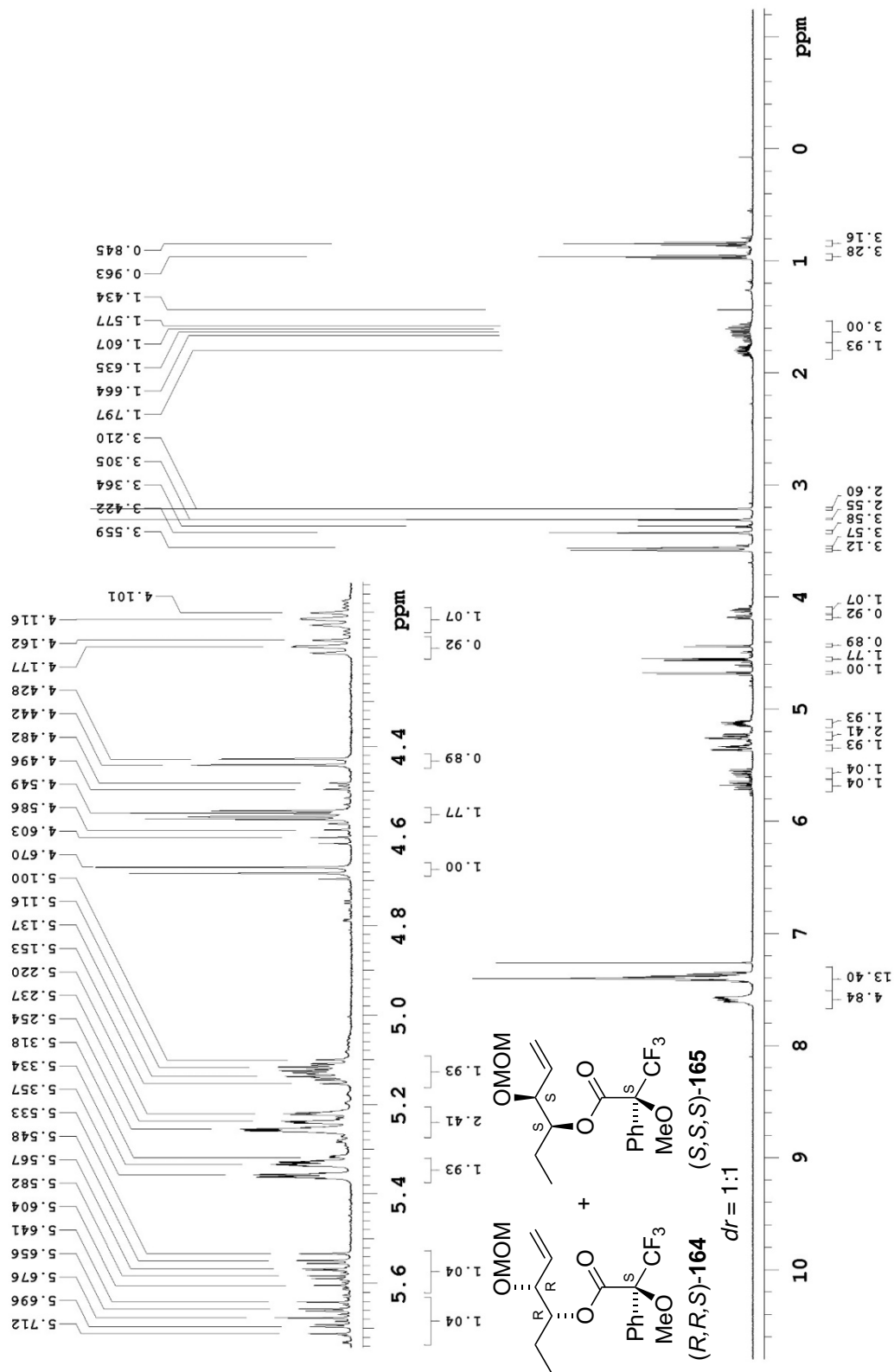
499.815 MHz ¹H PRESAT in cdcl3 (ref. to CDCl3 @ 7.26 ppm), temp 27.7 C -> actual temp = 27.0 C, colddual probe



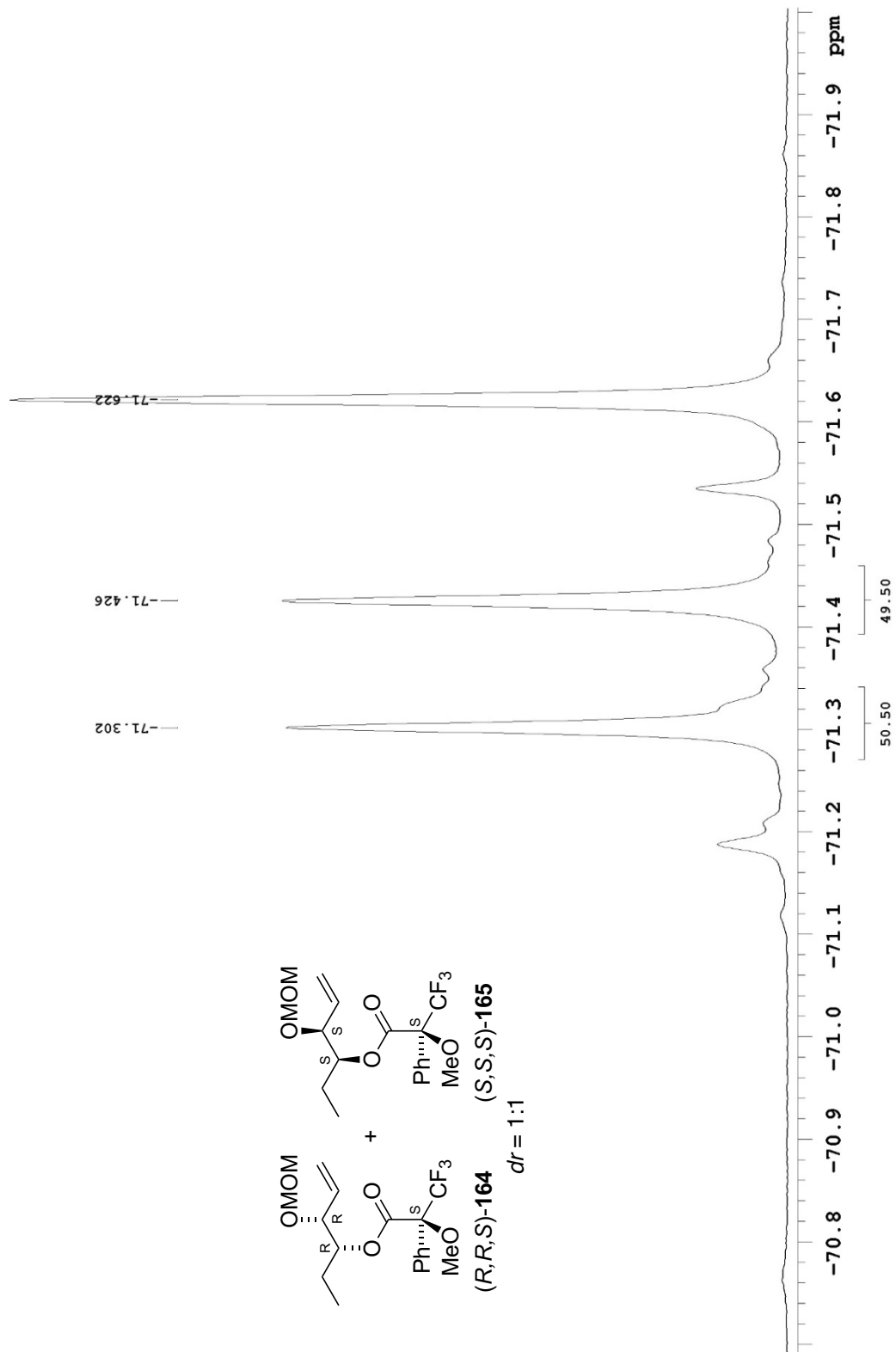
125.692 MHz C13[H1] APT_ad in cdcl3 (ref. to CDCl3 @ 77.16 ppm), temp 27.7 C -> actual temp = 27.0 C, coldddual probe
C & CH2 same, CH & CH3 opposite side of solvent signal



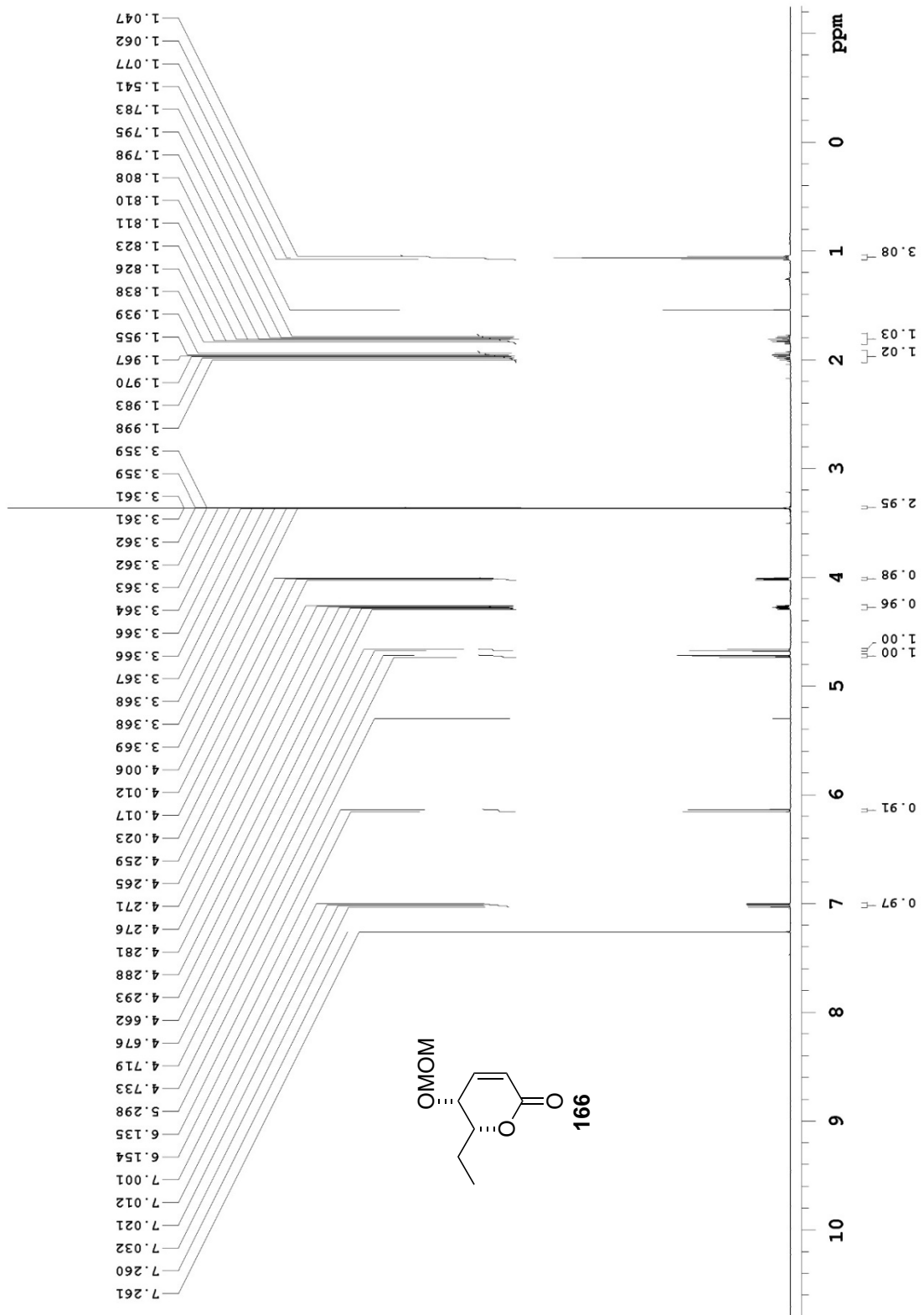
498.118 MHz ¹H ID in cdcl₃ (ref. to cdcl₃ @ 7.26 ppm), temp 26.4 C → actual temp = 27.0 C, autotxdb probe



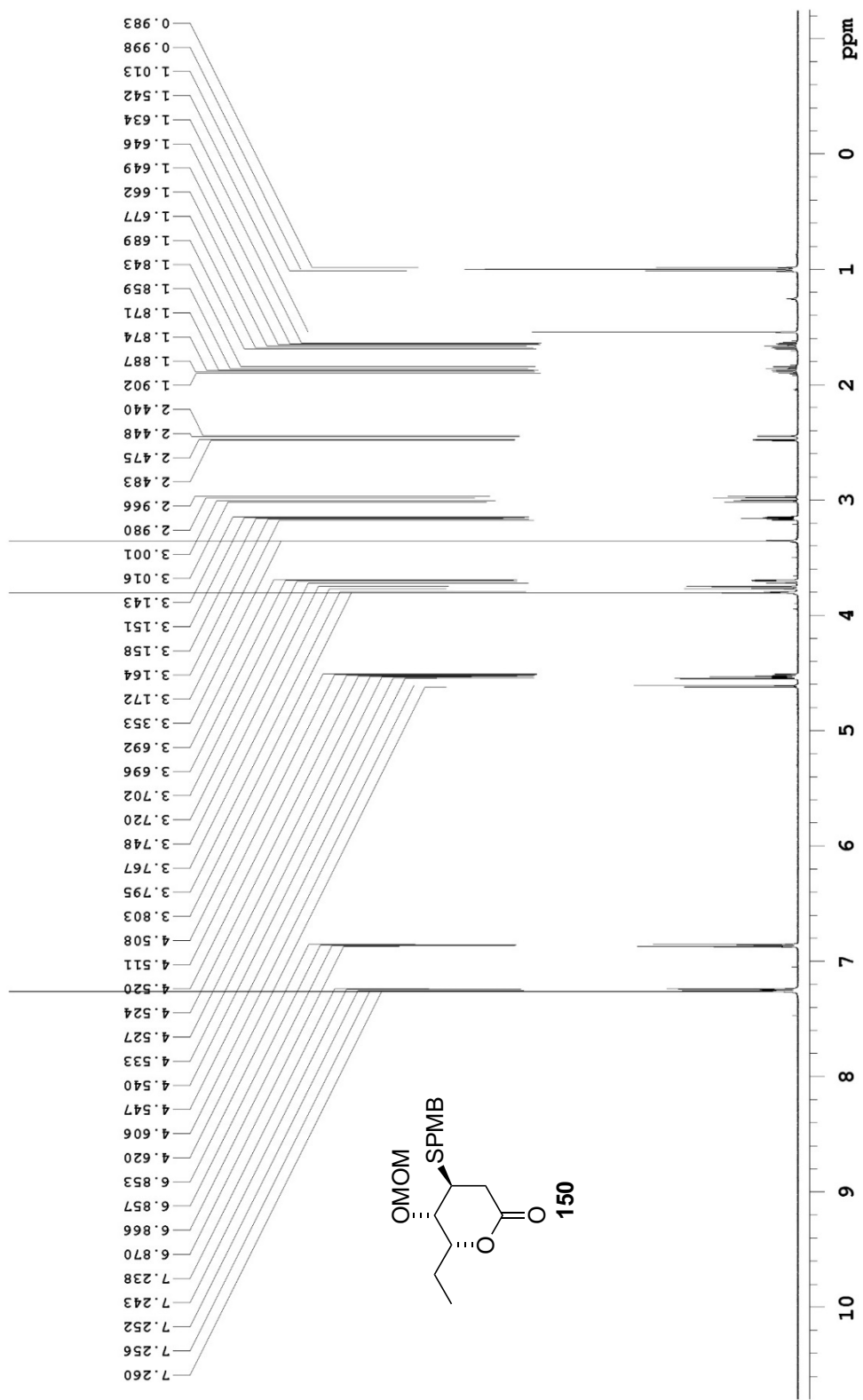
468.652 MHz F19 1D in cdcl3, temp 26.4 C -> actual temp = 27.0 C, autoxdbc probe



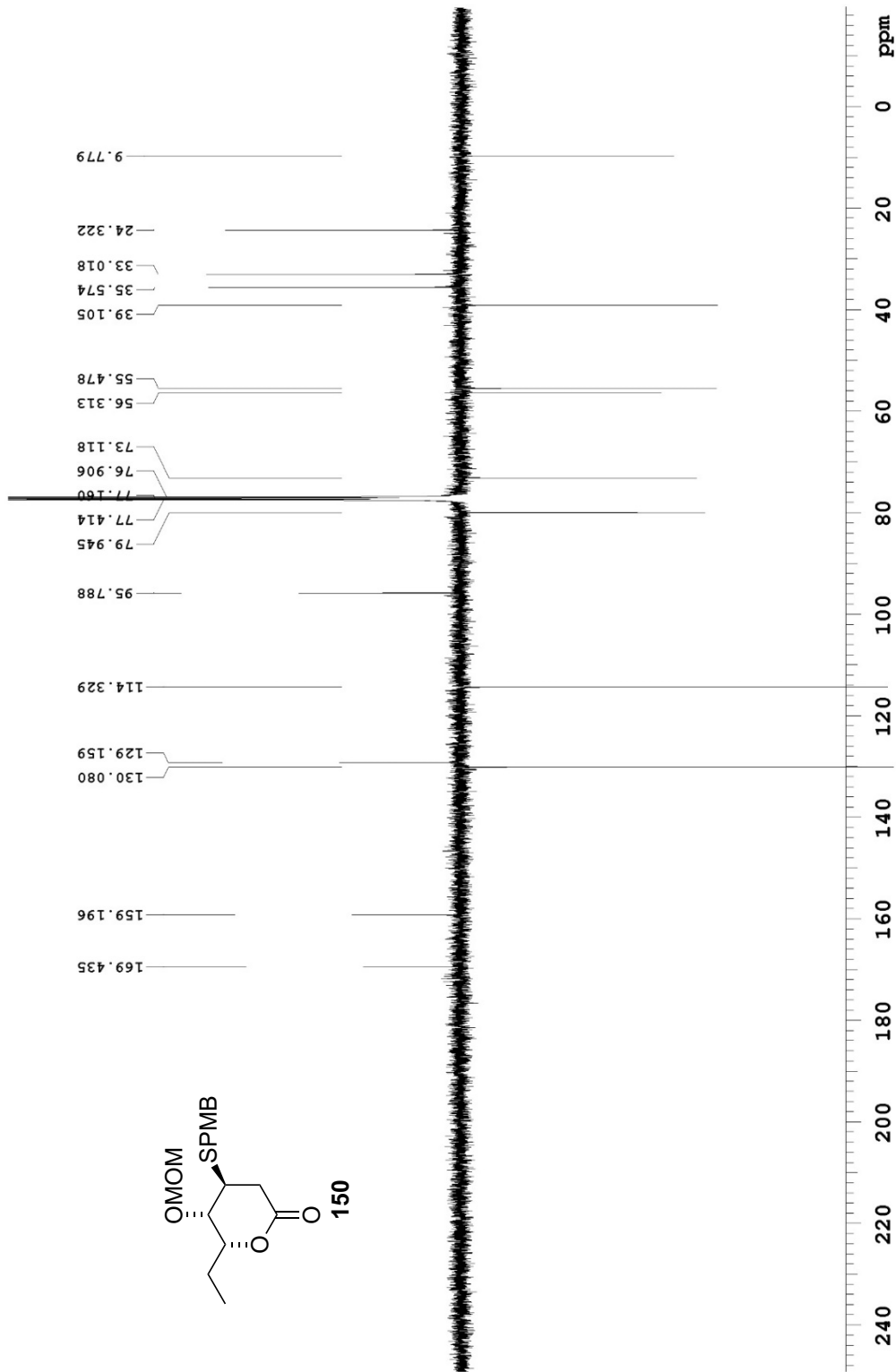
498.118 MHz H1 1D in cdcl3 (ref. to CDCl3 @ 7.26 ppm), temp 27.2 C -> actual temp = 27.0 C, autoxdb probe



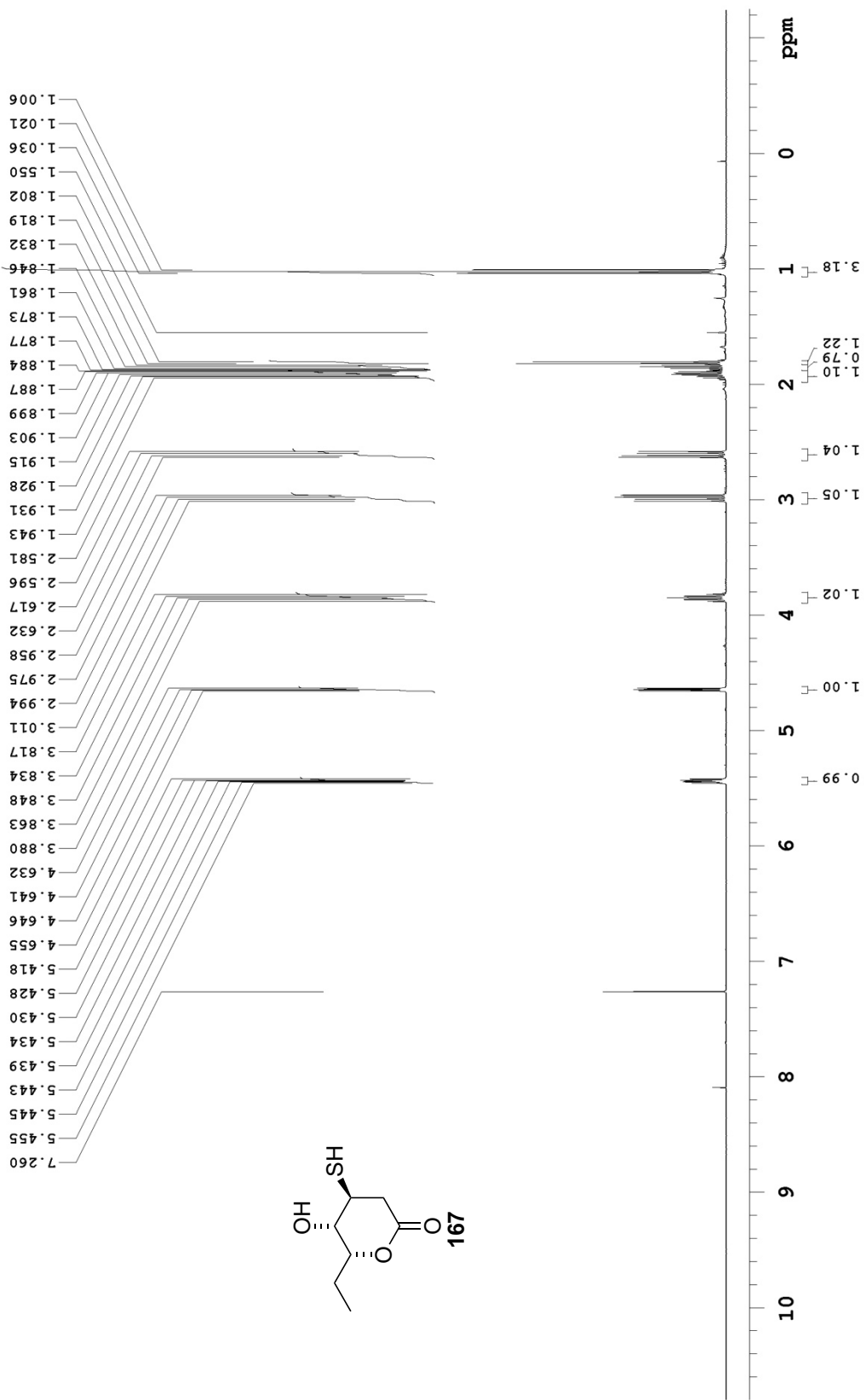
498.118 MHz H1 1D in cdcl3 (ref. to CDC13 @ 7.26 ppm), temp 26.4 C -> actual temp = 27.0 C, autoxdbc probe



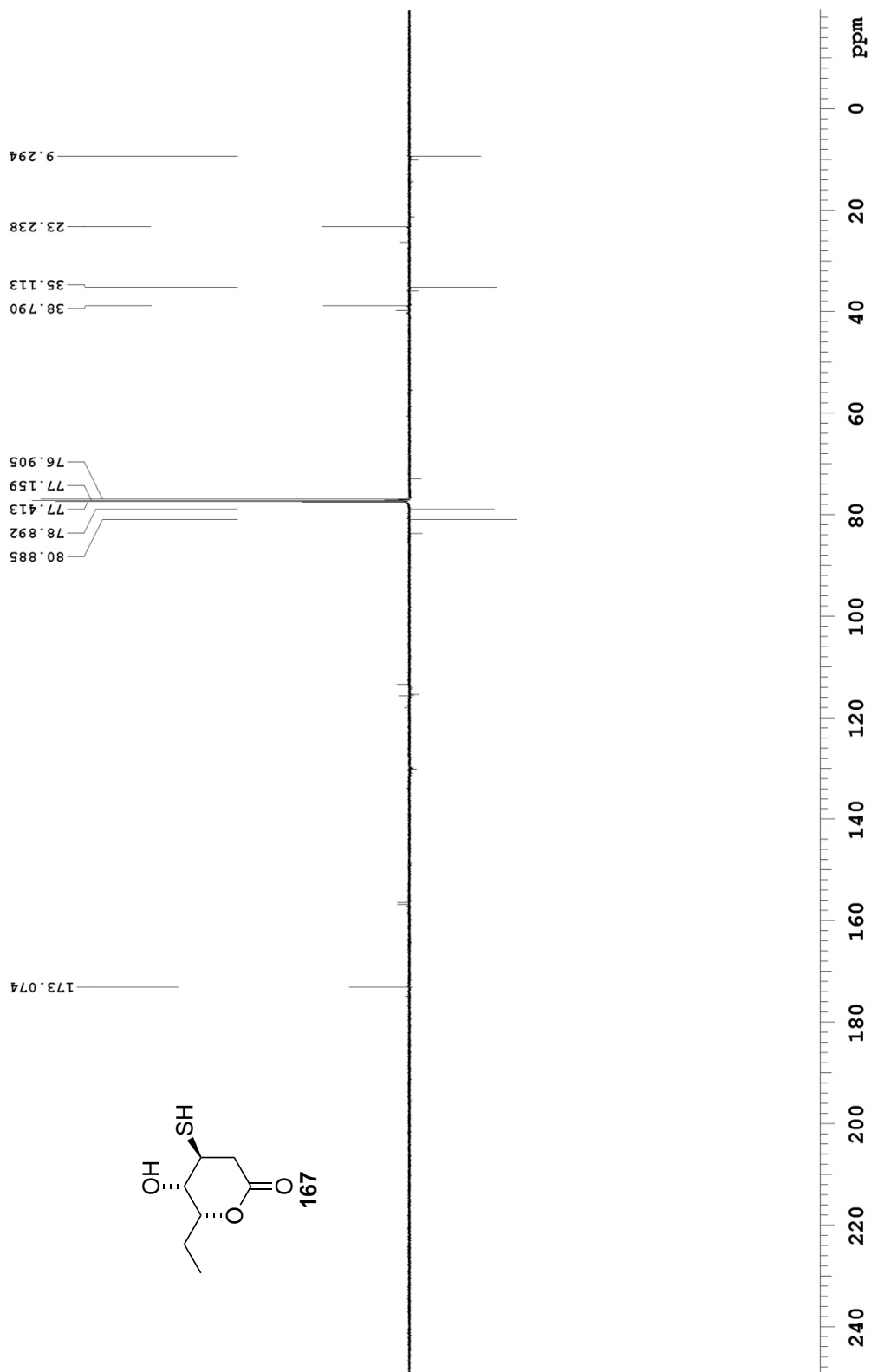
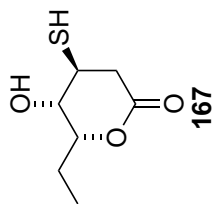
125.690 MHz C13[HI] APT_ad in cdcl3 (ref. to CDCl3 @ 77.16 ppm), temp 27.7 C -> actual temp = 27.0 C, coldddual probe
 C & CH2 same, CH & CH3 opposite side of solvent signal



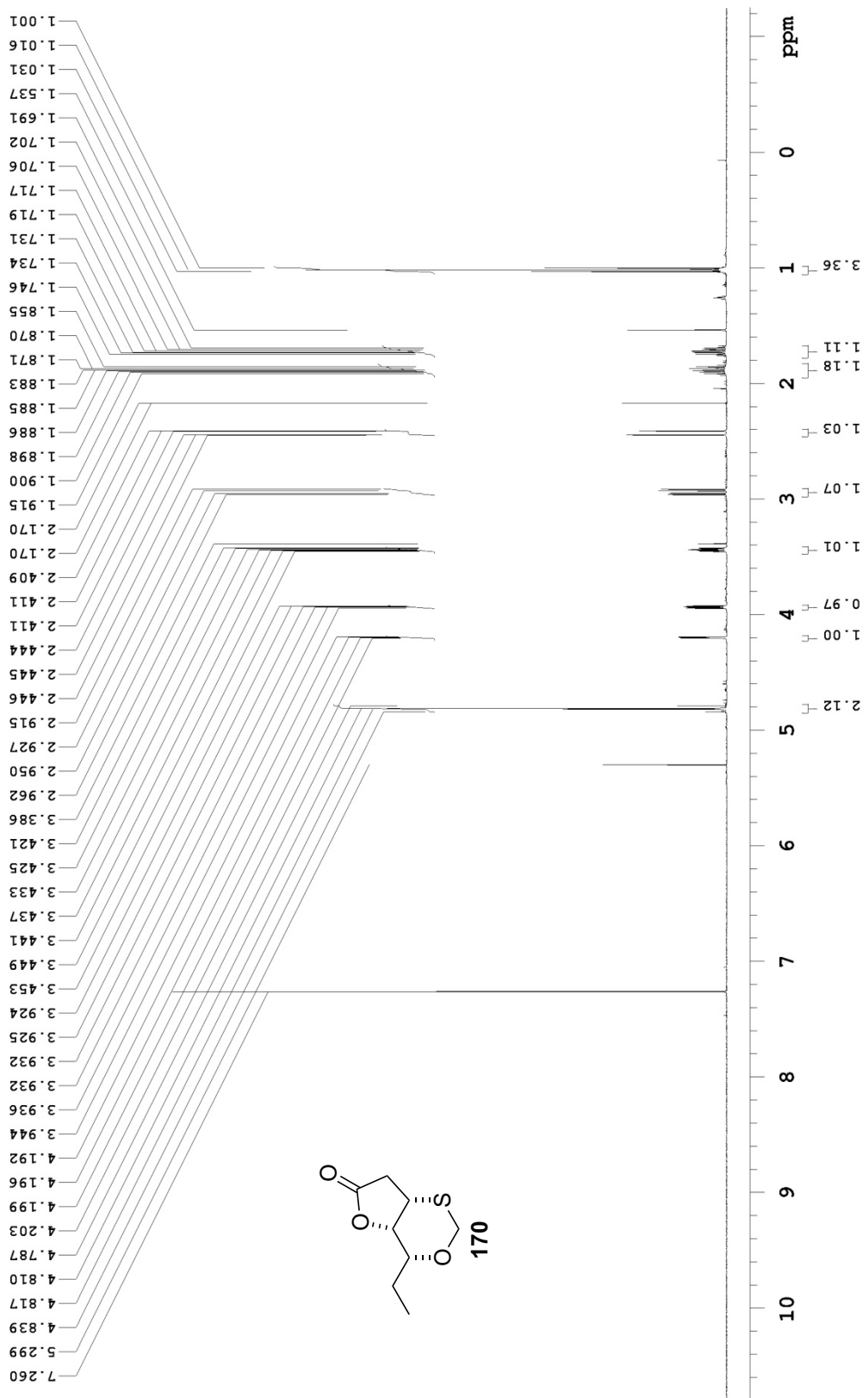
498.118 MHz H1 1D in cdcl3 (ref. to CDCl3 @ 7.26 ppm), temp 26.4 C -> actual temp = 27.0 C, autotxdb probe



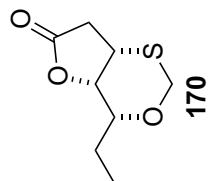
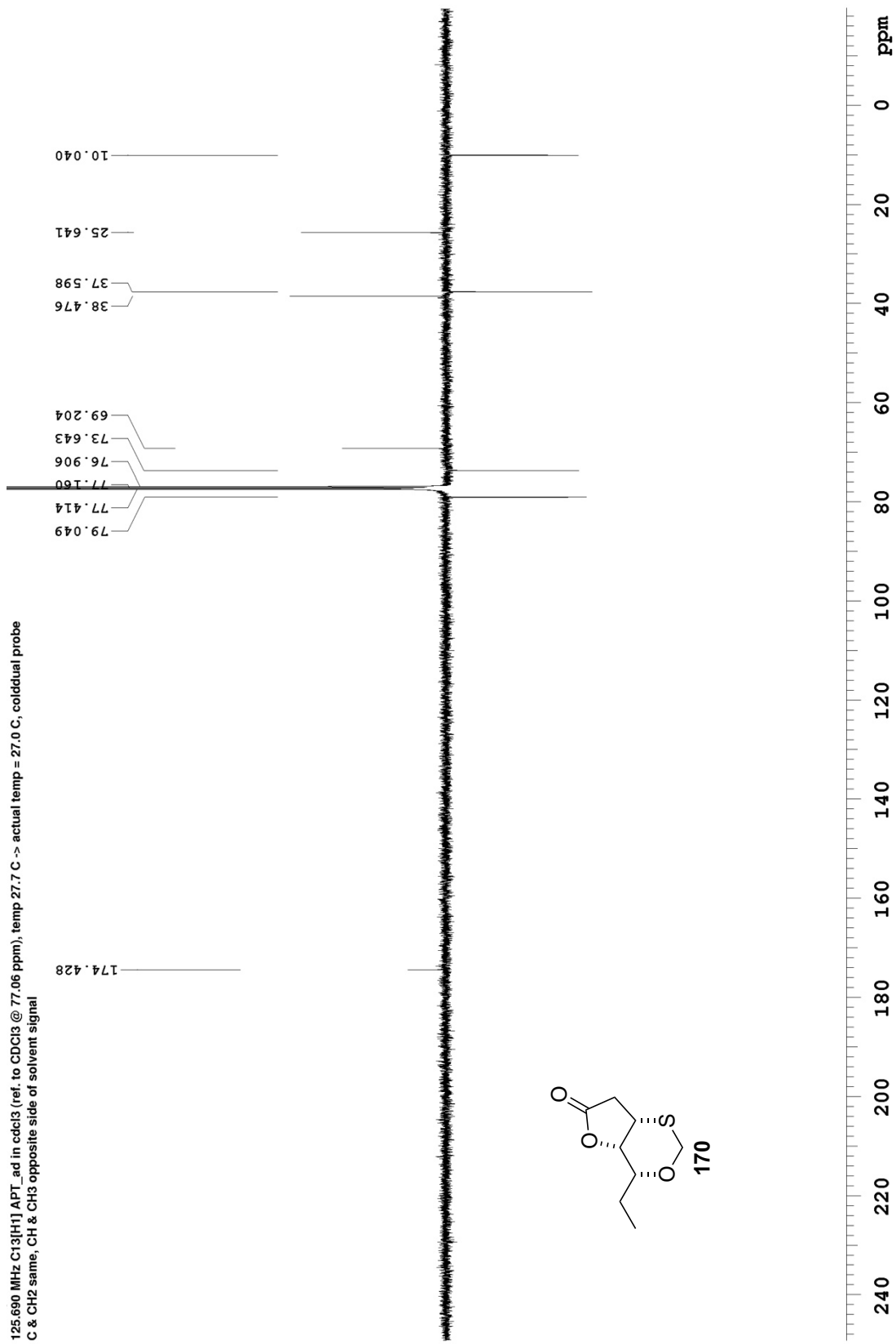
125.690 MHz C13{H1}APT_ad in cdcl3 (ref. to CDC13 @ 77.06 ppm), temp 27.7 C -> actual temp = 27.0 C, coldlual probe
C & CH2 same, CH & CH3 opposite side of solvent signal



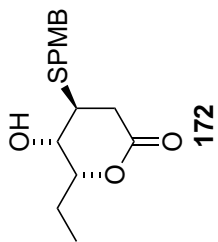
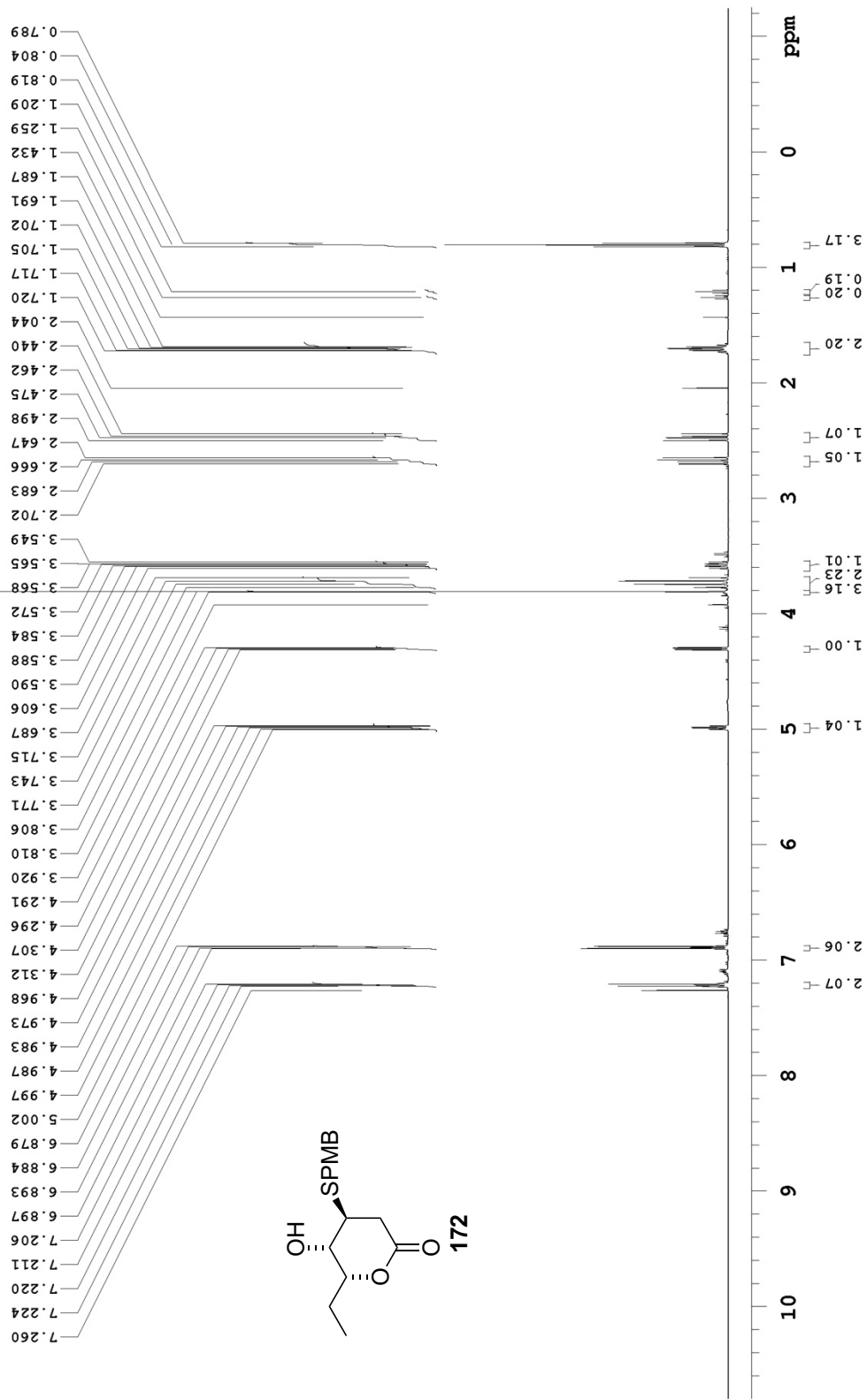
498.118 MHz H1 1D in cdcl3 (ref. to CDC13 @ 7.26 ppm), temp 27.2 C -> actual temp = 27.0 C, autoxdb probe



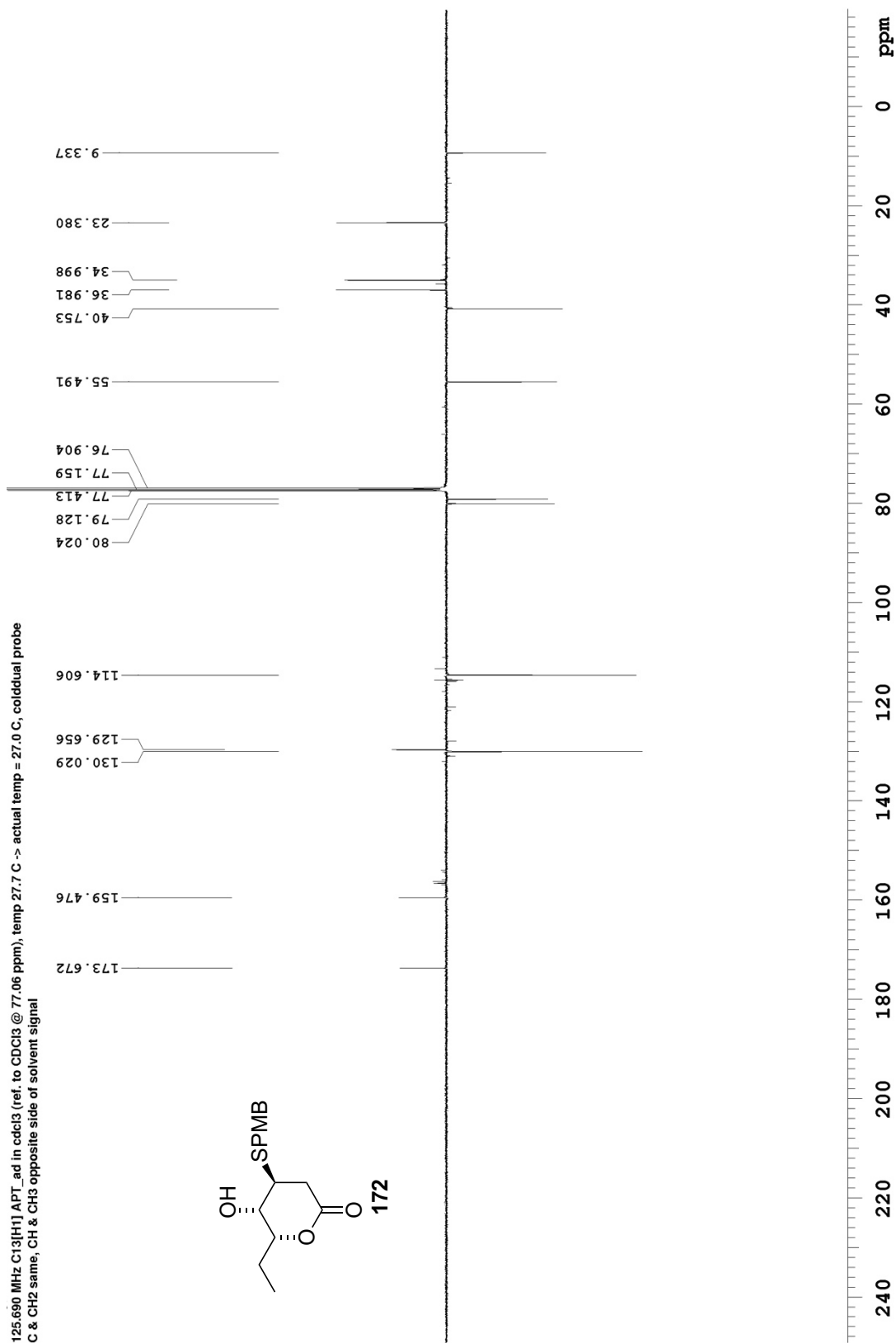
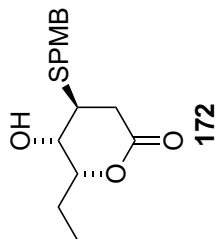
125.690 MHz C13{H1} APT ad in cdcl3 (ref. to CDCl3 @ 77.06 ppm), temp 27.7 C -> actual temp = 27.0 C, cold dual probe
C & CH2 same, CH & CH3 opposite side of solvent signal



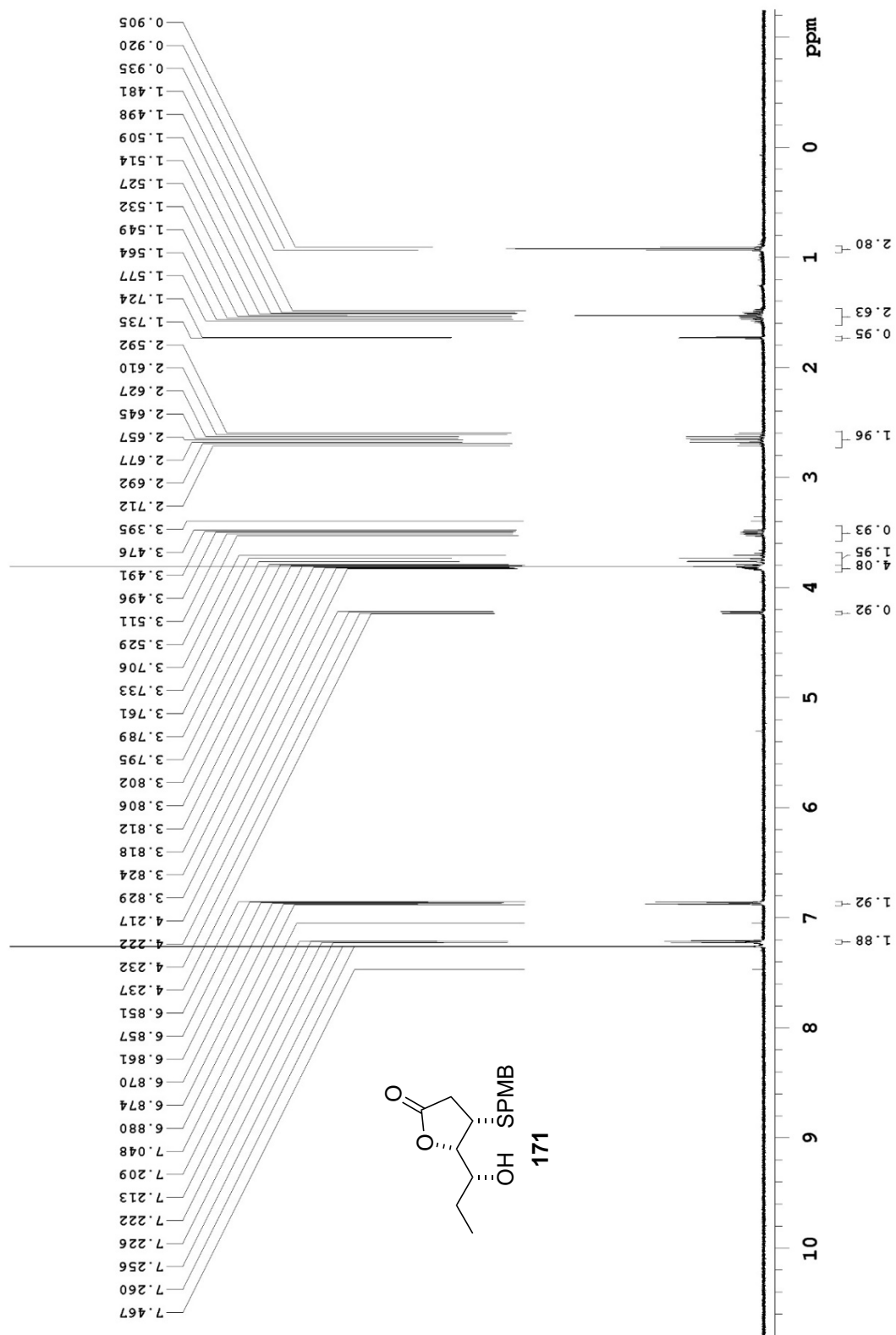
498.118 MHz H1 1D in cdcl3 (ref. to CDC13 @ 7.26 ppm), temp 27.2 C -> actual temp = 27.0 C, autotxdb probe



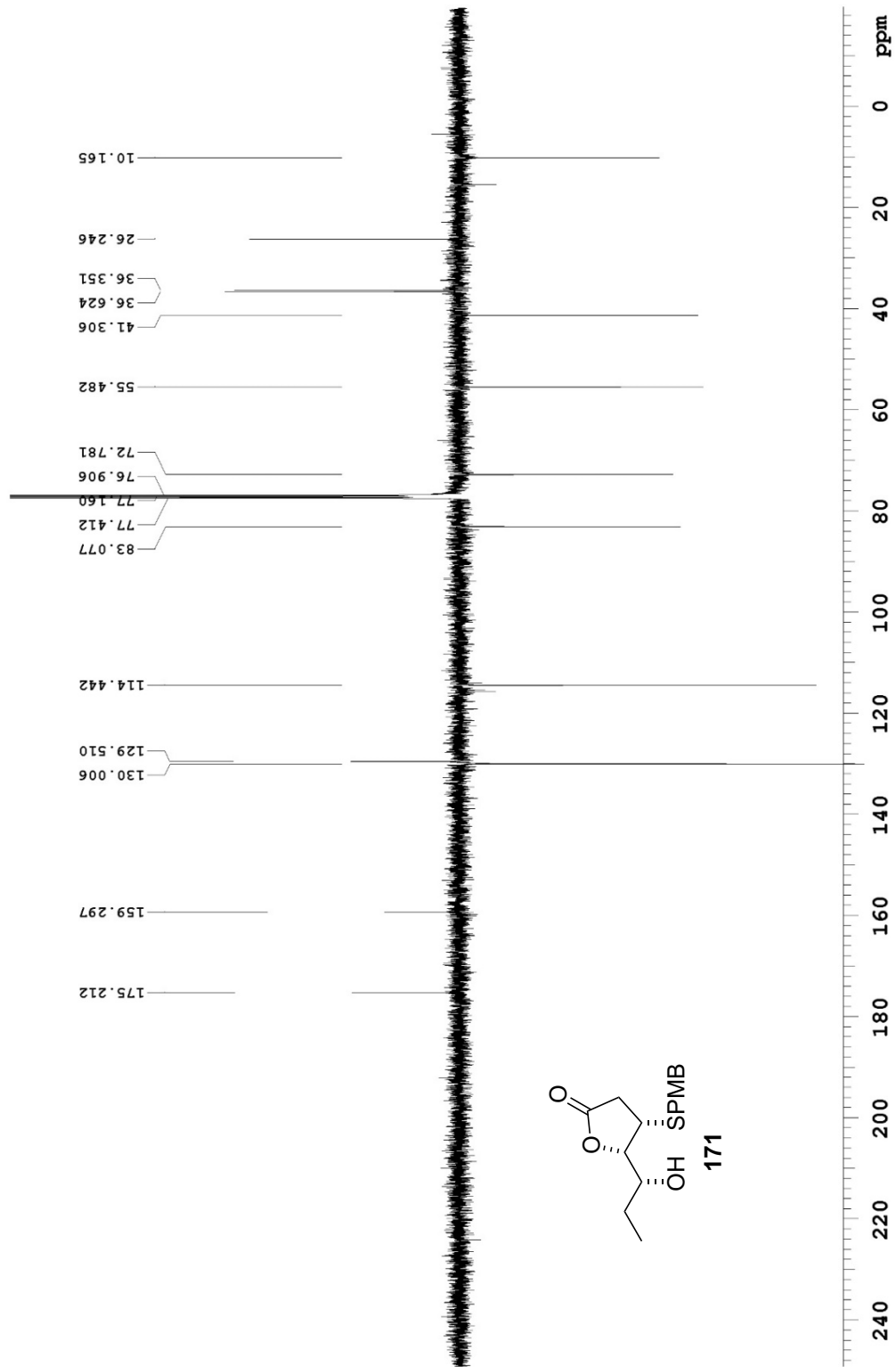
125.690 MHz C13[H1] APT_ad in cdcl3 (ref. to CDCl3 @ 77.06 ppm), temp 27.7 C -> actual temp = 27.0 C, coldddual probe
C & CH2 same, CH & CH3 opposite side of solvent signal



498.118 MHz H1 ID in cdcl3 (ref. to CDCl3 @ 7.26 ppm), temp 26.4 C -> actual temp = 27.0 C, autoxdbc probe



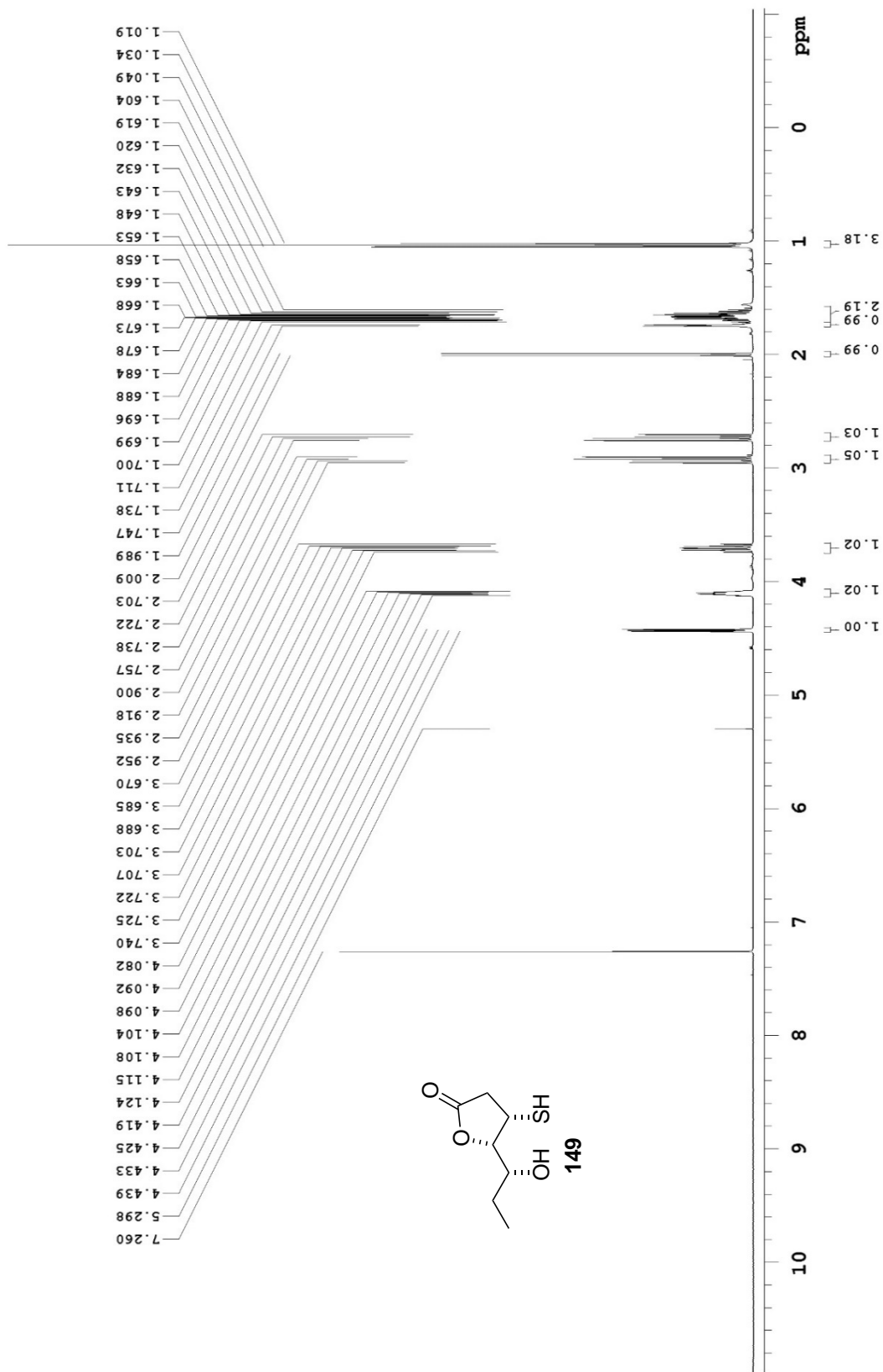
125.690 MHz C13[H1] APT_ad in cdcl3 (ref. to CDCl3 @ 77.16 ppm), temp 27.7 C -> actual temp = 27.0 C, coldddual probe
 C & CH2 same, CH & CH3 opposite side of solvent signal



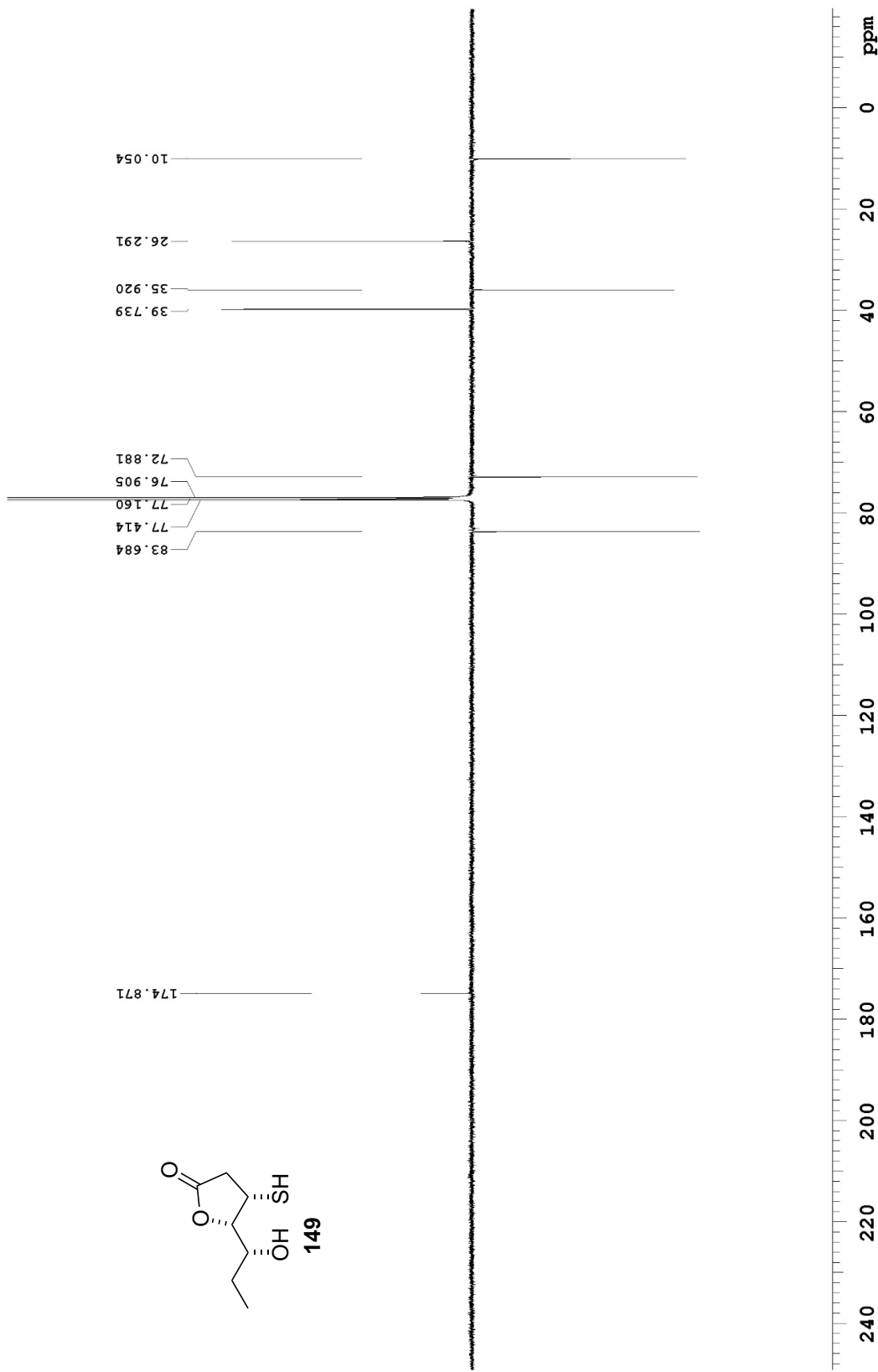
Pulse Sequence: APT_ad

Department of Chemistry, University of Alberta

499.806 MHz ¹H PRESAT in cdcl3 (ref. to CDCl3 @ 7.26 ppm), temp 27.7 C -> actual temp = 27.0 C, coldludal probe



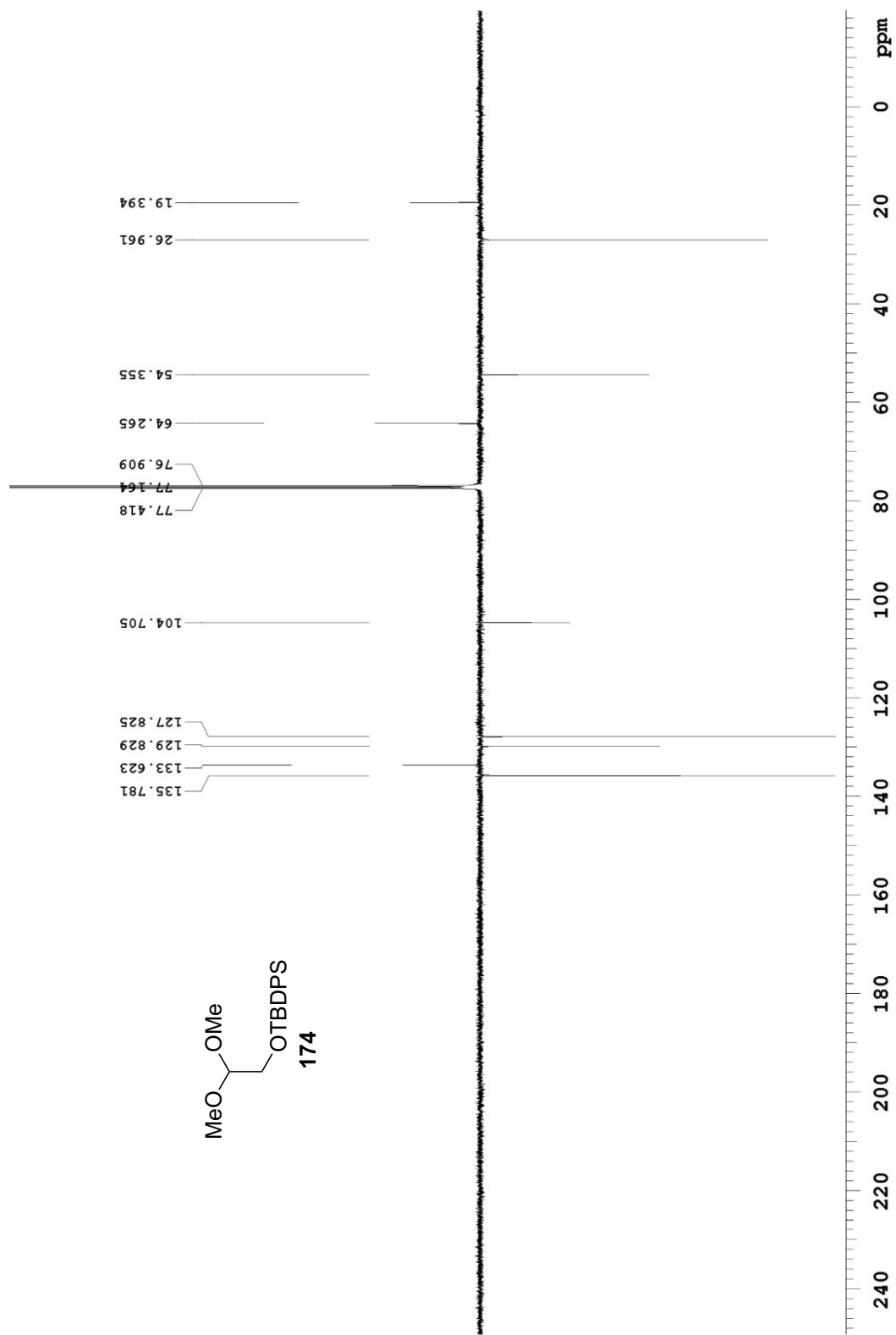
125.690 MHz C13[H1] APT_ad in cdcl3 (ref. to CDCl3 @ 77.16 ppm), temp 27.7 C -> actual temp = 27.0 C, coldddual probe
C & CH2 same, CH & CH3 opposite side of solvent signal



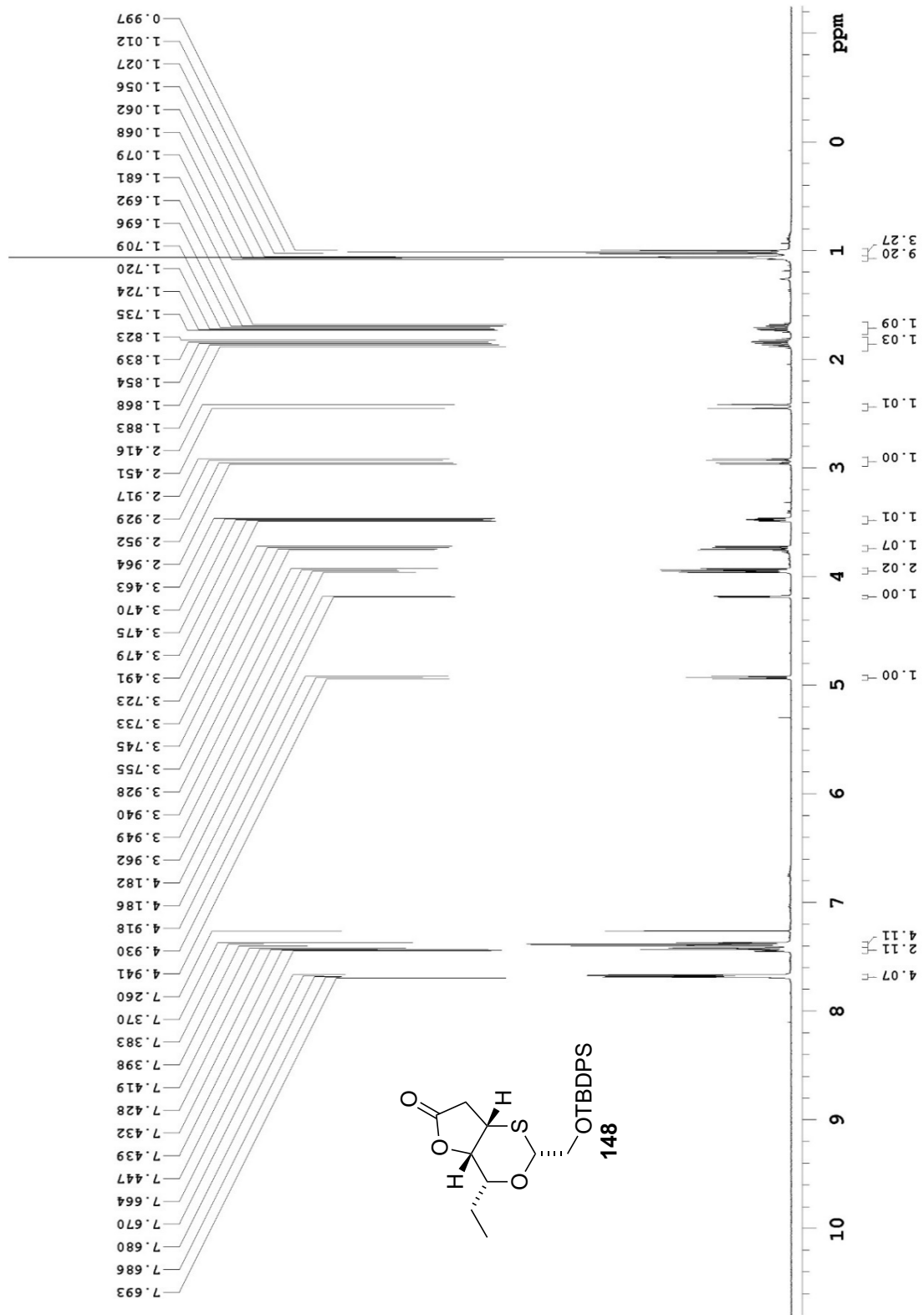
Pulse Sequence: APT_ad

Department of Chemistry, University of Alberta

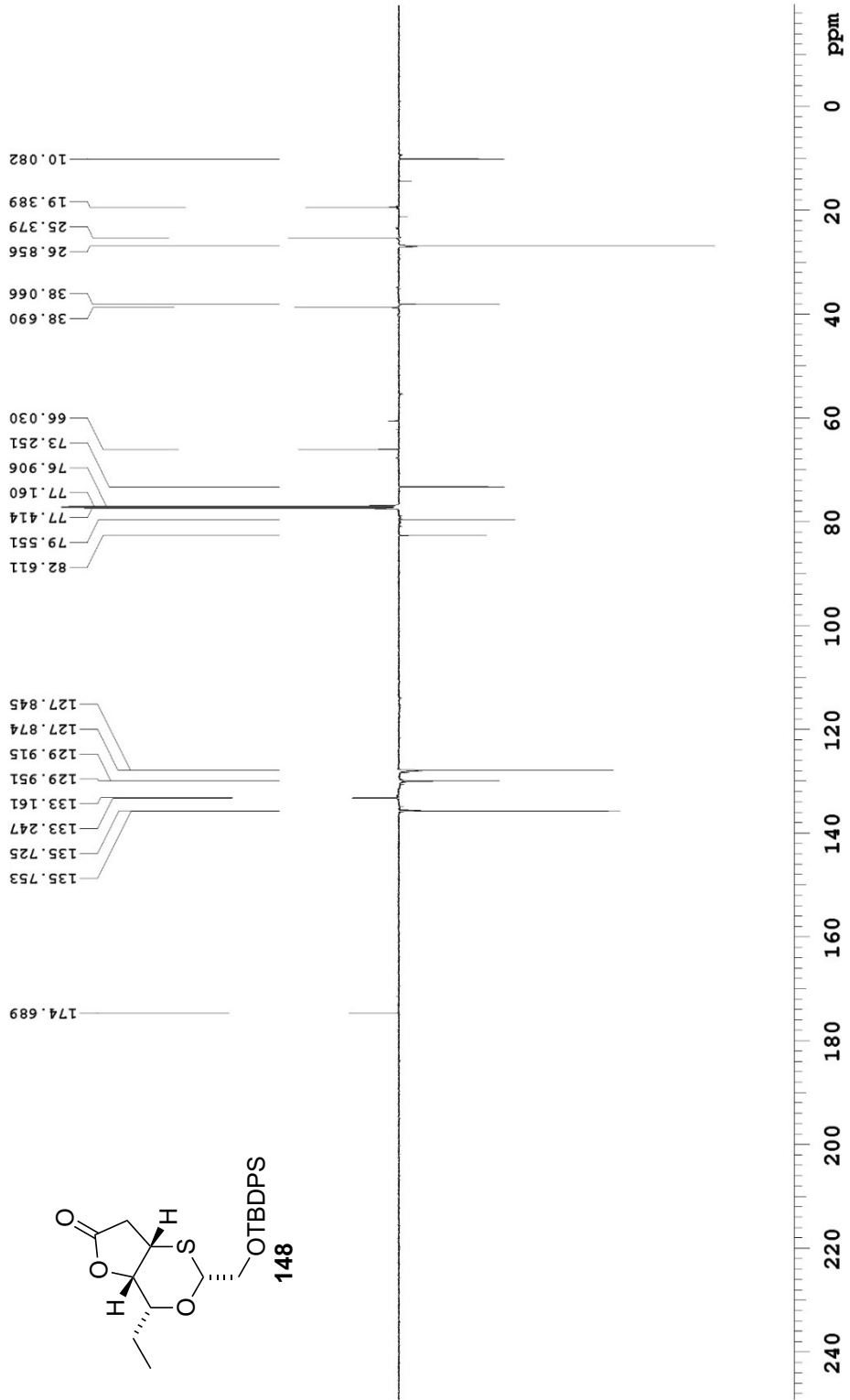
125.690 MHz C13[H1] APT_ad in cdcl3 (ref. to CDCl3 @ 77.16 ppm), temp 27.7 C -> actual temp = 27.0 C, coldddual probe
C & CH2 same, CH & CH3 opposite side of solvent signal



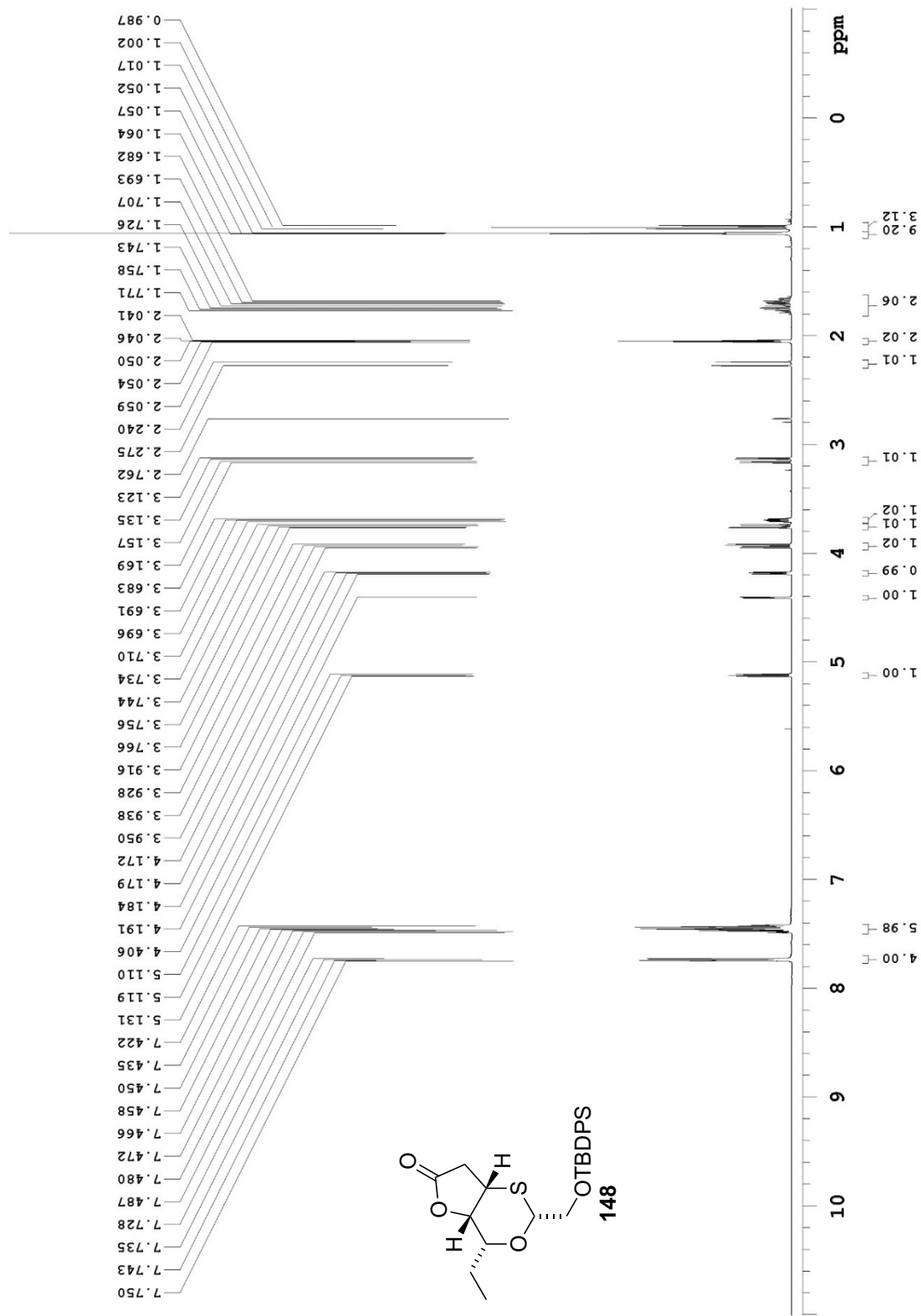
498.118 MHz H1 1D in cdcl3 (ref. to CDCl3 @ 7.26 ppm), temp 26.4 C -> actual temp = 27.0 C, autotxdbc probe



125.692 MHz C13[H1] APT_ad in cdcl3 (ref. to CDC13 @ 77.16 ppm), temp 27.7 C -> actual temp = 27.0 C, colddual probe
 C & CH2 same, CH & CH3 opposite side of solvent signal



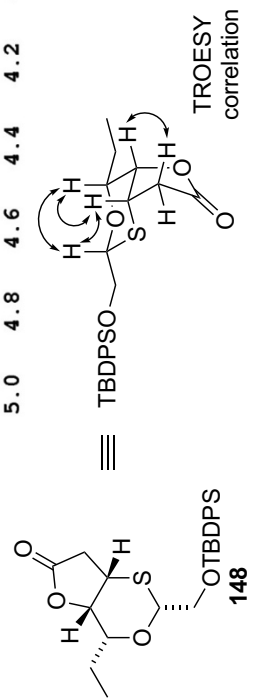
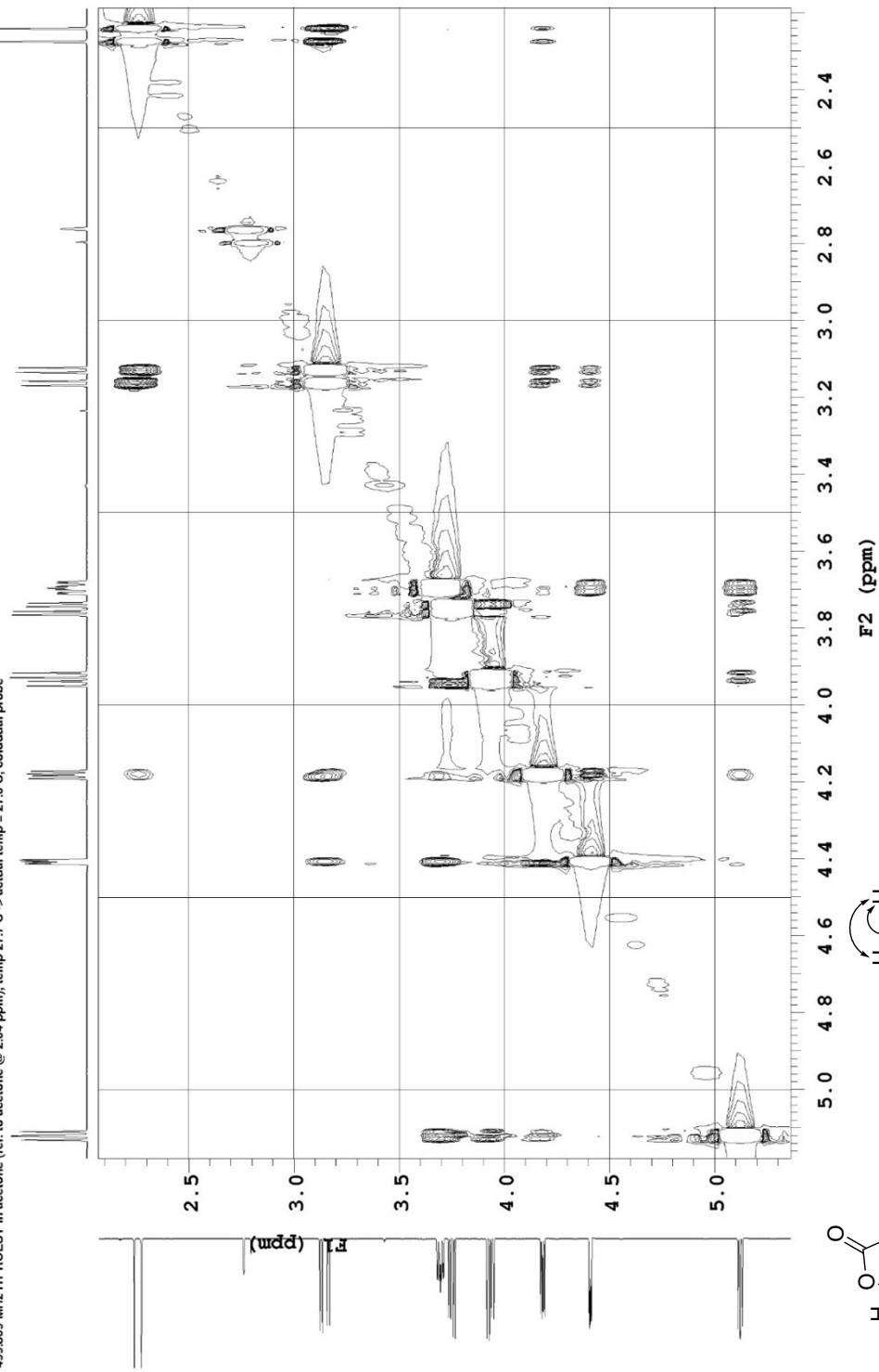
499.809 MHz H1 PRESAT in acetone (ref. to acetone @ 2.05 ppm), temp 27.7 C -> actual temp = 27.0 C, cold dual probe



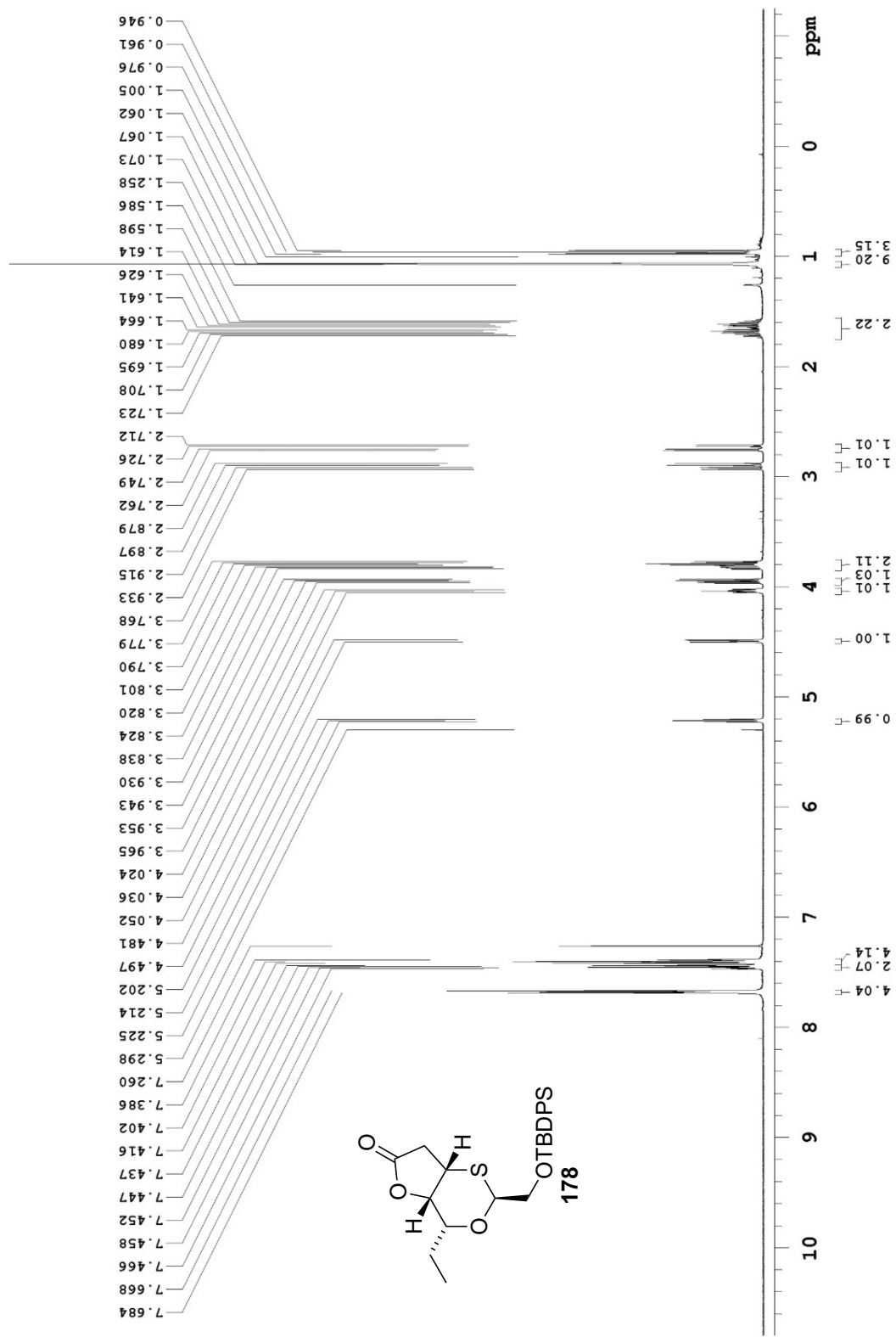
Pulse Sequence: PRESAT

Department of Chemistry, University of Alberta

499.809 MHz ¹H ROESY in acetone (ref. to acetone @ 2.04 ppm), temp 27.7 C -> actual temp = 27.0 C, coldludal probe



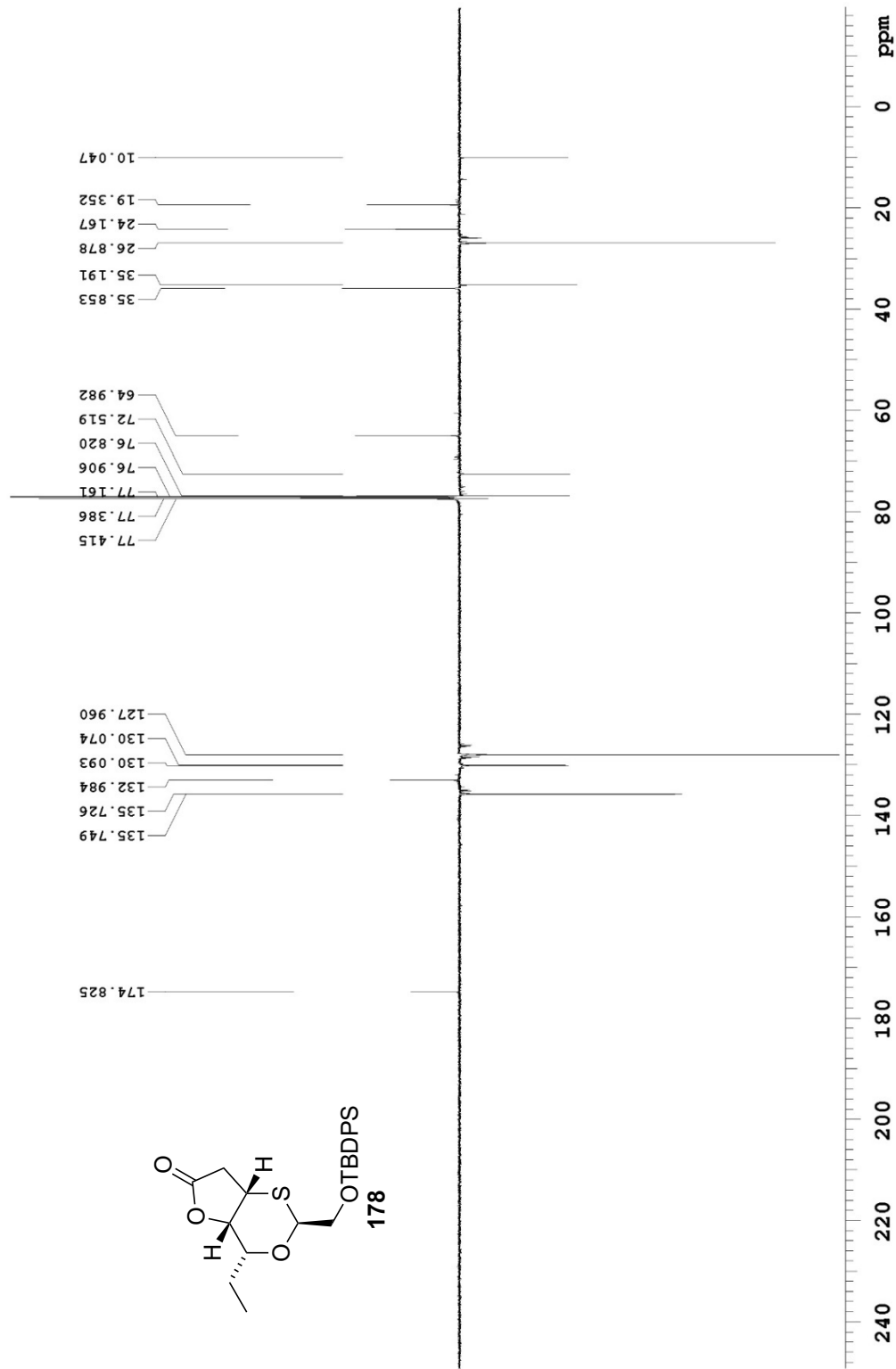
498.118 MHz ¹H 1D in cdcl3 (ref. to CDCl3 @ 7.26 ppm), temp 26.4 C -> actual temp = 27.0 C, autoxdbc probe



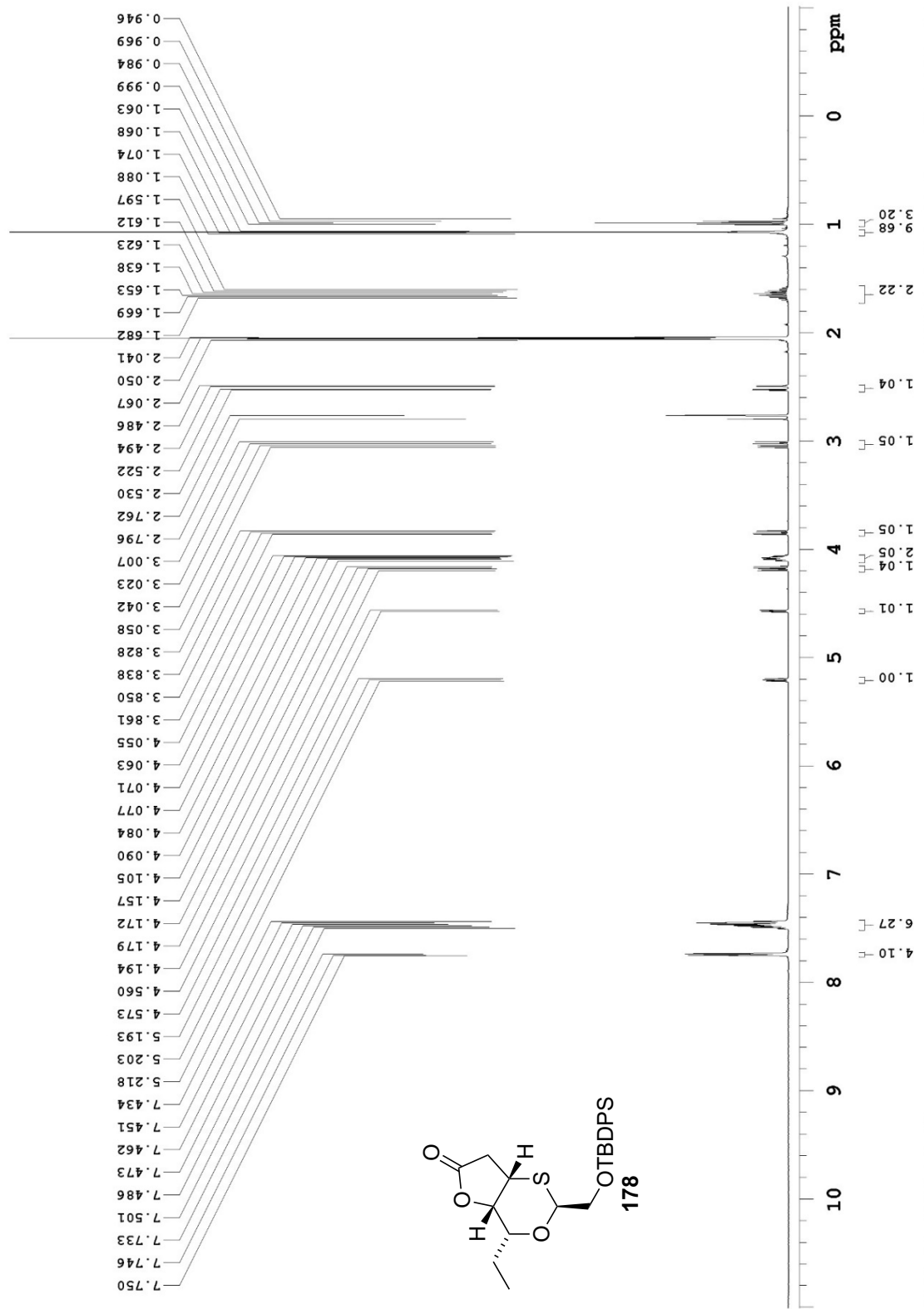
Pulse Sequence: s2pul

Department of Chemistry, University of Alberta

125.690 MHz C13[H1] APT_ad in cdcl3 (ref. to cdcl3 @ 77.16 ppm), temp 27.7 C -> actual temp = 27.0 C, coldddual probe
 C & CH2 same, CH & CH3 opposite side of solvent signal



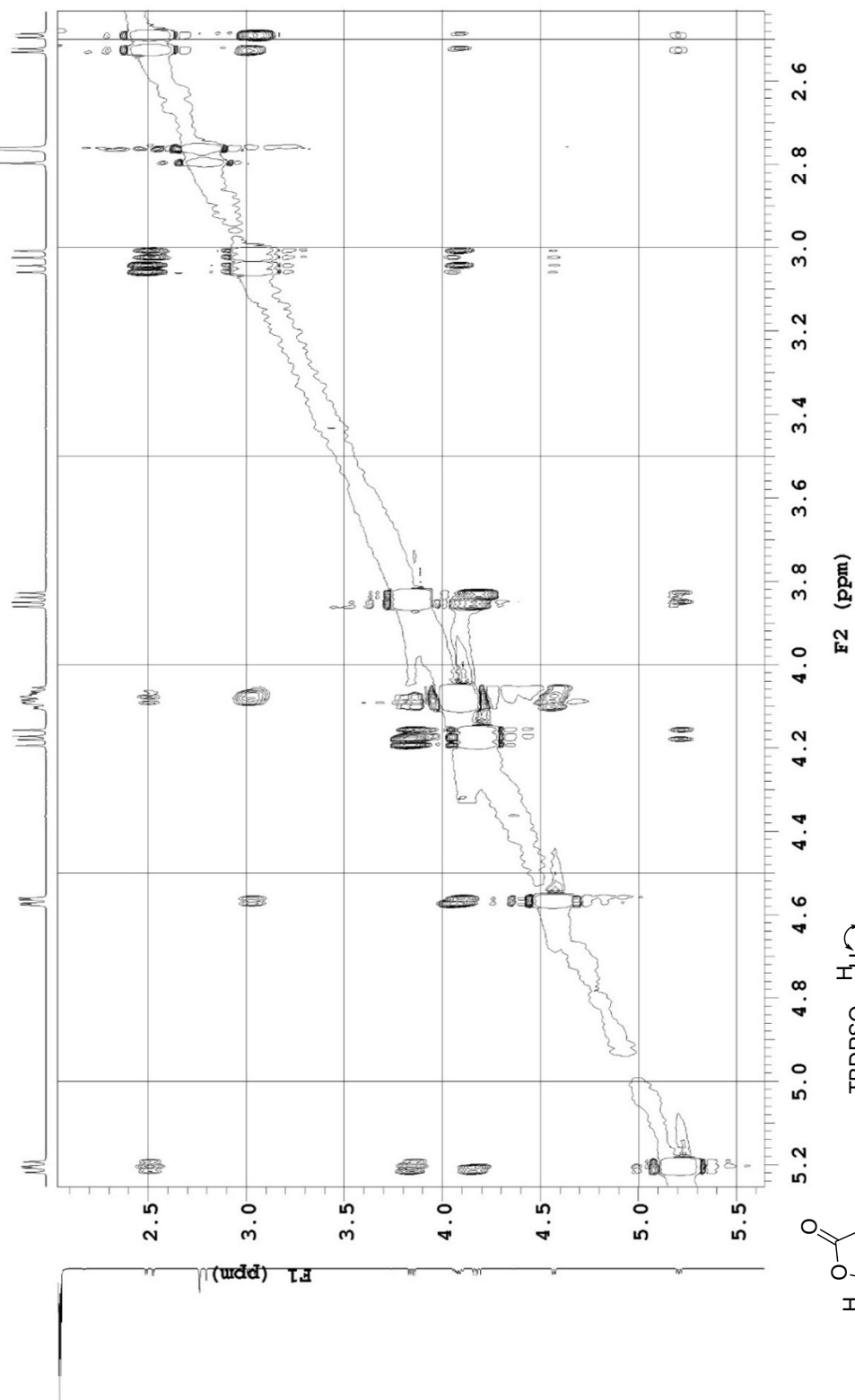
499.809 MHz ¹H PRESAT in acetone (ref. to acetone @ 2.05 ppm), temp 27.7 C -> actual temp = 27.0 C, cold dual probe

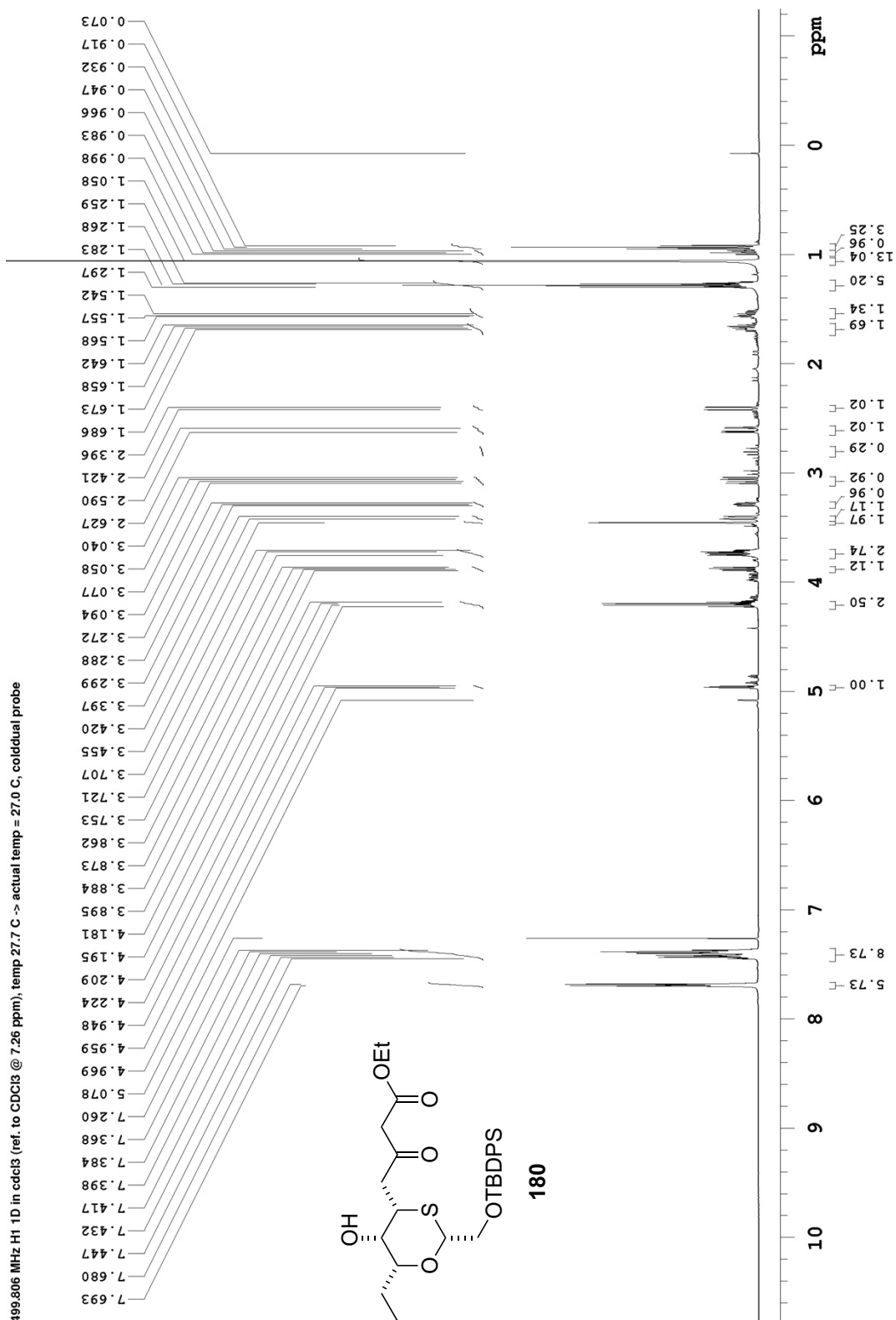


Department of Chemistry, University of Alberta

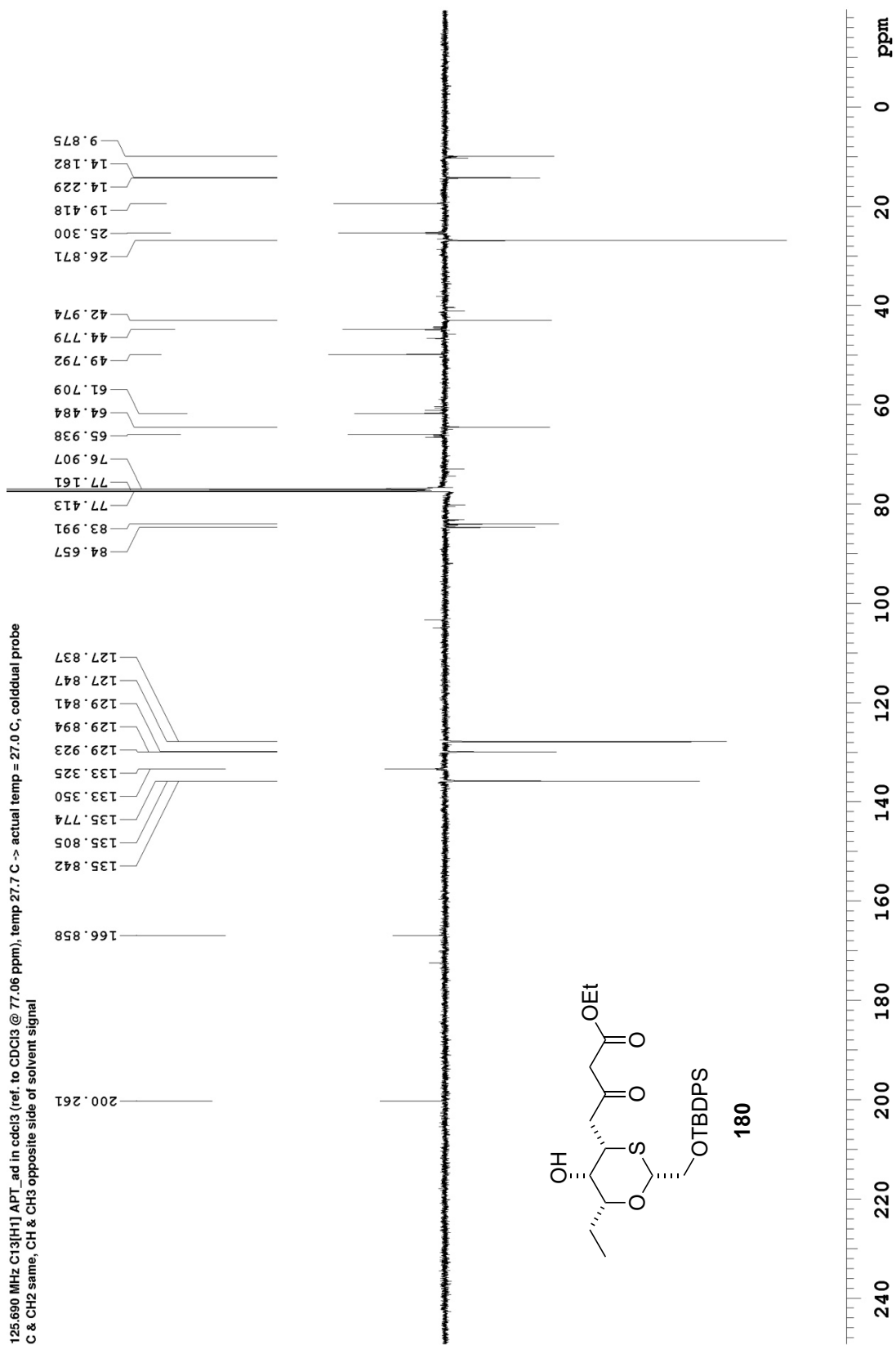
Pulse Sequence: PRESAT

499.809 MHz ¹H ROESY in acetone (ref. to acetone @ 2.05 ppm), temp 27.7 C -> actual temp = 27.0 C, coldliald probe

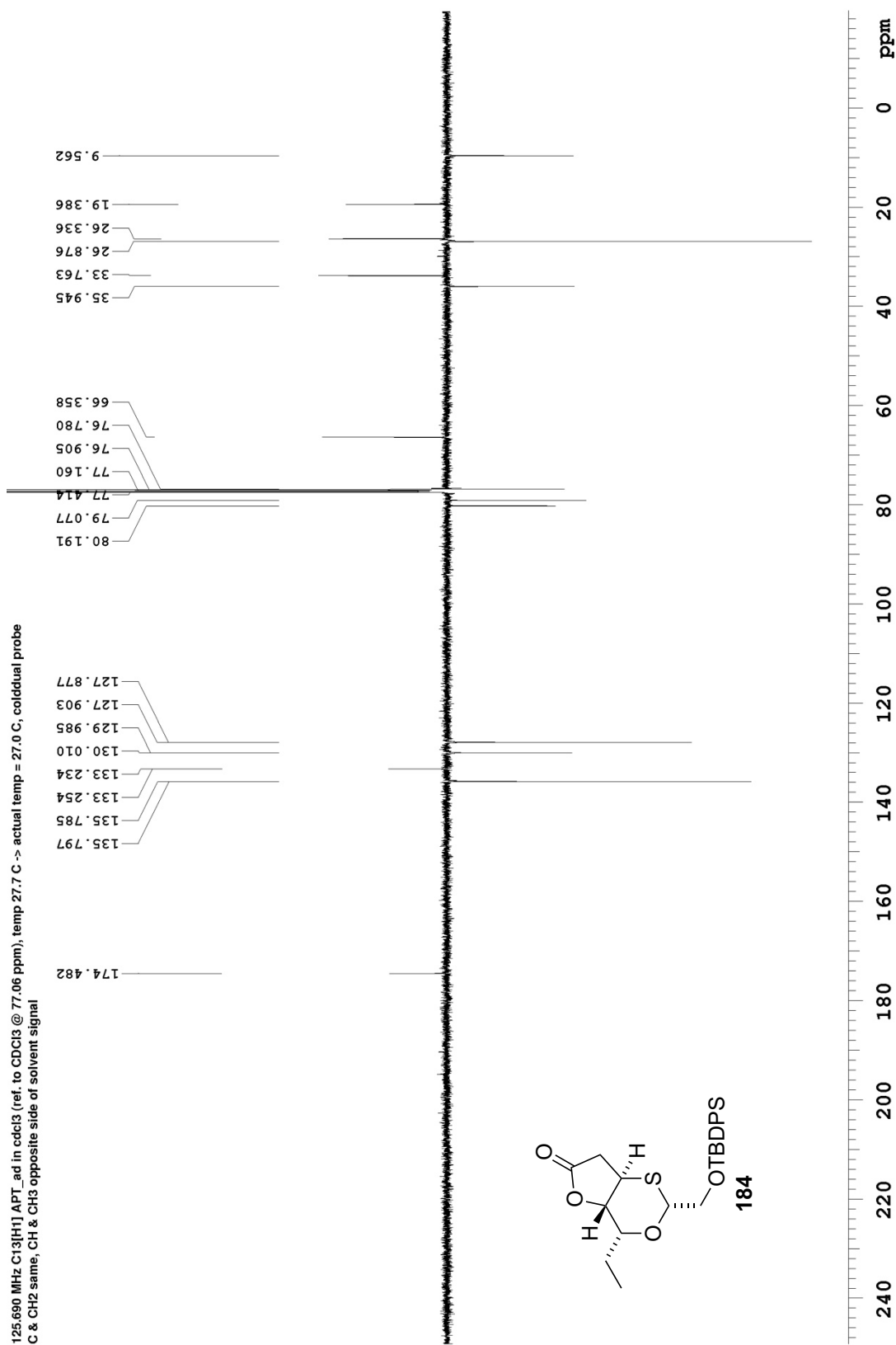




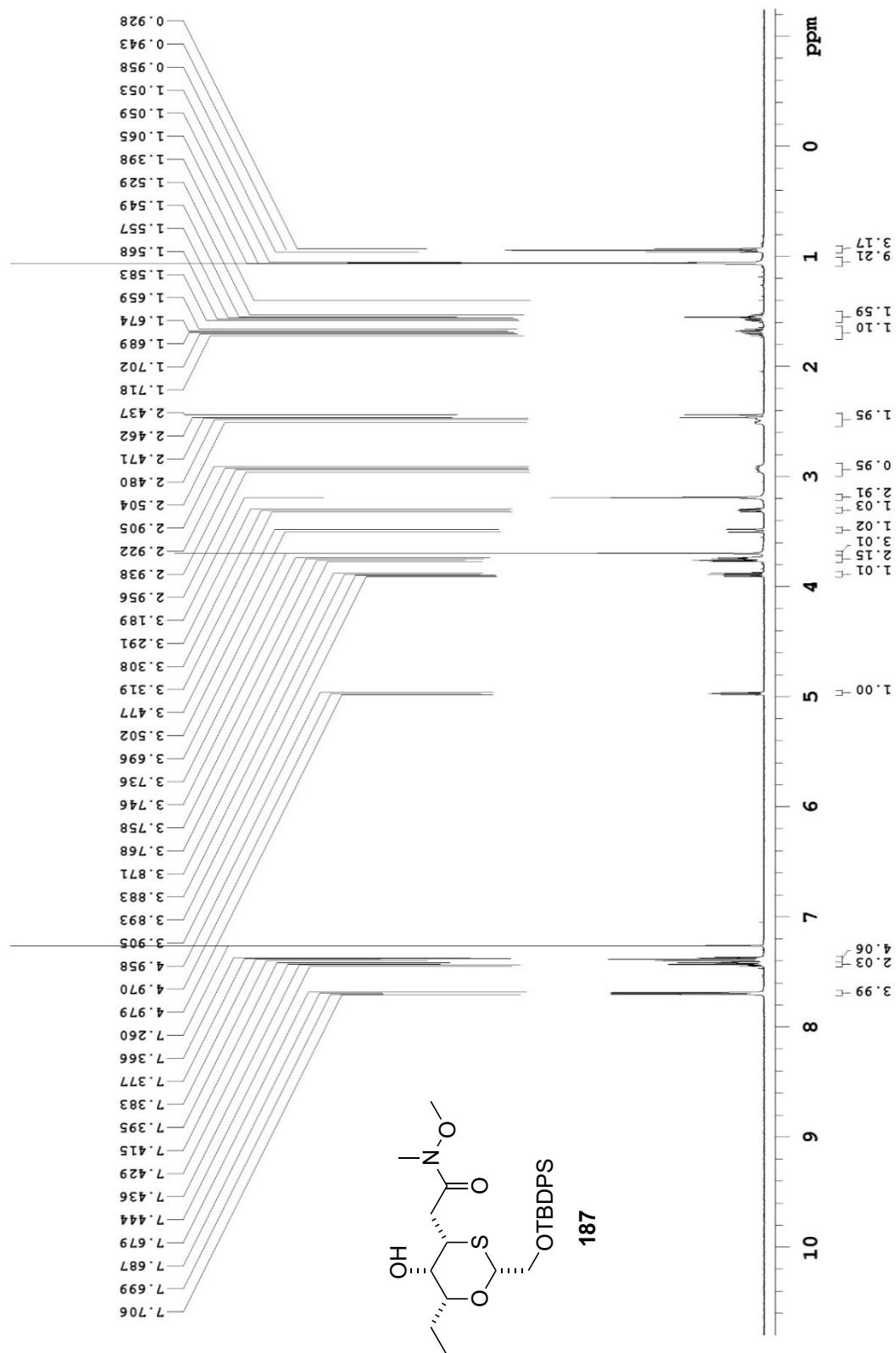
125.690 MHz C13[H1] APT, ad in cdcl3 (ref. to CDCl3 @ 77.06 ppm), temp 27.7 C -> actual temp = 27.0 C, coldluald probe
 C & CH2 same, CH & CH3 opposite side of solvent signal



125.690 MHz C13[H1] APT_ad in cdcl3 (ref. to CDCl3 @ 77.06 ppm), temp 27.7 C -> actual temp = 27.0 C, cold dual probe
C & CH2 same, CH & CH3 opposite side of solvent signal



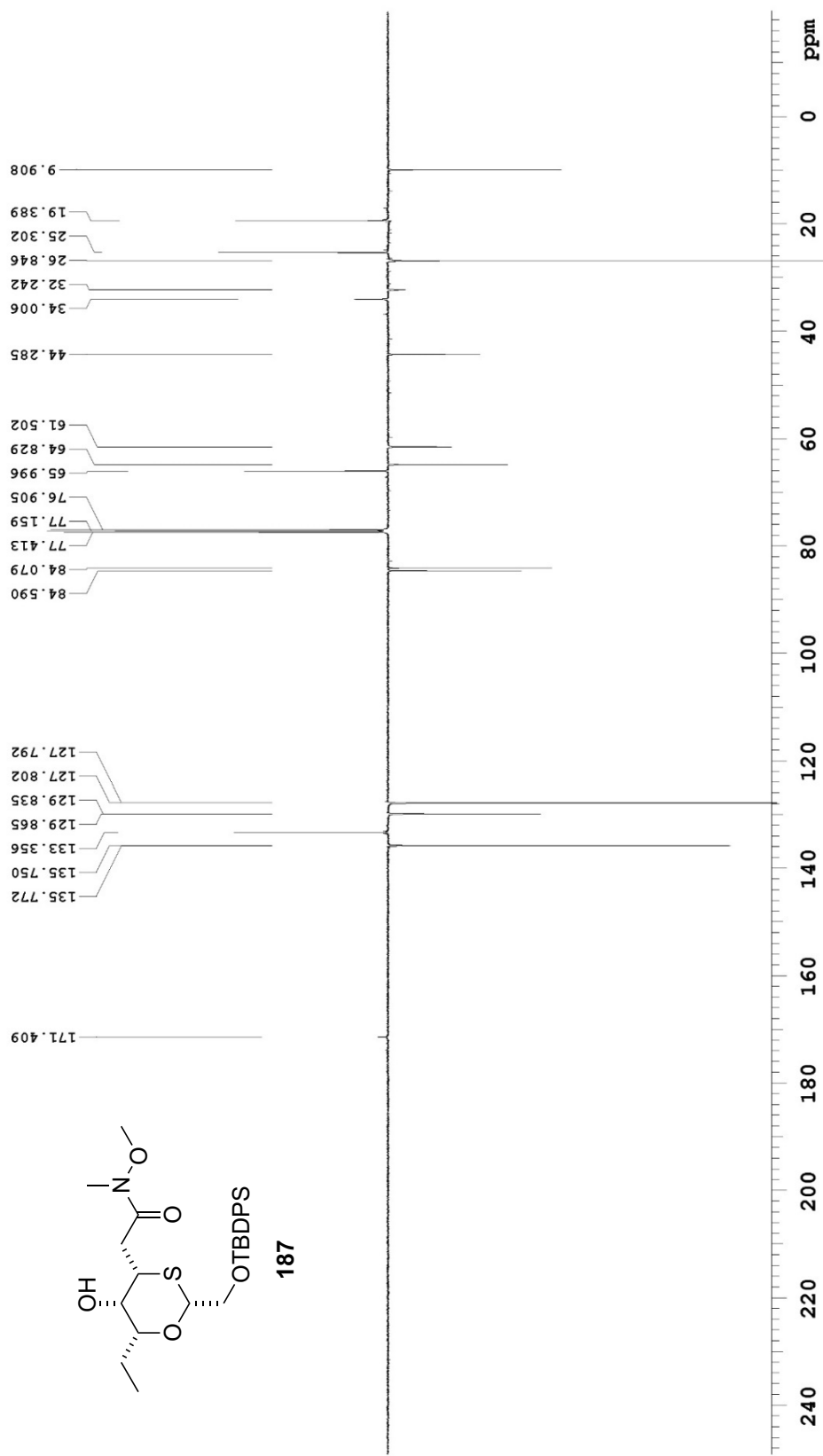
498.118 MHz H1 1D in cdcl3 (ref. to CDCl3 @ 7.26 ppm), temp 26.4 C -> actual temp = 27.0 C, autoxdbc probe



Pulse Sequence: s2pul

Department of Chemistry, University of Alberta

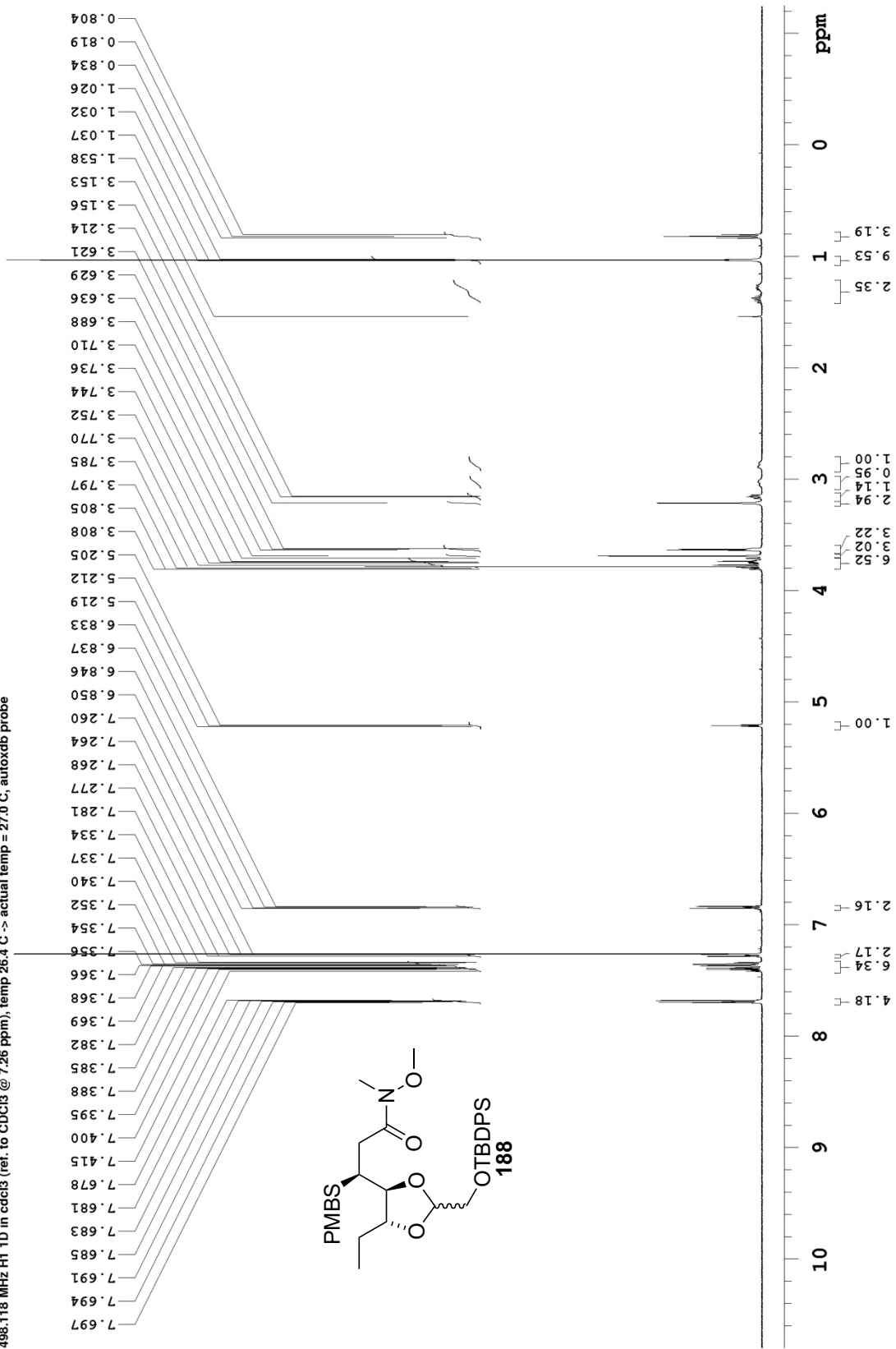
125.690 MHz C13[H1] APT_ad in cdcl3 (ref. to cdcl3 @ 77.16 ppm), temp 27.7 C -> actual temp = 27.0 C, coldddual probe
C & CH2 same, CH & CH3 opposite side of solvent signal



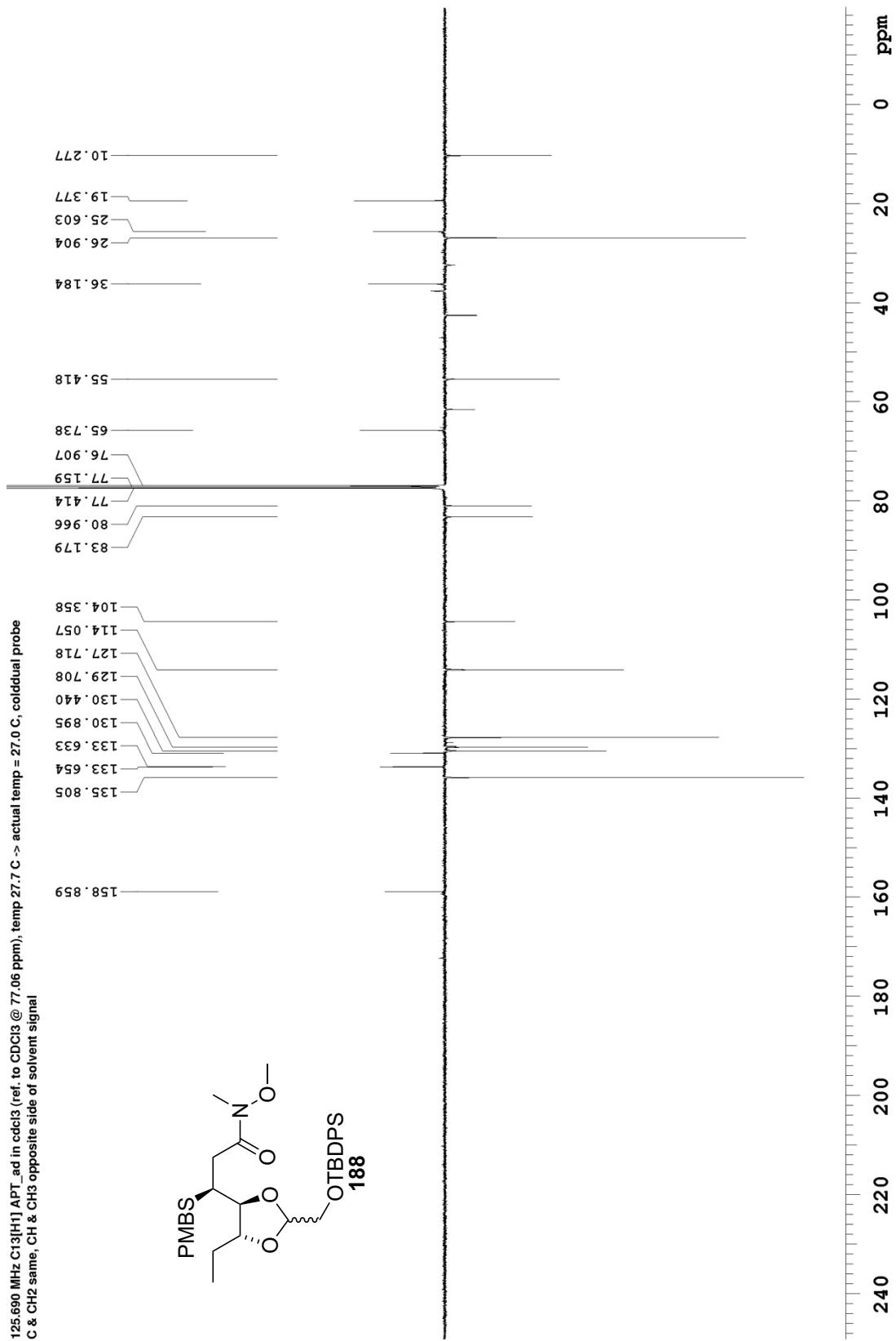
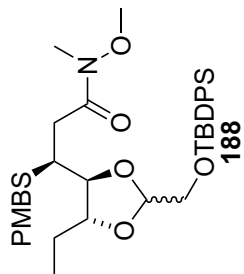
Pulse Sequence: APT_ad

Department of Chemistry, University of Alberta

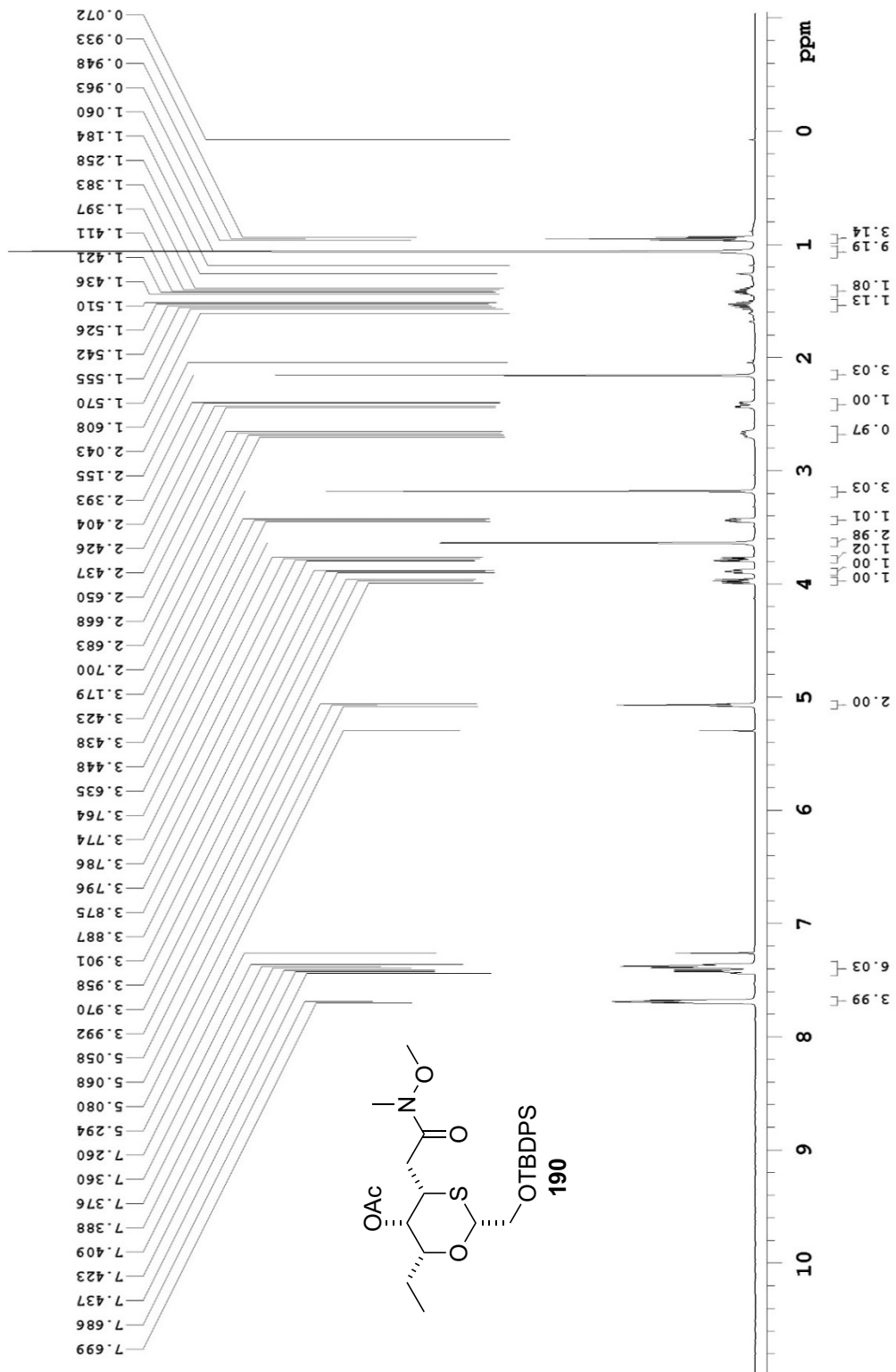
498.118 MHz H1 1D in cdcl3 (ref. to CDC13 @ 7.26 ppm), temp 26.4 C -> actual temp = 27.0 C, autotdb probe



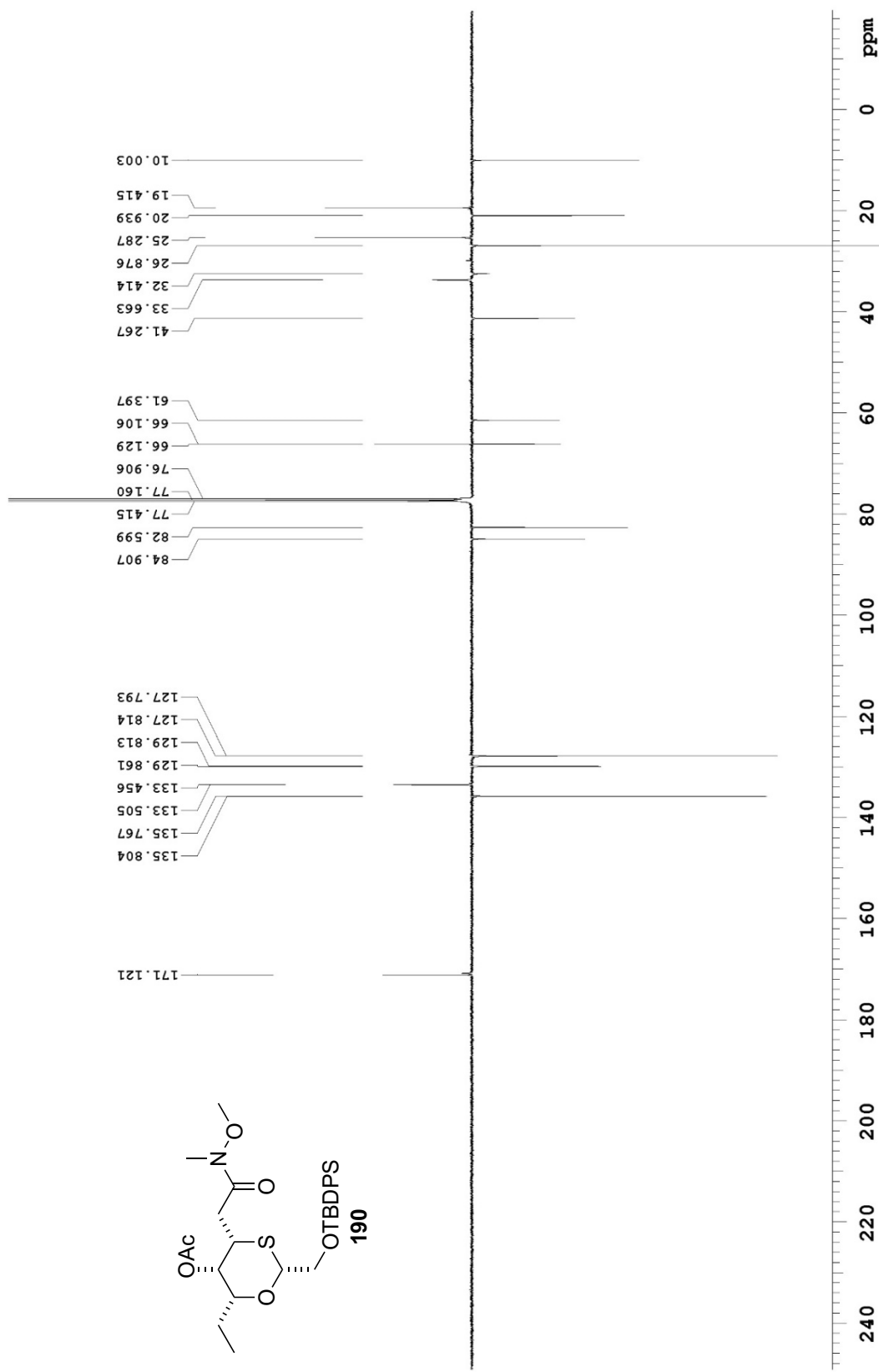
125.690 MHz C13{H1} APT_ad in cdcl3 (ref. to CDCl3 @ 77.06 ppm), temp 27.7 C -> actual temp = 27.0 C, coldlual probe
 C & CH2 same, CH & CH3 opposite side of solvent signal



499.806 MHz H1 PRESAT in cdcl3 (ref. to CDCl3 @ 7.26 ppm), temp 27.7 C -> actual temp = 27.0 C, coldlual probe



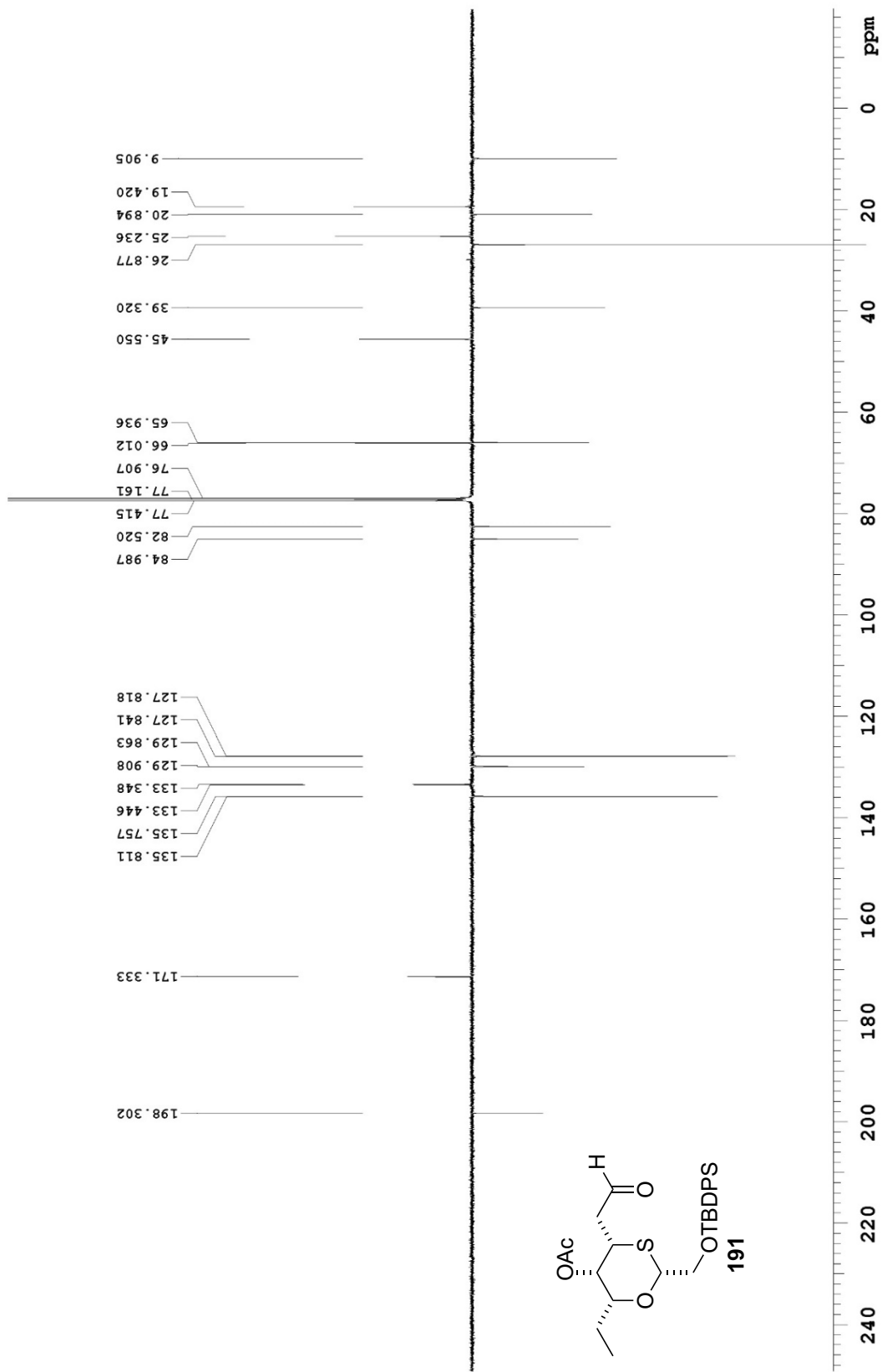
125.690 MHz ¹³C{¹H} APT_{ad} in cdcl3 (ref. to cdcl3 @ 77.16 ppm), temp 27.7 C -> actual temp = 27.0 C, coldddual probe
C & CH2 same, CH & CH3 opposite side of solvent signal



Pulse Sequence: APT_{ad}

Department of Chemistry, University of Alberta

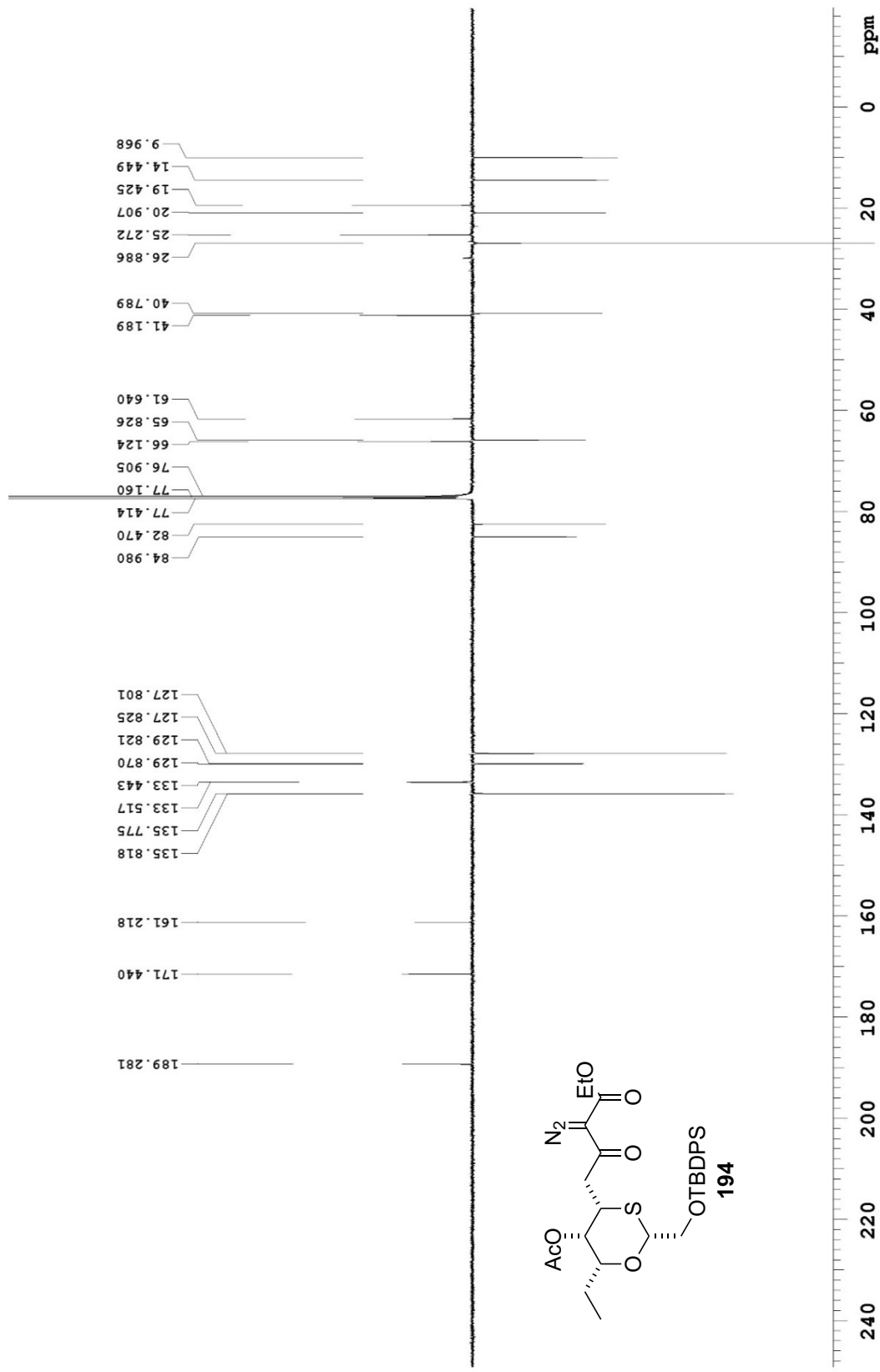
125.690 MHz $^{13}\text{C}\{^1\text{H}\}$ APT_{ad} in cdcl_3 (ref. to CDCl_3 @ 77.16 ppm), temp 27.7 C -> actual temp = 27.0 C, coldddual probe
 C & CH2 same, CH & CH3 opposite side of solvent signal



Pulse Sequence: APT_{ad}

Department of Chemistry, University of Alberta

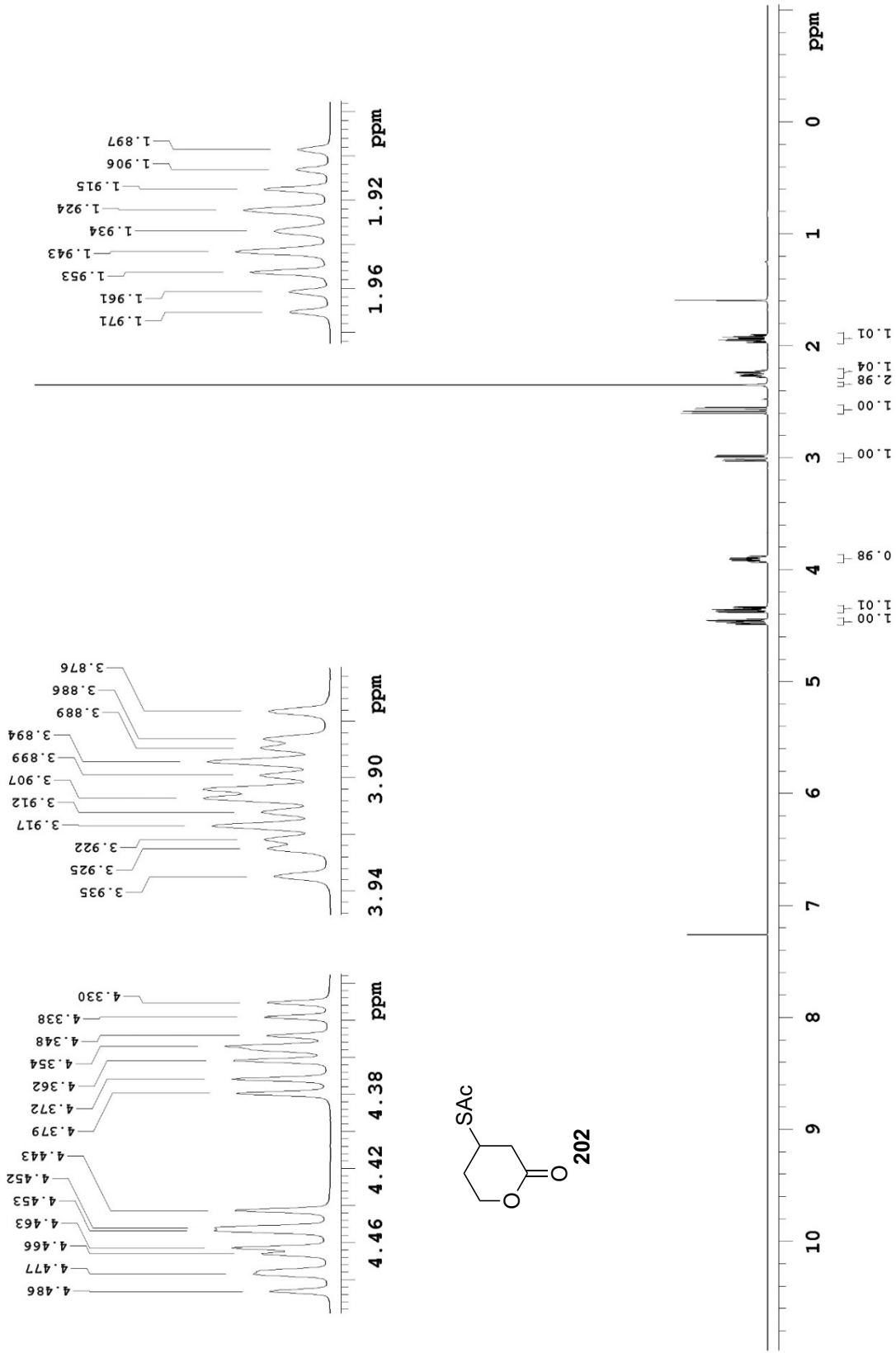
125.690 MHz C13{H1} APT_ad in cdcl3 (ref. to CDC13 @ 77.16 ppm), temp 27.7 C -> actual temp = 27.0 C, coldddual probe
 C & CH2 same, CH & CH3 opposite side of solvent signal



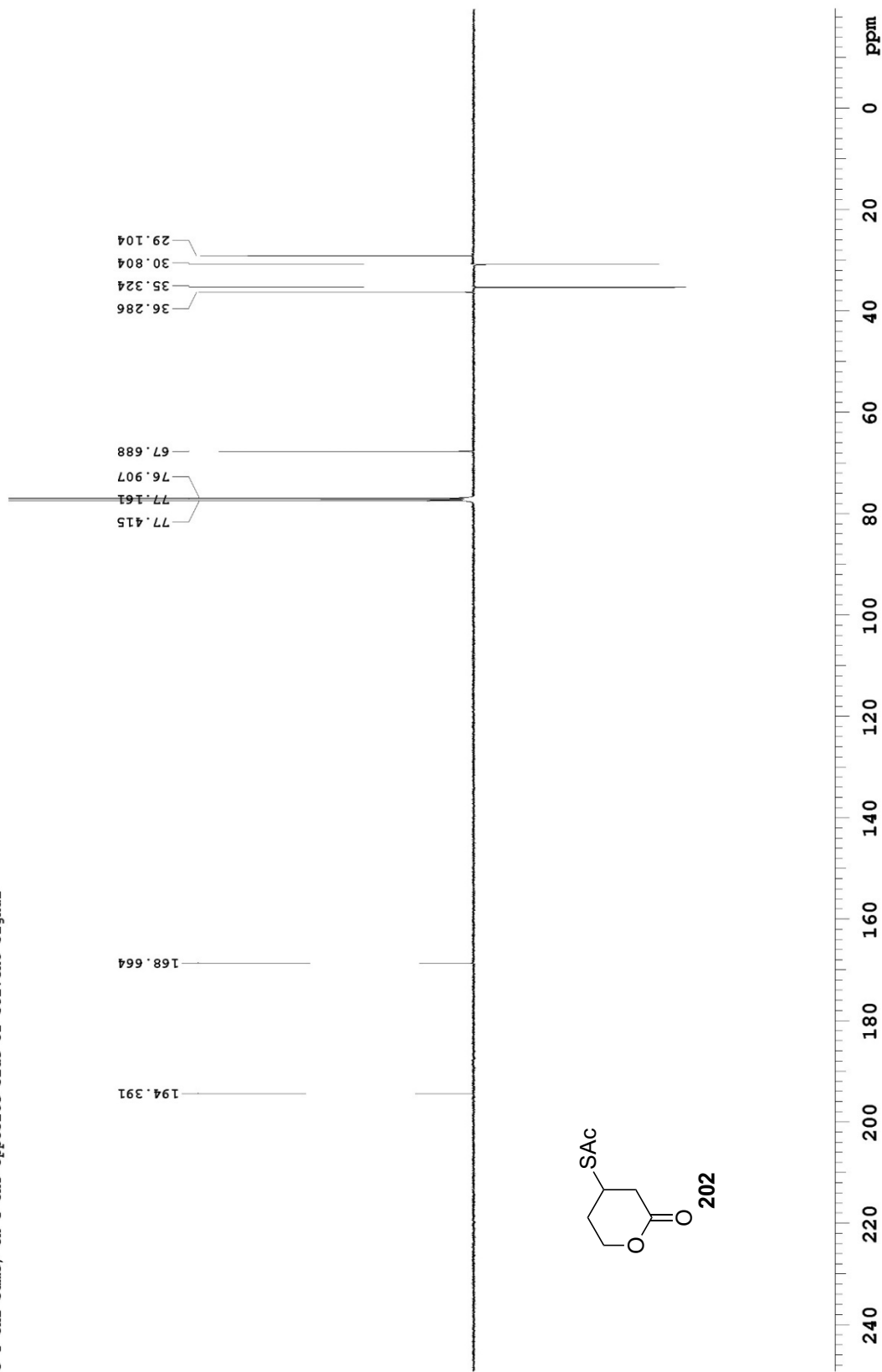
Pulse Sequence: APT_ad

Department of Chemistry, University of Alberta

499.806 MHz ¹H PRESAT in cdcl3 (ref. to CDCl3 @ 7.26 ppm), temp 27.7 C -> actual temp = 27.0 C, colddual probe



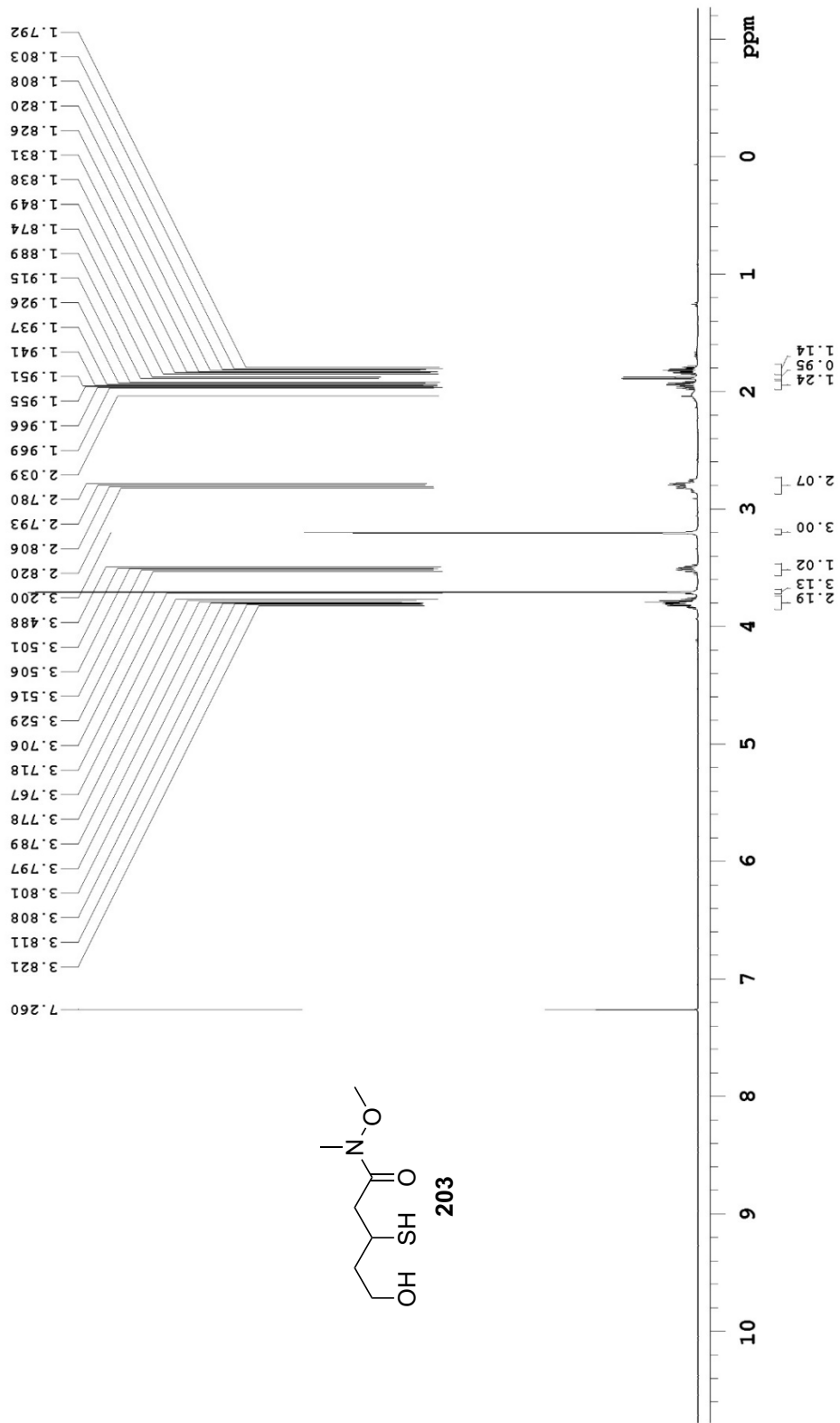
125.690 MHz C13[HL] APT_ad in cdcl3 (ref. to CDCl3 @ 77.06 ppm), temp 27.7 C -> actual temp = 27.0 C, coldddual probe
C & CH2 same, CH & CH3 opposite side of solvent signal



Pulse Sequence: APT_ad

Department of Chemistry, University of Alberta

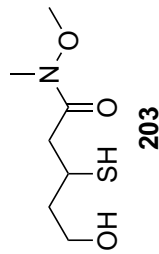
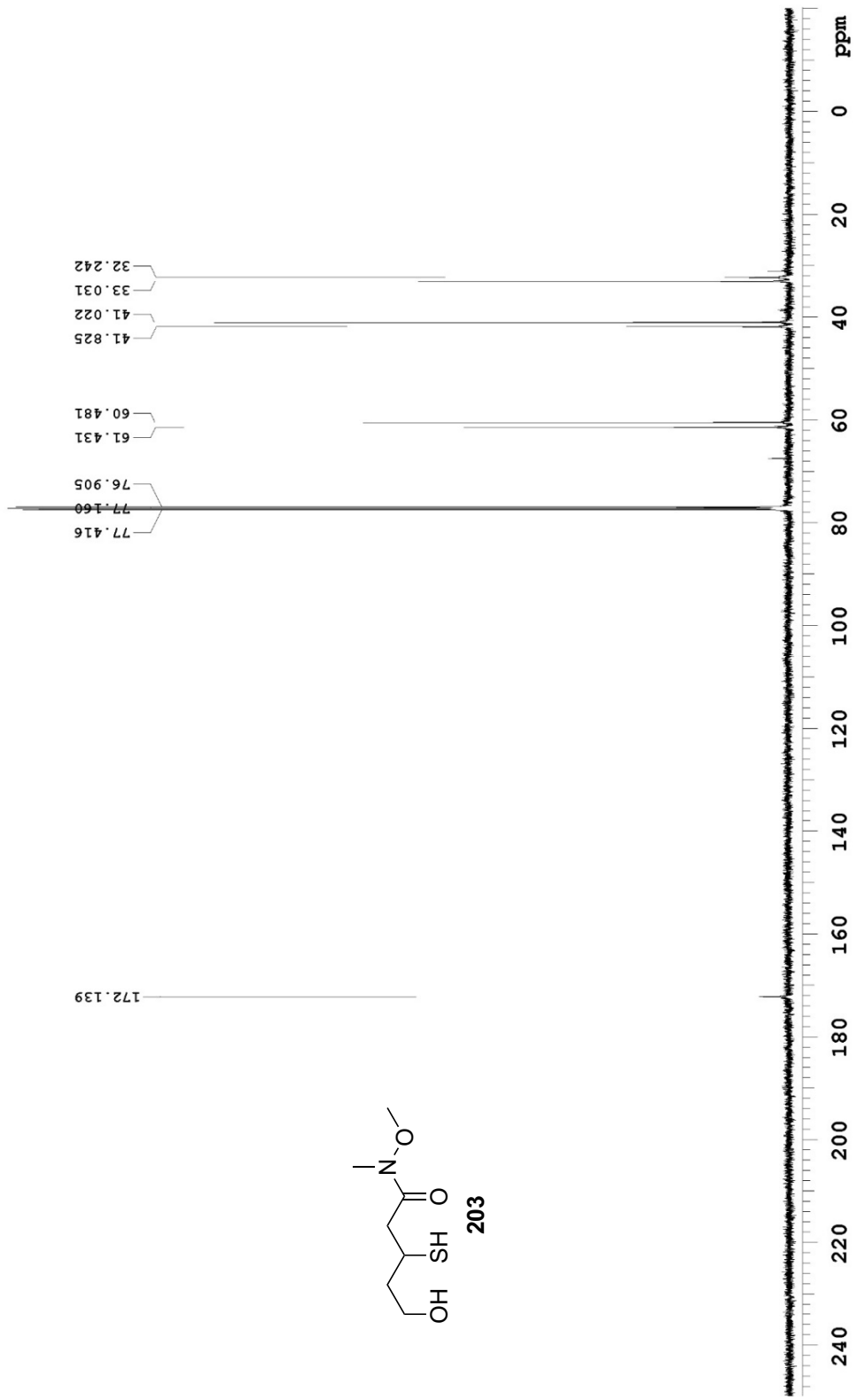
500 MHz 1D in CDCl3 (ref. to CDCl3 @ 7.26 ppm), temp 27.2 C -> actual temp = 27.0 C, sw500 probe



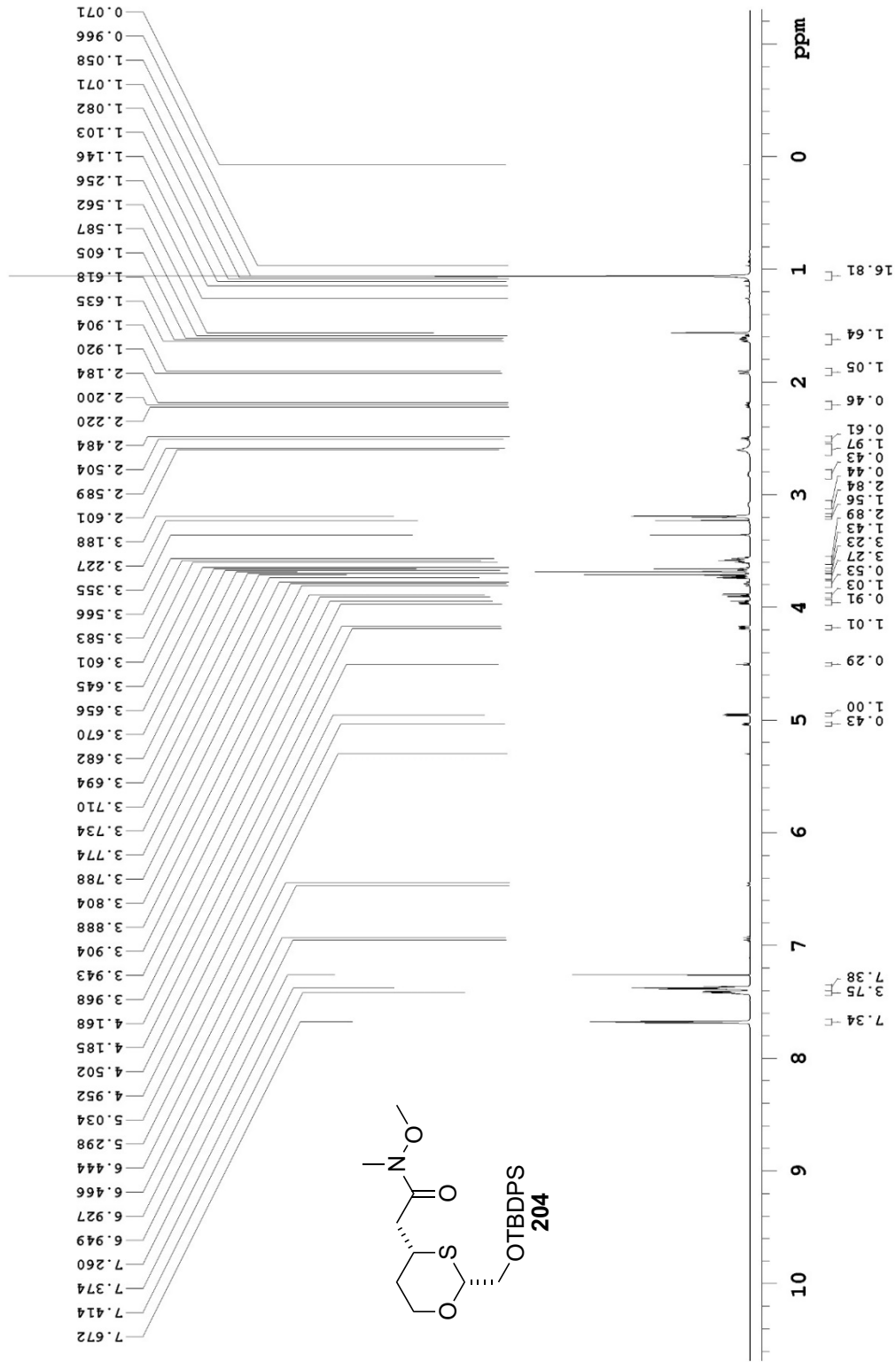
Pulse Sequence: s2pul

Department of Chemistry, University of Alberta

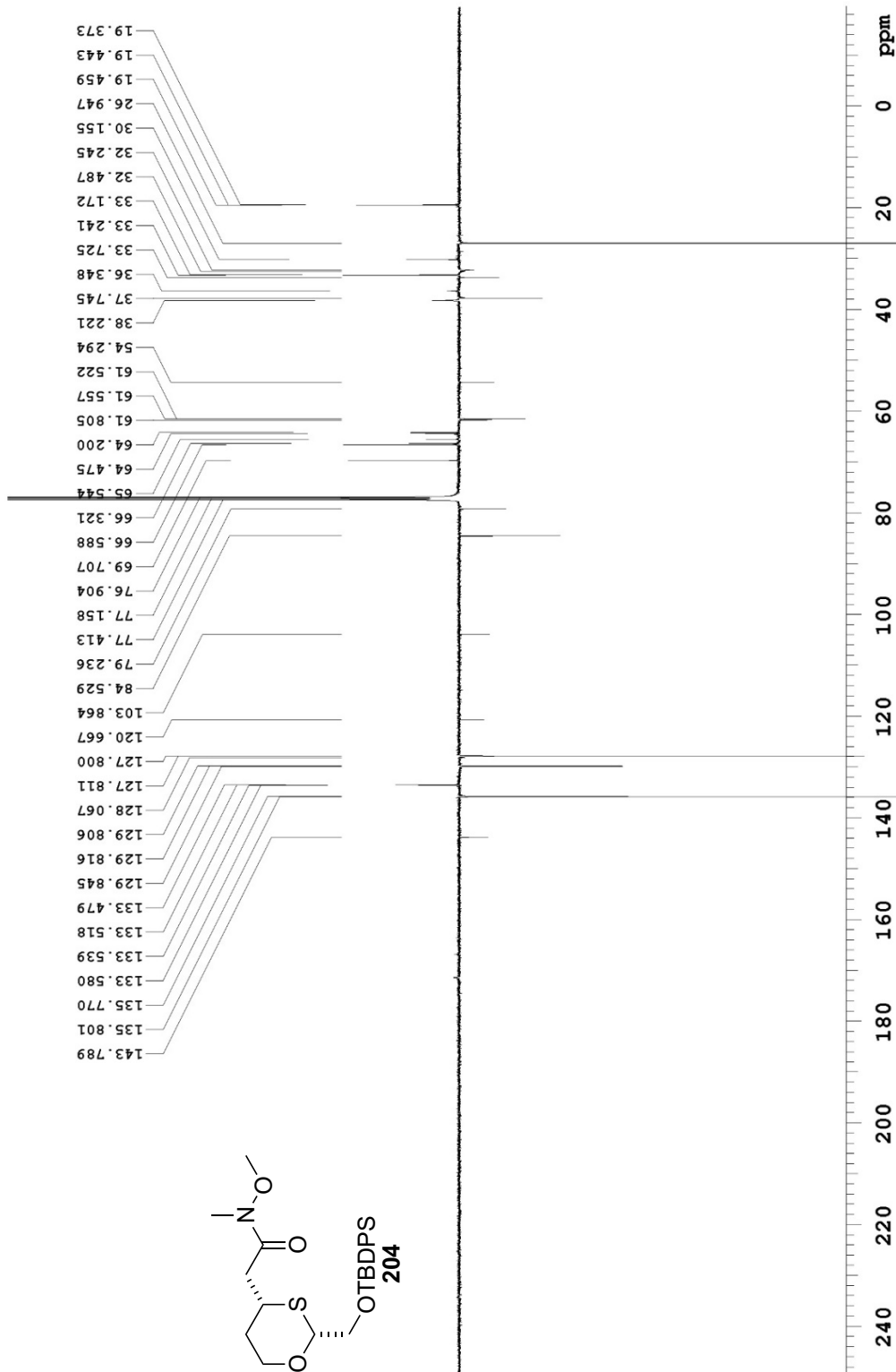
125 MHz 1D C13 in CDCl3 (ref. to CDCl3 @ 77.16 ppm), temp 27.2 C -> actual temp = 27.0 C, sw probe



699.762 MHz H1 PRESAT in cdcl3 (ref. to CDCl3 @ 7.26 ppm), temp 27.5 C -> actual temp = 27.0 C, coldid probe



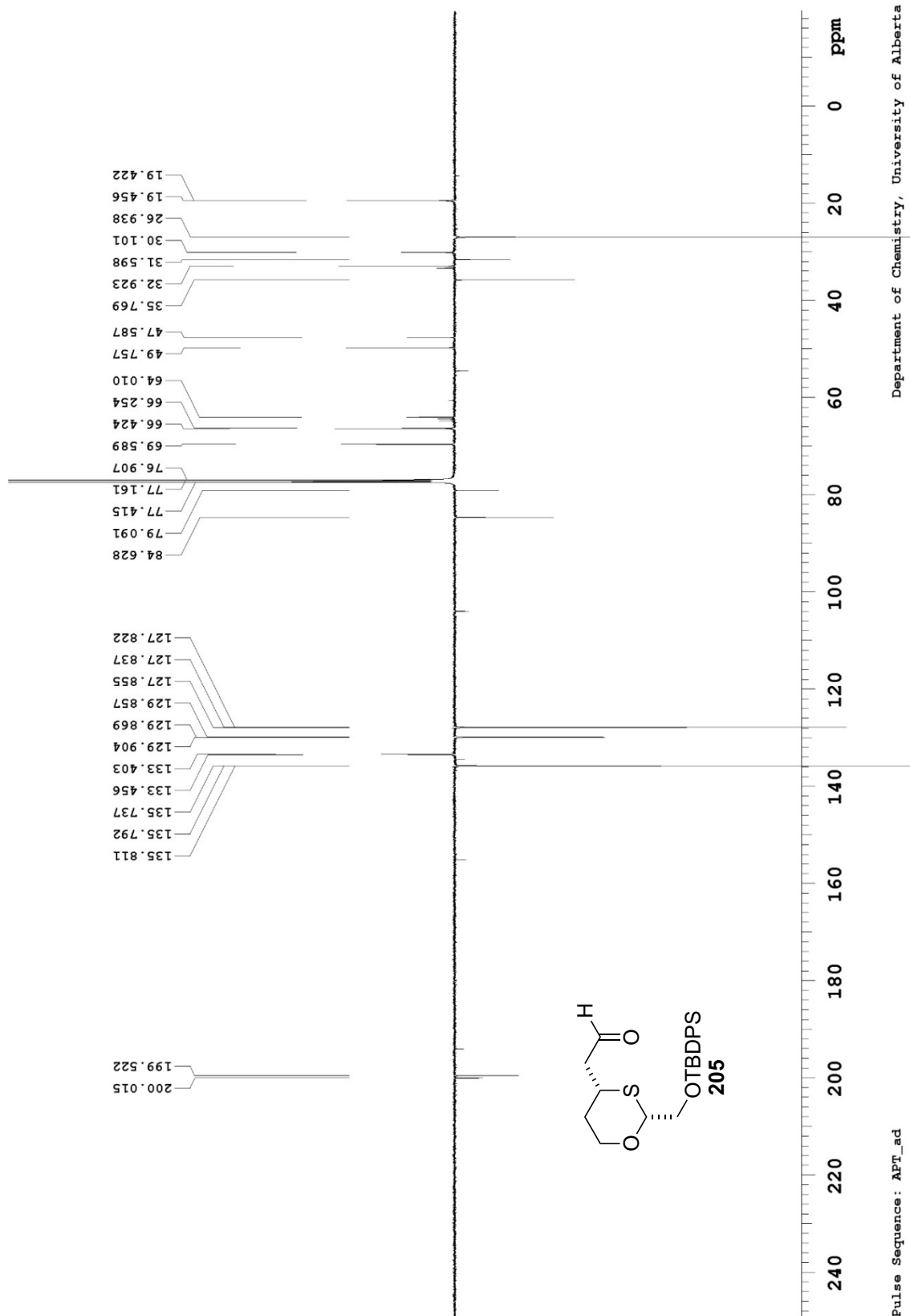
125.688 MHz ¹³C{¹H} APT_{ad} in cdcl3 (ref. to CDCl₃ @ 77.16 ppm), temp 27.7 C -> actual temp = 27.0 C, coldddual probe
 C & CH₂ same, CH & CH₃ opposite side of solvent signal



Pulse Sequence: APT_{ad}

Department of Chemistry, University of Alberta

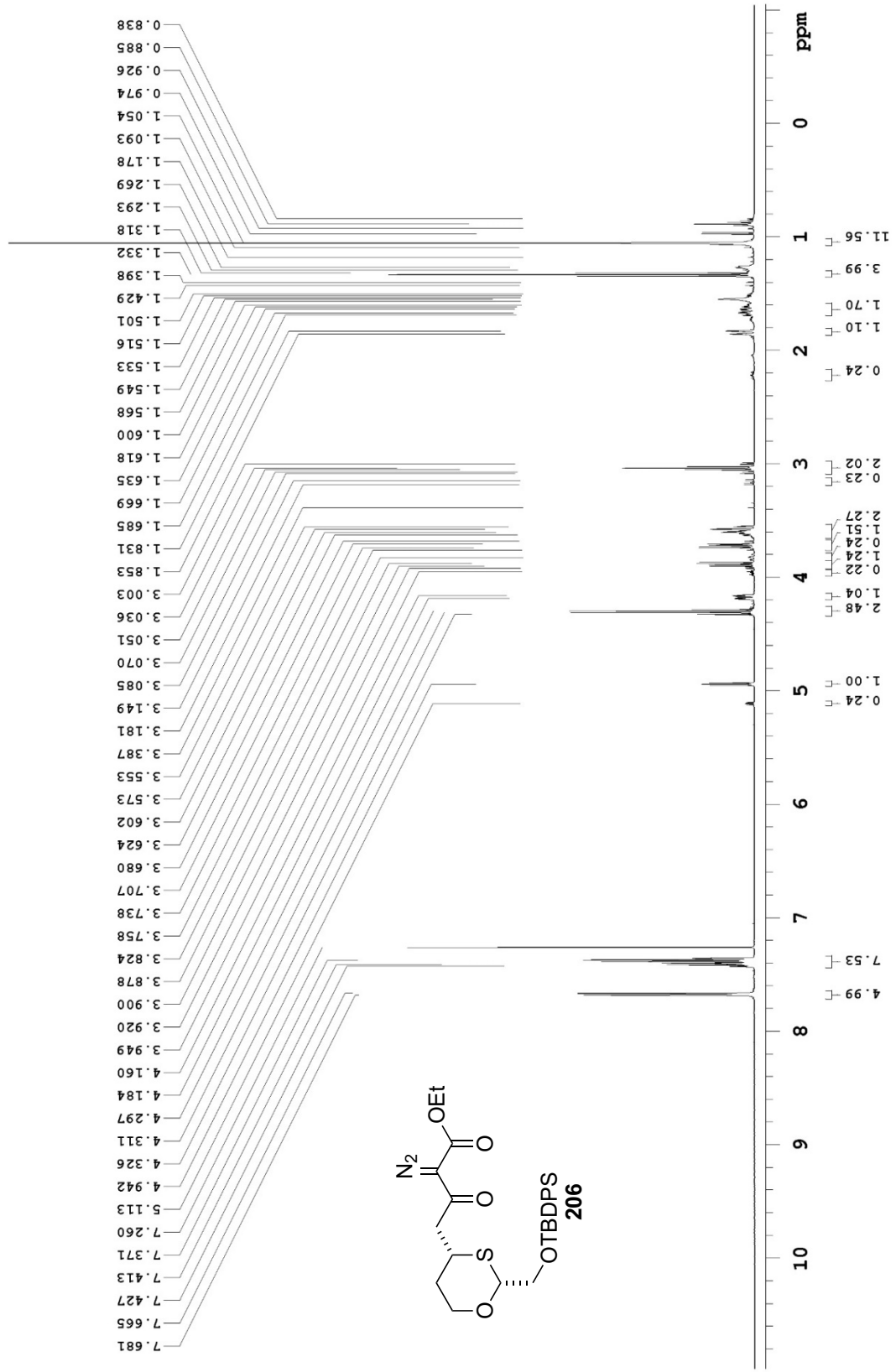
125.690 MHz C13[HL] APT_ad in cdc13 (ref. to CDC13 @ 77.16 ppm), temp 27.7 C -> actual temp = 27.0 C, coldddual probe
 C & CH2 same, CH & CH3 opposite side of solvent signal



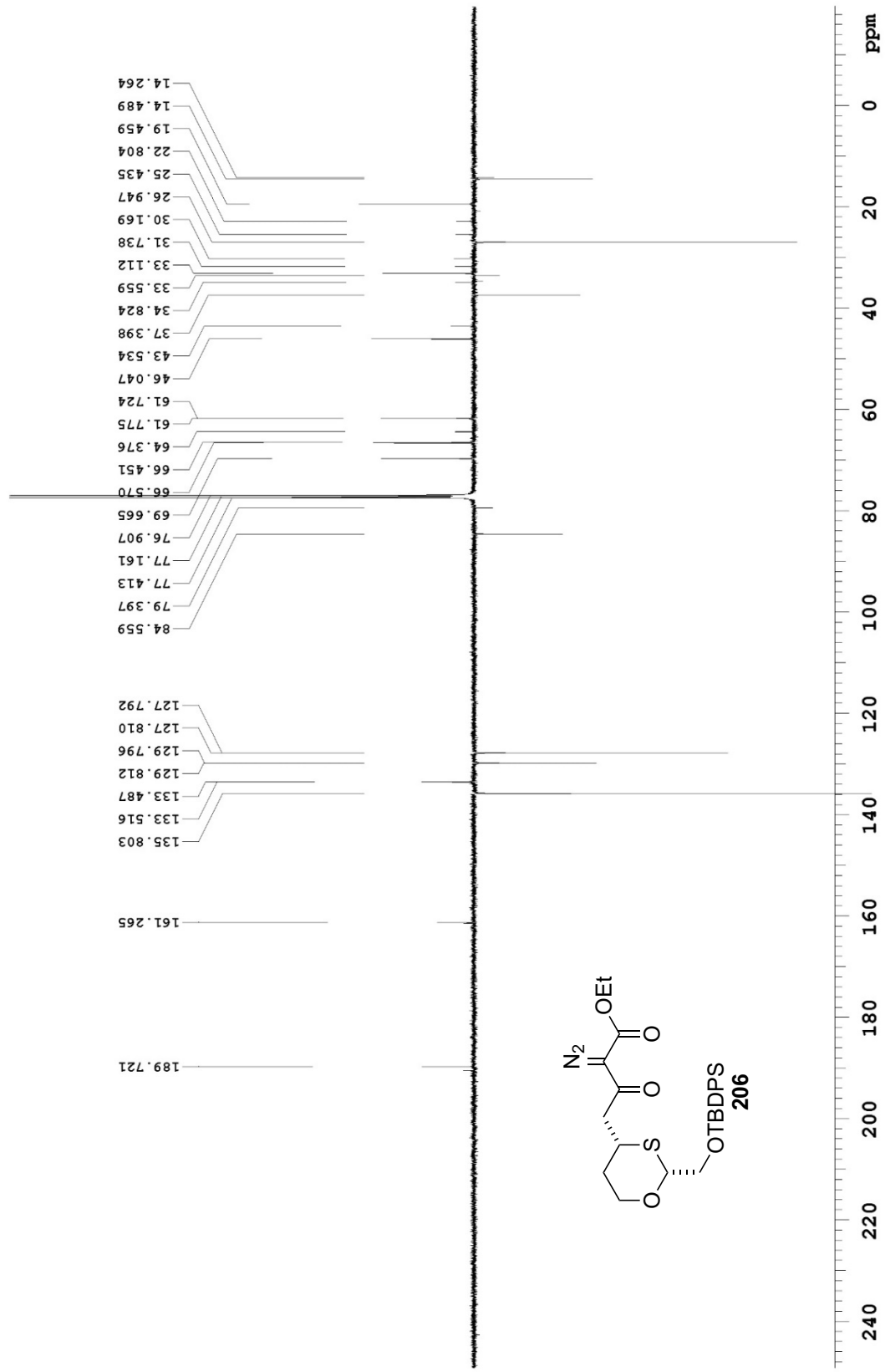
Pulse Sequence: APT_ad

Department of Chemistry, University of Alberta

499.806 MHz H1 PRESAT in cdcl3 (ref. to CDCl3 @ 7.26 ppm), temp 27.7 C -> actual temp = 27.0 C, coldddual probe

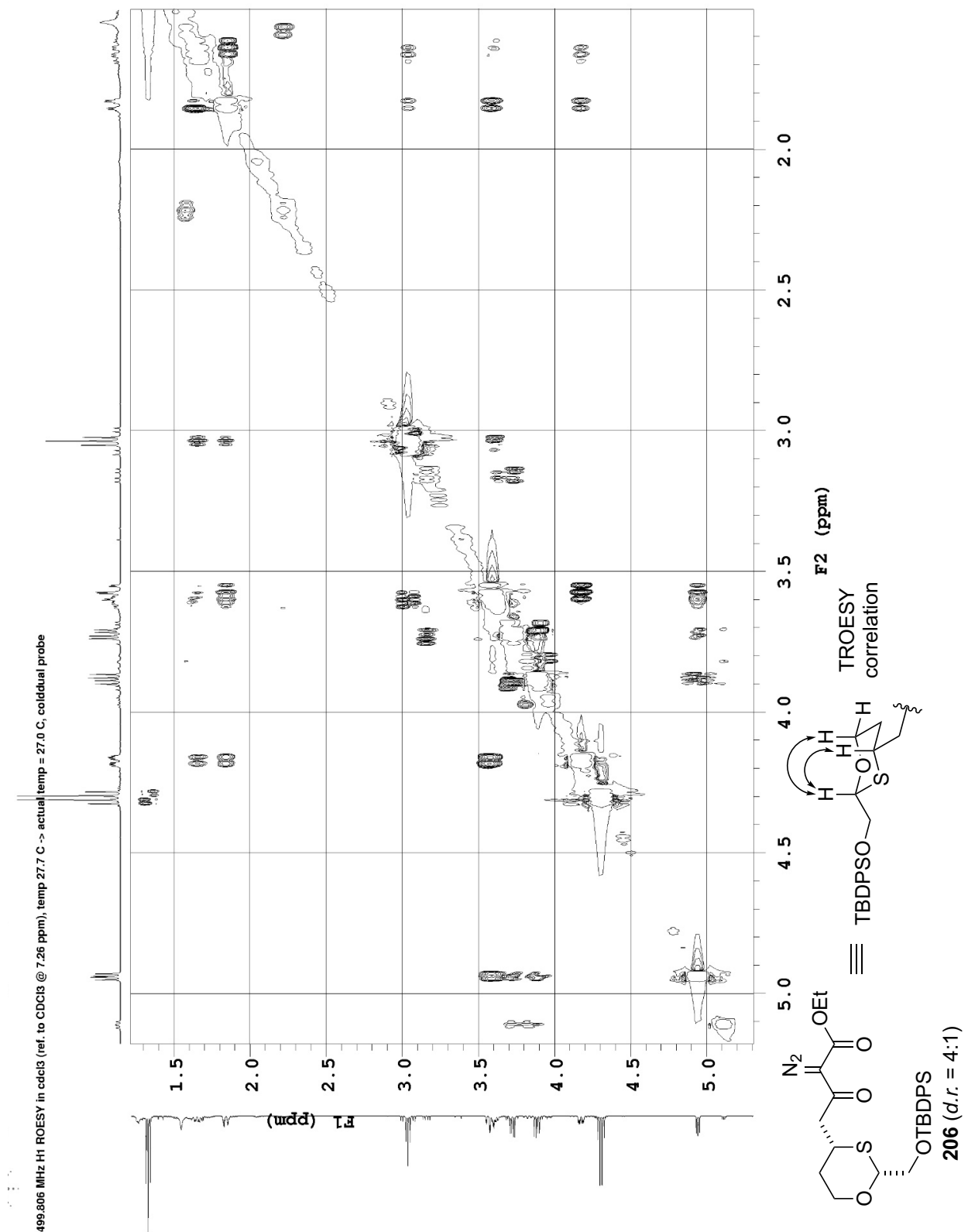


125.690 MHz ¹³C{¹H} APT_ad in cdcl3 (ref. to CDCl3 @ 77.16 ppm), temp 27.7 C -> actual temp = 27.0 C, cold dual probe
 C & CH2 same, CH & CH3 opposite side of solvent signal

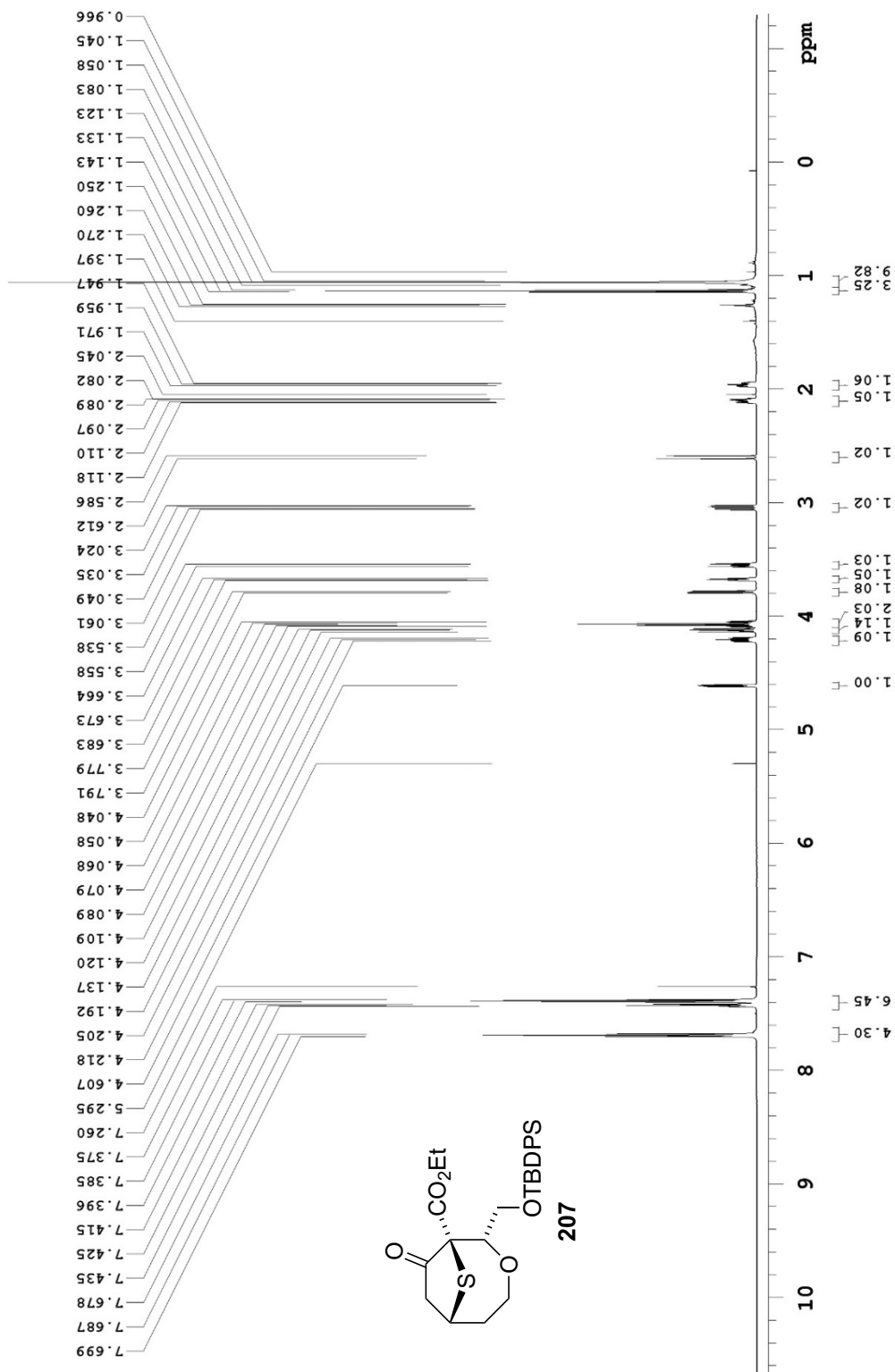


Pulse Sequence: APT_ad

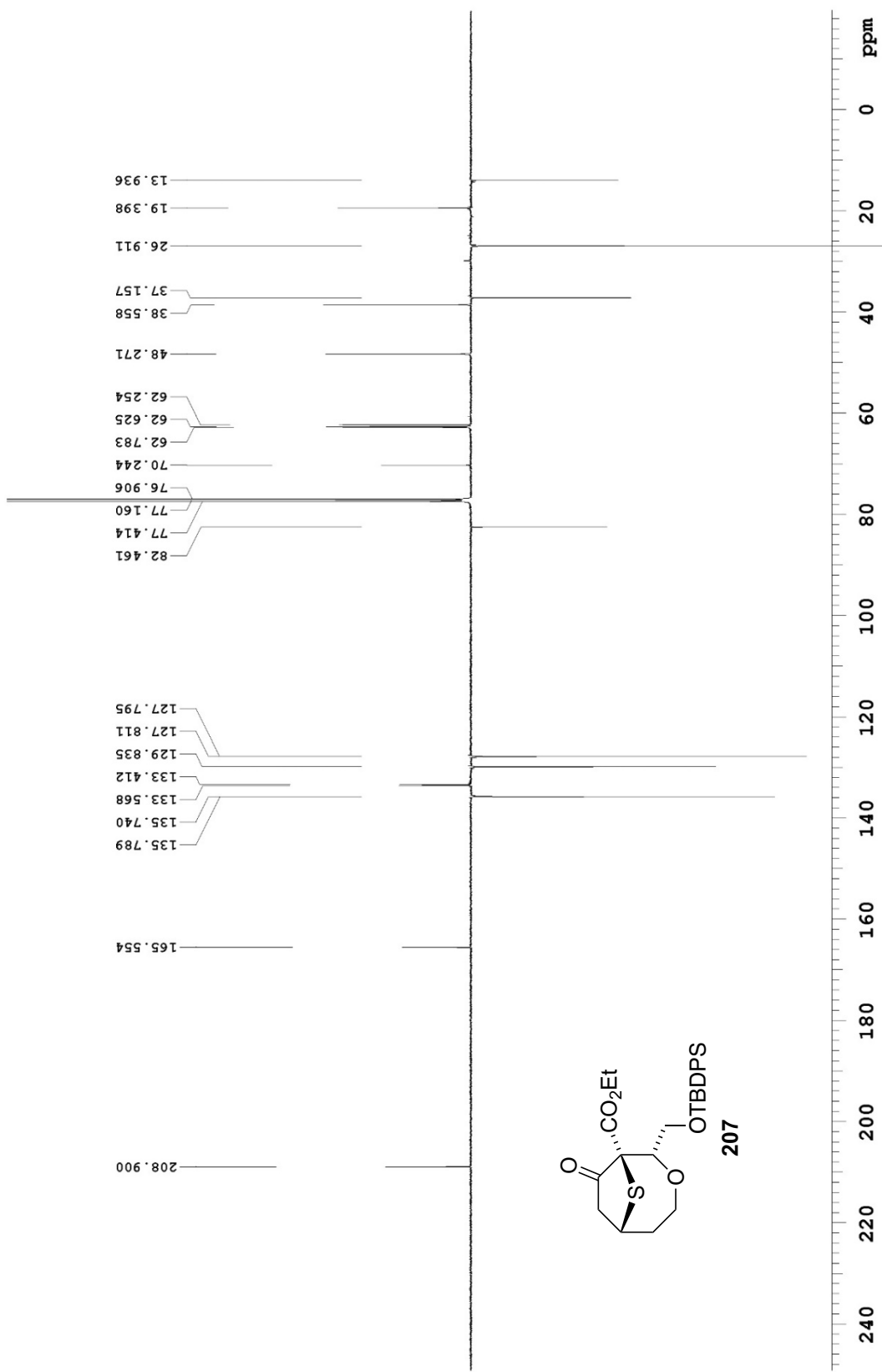
Department of Chemistry, University of Alberta



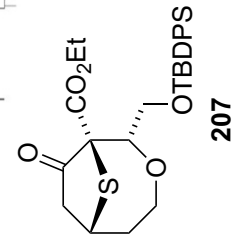
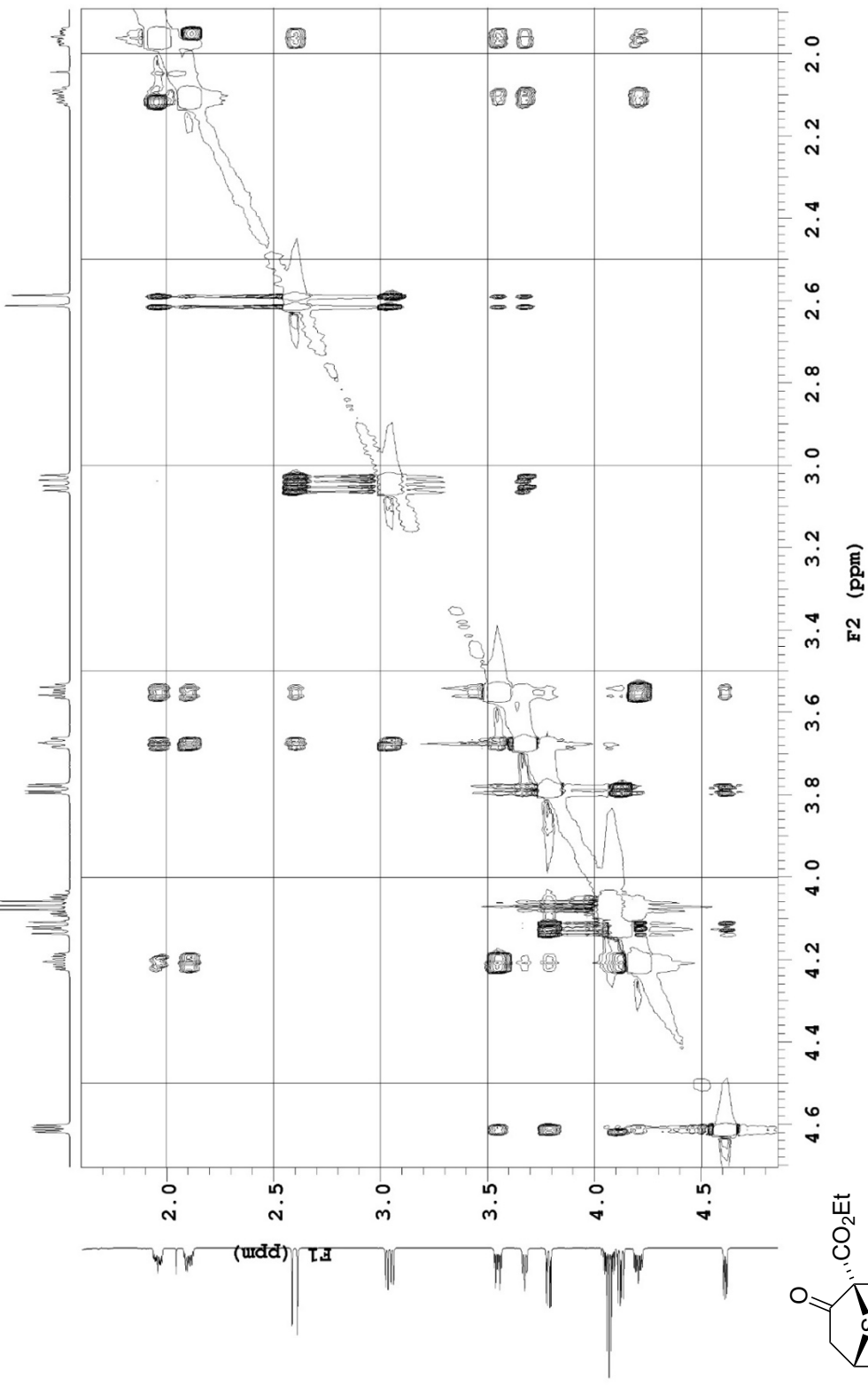
699.762 MHz H1 PRESAT in cdcl3 (ref. to CDCl3 @ 7.26 ppm), temp 27.5 C -> actual temp = 27.0 C, coldid probe



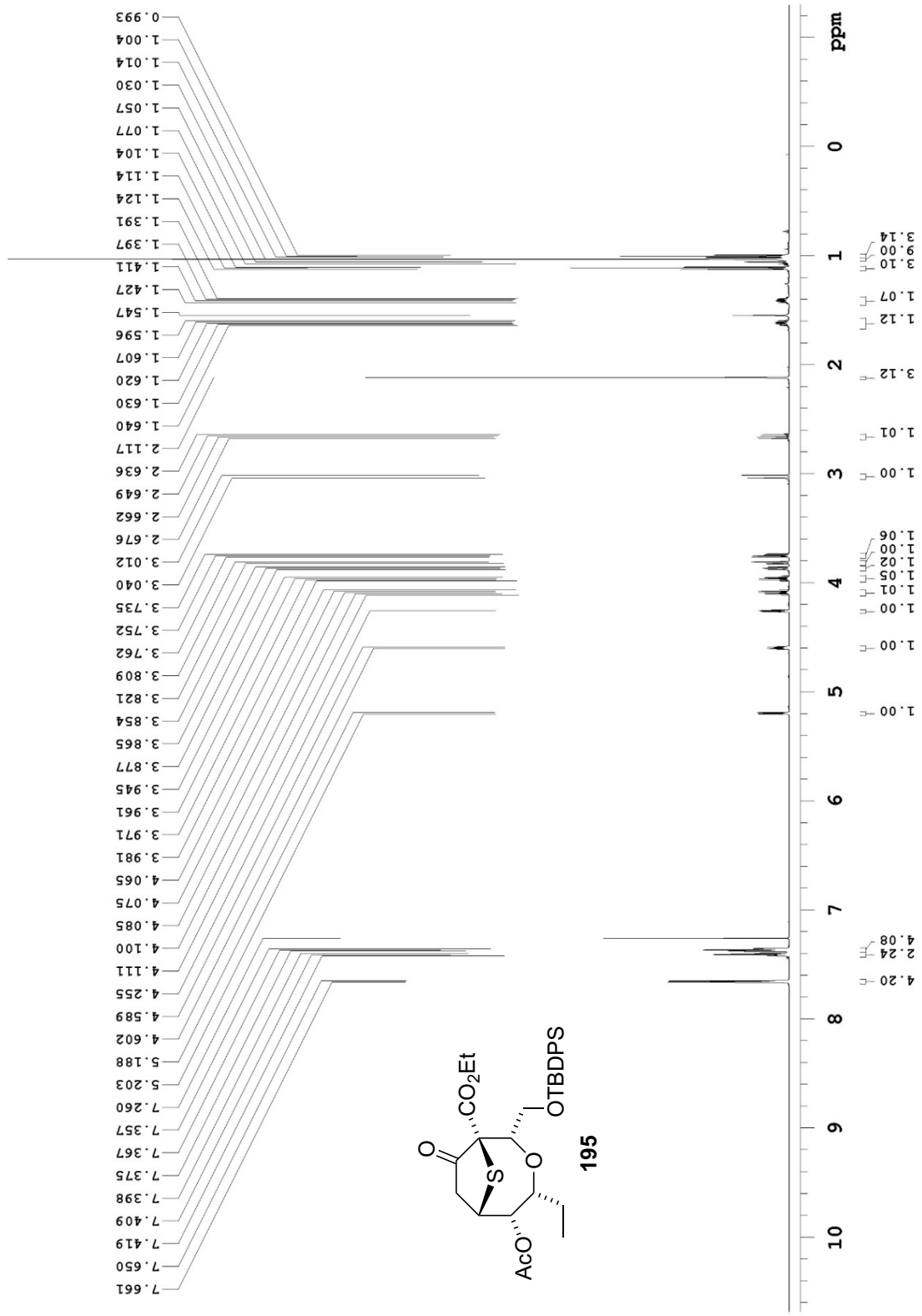
125.690 MHz C13[H1] APT_ad in cdcl3 (ref. to CDCl3 @ 77.16 ppm), temp 27.7 C -> actual temp = 27.0 C, coldddual probe
 C & CH2 same, CH & CH3 opposite side of solvent signal



699.762 MHz H1 ROESY in cdcl3 (ref. to CDCl3 @ 7.26 ppm), temp 27.5 C -> actual temp = 27.0 C, coldid probe



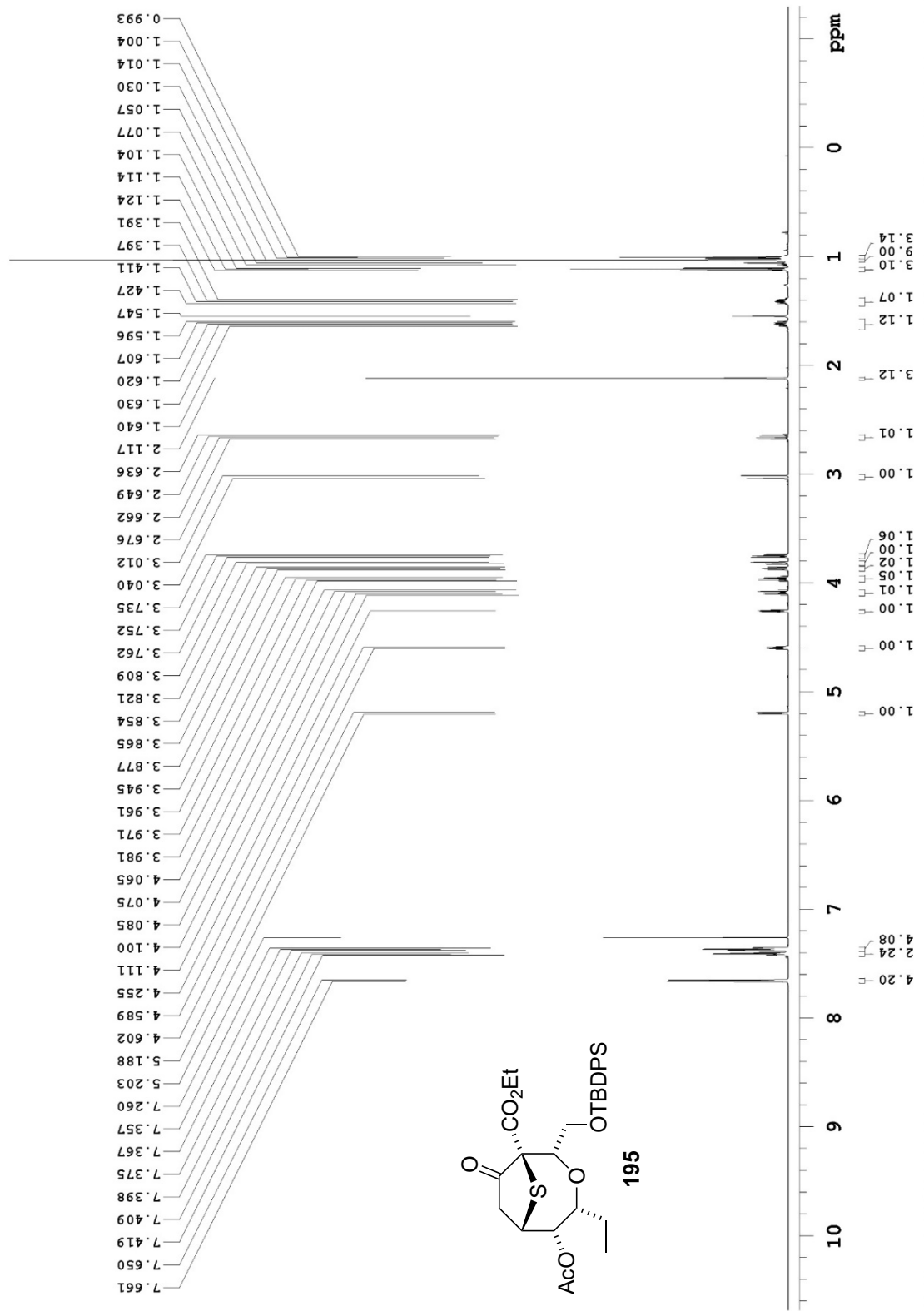
699.762 MHz H1 PRESAT in cdcl3 (ref. to CDCl3 @ 7.26 ppm), temp 27.5 C -> actual temp = 27.0 C, coldidid probe



Department of Chemistry, University of Alberta

Pulse Sequence: PRESAT

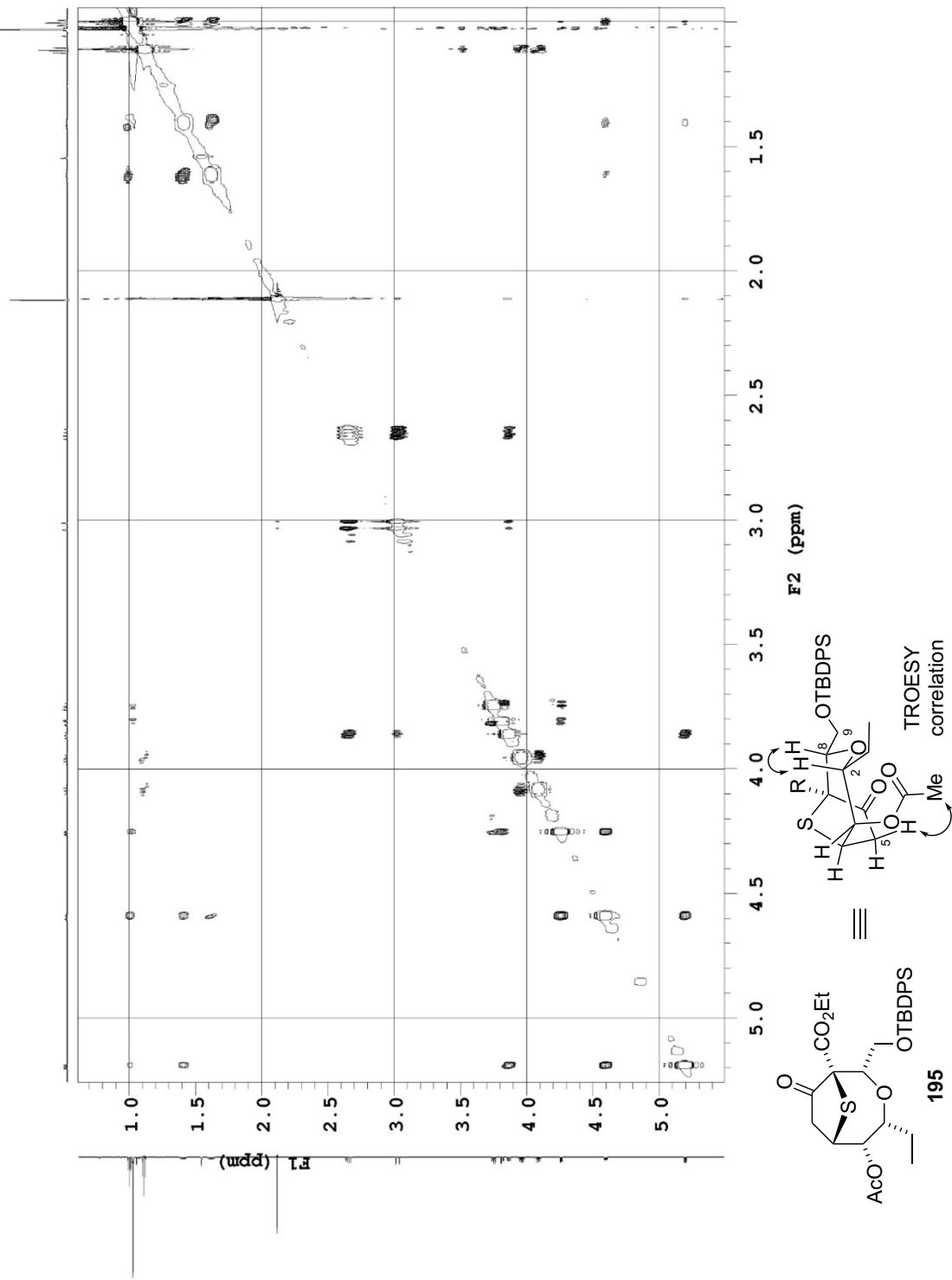
699.762 MHz H1 PRESAT in cdcl3 (ref. to CDCl3 @ 7.26 ppm), temp 27.5 C -> actual temp = 27.0 C, coldid probe



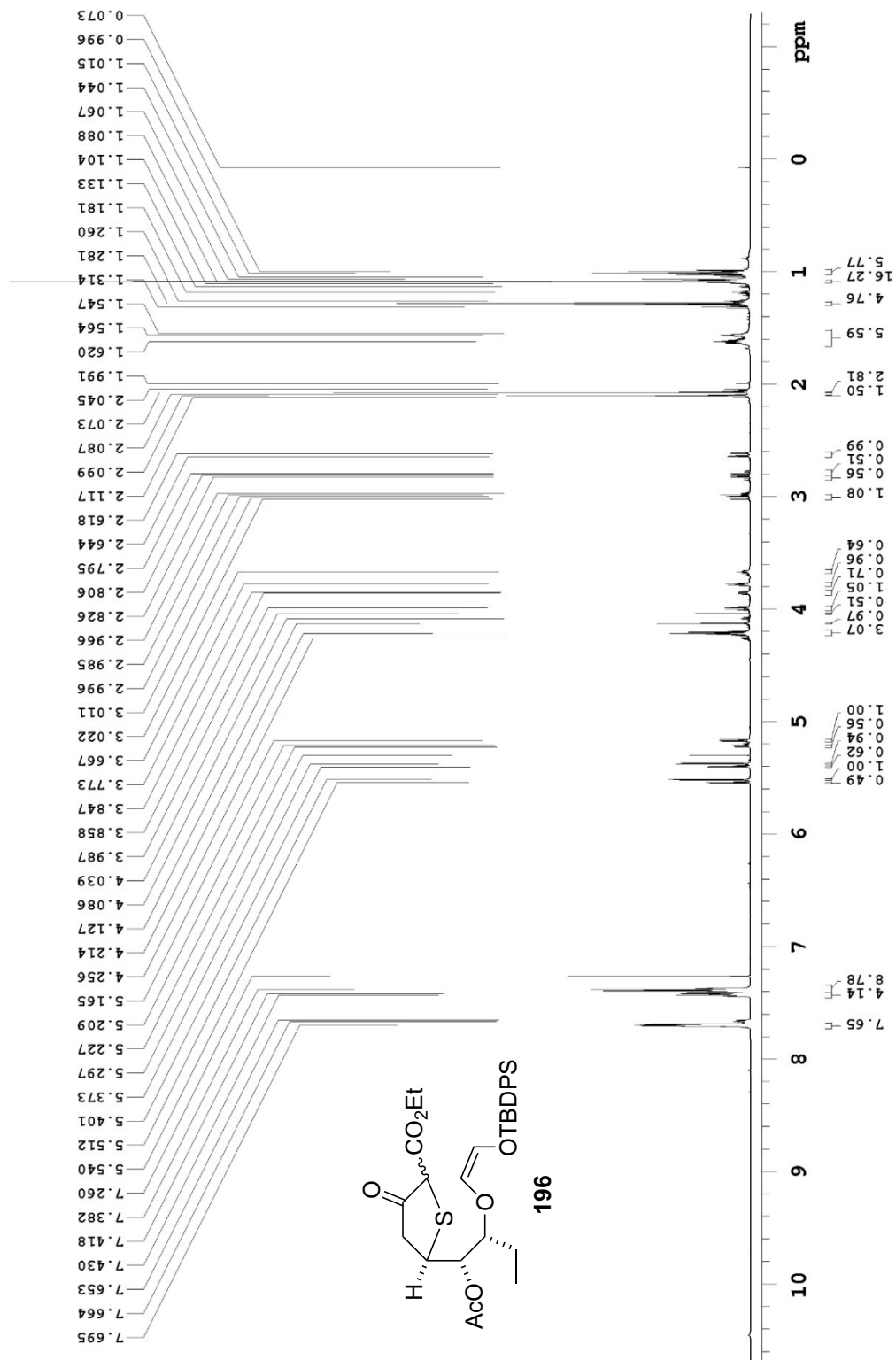
Department of Chemistry, University of Alberta

Pulse Sequence: PRESAT

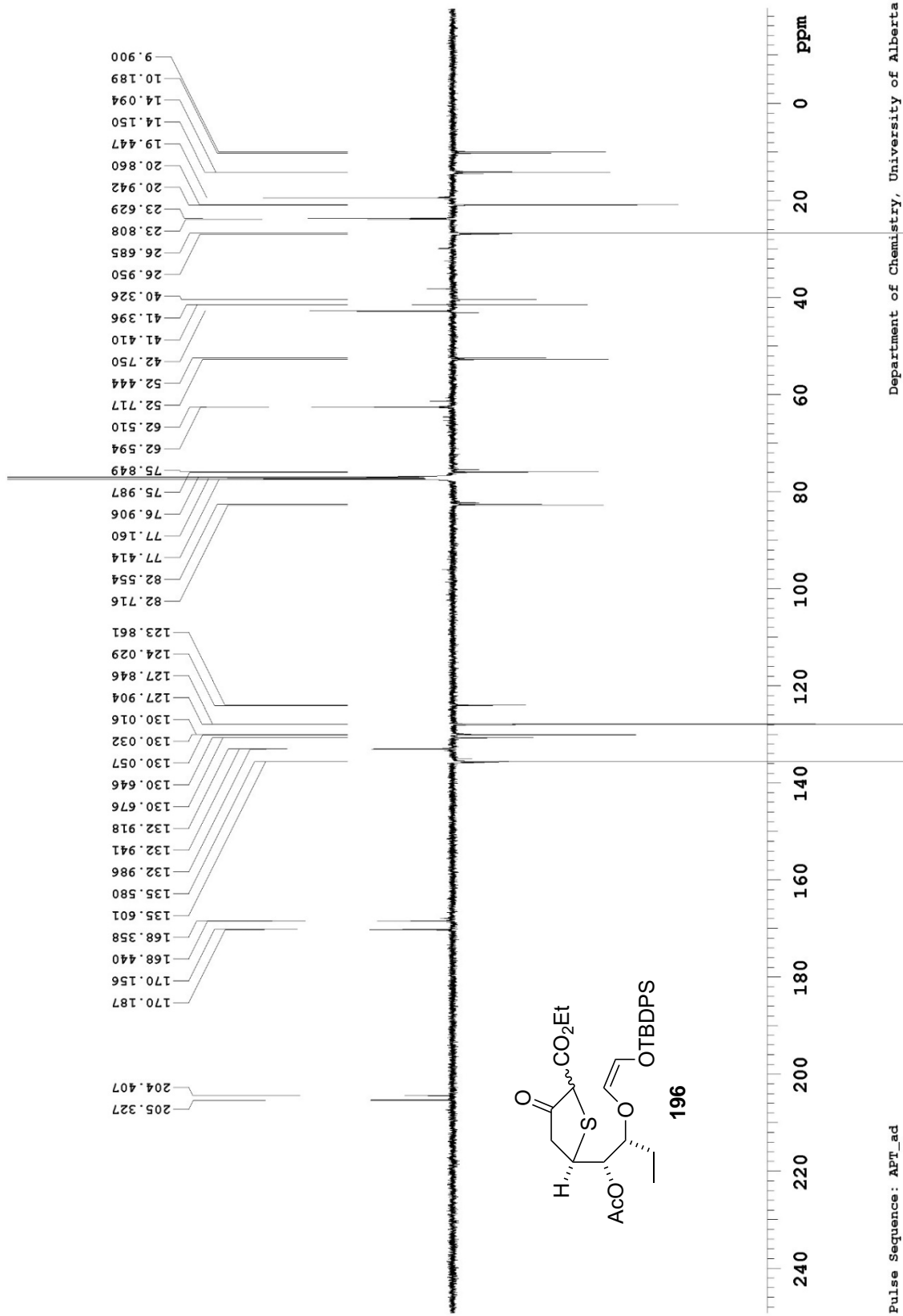
699.762 MHz ¹H ROESY in cdcl₃ (ref. to CDC13 @ 7.26 ppm), temp 27.5 C -> actual temp = 27.0 C, coldfil probe



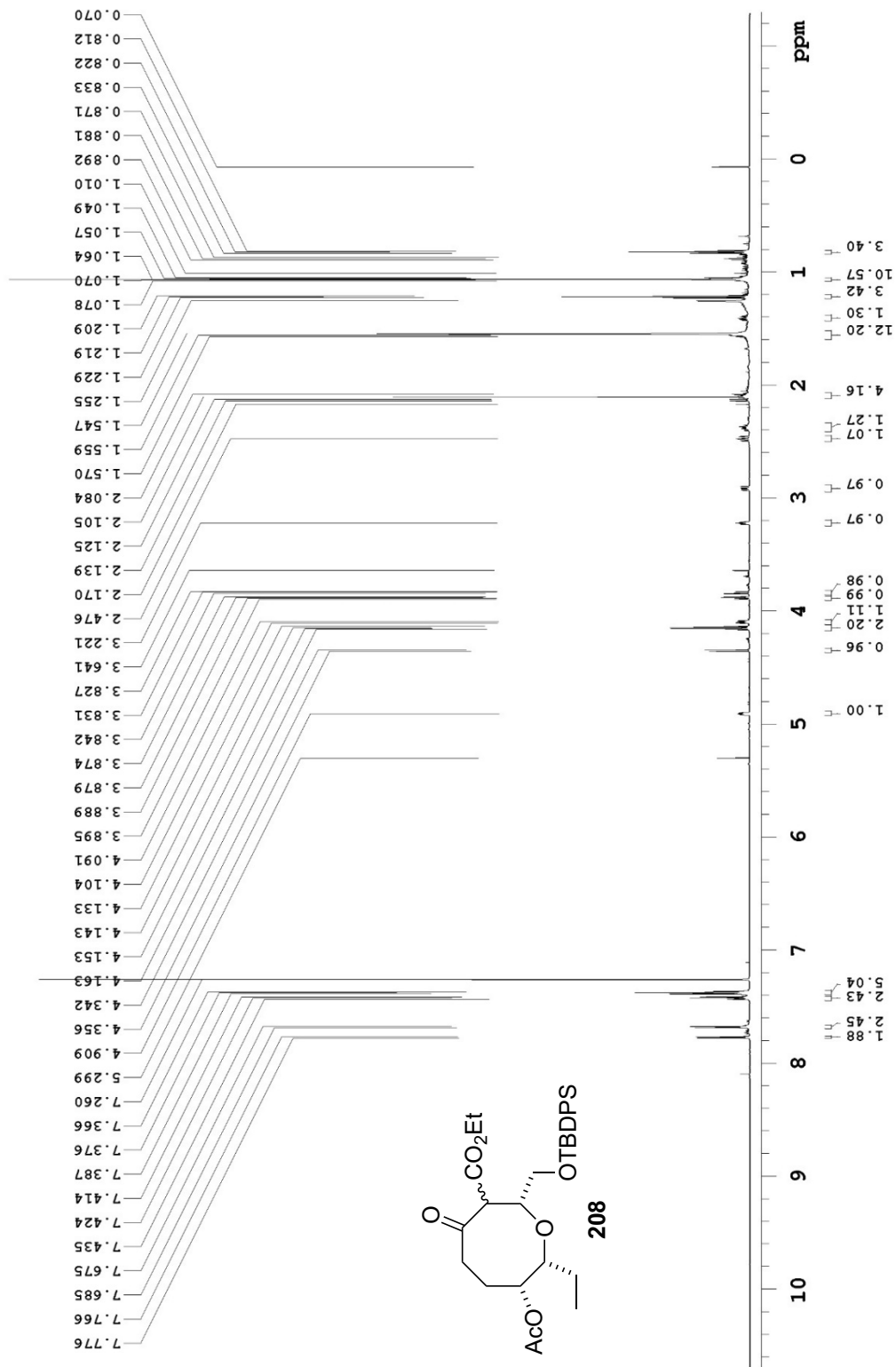
699.762 MHz ¹H PRESAT in cdcl3 (ref. to CDCl3 @ 7.26 ppm), temp 27.5 C -> actual temp = 27.0 C, coldid probe



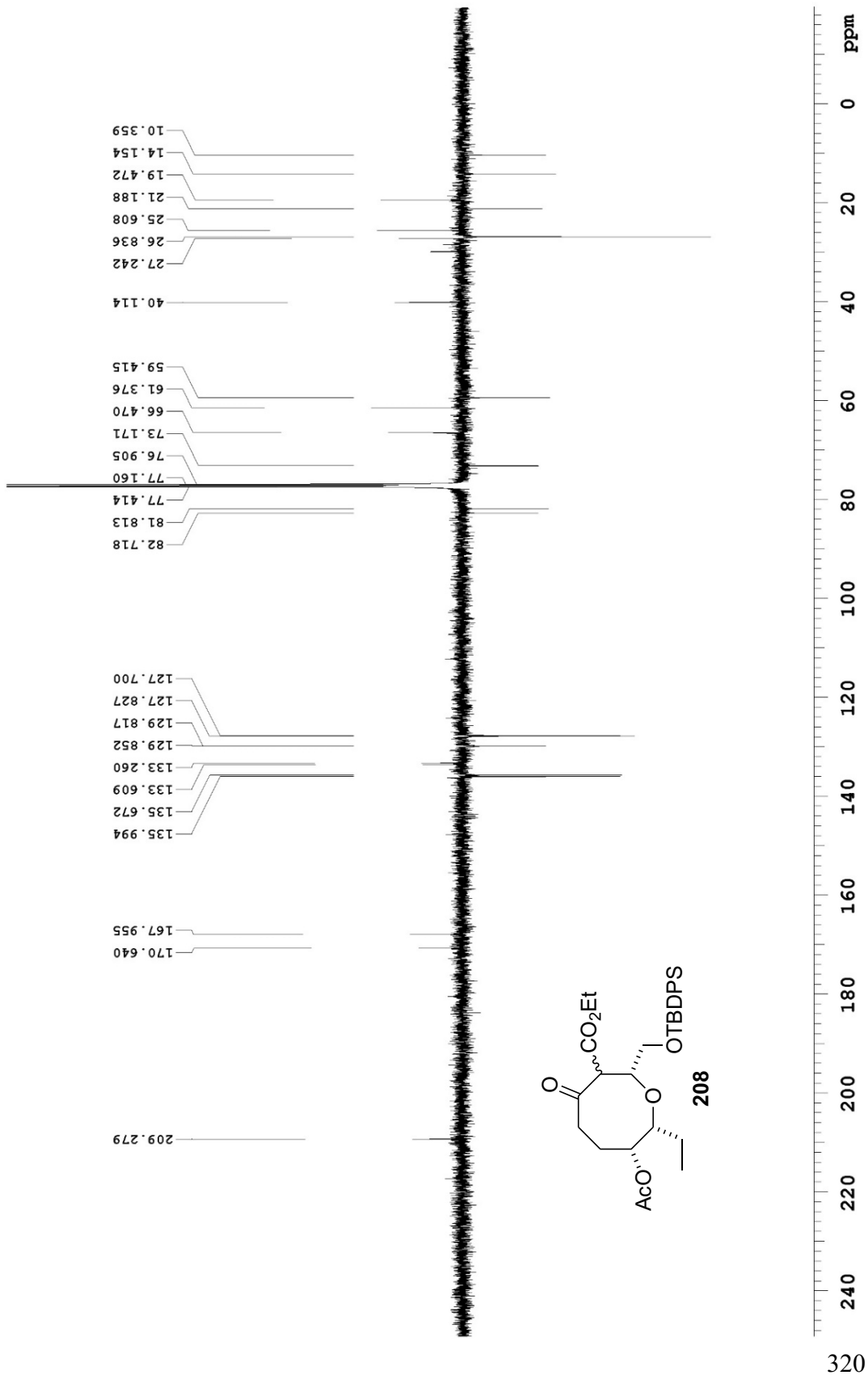
125.690 MHz C13[HI] APT_ad in cdcl3 (ref. to cdcl3 @ 77.16 ppm), temp 27.7 C -> actual temp = 27.0 C, coldddual probe
 C & CH2 same, CH & CH3 opposite side of solvent signal



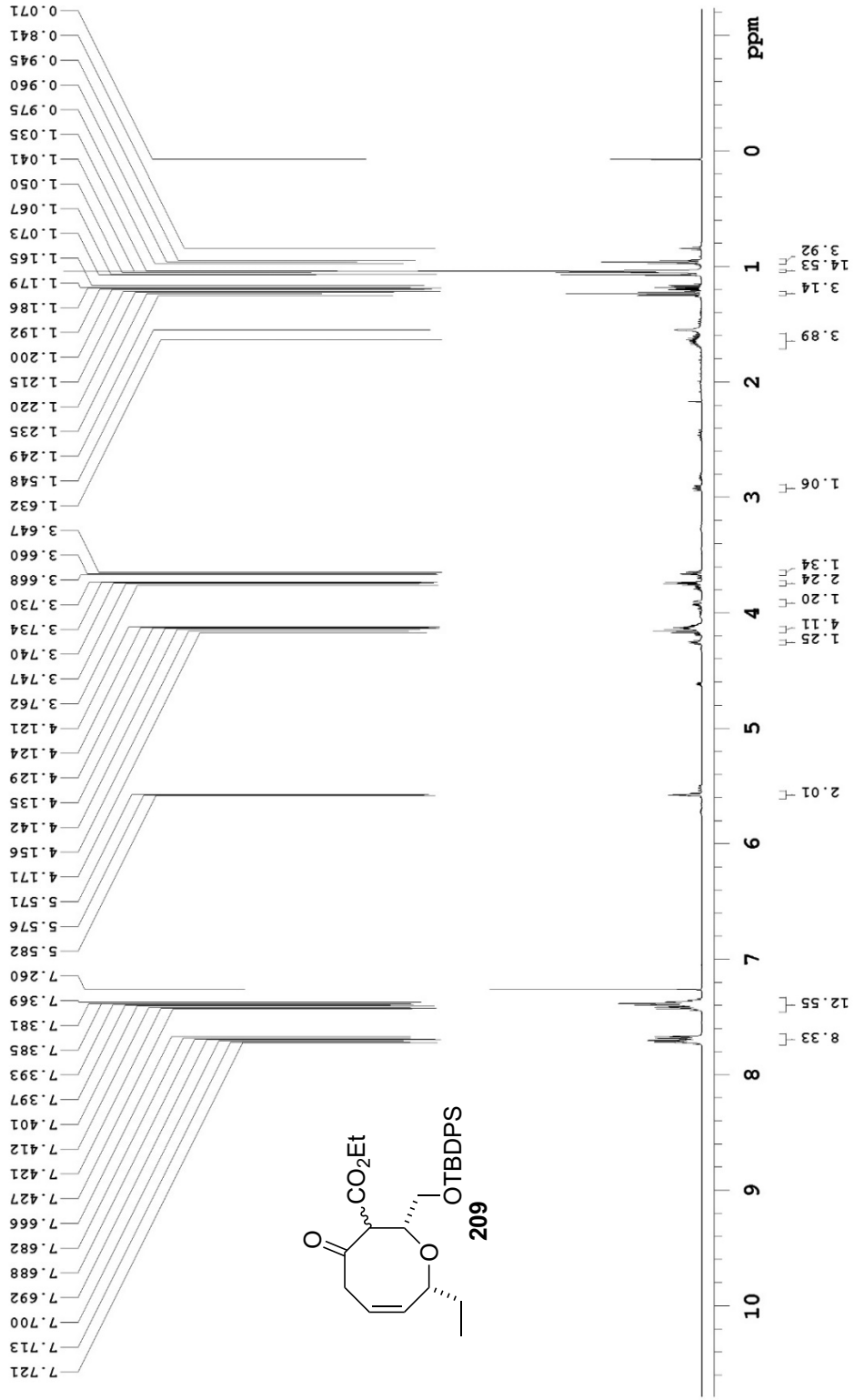
699.769 MHz H1 PRESAT in cdcl3 (ref. to CDCl3 @ 7.26 ppm), temp 27.5 C -> actual temp = 27.0 C, coldid probe



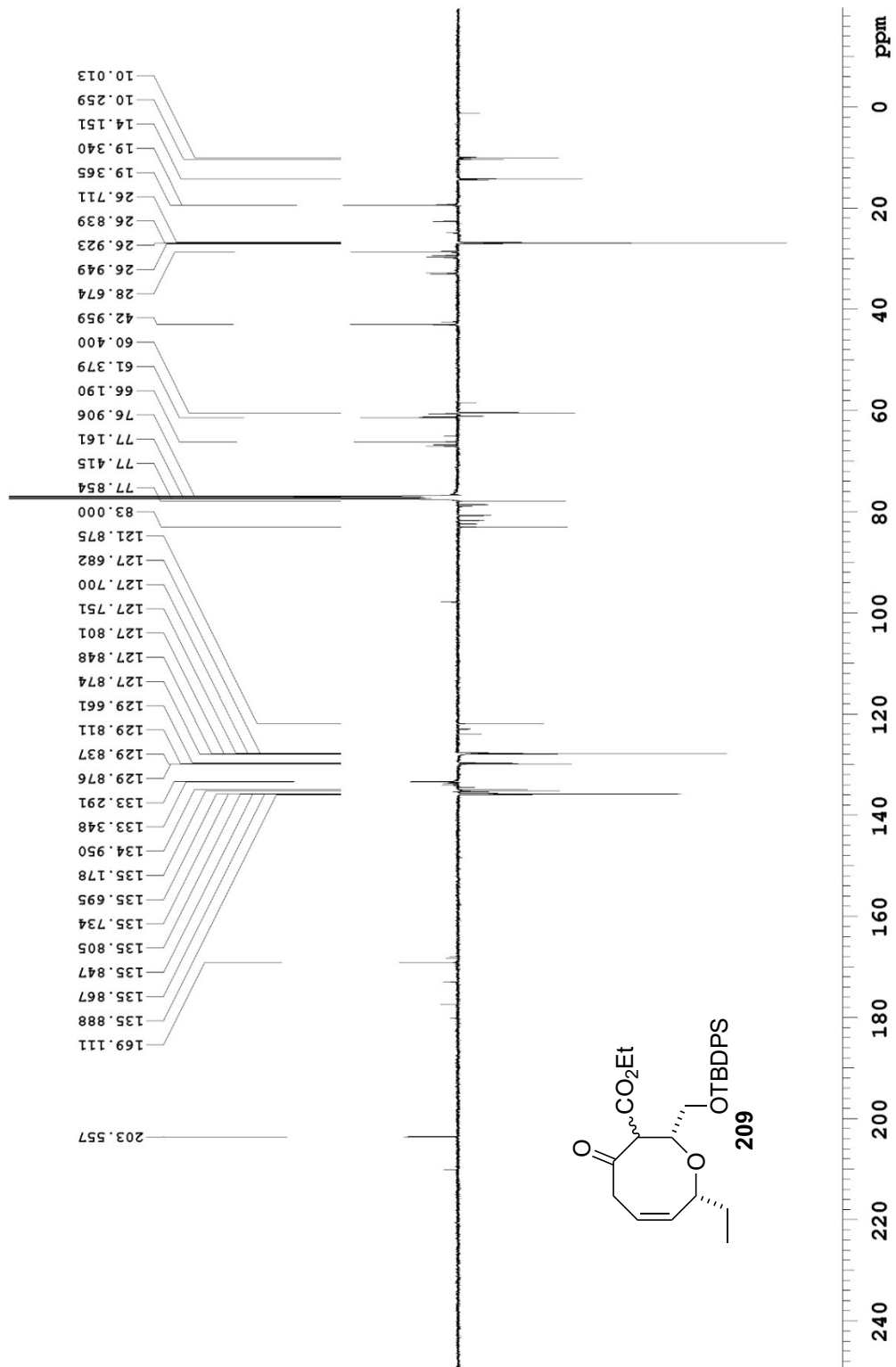
125.690 MHz C13[H1] APT_ad in cdcl3 (ref. to CDCl3 @ 77.16 ppm), temp 27.7 C -> actual temp = 27.0 C, coldddual probe
 C & CH2 same, CH & CH3 opposite side of solvent signal



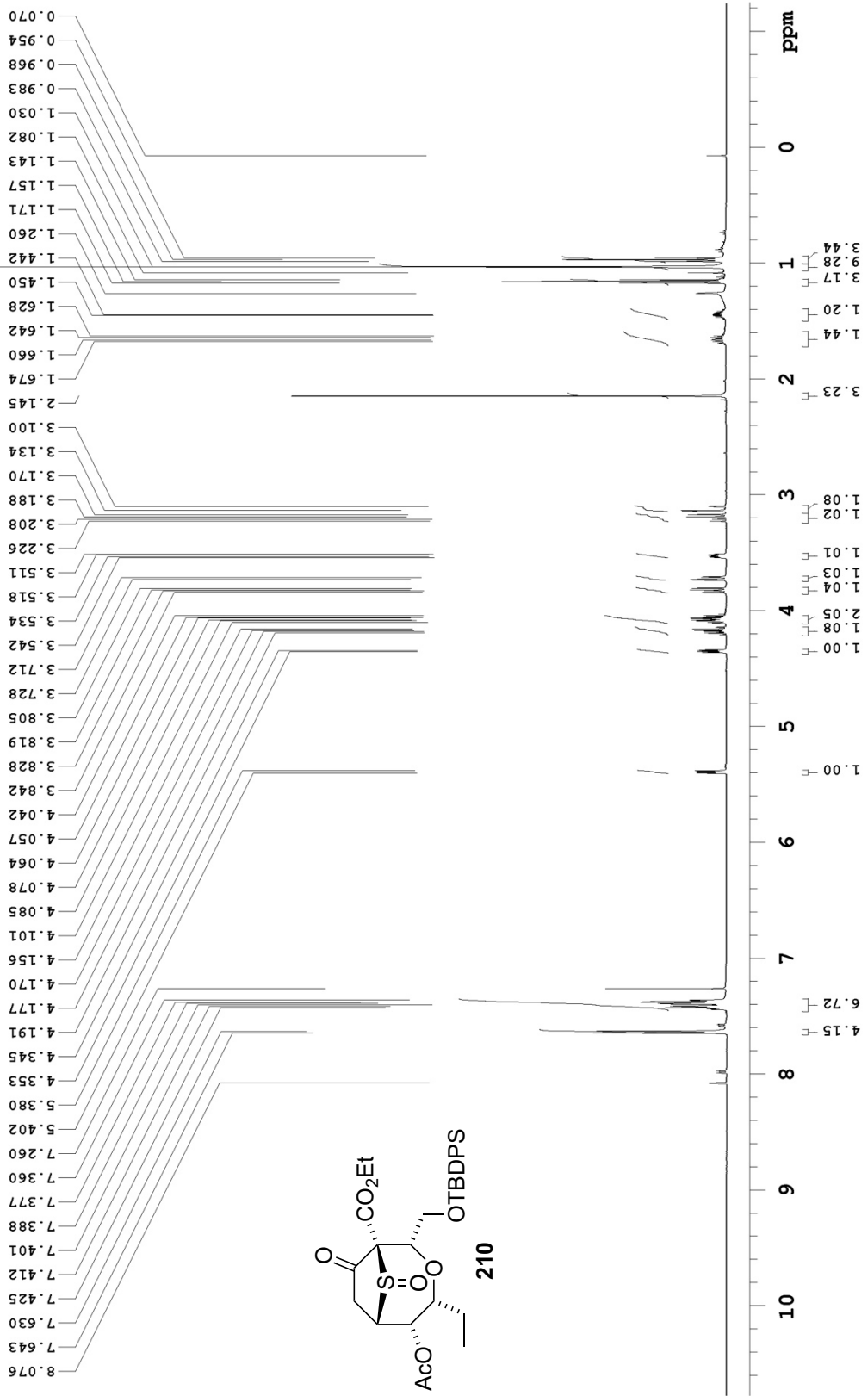
499.797 MHz ¹H PRESAT in cdcl3 (ref. to CDCl3 @ 7.26 ppm), temp 27.7 C -> actual temp = 27.0 C, coldddual probe



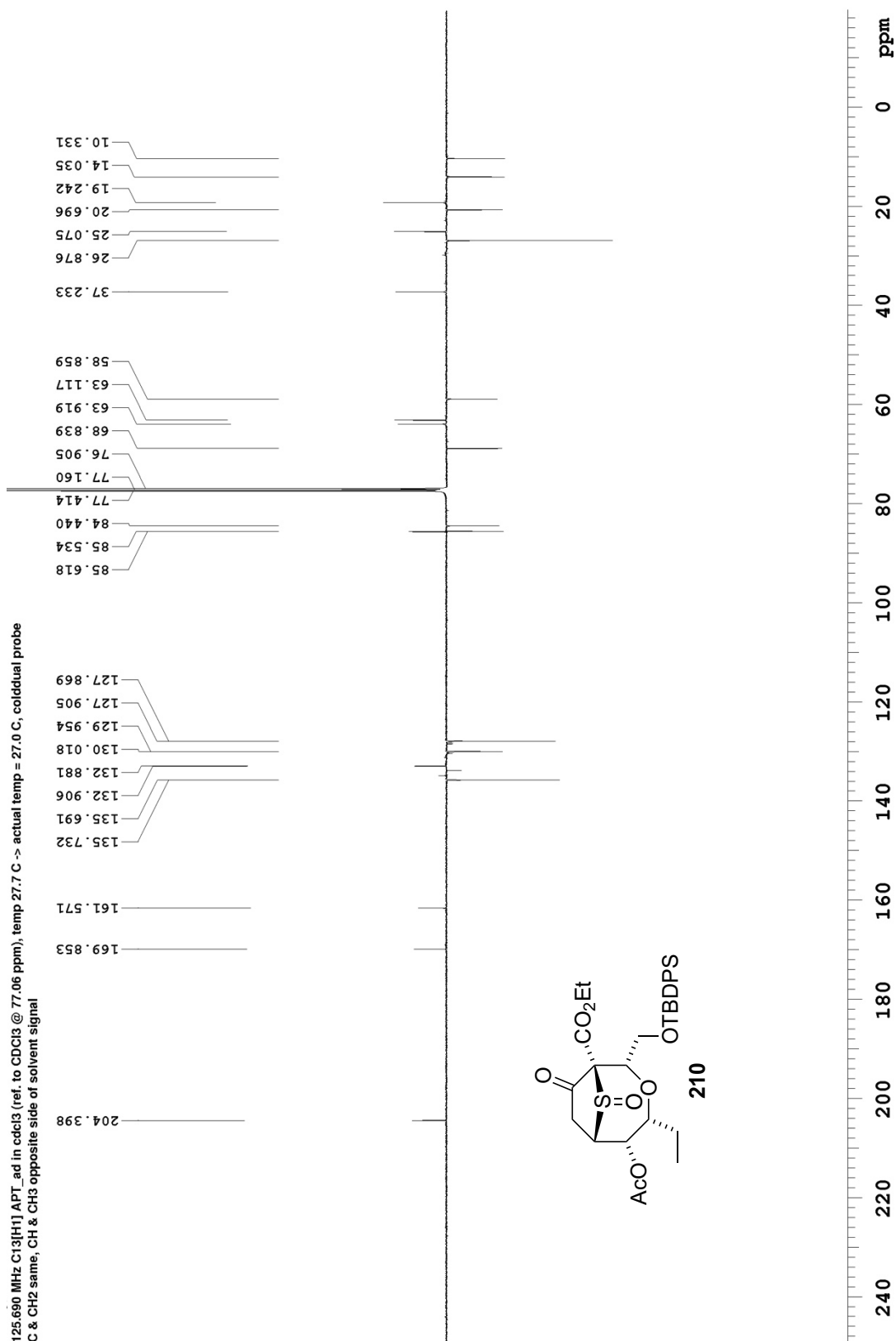
125.688 MHz C13[H1] APT_ad in cdcl3 (ref. to CDCl3 @ 77.16 ppm), temp 27.7 C -> actual temp = 27.0 C, cold dual probe
 C & CH2 same, CH & CH3 opposite side of solvent signal



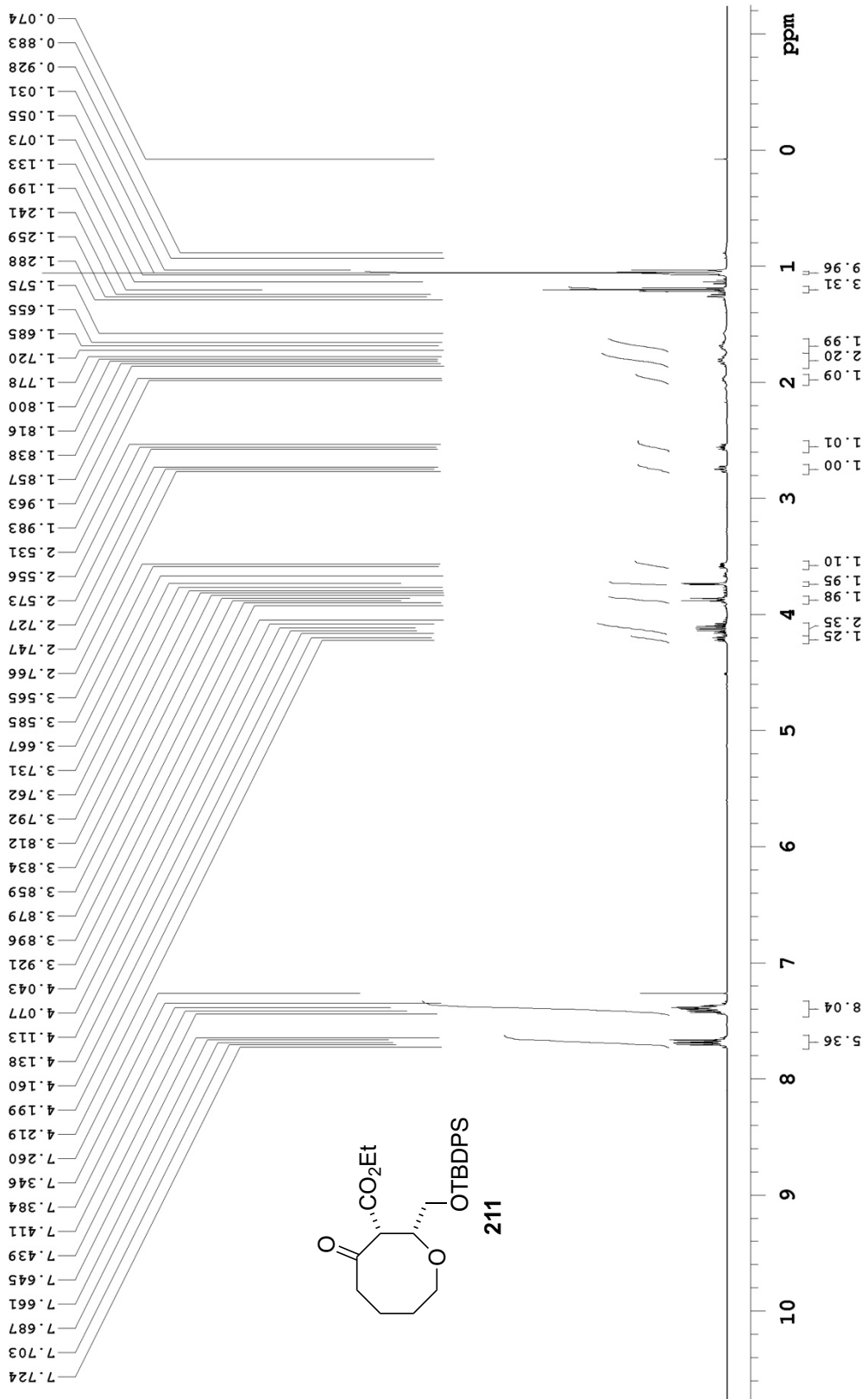
499.806 MHz H1 PRESAT in cdcl3 (ref. to CDC13 @ 7.26 ppm), temp 27.7 C -> actual temp = 27.0 C, coldlual probe



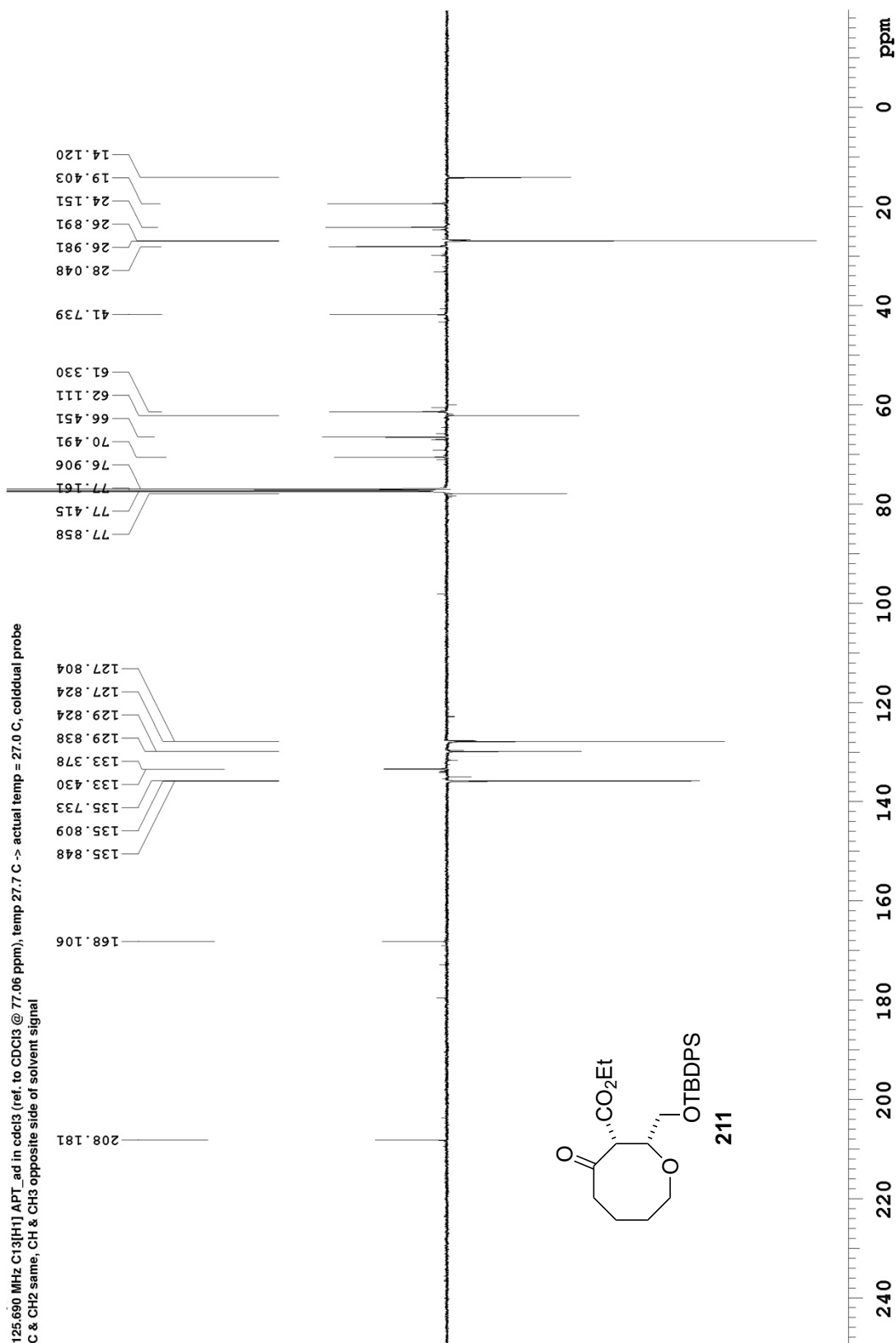
125.690 MHz C¹³[H1] APT_ad in cdcl3 (ref. to CDC13 @ 77.06 ppm), temp 27.7 C -> actual temp = 27.0 C, coldddual probe
C & CH2 same, CH & CH3 opposite side of solvent signal



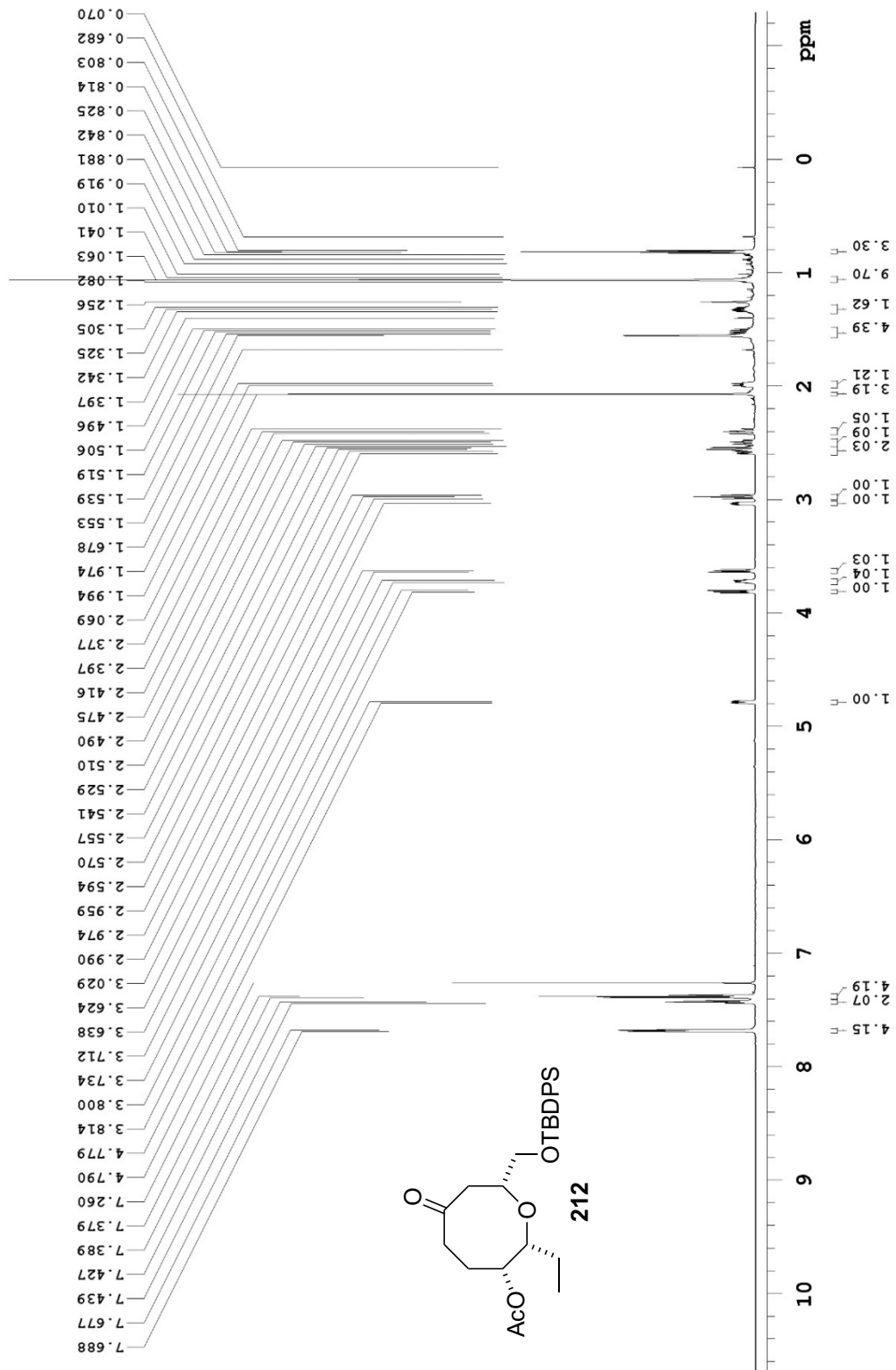
499.806 MHz H1 PRESAT in cdcl3 (ref. to CDC13 @ 7.26 ppm), temp 27.7 C -> actual temp = 27.0 C, coldddual probe



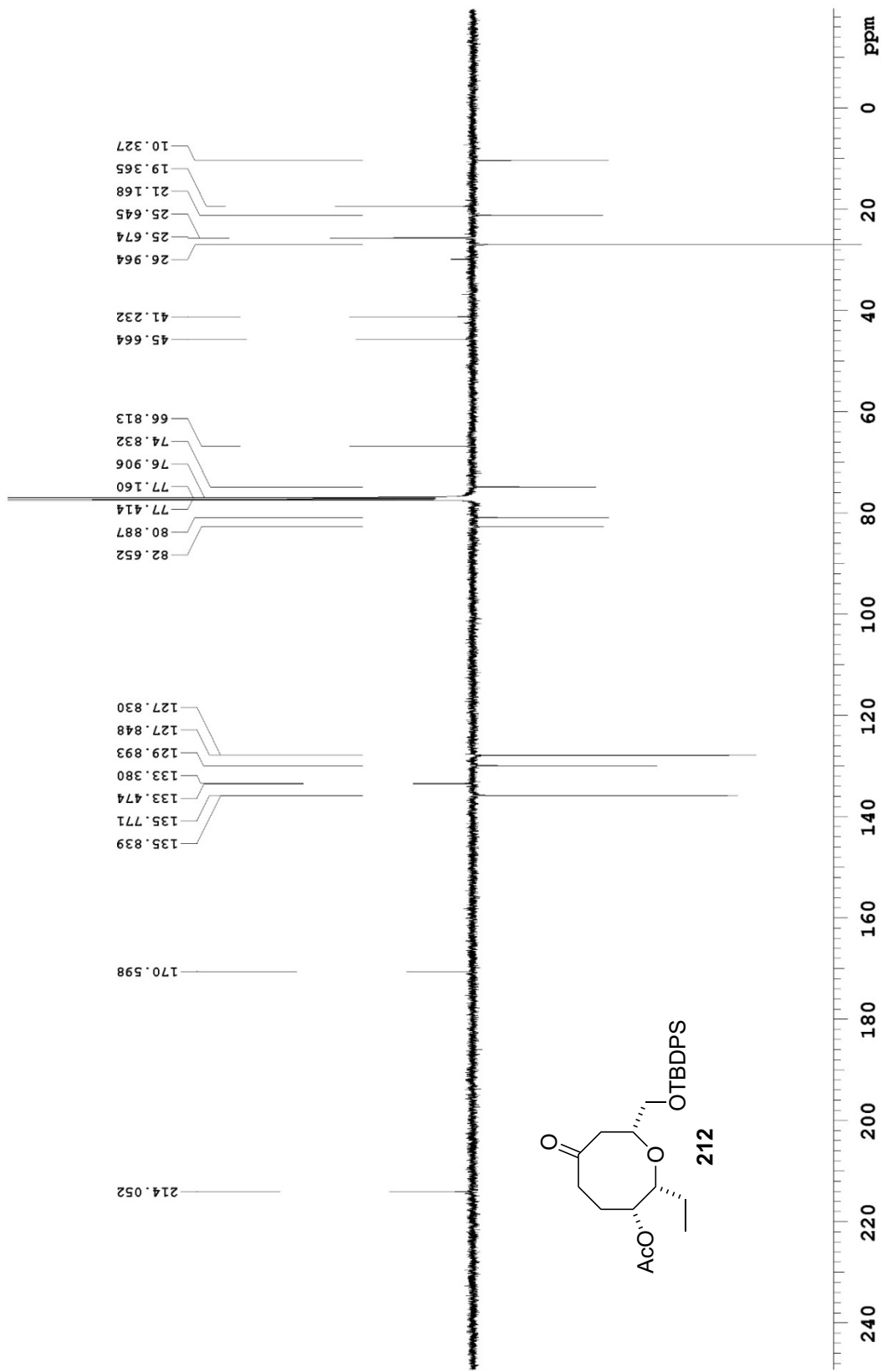
125.690 MHz C{13}H1] APT_ad in cdcl3 (ref. to CDCl3 @ 77.06 ppm), temp 27.7 C -> actual temp = 27.0 C, cold dual probe
C & CH2 same, CH & CH3 opposite side of solvent signal



699.762 MHz H1 PRESAT in cdcl3 (ref. to CDCl3 @ 7.26 ppm), temp 27.5 C -> actual temp = 27.0 C, coldidid probe



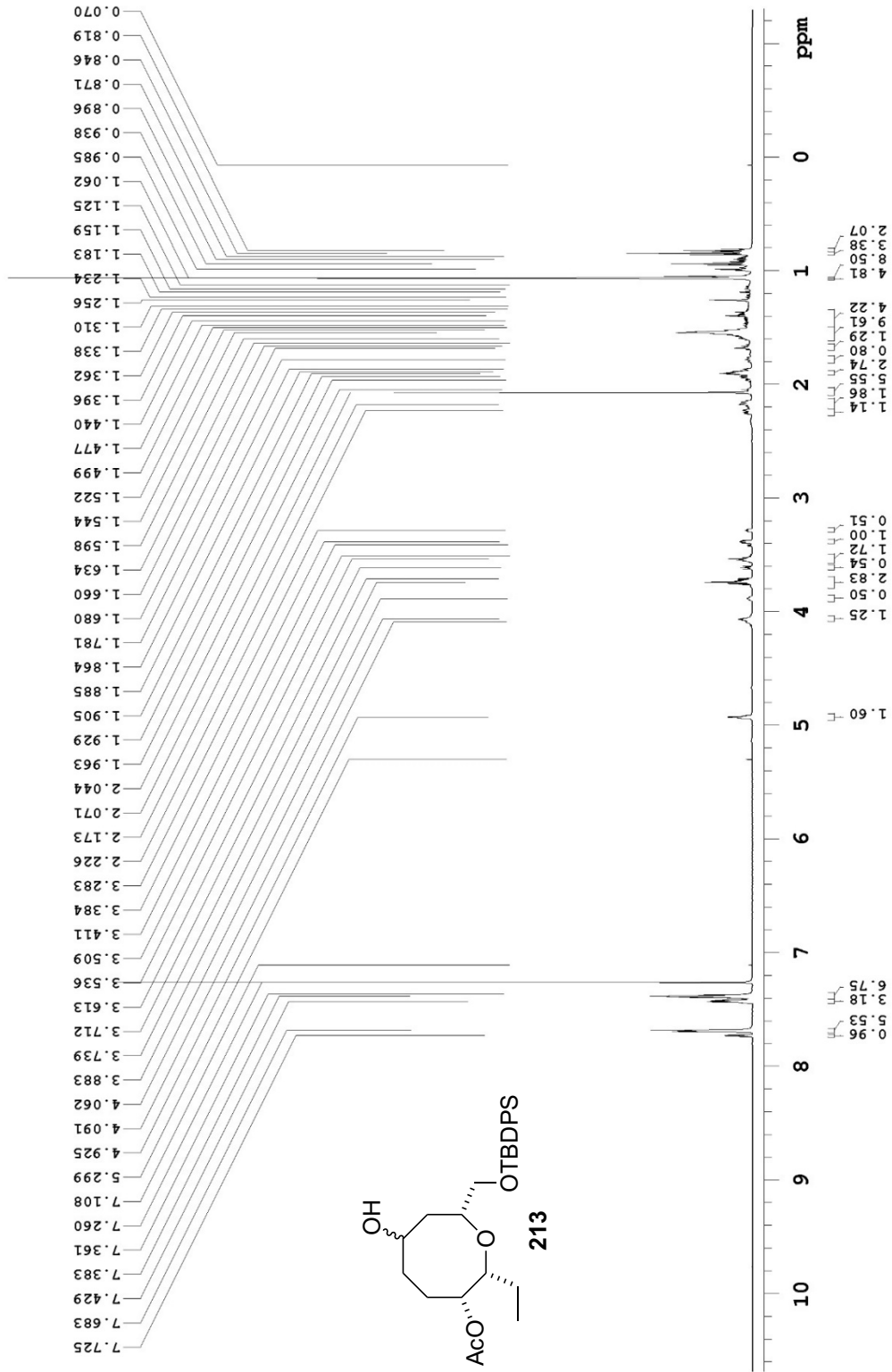
125.690 MHz ¹³C{¹H} APT-ad in cdcl3 (ref. to CDCl3 @ 77.16 ppm), temp 27.7 C -> actual temp = 27.0 C, ccolddual probe
 C & CH2 same, CH & CH3 opposite side of solvent signal



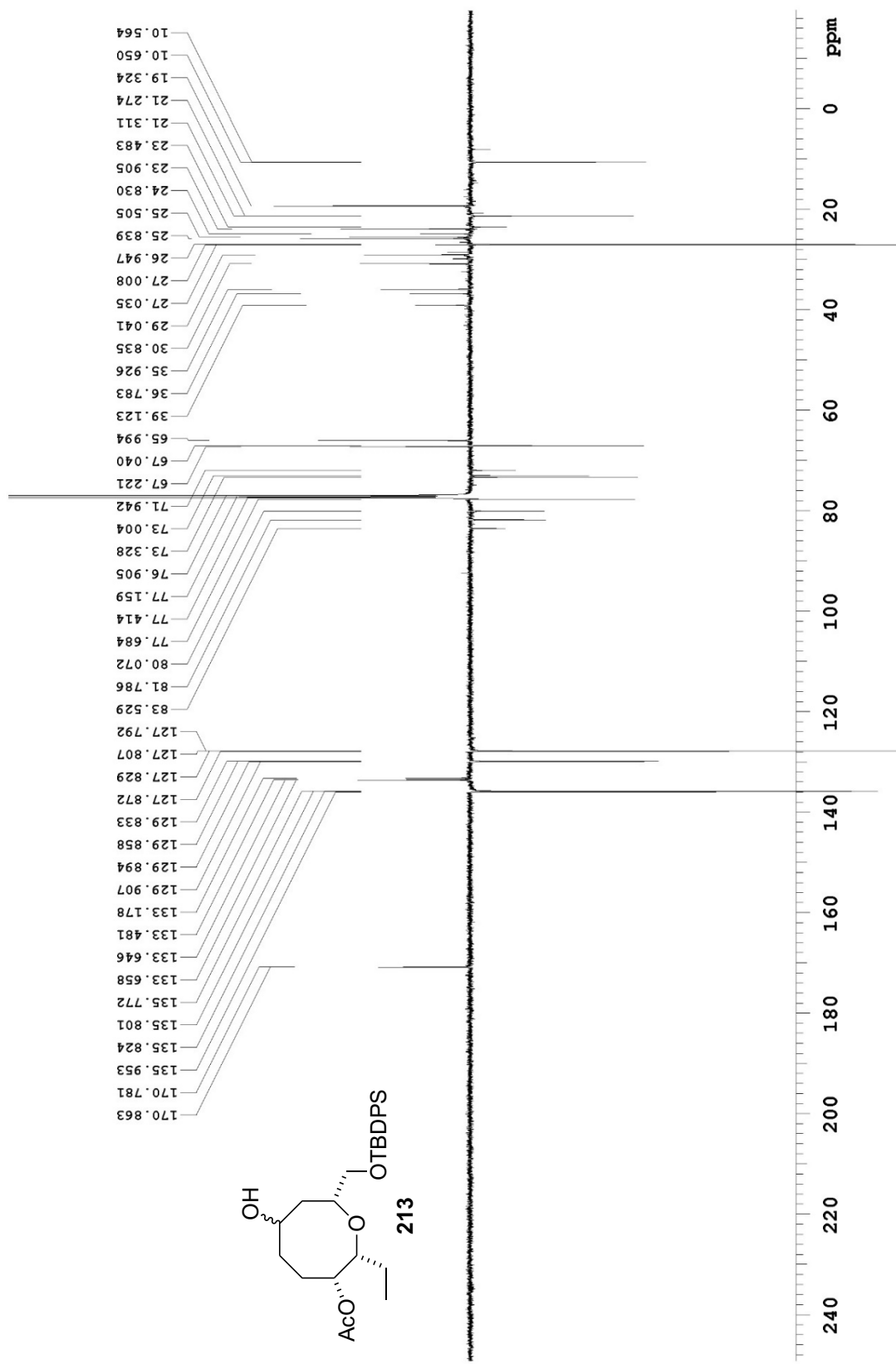
Pulse Sequence: APT-ad

Department of Chemistry, University of Alberta

699.762 MHz H1 PRESAT in cdcl3 (ref. to CDCl3 @ 7.26 ppm), temp 27.5 C -> actual temp = 27.0 C, coldid probe



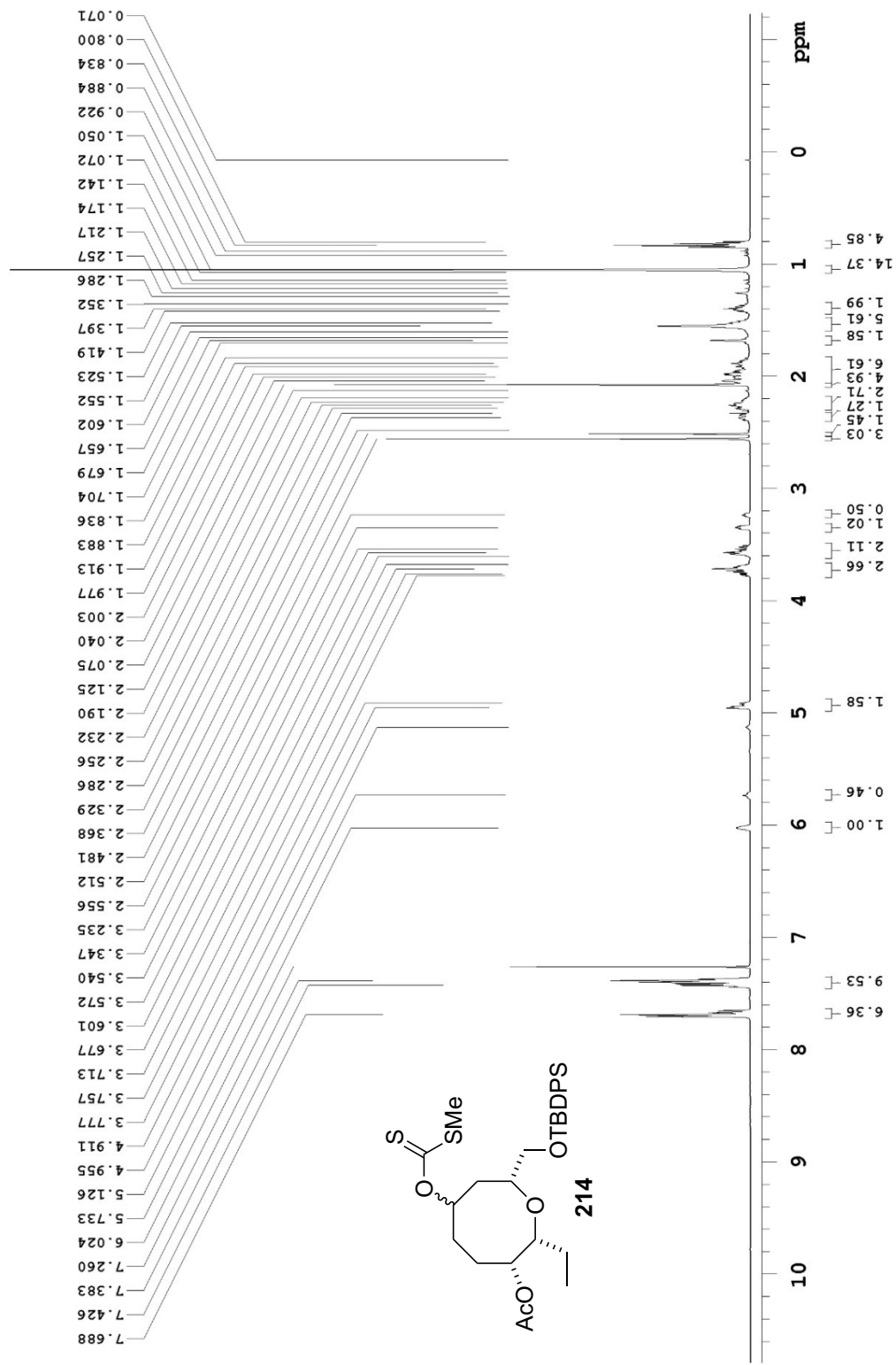
125.690 MHz C13[H1] APT_ad in cdcl3 (ref. to CDCl3 @ 77.16 ppm), temp 27.7 C -> actual temp = 27.0 C, coldddual probe
 C & CH2 same, CH & CH3 opposite side of solvent signal



Pulse Sequence: APT_ad

Department of Chemistry, University of Alberta

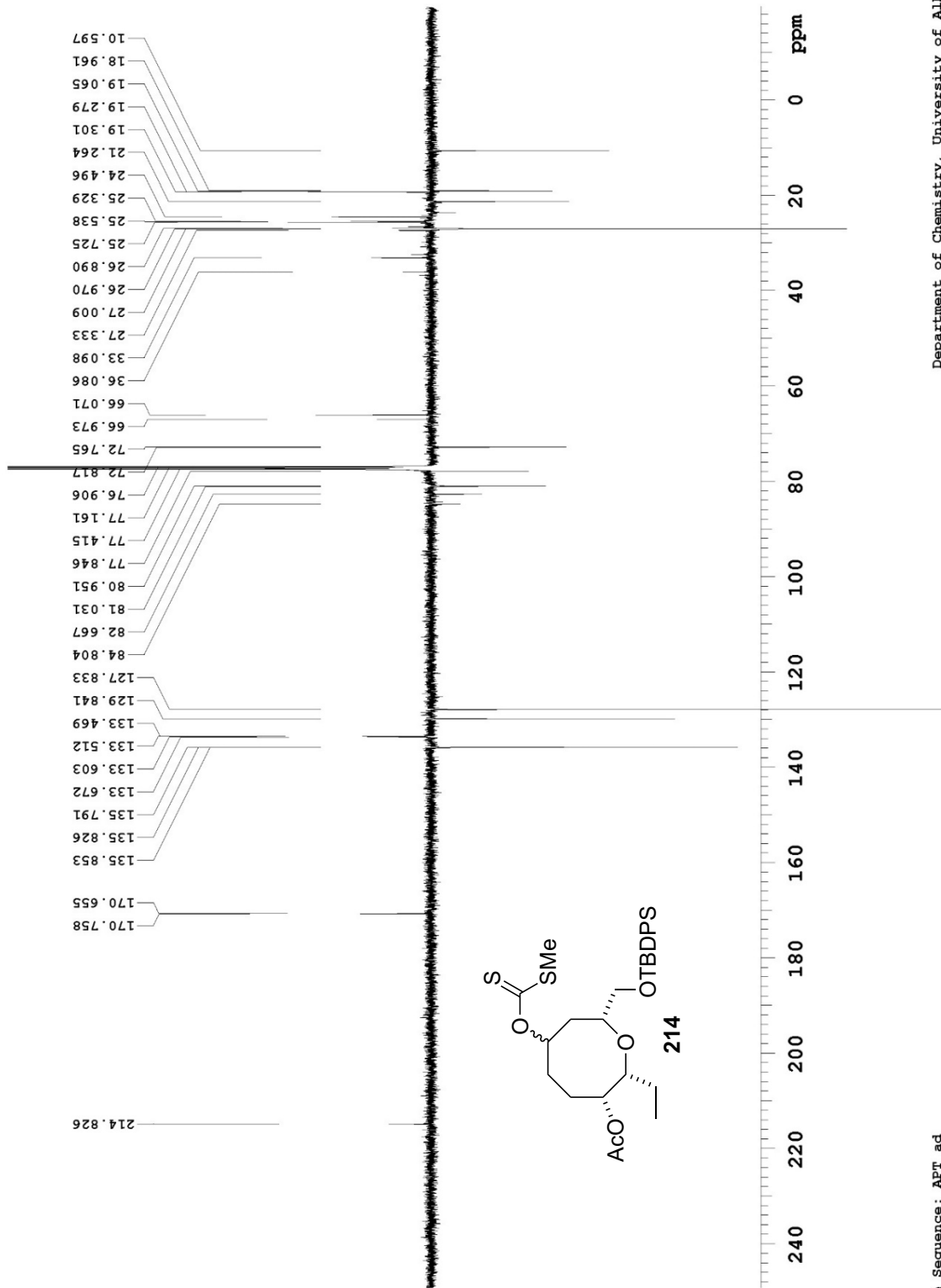
499.797 MHz H1 PRESAT in cdcl3 (ref. to CDCl3 @ 7.26 ppm), temp 27.7 C -> actual temp = 27.0 C, coldddual probe



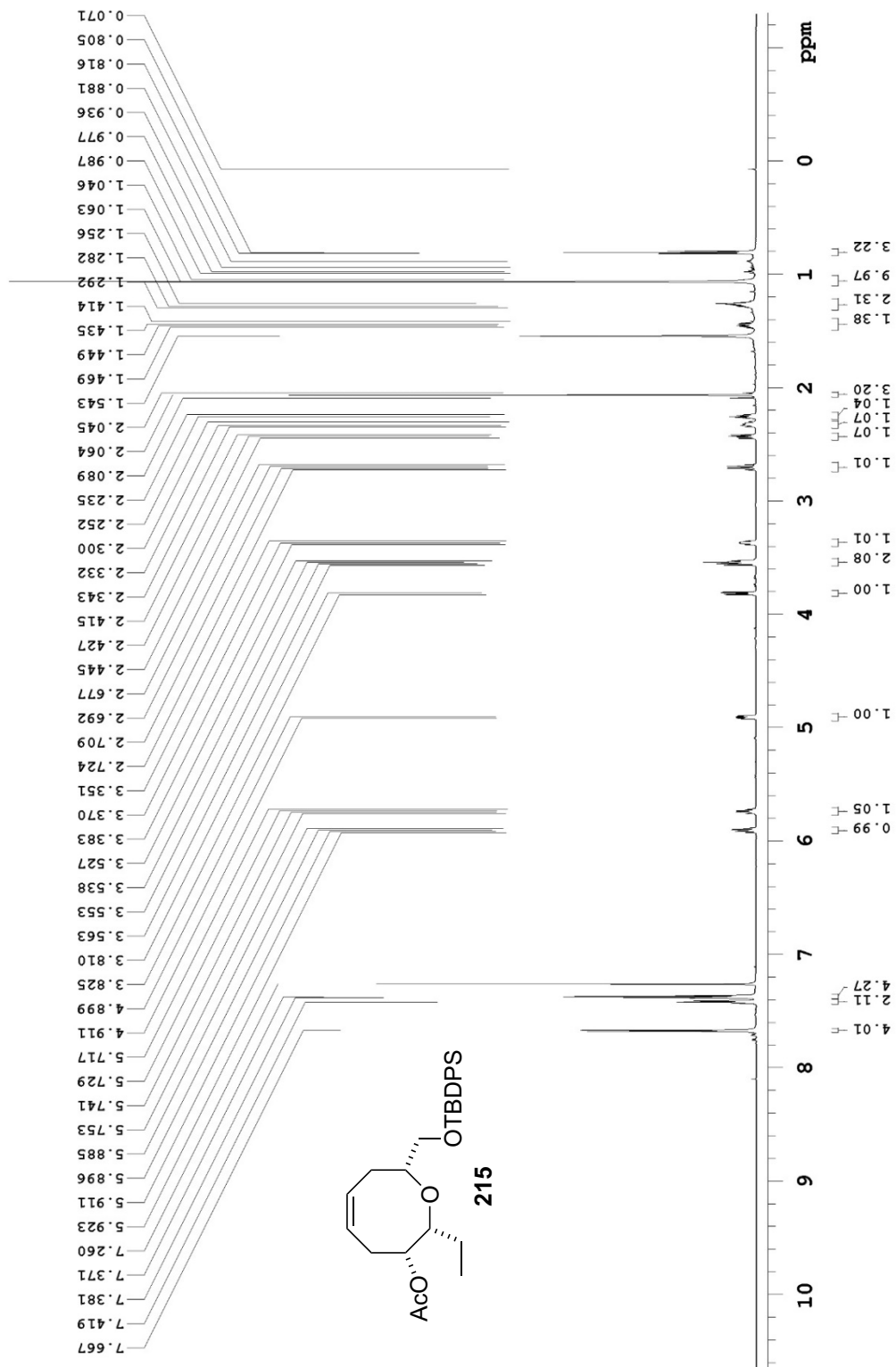
Pulse Sequence: PRESAT

Department of Chemistry, University of Alberta

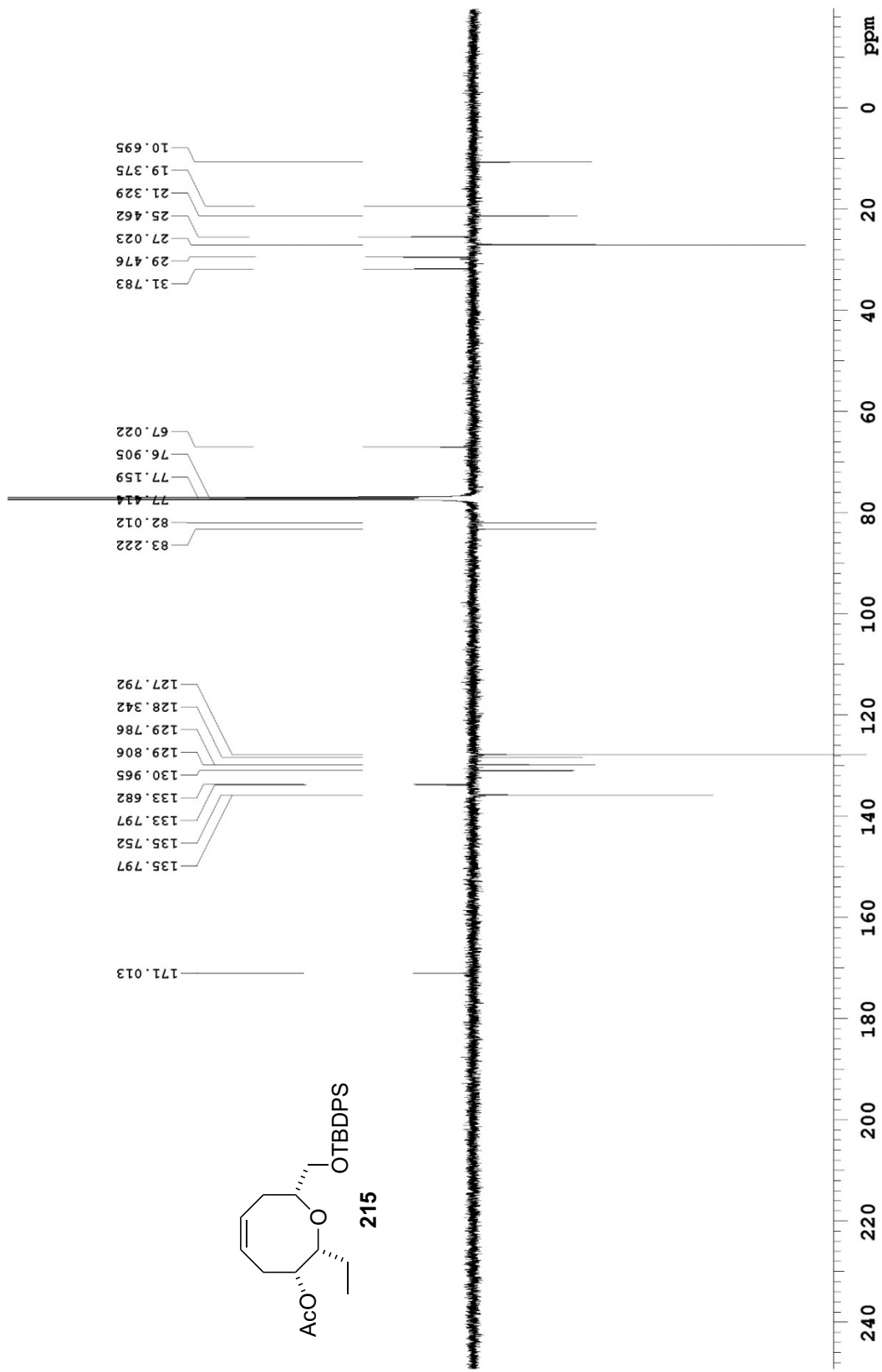
125.688 MHz C13[HL] APT_ad in cdcl3 (ref. to CDCl3 @ 77.16 ppm), temp 27.7 C -> actual temp = 27.0 C, coldddual probe
 C & CH2 same, CH & CH3 opposite side of solvent signal



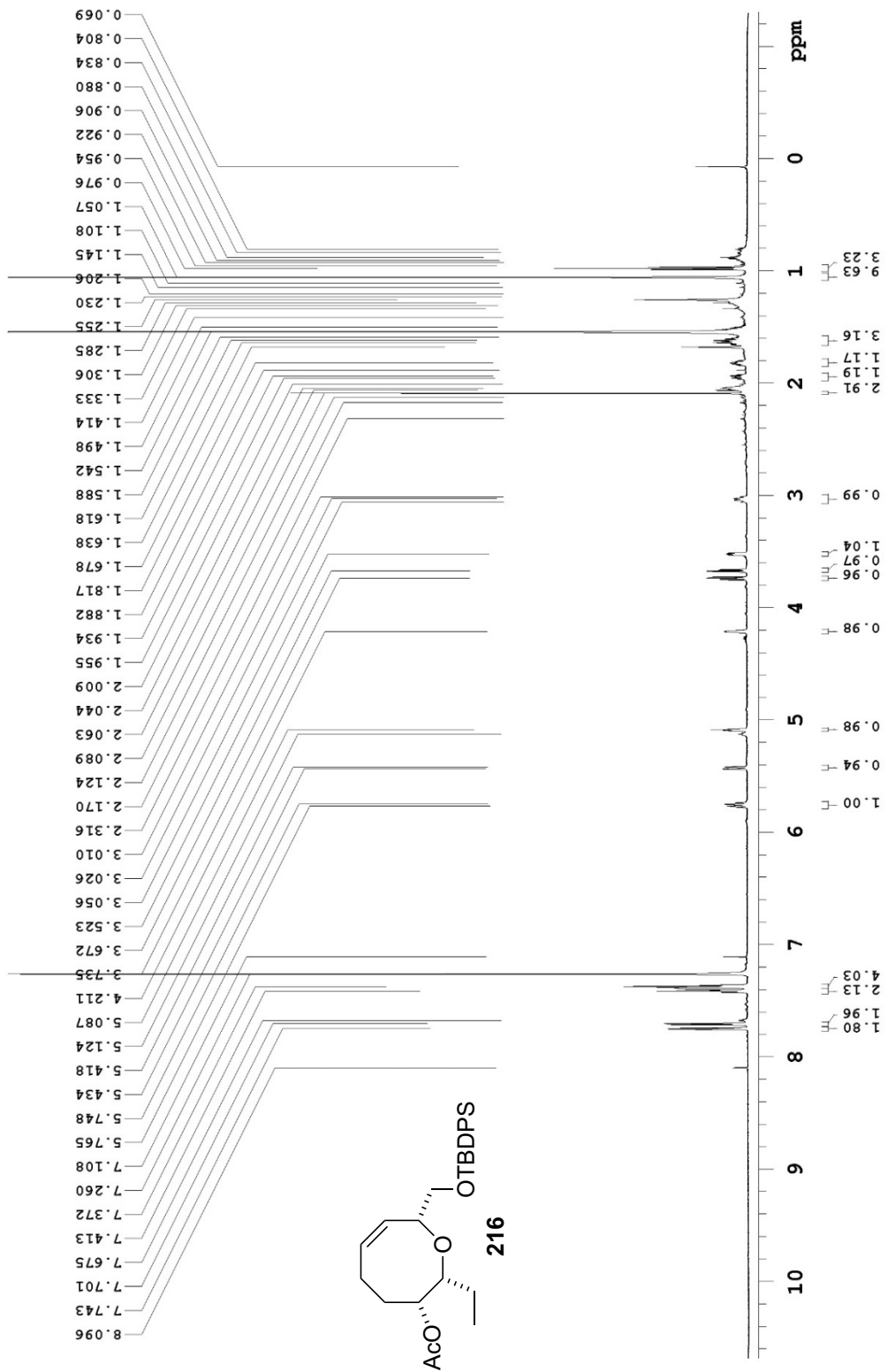
699.762 MHz H1 PRESAT in cdcl3 (ref. to CDCl3 @ 7.26 ppm), temp 27.5 C -> actual temp = 27.0 C, coldid probe



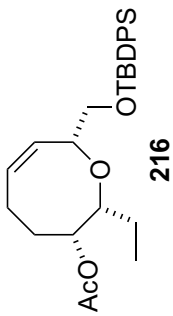
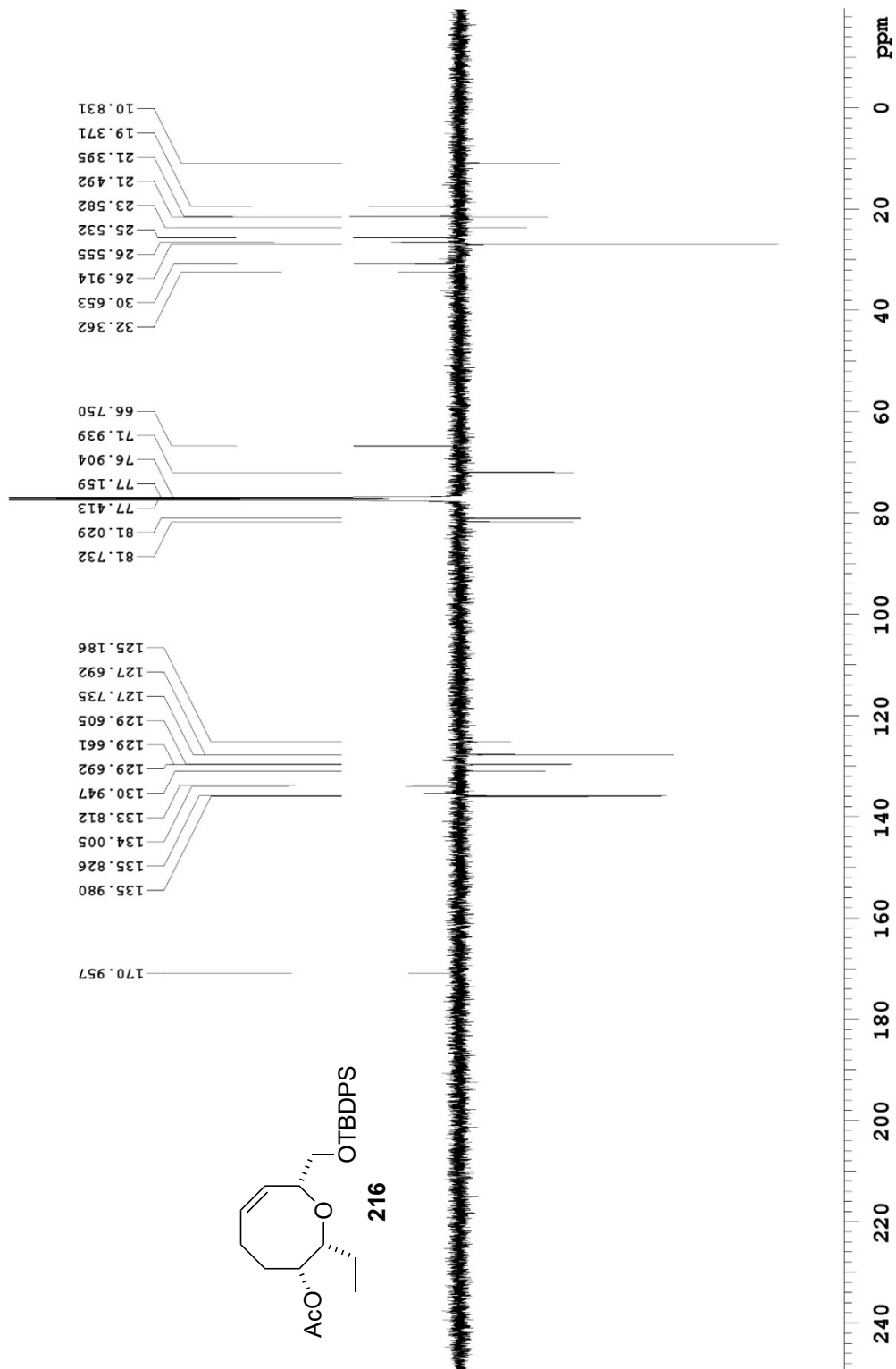
125.690 MHz ¹³C{¹H} APT-ad in cdcl3 (ref. to cdcl3 @ 77.16 ppm), temp 27.7 C -> actual temp = 27.0 C, coldddual probe
 C & CH2 same, CH & CH3 opposite side of solvent signal



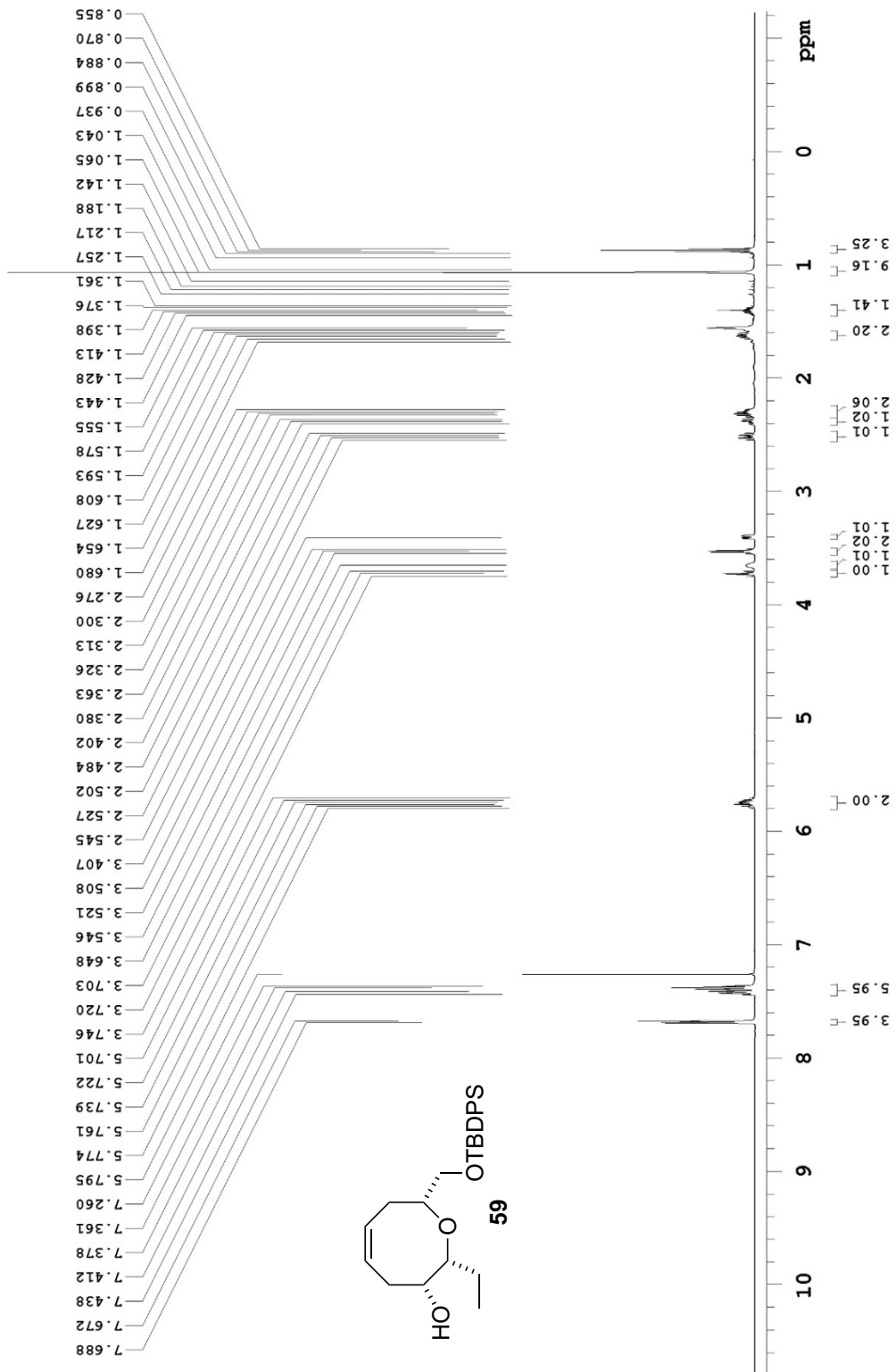
699.762 MHz H1 PRESAT in cdcl3 (ref. to CDCl3 @ 7.26 ppm), temp 27.5 C -> actual temp = 27.0 C, coldid probe



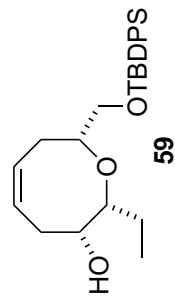
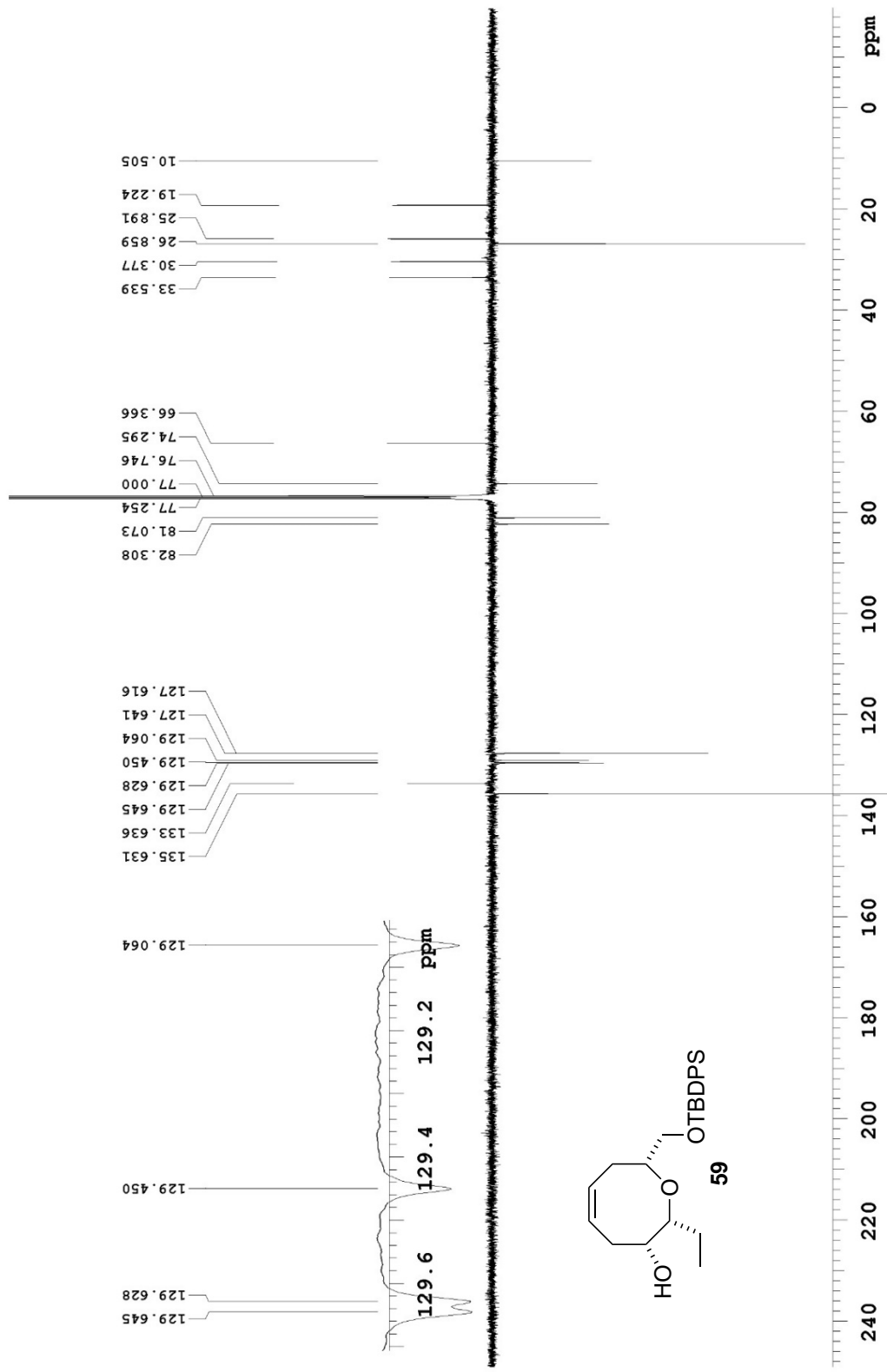
125.688 MHz C13[HI] APT_ad in cdcl3 (ref. to CDCl3 @ 77.16 ppm), temp 27.7 C -> actual temp = 27.0 C, coldddual probe
 C & CH2 same, CH & CH3 opposite side of solvent signal



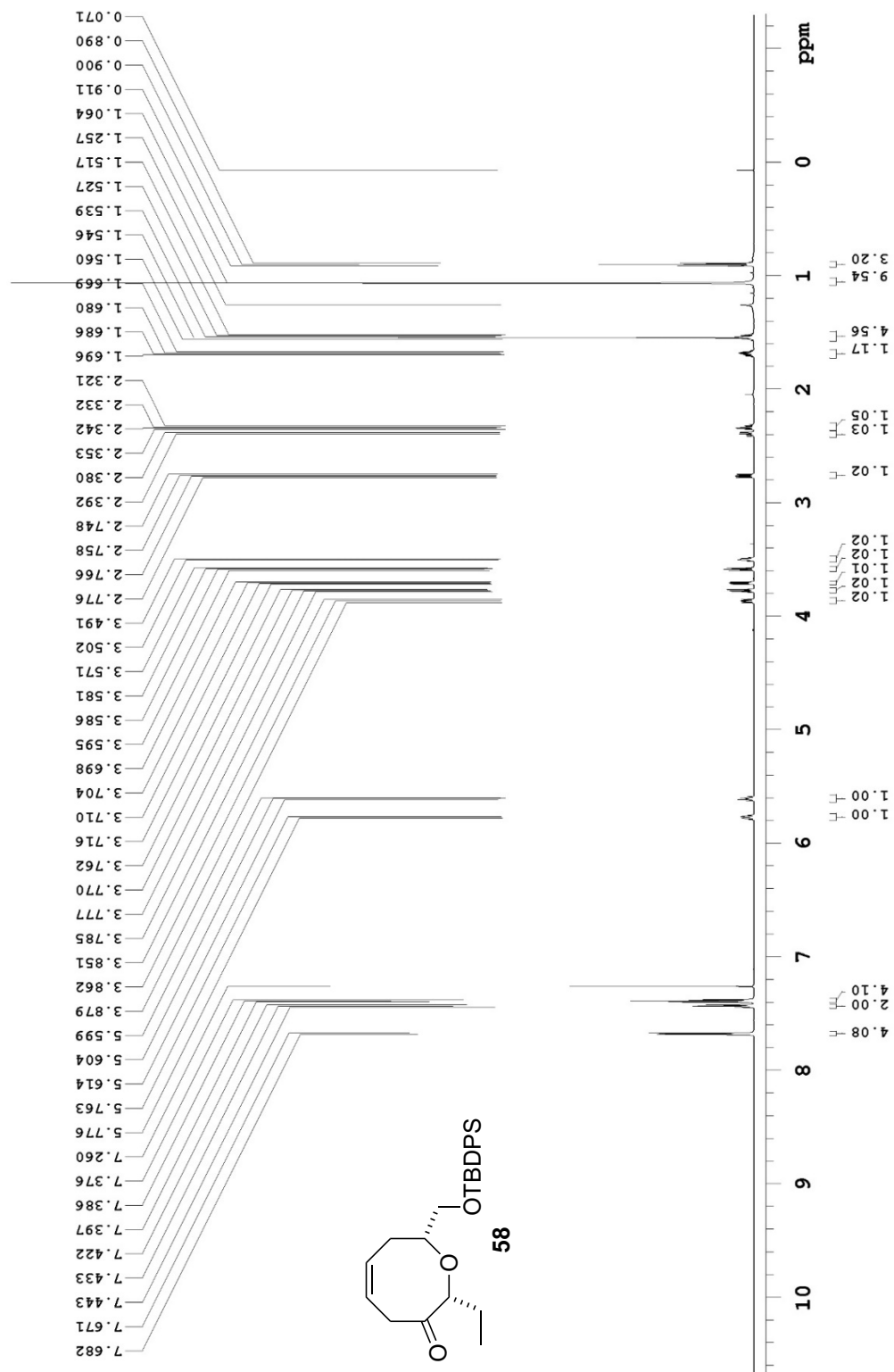
499.797 MHz H1 PRESAT in cdcl3 (ref. to CDCl3 @ 7.26 ppm), temp 27.7 C -> actual temp = 27.0 C, coldhdal probe



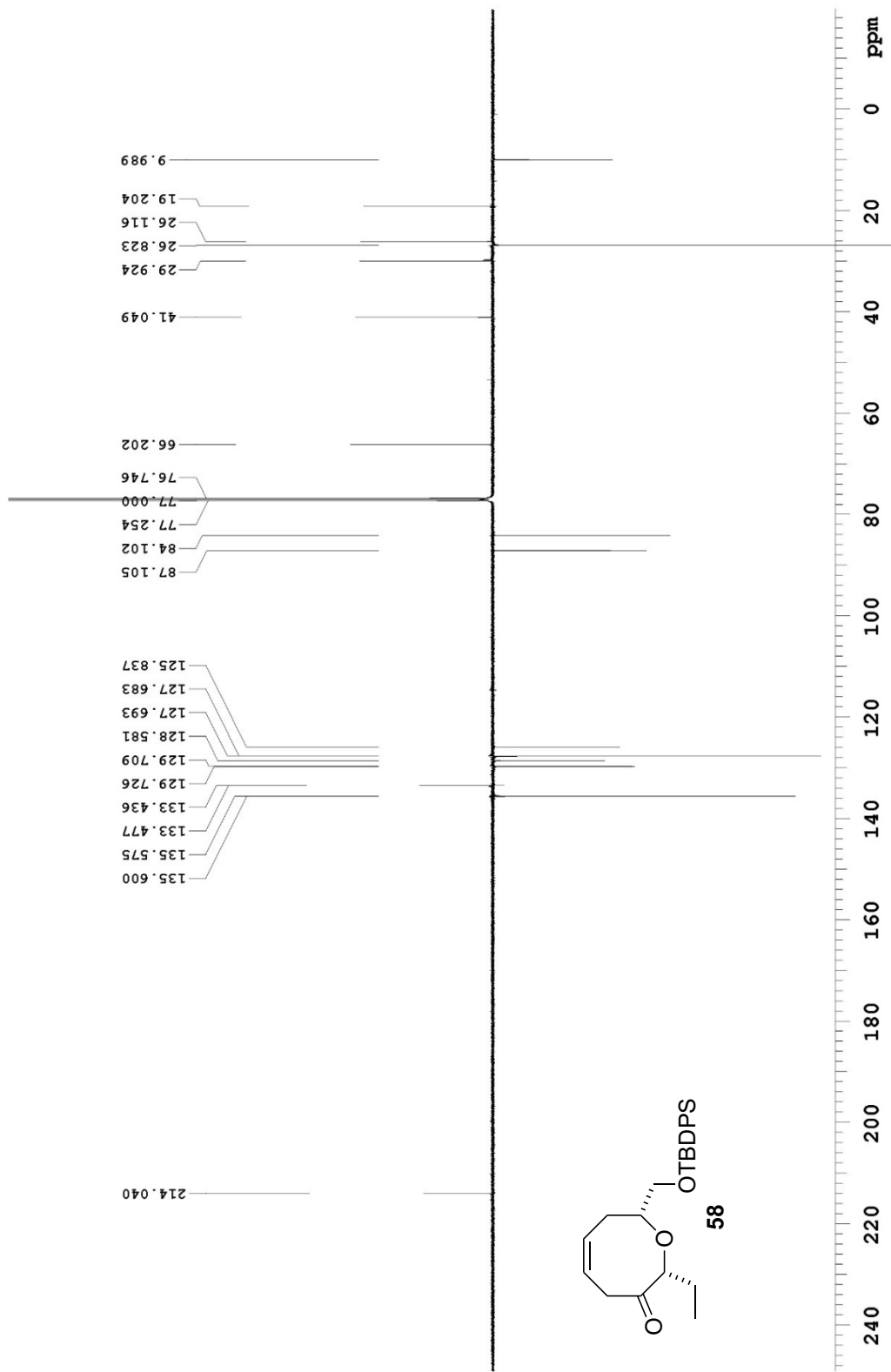
125.690 MHz ¹³C{¹H} APT_{ad} in cdcl3 (ref. to cdcl3 @ 77.0 ppm), temp 27.7 C -> actual temp = 27.0 C, coldddual probe
 C & CH2 same, CH & CH3 opposite side of solvent signal



699.762 MHz H1 PRESAT in cdcl3 (ref. to cdcl3 @ 7.26 ppm), temp 27.5 C -> actual temp = 27.0 C, coldid probe

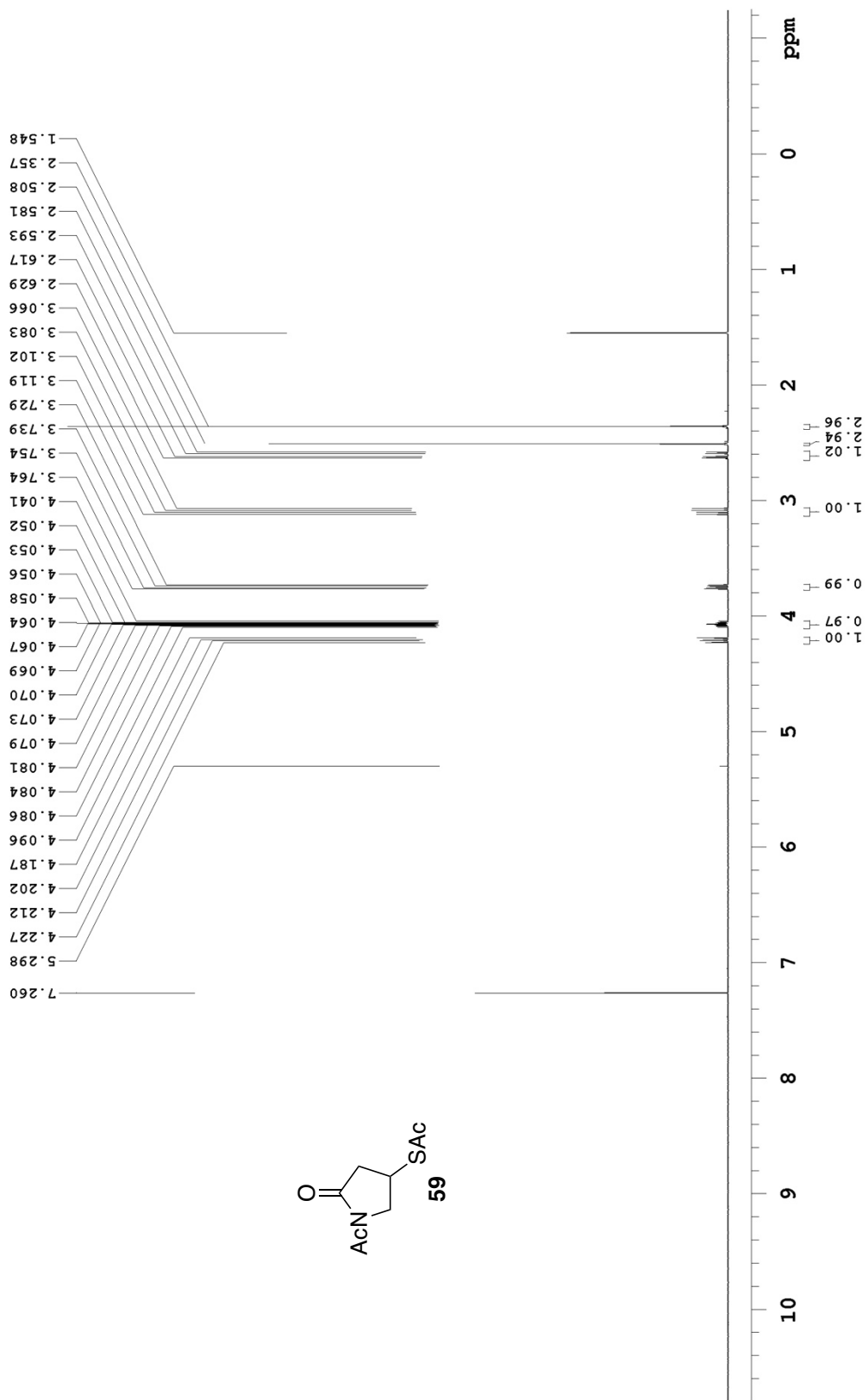


125.688 MHz C13[H1] APT_ad in cdcl3 (ref. to CDCl3 @ 77.0 ppm), temp 27.7 C -> actual temp = 27.0 C, coldddual probe
 C & CH2 same, CH & CH3 opposite side of solvent signal

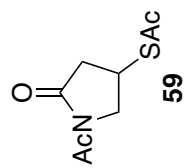
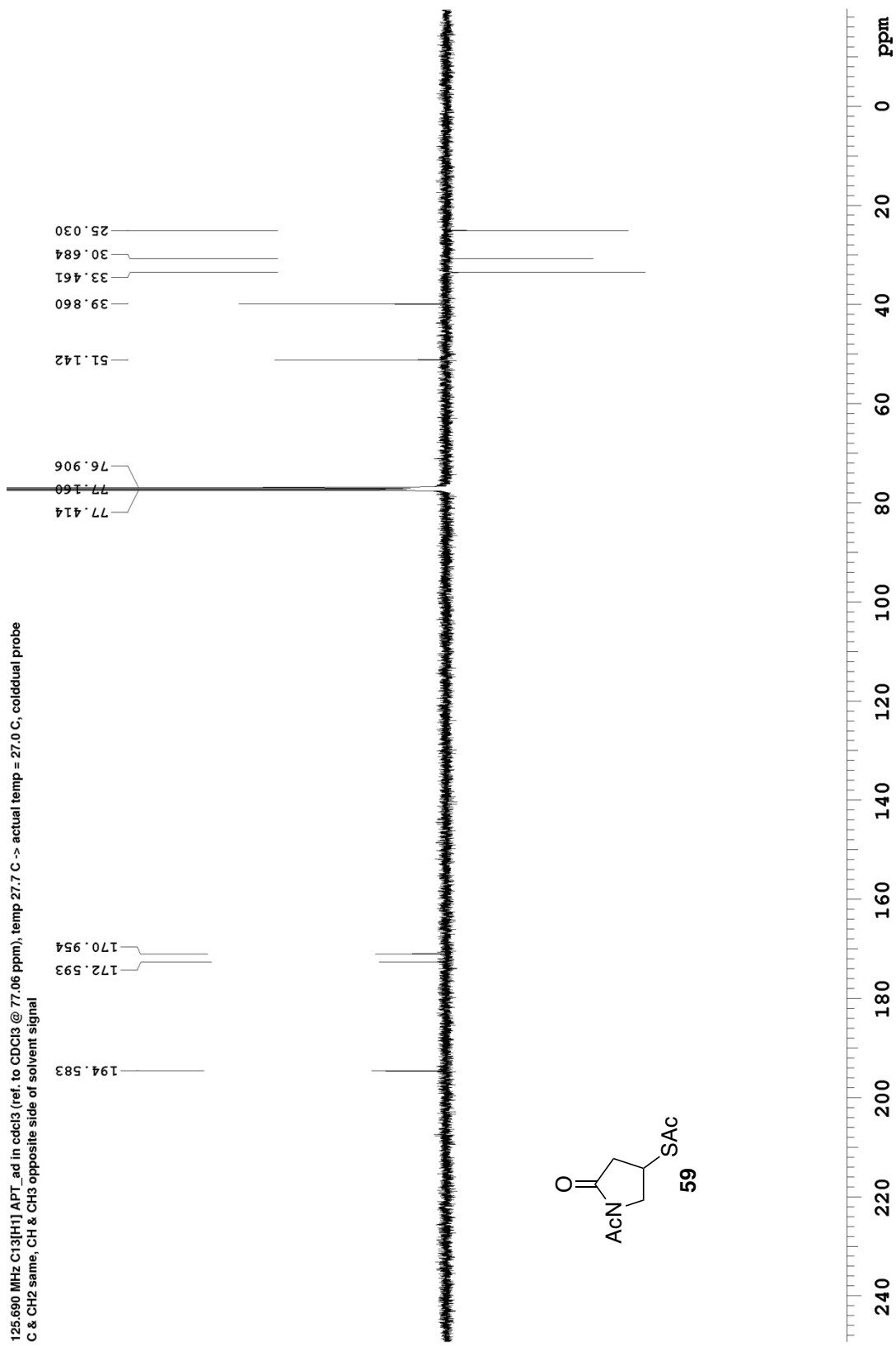


Appendix II: Selected NMR Spectra (Chapter 3)

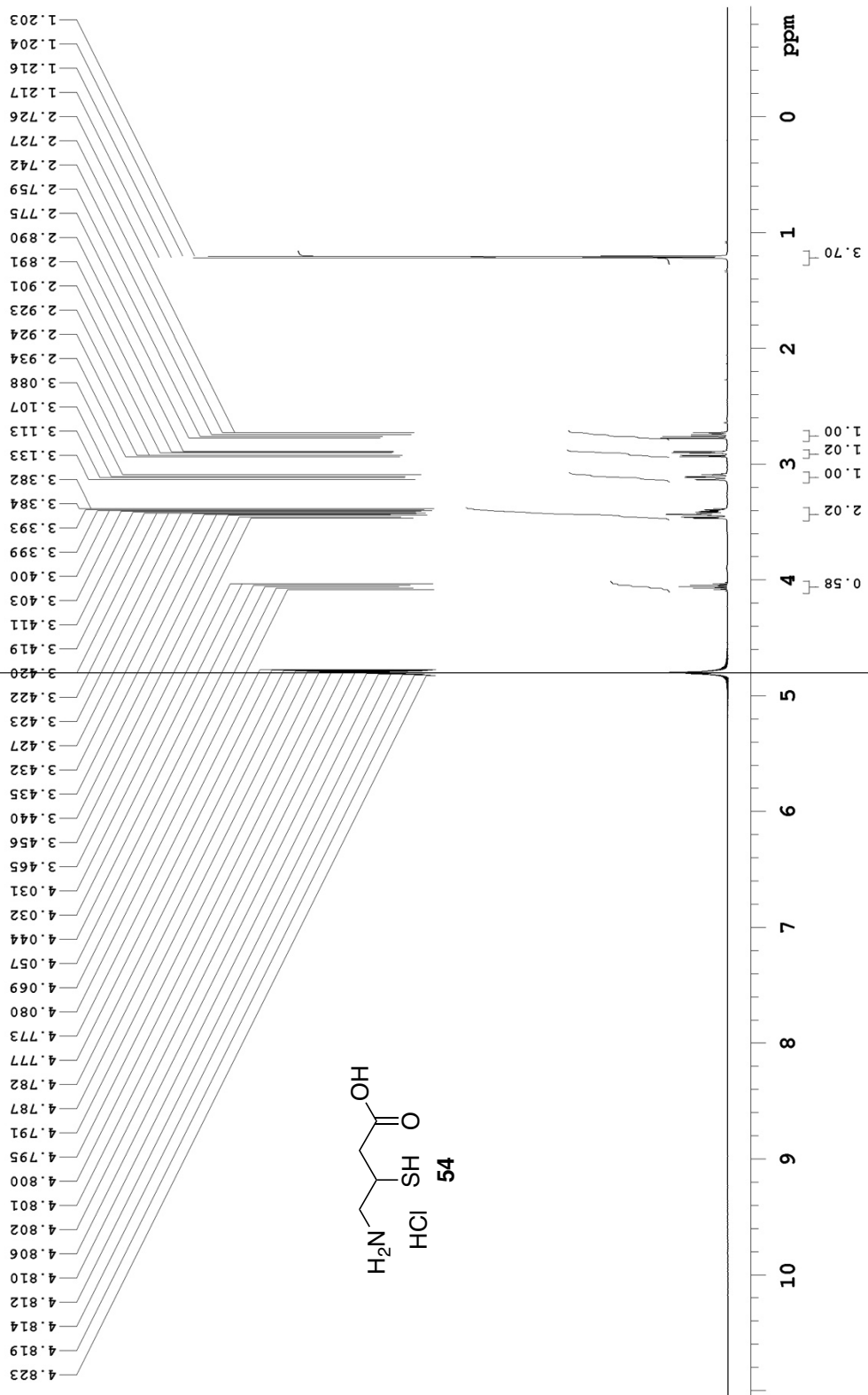
498.118 MHz H1 1D in cdcl3 (ref. to CDC13 @ 7.26 ppm), temp 26.4 C -> actual temp = 27.0 C, autoxdb probe



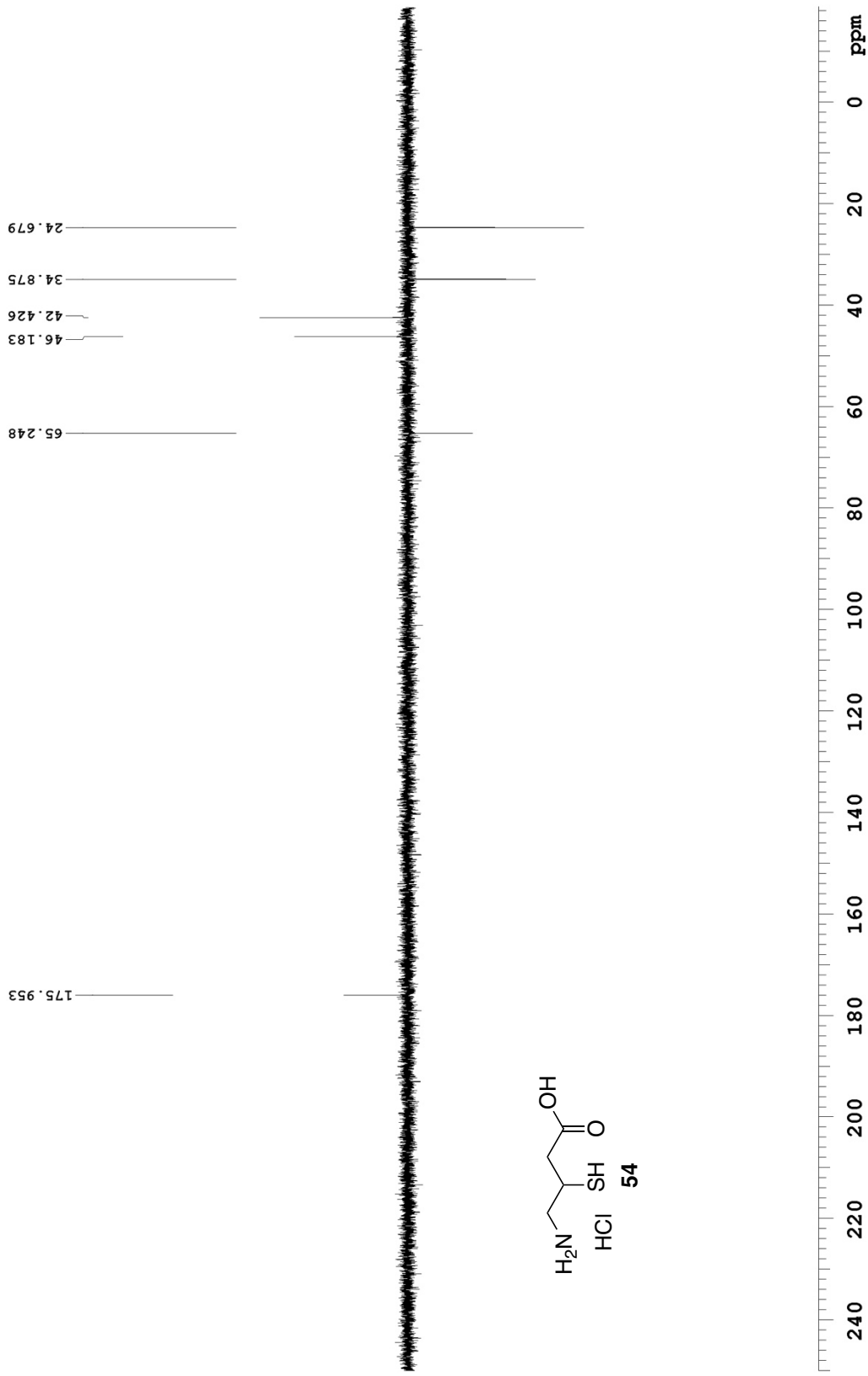
125.690 MHz C13{H1} APT ad in cdcl3 (ref. to CDCl3 @ 77.06 ppm), temp 27.7 C -> actual temp = 27.0 C, cold dual probe
C & CH2 same, CH & CH3 opposite side of solvent signal



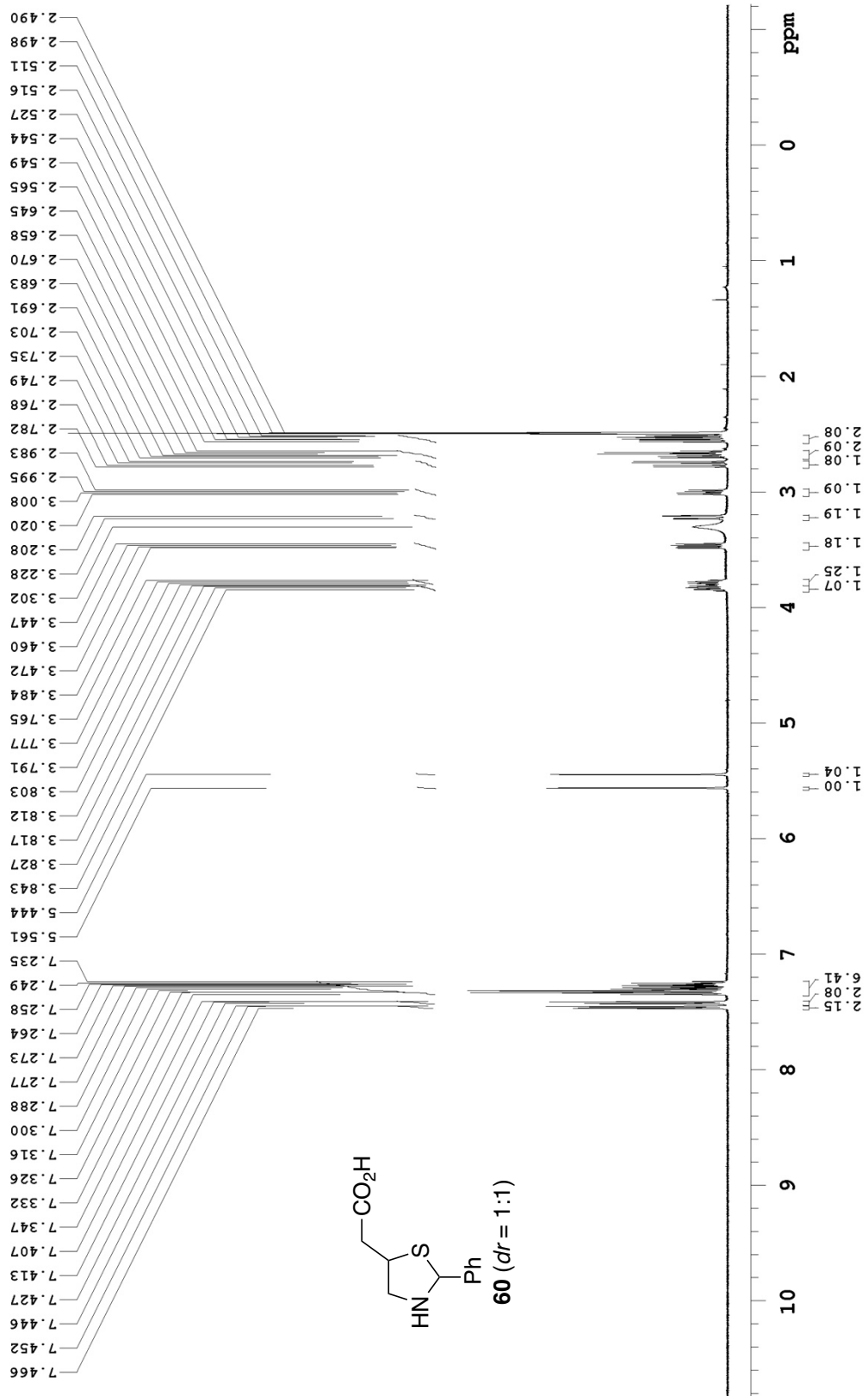
499.808 MHz ¹H PRESAT in d₂O (ref. to external acetone @ 2.225 ppm), temp 27.7 C -> actual temp = 27.0 C, coldidial probe



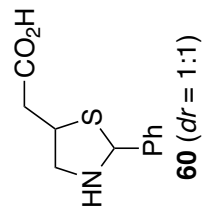
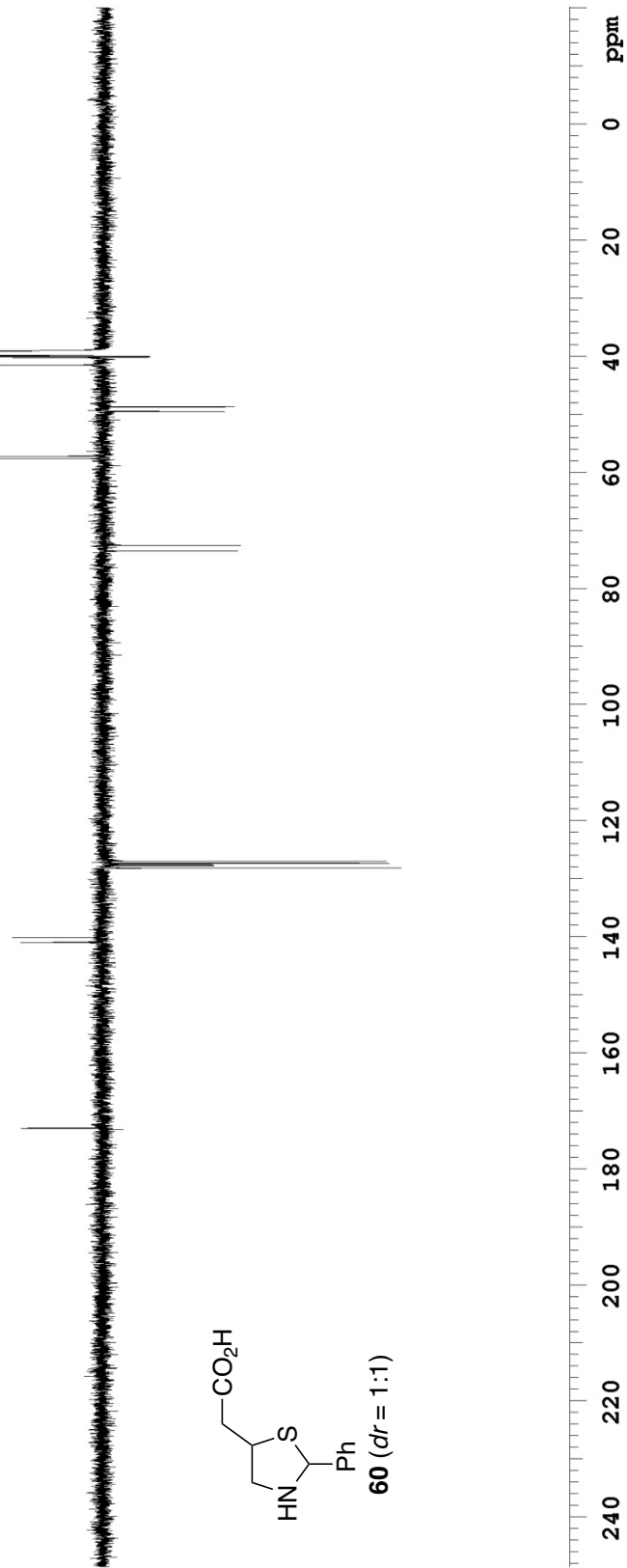
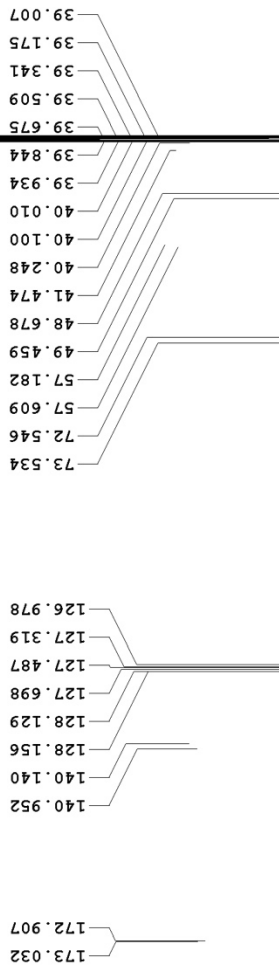
125.691 MHz C13[H1] APT_ad in d2o (ref. to external acetone @ 31.07 ppm), temp 27.7 C -> actual temp = 27.0 C, cold dual probe
C & CH2 same, CH & CH3 opposite side of solvent signal



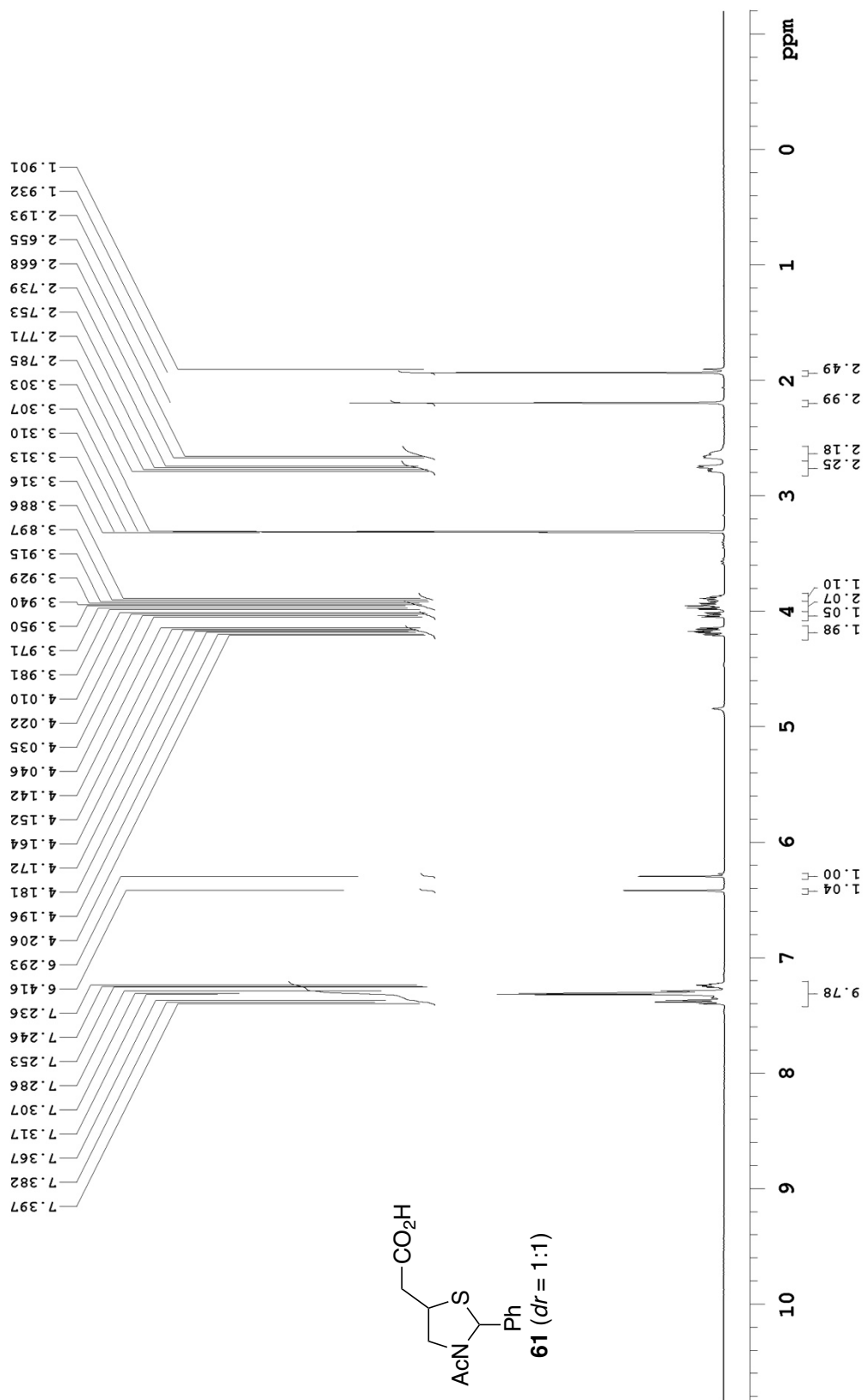
498.120 MHz H1 1D in dimso (ref. to DMSO @ 2.49 ppm), temp 26.4 C -> actual temp = 27.0 C, autotxdb probe



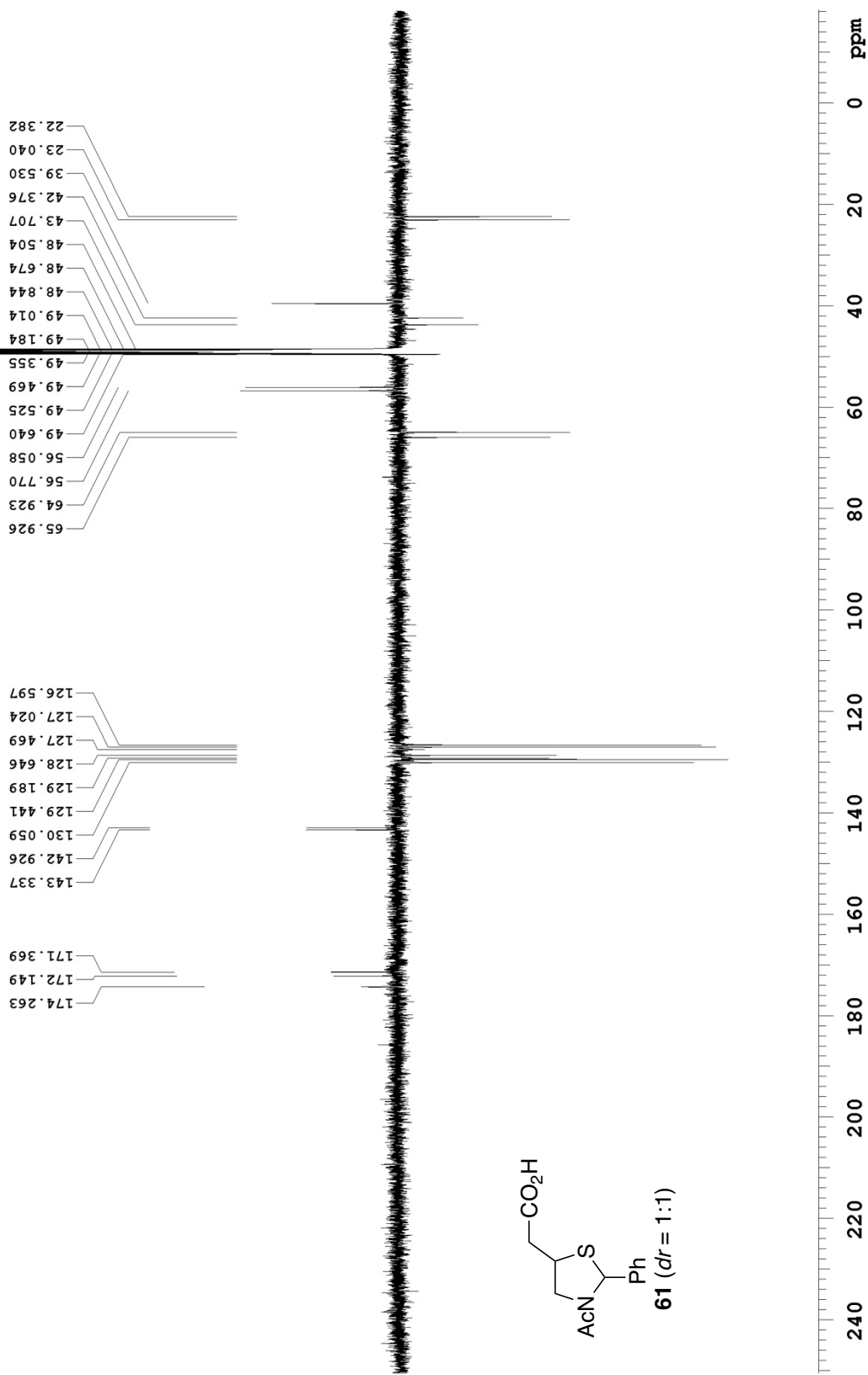
125.691 MHz C13[1H]APT ad in dimso (ref. to DMSO @ 39.5 ppm), temp 27.7 C -> actual temp = 27.0 C, cold dual probe
C & CH2 same, CH & CH3 opposite side of solvent signal



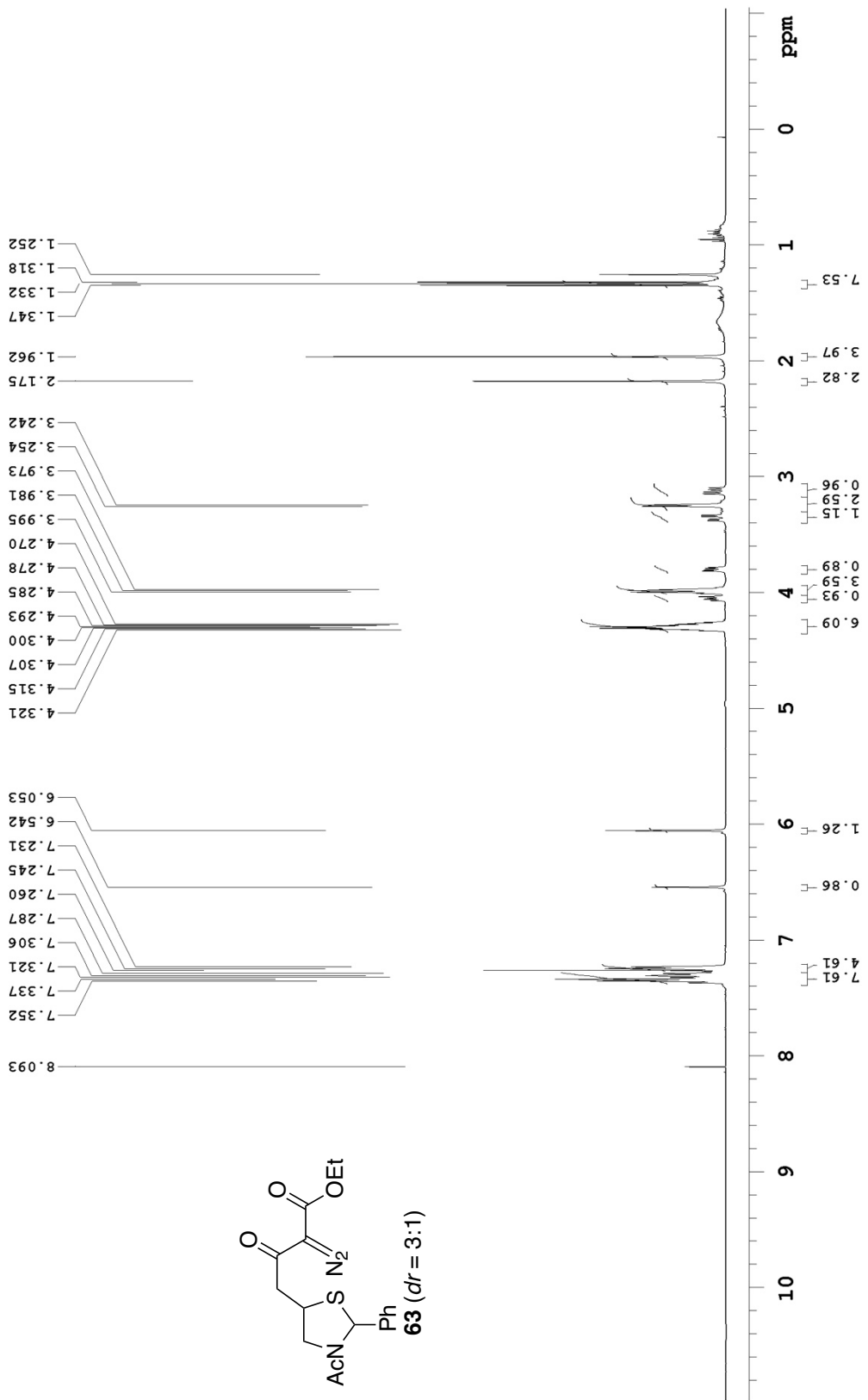
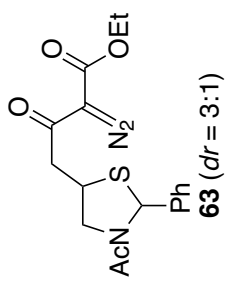
498.120 MHz H1 1D in cd3od (ref. to CD3OD @ 3.30 ppm), temp 26.4 C -- actual temp = 27.0 C, autotxdb probe



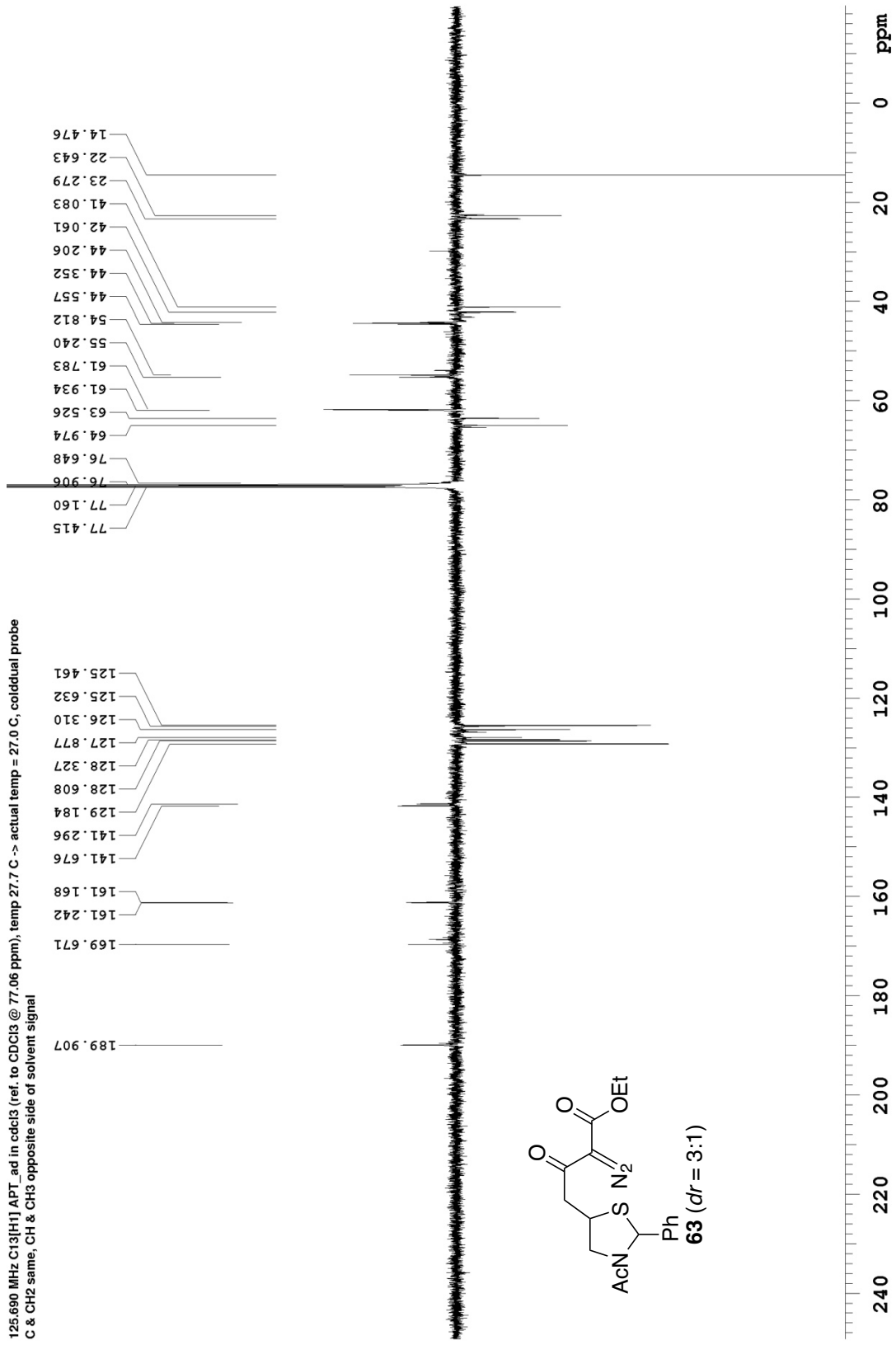
125.691 MHz C13[H1] APT_ad in cd3od (ref. to CD3OD @ 49.0 ppm), temp 27.7 C -> actual temp = 27.0 C, coldlual probe
 C & CH2 same, CH & CH3 opposite side of solvent signal



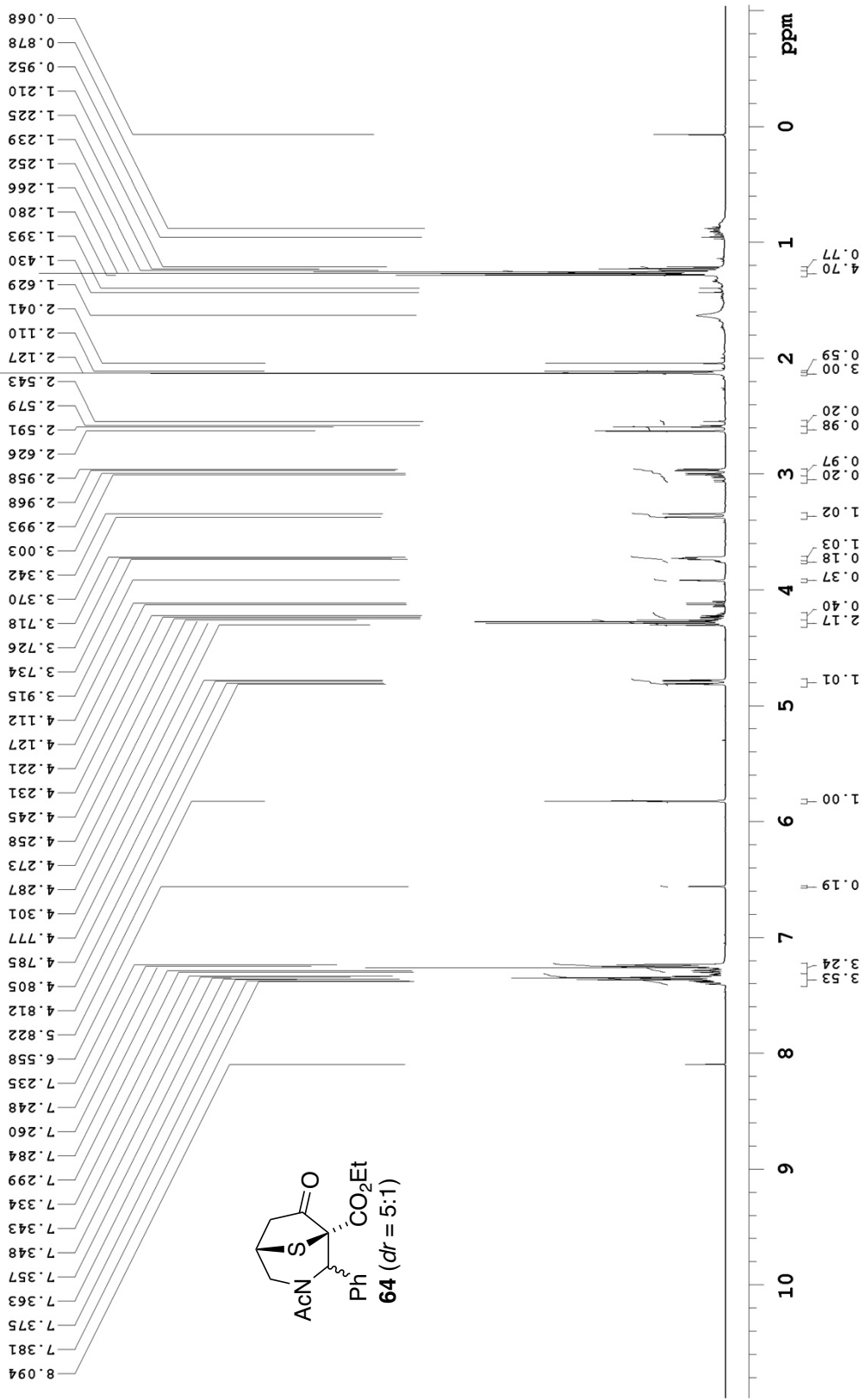
499.806 MHz H1 PRESAT in cdcl3 (ref. to CDC13 @ 7.26 ppm), temp 27.7 C -> actual temp = 27.0 C, coldddual probe



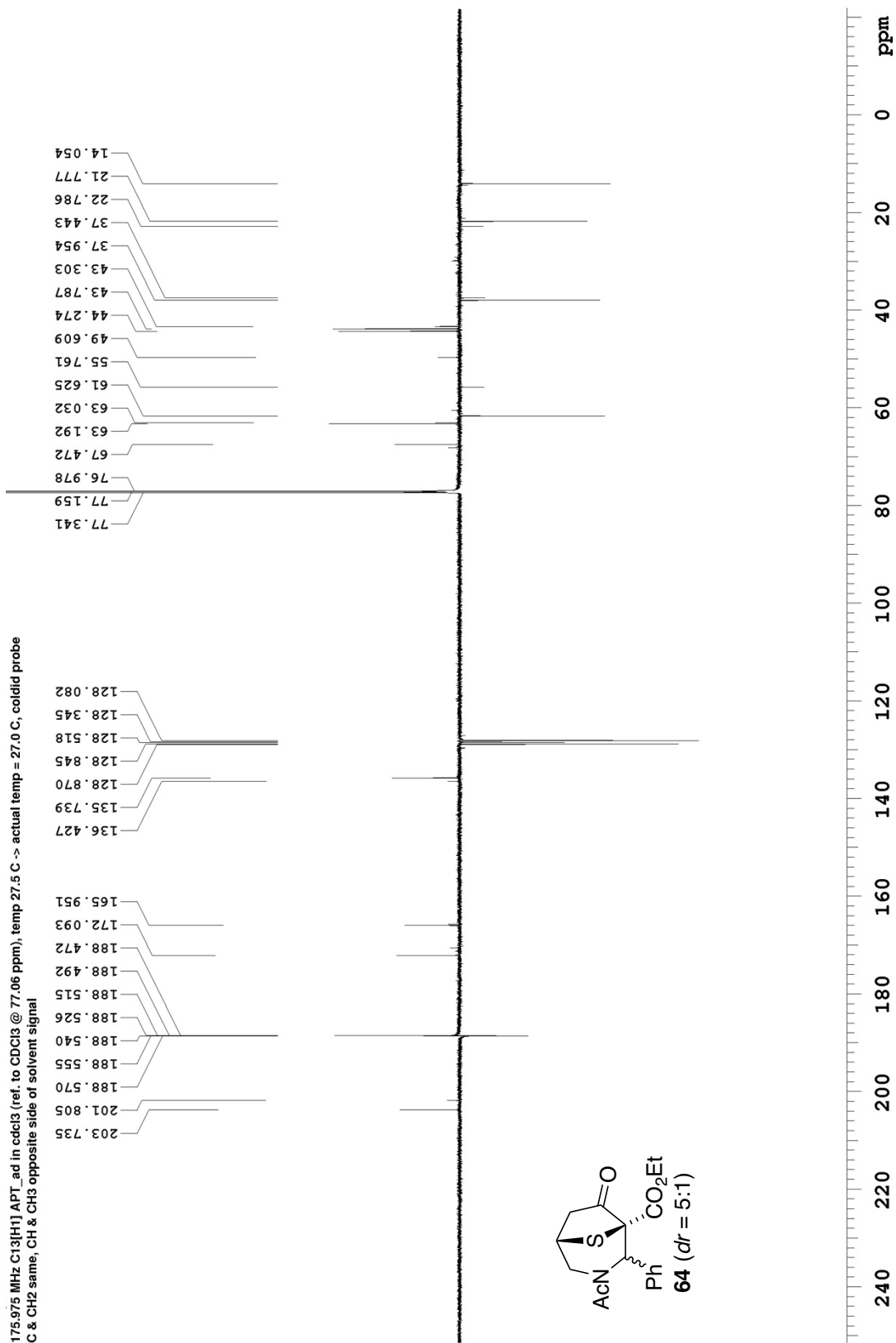
125.690 MHz C13{H1} APT, ad in cdcl3 (ref. to CDCl3 @ 77.06 ppm), temp 27.7 C -> actual temp = 27.0 C, coldlial probe
 C & CH2 same, CH & CH3 opposite side of solvent signal

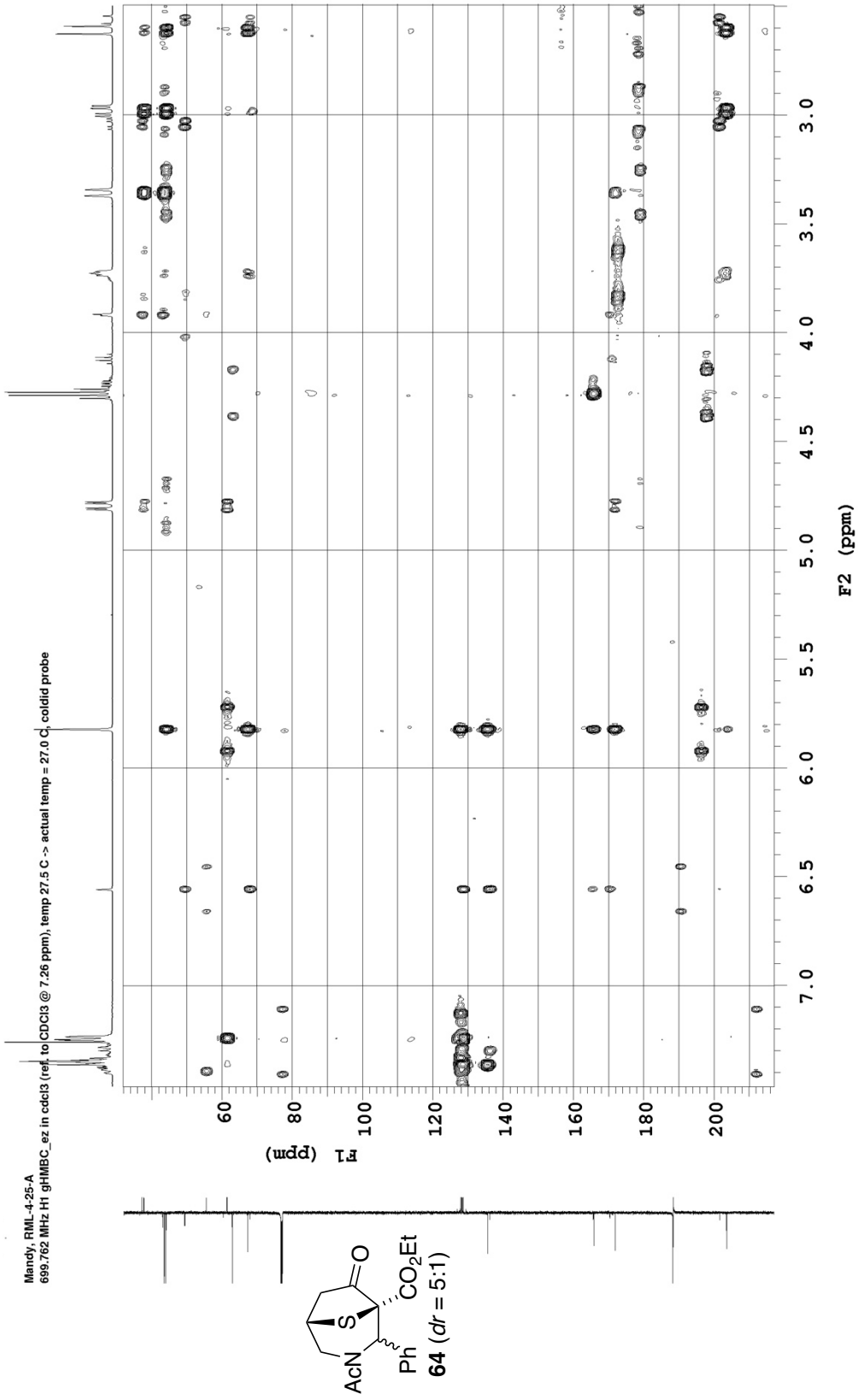


499.806 MHz H1 PRESAT in cdcl3 (ref. to CDCl3 @ 7.26 ppm), temp 27.7 C -> actual temp = 27.0 C, coldlual probe

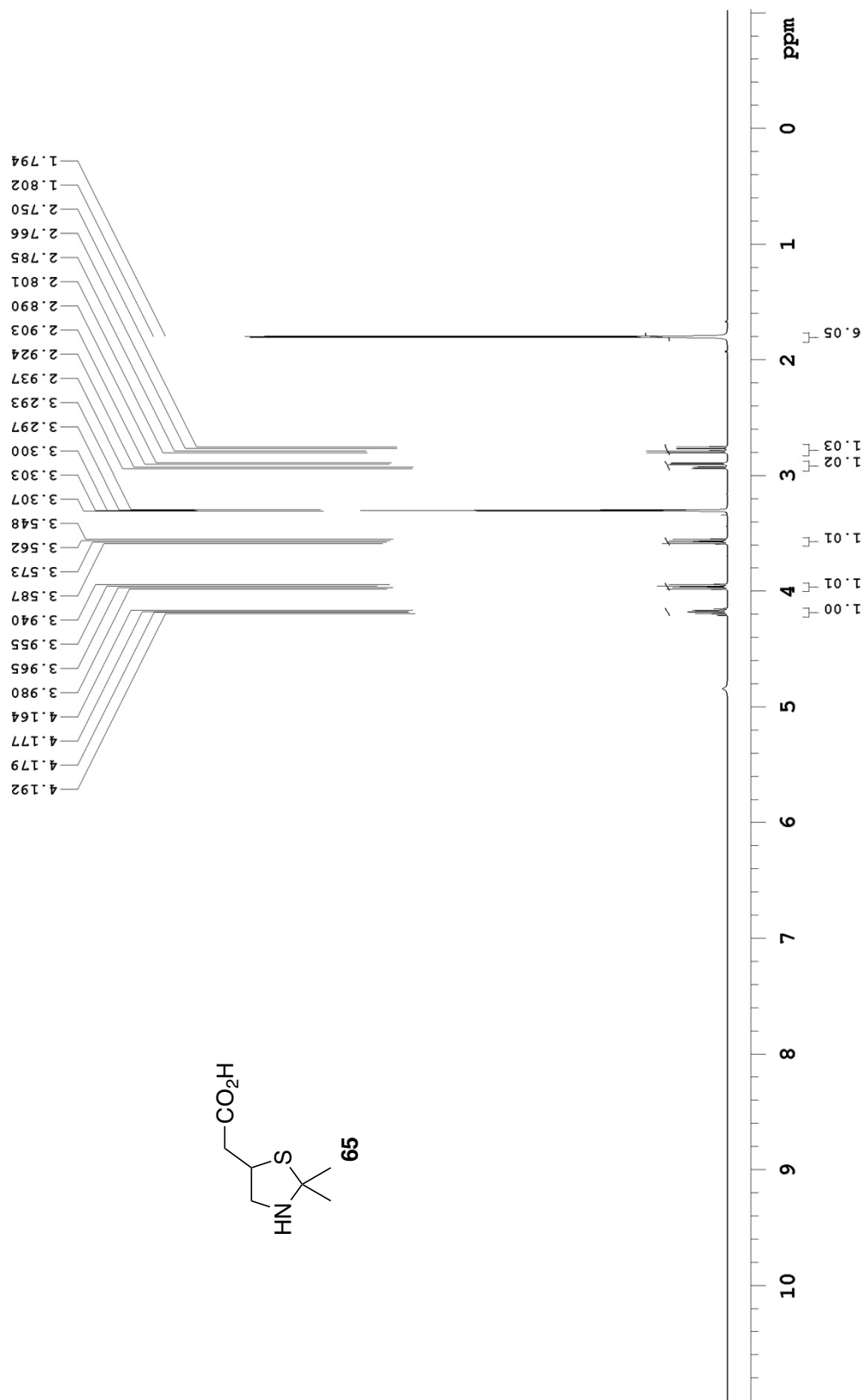


175.975 MHz C13{H1} APT_ad in cdc13 (ref. to cdc13 @ 77.06 ppm), temp 27.5 C -> actual temp = 27.0 C, coldid probe
 C & CH2 same, CH & CH3 opposite side of solvent signal

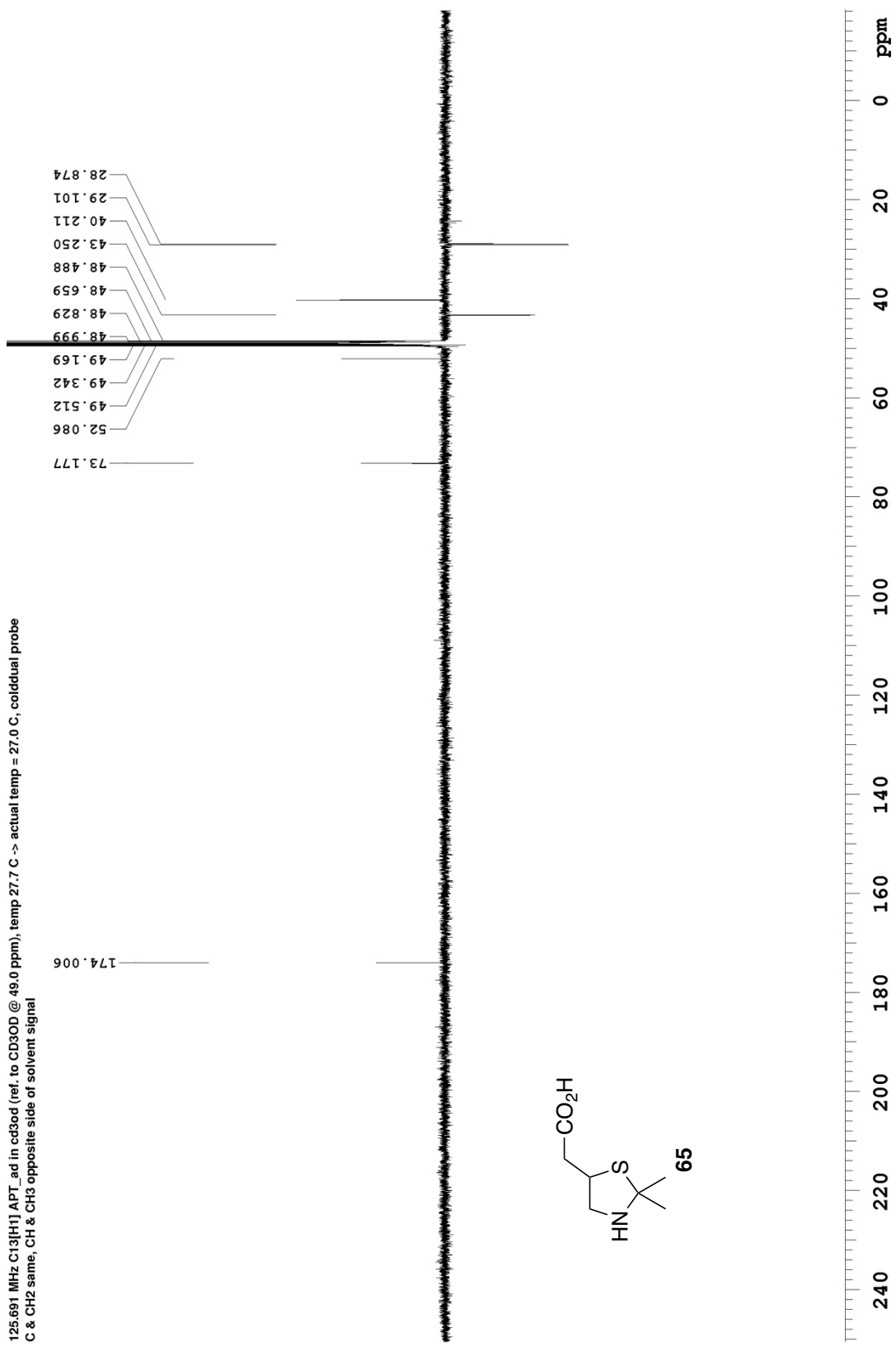




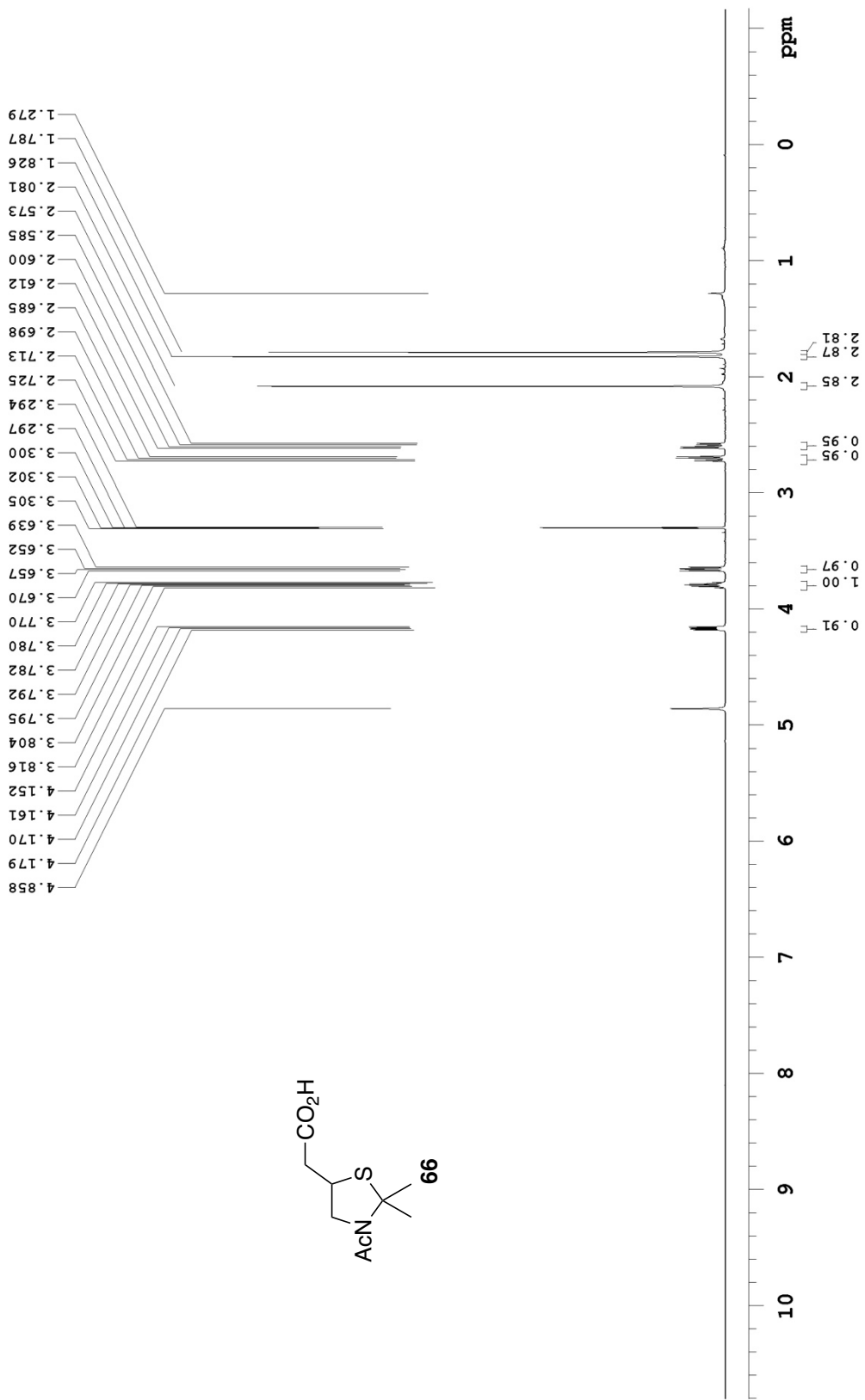
499.808 MHz ¹H PRESAT in cd3od (ref. to CD3OD @ 3.30 ppm), temp 27.7 C -> actual temp = 27.0 C, coldlual probe



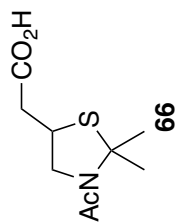
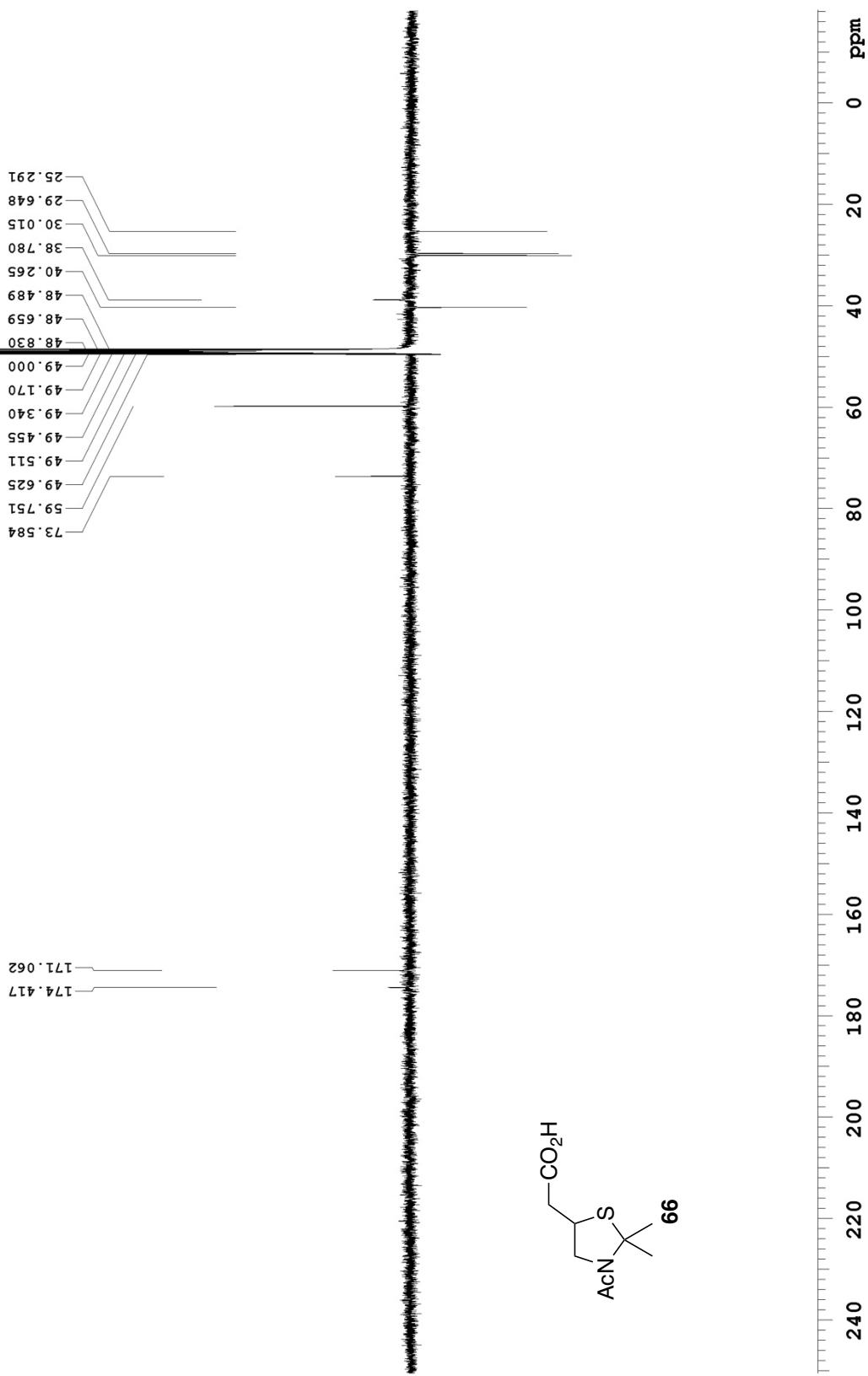
125.691 MHz C13[H1] APT ad in cd3od (ref. to CD3OD @ 49.0 ppm), temp 27.7 C -> actual temp = 27.0 C, cold dual probe
C & CH2 same, CH & CH3 opposite side of solvent signal



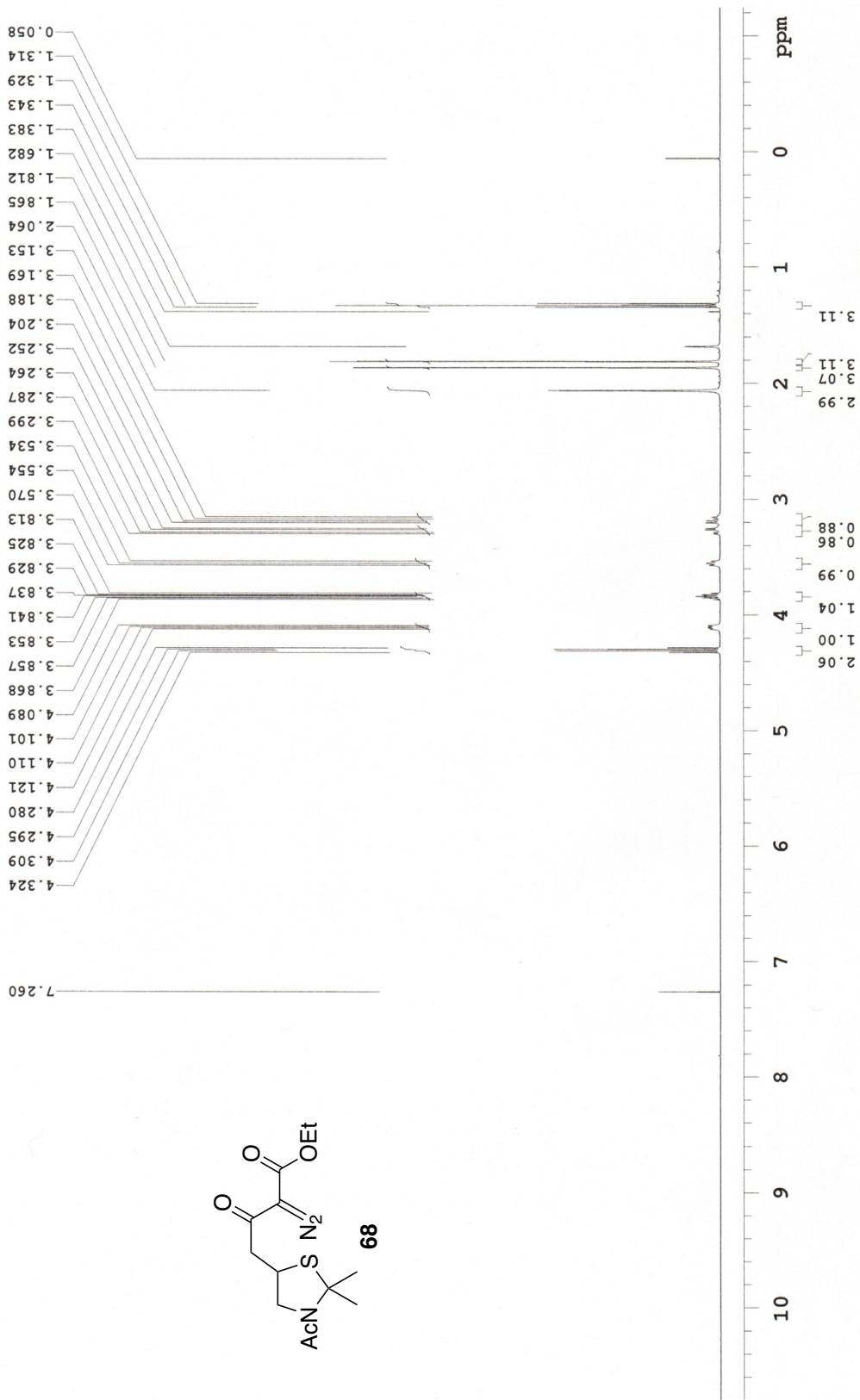
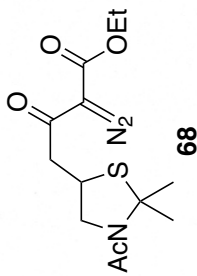
599.928 MHz H1 1D in cd3od (ref. to CD3OD @ 3.30 ppm), temp 25.8 C -> actual temp = 27.0 C, autoxid probe



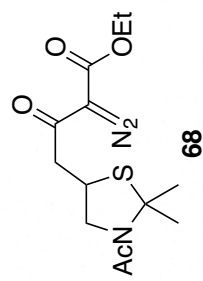
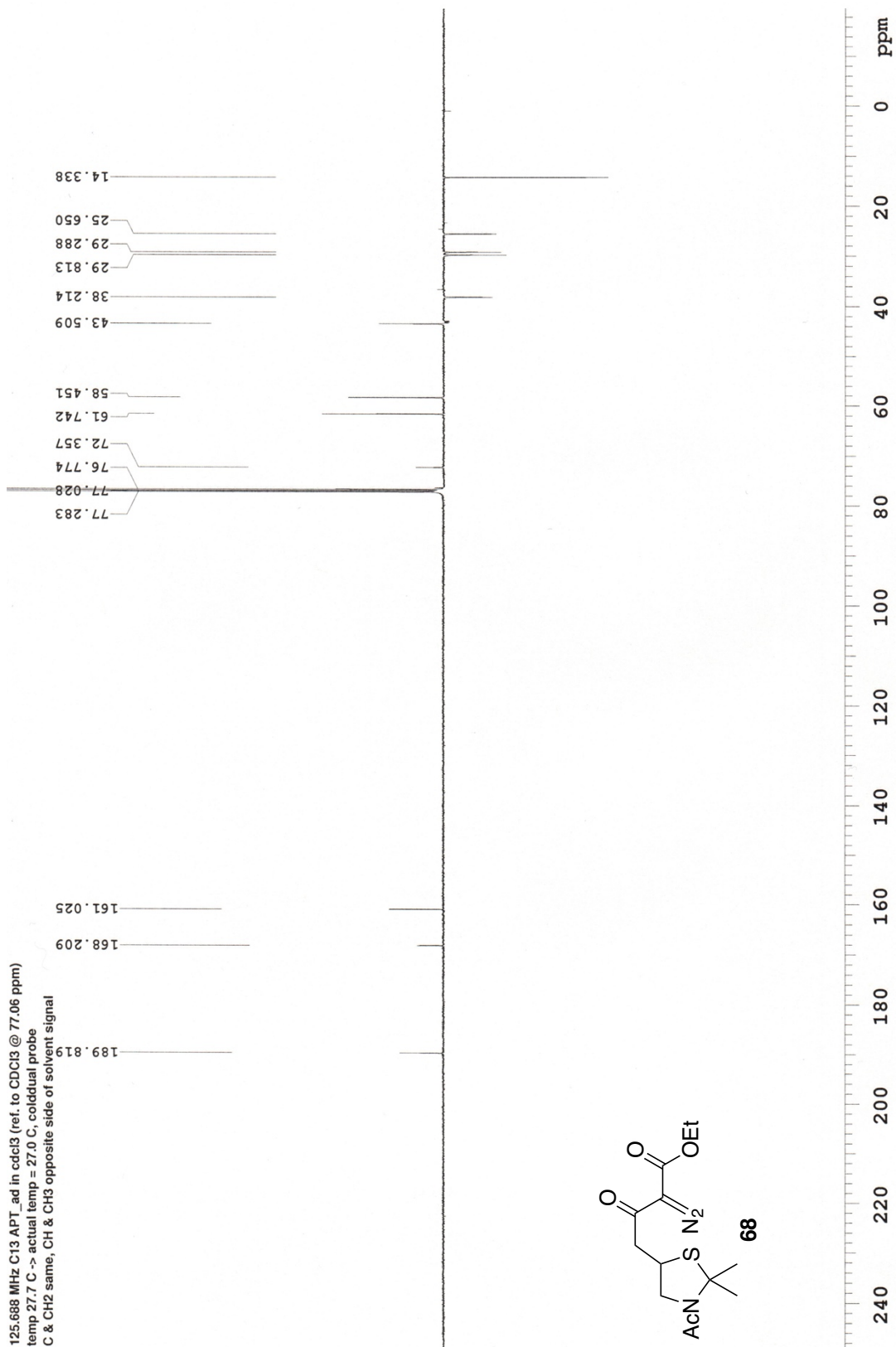
125.691 MHz C13{H1} APT ad in cd3od (ref. to CD3OD @ 49.0 ppm), temp 27.7 C -> actual temp = 27.0 C, cold dual probe
C & CH2 same, CH & CH3 opposite side of solvent signal



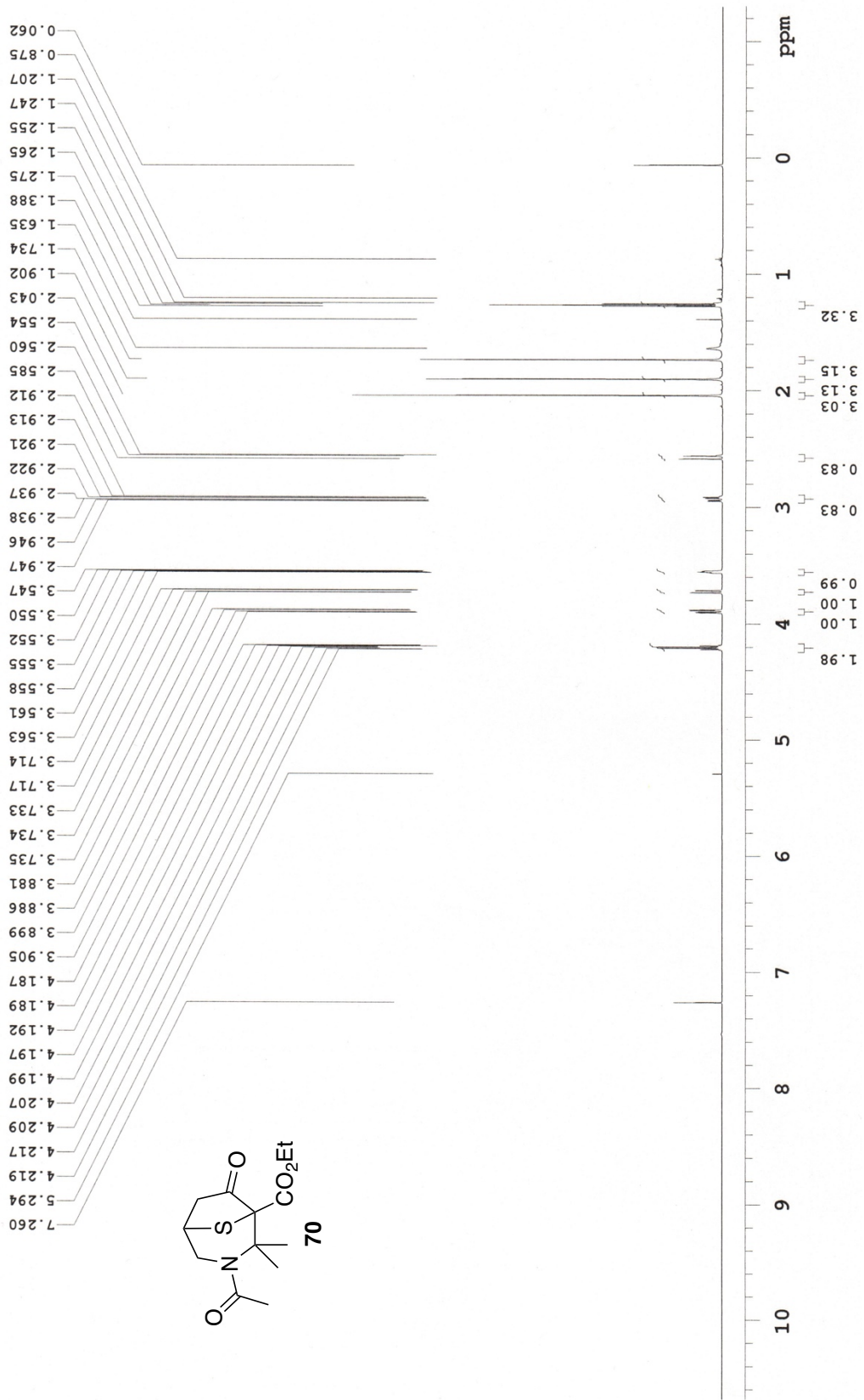
498.118 MHz ¹H 1D in cdcl₃ (ref. to CDCl₃ @ 7.26 ppm)
temp 26.9 C -> actual temp = 27.0 C, autotxdb probe



125.688 MHz C13 APT .ad in cdcl3 (ref. to CDCl3 @ 77.06 ppm)
temp 27.7 C -> actual temp = 27.0 C, coldlual probe
C & CH2 same, CH & CH3 opposite side of solvent signal



699.762 MHz H1 1D in cdcl3 (ref. to CDCl3 @ 7.26 ppm)
temp 27.5 C -> actual temp = 27.0 C, coldid probe



100.689 MHz C13 APT, ad in cdcl3 (ref. to CDC13 @ 77.06 ppm)
temp 27.0 C -> actual temp = 27.0 C, m400gz probe
C & CH2 same, CH & CH3 opposite side of solvent signal

